

**UNIVERSIDAD AUTÓNOMA DE MADRID**

**FACULTAD DE CIENCIAS**

**Dpto. de Biología Molecular**

**ENDOTHELIAL ADHESIVE PLATFORMS AND DOCKING STRUCTURES:  
MOLECULAR COMPOSITION, BIOPHYSICAL PROPERTIES, DYNAMICS  
AND INVOLVEMENT IN LEUKOCYTE FIRM ADHESION**

**Memoria que para optar al grado de Doctora en Ciencias Biológicas**

**con mención de Doctora Europea presenta la Licenciada:**

**Olga Barreiro del Río**

**Director: Dr. Francisco Sánchez-Madrid**

**Catedrático de Inmunología de la Universidad Autónoma de Madrid**

**Madrid 2007**

---

<b>INDEX.....</b>	<b>1</b>
<b>SUMMARY.....</b>	<b>4</b>
<b>INTRODUCCIÓN</b>	
<b>EL PROCESO DE EXTRAVASACIÓN.....</b>	<b>5</b>
. <i>Interacciones iniciales entre leucocitos circulantes y el endotelio: tethering y rodamiento mediado por selectinas y sus ligandos.....</i>	<b>6</b>
. <i>Papel central de las integrinas leucocitarias y sus ligandos endoteliales en los procesos de activación, parada, adhesión firme y locomoción.....</i>	<b>7</b>
. <i>Integrinas y sus ligandos durante la transmigración endotelial.....</i>	<b>13</b>
<b>MICRODOMINIOS DE TETRASPANINAS.....</b>	<b>15</b>
<b>ESTUDIO DE LAS PROPIEDADES BIOFÍSICAS DE LAS PROTEÍNAS MEDIANTE TÉCNICAS DE MICROSCOPIA ANALÍTICA.....</b>	<b>18</b>
<b>INTRODUCTION</b>	
<b>EXTRAVASATION PROCESS.....</b>	<b>21</b>
. <i>Initial interactions between circulating leukocytes and the endothelium: tethering and rolling mediated by selectins and their ligands.....</i>	<b>21</b>
. <i>Central role of leukocyte integrins and their endothelial ligands in the activation, arrest, firm adhesion and locomotion processes.....</i>	<b>23</b>
. <i>Integrins and their ligands during transendothelial migration .....</i>	<b>32</b>
<b>TETRASPANIN MICRODOMAINS.....</b>	<b>34</b>
<b>STUDY OF THE BIOPHYSICAL PROPERTIES OF PROTEINS USING ANALYTICAL MICROSCOPY TECHNIQUES.....</b>	<b>37</b>
<b>OBJECTIVES.....</b>	<b>40</b>
<b>MATERIALS AND METHODS.....</b>	<b>41</b>

**RESULTS**

. <i>VCAM-1 interacts with moesin and ezrin at the apical surface of activated endothelial cells</i> .....	<b>57</b>
. <i>Differential contribution of VCAM-1, ICAM-1, and ERM proteins to the extravasation process</i> .....	<b>58</b>
. <i>Redistribution of VCAM-1, ICAM-1 and ERM proteins at a docking structure during endothelium-leukocyte interaction</i> .....	<b>62</b>
. <i>Relocation of cytoskeletal components to the endothelial docking structure</i> .....	<b>65</b>
. <i>The docking structure is regulated by PI(4,5)P<sub>2</sub> and Rho/p160 ROCK</i> .....	<b>67</b>
. <i>Tetraspanins are components of the endothelial docking structure for adherent leukocytes by their association with ICAM-1 and VCAM-1</i> .....	<b>71</b>
. <i>Tetraspanin microdomains are critical for a proper expression and function of ICAM-1 and VCAM-1</i> .....	<b>75</b>
. <i>Tetraspanin soluble peptides interfere with ICAM-1 and VCAM-1 function without affecting their surface expression</i> .....	<b>78</b>
. <i>Enhanced ICAM-1 and VCAM-1 adhesive function requires an appropriate tetraspanin environment</i> .....	<b>82</b>
. <i>Endothelial ICAM-1 and VCAM-1 cluster at the docking structure independently of counterreceptor engagement and actin anchorage</i> .....	<b>85</b>
. <i>Analysis of ICAM-1 and VCAM-1 hetero- and homo-dimers in living endothelial cells</i> .....	<b>88</b>
. <i>Tetraspanin microdomains mediate the association of endothelial adhesion receptors to form specialized endothelial adhesive platforms</i> .....	<b>90</b>
. <i>Diffusional properties of endothelial adhesive platforms at nude membrane and at docking structures</i> .....	<b>92</b>
. <i>Diffusional characteristics of individual endothelial adhesive platform constituents determined by FCS and FCCS single-molecule measurements</i> .....	<b>98</b>
. <i>Complexity of inter-molecular interactions within endothelial adhesive platforms</i> .....	<b>101</b>
. <i>Modulation of nanoclustering and diffusion within the endothelial adhesive platforms by tetraspanin blocking peptides</i> .....	<b>106</b>

**DISCUSSION**

*. Identification and characterization of the endothelial docking structure for adherent leukocytes.....112*

*. Functional role of the inclusion of endothelial adhesion receptors in tetraspanin-enriched microdomains.....116*

*. Endothelial adhesive platforms as a model for the biophysical study of tetraspanin-enriched microdomains.....122*

*. Regulation of the avidity of endothelial adhesion receptors by their inclusion in tetraspanin-enriched endothelial adhesive platforms.....127*

**CONCLUSIONS.....131**

**CONCLUSIONES.....133**

**REFERENCES..... 135**

**APPENDIX I (SUPPLEMENTAL MATERIAL).....151**

**APPENDIX II (ABBREVIATIONS) .....160**

**APPENDIX III (LIST OF PUBLICATIONS).....162**

**SUMMARY**

Endothelial adhesion receptors ICAM-1 and VCAM-1 are key molecules for leukocyte extravasation to inflammatory foci. In this work, we demonstrate that both receptors together with the actin-cytoskeleton and related proteins such as ezrin, moesin,  $\alpha$ -actinin, vinculin and VASP participate in the formation of a three-dimensional structure (endothelial docking structure) that arises from the apical surface of activated endothelial cells to partially embraced and firmly attached adherent lymphocytes, preventing their detachment under physiological hemodynamic conditions. The formation and maintenance of this cup-like structure is regulated by Rho/ROCK and phosphoinositide PIP<sub>2</sub>. Furthermore, tetraspanin proteins CD9 and CD151 laterally associate with ICAM-1 and VCAM-1 at the plasma membrane, co-localizing with these adhesion receptors at the endothelial docking structures. The insertion of ICAM-1 and VCAM-1 in tetraspanin microdomains is crucial for the proper adhesive functions of these endothelial receptors. In addition, ICAM-1 and VCAM-1 are able to co-cluster at docking structures in the absence of ligand engagement, actin anchorage and heterodimer formation. This phenomenon can be explained by their specific interactions within the tetraspanin microdomains (ICAM-1/CD9, VCAM-1/CD151, CD9/CD151). The analysis of the biophysical properties of tetraspanin and adhesion receptors demonstrate the existence of these organized microdomains containing CD9, CD151, ICAM-1 and VCAM-1 at the apical endothelial plasma membrane of living cells, with different diffusional properties compared to lipid rafts. These particular kind of microdomains has been termed endothelial adhesive platforms (EAP). Finally, EAP-induced nanoclustering of VCAM-1 and ICAM-1 represents a novel mechanism of supramolecular organization that regulate the efficient leukocyte integrin-binding capacity of both endothelial receptors.

## **INTRODUCCIÓN**

### **EL PROCESO DE EXTRAVASACIÓN**

El proceso de extravasación leucocitaria, que tiene lugar durante la recirculación linfoide o la respuesta inflamatoria, requiere de cambios morfológicos drásticos que implican el agrupamiento de receptores de adhesión en estructuras protrusivas de la membrana plasmática, tanto en leucocitos como en células endoteliales. La extravasación es un proceso activo no sólo para los leucocitos sino también para el endotelio, lo que promueve la rápida y eficiente llegada de los leucocitos a los tejidos diana sin comprometer la integridad de la barrera endotelial.

Los receptores de adhesión regulan muchos procesos tales como la activación, migración, crecimiento, diferenciación y muerte celular (Frenette and Wagner, 1996a; Frenette and Wagner, 1996b) mediante la transducción directa de señales y la modulación de otras cascadas de señalización intracelular desencadenadas por diferentes factores de crecimiento (Aplin et al., 1998). Las interacciones celulares son críticas para la regulación de la hematopoyesis (Levesque et al., 1999; Verfaillie, 1998) y la respuesta inflamatoria (Butcher, 1991; Butcher and Picker, 1996). El funcionamiento coordinado de los receptores de adhesión, el citoesqueleto y las moléculas de señalización es crucial para la extravasación leucocitaria, un proceso central en la inmunidad. Así, la correcta integración de señales “del exterior al interior” y “del interior al exterior” en leucocitos y endotelio durante cada paso de la extravasación es crítico para permitir la consecución de este fenómeno, el llamado paradigma multi-secuencial (Butcher, 1991; Springer, 1994).

## **Interacciones iniciales entre leucocitos circulantes y el endotelio: tethering y rodamiento mediado por selectinas y sus ligandos**

Los leucocitos circulantes en el torrente sanguíneo deben establecer contacto y adherirse a la pared vascular soportando fuerzas de cizalla, para iniciar la respuesta inflamatoria o migrar a órganos linfoides secundarios (recirculación). El “tethering” y el rodamiento de los leucocitos sobre el endotelio activado son los primeros pasos del proceso secuencial de extravasación, seguidos de la adhesión firme y la migración transendotelial. Estos contactos iniciales están mediados mayoritariamente por selectinas y sus ligandos. Las selectinas (P-, E- y L-selectina) son glicoproteínas transmembrana tipo I que se unen a carbohidratos sialilados presentes en sus ligandos de forma dependiente de  $Ca^{2+}$ . Aunque las selectinas y sus ligandos tienden a interactuar con afinidad variable, la elevada frecuencia de asociación-disociación de sus interacciones les permiten mediar contactos transitorios entre leucocitos y endotelio (“tethering”) (Mehta et al., 1998; Nicholson et al., 1998). Estos contactos provocan la disminución de velocidad de los leucocitos y permiten su rodamiento sobre la superficie endotelial, lo que favorece las interacciones subsiguientes mediadas por integrinas y sus ligandos, aumentando la adherencia de los leucocitos, lo que finalmente provoca su parada en la pared venular (Evans and Calderwood, 2007). Además de las selectinas y sus ligandos, las integrinas  $\alpha 4\beta 1$  y  $\alpha 4\beta 7$  a través de su interacción con VCAM-1 y MAdCAM-1, respectivamente, pueden mediar de manera independiente estos contactos iniciales (Alon et al., 1995; Berlin et al., 1995). Por otra parte, la interacción LFA-1/ICAM-1 coopera con la función de L-selectina, estabilizando la fase de tethering y disminuyendo la velocidad de rodamiento (Henderson et al., 2001; Kadono et al., 2002).

La localización topográfica de los receptores de adhesión es necesaria para su correcto funcionamiento durante el tráfico leucocitario (von Andrian et al., 1995). Por

ello, las selectinas, sus ligandos y las integrinas  $\alpha 4$  se encuentran agrupadas en los extremos de los microvilli. Por otra parte, el anclaje de las selectinas al citoesqueleto de actina mediante proteínas como  $\alpha$ -actinina o moesina es necesario para su adecuado funcionamiento (Dwir et al., 2001; Ivetic et al., 2002; Pavalko et al., 1995).

### **Papel central de las integrinas leucocitarias y sus ligandos endoteliales en los procesos de activación, parada, adhesión firme y locomoción**

El tráfico de los leucocitos a través de los diferentes tejidos y órganos, y su interacción posterior con otras células inmunes es esencial para el desarrollo de la inmunidad innata y adquirida (von Andrian and Mackay, 2000). Las integrinas son moléculas clave en la migración celular que controlan las interacciones intercelulares y célula-matriz extracelular durante la recirculación y la inflamación. Una de sus características más importantes estriba en la regulación de su actividad adherente de manera independiente a su nivel de expresión en membrana (Hynes, 2002). Así, los leucocitos circulantes en sangre mantienen sus integrinas en conformación inactiva para evitar contactos inespecíficos con paredes vasculares no inflamadas, pero cuando encuentran un foco inflamatorio, se produce una rápida activación *in situ* de sus integrinas (Campbell et al., 1998). Como en el caso de las selectinas, la distribución espacial de las integrinas y sus ligandos en estructuras de membrana especializadas es esencial para su apropiado funcionamiento. Esta organización topográfica requiere una precisa regulación del citoesqueleto para permitir el reclutamiento de intermediarios de señalización y segundos mensajeros que desencadenen la activación celular (Vicente-Manzanares and Sanchez-Madrid, 2004).

Las integrinas constituyen una familia de 24 receptores heterodiméricos, compuesto cada uno de ellos por una subunidad  $\alpha$  y otra  $\beta$ . Son moléculas que regulan

dinámicamente sus propiedades adherentes mediante cambios conformacionales (afinidad) así como por redistribución espacial en la superficie celular (avidéz) (Carman and Springer, 2003). Datos recientes predicen la existencia de tres estados conformacionales (plegado/con baja afinidad, extendido con afinidad intermedia y extendido con alta afinidad) (Beglova et al., 2002; Nishida et al., 2006). Las integrinas más relevantes para la adhesión leucocitaria al endotelio son miembros de la subfamilia  $\beta 2$ , particularmente LFA-1 (CD11a/CD18 o  $\alpha L\beta 2$ ) y la integrina específica de linaje mielóide Mac-1 (CD11b/CD18 o  $\alpha M\beta 2$ ), así como las integrinas  $\alpha 4$  VLA-4 ( $\alpha 4\beta 1$ ) y  $\alpha 4\beta 7$ . La mayoría de sus ligandos son proteínas transmembrana que pertenecen a la superfamilia de las inmunoglobulinas. LFA-1 puede unirse a cinco moléculas de adhesión intercelular (ICAM-1 a -5), aunque las más relevantes son ICAM-1 e ICAM-3 (Gahmberg et al., 1990). ICAM-1 se expresa en leucocitos, células dendríticas y células epiteliales. Además, su expresión es baja en células endoteliales quiescentes, aumentando con estímulos pro-inflamatorios (Dustin et al., 1986). ICAM-3 es expresado constitutivamente por todos los leucocitos (Acevedo et al., 1993), mientras que la molécula de adhesión de uniones intercelulares JAM-1, un ligando adicional de LFA-1, se concentra selectivamente en la región apical de las uniones estrechas (“tight junctions”) en células endoteliales (Ostermann et al., 2002). Por otra parte, Mac-1 interacciona con ICAM-1, JAM-C y el receptor RAGE (Chavakis et al., 2003; Lamagna et al., 2005). La integrina VLA-4 interacciona con VCAM-1 (Elices et al., 1990), que es una molécula de adhesión que se expresa *de novo* tras la activación endotelial (Carlos and Harlan, 1994), y también se une a JAM-B (Cunningham et al., 2002). Además, VLA-4 interacciona con ADAM-28, fibronectina, osteopontina, trombospondina, el factor de coagulación von Willebrand y la proteína bacteriana invasina (Mittelbrunn et al., 2006). Finalmente, la integrina  $\alpha 4\beta 7$ , aparte de interaccionar con VCAM-1 y

fibronectina, reconoce específicamente a MAdCAM-1, un receptor expresado en los tejidos linfoides de las mucosas (Berlin et al., 1993).

#### Modulación de la actividad de las integrinas mediada por quimioquinas

Durante el establecimiento de los contactos iniciales con el endotelio vascular, los leucocitos disminuyen su velocidad de rodamiento y se activan al encontrar quimioquinas inmovilizadas y ligandos de integrinas expuestos en la superficie apical endotelial. Este paso de activación permite la parada y adhesión firme de los leucocitos al endotelio en condiciones de flujo fisiológico (Alon et al., 2003; Rot and von Andrian, 2004). La activación del leucocito implica un marcado cambio morfológico: la célula redondeada circulante se transforma en una célula pro-migratoria con morfología polarizada en la cual se distinguen al menos dos regiones, el frente de avance y el urópodo (del Pozo et al., 1995). La polarización del leucocito permite a la célula la coordinación de las fuerzas intracelulares para producir la locomoción celular necesaria durante el proceso de extravasación (Geiger and Bershadsky, 2002).

Las quimioquinas unidas a los glicosaminoglicanos de la membrana apical endotelial actúan señalizando a través de receptores acoplados a proteínas G (GPCRs) localizados en los microvilli del leucocito, induciendo una gran variedad de señales “del interior al exterior” en fracciones de segundo, que conducen a cambios conformacionales múltiples en las integrinas (Constantin et al., 2000; Sanchez-Madrid and del Pozo, 1999; Shamri et al., 2005). Debido a la complejidad y al corto margen de tiempo de los mecanismos de señalización inducidas por quimioquinas que controlan la activación de integrinas, es posible la existencia de redes protéicas compartimentalizadas y pre-formadas (“signalosomas”) en los leucocitos (Laudanna and Alon, 2006). La presencia de quimioquinas específicas de diferentes lechos vasculares

contribuye a orquestar el reclutamiento selectivo de las diferentes subpoblaciones leucocitarias a los focos inflamatorios o a los órganos linfoides secundarios (Luster, 1998). Además, las quimioquinas pueden ejercer un efecto diferencial sobre integrinas específicas dentro del mismo micro-ambiente (Laudanna, 2005).

#### Modulación de la afinidad de las integrinas mediada por sus ligandos

Tras la activación inducida por las quimioquinas, la conformación de las integrinas cambia de manera reversible de inactiva (plegada) a extendida con afinidad intermedia. Este evento prepara a la integrina para unirse a su ligando endotelial. Las integrinas que contienen un dominio I insertado en sus subunidades  $\alpha$  sufren un ulterior cambio conformacional tras la unión a ligando, que culmina en la activación total de la integrina y la parada del leucocito (Cabanas and Hogg, 1993; Jun et al., 2001; Salas et al., 2004). Por tanto, el estado conformacional de alta afinidad para la parada inmediata del leucocito sobre el endotelio requiere una inducción bidireccional por parte de las quimioquinas inmobilizadas y los ligandos de integrinas (Grabovsky et al., 2000; Shamri et al., 2005). Sin embargo, las integrinas  $\alpha_4$ , que contienen un dominio “I-like” en sus cadenas  $\beta$ , pueden interactuar espontáneamente con sus ligandos endoteliales sin estimulación quimiotáctica previa (Alon et al., 1995).

La señalización inducida por la unión a ligando conlleva la separación de las regiones citoplásmicas de las subunidades de la integrina, lo que favorece su asociación con el citoesqueleto cortical de actina. Además, la unión al ligando aumenta el reclutamiento de integrinas adicionales para incrementar la adhesión firme del leucocito en condiciones de estrés de flujo (Dobereiner et al., 2006). Este agrupamiento de integrinas depende de la liberación de su anclaje al citoesqueleto de actina, que está mediada por la proteína quinasa C (PKC) y calpaína, para aumentar su movilidad lateral en la membrana (Stewart et al., 1998). En este sentido, se ha sugerido la presencia de

nano-agrupamientos de LFA-1 no unidos a ligando en la membrana plasmática de los leucocitos, que promueven la formación eficiente de los micro-agrupamientos inducidos por unión a ligando (Cambi et al., 2006). Por otra parte, varios estudios sugieren que el estrés de flujo también regula a las integrinas, reforzando sus enlaces e, incluso, aumentando su afinidad (Marschel and Schmid-Schonbein, 2002; Zwartz et al., 2004). La integración de la señalización derivada de las quimioquinas y las fuerzas externas para favorecer la transmigración se ha definido como el fenómeno de quimio-reotaxis (Cinamon et al., 2001).

#### Regulación de la locomoción de los leucocitos por integrinas

Las señales implicadas en la adhesión firme de los leucocitos al endotelio mediadas por integrinas deben ser atenuadas para permitir la migración del leucocito hacia un sitio apropiado de transmigración. Las integrinas  $\beta 2$  parecen tener una implicación crítica en este proceso de locomoción, ya que su bloqueo o el de sus ligandos provoca migración al azar, fallo de posicionamiento en las uniones inter-endoteliales y diapedesis defectiva (Schenkel et al., 2004). Tras su activación por unión a ligando, las integrinas activan diferentes efectores de contractilidad de miosina, GTPasas remodeladoras de actina y moléculas implicadas en la regulación de la red de microtúbulos tanto en el frente de avance como en el urópodo. Así, la integración de señales generadas en ambos polos celulares lleva a un movimiento coordinado del leucocito (Vicente-Manzanares and Sanchez-Madrid, 2004).

#### Papel funcional de VCAM-1 e ICAM-1 en la captura de leucocitos

VCAM-1 e ICAM-1, miembros de la superfamilia de las inmunoglobulinas, son las principales moléculas de adhesión endotelial implicadas en la unión a las integrinas

VLA-4 y LFA-1, respectivamente (Elices et al., 1990; Marlin and Springer, 1987). Solamente ICAM-1 se expresa a bajo nivel en endotelio quiescente, mientras que se induce la expresión de ambas moléculas tras la activación celular por citoquinas pro-inflamatorias tales como IL-1 y TNF- $\alpha$  (Carlos and Harlan, 1994; Dustin et al., 1986). Además, se ha descrito la unión de VCAM-1 e ICAM-1 al citoesqueleto de actina a través de dos miembros de la familia ERM, ezrina y moesina (Barreiro et al., 2002; Heiska et al., 1998). Estas moléculas funcionan como conectores de la membrana con el citoesqueleto de actina regulando la morfogénesis cortical y la adhesión celular. Las proteínas ERM están implicadas en la formación de estructuras protrusivas de la membrana plasmática tales como filopodia, microespículas o microvilli (Mangeat et al., 1999; Yonemura and Tsukita, 1999). Estructuralmente, todos los miembros de la familia son muy parecidos entre sí y parecen ser funcionalmente redundantes, como lo sugiere el fenotipo aparentemente normal del ratón knockout para moesina (Doi et al., 1999). El dominio N-terminal de las ERM es capaz de interaccionar con proteínas integrales de membrana, mientras que su extremo C-terminal se une a F-actina (Turunen et al., 1994). Su funcionamiento está conformacionalmente regulado, cambiando reversiblemente de la forma plegada o inactiva a la forma extendida o activa. La unión de fosfatidilinositol 4,5-bisfosfato y la fosforilación de un residuo específico de treonina en su porción C-terminal promueven la conformación activa de las ERM (Barret et al., 2000; Nakamura et al., 1999). La ruta de señalización Rho/ROCK y la producción de PIP<sub>2</sub> son los principales mecanismos de regulación para la activación de las ERM, induciendo su fosforilación y translocación a la membrana (Hirao et al., 1996; Matsui et al., 1998; Shaw et al., 1998). Por otra parte, las proteínas ERM activadas pueden

secuestrar Rho-GDI, permitiendo la activación de Rho, lo que a su vez promueve un mecanismo positivo de retro-alimentación de su propia activación (Takahashi et al., 1997).

En cuanto a la transducción de señales, VCAM-1 e ICAM-1 son capaces de transmitir señales tras su unión con el ligando. VCAM-1 está implicada en la apertura de las uniones interendoteliales para facilitar la extravasación de los leucocitos. De hecho, VCAM-1 induce la activación de la NADPH oxidasa y la producción de especies reactivas de oxígeno (ROS) de manera dependiente de Rac GTPasa, con la consiguiente activación de metaloproteinasas de matriz y pérdida de la adhesión mediada por VE-cadherina (Cook-Mills, 2002; van Wetering et al., 2002; van Wetering et al., 2003). Por otra parte, VCAM-1 e ICAM-1 son capaces de inducir un rápido incremento de las concentraciones de  $\text{Ca}^{2+}$  intracelular, produciendo la activación de Src kinasa y la subsiguiente fosforilación de cortactina (Etienne-Manneville et al., 2000; Lorenzon et al., 1998). ICAM-1 también puede activar RhoA induciendo la formación de fibras de estrés y la fosforilación de FAK, paxilina y p130<sup>Cas</sup>, que a su vez, están implicados en rutas de señalización que implican a JNK y p38 (Greenwood et al., 2002; Hubbard and Rothlein, 2000; Thompson et al., 2002a; Wang and Doerschuk, 2002). Además, también se ha descrito la inducción de la transcripción de c-fos y rhoA via ICAM-1 (Thompson et al., 2002). Finalmente, ICAM-1 también puede inducir su propia expresión y la de VCAM-1, como un mecanismo de regulación para facilitar la trans migración leucocitaria (Clayton et al., 1998).

### **Integrinas y sus ligandos durante la trans migración endotelial**

Las señales implicadas en la adhesión firme de los leucocitos al endotelio deben ser revertidas, debilitando los contactos originales lo suficiente para permitir la

migración y extravasación de los leucocitos. Durante la transmigración endotelial (TEM), las uniones endoteliales se deshacen parcialmente, evitando el daño de la monocapa o importantes cambios de permeabilidad. Así, las membranas del leucocito y el endotelio se mantienen en estrecho contacto durante la diapedesis y, posteriormente, las membranas endoteliales vuelven a sellar sus conexiones.

Una vez que los leucocitos encuentran un sitio apropiado para transmigrar (preferencialmente en las uniones intercelulares), extienden pseudópodos exploratorios entre dos células endoteliales adyacentes. A continuación, los pseudópodos evolucionan a una lamella que va atravesando el espacio abierto en la monocapa. Durante este proceso, LFA-1 es la integrina que tiene el papel preponderante. Esta molécula se relocaliza rápidamente, formando un agrupamiento en forma de anillo en la interfase de contacto leucocito-endotelio, donde interacciona con ICAM-1 y, en algunos otros modelos celulares, con JAM-A. Cuando el proceso de transmigración concluye, LFA-1 se concentra finalmente en el urópodo (Sandig et al., 1999; Shaw et al., 2004).

En el contexto de transmigración leucocitaria, además de la ruta clásica de diapedesis, en la que los leucocitos cruzan a través de uniones interendoteliales (ruta paracelular), existen crecientes evidencias que indican la existencia de una ruta alternativa, en la que los leucocitos podrían migrar a través de células endoteliales individuales (ruta transcelular) (Carman and Springer, 2004; Engelhardt and Wolburg, 2004). Este proceso tiene lugar preferencialmente en células endoteliales de microvasculatura. Nuevos datos sobre el mecanismo de este proceso de migración transcelular han sido aportados recientemente. Parece que, inicialmente, los leucocitos generan podosomas invasivos dependientes de la actividad de Src kinasa y de WASP para palpar la superficie endotelial que, posteriormente, evolucionan para formar el poro transcelular. En el endotelio es necesaria la fusión de membranas regulada por calcio y

complejos que contienen SNARE (Carman et al., 2007). Otro estudio describe la translocación de ICAM-1 a caveolas tras la adhesión leucocitaria y la posterior formación de una especie de canal multivesicular, que contiene ICAM-1 y caveolina-1, alrededor del pseudópodo leucocitario que penetra a través de la célula endotelial. Ambas proteínas, ICAM-1 y caveolina, siguen el paso de todo el leucocito, moviéndose hacia la membrana endotelial basal (Millan et al., 2006). Además, la proteína de filamentos intermedios vimentina también parece tener un papel importante en la ruta transcelular (Nieminen et al., 2006).

### **MICRODOMINIOS DE TETRASPANINAS**

Las tetraspaninas son una superfamilia de proteínas que cuenta con al menos 28 genes clonados en humanos. Son proteínas de bajo peso molecular, con una estructura secundaria común que atraviesa cuatro veces la membrana plasmática y con ambos extremos N- y C-terminal en el citosol. Estas proteínas presentan baja homología en su secuencia exceptuando varios dominios de carácter probablemente estructural, la mayoría en las regiones transmembrana, y algunas cisteínas implicadas en putativos puentes disulfuro en el segundo bucle extracelular (Maecker et al., 1997). Estas proteínas, que son bastantes ubicuas, son capaces de asociarse consigo mismas formando homo- y hetero-multímeros (Kovalenko et al., 2005; Stipp et al., 2003). Además, pueden asociarse lateralmente en la membrana plasmática con diversas proteínas transmembrana, principalmente a través de su segundo bucle extracelular, y, así, modular las funciones de los receptores asociados. Entre estas proteínas asociadas se incluyen moléculas endoteliales y leucocitarias de adhesión (Barreiro et al., 2005; Feigelson et al., 2003; Levy et al., 1998; Mannion et al., 1996; VanCompernelle et al., 2001), integrinas relacionadas con uniones intercelulares y célula-matriz extracelular

(Berditchevski, 2001; Lammerding et al., 2003; Yanez-Mo et al., 1998), el complejo CD19/CD21-BCR (receptor de células B) (Cherukuri et al., 2004), el complejo principal de histocompatibilidad (MHC) unido a péptido (Kropshofer et al., 2002; Vogt et al., 2002), receptores Fc (Moseley, 2005), receptores acoplados a proteínas G (Little et al., 2004), y metaloproteinasas (Andre et al., 2006; Takino et al., 2003; Yan et al., 2002). Las asociaciones de las tetraspaninas con receptores de membrana ocurren a través del segundo bucle extracelular que es muy divergente, lo que apoya la idea de que dichas asociaciones son realmente muy específicas. Las tetraspaninas también pueden asociarse a través de sus dominios intracelulares con mediadores de señalización citoplásmicos tales como la PI4K tipo II o diferentes isoformas de PKC (Yauch and Hemler, 2000; Zhang et al., 2001).

Recientes estudios bioquímicos, proteómicos y estructurales apoyan la existencia de microdominios ricos en tetraspaninas que podrían desempeñar una labor como organizadores de complejos moleculares en la membrana plasmática, integrando receptores de membrana y moléculas intracelulares de señalización, y con una composición específica y diferente a la de las balsas lipídicas (Hemler, 2005; Le Naour et al., 2006; Min et al., 2006; Nydegger et al., 2006). Estos microdominios ricos en tetraspaninas se formarían gracias a la habilidad de estas proteínas para interactuar simultáneamente entre ellas y con una gran variedad de moléculas, organizando compartimentos definidos pero dinámicos en la membrana plasmática. Aparte de su capacidad para actuar como adaptadores en la organización de la membrana, las tetraspaninas también están implicadas en la regulación del tráfico y el procesamiento biosintético de sus receptores asociados (Berditchevski and Odintsova, 2007). Aunque los microdominios enriquecidos en tetraspaninas difieren en sus propiedades de las balsas lipídicas, no están carentes de interacciones lipídicas, ya que son proteínas

altamente palmitoiladas que unen colesterol y gangliósidos (Charrin et al., 2003; Hakomori, 2002; Yang et al., 2004). La composición de estos microdominios así como otras características específicas, pueden variar en función del tipo celular. La delección génica, el silenciamiento o la sobre-expresión protéica y los experimentos de mutagénesis han revelado el papel principal de las tetraspaninas en muchos procesos fisiológicos fundamentales. Entre ellos, cabe destacar la fusión óvulo-espermatozoide (Le Naour et al., 2000; Rubinstein et al., 2006), la presentación antigénica (Delaguillaumie et al., 2004; Levy and Shoham, 2005b; Mittelbrunn et al., 2002; Unternaehrer et al., 2007), diversos procesos que tienen lugar durante la infección viral (Gordon-Alonso et al., 2006; Martin et al., 2005; Pileri et al., 1998), la actividad metaloproteínasa (Fujita et al., 2006; Hong et al., 2006; Hong et al., 2005; Takino et al., 2003), la angiogénesis (Takeda et al., 2007; Wright et al., 2004), la función renal (Sachs et al., 2006), el crecimiento de neuritas (Stipp and Hemler, 2000), la organización de hemidesmosomas (Sterk et al., 2000), la unión específica de los exosomas a las células dendríticas (Morelli et al., 2004), y la adhesión celular, migración e invasión (Barreiro et al., 2005; Chattopadhyay et al., 2003; Garcia-Lopez et al., 2005; Hemler, 2003; Kovalenko et al., 2007; Longo et al., 2001; Yanez-Mo et al., 1998; Yanez-Mo et al., 2001). El hecho de que se hayan encontrado muy pocos ligandos de tetraspaninas en “trans” sugiere que el papel regulador de las tetraspaninas en los procesos citados anteriormente ocurre de manera indirecta, a través de la unión en “cis” a sus receptores asociados (Hemler, 2001). Sin embargo, continúan siendo desconocidos los mecanismos moleculares subyacentes a esta actividad reguladora de las tetraspaninas.

## **ESTUDIO DE LAS PROPIEDADES BIOFÍSICAS DE LAS PROTEÍNAS MEDIANTE TÉCNICAS DE MICROSCOPIA ANALÍTICA**

Para comprender la complejidad y la dinámica de los procesos biológicos es necesario entender cómo las células organizan y compartimentalizan físicamente los receptores de adhesión y las moléculas señalizadoras en redes especializadas y eficientemente reguladas. En este sentido, se propone que las balsas lipídicas ricas en colesterol y esfingolípidos funcionan como plataformas para exportar componentes específicos a la membrana, incluyendo proteínas ancladas a membrana por glicosilfosfatidilinositol (GPI), y para proporcionar sitios específicos para el ensamblaje de complejos citoplásmicos de señalización (Anderson and Jacobson, 2002; Simons and Toomre, 2000). La existencia de las balsas lipídicas ha sido estudiada de manera extensiva haciendo uso de innovadores métodos de microscopía analítica (Kenworthy et al., 2004; Larson et al., 2005; Sharma et al., 2004; Suzuki et al., 2007a; Suzuki et al., 2007b). Sin embargo, no se ha documentado hasta la fecha ningún estudio demostrando la existencia de microdominios ricos en tetraspaninas en la membrana plasmática de células vivas y caracterizando sus propiedades dinámicas.

Las propiedades dinámicas de una proteína son cruciales para determinar su función dentro de la célula y para entender cómo, cuándo y dónde puede interactuar físicamente con otras proteínas y macromoléculas en respuesta a estímulos extracelulares. El reciente desarrollo de potentes técnicas analíticas microscópicas y espectroscópicas complementarias permite el análisis espacio-temporal de complejos proteicos, así como el estudio de su composición y el cálculo de su estequiometría, estado de oligomerización, propiedades difusivas, etc.

Los complejos macromoleculares tienen dimensiones nanométricas, por lo que no son directamente accesibles mediante estudios de colocalización con microscopía

confocal convencional, que se encuentra limitada por su resolución óptica. Sin embargo, la detección de interacciones moleculares en células vivas se puede llevar a cabo fusionando una proteína fluorescente donadora a una de las proteínas de interés y una proteína fluorescente aceptora a la otra proteína del par protéico en estudio, y midiendo la transferencia de energía de resonancia de Förster (FRET) del fluoróforo donador al aceptor, que ocurre en un rango de decenas de angstroms, y que sólo puede tener lugar si las proteínas se encuentran interaccionando de manera directa. Como consecuencia del FRET, el tiempo de vida de la fluorescencia del donador decrece y éste es un parámetro que se puede medir en células vivas mediante la técnica microscópica denominada FLIM. Esta técnica es mucho más reproducible y sensible que los métodos clásicos para medir FRET basados en intensidad de fluorescencia. Además, el método de FLIM es lo suficientemente rápido para ser aplicado en células vivas (Caiolfa et al., 2007; Wallrabe and Periasamy, 2005).

Las proteínas se localizan en dominios en equilibrio dinámico en la membrana plasmática. La difusión protéica se puede estudiar a escala microscópica considerando una población molecular en su conjunto. Para ello, se utiliza una técnica denominada recuperación de fluorescencia tras el fotoblanqueo (FRAP) que consiste en el quemado de la fluorescencia en una región de interés dentro de una célula viva y, a continuación, la medida de la tasa de recuperación de fluorescencia en esa región para obtener un coeficiente de difusión aparente de la proteína marcada fluorescentemente (Phair and Misteli, 2001). Alternativamente, se pueden utilizar proteínas fotoactivables o fotoconvertibles para marcar de manera específica una subpoblación molecular en una célula viva y estudiar su movilidad en el tiempo. Por otro lado, se pueden realizar estudios de difusión a nivel de molécula individual utilizando el método denominado espectroscopía de correlación de fluorescencia (FCS), o bien, extender el análisis

cuantitativo a dos especies moleculares que co-difunden en los mismos complejos usando espectroscopía de cross-correlación de fluorescencia (FCCS). La técnica de FCS analiza las fluctuaciones de la intensidad de fluorescencia de un sistema en equilibrio. De este modo, la FCS y el análisis del histograma del conteo de fotones (PCH) permiten obtener información dinámica de una región específica en la célula (un femto-volumen), así como la estimación de la concentración local y el estado de oligomerización de las especies moleculares difusibles. Finalmente, la variante para doble color (FCCS), complementa los estudios de FLIM-FRET, monitorizando las interacciones moleculares entre especies difusibles y obteniendo la estequiometría de los complejos, así como la cinética de dichas interacciones (Muller et al., 2003).

## **INTRODUCTION**

### **EXTRAVASATION PROCESS**

Leukocyte extravasation during homing and inflammation requires drastic cell morphological changes, involving cytoskeletal-directed clustering of adhesion receptors in specialized protrusive membrane structures in leukocytes and endothelial cells. Extravasation is an active process not only for leukocytes but also for endothelial cells, which promote the rapid and efficient entry of leukocytes to the target tissues, without disturbing the integrity of the endothelial barrier.

Cell adhesion receptors regulate many cellular processes such as activation, migration, growth, differentiation and death (Frenette and Wagner, 1996a; Frenette and Wagner, 1996b), by both signal transduction and the modulation of intracellular signaling cascades triggered by different growth factors (Aplin et al., 1998). Cellular interactions are critical for regulation of hematopoiesis (Levesque et al., 1999; Verfaillie, 1998) and inflammatory responses (Butcher, 1991; Butcher and Picker, 1996). The coordinate function of adhesion receptors, cytoskeleton and signaling molecules is crucial for leukocyte extravasation, a central process in immunity. Hence, the correct integration of “outside-in” and “inside-out” signals in leukocytes and endothelium during each stage of extravasation is critical to allow the completion of this phenomenon, the so-called “multi-step paradigm” (Butcher, 1991; Springer, 1994).

#### **Initial interactions between circulating leukocytes and the endothelium: tethering and rolling mediated by selectins and their ligands**

Free-flowing leukocytes contact with and adhere to the vascular wall under shear forces to initiate an inflammatory response or to migrate into a secondary lymphoid organ

(homing). Leukocyte tethering and rolling on activated endothelial cells are the first steps of the sequential process of extravasation, followed by the firm adhesion and transendothelial migration of leukocytes. These initial contacts are largely mediated by selectins and their ligands. Selectins (P-, E- and L-selectin) are type I transmembrane glycoproteins that bind to sialylated carbohydrate moieties present on ligand molecules in a calcium-dependent manner. Although selectins and their ligands tend to interact with a variable affinity, their rapid association and dissociation rates mediate transient contacts between leukocytes and endothelium (“tethering”) (Mehta et al., 1998; Nicholson et al., 1998). Tethering results in the slowing of leukocytes in the bloodstream and their rolling on the surface of endothelium, which favors subsequent interactions with endothelial cells mediated by integrins and their ligands, increasing the adhesiveness of leukocytes, that leads to their final arrest on the vessel wall (Evans and Calderwood, 2007). In addition to selectins and their ligands,  $\alpha 4$  integrins ( $\alpha 4\beta 1$  and  $\alpha 4\beta 7$ ) through their interaction with VCAM-1 and MAdCAM-1, respectively, support leukocyte tethering, rolling, and arrest (Alon et al., 1995; Berlin et al., 1995). Moreover, the interaction of LFA-1/ICAM-1 cooperates with L-selectin, by stabilizing the tethering phase and decreasing the rolling velocity (Henderson et al., 2001; Kadono et al., 2002).

Adhesion receptor distribution on cell membrane has a key role in leukocyte interactions and is an important regulatory mechanism for leukocyte trafficking (von Andrian et al., 1995). Selectins, their ligands and  $\alpha 4$  integrins are clustered at the tips of microvilli, and this localization is critical for tethering and rolling. L-selectin is anchored to the actin cytoskeleton through the constitutive association of its cytoplasmic tail to alpha-actinin, and its cell activation-dependent binding to moesin (Ivetic et al., 2002; Pavalko et al., 1995). Although the association with alpha-actinin is not essential for its targeting to microvilli (Pavalko et al., 1995), its cytoplasmic anchorage to the actin

cytoskeleton is necessary to control L-selectin function (Alon and Feigelson, 2002; Dwir et al., 2001).

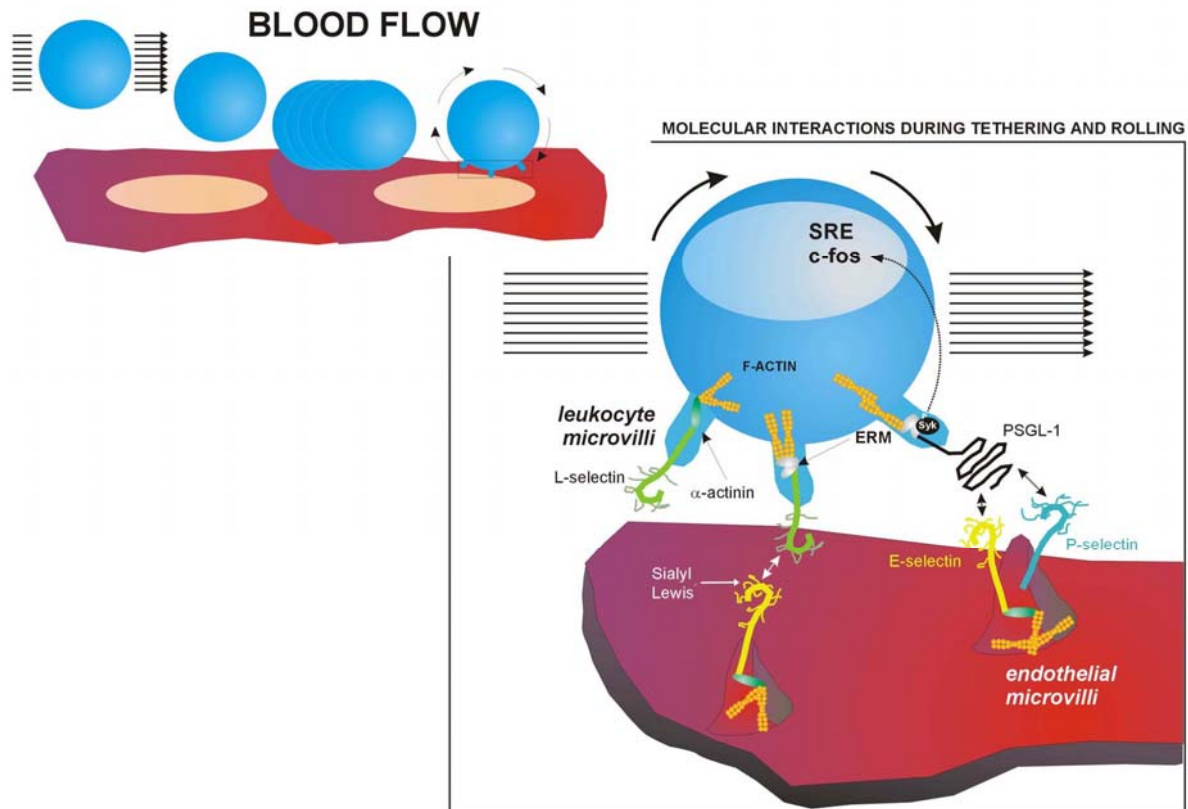


**Figure 1.** The first step of the extravasation process. As shown in the diagram, free-flowing leukocytes establish transient contacts with activated endothelial cells (tethering), being slowed down. These initial contacts allow leukocytes to roll on the endothelial wall to become activated and finally arrest. The main molecules that participate during this process are presented in detail in the inset: E- and P-selectin in endothelium as well as L-selectin and PSGL-1 in leukocytes are localized at specialized protrusions (microvilli) supported by the actin cytoskeleton, which is linked to the adhesion receptors via ERM proteins, alpha-actinin and other cytoskeletal components. All these molecules interact with their corresponding receptors through carbohydrate residues such as Sialyl Lewis<sup>x</sup>. Thus, L-selectin binds to several endothelial counterreceptors (E-selectin among them) and leukocyte PSGL-1 interacts with endothelial E- and P-selectin. In addition, The binding of PSGL-1 with its ligands allows the recruitment of the tyrosine kinase Syk via ERM proteins, which triggers signaling cascades that culminate in the activation of expression of several genes (e.g., SRE and c-fos) in leukocytes.

### **Central role of leukocyte integrins and their endothelial ligands in the activation, arrest, firm adhesion and locomotion processes**

Trafficking of leukocytes throughout different tissues and organs, and their subsequent interactions with other immune cells are crucial for the development of innate and adaptive immunity (von Andrian and Mackay, 2000). In this regard, integrins have a

central role in cell migration by controlling intercellular and cell-matrix interactions during homing and inflammation. One of the most important features of these receptors relies on the regulation of their adhesion activity independently of their membrane expression. Thus, leukocytes modify their adhesive properties to be properly adapted to every immune scenario (Hynes, 2002). Hence, free-flowing leukocytes maintain their integrins in non-adhesive conformation, to avoid unspecific contacts with non-inflamed vascular walls, but upon encountering localized inflammatory foci, a rapid *in situ* activation of leukocyte integrins by endothelium-displayed activating signals takes place (Campbell et al., 1998). The spatial distribution of integrins and their ligands in specialized membrane structures is also of key importance for the proper accomplishment of their adhesive functions. This topographic organization requires a finely regulated cellular cytoskeleton that also enables the recruitment of signaling intermediates and second messengers that lead to cellular activation (Vicente-Manzanares and Sanchez-Madrid, 2004).

Integrins constitute a large family of 24 heterodimeric adhesion receptors, each one composed of an  $\alpha$  and a  $\beta$  subunits. These molecules regulate dynamically their adhesiveness by conformational changes as well as by redistribution on cell surface (Carman and Springer, 2003). Recent data predict the existence of three conformational states for integrins, which differ in their localization on the plasma membrane and in conformation (folded/low affinity, extended with intermediate affinity and extended with high affinity) (Beglova et al., 2002; Nishida et al., 2006). The overall strength of adhesiveness (avidity) depends on the affinity of each individual receptor-ligand bond and the number of these interactions. Therefore, the regulation of integrin avidity involves both the modulation of receptor and ligand density and their redistribution on specialized membrane structures (Carman and Springer, 2004).

The most relevant integrins for leukocyte adhesion to endothelium are members of the  $\beta 2$  subfamily, particularly LFA-1 (CD11a/CD18 or  $\alpha L\beta 2$ ) and the myeloid specific integrin Mac-1 (CD11b/CD18 or  $\alpha M\beta 2$ ), as well as the  $\alpha 4$  integrins VLA-4 ( $\alpha 4\beta 1$ ) and  $\alpha 4\beta 7$ . Most of the cellular counterreceptors for leukocyte integrins are transmembrane proteins that belong to the immunoglobulin superfamily. LFA-1 binds five distinct intercellular cell adhesion molecules (ICAM-1 to -5), although the most relevant among them seem to be ICAM-1 and ICAM-3 (Gahmberg et al., 1990). ICAM-1 is found in leukocytes, dendritic cells, epithelial cells and is expressed at low levels in resting endothelial cells, becoming highly upregulated upon inflammatory stimuli (Dustin et al., 1986). ICAM-3 is constitutively expressed by all leukocytes (Acevedo et al., 1993), whereas the junctional adhesion molecule JAM-A, an additional ligand for LFA-1, is selectively concentrated at the apical region of intercellular tight junctions in endothelial cells (Ostermann et al., 2002). On the other hand, Mac-1 interacts with ICAM-1, JAM-C, and the endothelial receptor RAGE (Chavakis et al., 2003; Lamagna et al., 2005). The integrin VLA-4 interacts with VCAM-1 (Elices et al., 1990), which is expressed *de novo* upon endothelial cell activation (Carlos and Harlan, 1994) and also binds JAM-B (Cunningham et al., 2002). Alternatively, VLA-4 interacts with ADAM-28, fibronectin, osteopontin, thrombospondin, von Willebrand Factor, and the bacterial protein invasins (Mittelbrunn et al., 2006). Finally, the  $\alpha 4\beta 7$  integrin, apart from its interaction with fibronectin and VCAM-1, specifically recognizes MadCAM-1, a receptor expressed in mucosal lymphoid tissues (Berlin et al., 1993).

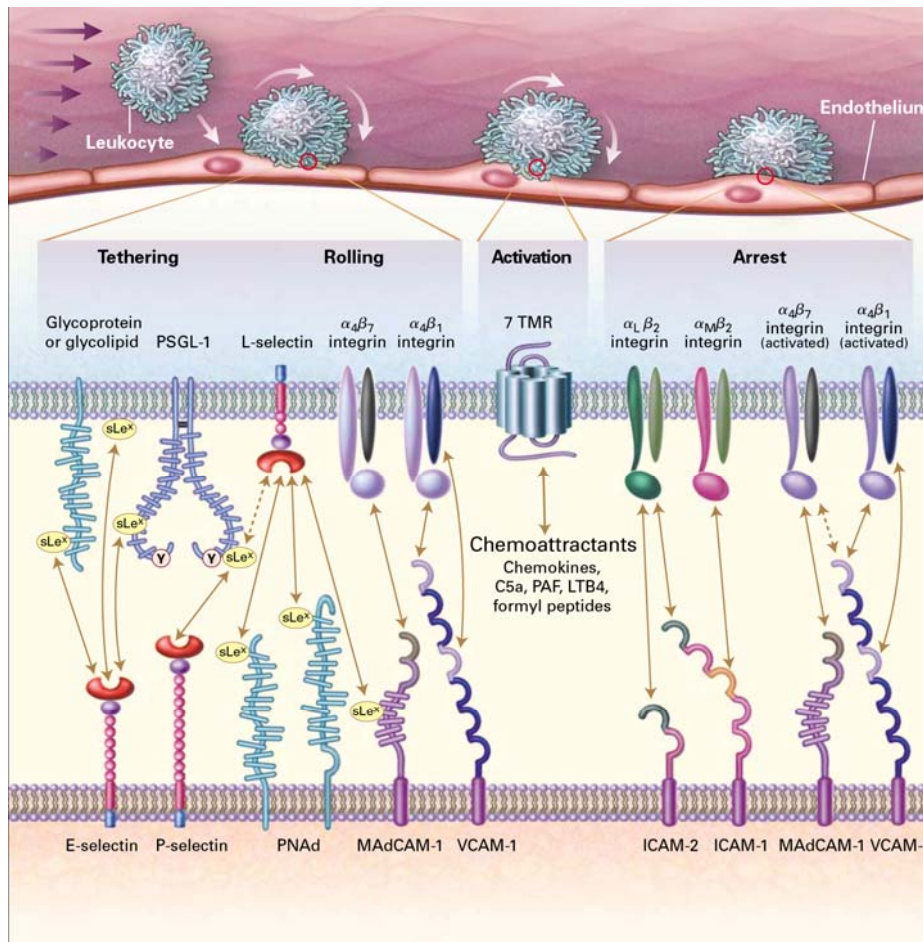


**Figure 2. Main molecules involved in tethering, rolling, activation and firm arrest.** Image adapted from (von Andrian and Mackay, 2000).

### Chemokine modulation of integrin activity

During the initial establishment of contacts with the vascular endothelium, leukocytes slow down their rolling velocity and become activated by encountering immobilized chemokines and integrin ligands displayed at the endothelial apical surface. This activation step allows the arrest and firm adhesion of leukocytes to endothelium under shear flow (Alon et al., 2003; Rot and von Andrian, 2004). Leukocyte activation involves a marked shape change from the round free-flowing cell to a polarized promigratory morphology with two distinct regions: the leading edge and the uropod (del Pozo et al., 1995). Leukocyte polarization enables the cell to turn intracellular forces into

net cell locomotion necessary to accomplish the extravasation process (Geiger and Bershadsky, 2002).

The chemokines coupled to apical endothelial glycosaminoglycans act by signaling through leukocyte GPCRs and induce an array of “inside-out” signals within fractions of seconds, leading to multiple conformational changes of integrins with important effects on leukocyte adhesion and morphology (Constantin et al., 2000; Sanchez-Madrid and del Pozo, 1999; Shamri et al., 2005). Both, the endothelium-immobilized chemokines and the chemokine receptors expressed on leukocytes are concentrated on microvilli to facilitate their interaction. Due to the complexity and timeframes of the signaling mechanisms controlling integrin activation, it is conceivable the existence of preformed compartmentalized protein networks (“signalosomes”) in leukocytes encountering endothelial chemokines (Laudanna and Alon, 2006). The presence of specific chemokines on different vascular beds contributes to orchestrate the selective recruitment of leukocyte subsets to inflammation foci or secondary lymphoid organs (Luster, 1998). In addition, chemokines may exert a differential effect on specific integrins within the same microenvironment. Accordingly, it has been described that chemokines can only mediate lymphocyte arrest dependent on VLA-4/VCAM-1 when binding their GPCRs with high affinity and with high relative occupancy, but this signal threshold-dependent effect is not observed with chemokine-stimulated  $\beta 2$  integrins (Laudanna, 2005).

#### Ligand modulation of integrin affinity

Upon the “inside-out” chemokine-mediated signaling in leukocytes, integrin conformation reversibly and readily switches from the inactive (folded) to the extended conformation with intermediate affinity. This event primes the integrin to bind its endothelial ligand. Integrins containing the “inserted” I-domain in their  $\alpha$  subunits

undergo a further conformational shift from this intermediate affinity extended conformation upon ligand binding, resulting in full integrin activation and leukocyte arrest (Cabanas and Hogg, 1993; Jun et al., 2001; Salas et al., 2004). Therefore, high affinity conformational state for leukocyte immediate arrest requires bidirectional induction from both immobilized chemokines and integrin ligands (Grabovsky et al., 2000; Shamri et al., 2005). However,  $\alpha 4$  integrins, which contain an I-like domain in their  $\beta$  subunits, can spontaneously interact with their endothelial ligands without previous chemokine stimulation (Alon et al., 1995). Therefore, it is possible that these integrins exist in overall extended conformations with high accessibility to their ligands, due to their preferential localization at microvilli. Finally, the “outside-in” ligand-driven signaling results in further separation of the integrin subunit cytoplasmic tails (unclasping), which favors their association with the cortical actin cytoskeleton (Nishida et al., 2006).

Ligand binding enhances the recruitment of additional integrins (microclustering), further increasing the integrin-dependent adhesiveness of leukocytes under shear stress, to support their firm adhesion to endothelium (Dobereiner et al., 2006). This clustering is dependent on integrin release from the actin cytoskeleton by PKC and calpain in order to increase their lateral mobility (Stewart et al., 1998). In this regard, it has been suggested the presence of ligand-independent LFA-1 nanoclusters at the plasma membrane of leukocytes, which promote the efficient formation of ligand-triggered microclusters (Cambi et al., 2006). Accordingly, a recent study has revealed that a large proportion of LFA-1 molecules in extended conformation rather than low affinity folded molecules are anchored to the cytoskeleton prior to ligand binding (Cairo et al., 2006). However, key differences between  $\alpha 4$  and  $\beta 2$  integrins regarding their increase in avidity mediated by cytoskeleton may occur. The  $\alpha 4$  integrins can bind paxillin upon dephosphorylation of

Ser988 in their cytoplasmic domain. Paxillin regulates  $\alpha 4$  integrin function (tethering and firm adhesion) in immune cells (Yang et al., 2005), enhancing their rate of migration and reducing their spreading. On the other hand, it has been described that LFA-1 and Mac-1 may use the adaptor molecules talin,  $\alpha$ -actinin, filamin and 14-3-3 to properly anchor to the actin cytoskeleton (Fagerholm et al., 2005; Pavalko and LaRoche, 1993).

On the other hand, several studies suggest that integrins are directly regulated by shear stress (Marschel and Schmid-Schonbein, 2002). Shear flow promotes additional stretching of integrin bonds, increasing outside-in signals that coordinate leukocyte and endothelial adhesion machineries to promote productive diapedesis. Recent findings also point out to a shear stress-mediated conformational activation of VLA-4, resulting in increased affinity (Zwartz et al., 2004). The integration of chemokine- and external force-derived signaling to enhance migration has been defined as the phenomenon of chemorheotaxis (Cinamon et al., 2001). In terms of subcellular localization, the integrins displayed on leukocyte microvilli distribute more readily high disruptive forces along the microvillar axis. Remarkably, it has been recently addressed the importance of shear forces for the integration of signals from apical and subendothelial chemokines, rendering an increase in chemotaxis towards the subendothelial compartment (Schreiber et al., 2006).

#### Regulation of leukocyte locomotion by integrins

The signals involved in leukocyte firm adhesion to endothelium mediated by integrins are subsequently attenuated to allow leukocyte migration towards an appropriate site of transmigration.  $\beta 2$  integrins appear to have a critical involvement in this process of locomotion, since blockade of these integrins or their correspondent endothelial ligands

results in random locomotion, failure in correct positioning at the endothelial junction and defective diapedesis (Schenkel et al., 2004).

Upon interaction with their ligands, integrins activate distinct myosin contractility effectors, actin-remodeling GTPases and molecules involved in microtubule network regulation at the leading and trailing edges of motile leukocytes (Hogg et al., 2003; Smith et al., 2003). During cell polarization, Cdc42, MLCK, Rac, RAPL, Rap1, mDia, Myosin-IIA and chemokine receptors are redistributed to the cellular front, participating in the formation of exploratory filopodia and in the extension of lamellipodia. In contrast, Rho and ROCK (both involved in trailing edge retraction), the microtubule-organizing center (MTOC) and the adhesion receptors ICAM-1, ICAM-3, CD44 and CD43 move towards the rear pole (Vicente-Manzanares and Sanchez-Madrid, 2004). Interestingly, the redistribution of integrin ligands to the uropod seems to be involved in the recruitment of bystander leukocytes through this cellular structure (del Pozo et al., 1996). Hence, the integration of signals generated in both cellular poles leads to a coordinate movement of the leukocyte.

#### VCAM-1 and ICAM-1 play an essential role in leukocyte capture

VCAM-1 and ICAM-1, members of the Ig superfamily, are the two major endothelial adhesion molecules involved in the binding to leukocyte integrins VLA-4 and LFA-1, respectively (Elices et al., 1990; Marlin and Springer, 1987b). ICAM-1 but not VCAM-1 is expressed at low levels in resting endothelium, and both molecules are induced upon cell activation by pro-inflammatory cytokines such as IL-1 and TNF- $\alpha$  (Carlos and Harlan, 1994; Dustin et al., 1986). Furthermore, it has been described that VCAM-1 and ICAM-1 are anchored to the actin cytoskeleton through members of the ERM family, mainly ezrin and moesin (Barreiro et al., 2002; Heiska et al., 1998;

Helander et al., 1996). These molecules function as membrane-actin cytoskeleton linkers regulating cortical morphogenesis and cell adhesion. Accordingly, they play a key role in the formation of protrusive plasma membrane structures such as filopodia, microspikes or microvilli (Arpin et al., 1994; Vaheri et al., 1997; Yonemura and Tsukita, 1999). Structurally, they are closely related to each other and seem to be functionally redundant, as suggested by the apparently normal phenotype of moesin knockout mice (Doi et al., 1999). Their amino-terminal domains interact with integral membrane proteins, whereas their carboxy-terminal domains bind F-actin (Tsukita and Yonemura, 1997; Turunen et al., 1994). These functions are conformationally regulated by reversible changes from inactive to functionally active forms. Binding of PI(4,5)P<sub>2</sub> and phosphorylation of a specific C-terminal threonine residue unmask the F-actin and membrane binding sites and stabilize the active conformation (Barret et al., 2000; Nakamura et al., 1999; Simons et al., 1998). The Rho/p160 ROCK signaling pathway and the phosphatidylinositol turnover are the major regulatory mechanisms for ERM activation inducing their phosphorylation and translocation into apical membrane/actin protrusions (Hirao et al., 1996; Matsui et al., 1998; Shaw et al., 1998). On the other hand, activated ERM proteins can sequester Rho-GDI to permit Rho activation, providing a positive feedback pathway (Takahashi et al., 1997).

VCAM-1 and ICAM-1 are capable of transducing signals after ligand binding. VCAM-1 is involved in the opening of the “endothelial passage” through which leukocytes can extravasate. In this regard, VCAM-1 ligation induces NADPH oxidase activation and the production of reactive oxygen species (ROS) in a Rac-mediated manner, with subsequent activation of matrix metalloproteinases and loss of VE-cadherin-mediated adhesion. This signaling pathway can be blocked by TGFβ1 and IFNγ (Cook-Mills, 2002; Hordijk, 2003; van Wetering et al., 2002; van Wetering et

al., 2003). On the other hand, cross-linking of both VCAM-1 and ICAM-1 induces a rapid increase in intracellular  $\text{Ca}^{2+}$  concentration (Etienne-Manneville et al., 2000; Lorenzon et al., 1998). ICAM-1-mediated calcium signaling has been mostly studied in brain endothelial cells. In this cellular model, it has been found that ICAM-1-mediated calcium increase triggers activation of Src and subsequent phosphorylation of cortactin (Etienne-Manneville et al., 2000). ICAM-1 is also able to activate RhoA inducing stress fiber formation (Thompson et al., 2002b) and phosphorylation of FAK, paxillin and  $\text{p130}^{\text{Cas}}$ , which in turn trigger different signaling pathways involving JNK or p38 (Greenwood et al., 2002; Hubbard and Rothlein, 2000; Wang and Doerschuk, 2002). Moreover, ICAM-1 cross-linking stimulate c-fos and rhoA transcription (Thompson et al., 2002b). Finally, the ICAM-1 cross-linking can also induce its own expression as well as that of VCAM-1, as a regulatory mechanism to facilitate leukocyte transendothelial migration (TEM) (Clayton et al., 1998).

### **Integrins and their ligands during transendothelial migration**

The signals involved in the firm adhesion of leukocytes to endothelium must be reverted, weakening the original contact sufficiently to allow the migration and extravasation of leukocytes. During TEM, endothelial junctions must be loosened to a limited extent, thereby avoiding cell monolayer damage or important changes in permeability. Thus, the leukocyte and endothelium membranes are kept in close contact and show prominent associated cytoskeletal structures. Subsequently, the endothelial membranes reseal their connections over the trailing end of the leukocyte.

Once the leukocyte finds a proper site for transmigration, mostly at intercellular junctions, it extends exploratory pseudopodia in between the two adjacent endothelial cells. Subsequently, pseudopodia evolve into a lamella squeezed into the monolayer gap.

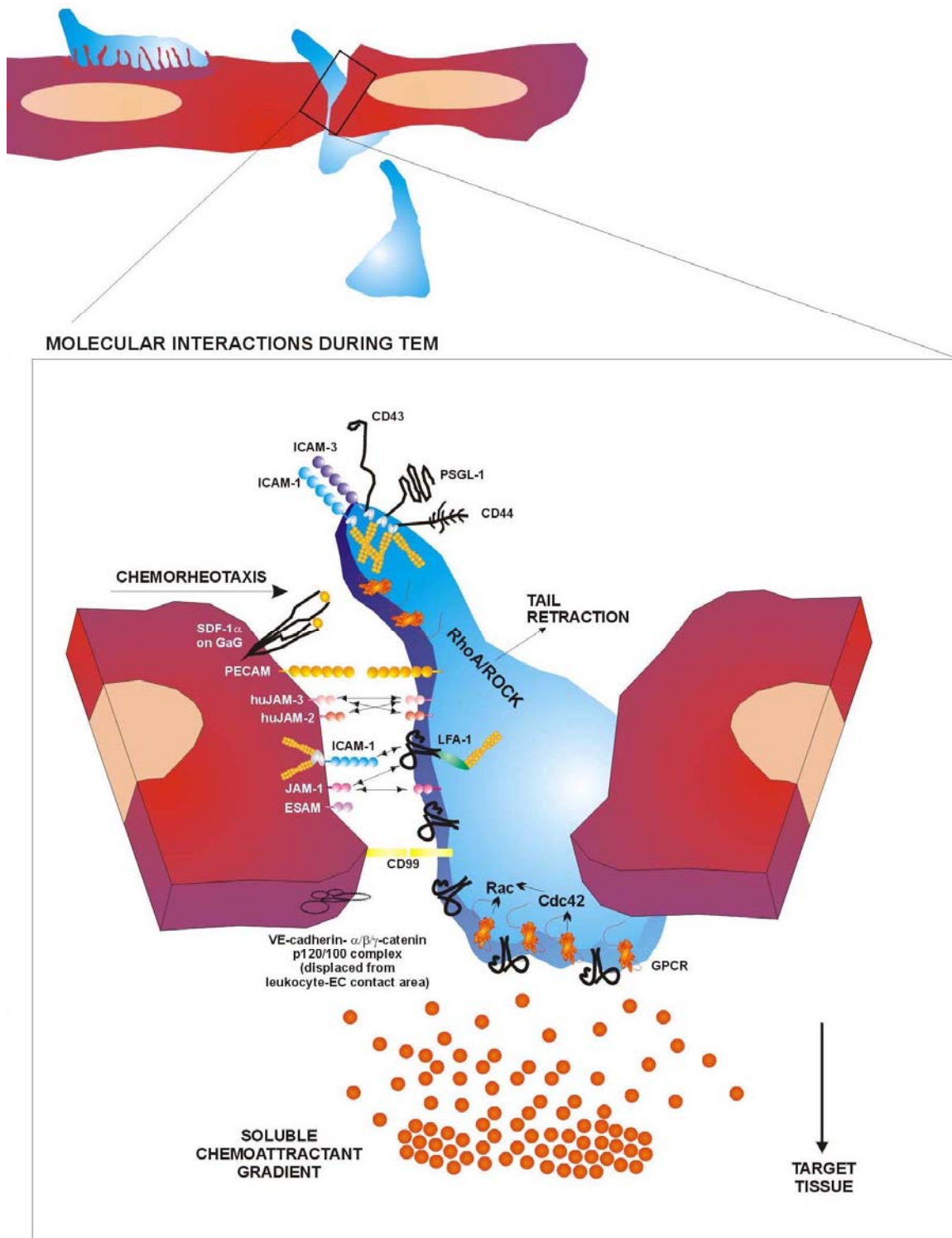


**Figure 3. The heterotypic leukocyte-endothelium interactions during transendothelial migration.** Most of the crucial molecules involved in leukocyte transmigration are shown, including members of the tight junctions (ESAM and the JAM family), the VE-cadherin complex and other molecules such as PECAM-1 and CD99. Most of them interact homophilically, being express by the endothelium as well as by leukocytes. On the other hand, the processes of lamellipodia formation at the leukocyte leading edge and tail retraction, the phenomenon of chemorheotaxis and the existence of a subendothelial soluble chemoattractant gradient to guide the extravasated leukocytes to the target tissue are also illustrated.

During this process, LFA-1 is the integrin with a more prominent role. This molecule is rapidly relocalized, forming a ring-like cluster at the leukocyte-endothelial interface, where it interacts with ICAM-1 and, in some cellular models, with JAM-A. When the transmigration process is over, LFA-1 is finally concentrated at the uropod (Sandig et al., 1997; Shaw et al., 2004).

In the context of leukocyte transmigration, in addition to the classical pathway of diapedesis, in which the leukocytes cross through inter-endothelial junctions without disrupting the integrity of the endothelium (paracellular pathway), there are increasing evidences indicating the existence of an alternative pathway, in which leukocytes could migrate across an individual endothelial cell (transcellular pathway) (Carman and Springer, 2004; Engelhardt and Wolburg, 2004). New insights into the mechanism of this process have been recently reported. It seems that lymphocytes used invasive podosomes to palpate the surface of endothelium and form transcellular pores. These lymphoid structures are dependent on Src kinase and WASP, whereas membrane fusion events dependent on the SNARE-containing membrane fusion complex and intracellular calcium are required in endothelium (Carman et al., 2007). Another study describes the translocation of ICAM-1 to caveolae upon leukocyte adhesion, and the subsequent formation of a sort of multivesicular channel, containing ICAM-1 and caveolin-1 around the penetrating leukocyte pseudopod. Both proteins follow the passage of the whole cell, moving towards the basal side of the endothelial membrane (Millan et al., 2006). In addition, the protein of intermediate filaments vimentin also seems to play a role in the transcellular pathway (Nieminen et al., 2006).

## **TETRASPANIN MICRODOMAINS**

Tetraspanins are a superfamily of proteins with, at least, 28 genes cloned in humans. They are proteins of low molecular weight, with a common secondary structure that spans four times the plasma membrane and with both N- and C-terminal domains in the cytoplasm. Tetraspanins present little homology in their sequence, except for several structural domains, most of them in transmembrane regions, and several cysteines involved in disulphide bonds from the large second extracellular loop (Maecker et al., 1997). Tetraspanins are ubiquitous proteins able to organize themselves by homo- and hetero-oligomerization (Kovalenko et al., 2005; Stipp et al., 2003). These molecules can also associate laterally at the plasma membrane with partners via their second extracellular loop, modulating partner functions, as reported for a plethora of membrane integral receptors such as leukocyte and endothelial adhesion molecules (Barreiro et al., 2005; Feigelson et al., 2003; Levy et al., 1998; Mannion et al., 1996; VanCompernelle et al., 2001), intercellular junction- and extracellular matrix-related integrins (Berditchevski, 2001; Lammerding et al., 2003; Yanez-Mo et al., 1998), CD19/CD21-B cell antigen receptor complex (Cherukuri et al., 2004), MHC-peptide complex (Kropshofer et al., 2002b; Vogt et al., 2002), Fc receptors (Moseley, 2005), G-protein-coupled receptors (Little et al., 2004), or metalloproteinases (Andre et al., 2006; Takino et al., 2003; Yan et al., 2002). Tetraspanins also associate intracellularly with a number of cytoplasmic signalling mediators such as type II PI4K or different PKC isoforms (Yauch and Hemler, 2000; Zhang et al., 2001).

Recent biochemical, proteomics and structural studies have bolstered that tetraspanin-enriched microdomains (TEM) also play a key role in organizing molecular complexes at the plasma membrane with different protein composition compared to typical lipid rafts (Hemler, 2005; Le Naour et al., 2006; Min et al., 2006; Nydegger et al.,

2006). Thus, the concept of TEM emerges from the ability of tetraspanins to dynamically interact among them and simultaneously with a wide range of molecules, organizing discrete compartments throughout the plasma membrane. Apart from acting as adapters for membrane organization, tetraspanins are also involved in the regulation of trafficking and biosynthetic processing of associated receptors (Berditchevski and Odintsova, 2007). Although TEM nature seems to be different from lipid rafts, they are not devoid of lipid interactions, since tetraspanins are highly palmitoylated proteins that bind cholesterol and gangliosides (Charrin et al., 2003; Hakomori, 2002; Yang et al., 2004). Tetraspanin and associated partner composition as well as specific characteristics of TEM may vary depending on the cellular type. A number of experimental strategies including tetraspanin genetic deletion, knocking-down, over-expression, or mutation have unveiled a key functional role for these proteins in multiple central physiological processes, namely, egg-sperm fusion (Le Naour et al., 2000; Rubinstein et al., 2006), antigen presentation (Delaguillaumie et al., 2004; Levy and Shoham, 2005b; Mittelbrunn et al., 2002; Unternaehrer et al., 2007), leukocyte-endothelial adhesion and transendothelial migration (Barreiro et al., 2005), cellular entry and budding during viral infection as well as virus-promoted syncytia formation (Gordon-Alonso et al., 2006; Martin et al., 2005; Pileri et al., 1998), metalloproteinase activity (Fujita et al., 2006; Hong et al., 2006; Hong et al., 2005; Takino et al., 2003), angiogenesis (Takeda et al., 2007; Wright et al., 2004), renal function (Sachs et al., 2006), neurite outgrowth (Stipp and Hemler, 2000), hemidesmosomes organization (Sterk et al., 2000), exosome targeting to dendritic cells (Morelli et al., 2004), or cell adhesion, migration and invasion (Chattopadhyay et al., 2003; Garcia-Lopez et al., 2005; Hemler, 2003; Kovalenko et al., 2007; Longo et al., 2001; Yanez-Mo et al., 1998; Yanez-Mo et al., 2001). Since there are very few described ligands in *trans* for tetraspanins, most of the reported regulatory effects may be exerted in

*cis* on their laterally-associated partners (Hemler, 2001). However, the molecular mechanisms underlying the regulation by tetraspanins still remain elusive.

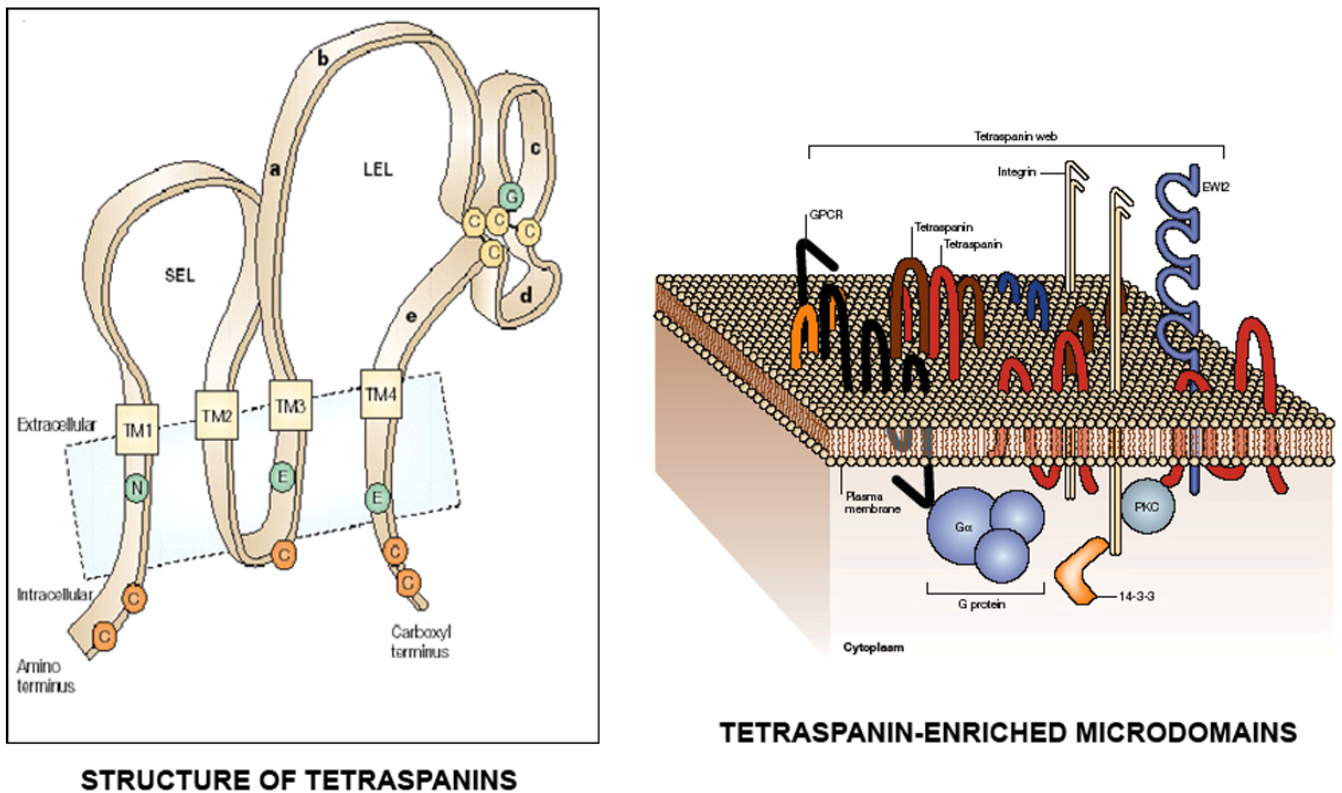


**Figure 4.** Scheme of the molecular structure of tetraspanins and a model of tetraspanin-enriched microdomain at the plasma membrane. Images adapted from Levy and Shoham, *Nat Rev Immunol* 2005).

## STUDY OF THE BIOPHYSICAL PROPERTIES OF PROTEINS USING ANALYTICAL MICROSCOPY TECHNIQUES

How cells physically organize and compartmentalize receptors and signalling molecules into specialized, efficient, regulated networks is of critical importance to understand complexity and dynamics of biological processes. In this regard, cholesterol and sphingolipid-enriched rafts have been proposed as platforms for the sorting of specific membrane components including glycosylphosphatidylinositol (GPI)-anchored proteins and to provide sites for the assembly of cytoplasmic signalling complexes (Anderson and Jacobson, 2002; Simons and Toomre, 2000). The existence and physical

properties of lipid rafts has been extensively studied taking advantage of innovative analytic methods (Kenworthy et al., 2004; Larson et al., 2005; Sharma et al., 2004; Suzuki et al., 2007a; Suzuki et al., 2007b). Nonetheless, no study demonstrating the existence of tetraspanin-enriched microdomains on the plasma membrane of living cells and characterizing their dynamic features has been documented so far.

The dynamic properties of a protein have a crucial role in determining what its cellular function and how, when and where it may physically interact with other proteins and macromolecules in response to extracellular stimuli. The combination of several complementary analytical microscopy and spectroscopy approaches allow the spatial and temporal analysis of complex protein assemblies within living cells, leading to the determination of their stoichiometry, oligomerization state, molecular composition, and diffusional mechanisms.

Microscopy techniques are intrinsically limited by optical resolution. Therefore, molecular complexes that occur on the scale of nanometers are not directly accessible by colocalization studies performed with standard confocal microscopes. The detection of molecular interactions within living cells, however, can be achieved by fluorescently tagging the pair of proteins of interest and measuring the Förster resonance energy transfer (FRET) from the donor fluorophore to the acceptor one, that occurs in the range of tenths of angstroms (i.e., few nanometers), only attainable if proteins directly interact. As consequence of FRET, the fluorescence lifetime of the donor molecule decreases. The fluorescence lifetime is of the order of few nanoseconds for all fluorescent genetically encoded dyes, and it can be measured in live cells by Fluorescence Lifetime Imaging Microscopy (FLIM). This technique is a more reliable and sensitive than the classical fluorescence intensity-based FRET approaches. This method is fast enough for being applied to live cells, in that avoids the approximate

decomposition of complex fluorescence decays, and recovers robust FRET efficiencies between fluorescent protein-tagged interacting molecules (Caiolfa et al., 2007; Wallrabe and Periasamy, 2005).

The proteins that localize in the plasma membrane at steady state are in dynamic domains, which might control functions such as ligand binding and signaling. Diffusion of proteins can be studied considering an overall molecular population at a microscopic scale. For this purpose, a technique termed fluorescence recovery after photobleaching (FRAP) is used. FRAP method is based on the photobleaching of a region of interest within a living cell and the measurement of fluorescence recovery rate to obtain an apparent diffusion coefficient for the fluorescently tagged protein. Alternatively, photoactivatable or photoconvertible fluorescent proteins might be used for the specific labelling of a molecular subpopulation within a living cell and the study of its mobility over time. On the other hand, studies of the diffusion of single protein species can be approached by FCS (fluorescence correlation spectroscopy), and extended to the quantitative analyses of co-diffusing protein assemblies, using the FCCS variant approach. FCS analyzes the fluctuation of the fluorescence intensity of a system at equilibrium. Thus, FCS recovers dynamic information on a specific region of a cell (a femto-volumen) together with the estimation of the local concentration of the diffusing species. In addition, coupled with the analysis of the photon counting histogram (PCH), FCS can better explore the state of oligomerization of the diffusing particles. Finally, using the dual-color variant, FCCS, complements FRET-FLIM studies by monitoring molecular interactions between diffusing molecules and recovering the stoichiometry of the diffusing protein assemblies, as well as the kinetics of the interactions (Muller et al., 2003).

## **OBJECTIVES**

Aims to study:

- 1.** Dynamic recruitment of endothelial adhesion receptors VCAM-1 and ICAM-1 during lymphocyte firm adhesion and transendothelial migration, and their binding to actin-cytoskeleton through ERM proteins.
- 2.** Endothelial docking structures formed to adhere firmly leukocytes and prevent their detachment under physiological flow conditions. Structural and regulatory components.
- 3.** Localization of endothelial tetraspanins CD9 and CD151 during leukocyte-endothelium adhesion. Biochemical association between tetraspanins and adhesion receptors and functional role of CD9 and CD151 in the regulation of the adhesive properties of ICAM-1 and VCAM-1.
- 4.** Recruitment of ICAM-1 or VCAM-1 adhesion receptors to the docking structure in the absence of ligand engagement and actin anchorage. Involvement of tetraspanin microdomains.
- 5.** Biophysical properties, dynamics and molecular features of organized microdomains at the apical membrane of human primary living endothelial cells containing tetraspanin and adhesion receptors.
- 6.** Tetraspanin regulation of endothelial adhesion receptor avidity within endothelial adhesive platforms.

## **MATERIALS AND METHODS**

### **Cells and cell cultures**

Human umbilical vein endothelial cells (HUVEC) were obtained and cultured as previously described (Yanez-Mo et al., 1998). Cells were used up to the third passage in all assays. To activate HUVEC, TNF- $\alpha$  (20 ng/ml)(R&D Systems, Minneapolis, MN) was added to the culture media 20 h before the assays were performed. K562 erythroleukemic cells, which endogenously express  $\beta$ 1 integrin, were stably transfected with the  $\alpha$ 4 (termed as 4M7 cells or K562  $\alpha$ 4 and expressing functional VLA-4 at the plasma membrane) or LFA-1 integrins (Munoz et al., 1996; Nueda et al., 1995). K562 transfectants were grown in RPMI 1640 medium (Gibco BRL, Gaithersburg, MD) supplemented with 10% FCS, 50 IU/ml penicillin, 50  $\mu$ g/ml streptomycin, and 1 mg/ml of G418 (Calbiochem, La Jolla, CA). Human peripheral blood lymphocytes (PBLs), monocytes and neutrophils were obtained and cultured as described (Barreiro et al., 2002). T lymphoblasts were derived from freshly isolated human peripheral blood lymphocytes (PBLs) by activation with phytohemagglutinin-L (PHA-L) (1  $\mu$ g/ml; Sigma-Aldrich, St Louis, MO) for 48 h followed by culture for 5-7 days in the presence of recombinant human interleukin-2 (rhIL-2; 100 U/ml) provided by the National Institutes of Health AIDS Research and Reference Reagent program, Division of AIDS. Adhesion of K562 LFA-1 transfectants to Colo320 cells colocal carcinoma cell line or to activated endothelial cells was performed in the presence of 1mM  $Mn^{2+}$  to induce integrin activation. Colo320-CD9 and chimeric Colo320-CD9x82 and Colo320-CD82CCG9 are stably transfected clones derived from those previously described (Gutierrez-Lopez et al., 2003). Integrin inhibitors BIO5192 and BIRT377 were kindly provided by Biogen Idec

(Cambridge, MA) and Boehringer-Ingelheim Pharmaceuticals (Ridgefield, CT), respectively.

### **Antibodies and reagents**

The TEA1/31 anti-VE cadherin and TS2/16 anti- $\beta$ 1 integrin (Yanez-Mo et al., 1998), the HP2/1 anti- $\alpha$ 4 integrin, TS1/11 anti- $\alpha$ L integrin, and TP1/24 anti-ICAM-3 (Serrador et al., 1997) mAb have been described elsewhere. The 4B9 and P8B1 (anti-VCAM-1), Hu5/3 (anti-ICAM-1) and 297S (anti-phosphorylated forms of ERM proteins) mAb were kindly provided by Dr. R. R. Lobb (Biogen Inc., Cambridge, MA), Dr. E. A. Wayner (Fred Hutchinson Cancer Research Center, Seattle, WA), Dr. F. W. Luscinskas (Brigham and Women's Hospital and Harvard Medical School, Boston, MA), and Dr. S. Tsukita (Faculty of Medicine, Kyoto University, Japan), respectively. The moesin-specific polyclonal antiserum 95/2 and the ezrin-polyclonal antiserum 90/3 have been previously described (Serrador et al., 2002). The anti-tubulin and anti-vinculin mAb were purchased from Sigma (St Louis, MO). The anti-talin pAb was a kind gift of Dr. K. Burrige (University of North Carolina at Chapel Hill, NC). Monoclonal antibodies (mAb) anti-CD151 (LIA1/1), anti-E-Selectin (TEA2/1), anti-CD44 (HP2/9) anti-CD63 (Tea3/18) and anti-CD9 (VJ1/20) have been previously described (Montoya et al., 1999; Penas et al., 2000; Serrador et al., 1997; Yanez-Mo et al., 1998). TS82 (anti-CD82), 10B1 (anti-CD9), 8C3 (anti-CD151), I.33.22 (anti-CD81) mAb were kindly provided by Dr. E. Rubinstein (INSERM U268, Villejuif, France), Dr. K. Sekiguchi (Osaka University, Japan), and Dr. R. Vilella (Hospital Clinic, Barcelona, Spain), respectively. Anti-GST goat polyclonal Ab was purchased from Amersham Biosciences (Uppsala, Sweden), and anti-vimentin mAb from Sigma Chemical Co. (St. Louis, MO). Anti-caveolin Ab was purchased from Sigma. The 40 nm gold-coupled anti-mouse and 15 nm gold-coupled

streptavidin were purchased from British Biocell. International (Cardiff, UK). The monoclonal IgG1, $\kappa$  from the P3X63 myeloma cell line was used as negative control. Recombinant human fibronectin (FN) was purchased from Sigma. The p160 ROCK inhibitor Y-27632, the PI3K inhibitor Ly 294002, and the classic PKCs inhibitor Gö6976 were purchased from Calbiochem. The LEL-GST peptides of wild type human CD9 or the mutated forms in the Cys residues have been described (Higginbottom et al., 2003). The corresponding CD151-LEL-GST peptide presented a low rate of proper folding in solution which precluded its use in functional studies.

### **Recombinant DNA constructs and proteins, cell transfections**

The fusion protein GST-VC, containing the cytoplasmic tail of VCAM-1, was obtained by PCR amplification using as template the human VCAM-1 cDNA, and [TATGGATCCAGAAAAGCCAACATGAAG] and [TGGAATTCATAGATGGGCATTTTC] as 5' and 3' primers, respectively. The PCR product was cloned as a BamHI/EcoRI fragment into pGEX-4T (Pharmacia LKB biotechnology, Uppsala, Sweden). The cytoplasmic tail of ICAM-3 fused to GST (GST-IC3) and a truncated form of it (GST-Y9, Y490stop) have been described elsewhere (Serrador et al., 1997).

VCAM-1-GFP and ICAM-1-GFP were obtained using the corresponding human cDNAs as templates to amplify by PCR the complete encoding region of these molecules without the stop codon. A Xho I site was added to the 5' end and a Xma I site at the 3' end of VCAM-1 cDNA. Likewise, HindIII and BamHI sites were added to the 5' and 3' ends of ICAM-1 cDNA, respectively. The PCR products were then cloned into pEGFP-N1 (Clontech Laboratories, Inc. Palo Alto, CA) resulting in an in-frame fusion of EGFP

to the C-terminus of VCAM-1 and ICAM-1. The VCAM-1- and ICAM-1-GFP proteins behaved similarly to the corresponding endogenous proteins in terms of their binding to ezrin and moesin. The generation of the GFP fusion construct containing the GFP cDNA inserted at the carboxy-terminal end of the rat full length moesin (moesin-GFP, residues 1-577) has been previously described (Amieva et al., 1999).  $\alpha$ -actinin-GFP and paxillin-GFP were kind gifts of Dr. A. F. Horwitz (University of Virginia, Charlottesville, VA). VASP-GFP, PLC $\delta$ -PH-GFP, and GRP1-PH-GFP, were kindly provided by Dr. J. V. Small (Institute of Molecular Biology, Salzburg, Austria), Dr. T. Balla (NICHD, National Institutes of Health, Bethesda, MA), and Dr. A. Gray (University of Dundee, Dundee, U. K.), respectively.

CD9-, and CD151-EGFP tagged proteins have been described (Barreiro et al., 2002; Garcia-Lopez et al., 2005; Longo et al., 2001). The VCAM-1 truncated protein lacking its cytoplasmic tail (VCAM $\Delta$ Cyt) (that retains only the first cytoplasmic charged residue for proper membrane insertion) was generated by PCR using as template the human VCAM-1 cDNA, and [CTCGAGTCTCATCACGACAGCAAC] and [CTATCTTGCAAAGTAAATTATC] as 5' and 3' primers, respectively. The PCR product containing a stop codon at position 722 was cloned into pcDNA3.1/V5-His-TOPO vector (Invitrogen, Carlsbad, CA) and the correct expression of the protein at the plasma membrane was tested. The ICAM-1-tailless construct was a kind gift of Dr. W.F. Luscinskas (Yang et al., 2005). For the FCS, FCCS, FLIM-FRET studies, monomeric green and red variants of ICAM-1, VCAM-1, CD9 and CD151 were generated. Monomeric EGFP constructs were obtained by point mutation at the position A206K (Zacharias et al., 2002; Zhang et al., 2002) using the Quick Mutagenesis Kit (Stratagene, La Jolla, CA). The mRFP variants were generated by subcloning of the corresponding EGFP constructs into the mRFP vector that was kindly provided by Dr. Tsien (UCSD, La

Jolla CA). GPI-EGFP construct was a kind gift of Dr. M.A. del Pozo (CNIC, Madrid, Spain).

Expression of GST-fusion proteins in BL21 bacteria and purification were carried out following the manufacturer's instructions. The LEL of wild type human CD9 was cloned in the pGX-KG vector and expressed in protease negative BL21 cells. LEL-GST fusion proteins were obtained as previously described (Barreiro et al., 2005).

Transiently transfected HUVEC were generated by electroporation at 200 V and 975  $\mu$ F using a Gene Pulser (Bio-Rad Labs, Hercules, CA), and adding 20  $\mu$ g of each DNA construct or using lipofectin (Invitrogen) following manufacturer's protocol. Transfected cells were grown to confluence on glass bottom dishes for 24-48 h (WillCo Wells, Amsterdam, The Netherlands) pre-coated with fibronectin (20  $\mu$ g/ml). Cells were activated with TNF- $\alpha$  for 20 h and subsequently used for FRAP, FLIM-FRET or FCS experiments.

### **Flow cytometry analysis, immunofluorescence and confocal microscopy**

For flow cytometry analysis and immunofluorescence experiments, cells were treated as previously described (Yanez-Mo et al., 1998). Rhodamine Red-X-Affinipure goat anti-mouse IgG (H+L), Rhodamine Red-X-Affinipure streptavidin, Alexa Fluor 488 rabbit anti-mouse, goat anti-mouse IgG (H+L) or goat anti-rabbit IgG (H+L) conjugate highly cross-adsorbed, and Phalloidin Alexa Fluor 568 were used as fluorescent reagents (Molecular Probes, Eugene, OR). Staining with the 297S mAb was performed as previously described (Hayashi et al., 1999). Series of optical sections were obtained with a Leica TCS-SP1, SP2 or SP5 confocal laser scanning unit equipped with Ar and He/Ne laser beams and attached to a Leica DMIRBE inverted epifluorescence microscope (Leica Microsystems, Heidelberg, Germany), using a 63x oil or glycerol immersion

objective (NA: 1.4 or 1.3, respectively). Image analysis and colocalization histograms were obtained with Leica Confocal Software.

### **Co-immunoprecipitation, Western blot, in vitro translation, and protein binding assays**

Lysates from activated HUVEC, immunoprecipitation and Western blot were performed as described (Serrador et al., 1997). The pCR3 plasmids carrying the inserts of untagged moesin and ezrin amino-terminal regions (amino acid residues 1-310) were transcribed, translated and isotope-labeled *in vitro* using a TNT-coupled rabbit reticulocyte lysate system (Promega, Madison, WI). Then, binding assays using these isotope-labeled recombinant proteins and the GST-fusion proteins (GST-VC, GST-IC3, GST-Y9, and GST alone) were carried out as previously described (Serrador et al., 1997). Coimmunoprecipitation experiments of tetraspanins and adhesion receptors were performed as previously described (Yanez-Mo et al., 1998) with TNF- $\alpha$ -activated HUVEC lysates obtained in 1% Brij96 in 1 mM Ca<sup>2+</sup>, 1 mM Mg<sup>2+</sup> TBS with protease inhibitors.

### **Adhesion and transendothelial migration assays**

For cellular adhesion assays, HUVEC were grown to confluence in 96-microwell plates (Costar) and activated with TNF- $\alpha$  for 20 h. K562 cells or human PBLs were labeled with 1  $\mu$ M of BCECF-AM for 15 min at 37°C, pre-incubated with different purified mAb and allowed to adhere to activated HUVEC for 15 min at 37°C as previously described (Yanez-Mo et al., 1998). Fluorescence intensity was measured in a microplate reader (Biotek FL500).

Alternatively, HUVEC were grown to confluence onto coverslips pre-coated with FN (20 µg/ml). Then, cells were activated with TNF-α (20 ng/ml) for 20 h. For adhesion experiments, medium was removed and K562 stable transfectants or T lymphoblasts resuspended in 500 µl of complete 199 medium were added. Adhesion of K562 LFA-1 transfectants to activated HUVEC monolayers was performed in the presence of 1mM Mn<sup>2+</sup> to induce integrin activation. Pretreatment of T lymphoblasts with BIO5192 (10 µg/ml) or BIRT377 (10 µM) for 5 min prior to adhesion assays was performed when indicated. After incubation time (5-10 min for lymphoblasts, at least 30 min for K562 cells), samples were washed and fixed with 4% paraformaldehyde to proceed with immunofluorescence. Alternatively, TNF-α-activated HUVEC cells were incubated for 30 min with anti-tetraspanin, anti-VCAM-1 or anti-VE-cadherin mAb-coated dynabeads (Dynal Biotech ASA, Oslo, Norway), fixed and stained with biotinylated anti-ICAM-1 mAb. Representative confocal sections are shown. Arrows point to the position of the attached beads.

T lymphoblast or PBL migration through a confluent monolayer of activated HUVEC was assayed in 3 µm-pore Transwell cell culture chambers (Costar, Corning Inc., Corning, NY). HUVEC were seeded and grown to confluence on these Transwell inserts pre-coated with 1% gelatin or 20 µg/ml of fibronectin and activated with TNF-α for 20 h. In some experiments, 150 µg/ml of the LEL-GST fusion proteins were added at the time of TNF-α stimulation, and other times endothelial cells were previously treated to knock down tetraspanin proteins. Cultured lymphoblasts ( $2 \times 10^5$  in 100 µl of complete 199 medium/well) were incubated with 10 µg/ml of different purified mAbs for 20 min at 4°C, and then added to the upper chambers. Alternatively, freshly isolated PBLs ( $2 \times 10^5$  in 100 µl /well) were added to the upper chambers. In the lower well, 600 µl of complete 199 medium, containing or not 100 ng/ml of human recombinant SDF-1α (R&D

Systems), were poured. Cells were incubated for 90 min at 37°C (lymphoblasts) or for 2-7h (PBLs), and migrated cells were recovered from the lower chamber. The number of migrated lymphocytes, that ranged from 5 to 20%, were recovered from the lower chamber was estimated by flow cytometry.

### **Time-lapse fluorescence confocal microscopy**

HUVEC transfected with different GFP constructs were grown to confluence on glass-bottomed dishes (WillCo Wells, Amsterdam, The Netherlands) pre-coated with fibronectin (20 µg/ml). Then, cells were activated with TNF-α for 20 h, and placed on the microscope stage. 4M7 cells or T lymphoblasts resuspended in 500 µl of complete 199 medium were added. During the observation time, plates were maintained at 37°C in a 5% CO<sub>2</sub> atmosphere using an incubation system (La-con GBr Pe-con GmbH). Confocal series of fluorescence and differential interference contrast (DIC) images, distanced 0.4 µm in the z axis, were simultaneously obtained at 30 s or 1 min intervals, with a 63x oil immersion objective. Images were processed and assembled into movies using the Leica Confocal Software.

### **Parallel plate flow chamber analysis of endothelial-lymphocyte interactions**

The parallel plate flow chamber used for leukocyte adhesion and transmigration under defined laminar flow has been described in detail (Luscinskas et al., 1994). PBLs ( $1 \times 10^6$ /ml) were drawn across activated confluent monolayers at an estimated wall shear stress of 1.8 dynes/cm<sup>2</sup> for perfusion times from 30 s to 10 min. Lymphocyte rolling on the endothelium were easily visualized since they travelled more slowly than free-flowing cells. Lymphocytes were considered to be adherent after 20 s of stable contact

with the monolayer. Transmigrated lymphocytes were determined as being beneath the endothelial monolayer. Lymphocytes were considered to be detached when they returned to free-flowing after having been completely arrested on endothelium. The number of rolling, adhered, transmigrated and detached cells was quantified by direct visualization of different fields (20x phase-contrast objective), each one observed for 30 s starting at min 3,5 and ending at time point 6,5. Digitalization was performed with Optimas software (Bioscan). Coverslips were fixed immediately in PFA 4% at room temperature for 10 min, washed with HBSS, and stained for VCAM-1, ICAM-1 or ezrin.

For detachment experiments, peripheral blood lymphocytes were allowed to adhere for 15 min at 37°C to activated HUVEC monolayers, either incubated with LEL-GSTs for 20h, or transfected with siRNA oligos. Then, shear stress was applied by pulling assay buffer (HBSS buffer with 2% FCS) through the flow chamber with a programmable syringe pump, starting at 2 dyn/cm<sup>2</sup> and increasing up to 30 dyn/cm<sup>2</sup> at 1 min intervals. The number of cells attached after each shear stress interval was quantified in 4-8 fields (20x phase-contrast objective). Cell detachment was obtained from the difference in adhered cells after subtracting the percentage of cells that had transmigrated during the assay.

### **Small interference RNA assay**

To selectively knock down the expression of endothelial tetraspanins CD9 and CD151, a screening of different target sequences for each protein was performed using siRNA expression cassettes (Ambion, Austin, TX). We found the silencing sequences GAGCATCTTCGAGCAAGAA and CATGTGGCACCGTTTGCCCT for CD9 and CD151, respectively. RNA duplexes corresponding to these target sequences, as well as a negative oligonucleotide that does not pair with any human mRNA, designed by

Eurogentec (Seraing, Belgium) were used. Oligos were transfected in HUVEC with oligofectamine (Invitrogen, Carlsbad, CA) following manufacturer's instructions. For CD9 interference, cells were transfected on day 0, further splitted on day 2 and retransfected on day 3. In parallel, on day 3, cells were transfected only once for CD151 knocking down. Then cells were trypsinized on day 6 and negatively selected with anti-CD9 or anti-CD151 magnetic coated beads (Dynabeads M450 Goat anti-Mouse IgG, DYNAL BIOTECH ASA, Oslo, Norway), in order to enrich the tetraspanin low-expressing population. Cells thus selected were counted, seeded to confluence for the different experiments and activated or not with TNF- $\alpha$  for 20h.

#### **Paracellular monolayer permeability measurements**

HUVEC monolayer paracellular permeability measurements were performed in 0.4  $\mu$ m pore diameter Transwells (Costar) with 77 KDa FITC-labelled dextran (Sigma) as described (Dominguez-Jimenez et al., 2001).

#### **Heterotypic intercellular binding assays**

Colo320 colocal carcinoma cells or different stable transfectants derived from this cell line were transiently transfected with ICAM-1-GFP or VCAM-1-GFP by electroporation in an ElectroSquarePorator ECM 830 (BTX, VWR Int., San Diego, CA). A total of  $5 \times 10^5$  cells of each condition were mixed with  $2 \times 10^5$  of K562 cells, either untransfected or stably transfected with  $\alpha 4$  or LFA-1 integrins, which had been previously loaded with the CM-TMR red fluorescent dye (Molecular Probes). Then, cells were allowed to adhere at room temperature under rotatory conditions for 90 min in RPMI medium without

supplements. The relative number of heterotypic intercellular binding was estimated by flow cytometry.

### **Sucrose density gradient fractionation**

Confluent TNF- $\alpha$ -activated HUVEC were rinsed with phosphate-buffered saline (PBS) and lysed for 20 min in 250  $\mu$ l of 25 mM Tris-HCl, pH 7.5, 150 mM NaCl, 1 % Brij96 at 4°C. The cell lysate was homogenized by passing the sample through a 22-gauge needle. The extract was brought to 40% sucrose (w/w) in a final volume of 4 ml and placed at the bottom of an 8-ml 5-30% linear sucrose gradient. Gradients were ultracentrifuged to equilibrium for 20 h at 39,000 rpm at 4°C in a Beckman SW41 rotor (Beckman Coulter, Fullerton, CA). Fractions (1ml) were harvested from the bottom of the tube. Aliquots from each fraction were subjected to SDS-PAGE and Western blot with appropriate Abs.

### **Fluorescence Recovery after Photobleaching**

Cells transfected with EGFP-fusion proteins (VCAM-1-, ICAM-1-, CD9-, CD151-, ICAM-1 $\Delta$ Cyt-, GPI-EGFP) were plated on 25mm glass coverslips coated with 20  $\mu$ g/ml of FN. After 24h, cells were stimulated with 20 ng/ml TNF- $\alpha$  in the presence or absence of CD9-LEL-GST and FRAP experiments were performed before 48h after plating. To analyse FRAP at the endothelial docking structure, an adhesion assay was conducted under static conditions using K562 cells expressing VLA-4 ( $\alpha$ 4 $\beta$ 1) or LFA-1 ( $\alpha$ L $\beta$ 2) at the plasma membrane. Live-cell microscopy was performed with a Leica SP2 laser scanning confocal microscope using the 488-nm Ar laser line and an X 63 glycerol objective. During the observation period, plates were maintained at 37°C in a 5% CO<sub>2</sub> atmosphere using an incubation system (La-con GBr Pe-con GmbH). Laser

power for bleaching was maximal, whereas it was attenuated to 10% of the bleach intensity for imaging. Ten single-section prebleach images were acquired, followed by three iterative bleach pulses of 1.686 sec each. Then, ten single-section images were collected at 1.686 sec intervals, followed by 20 images collected every 10 sec and, finally, 15 images every 30 sec for a total experimental time of 650 sec approx.

Fluorescence recovery in the bleached region was measured as average signal intensity. Although the size of the measured region was dependent on docking structure dimension, it was very homogenous. Signal loss in unbleached regions during the recovery period was less than 5 % of the initial fluorescence signal. All recovery curves were generated from background-subtracted and bleaching-corrected images. Fluorescence signal measured in a region of interest (ROI) was normalized to the prebleach signal in the same ROI.

The mobile fraction (Mf) corresponds to the final value of the recovered fluorescence intensity, and the immobile fraction is obtained as 1-Mf. The half-time of recovery is the time from the bleach to the time point where the fluorescence intensity reaches the half of the final recovered intensity. All these three variables were directly obtained from the normalized mean fluorescence recovery curves. To assess the statistical significance of differences found between two given families of curves characterized by measurements at identical time-points, a point-to-point comparison based on a Student's t-test was implemented. The Benjamini and Hochberg (BH) method (Benjamini and Hochberg, 1995) was employed to control for the false discovery rate associated with multiple testing. The analysis was accomplished using R (R Development Core Team, 2006).

## **Hetero-fluorescence resonance energy transfer by donor fluorescence lifetime imaging microscopy in intact living cells**

HUVEC were single transfected with different mEGFP standards or co-transfected with combinations of mEGFP-mRFP1 pairs and seeded on FN-coated glass-bottomed Petri-dishes as described above. After 24h, and without TNF- $\alpha$  treatment, culture medium was replaced with phenol red-free medium for optimal image acquisition. FLIM was performed using a laser scanning microscope assembled at the Laboratory for Fluorescence Dynamics, (Irvine, CA, USA) using the photon counting regime of the photomultiplier detector in conjunction with time-resolved frequency-domain data acquisition hardware (Colyer et al., submitted). The data is processed automatically by software which accumulates a phase histogram of photon counts across the cross-correlation period, and then automatically calculates the phase and modulation of the emission. From the phase and modulation, the fluorescence lifetime ensembles in live cells was analyzed using the phasor-FLIM approach recently described (Digman et al., submitted; Caiolfa et al., 2007). The system was based on an Olympus Fluoview 1000 microscope, connected to a modulated ISS 471nm diode laser and equipped with a 470 +/- 5 nm excitation filter and a BA 505-525 nm emission filter (ISS Inc., Champaign, IL, USA). The laser was guided into the microscope by x-y galvano-scanner mirrors (Model 6350; Cambridge Technology, Watertown, MA), driven in a raster scan movement using the ISS 3-axis card (ISS, Inc. Champaign, IL) and synchronized with data acquisition with a Becker and Hickl SPC830 card. Data were acquired and processed by the SimFCS software developed at the LFD. A photomultiplier tube (R7862, Hamamatsu Photonics, Battlesboro, NJ) was used for the detection in the photon counting mode. The objective was a 40X water immersion (Zeiss, Germany) with 1.2 N.A. The scan area (256x256 pixels) corresponds to 32x32

$\mu\text{m}^2$ . Before measurement, a slide with concentrated fluorescein at pH 9 was measured. The lifetime of fluorescein, 4.04 ns, was determined separately in an ISS Inc fluorometer.

### **Fluorescence Correlation Spectroscopy**

Endothelial cells were transiently single or double transfected as for FLIM analysis. The dual-channel confocal fluorescence correlation spectrometer, ALBA (ISS Inc., Champaign, IL, USA), was equipped with avalanche photodiodes and interfaced to a Nikon TE2000 inverted microscope equipped with a dichroic set C-74610 (z488/594 dbx z488/594rpc) + emission filter z 488/594m (Chroma Technology, USA). The objective used was a 60X Plan Apo (1.2 NA, water immersion). Excitation at 488 nm was provided by a tunable argon ion laser (Melles Griot, USA) and at 594 nm by a HeNe Laser (Melles Griot, USA). The diameter and power of the two beams were controlled by the ISS laser launcher system. The two laser lines were combined by a suitable external dichroic mirror (Chroma Technology, USA). Inside the ALBA box an additional dichroic (Chroma Technology, USA) separated the mRFP1 and mEGFP emissions in the two channels (set C74612 (570 dclp, 520/30m, 610 lp). Every day, the power of the light passing through the objective in the absence of any immersion liquid was adjusted to 1 microW. An x,y,z computer-controlled piezoelectric actuator with a step resolution of less than 50 nm warranted the nanometric positioning. An ISS acquisition card received the data stream from the detectors. Data were stored for further processing by VISTA (ISS Inc.) and simFCS (LFD). Acquisition was in time-mode, and sampling frequency was 20 kHz. The waist ( $\omega_0$ ) of the excitation beam was

calibrated before each day's experiments using Rhodamine 110 at 488 nm and Sulphorhodamine at 594 nm. Typical  $\omega_0$  values were 0.34-0.38  $\mu\text{m}$ .

The autocorrelation functions (ACFs) were best-fitted using the anomalous diffusion model (Banks and Fradin, 2005), according to the equation:

$$G(\tau) = \frac{1}{N} \cdot \frac{1}{1 + \left(\frac{\tau}{\tau_D}\right)^\alpha}$$

where N is the average number of molecules in the excitation volume,  $\tau_D$  is the diffusion time, and  $\alpha$  is the anomaly coefficient.

Accordingly, the diffusion coefficient (D) is derived from the relationship:

$$D = \omega^2 / 4\tau^\alpha$$

### **Scanning electron microscopy**

Endothelial monolayers were activated for 20h with TNF- $\alpha$  20 ng/ml in the absence or presence of 250  $\mu\text{g/ml}$  of active or heat-inactivated (5 min, 90°C) CD9-LEL-GST peptide. Cells were then fixed in 2% paraformaldehyde in PBS and subjected to regular immunolabeling with P8B1 (anti-VCAM-1), Hu5/3 (anti-ICAM-1) or biotinylated MEM-111 (anti-ICAM-1) as primary antibodies and 40 nm gold-coupled anti-mouse antibody or 15 nm gold-coupled streptavidin (BBInt.) as detection reagents. After immunolabeling, samples were fixed in 2.5% glutaraldehyde in PBS and then dehydrated by sequential passages through 30, 50, 70, 90%, and absolute ethanol. The ethanol was substituted by liquid CO<sub>2</sub>, and the specimens were critical-point dried using a Polaron E3000 apparatus. Then, samples were transferred onto appropriate microscope slides and covered with a carbon layer up to 5 nm using a high vacuum evaporator (Edwards 12E6/1266). Images were obtained with a Hitachi S-4100

scanning electron microscope at an acceleration voltage of 12kV and a working distance of 4mm. Images were processed with Metamorph software (Universal Imaging Corporation, Molecular Devices Corporation, Downingtown, PA). Receptor clustering was evaluated by nearest neighbour analysis using a custom-written software based on R software. The developed method allowed us to establish similarities and discrepancies between different treatments in terms of aggregation and dispersion of the objects (gold particles) in the images.

## RESULTS

### VCAM-1 interacts with moesin and ezrin at the apical surface of activated endothelial cells

The subcellular distribution of VCAM-1, ezrin and moesin was analyzed by confocal microscopy in TNF- $\alpha$  activated HUVEC. VCAM-1 colocalized with ezrin (Fig. 5 a-c) and moesin (Fig. 5 e-g) in the microspikes and microvilli that protrude from the apical surface of these cells.

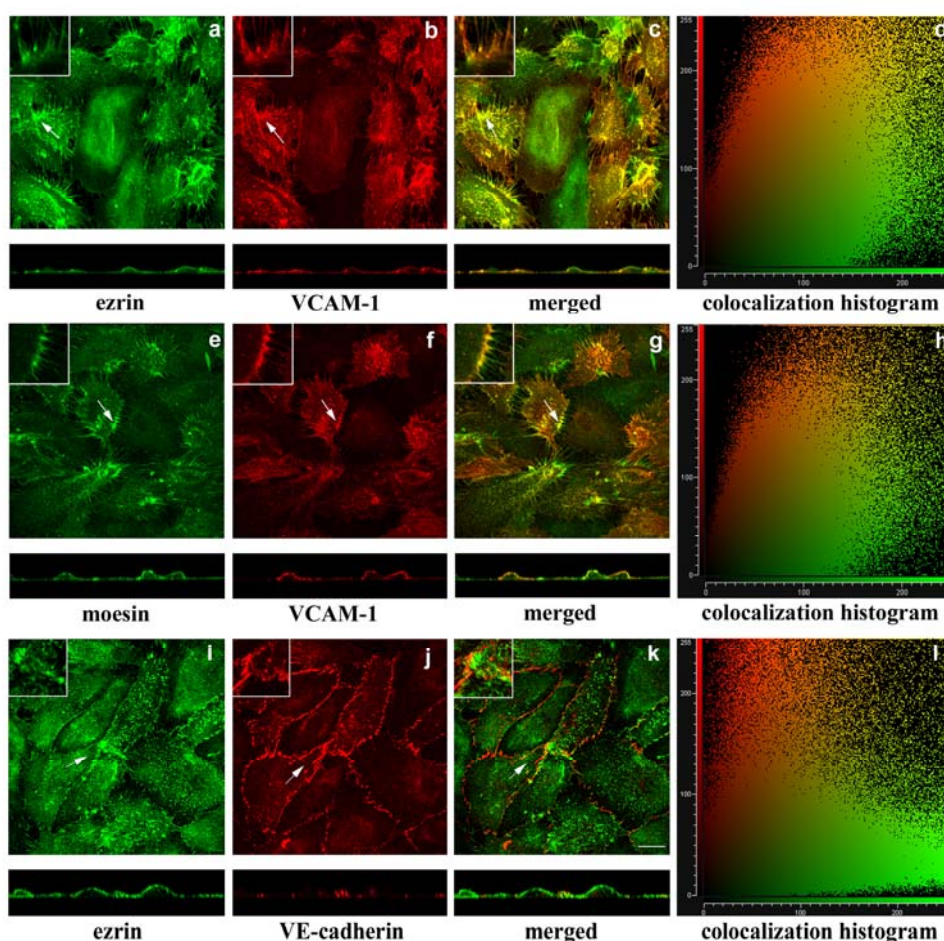


**Fig. 5.- VCAM-1 colocalizes with moesin and ezrin at the apical surface of activated HUVEC.**

Confluent HUVEC were activated with 20 ng/ml TNF- $\alpha$  for 20 h. Thereafter, cells were fixed, permeabilized and stained with the anti-ezrin pAb 90/3 (a and i) (green), anti-moesin pAb 95/2 (e) (green), anti-VCAM-1 mAb P8B1 (b and f) (red) or anti-VE-cadherin mAb Tea1/31 (j) (red). Merged images are shown in panels c, g and k, where colocalizations are observed (yellow). Images represent confocal laser scanning micrographs showing horizontal projections or the corresponding orthogonal section of the same field. Insets correspond to the amplified image of the zones pointed to by arrows. Colocalization histograms of green and red signals corresponding to these images are shown on the right (d, h, l). The corresponding colocalization percentages are 65.7% (d), 67.6% (h) and 13.3% (l). Bar: 20  $\mu$ m.

Colocalization analysis confirmed these observations (Fig. 5 d, h). By contrast, VE-cadherin did not colocalize with ERM proteins (Fig. 5 i-k).

To assess whether this codistribution in activated HUVEC is correlated with the formation of complexes between VCAM-1 molecules and ERM proteins, immunoprecipitation assays were carried out. As shown in Fig. 6A, moesin and ezrin co-immunoprecipitated with VCAM-1. To determine whether these interactions are direct, binding assays were performed using a GST fusion protein containing the cytoplasmic tail of VCAM-1 (GST-VC). The fusion protein containing the cytoplasmic tail of ICAM-3, GST-IC3, which has been demonstrated to bind ERM, as well as the partially truncated form GST-Y9, which shows a considerable reduced binding to moesin and ezrin (Serrador et al., 2002), were used as positive and negative controls, respectively. <sup>35</sup>S-Met-labeled N-moesin and N-ezrin were added to Sepharose beads coupled to the GST fusion proteins. Strong binding of VCAM-1 to ezrin and moesin was observed, which was much higher in comparison to ICAM-3 (Fig. 6B). Altogether these data demonstrate that VCAM-1 can directly associate with ezrin and moesin *in vitro* and presumably also at the apical membrane sites of endothelial cells.

### **Differential contribution of VCAM-1, ICAM-1, and ERM proteins to the extravasation process.**

The functional role of the VCAM-1/ERM association in the endothelial cell-lymphocyte interaction was analyzed and compared with another adhesion receptor that also interacts with ERM proteins, namely ICAM-1 (Heiska et al., 1998). For this purpose, we used T lymphoblasts, that express high levels of VLA-4 and LFA-1, ligands of VCAM-1 and ICAM-1, respectively (Fig. 7A).

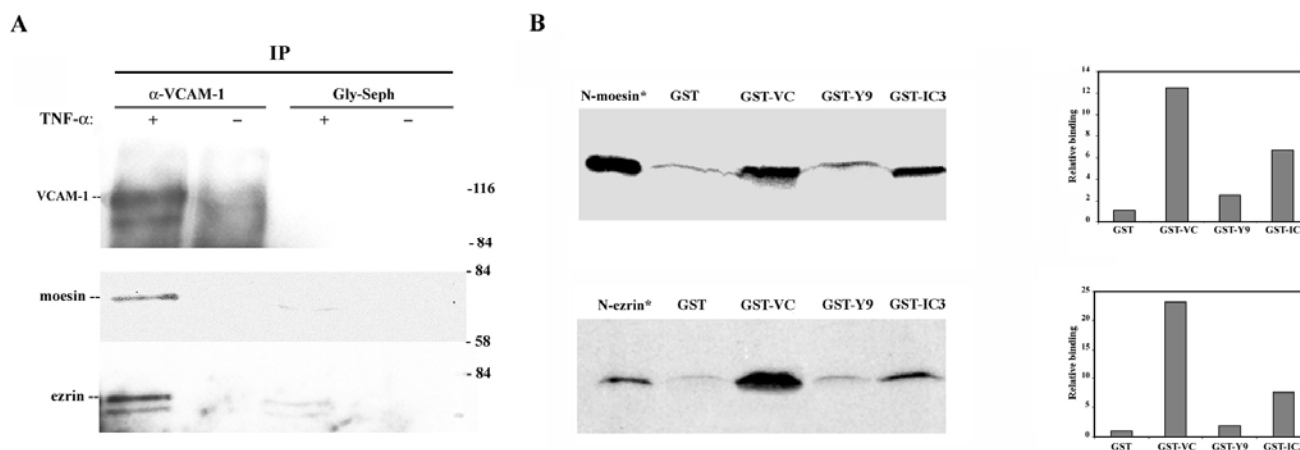


**Fig. 6.- Association of VCAM-1 with moesin and ezrin.**

**A.** Cytokine-activated HUVEC were lysed and immunoprecipitated with the anti-VCAM-1 mAb 4B9 or Gly-Sepharose. Immunoprecipitates were then resolved on a 10% SDS-PAGE, and sequentially immunoblotted with the anti-VCAM-1 mAb 4B9, the anti-moesin pAb 95/2, and the anti-ezrin pAb 90/3. Molecular weights (kDa) are indicated on the right side.

**B.** GST or the GST fusion proteins GST-VC, GST-IC3 and GST-Y9 were bound to glutathione-Sepharose beads and incubated with  $^{35}\text{S}$ -Met-N-moesin or  $^{35}\text{S}$ -Met-N-ezrin (upper and lower panels, respectively). After incubation, beads were boiled in sample buffer and eluted proteins were analyzed by 10% SDS-PAGE, autoradiography and fluorography. Lanes with isotope-labeled N-moesin and N-ezrin (\*) indicate the molecular mass of these truncated proteins. Densitometric diagrams normalized to the loading controls of GST-proteins are shown on the right.

Both integrins were active since mAb against them blocked T lymphoblast TEM (Fig. 7B). These cells were allowed to adhere and migrate across an activated HUVEC monolayer and confocal microscopic analysis of endogenous endothelial VCAM-1 and ICAM-1 distribution was performed. When lymphoblasts were spread on the apical surface of endothelium, VCAM-1 clustered around these cells (Fig. 7C, a). However, such VCAM-1 clusters were neither observed during the passage of lymphoblasts across the endothelium nor after transmigration (Fig. 7C, b). The orthogonal section showed two lymphoblasts migrating across adjacent endothelial cells, where clustered VCAM-1 molecules colocalized with endothelial ezrin only at the apical surface of the lymphoblast-endothelial cell contact area (Fig. 7C, c). On the other hand, ICAM-1 was clustered around lymphoblasts during all the lymphoblast adhesion and transmigration processes (Fig. 7C, d and e), colocalizing with endothelial ezrin (Fig. 7C, f).

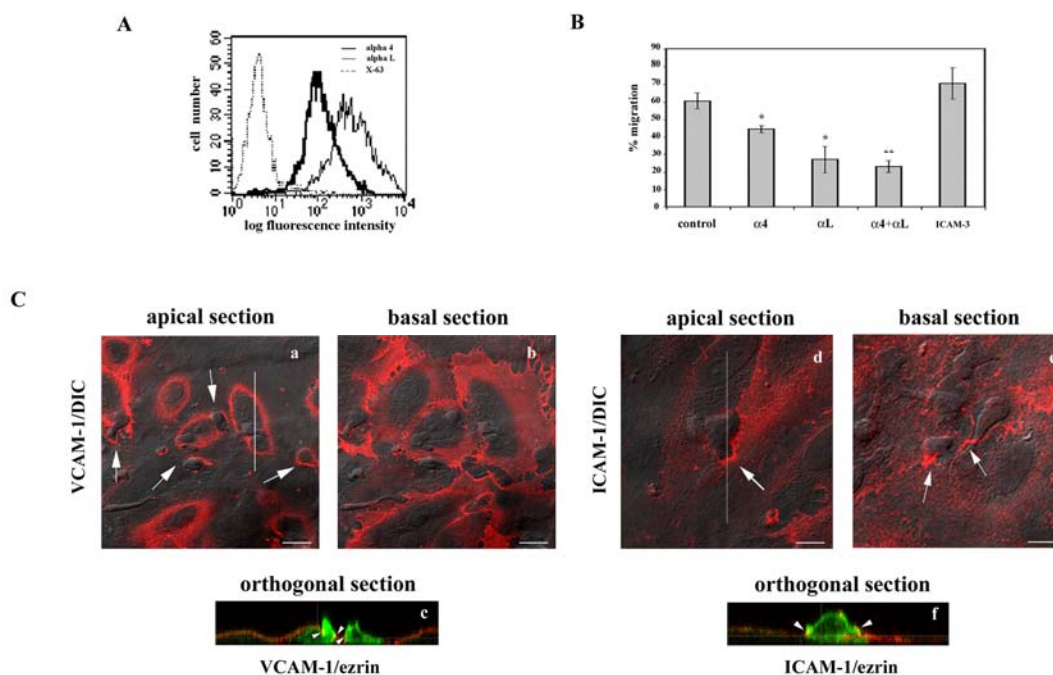


**Fig. 7.- Distribution of endogenous VCAM-1, ICAM-1 and ezrin during lymphoblast TEM.**

**A.** Expression of  $\alpha 4$ -integrin (thick line), and  $\alpha L$ -integrin (thin line) on T lymphoblasts as determined by flow cytometry analysis. P3X63 (dotted line) was used as negative control.

**B.** Transendothelial migration assay of T lymphoblasts pre-treated with the blocking anti- $\alpha 4$  mAb HP2/1, the blocking anti- $\alpha L$  mAb TS1/11, the mixture of anti- $\alpha 4$  plus  $\alpha L$  mAb, or the anti-ICAM-3 mAb TP1/24 as negative control. Values correspond to the arithmetic mean  $\pm$  SD of a representative experiment run by duplicate out of 3 independent ones. Statistically significant values, as defined by unpaired Student's t-test, are indicated with \* ( $p < 0.05$ ) or \*\* ( $p < 0.015$ ) compared with no Ab treatment.

**C.** T lymphoblasts were allowed to transmigrate across an activated HUVEC monolayer, and then cells were fixed, permeabilized and stained with the anti-VCAM-1 mAb P8B1 (a-c) (red), the anti-ICAM-1 mAb Hu5/3 (d-f) (red) or the anti-ezrin pAb 90/3 (c and f) (green). Representative confocal horizontal images showing an apical section of endothelium with adhered lymphoblasts on top (a, d) and a basal section with transmigrated lymphoblasts beneath the endothelium (b, e) are presented. DIC images are shown overlaid with VCAM-1 (a, b) or ICAM-1 staining (d, e). Arrows point to VCAM-1 or ICAM-1 clusters at the contact area. Representative orthogonal sections corresponding to the white line in panel a or panel d are shown in panels c and f, respectively. Green signal corresponds to ezrin staining both in lymphoblasts and endothelium. Arrowheads point to the sites of VCAM-1/ezrin or ICAM-1/ezrin clustering at the apical surface of endothelial cells. Bars: 20  $\mu$ m (a-b), 8  $\mu$ m (d-e).

To dynamically assess the changes in distribution of VCAM-1, ICAM-1, and ERM proteins, HUVEC transiently transfected with VCAM-1-, ICAM-1-, or moesin-GFP were separately monitored by live time-lapse confocal microscopy after addition of lymphoblasts. As observed previously for endogenous molecules, VCAM-1- and moesin-GFP fusion proteins redistributed to sites of contact during lymphoblast initial adhesion and spreading. However, only moesin was concentrated in the transmigration cleft and

apparently participated in subsequent interactions, when lymphoblasts migrated beneath the activated endothelium (Fig. 8A). Interestingly, moesin-GFP exhibited a dynamic behavior similar to ICAM-1-GFP (Fig. 8B), presumably because this adhesion molecule binds to ERM proteins to actively participate in TEM. Digital movies showing more clearly the differential dynamic distribution of these molecules are included as additional material.

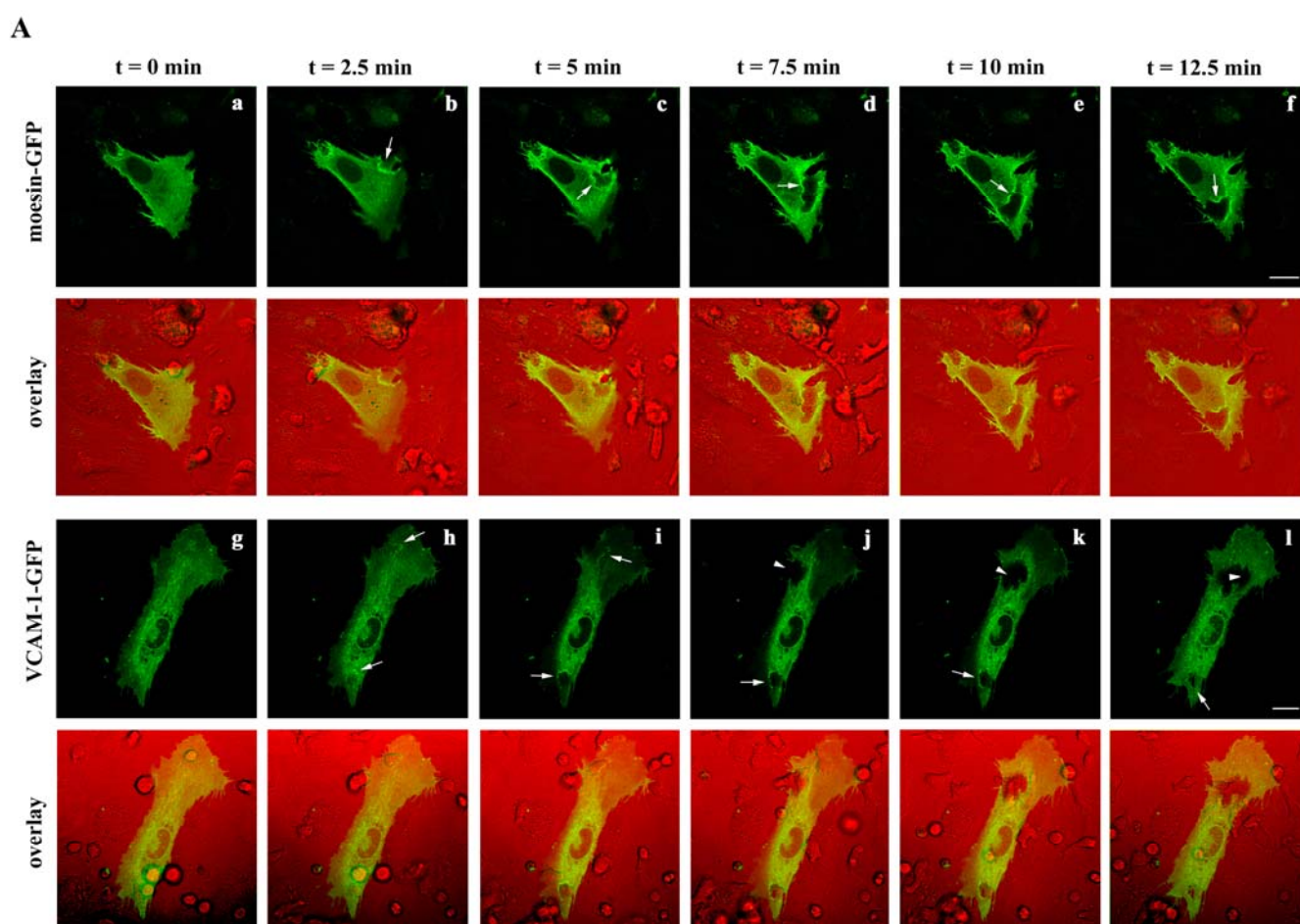


**Fig. 8A.- Dynamic changes in the localization of VCAM-1, ICAM-1 and moesin during lymphoblast TEM.**

**A.** Lymphoblasts were allowed to transmigrate across activated HUVEC transfected with moesin- or VCAM-1-GFP. Videosequences tracking the spatial and temporal distribution of moesin (a-f) and VCAM-1 (g-l) were obtained using live time-lapse fluorescence confocal microscopy. Each image represents a projection of several representative horizontal sections of a confocal image-stack depicted from the videosequence at the specified times. DIC and fluorescence images are merged and presented at the lower side of each panel. Arrows point to the GFP proteins clustering during the lymphoblast-endothelium interaction. Arrowheads indicate the absence of VCAM-1-GFP from the contact area between the transfected endothelial cell and a migrated lymphoblast placed beneath the endothelial monolayer. Corresponding digital videosequences are available in Appendix I Supplemental material. Bars: 20  $\mu$ m.

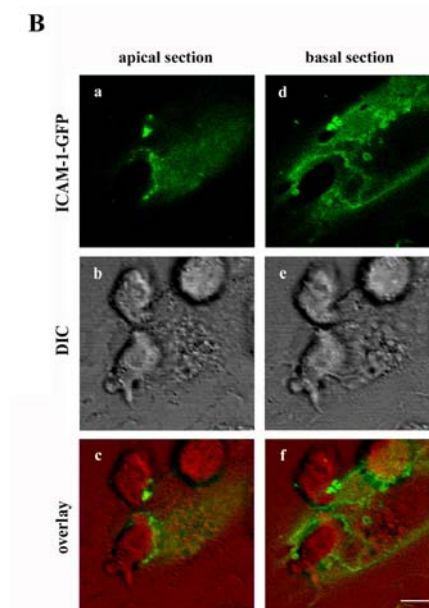


**Fig. 8B.- Dynamic changes in the localization of VCAM-1, ICAM-1 and moesin during lymphoblast TEM.**

**B.** Lymphoblast transmigration across activated HUVEC transfected with ICAM-1-GFP was analyzed by live time-lapse fluorescence confocal microscopy. Two representative horizontal sections from the apical and the basal side of the endothelial cell belonging to the same confocal stack depicted from the videosequence are presented. ICAM-1-GFP signal is shown in panels a and d. DIC images and the overlaid images are presented in panels b, e and c, f, respectively. The corresponding videosequence is available in Appendix I Supplemental Material. Bar: 5  $\mu$ m.

### **Redistribution of VCAM-1, ICAM-1 and ERM proteins at a docking structure during endothelium-leukocyte interaction.**

To focus our study on the role of ERM interaction with endothelial adhesion receptors during the initial adhesion of leukocytes to the endothelium, to which VCAM-1 involvement was mainly restricted, we used K562 cells stably transfected with  $\alpha$ 4 integrin (4M7 cells) (Munoz et al., 1996). These cells expressed high levels of VLA-4, but negligible amounts of LFA-1 (Fig. 9A). In addition, their adhesion to activated endothelium was dependent on VLA-4, since it was inhibited by the blocking anti- $\alpha$ 4 HP2/1 mAb, and induced by the activating anti- $\beta$ 1 TS2/16 mAb (Fig. 9B). 4M7 cells adhered to activated endothelium mainly via VLA-4, but these cells were unable to progress to TEM (data not shown). When the distribution of endogenous endothelial VCAM-1 was examined during 4M7 cell adhesion, we found that it was strongly

concentrated around attached leukocytes (Fig. 9C, c). Endogenous ezrin colocalized with VCAM-1 at the endothelial-leukocyte contact area (Fig. 9C, d), and antibodies to ezrin also stained the leukocyte membrane (Fig. 9C, b). Furthermore, a three-dimensional reconstruction of the site of adhesion showed that VCAM-1 and ezrin were contained in a unique docking structure that was raised above the level of the endothelial cell surface and that surrounded the adherent leukocyte in a cup-like fashion. Both proteins were preferentially concentrated in microspikes of this structure that presumably served to anchor the attached leukocyte (Fig. 9C, e-g). The redistribution of VCAM-1 and moesin to the leukocyte-endothelium contact area was tracked separately by live time-lapse fluorescence confocal microscopy during the interaction of 4M7 cells with VCAM-1- or moesin-GFP transfected HUVEC. The dynamic studies demonstrated that VCAM-1/VLA-4 engagement was associated with the progressive concentration of VCAM-1 and moesin at the specialized anchoring structure formed between the two interacting cells, which was progressively strengthened and sustained with time (Fig. 9D).

To ascertain the physiological relevance of this docking structure, we analyzed the redistribution of VCAM-1, ICAM-1, and ezrin to the contact area of migrating peripheral blood lymphocytes (PBLs) allowed to adhere under fluid shear conditions, using a physiological wall shear stress ( $1.8 \text{ dyn/cm}^2$ ) for perfusion periods from 30s to 10 min. We found these endothelial molecules colocalizing in clusters at the docking structures formed around spreaded PBLs (Fig. 10A), at early time points during the arrest of lymphocytes. This structure was also observed during the interaction of activated HUVEC with T lymphoblasts in static conditions (Fig. 10B, and data not shown). Similarities in three-dimensional VCAM-1 distribution around 4M7 cells, T lymphoblasts or peripheral blood lymphocytes supported the generality of the docking structure (Fig. 10B).

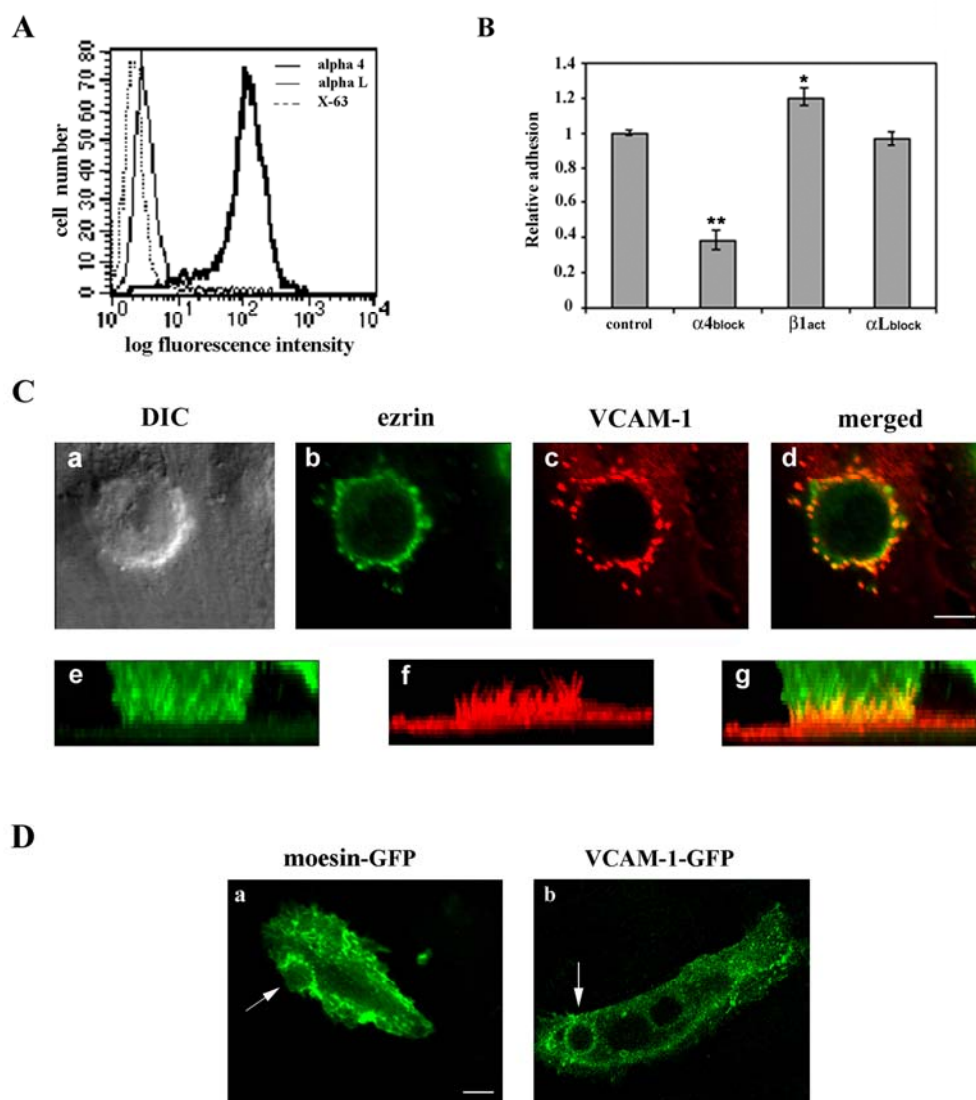


**Fig. 9.- Localization of VCAM-1 and ezrin at the contact area of activated HUVEC with leukocytes.**

**A.** Expression of  $\alpha 4$ -integrin (thick line), and  $\alpha L$ -integrin (thin line) on 4M7 cells as determined by flow cytometry analysis. P3X63 (dotted line) was used as negative control.

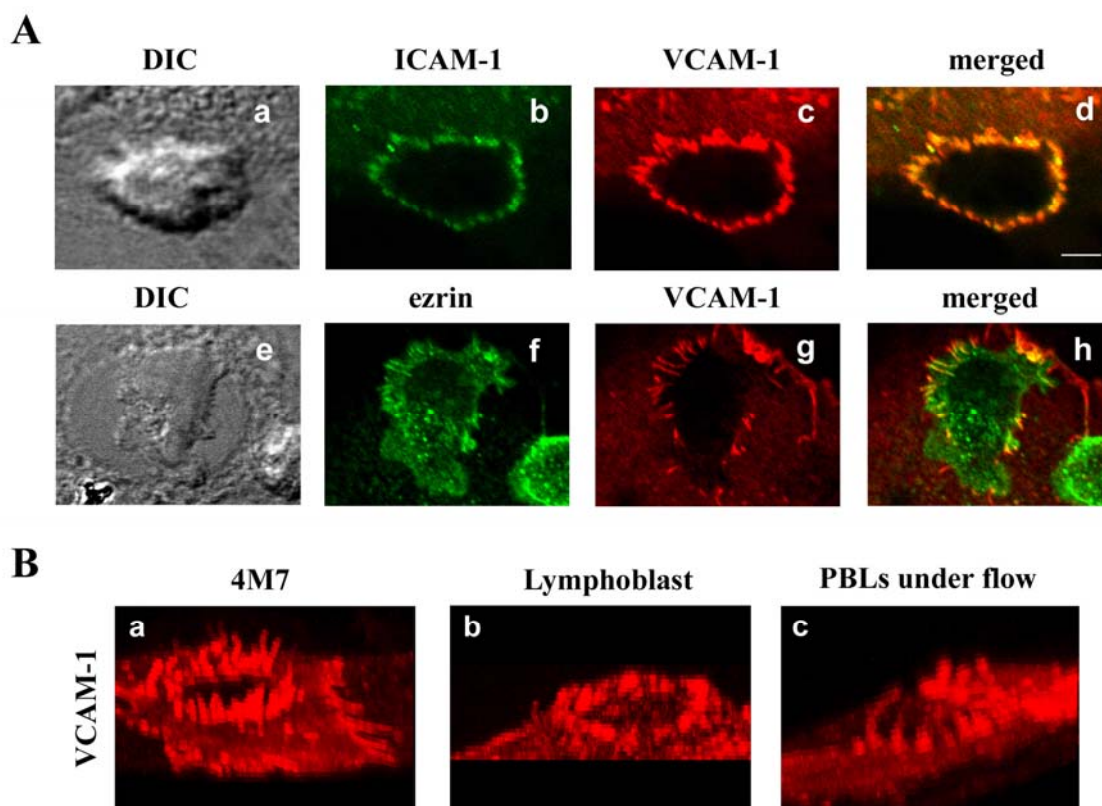
**B.** Adhesion to activated HUVEC of 4M7 cells pre-treated with the blocking anti- $\alpha 4$  mAb HP2/1, the activating anti- $\beta 1$  mAb TS2/16, or the blocking anti- $\alpha L$  mAb TS1/11. Values correspond to the arithmetic mean  $\pm$  SD of a representative experiment run by triplicate out of 3 independent ones. Statistically significant values, as defined by unpaired Student's t-test, are indicated with \* ( $p < 0.005$ ) or \*\* ( $p < 0.0001$ ), compared with no Ab treatment.

**C.** 4M7 cells interacting with activated endothelial cells were fixed, permeabilized and stained with the anti-ezrin pAb 90/3 (green) and the anti-VCAM-1 mAb P8B1 (red). Representative horizontal sections of confocal laser scanning images (b,c) are merged in panel d. The corresponding DIC image is shown in panel a. The corresponding three-dimensional reconstruction is presented in panels e-g. Bar: 5  $\mu$ m.

**D.** 4M7 cells were allowed to adhere to activated HUVEC transfected with moesin- or VCAM-1-GFP. GFP staining was monitored using live time-lapse fluorescence confocal microscopy. Horizontal sections showing the staining of moesin- (a) or VCAM-1-GFP (b) after 60 min of leukocyte-endothelium interaction. Arrows point to the GFP proteins clustered in the anchoring structure. Bar: 20  $\mu$ m.

### Relocation of cytoskeletal components to the endothelial docking structure.

The cytoskeletal components involved in the generation of this endothelial structure were analyzed. Samples of 4M7 cells adhered to activated HUVEC and stained for VCAM-1 and F-actin revealed a considerable enrichment of endothelial actin within the docking structure (Fig. 11A, a-b). Interestingly, this apical actin scaffold appeared not to be connected to basal stress fibers (Fig. 11A, c-d). On the contrary, tubulin was not present with F-actin at the anchoring structure (Fig. 11A, e-h).

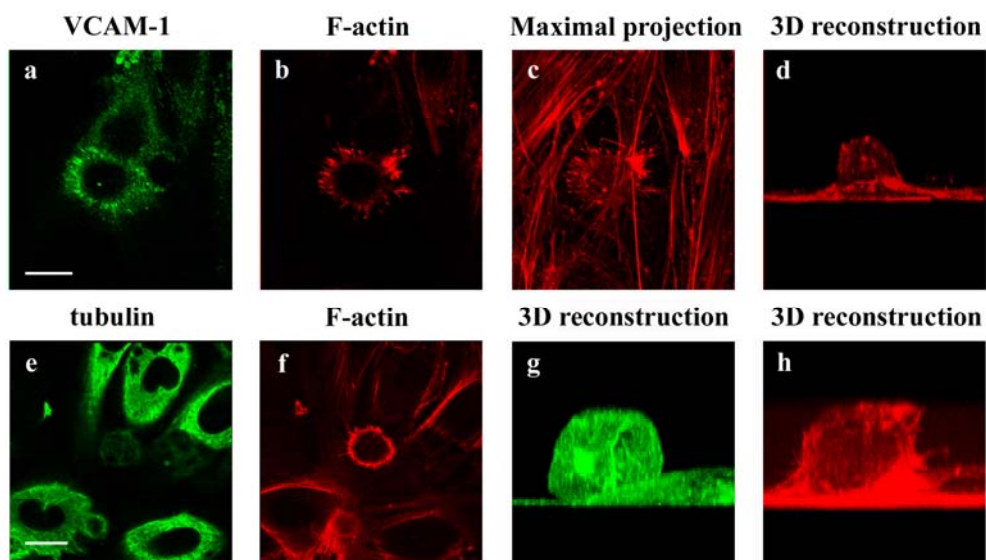
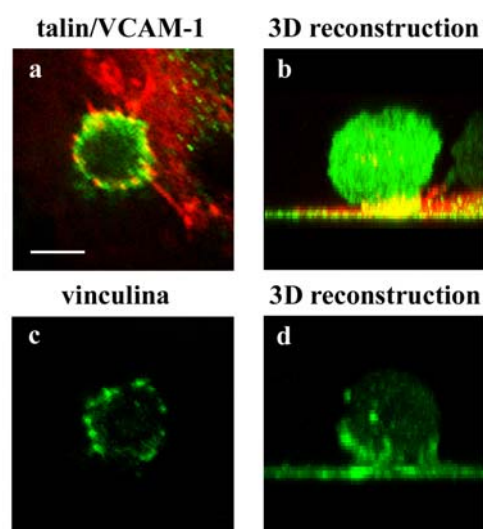


**Fig. 10.- Formation of the endothelial docking structure for adhered lymphocytes under flow.**

**A.** Transendothelial migration assay of peripheral blood lymphocytes under fluid shear conditions. After 10 min of perfusion, cells were fixed and stained for ICAM-1 (b, d) (green), VCAM-1 (c, d, g, h) (red), and ezrin (f, h) (green). The corresponding DIC images are shown in panels a and e. Merged images are shown in panels d and h. Bar: 3,5  $\mu$ m. **B.** Three-dimensional reconstruction of VCAM-1 staining during 4M7 cell (a), T lymphoblast (b), or PBLs under flow (c) adhesion.

Vinculin and  $\alpha$ -actinin-GFP also redistributed to this structure with a punctuate pattern (Fig. 11B, c-d, and Fig. 11C a-c). Likewise, VASP-GFP colocalized with VCAM-1 (Fig. 11C, f-g), whereas talin and paxillin-GFP were only found colocalizing with

VCAM-1 at some adhesion structures (Fig. 11B, a-b, and Fig. 11C, d-e). These data indicate that the endothelial docking structure was supported by the actin cytoskeleton, actin-bundling proteins such as  $\alpha$ -actinin, actin-nucleating proteins such as VASP, and focal adhesion proteins such as vinculin, talin or paxillin. The formation of this structure was associated with a remarkable change in distribution of several of these proteins, in particular vinculin, talin and paxillin, from their normal subcellular localization at focal adhesions at the basal surface to the docking structure at the apical surface.

**A****B**

C

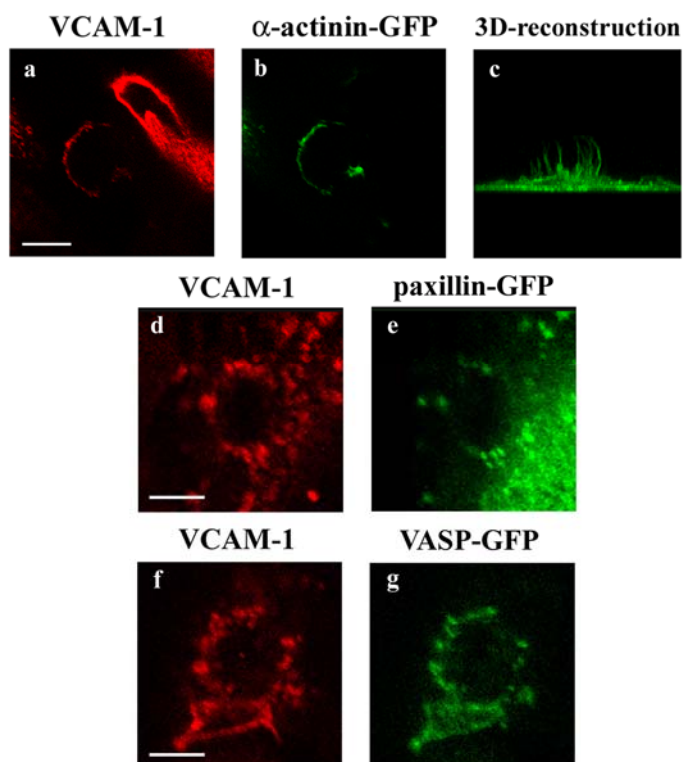


**Fig. 11.- Characterization of the endothelial docking structure formed during leukocyte adhesion.**

**A.** 4M7 cells were allowed to adhere to activated HUVEC cells, then fixed, permeabilized and stained for VCAM-1 (a) (green), F-actin (b-d, f, and h) (red), and tubulin (e and g) (green). Representative horizontal sections of confocal image-stacks are presented in panels (a-b, e-f). The panel c shows the projection of all the horizontal sections corresponding to the image presented in panels a-b. Three-dimensional reconstructions of F-actin (d, h) and tubulin (g) stainings are also shown. Bars: 20  $\mu\text{m}$ .

**B.** 4M7 cells adhered to activated HUVEC were fixed, permeabilized and stained for talin (a-b) (green), VCAM-1 (a-b) (red), or vinculin (c-d) (green). Representative horizontal sections of confocal images are presented in panels a and c. Three-dimensional reconstructions are shown in panels b and d. Bar: 5  $\mu\text{m}$ .

**C.** 4M7 cells were allowed to adhere to activated HUVEC transfected with  $\alpha$ -actinin, paxillin-, and VASP-GFP. Thereafter, cells were fixed and stained with the anti-VCAM-1 mAb P8B1 (a, d, f) (red). Green signal corresponds to GFP fusion proteins (b, c, e, g). Representative horizontal sections of confocal image-stacks are presented in all panels except for panel c, which shows the three-dimensional reconstruction of  $\alpha$ -actinin-GFP signal. Bars: 5  $\mu\text{m}$ .

### The docking structure is regulated by PI(4,5)P<sub>2</sub> and Rho/p160 ROCK.

To assess whether the clustering of ERM proteins at the endothelial-leukocyte contact area is associated with an activated state of these proteins, immunofluorescence studies using the 297S mAb, which recognizes a C-terminal threonine phosphorylated in ERM proteins (Matsui et al., 1998), were conducted. A high concentration of

phosphorylated ERM proteins was evident at the endothelial anchoring structure generated after VCAM-1/VLA-4 interaction (Fig. 12A).

We have also studied two important regulators of ERM activation, namely phosphoinositides and components of the Rho/p160 ROCK pathway. The subcellular localization of different phosphoinositides was determined by using as probes the PH domain of PLC $\delta$ , which binds PI(4,5)P $_2$ , and that of GRP1, which binds PI(3,4,5)P $_3$  and PI(3,4)P $_2$ , fused to GFP (Gray et al., 1999; Várnai et al., 1999). Upon endothelial cell transfection, both probes colocalized with VCAM-1 at the endothelial docking structure (Fig. 12B, a-b and d-e). PLC $\delta$ -PH-GFP showed a higher concentration at microspike tips

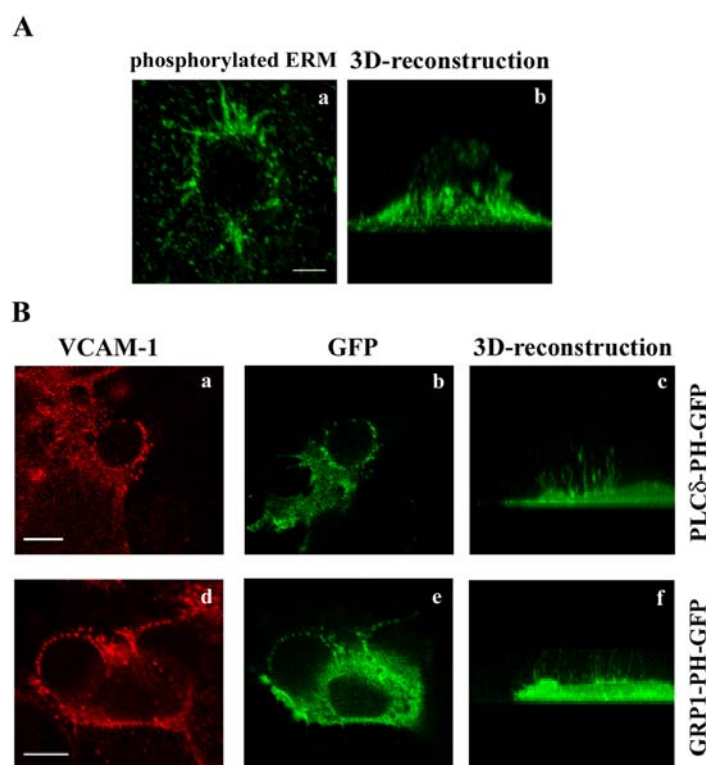


**Fig. 12.- Localization of phosphorylated ERM proteins and phosphoinositides at the anchoring structure.**

**A.** 4M7 cells adhered to activated HUVEC were fixed, permeabilized and stained with the mAb 297S. Representative horizontal section of a confocal micrograph (a), and a three-dimensional reconstruction of a series of horizontal sections (b) are shown. Bar: 5  $\mu$ m.

**B.** HUVEC cells were transfected with PLC $\delta$ -PH- and GRP1-PH-GFP and then, 4M7 cells were allowed to adhere. Thereafter, cells were fixed, permeabilized and stained with the anti-VCAM-1 mAb P8B1 (a, d). Green signal corresponds to GFP fusion proteins (b, e). Panels c and f show three-dimensional reconstructions of horizontal sections corresponding to the green signal. Bars: 5  $\mu$ m.

(Fig. 12B, c), whereas GRP1-PH-GFP appeared to be more diffusely distributed and localized throughout the entire structure (Fig. 12B, f).

Next, blocking studies with chemical inhibitors were carried out before and after HUVEC-leukocyte adhesion. The p160 ROCK inhibitor Y-27632 strongly inhibited the generation and maintenance of the anchoring structure (Fig. 13A). On the other hand, the PI3K inhibitor Ly 294002 only had a minor effect on the generation of this structure, but moderately inhibited its maintenance (Fig. 13A). The classic PKCs inhibitor Gö6976 did not exert a significant inhibitory effect neither on the generation nor in the maintenance of the anchoring structure (Fig. 13A). Dynamic studies using VCAM-1-GFP transfected HUVEC showed that the p160 ROCK inhibitor Y-27632 acted by destroying the docking structure, as observed in Fig. 13B. Finally, the effect of this inhibitor was assayed on endothelium during lymphocyte adhesion and transmigration under flow conditions. We found a diminished lymphocyte rolling and adhesion after Y-27632 treatment with regard to control conditions. Furthermore, some cells that were initially adhered, began to roll and finally detached from the monolayer, indicating an abnormal adhesion process. Accordingly, all these events led to a significant inhibition of transmigration (Fig. 13C). Furthermore, immunofluorescence analysis revealed that most of adhered lymphocytes were not tightly anchored by an endothelial docking structure (data not shown).

In conclusion, these findings suggest that both, PI(4,5)P<sub>2</sub> and the Rho/p160 ROCK pathway, are important for the generation as well as for the maintenance of the endothelial docking structure.

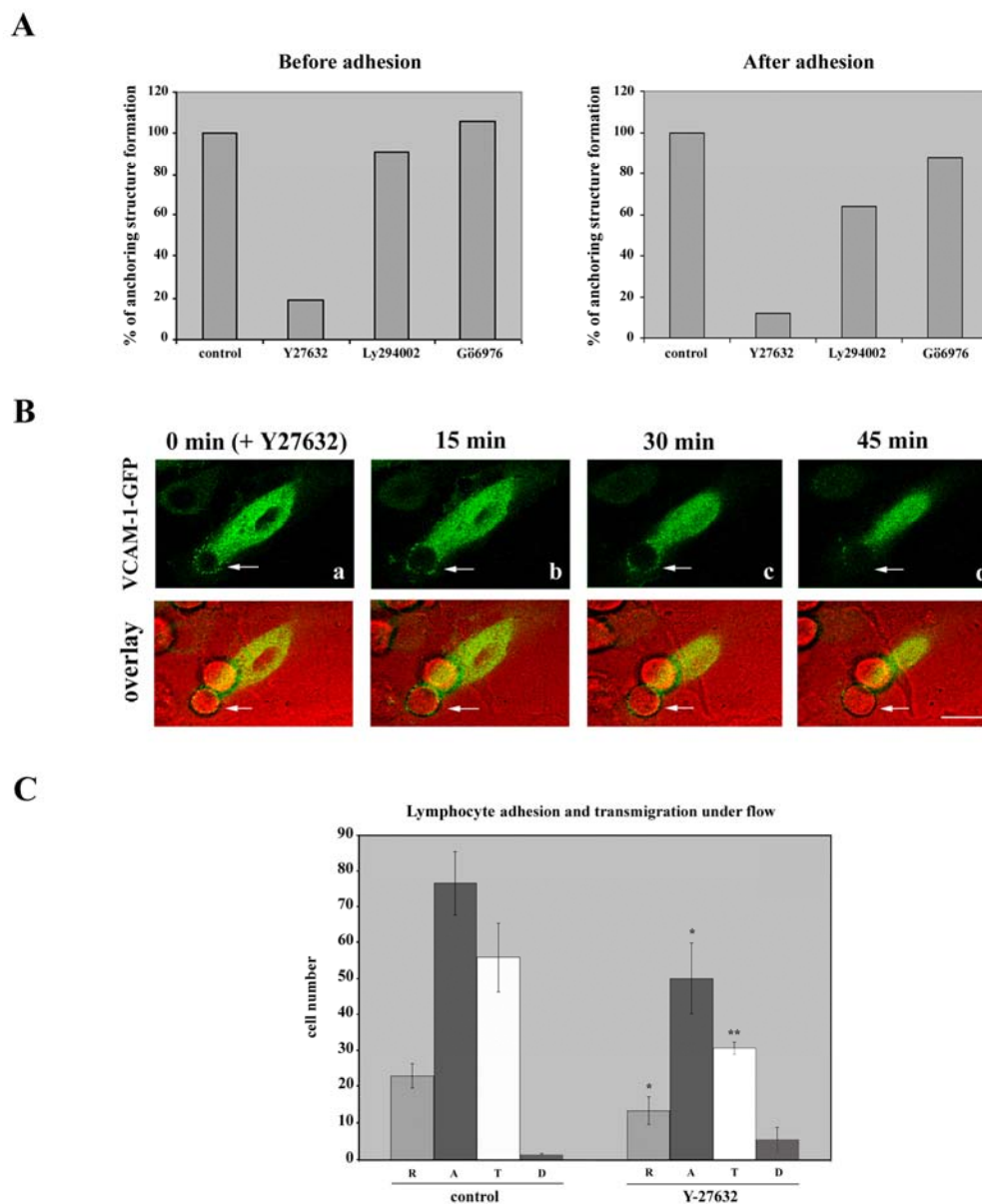


**Fig. 13.- Rho/p160 ROCK pathway regulates the generation and maintenance of the VCAM-1-mediated docking structure.**

**A.** Activated HUVEC were pretreated with Y27632 (30  $\mu$ M), Ly294002 (20  $\mu$ M), or Gö6976 (1  $\mu$ M) for 20 min before or 30 min after the addition of 4M7 cells. Total adhesion time was in both cases 60 min. Quantification of leukocyte adhesion and endothelial docking structure formation was carried out by staining with the mAb anti-VCAM-1 P8B1 and counting 300 adhered cells of each treatment. A representative experiment out of 4 independent ones is presented. **B.** Kinetics of the endothelial anchoring structure dissolution after the addition of the p160 ROCK inhibitor Y-27632. The inhibitor Y-27632 (30  $\mu$ M) was added after the formation of the docking structure in an adhesion assay performed as above. Representative horizontal sections captured every 15 min are shown in panels a-c. DIC and fluorescence images are merged and presented in the lower side of each panel. Arrows indicate the clustering of GFP proteins. Bar: 10  $\mu$ m. **C.** Effect of Y-27632 on lymphocyte adhesion and TEM under flow conditions. Activated endothelium was pretreated or not with Y-27632 (30 $\mu$ M) for 30 minutes. Thereafter, PBLs were allowed to adhere and transmigrate under flow conditions for 10 min. Quantification of rolling (R), adhesion (A), transmigration (T) and detachment (D) events during the last min of perfusion was carried out. Values correspond to the arithmetic mean  $\pm$  SD of 4 different fields belonging to a representative experiment. Statistically significant values, as defined by unpaired Student's t-test, are indicated with \*( $p < 0.01$ ) or \*\*( $p < 0.002$ ) compared with no inhibitory treatment.

### Tetraspanins are components of the endothelial docking structure for adherent leukocytes by their association with ICAM-1 and VCAM-1

Tetraspanin proteins are low molecular weight polypeptides that are able to associate with a variety of transmembrane proteins via their extracellular domain, forming multiproteic domains in the plasma membrane. They have been involved in several cellular functions including intercellular homotypic and heterotypic adhesion (Yanez-Mo et al., 2001), however genetic approaches directed to tetraspanins did not render clearcut information on their individual functional roles. HUVEC cells express several of these proteins (CD9, CD81, CD151, CD63), both at intercellular contacts and intracellular vesicles (Sincock et al., 1999; Yanez-Mo et al., 1998).

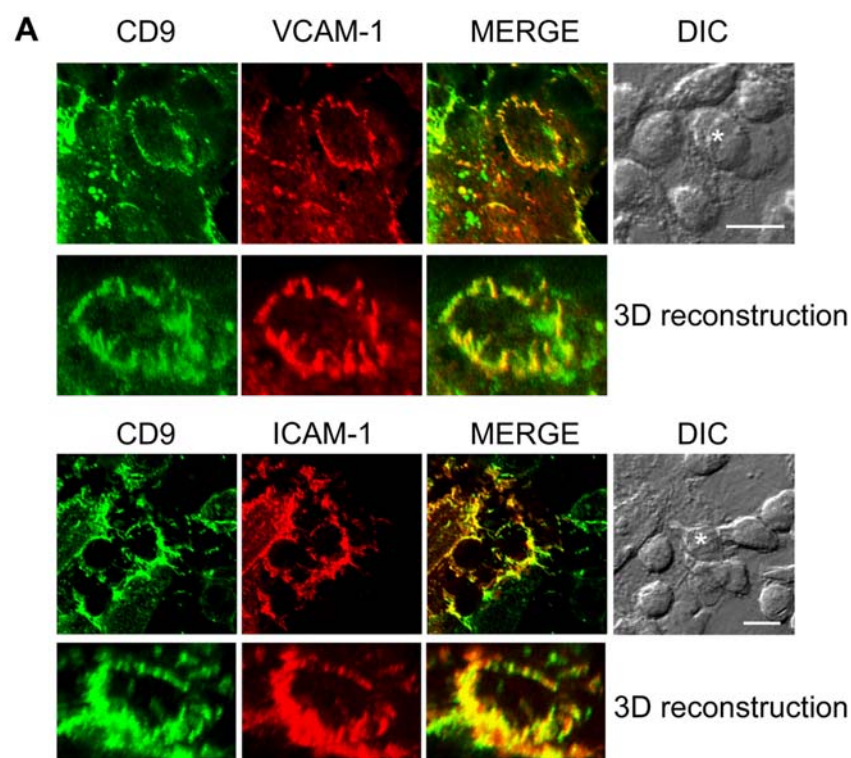


**Figure 14A. Endothelial tetraspanin proteins relocalize to the contact site with adherent leukocytes and associate with ICAM-1 and VCAM-1.**

A. T lymphoblasts were adhered to TNF- $\alpha$ -activated HUVEC monolayers, fixed, and double-stained for CD9 and VCAM-1 or ICAM-1. Maximum projections of the relevant sections from the confocal stacks and the merge of both channels are shown. Asterisks in differential interference contrast (DIC) images highlight the T lymphoblasts around which the docking structures shown in the 3-dimensional (3D) reconstructions are formed. Scale bars equal 10  $\mu$ m.

On the other hand, T lymphoblasts express CD81 and low levels of CD151, whereas the expression of CD9 is heterogeneous, ranging from completely negative to high expressing cells, and the relative amount of each population varies in different human donors. Upon T lymphoblast adhesion onto activated HUVEC monolayers, endothelial tetraspanins redistributed, together with ICAM-1 and VCAM-1, to the docking structure that emerges from the apical surface to firmly attach the transmigrating cell (Barreiro et al., 2004; Barreiro et al., 2002) (Figure 14A and B and data not shown). Tetraspanin redistribution was also observed under flow conditions around adherent peripheral blood lymphocytes, neutrophils or monocytes (Fig 14C for CD9, and data not shown).

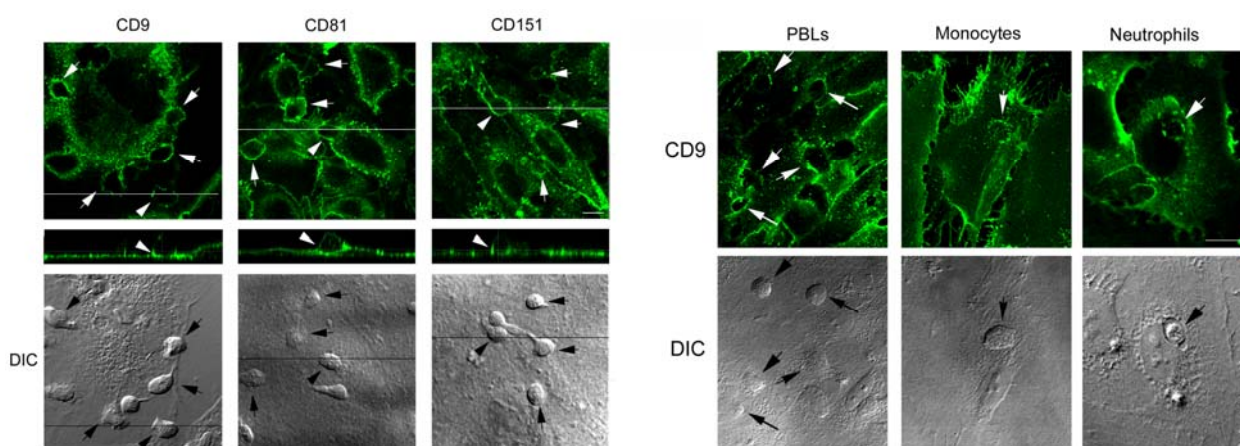


**Figure 14B (left) and C (right). Endothelial tetraspanin proteins relocate to the contact site with adherent leukocytes and associate with ICAM-1 and VCAM-1.**

**B.** T lymphoblasts were adhered to TNF- $\alpha$ -activated HUVEC monolayers, fixed, and stained with antitetraspanin mAbs VJ1/20 (anti-CD9), I.33.2.2 (anti-CD81), and LIA1/1 (anti-CD151). Confocal stacks were obtained and representative apical horizontal and vertical sections together with the corresponding DIC images are shown. Arrows point to the positions of the adhered lymphoblasts. Arrowheads and lines point to the position of the adhered lymphoblasts shown in the vertical sections. Scale bar equals 10  $\mu$ m. **C.** Human PBLs, neutrophils, or monocytes were perfused at physiologic flow rate (1.8 dyn/cm<sup>2</sup>), fixed, and stained with anti-CD9 VJ1/20 mAb. Confocal stacks were obtained and maximum projections of the whole series or a representative section together with the corresponding DIC images are shown. Arrows point to the position of the adhered leukocytes. Scale bar = 20  $\mu$ m.

To determine the subcellular localization of endothelial tetraspanins during the whole transendothelial migration process, T lymphoblasts were allowed to transmigrate across TNF- $\alpha$ -activated HUVEC monolayers. CD9 clustering was evident in those lymphocyte-endothelial interactions occurring at the apical surface of the monolayer (Fig

14D, white arrows). In contrast, almost no redistribution of CD9 could be observed at the ventral surface of endothelial cells in contact with transmigrated lymphoblasts (Fig 14D, grey arrows). On the other hand, CD151 relocation around lymphoblasts was clearly detected at both the apical and basal surface of the endothelial cell (Fig 14D; white and grey arrows, respectively) paralleling the behavior of ICAM-1.

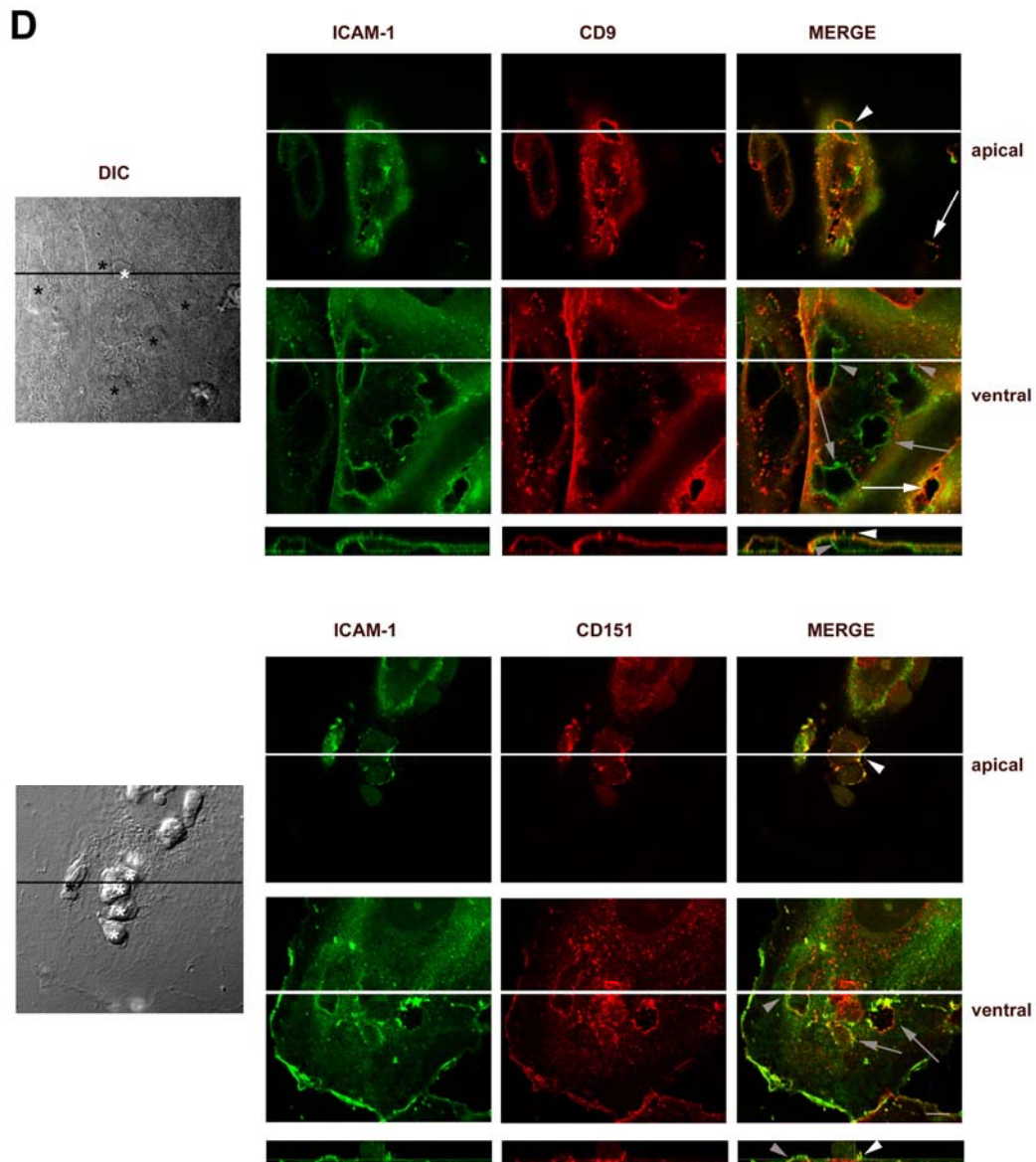


**Figure 14D. Endothelial tetraspanin proteins relocate to the contact site with adherent leukocytes and associate with ICAM-1 and VCAM-1.**

**D.** Analysis of the localization of endogenous endothelial CD9 or CD151, compared with ICAM-1, at apical and ventral contact sites with transmigrating lymphocytes. Human T lymphoblasts were allowed to transmigrate through TNF- $\alpha$ -activated HUVECs, fixed, and double-stained with antitetraspanin mAbs and biotin-conjugated anti-ICAM-1. Confocal stacks were obtained and representative sections at apical or ventral positions of the same field together with the corresponding DIC image are displayed. White arrows and asterisks mark apically adhered lymphocytes, and gray arrows and black asterisks mark those lymphocytes that have transmigrated. Arrowheads and lines point to the position of the adhered or transmigrated lymphoblast shown in the vertical sections. Scale bar equals 10  $\mu$ m.

Similarly to that observed with the endogenous protein stainings, CD9-GFP was more clearly relocalized to the contact site with T lymphoblasts at the endothelial apical surface, although some clustering occurred around transmigrated lymphoblasts locomoting underneath the endothelium. On the other hand, CD151-GFP was strongly concentrated at the contact with lymphoblasts throughout all the transmigration process. These data point to the existence of different tetraspanin microdomains at the apical and ventral endothelial surfaces and suggest a complex dynamic regulation of these membrane domains.

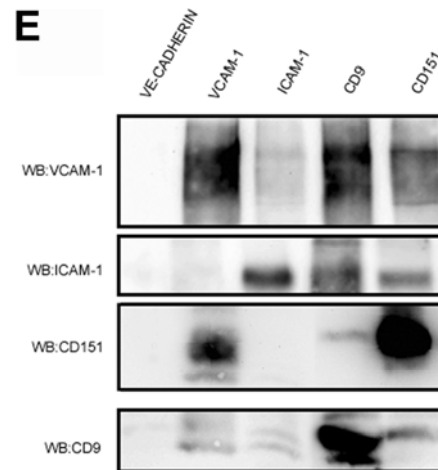


**Figure 14E. Endothelial tetraspanin proteins relocalize to the contact site with adherent leukocytes and associate with ICAM-1 and VCAM-1.**

**E.** ICAM-1 and VCAM-1 are associated with tetraspanins in TNF- $\alpha$ -activated HUVECs. Cell lysates were obtained in 1% Brij96 and immunoprecipitated with the different mAbs specific for endothelial adhesion molecules or tetraspanins. After washing, immunoprecipitates were resolved in sodium dodecyl sulfate–polyacrylamide gel electrophoresis (SDS-PAGE) gels and revealed by Western blot for VCAM-1 (P8B1), ICAM-1 (HU5/3), CD151 (8C3) or CD9 (VJ1/20).

Tetraspanin interactions are biochemically detected by extraction with Brij 96/97 detergents. Although HUVEC tetraspanins were mostly associated with EWI-F and  $\beta$ 1 integrins ((Yanez-Mo et al., 1998) and data not shown), CD9 and CD151 were also able to pull down ICAM-1 and VCAM-1 (Fig 14E). Conversely, ICAM-1 mAbs were also able to coprecipitate CD9, whereas VCAM-1 coprecipitated mainly CD151. No detectable signal for ICAM-1 was observed in  $\beta$ 1 immunoprecipitates (not shown),

suggesting that tetraspanin-integrin complexes are different to tetraspanin/ICAM-1/VCAM-1 complexes. Coprecipitation of CD9 and CD151 with ICAM-1 and VCAM-1 could also be faintly detected upon extraction with 1% digitonin (not shown), conditions in which most interactions among tetraspanins are lost and direct tetraspanin-partner associations are observed (Serru et al., 1999). These results indicate that ICAM-1 and VCAM-1 are included into tetraspanin microdomains.

### **Tetraspanin microdomains are critical for a proper expression and function of ICAM-1 and VCAM-1**

In order to gain insights in the relevance of the inclusion of ICAM-1 and VCAM-1 into tetraspanin microdomains at endothelial cells, we used a siRNA approach against tetraspanins CD9 and CD151 in primary human endothelial cells. Endothelial tetraspanin CD9 and CD151 expression was considerably knocked down with specific siRNA oligos. In no case was the expression completely abolished, but a significant reduction (40-70%) was attained (Fig 15A and B, flow cytometry analysis being depicted in logarithmic scale and mean fluorescence quantified in Figure 15C). In immunofluorescence analyses a clear reduction of tetraspanin staining could be observed, with some cells showing expression levels even below the detection threshold (Fig 15D). A compensation effect on the expression of other tetraspanins was observed (Fig 15B, C and D).

HUVEC cells thus treated were viable and clearly responded to TNF- $\alpha$  increasing ICAM-1, VCAM-1 and E-Selectin expression over resting levels (ICAM-1 expression increases 10-30 folds upon TNF- $\alpha$  treatment, whereas VCAM-1 and E-Selectin are undetectable in resting cells) (Fig 16A dotted line). The siRNA transfection procedure slightly affected the inducible expression of these adhesion receptors when compared to untransfected cells, as determined with a negative oligonucleotide control that does not

pair with any human mRNA (not shown). In CD9 or CD151 tetraspanin-interfered cells, a selective reduction in the expression of ICAM-1 and VCAM-1, but not that of E-selectin or CD44 was observed (Fig 16A, thick versus thin line). This reduction was of 60% for ICAM-1 and 80% for VCAM-1 when compared to their expression in negative oligonucleotide-transfected cells to exclude any off-target effect due to siRNA transfection (Fig 16B).

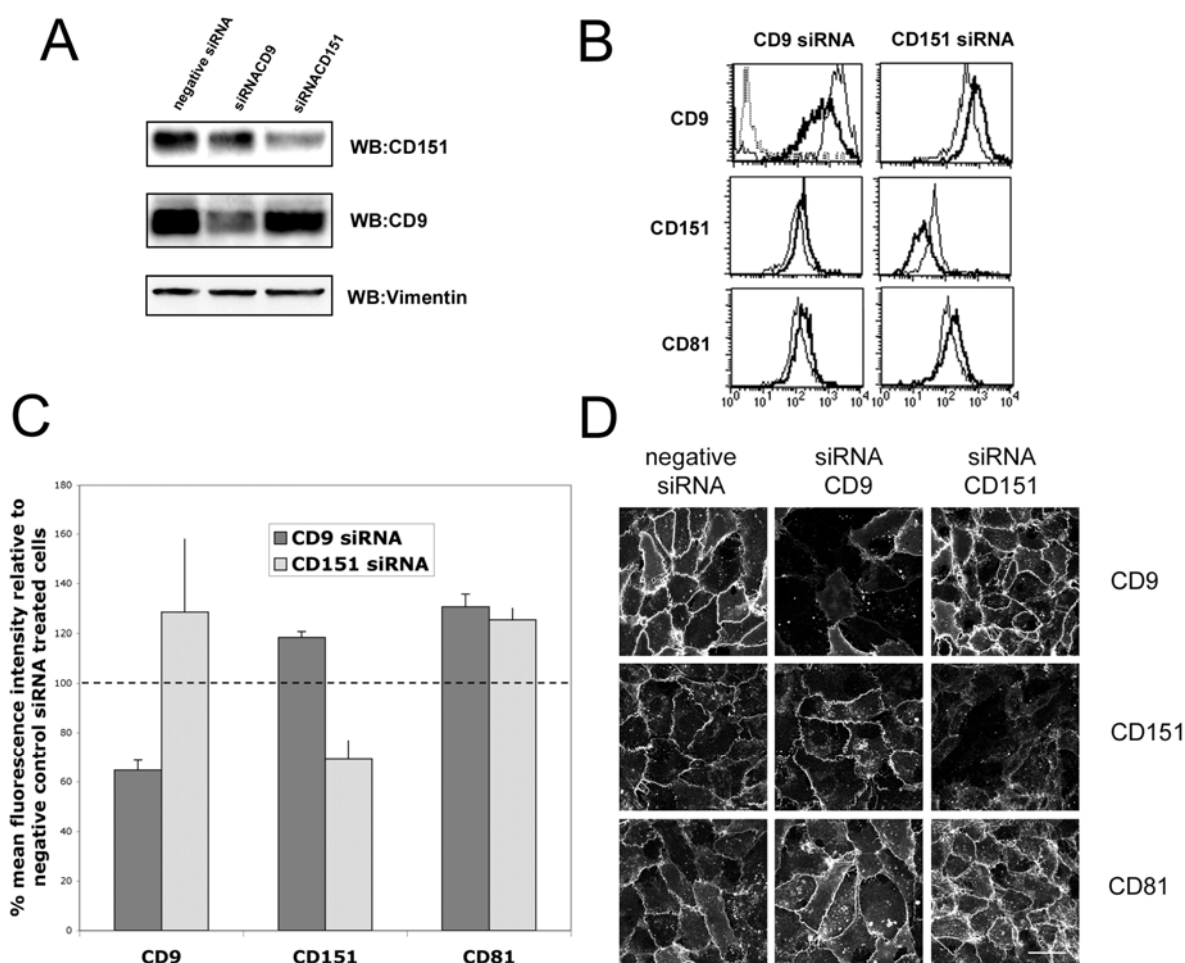


**Figure 15: siRNA knocking down of tetraspanins CD9 and CD151 in HUVEC cells.** **A.** Analysis by Western blot of the expression of tetraspanins CD9 and CD151 in total cell lysates of siRNA transfected cells. Loading control for vimentin is also shown. Densitometric analysis of the experiment shown gave a reduction in the total protein amount of 70% for CD151 and of 40% for CD9 expression. **B.** Flow cytometry analysis of the expression of tetraspanins (anti-CD9 VJ1/20, anti-CD151 LIA1/1, anti-CD81 I.33.2.2) in tetraspanin siRNA-treated HUVEC cells. Negative siRNA treated cells are shown in thin line. Thick line corresponds to the expression in tetraspanin siRNA transfected cells. Negative control PX63 is shown in dotted line. The histograms are depicted in a logarithmic scale. **C.** Quantitative analysis of the mean fluorescence intensity of CD9, CD151 and CD81 in tetraspanin siRNA transfected cells. Data represent the mean of two independent experiments  $\pm$ S.D. as the percentage of the expression referred to that of negative control siRNA transfected cells. **D.** Immunofluorescence analysis of CD9, CD151 expression and localization in HUVEC transfected with siRNA specific for endothelial tetraspanins CD9 and CD151. Images were acquired by confocal microscopy using the same photomultipliers parameters in control and tetraspanin-interfered cells. A maximal projection of the whole confocal image stack is shown. Bar 20 $\mu$ m.

These data further emphasize the importance of tetraspanin microdomains in ICAM-1 and VCAM-1 expression and suggest that their association with tetraspanins occurs early in the biosynthetic processing of these Ig adhesion molecules, or that it is necessary for their proper membrane insertion or retention.

Despite the expression of ICAM-1 and VCAM-1 being lower in tetraspanin-interfered HUVEC cells, no difference was observed in peripheral blood lymphocytes (PBL) adhesion to interfered monolayers when performed under static conditions (Fig 16C). However, when HUVEC cells treated with siRNA oligos were seeded onto transwell insets to perform chemotactic transmigration assays with human PBLs, a strong

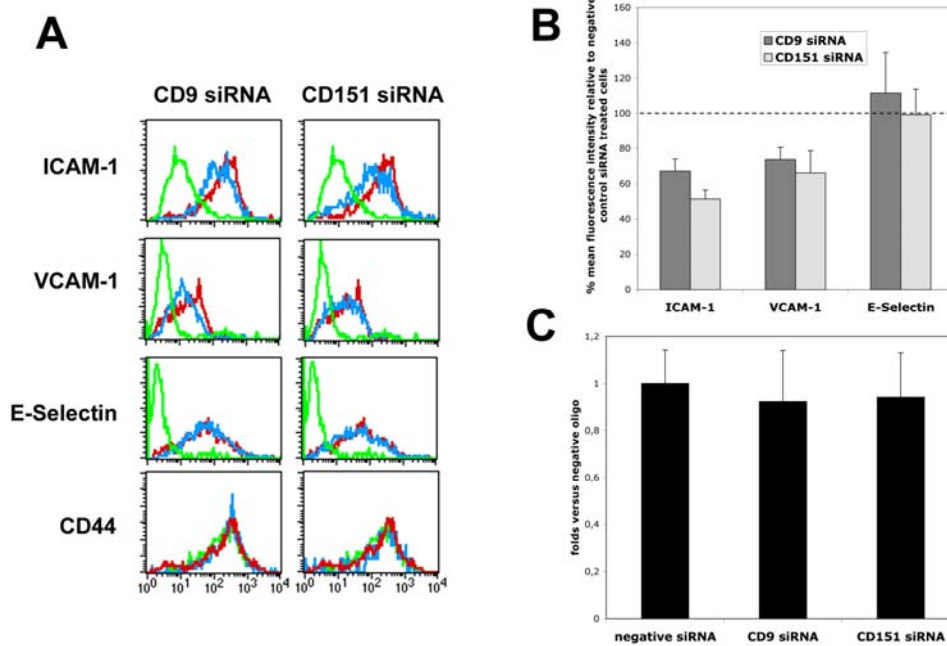


**Figure 16A, B and C: Tetraspanin-interference affects ICAM-1 and VCAM-1 expression and function.** **A.** Flow cytometry analysis of the expression of adhesion molecules ICAM-1 (HU5/3), VCAM-1 (P8B1), E-Selectin (TEA2/1) and CD44 (HP2/9) in tetraspanins siRNA-treated HUVEC. TNF- $\alpha$  activated negative siRNA-treated cells are shown in red line. Blue line corresponds to the expression in TNF- $\alpha$  activated tetraspanin siRNA-transfected cells. Expression of the different adhesion molecules in resting cells is shown in green line. The histograms are depicted in a logarithmic scale. **B.** Quantitative analysis of the mean fluorescence intensity of ICAM-1, VCAM-1 and E-Selectin in TNF- $\alpha$  activated tetraspanin siRNA transfected cells. Data represent the mean of two independent experiments  $\pm$ S.D. as the percentage of the expression referred to that of TNF- $\alpha$  activated negative control siRNA transfected cells. **C.** Analysis of the adhesion of PBLs to tetraspanin interfered cells under static conditions. PBLs were loaded with BCECF-AM fluorescent probe and let to adhere in serum free medium on confluent TNF- $\alpha$  activated HUVEC monolayers for 15 min at 37 $^{\circ}$ C. After washing the percentage of adhesion was quantified in a fluorimeter and depicted as the mean  $\pm$ S.D. respect to the adhesion levels of the negative siRNA transfected cells in three different experiments performed by triplicate.

inhibition of lymphocyte transmigration was observed with both CD9 and CD151 siRNA-treated endothelial monolayers as compared with cells transfected with the negative control oligonucleotide (Fig 16D).

Given that ICAM-1 and VCAM-1 are components of a docking structure whose relevance in leukocyte firm adhesion was unveiled under flow conditions (Barreiro et al., 2002), we assessed the role of tetraspanin microdomains on the strength of lymphocyte adhesion to endothelial cells by measuring their resistance to detachment under increasing shear stress. After 15 min, PBL adhesion to TNF- $\alpha$ -activated HUVEC cells was highly resistant to laminar flow, and most cells still remained attached at 10 dyn/cm<sup>2</sup> (5 folds over physiological shear stress) in control HUVEC monolayers (Fig 16E). In contrast, a great proportion of the PBLs adhered on tetraspanin-interfered monolayers started to detach even at low flow rates (Fig 16E). When extravasation assays using tetraspanin-interfered endothelium were performed under physiological flow conditions, a significant reduction in the number of adherent lymphocytes was also observed (Fig 16F). Furthermore, a tendency to decrease was consistently observed in rolling and transmigration. All these differences might be related to the lower ICAM-1 and VCAM-1 expression levels in tetraspanin interfered cells or, additionally, the insertion of these molecules into tetraspanin-based microdomains might be critical for their proper function under shear stress conditions.

### **Tetraspanin soluble peptides interfere with ICAM-1 and VCAM-1 function without affecting their surface expression**

Tetraspanin associations with other transmembrane proteins occur through their LEL (Stipp et al., 2003a). We thus generated soluble GST-LEL peptides from human

CD9 (Fig 17A) and point mutants to Ala of any of the four Cys residues in the LEL of CD9, which show altered disulphide bond formation and tertiary conformation (Fig 17A).

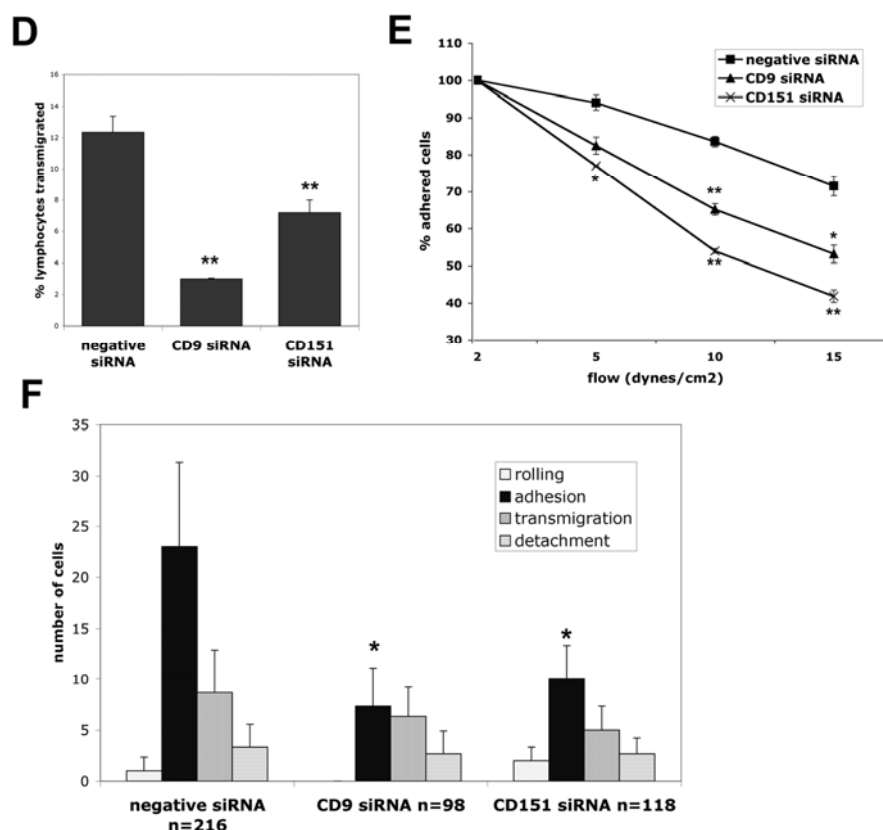


**Figure 16D, E and F: Tetraspanin-interference affects ICAM-1 and VCAM-1 expression and function.**

**D.** siRNA transfected HUVEC monolayers were seeded onto Transwell insets and activated with 20ng/ml of TNF- $\alpha$  for 20h. Then, human peripheral blood lymphocytes were added to the upper compartment and SDF-1 $\alpha$  (100 ng/ml) containing medium to the lower compartment. Cells were allowed to migrate for 2 h and analyzed by flow cytometry. Data represent the mean  $\pm$  S.D. of a representative experiment performed by triplicate. \*\*  $p < 0.005$  in a Student T-test.

**E.** Tetraspanin interference augments PBL detachment under shear stress. The percentage (mean  $\pm$  S.D.) of remaining adherent cells is represented for the different flow rates in 4 fields of a representative experiment. \*  $p < 0.02$ ; \*\*  $p < 0.005$  in a Student T-test.

**F.** Effect of tetraspanin siRNA on lymphocyte adhesion and transmigration under flow conditions. Activated endothelium transfected with specific siRNA oligos for tetraspanins CD9 or CD151 or the negative control oligonucleotide were activated with TNF- $\alpha$ . Thereafter, PBLs were allowed to adhere and transmigrate under physiological flow conditions (1.8 dyn/cm<sup>2</sup>) for 10 min. Quantification of rolling, adhesion, transmigration, and detachment events was performed from minutes 3,5 to min 6,5 of perfusion. Values correspond to the arithmetic mean  $\pm$  S.E.M. of the total number of PBLs interacting with the endothelial monolayer in the 6 different fields analyzed (20x objective) from a representative experiment. The total number of PBLs (n) interacting with the HUVEC monolayer in each condition is depicted in the legend of the X axis. \*  $p < 0.02$  in a Student T-test.

Although some degree of degradation of the soluble peptide occurs, a great proportion of the material eluted from the columns was reactive with CD9 mAb in Western blot under non-reducing conditions (Fig 17A). Incubation of HUVECs with GST-LEL peptides did neither affect the expression levels of ICAM-1 and VCAM-1 induced by TNF- $\alpha$  (Fig 17B), nor cell viability (Fig 17C) or monolayer permeability (Fig

17D). The soluble peptides were added to the preparations at the time of addition of TNF- $\alpha$  so that they were accessible at the earliest time of inducible expression of both adhesion receptors. Thus, these peptides allowed us to interfere with tetraspanin-based microdomains without altering the expression levels of ICAM-1 or VCAM-1 induced by TNF- $\alpha$ .

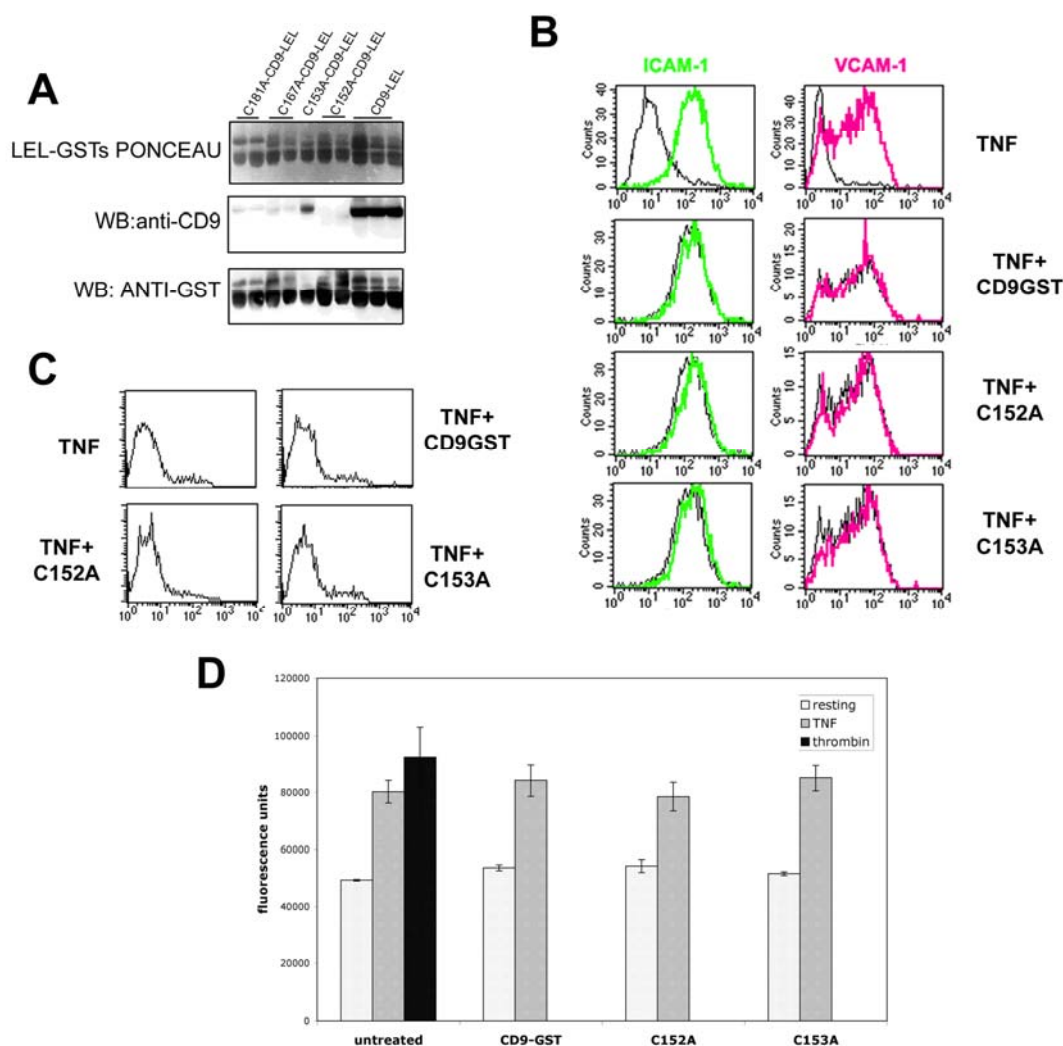


**Figure 17: Characterization of the soluble peptide CD9-LEL-GST and its mutants.** **A.** LEL-GST fusion proteins of human CD9, as well as point mutations to Ala of Cys 152, 153, 167 and 181 were generated, produced in bacterial cultures and isolated by affinity columns of Glutathion-Sepharose. Eluted purified proteins were then analyzed by Ponceau staining and Western blot against CD9 (VJ1/20 mAb) or GST. **B.** Flow cytometry analysis of the expression of ICAM-1 and VCAM-1 in HUVEC cells preincubated with CD9-GST or its point mutants. Thin line in the upper panel corresponds to the expression of resting cells. Thin line on the following panels corresponds to cells treated with TNF- $\alpha$  alone. Thick line corresponds to the expression in cells treated for 20h with TNF- $\alpha$  alone (upper panels) or in combination with the different soluble LEL-GST peptides. **C.** Propidium iodide profiles of cells treated with for 20h with TNF- $\alpha$  alone or in combination with the different soluble LEL-GST peptides. **D.** Paracellular permeability analysis of HUVEC monolayers preincubated with the different soluble LEL-GST peptides. Thrombin was added at 0.1 U/ml at the time of addition of the fluorescent dextran. Data represent the mean  $\pm$ S.D. of a representative experiment performed by duplicate.

Incubation of HUVEC cells with CD9-LEL-GST, but not the mutated forms, significantly inhibited transendothelial migration of lymphocytes (Fig 18A), whereas they did not affect lymphocyte chemotaxis across nude transwells (data not shown). When adhered PBLs were subjected to increasing shear stress, a higher PBL detachment rate was also observed upon treatment of HUVEC cells with CD9-LEL-GST (Fig 18B), but not with the point mutants. In these experiments the number of lymphocytes that transmigrated along the assay was also significantly reduced in those preparations treated with CD9-GST (not shown). All these data demonstrate that tetraspanin microdomains are important not only for proper ICAM-1 and VCAM-1 expression on the plasma membrane but also for their efficient adhesive function under flow conditions.

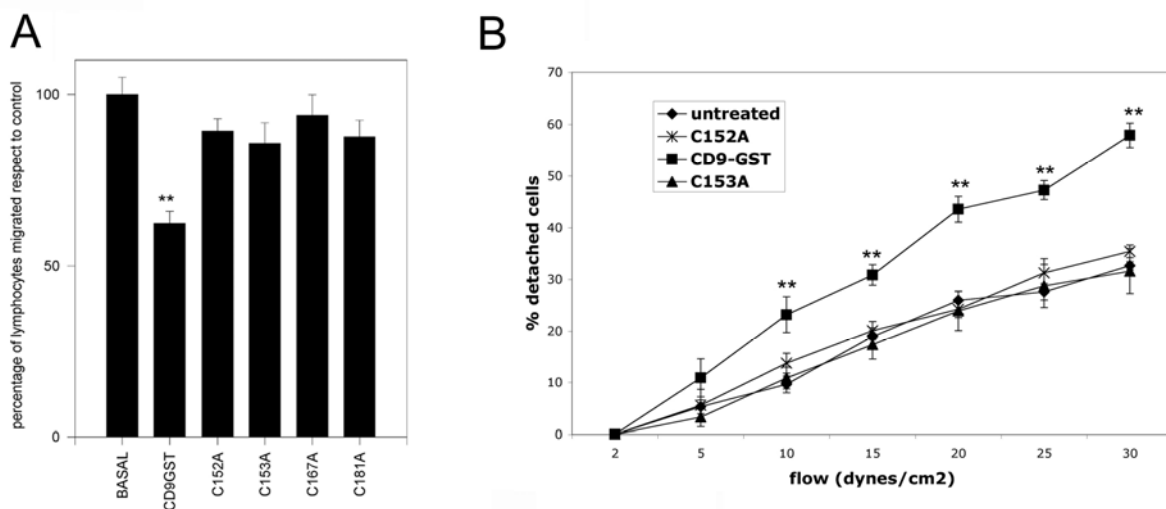


**Figure 18: CD9-LEL-GST inhibits leukocyte transendothelial migration and promotes cell detachment under flow.** **A.** CD9-LEL-GST peptide inhibits transendothelial lymphoid migration in Transwells. HUVEC monolayers were activated with TNF- $\alpha$  alone or in combination with the different LEL-GST peptides. Then, human PBLs were added to the upper compartment and allowed to migrate for 5-7 h. Cell migration was analyzed by flow cytometry and represented as the mean  $\pm$  S.E.M. respect to control untreated monolayers, of four independent experiments performed by duplicate. \*\*  $P < 0.005$  in a t-Student test. **B.** Preincubation with CD9 LEL-GST fusion protein augments detachment under flow conditions. The percentage of detachment of PBLs was analysed in 8-10 fields under increasing flow rates and represented as the mean  $\pm$  S.E.M. \*\*  $p < 0.005$  in a Student T-test.

### **Enhanced ICAM-1 and VCAM-1 adhesive function requires an appropriate tetraspanin environment**

To address the relevance of the repertoire of tetraspanin microdomains in the presentation of ICAM-1 and VCAM-1 adhesion molecules, we used Colo320 colocal carcinoma cells and a CD9 stable transfectant in this cell line. Colo320 cells express similar levels of CD151 and CD81, CD63 and CD82 on the plasma membrane than endothelial cells, without expression of CD9, ICAM-1 or VCAM-1 (Fig 19A). A downregulation of CD81 and CD63 was also observed upon stable transfection of these cells with CD9 (Fig 19A). Then, Colo320 and Colo320-CD9 were transiently transfected with VCAM-1- or ICAM-1- GFP to allow their heterotypic binding to  $\alpha 4$ - or LFA-1- transfected K562 cells. The levels of ICAM-1 and VCAM-1 expression attained by transient transfection varied among the different cell lines and experiments, but only cells with comparable high expression were analyzed in functional assays. This cell system allowed us to assess the adhesion mediated independently by ICAM-1 or VCAM-1 in the presence or the absence of CD9. As shown in Fig. 19B, binding of K562 transfectants to Colo320 cells was selective and completely dependent on the expression of ICAM-1 or VCAM-1, since no significant binding was observed with untransfected K562 cells or to untransfected Colo320 or Colo320CD9 cells (Fig 19B and data not shown). Interestingly, VCAM-1 and ICAM-1-mediated binding was augmented by the presence of CD9 on Colo320 cells (Fig 19B). In the case of ICAM-1/LFA-1 binding, the experiments required the addition of  $Mn^{2+}$  for LFA-1 activation on K562 cells, that resulted in a strong aggregation with Colo320 cells which partially masks the effect of CD9 (Figure 19B).

To further assess the specific contribution of CD9 in the generation of adhesion molecules/tetraspanins microdomains, we assayed the heterotypic binding of K562  $\alpha 4$

transfectants with Colo320 cells that stably express chimeric proteins made up of CD9 and CD82. All chimeric proteins were efficiently expressed at the plasma membrane (Fig 19C, flow cytometry analysis). The first chimera used coded for the N-terminal region of CD9 and the whole LEL and fourth transmembrane region belonged to CD82 (Colo320-CD9x82) and behaved as Colo320 wt cells in regard to VCAM-1 mediated binding (Fig 19C).

To map the functionally relevant region of CD9, we used a second chimera with a chimeric LEL comprising the first half of CD82 LEL and the second half of CD9 LEL, where important residues for association with other transmembrane proteins reside (Colo320-CD82CCG9). This chimeric protein was able to enhance VCAM-1-mediated adhesion, even though not to the same extent that wild-type CD9 (Fig.19C). These data suggest that CD82 is not capable to replace CD9 in the organization of endothelial-like tetraspanin-based domains in Colo320 cells and confirm that the LEL is an important functional region in CD9. Altogether, these data indicate that proper tetraspanin microdomains are necessary for the adhesive function of VCAM-1 and ICAM-1.

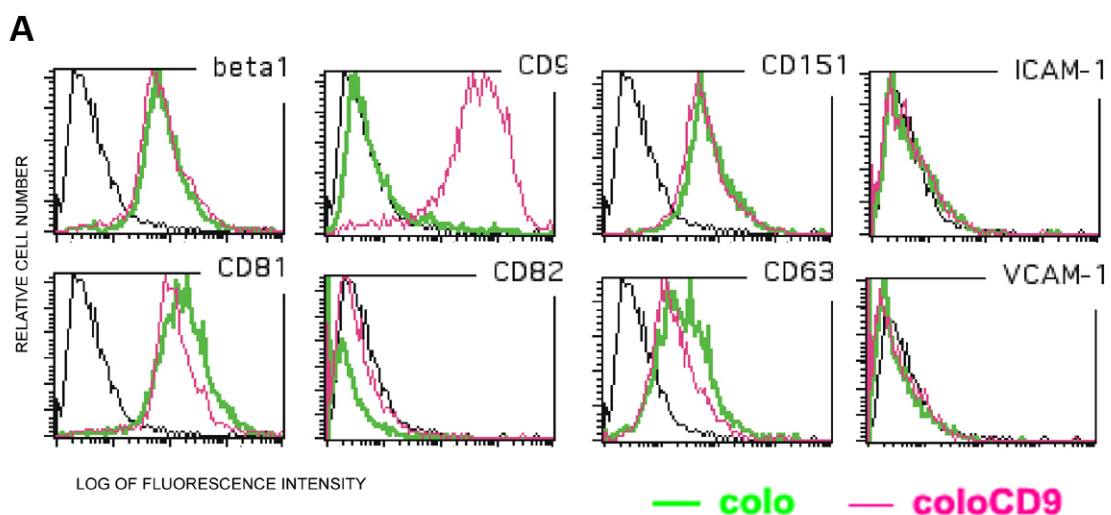


**Figure 19A: Enhanced ICAM-1 and VCAM-1 adhesive function requires an appropriate tetraspanin environment.** A. Flow cytometry analysis of the expression of  $\beta$ 1 integrin (TS2/16 mAb), tetraspanins (anti-CD9 VJ1/20, anti-CD151 LIA1/1, anti-CD81 I.33.2.2, anti-CD82 TS82, anti-CD63 TEA3/18 mAbs), ICAM-1 (HU5/3) and VCAM-1 (P8B1) in Colo320 cells (green line) or CD9-stably transfected Colo320 cell line (pink line). Negative control PX63 is shown in black thin line.

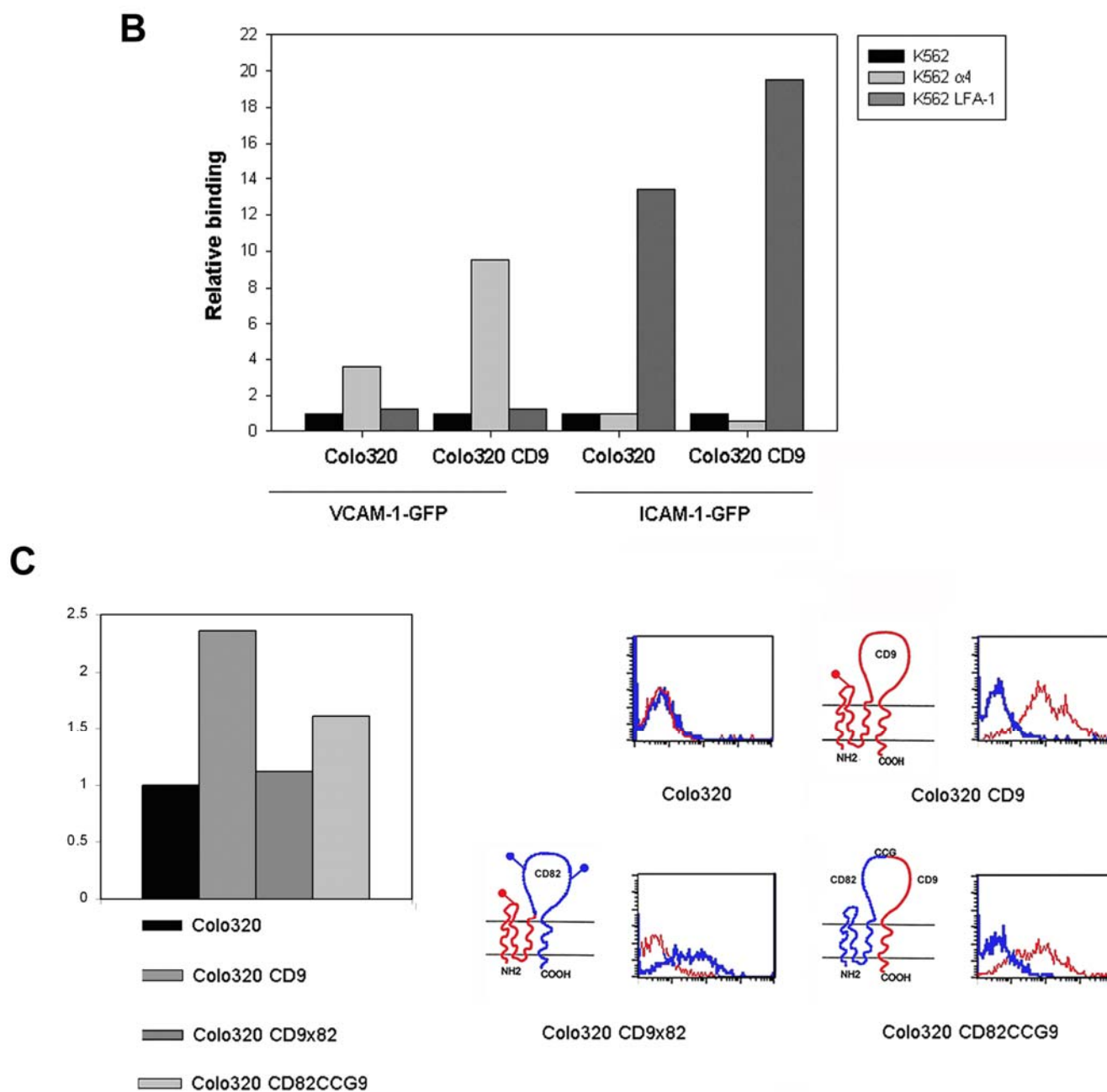


**Figure 19B and C: Enhanced ICAM-1 and VCAM-1 adhesive function requires an appropriate tetraspanin environment.** **B.** Heterotypic intercellular binding of K562 cell lines (parental and K562  $\alpha$ 4 and K562 LFA-1 integrin transfectants) to Colo320 and Colo320CD9 cells transiently transfected with GFP-tagged versions of VCAM-1 and ICAM-1. Data are calculated as the ratio of double positive aggregates (GFP-Colo320/CM-TMR K562) versus the non aggregated GFP<sup>+</sup> cells. Graph depicts the relative binding referred to the aggregation obtained with parental K562 cells (that ranged from 10 to 20% of the total GFP<sup>+</sup> cells in the different transient transfections in the experiment shown). **C.** Heterotypic intercellular binding of K562 $\alpha$ 4 integrin stable transfectant to VCAM-1-GFP transiently transfected Colo320 cells and the different chimeric clones of CD9/CD82. Data are calculated as the ratio of double positive aggregates (GFP-Colo320/CM-TMR K562) versus the total number of GFP<sup>+</sup> cells. Graph depicts relative binding referred to the aggregation of Colo320-VCAM-1-GFP cells (11% of the total GFP<sup>+</sup> cells in the experiment depicted). On the right, flow cytometry analysis of the expression with anti-CD9 (10B1, that also recognizes the chimeric CD9/CD82 loop) (red line) and CD82 (TS82) (blue line) of the different chimeric clones is shown.

---

**Endothelial ICAM-1 and VCAM-1 cluster at the docking structure independently of counterreceptor engagement and actin anchorage**

At contacts with adherent leukocytes, activated endothelial cells form three-dimensional actin-based docking structures which cluster endothelial VCAM-1 and ICAM-1. To analyze the mechanisms regulating the dynamic recruitment of adhesion molecules to these endothelial docking structures, we induced their formation with K562 leukocytes stably expressing either  $\alpha 4\beta 1$  (K562  $\alpha 4$ ) or  $\alpha L\beta 2$  (K562 LFA-1) integrins, which adhere to activated endothelial cells exclusively via VCAM-1 or ICAM-1, respectively. Remarkably, both ICAM-1 and VCAM-1 clustered at the docking structure formed around both types of K562 transfectant cells, regardless of whether they were directly engaged by their corresponding integrin receptor (Fig. 20A). Furthermore, similar co-recruitment effects were observed in a more physiological setting, in which lymphoblasts, which express significant amounts of LFA-1 and VLA-4, were treated with specific inhibitors of either LFA-1 (BIRT377) or VLA-4 (BIO5192) (Fig. 20B).

To assess the extent to which this ligand-independent adhesion molecule clustering is dependent on the actin cytoskeleton, we transiently transfected resting HUVEC with a cytoplasmic tail-truncated mutant of VCAM-1 (VCAM $\Delta$ Cyt). Under these conditions, HUVEC bear low levels of ICAM-1 and negligible levels of endogenous VCAM-1. Upon engagement of VCAM $\Delta$ Cyt by either K562  $\alpha 4$  cells or anti-VCAM-1 coated beads, discrete clusters containing VCAM $\Delta$ Cyt and ICAM-1 were observed around adhered cells, but in no case was a well developed three-dimensional structure formed (Fig. 20C and data not shown).

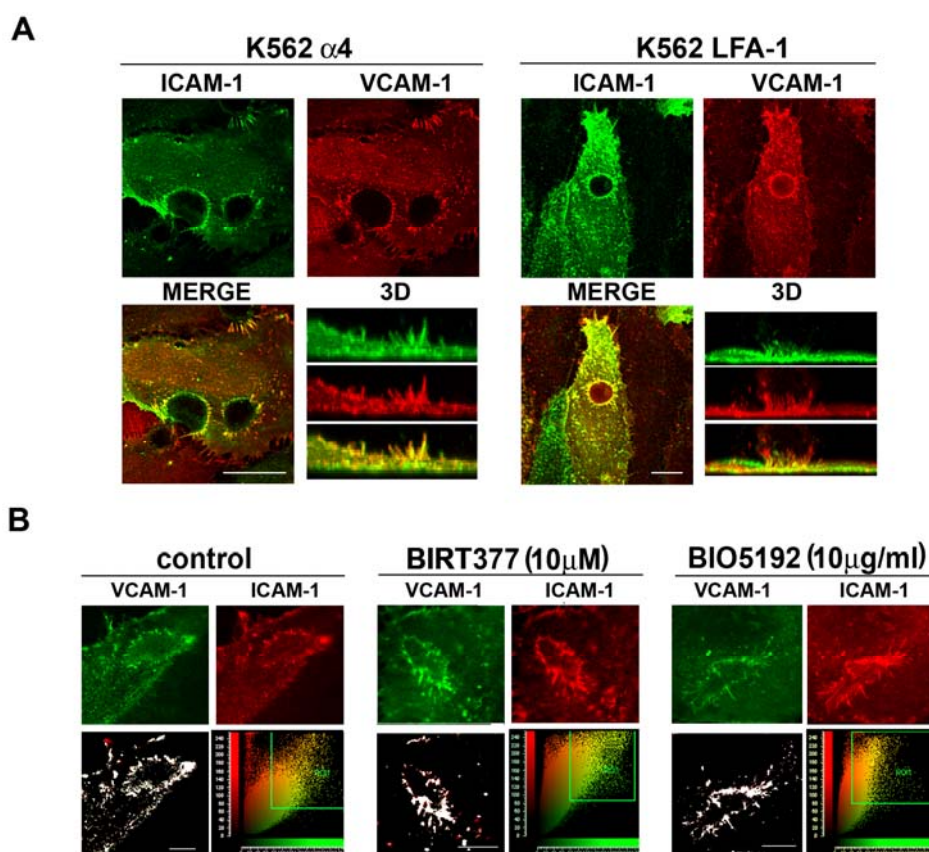


**Figure 20A and B: VCAM-1 and ICAM-1 are co-presented at lymphocyte-endothelium contact independently of ligand binding and actin anchorage.**

**A.** VCAM-1 and ICAM-1 co-localize at the endothelial docking structure in the absence of integrin engagement. K562 transfected with  $\alpha 4$  or LFA-1 integrin were allowed to adhere to TNF- $\alpha$ -activated HUVEC for 30 min, and cells were fixed and double stained with anti-VCAM-1 (P8B1) and biotin-conjugated anti-ICAM-1 (MEM111). Confocal stacks were obtained and orthogonal maximal projections and vertical 3D reconstructions of the whole series are displayed. Scale bars = 20  $\mu$ m. **B.** VCAM-1 and ICAM-1 are co-recruited to the endothelial contact area with human T lymphoblasts previously treated to inactivate VLA-4 or LFA-1. Human T lymphoblasts were pre-treated for 5 minutes with the LFA-1 inhibitor BIRT377 (10 $\mu$ M) or the VLA-4 inhibitor BIO5192 (10 $\mu$ g/ml) and then added to a TNF- $\alpha$  activated HUVEC monolayer for 5 min. Cells were fixed and double stained for VCAM-1 and ICAM-1 as in 1A. Confocal stacks were obtained and a representative section from each treatment is shown together with its corresponding colocalization histogram and a mask showing the distribution within the cell of double green-red pixels from the region marked on the histogram. Scale bars = 10  $\mu$ m.

In contrast, when ICAM-1 was directly engaged by K562  $\alpha L\beta 2$  transfectants, a proper docking structure was formed, also containing VCAM $\Delta$ Cyt (Fig. 20C). These data indicate that the engagement of one endothelial adhesion receptor (ICAM-1 or VCAM-1) by its corresponding leukocyte integrin is sufficient to induce the co-recruitment of the other endothelial receptor towards the contact area with the leukocyte. This co-clustering must involve the extracellular and/or transmembrane

domains of both adhesion molecules, because it occurs with cytoplasmic-truncated forms. However, the subsequent reorganization of the endothelial actin cytoskeleton into the protrusive cup depends on actin anchorage of the cytoplasmic tail of the endothelial adhesion molecule bound to its ligand, as indicated by quantitative analysis of the formation of VCAM-1-mediated docking structures in VCAM-1wt- vs. VCAM-1 $\Delta$ Cyt-transfected resting HUVEC (50.33% vs. 6%, respectively).

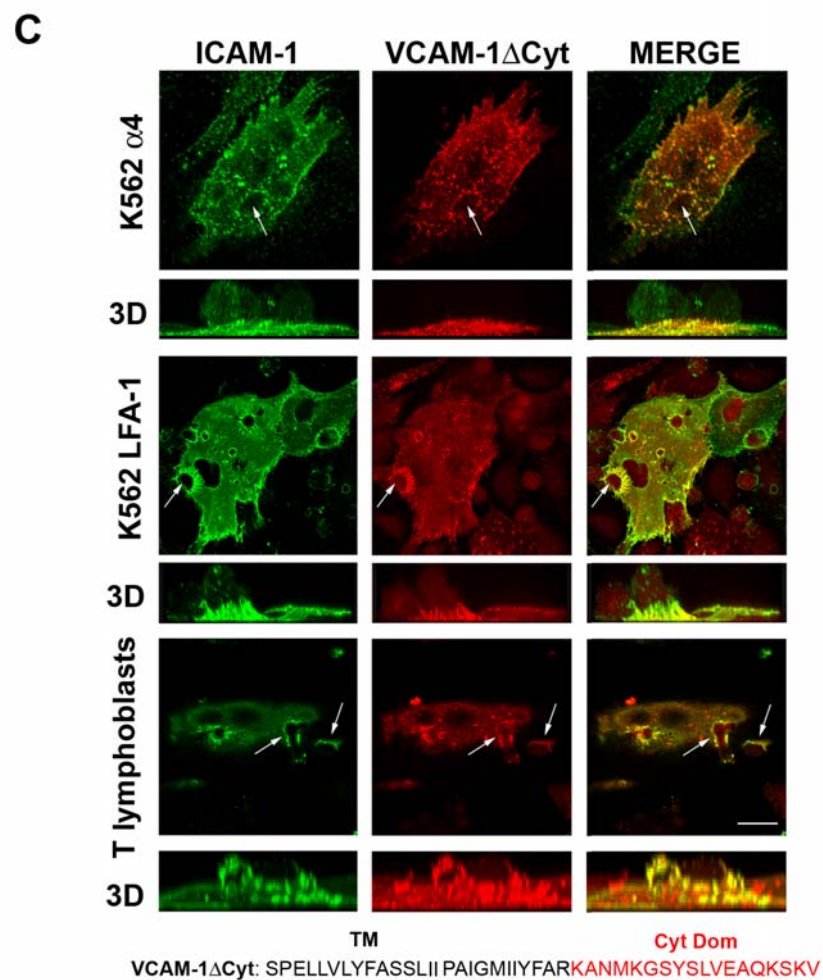


**Figure 20C: VCAM-1 and ICAM-1 are co-presented at lymphocyte-endothelium contact independently of ligand binding and actin anchorage.**

**C.** VCAM $\Delta$ Cyt is co-recruited to ICAM-1-mediated docking structures but is unable to trigger the formation of VCAM-1-mediated docking structures. Resting HUVEC were transfected with the VCAM $\Delta$ Cyt construct and incubated either with K562 leukocytes expressing VLA-4 (K562  $\alpha$ 4) or LFA-1 integrin or with T-lymphoblasts. Cells were then fixed and double stained with anti-VCAM-1 (VCAM $\Delta$ Cyt being the only VCAM-1 molecular species detected) and biotin-conjugated anti-ICAM-1. Confocal stacks were obtained and a representative section or vertical reconstructions of the whole series are displayed. Arrows point to the position of the adhered leukocytes. Scale bars = 20  $\mu$ m.

---

## **Analysis of ICAM-1 and VCAM-1 hetero- and homo-dimers in living endothelial cells**

Since cytoskeletal anchorage cannot account for adhesion receptor co-recruitment, we investigated the potential formation of VCAM-1/ICAM-1 heterodimers at the apical membrane of intact, living primary endothelial cells. This analysis was based on hetero-FRET, assessed by the donor fluorescence lifetime quenching in TCSPC-FLIM measurements. We generated functional VCAM-1 and ICAM-1 chimaeras fused to monomeric enhanced green (mEGFP, donor, termed also green) or red (mRFP1, acceptor, termed also red) fluorescent proteins (Campbell et al., 2002; Zacharias et al., 2002). The spontaneous dimerization of EGFP, which could interfere with “*bona fide*” protein-protein interactions, was avoided by introducing the A206K point mutation in the sequence. The constructs were transiently co-transfected into primary HUVEC under resting conditions, to prevent up-regulation of endogenous VCAM-1 and ICAM-1 expression and thus minimize possible interference that might decrease the efficiency of dimer formation by exogenous molecules. We analyzed the percentage of FRET efficiency (FRET<sub>eff</sub>) of the following pairs: ICAM-1mEGFP/ICAM-1mRFP1, VCAM-1mEGFP/VCAM-1mRFP1, ICAM-1mEGFP/VCAM-1mRFP1 and VCAM-1mEGFP/ICAM-1mRFP1, comparing the fluorescence lifetime of the donor (mEGFP construct) in each co-transfection with that of ICAM-1mEGFP or VCAM-1mEGFP in single transfections. Representative experiments are shown in Fig. 21 and Supplemental Figure 1 (for donor standards). For each donor/acceptor pair in Figure 21, the fluorescence intensity image (in pseudocolour scale), phasor plots and the corresponding FLIM images (pink mask) are shown. As previously described (Caiolfa et al., 2007) for this representation, the fluorescence decay of the donor molecule in each pixel of the image gives a point in the phasor plot.

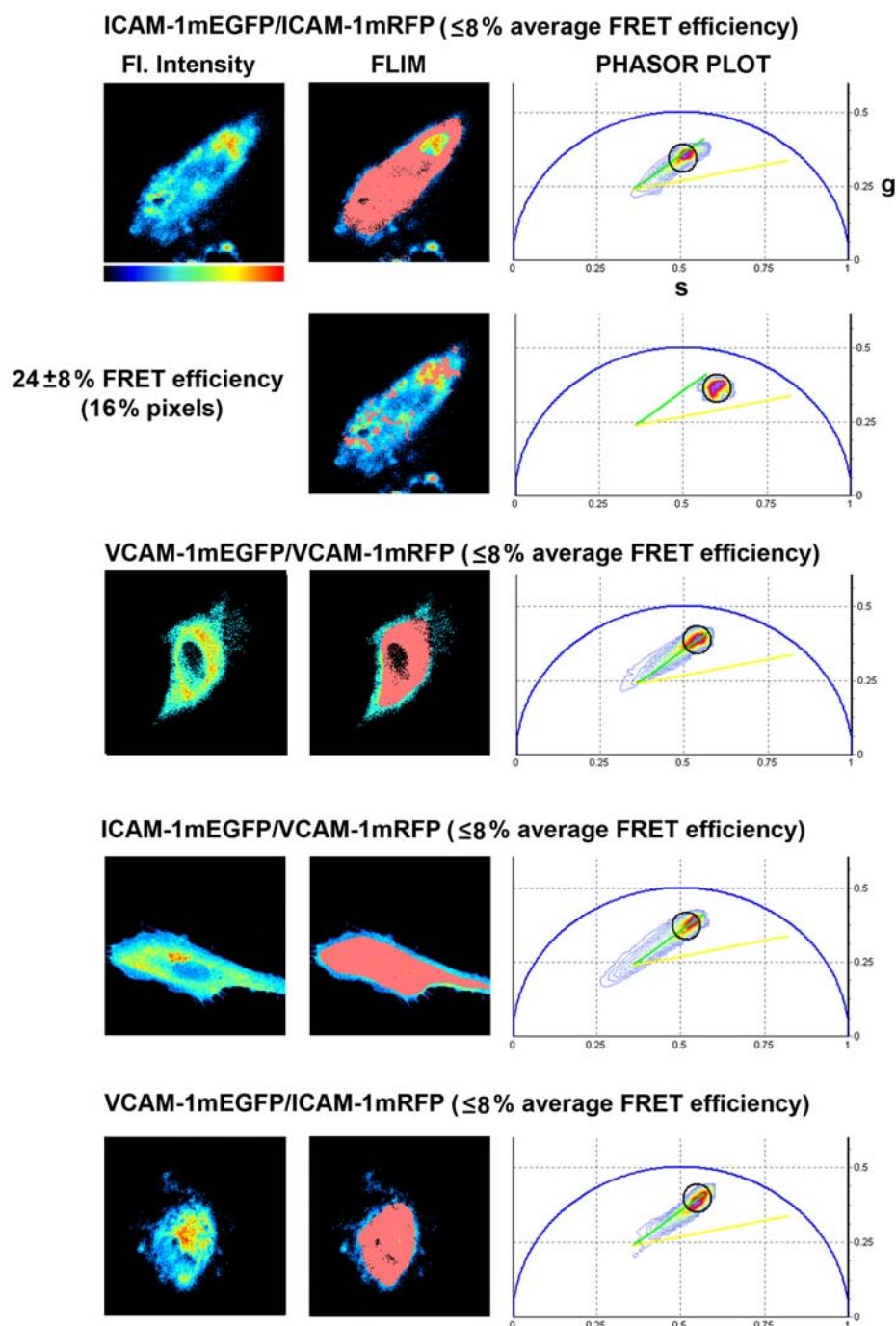


**Figure 21: VCAM-1 and ICAM-1 are not displayed as heterodimers at the plasma membrane.** Endothelial cells were co-transfected with different mEGFP-mRFP1 pairs (ICAM-1/ICAM-1, VCAM-1/VCAM-1, ICAM-1/VCAM-1 and VCAM-1/ICAM-1). FLIM-FRET analysis was performed using the phasor-FLIM analysis as explained in Material and Methods. For each pair of proteins, a representative analysis of a co-transfected cell is shown. The fluorescence intensity images of the scanned sections are in pseudocolour scale (left panels) and correspondent mEGFP lifetime distributions are shown in contour plots after the phasor transformation (phasor plots, right panels). In each phasor plot, the experimentally derived green-line represents the mean phasor distribution for unquenched mEGFP fluorescence lifetimes with different contribution of cell autofluorescence (see Suppl. Fig. 1). The yellow line marks the computed trajectory of mEGFP donors quenched by 50% FRET (Föster distance) and at different contribution of autofluorescence (Caiolfa et al., 2007). In the ICAM-1/ICAM-1 cell, two major phasor distributions are observed and selected in the phasor plot (black circles). The first one includes the majority, more than 80%, of the pixels in the image. In these pixels, which are rather homogeneously distributed at the cell membrane (their localization is shown in the FLIM image, pink mask), FRET is negligible ( $\leq 8\%$ ). The second distribution includes only 16% of pixels in which FRET varies from 16 to 32% (mean 24%), and localize few clusters on the cell membrane. The other protein pairs do not show significant quenching due to FRET, as their phasor distributions are not distinguishable from that of the correspondent pure donor cells (Suppl. Fig. 1). In each of these examples, more than 95% of pixels are selected (black circles) in the non-FRET area of the phasor plot and are localized in the correspondent FLIM image.

The ensemble of these donor phasors is represented as contour plot. This plot can be scanned by software (Digman et al., submitted) for localizing in the image pixels at high as well as low FRETeff. The black circle in the phasor plot selects a sub-population of pixels in which similar FRET efficiencies were observed, and highlights them in the correspondent image. For the ICAM-1-mEGFP/ICAM-1-mRFP1 pair depicted in Fig. 21, the majority of pixels do not show significant FRET (selection average  $\leq 8\%$  FRET). However, a small 16% of the pixels in the image, do show FRET efficiency in the range of  $24 \pm 8\%$  (fairly above the detection limit of the FRET analysis), which are localized in clusters at the membrane. We analyzed 4 replicate experiments and obtained average FRET efficiencies in the range from 5 to 15.5 in 65% of clustered pixels. In contrast, the other pairs of proteins, VCAM-1-mEGFP/VCAM-1-mRFP1, ICAM-1-mEGFP/VCAM-1-mRFP1 and VCAM-1-mEGFP/ICAM-1-mRFP1, did not show any significant quenching of the donor fluorescence lifetime (i.e., FRET) (Fig. 21), as compared to the phasor distribution of “pure” donor control cells (Suppl. Fig. 1). This analysis demonstrates that, under these conditions, VCAM-1/VCAM-1 homodimers and VCAM-1/ICAM-1 heterodimers are absent from the plasma membrane. These data thus suggest a separate organization of VCAM-1 and ICAM-1 at the plasma membrane, excluding the formation of VCAM-1/ICAM-1 heterodimers as a prerequisite for the recruitment of one of these receptors to the docking structure in the absence of integrin engagement and cytoskeleton anchorage.

### **Tetraspanin microdomains mediate the association of endothelial adhesion receptors to form specialized endothelial adhesive platforms**

Since ICAM-1 and VCAM-1 co-clustering at the docking structure is dependent on their extracellular and/or transmembrane domains, but does not result from direct

interaction, we examined the possible intermediary involvement of tetraspanin proteins. Several tetraspanins, such as CD9 and CD151, are concentrated at docking structures around primary human leukocytes together with VCAM-1 and ICAM-1, and can co-precipitate with these endothelial adhesion receptors (Barreiro et al., 2005). Tetraspanin proteins were also recruited to docking sites in the K562  $\alpha 4$  and LFA-1 adhesion models (Figure 22A). However, no specific tetraspanin ligand has been described in leukocytes.

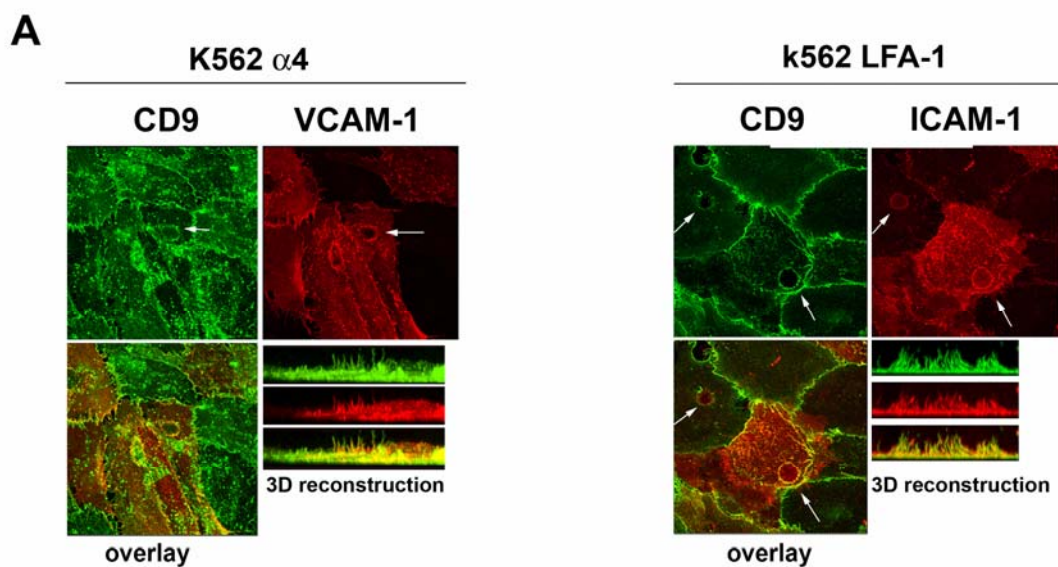


**Figure 22A: Tetraspanins are localized at docking structures mediated by the engagement of ICAM-1 or VCAM-1.** LFA-1<sup>+</sup> or  $\alpha 4$ <sup>+</sup> K562 cells were allowed to adhere to a TNF- $\alpha$ -activated endothelial monolayer for 30 min. *Left panels:* Cells were fixed and double stained for VCAM-1 (P8B1, red) and CD9 (biotinylated VJ1/20, green). *Right panels:* Cells were stained for CD9 (VJ1/20, green) and ICAM-1 (biotinylated MEM-111, red). Confocal stacks were obtained and orthogonal maximal projections and vertical 3D reconstructions of the whole series are displayed. White arrows point to endothelium-leukocyte contact areas (docking structures).

Furthermore, ICAM-1 and VCAM-1 were both recruited when either CD9 or CD151 was engaged with specific antibodies coupled to magnetic beads. In parallel, anti-VCAM-1- and anti-ICAM-1-coated beads were also able to cluster each other and the tetraspanins, whereas anti-VE-cadherin-coated beads did not induce significant recruitment of ICAM-1, VCAM-1 or tetraspanins above basal levels (Fig. 22B, quantified in Fig. 22C, and data not shown).

To assess the relationship between endothelial adhesion molecules and tetraspanin microdomains in more detail, Brij96 lysates of TNF- $\alpha$ -activated HUVEC were fractionated on a continuous 5-40% sucrose gradient. Most tetraspanins were soluble under these conditions and migrated with the heavy fractions (F1-F7) together with ICAM-1 and VCAM-1, which were not found in fractions containing caveolin (used as a marker of detergent-resistant membrane fractions, containing lipid rafts) (Fig. 22D). These results suggest that endothelial tetraspanin microdomains, containing VCAM-1 and ICAM-1 adhesion receptors, clearly stand apart from classical biochemically-defined lipid rafts and are in fact distinct organized membrane structures, which we term endothelial adhesive platforms (EAP).

#### **Diffusional properties of endothelial adhesive platforms at nude membrane and at docking structures**

Experimental evidence for the existence of tetraspanin microdomains is mainly based on biochemical approaches or microscopy techniques that analyze fixed cells (Claas et al., 2001; Min et al., 2006; Nydegger et al., 2006). In an attempt to demonstrate the existence of tetraspanin-based EAP in living cells, as physical entities with specific molecular dynamic features distinct from lipid rafts, we made use of the fluorescence recovery after photobleaching (FRAP) technique. First, we analyzed the dynamic behaviors of EGFP-tagged versions of CD9, CD151, VCAM-1 and ICAM-1 at the apical plasma membrane of primary HUVEC and compared these behaviors with that of GPI-EGFP, used as a lipid raft marker (Kenworthy et al., 2004; Sharma et al., 2004) (Fig. 22E).

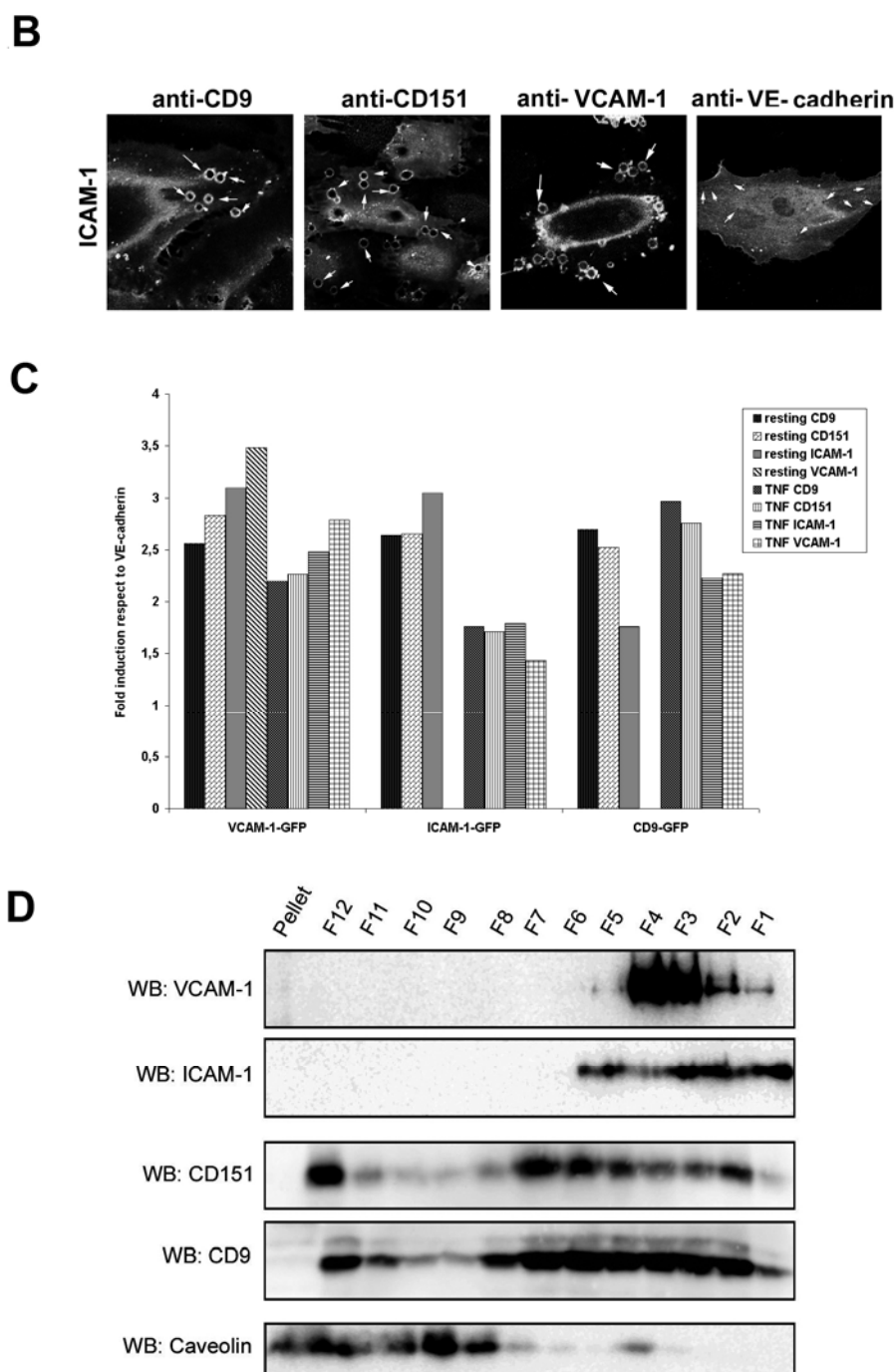


**Figure 22B, C and D: Dynamic behaviour of EAP components at the “nude” plasma membrane.**

**B.** Anti-tetraspanin-coated beads recruit both VCAM-1 and ICAM-1. TNF- $\alpha$ -activated HUVEC were incubated with magnetic beads coated with anti-CD9, anti-CD151, anti-VCAM-1 or anti-VE-cadherin for 30 min and then, stained with biotinylated anti-ICAM-1 mAb. Representative confocal sections are shown. Arrows point to the position of the attached beads. **C.** Quantification of ICAM-1-, VCAM-1- or CD9-EGFP clustering around beads coated with the indicated antibodies and attached to transfected resting or TNF- $\alpha$ -activated HUVEC. Data are the means  $\pm$  S.D. of two independent experiments. **D.** ICAM-1 and VCAM-1 are recovered together with tetraspanins in the heavy fractions of a continuous sucrose gradient. TNF- $\alpha$ -activated HUVEC were lysed in 1% Brij96 and lysates were loaded onto a continuous 5-40% sucrose gradient. After ultracentrifugation, samples were recovered in 1 ml fractions and analyzed by Western blot for VCAM-1, ICAM-1, CD151, CD9, or caveolin. Fractions were recovered from the bottom of the gradient, so that the soluble non-floating fractions were collected first.

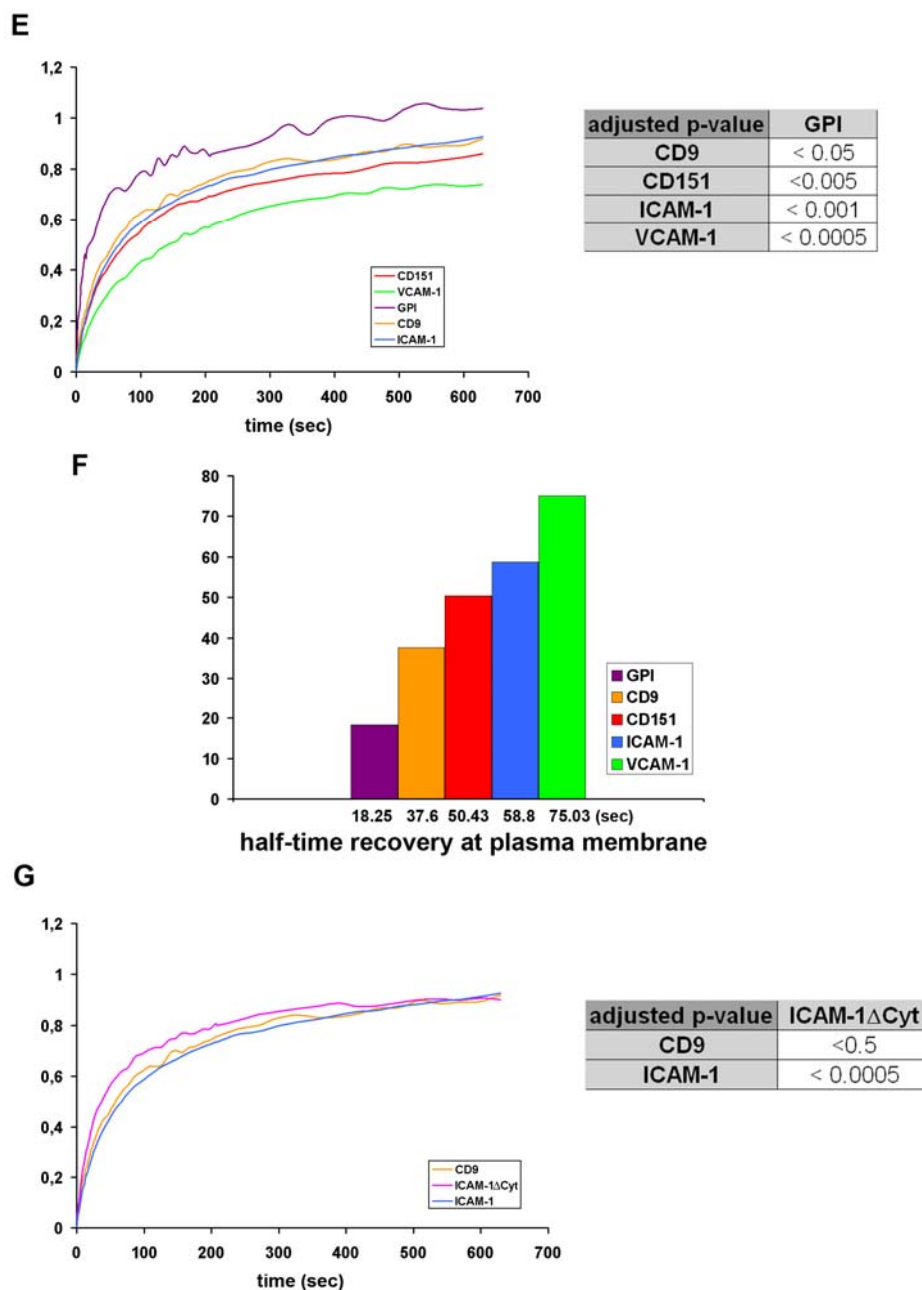


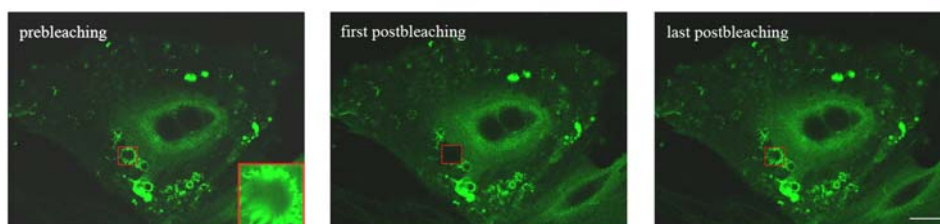
**Figure 22E, F and G: Dynamic behaviour of EAP components at the “nude” plasma membrane.**

**E.** FRAP analysis showing differences in the diffusion of tetraspanins and adhesion receptors compared with the lipid raft marker GPI at the plasma membrane. Endothelial cells were transiently transfected with the indicated EGFP-tagged protein constructs and activated with TNF- $\alpha$  20h before microscopy observation. Mean fluorescence recovery curves for CD9-, CD151-, ICAM-1-, VCAM-1- and GPI-EGFP were calculated (n ranged from 5 to 21 independent experiments for each protein) and are depicted together on the same graphic. Statistical significance was assessed by a point-to-point comparison based on a Student's t-test. p values were adjusted for multiple testing by using the Benjamini and Hochberg method to control for false discovery rate (fdr). Tests were considered to be significant when adjusted p values from 80% of the points out of the plateau were < 0.05. This ensures that the expected fdr is < 5%. (See Suppl. Fig. 2) **F.** Comparison of mobility parameters among tetraspanins, adhesion receptors and GPI-anchored protein at the endothelial plasma membrane. The average half-time recovery rate was calculated considering the mean mobility fraction for each protein. **G.** The retarded mobility of adhesion receptors compared with tetraspanins can be explained by their differential engagement to the actin cytoskeleton. Mean fluorescence recovery curves of ICAM-1 $\Delta$ Cyt-, ICAM-1- and CD9-EGFP were calculated (n ranged from 12 to 21) and are compared on the same graph. Deletion of the ICAM-1 cytoplasmic tail significantly increased recovery rate compared with wild-type protein. Statistical analysis was performed as in D.

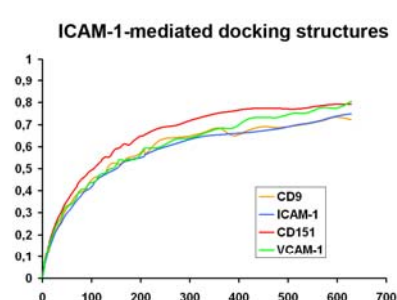
Quantification of recovery half-time data indicated that tetraspanin CD9 and CD151 diffuse 2-3 times more slowly than GPI-EGFP, and that VCAM-1 and ICAM-1 are even slower (3-4 times longer recovery half-time as compared with GPI-EGFP) (Fig. 22F). The differences observed between the diffusional behaviors of tetraspanin proteins and endothelial adhesion receptors might be due to differential anchorage to the actin cytoskeleton. To examine this possibility, we analyzed the dynamics of a C-terminally truncated EGFP-tagged ICAM-1 protein, ICAM-1 $\Delta$ Cyt-EGFP, which lacks the cytoplasmic domain and, therefore, lacks actin-cytoskeleton linking activity (Fig. 22G). This truncated ICAM-1, freed of cytoskeletal constraints, diffused more rapidly than the full-length receptor. Furthermore, ICAM-1 $\Delta$ Cyt-EGFP diffused faster than CD9, but in this case the difference was not significant, strengthening the notion of EAP as organized lateral-association domains at the plasma membrane.

To assess the influence of leukocyte adhesion on the dynamic behaviour of each EAP component, FRAP was used to examine endothelial docking structures induced by binding of  $\alpha$ 4<sup>+</sup>- or LFA-1<sup>+</sup>-K562 cells (Fig. 23A). The most notable effects were that, when endothelial adhesion receptors were dynamically and specifically bound to their ligands, a greater proportion were included in the immobile fraction and the mobility of the mobile fraction was retarded (Fig. 23B and C, for ICAM-1 and VCAM-1). The rest of EAP components analyzed were affected to a lesser extent, exhibiting a variable slow-down in fluorescence recovery compared with the FRAP analyses of the same molecules at other regions of the plasma membrane (Fig. 24). Statistical analyses showed that the effect on CD9 mobility was greater upon engagement of ICAM-1,

A

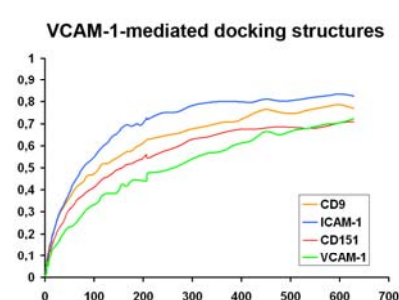


B



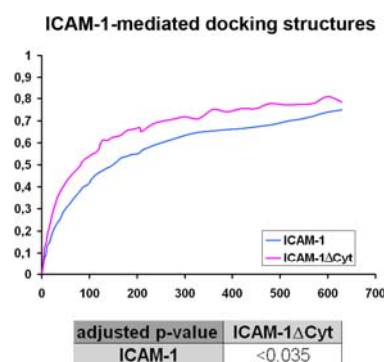
adjusted p-value	ICAM-1
CD9	<0.996
CD151	<0.05
VCAM-1	<0.9

C



adjusted p-value	VCAM-1
CD9	<0.003
CD151	<0.2
ICAM-1	<0.03

D



adjusted p-value	ICAM-1ΔCyt
ICAM-1	<0.035

**Figure 23: Dynamic behavior of endothelial adhesive platform components within the endothelial docking structure.**

**A.** Representative FRAP analysis of an endothelial docking structure. The prebleaching image shows a TNF- $\alpha$ -activated endothelial cell transiently transfected with ICAM-1-EGFP; docking structures formed around attached K562 LFA-1 cells are visible as circles of concentrated EGFP fluorescence. The docking structure in the boxed area, shown at high magnification in the inset, was selected for photobleaching measurements show the fluorescence recovery at the structure over time. Scale bar = 20  $\mu$ m. **B.** CD9 mobility is tightly regulated in ICAM-1-mediated docking structures. Mean fluorescence recovery curves are shown for ICAM-1-, VCAM-1-, CD9- and CD151-EGFP at docking structures formed around K562 cells expressing LFA-1 (activated by 1 mM  $Mn^{2+}$ , which does not affect endothelial molecule mobility); n ranged from 4 to 16 experiments for each transfected protein. Statistical analysis was based on p value adjusted for multiple testing (see Methods and Fig. 3D for details). **C.** CD151 and VCAM-1 mobilities are correlated at VCAM-1-mediated docking structures. Mean fluorescence recovery curves are shown for ICAM-1, VCAM-1-, CD9- and CD151-EGFP at docking structures formed around K562 cells expressing VLA-4 (K562  $\alpha$ 4); n ranged from 5 to 16 experiments for each protein. Statistical analysis was performed as in B. **D.** Actin-cytoskeleton anchorage stabilizes the interaction of ICAM-1 with its ligand LFA-1. Mean fluorescence recovery curves are shown for ICAM-1 $\Delta$ Cyt- and ICAM-1-EGFP at ICAM-1-mediated docking structures (n=7 for both proteins). Statistical analysis was performed as in B.

while CD151 was more affected by engagement of VCAM-1 (Numerical data on Fig. 23B and C). These data thus reveal a degree of specificity among tetraspanin-partner interactions within the endothelial tetraspanin microdomains. In contrast, GPI-EGFP diffusion was not altered at docking structures (data not shown).

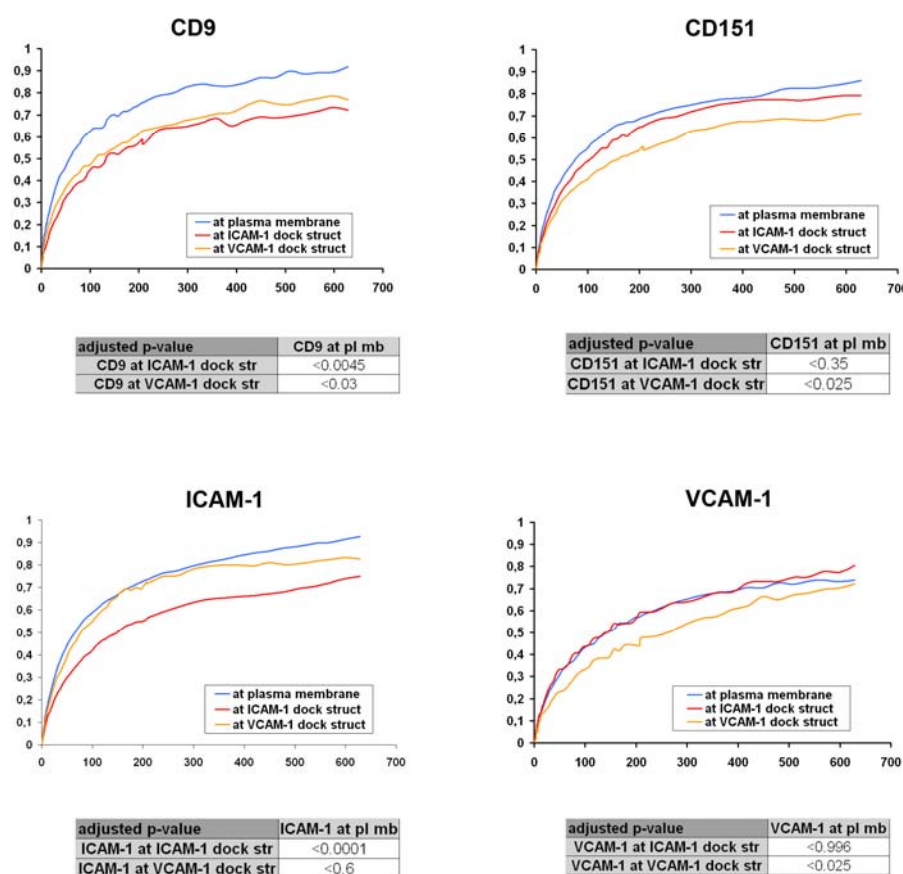


**Figure 24: Comparison of dynamic behaviors of each EAP constituent at nude plasma membrane and at ICAM-1- and VCAM-1-mediated docking structures.** The graphs show the mean fluorescence recovery curves at nude plasma membrane and at ICAM-1 and VCAM-1-mediated docking structures for each EAP component studied: CD9-, CD151-, VCAM-1- or ICAM-1-EGFP. Statistical analysis was performed as indicated in previous figures.

The tailless ICAM-1 mutant IC1 $\Delta$ Cyt-EGFP showed a faster fluorescence recovery rate than the wild-type molecule at docking sites with LFA-1<sup>+</sup>-K562 cells, which indicates that stabilization of the interaction between ICAM-1 and LFA-1 also

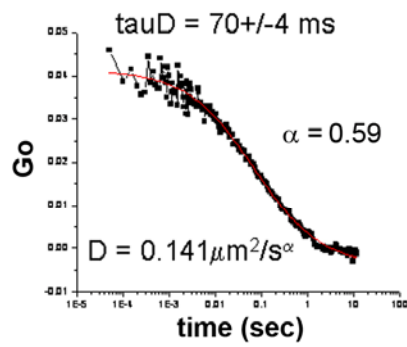
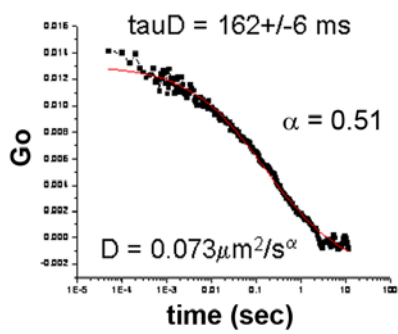
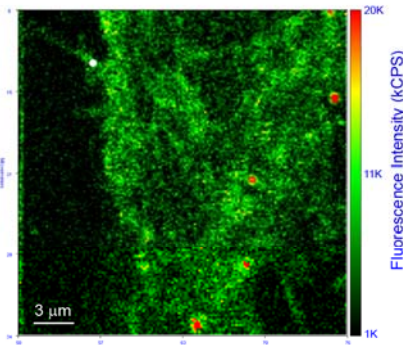
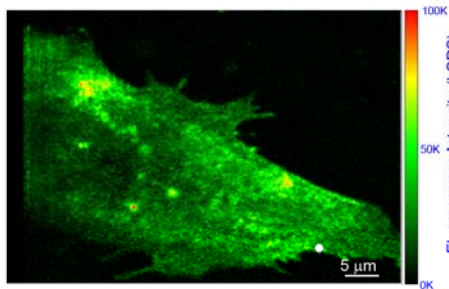
occurs on the endothelial side, by the anchorage of ICAM-1 to the F-actin cytoskeleton (Fig. 23D).

### **Diffusional characteristics of individual endothelial adhesive platform constituents determined by FCS and FCCS single-molecule measurements**

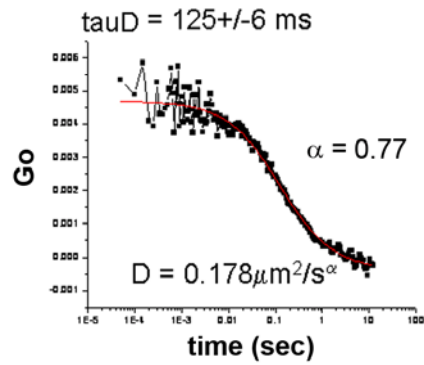
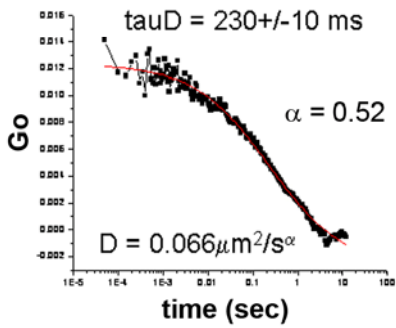
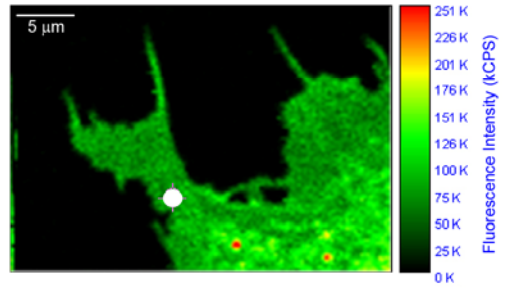
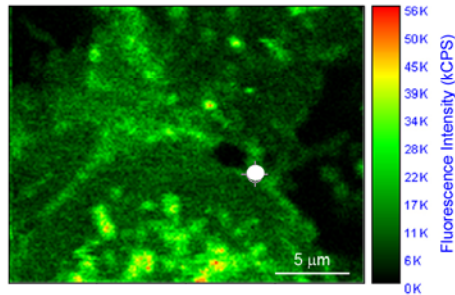
Because of technical limitations of FRAP, we could not accurately measure the diffusion coefficients of EAP components, which exhibit an anomalous diffusion because of cytoskeleton and ligand binding constraints. To overcome this limitation, we applied fluorescence correlation spectroscopy (FCS) on fluorescent protein-tagged ICAM-1, VCAM-1, CD9 and CD151 expressed in primary human living endothelial cells (Fig. 25A). The autocorrelation functions were always best-fitted using the anomalous diffusion model (see Materials and Methods section). The range of the diffusion ( $D$ ) and anomaly ( $\alpha$ ) coefficients was similar for all tested proteins (Fig. 25B). Nevertheless, the analysis in Fig. 5B indicates that, the diffusion of VCAM-1 and ICAM-1 is overall slower than that of CD9 and CD151. Hence, the FCS measurements of each individual EAP component was in agreement with previous FRAP analyses, indicating that tetraspanins are characterized by faster lateral mobility than adhesion receptors. Further analyses will be performed to sub-classify the results as corresponding to fast and slow molecular subsets. On the other hand, most of the  $D$  coefficients obtained for all these proteins are much slower than those reported for prototypic lipid raft proteins (Lenne et al., 2006). Finally, evidence of dynamic membrane complexes containing several EAP constituents was attained by fluorescence cross-correlation spectroscopy, as shown in Fig. 26.

A

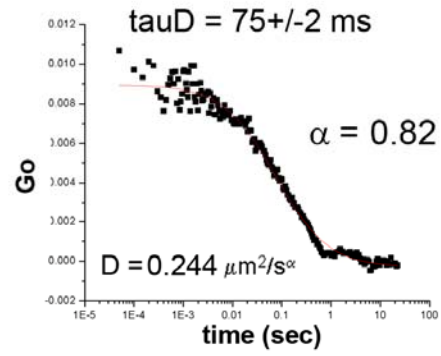
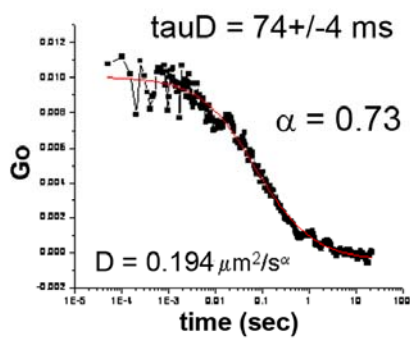
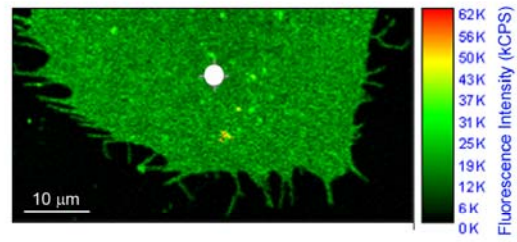
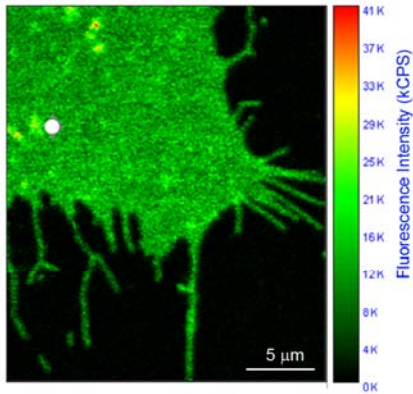
ICAM-1mEGFP



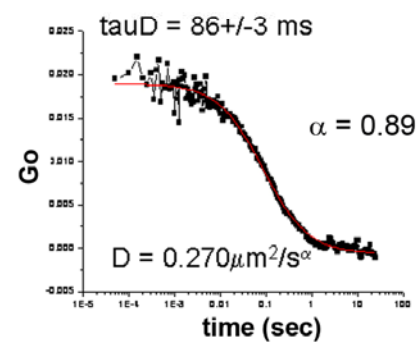
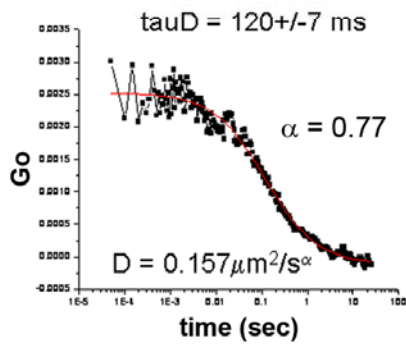
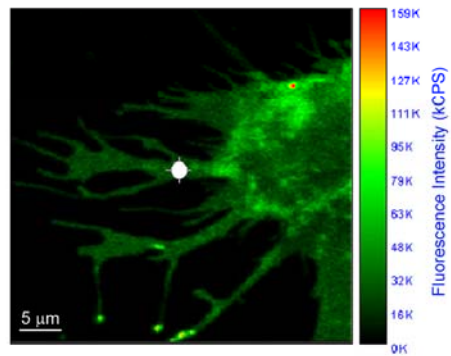
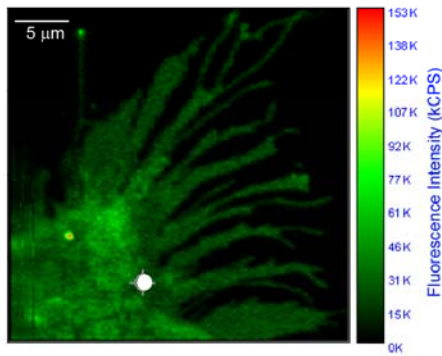
VCAM-1mEGFP



CD9mEGFP



CD151mEGFP



B

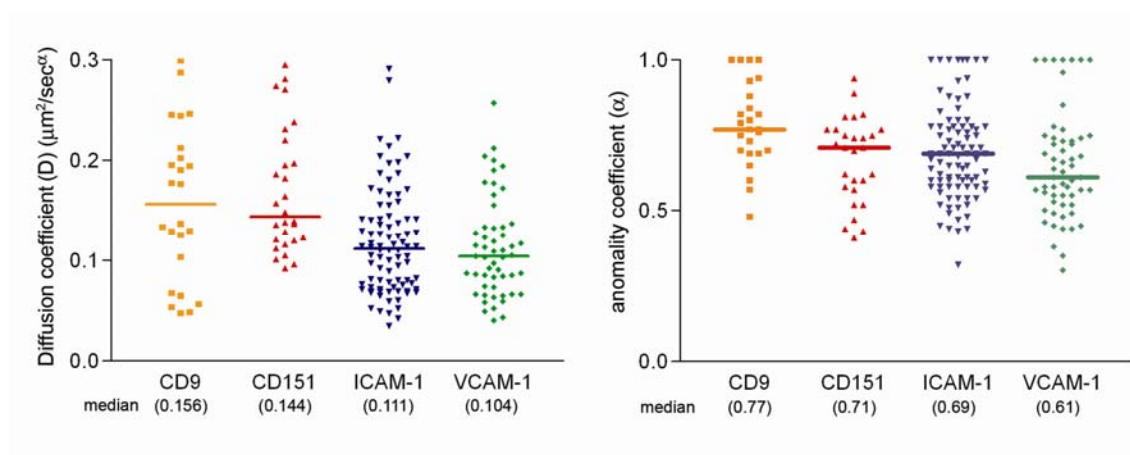


**Figure 25. FCS analysis on the components of endothelial adhesive platforms.**

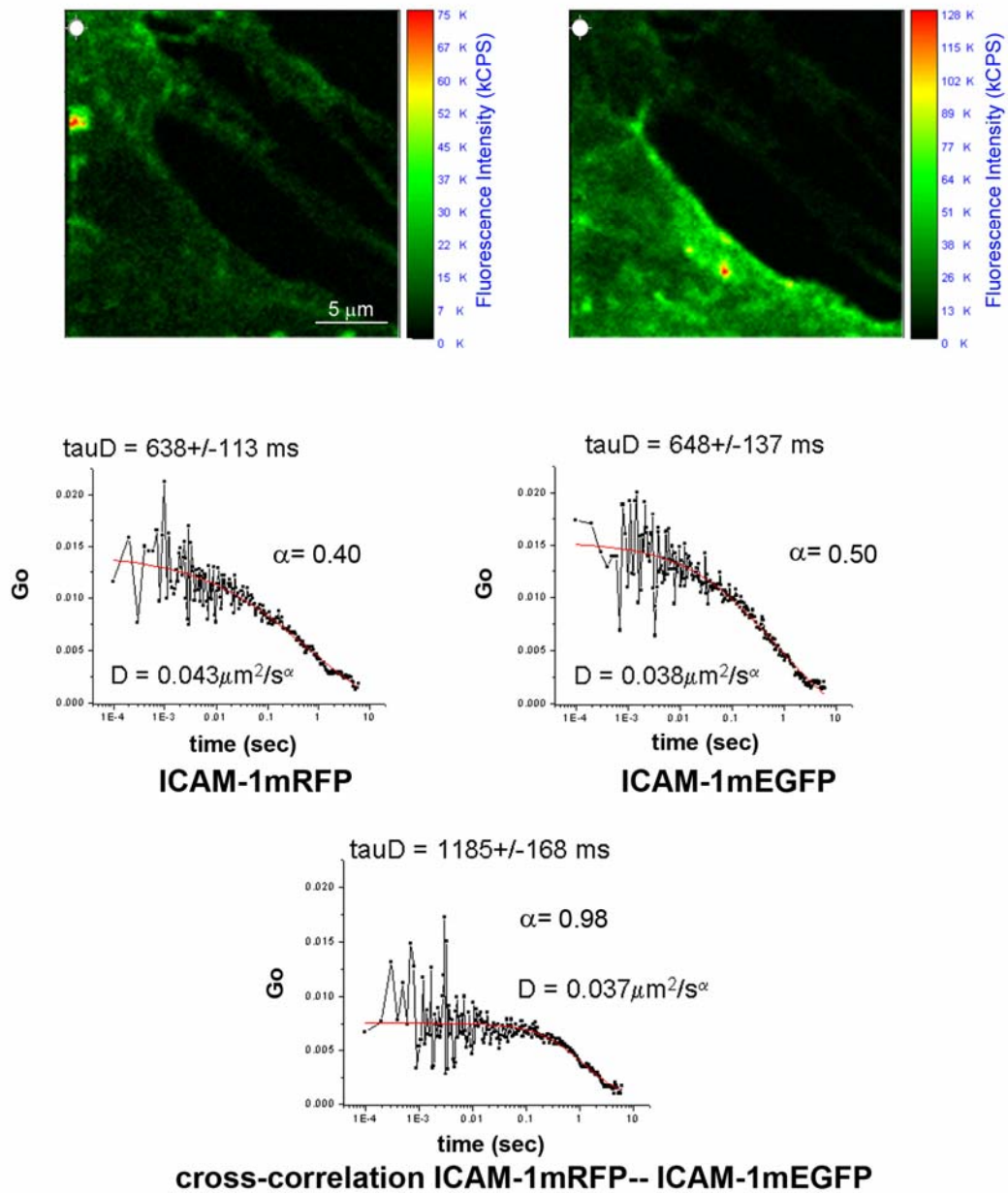
**A.** The panels show representative FCS measurements performed at the plasma membrane of transiently-transfected primary endothelial cells expressing very low levels of ICAM-1-, VCAM-1-, CD9-, and CD151-mEGFP. For each experiment are documented: the fluorescence intensity image, the point in which the laser beam was positioned for the measurement (white circle), the ACF (black line), the best-fitted curve (red line), and the fitted parameters, diffusion time (TauD) and anomaly coefficient ( $\alpha$ , ranging from 0 to 1), from which the diffusion coefficient (D) was derived as described (See under Materials and Methods section). The corresponding scale bar is shown in each image. kCPS: kilo counts per second. **B.** Scatter plots of the diffusion and anomaly coefficients determined by FCS analysis on the four proteins of interest. Each point is an individual measurement. Horizontal lines = medians.

### Complexity of inter-molecular interactions within endothelial adhesive platforms

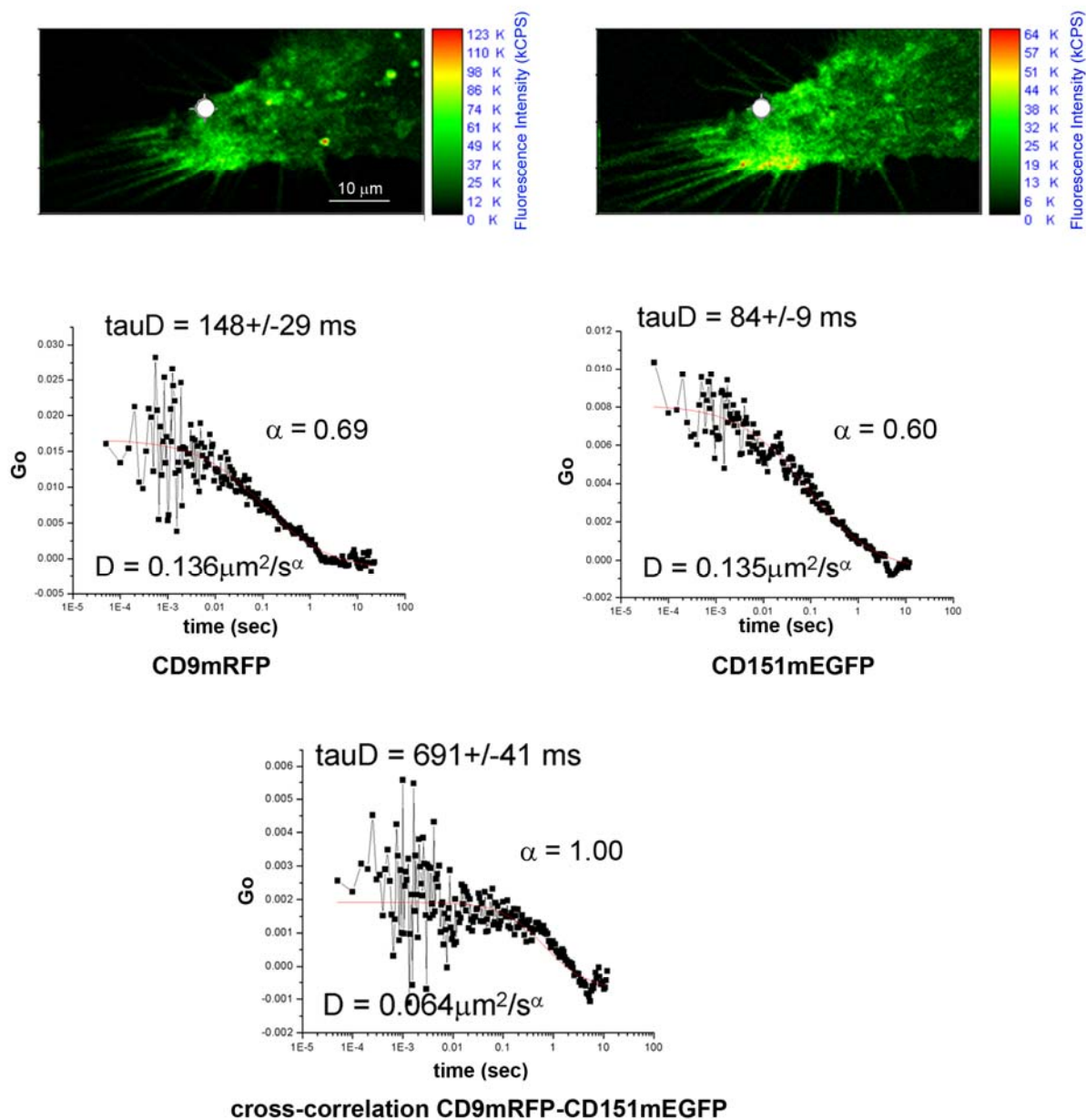
The colocalization studies previously performed with a conventional spectral confocal microscope, which has an optical resolution limit of 200-250 nm, cannot allow us to further discriminate between direct and indirect interactions within EAP. To explore the complex inter-relationships which might take place within the endothelial adhesive platforms and could account for the recruitment of adhesion receptors, we extended the FLIM-FRET analysis to determine whether direct associations occur among CD9, CD151, ICAM-1 and VCAM-1 molecules. First, we confirmed the formation of tetraspanin homo- and heterodimers (CD9mEGFP-CD9mRFP and CD9mEGFP-CD151mRFP) (Fig. 27A), which was previously suggested mainly on the basis of biochemical studies (Hemler, 2005). We then assessed the direct association of tetraspanins with their endothelial partners. Again, a certain degree of specificity was

found inside the microdomains, indicating that CD9 preferentially interacted with ICAM-1 and CD151 with VCAM-1; moreover, the FRET efficiencies of these

**A**

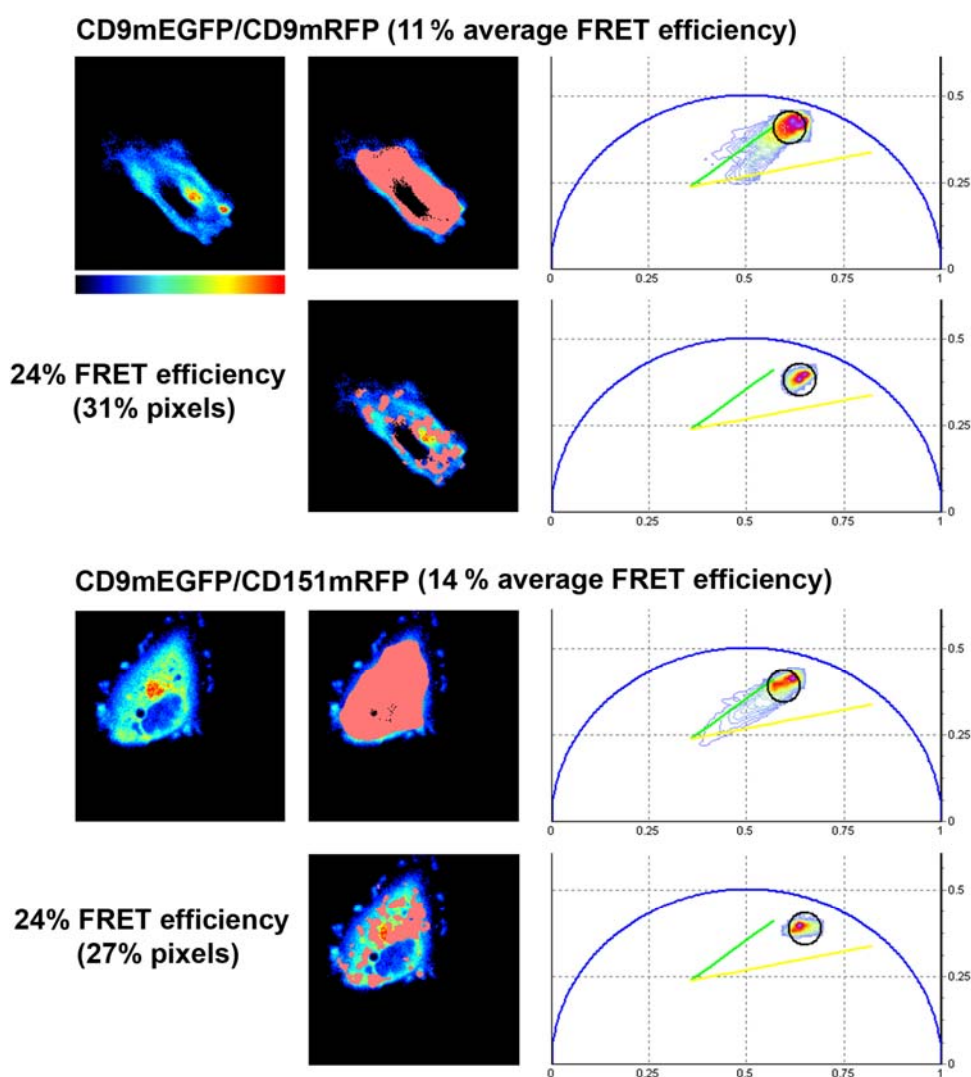


B



**Figure 26: Examples of Fluorescence Cross-correlation Spectroscopy measurements within endothelial adhesive platforms.** The figure shows representative measurements performed at the plasma membrane of HUVEC double transfected with ICAM-1mEGFP/ICAM-mRFP1 (A) or CD9mEGFP/CD151mRFP1 (B). For each experiment are documented: the fluorescence intensity image from both channels (red and green), the point in which the laser beam was positioned for the measurement (white circle), the ACF (black line), the best-fitted curve (red line), the cross-correlation function for the pair, and the fitted parameters, diffusion time ( $\tau_D$ ) and anomaly coefficient ( $\alpha$ ), from which the diffusion coefficient ( $D$ ) was derived. The corresponding scale bar is shown in the images. kCPS: kilo counts per second.

associations were close to those of tetraspanin pairs (Fig. 27B). In contrast, VCAM-1/CD9 and ICAM-1/CD151 pairs exhibited low occurrence of high FRETeff, and FRET in the remaining pixels of the cell was very close to the detection threshold of the technique (data not shown). Control experiments examining interaction between ICAM-1 and uPAR, a cell-surface receptor related to lipid rafts, showed the absence of interaction between these two molecules from distinct membrane microdomains (Fig.28). These results confirm the suggested specific intra-domain interactions in EAP observed in FRAP analysis and in the fluorescence cross-correlation measurements.

**A**

B

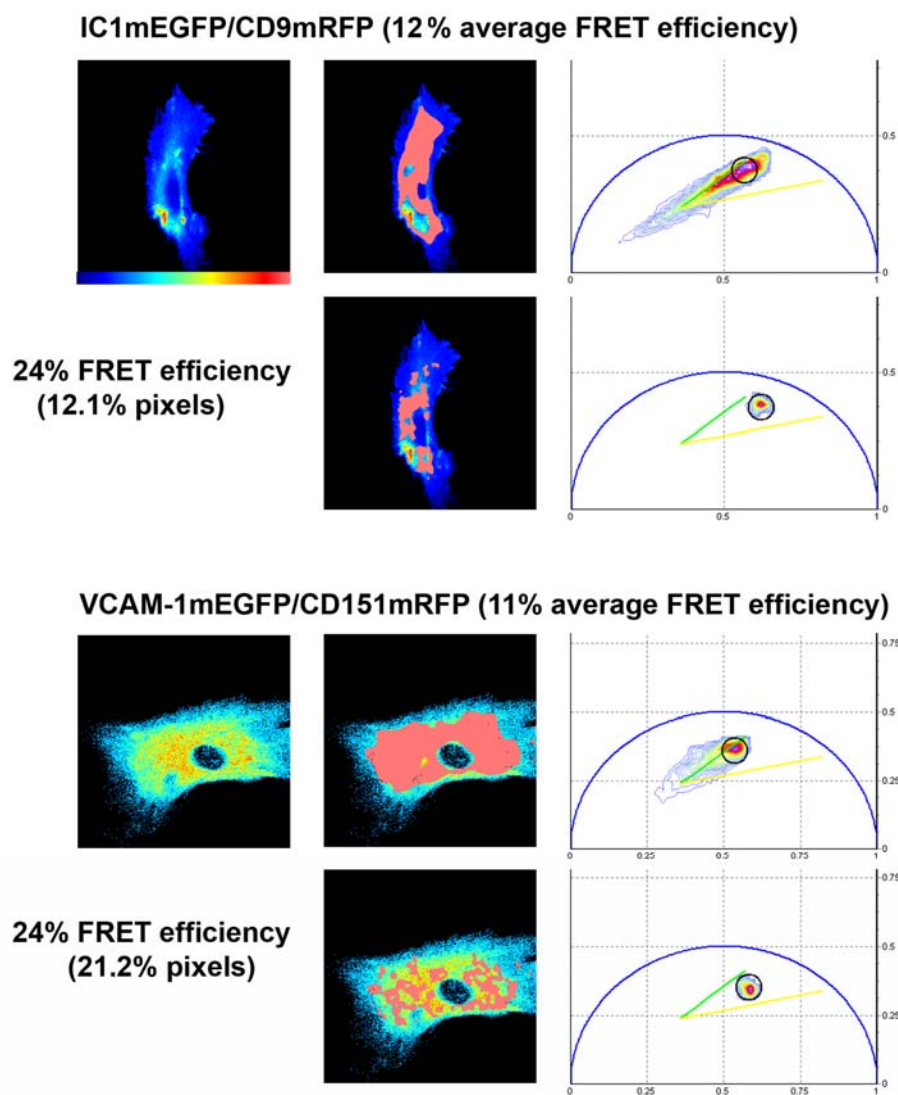


**Figure 27: Direct and indirect interactions within endothelial adhesive platforms.** Endothelial cells were co-transfected with different mEGFP-mRFP1 pair constructs (**A**: CD9/CD9 and CD9/CD151; **B**: ICAM-1/CD9 and VCAM-1/CD151). FLIM-FRET analysis was performed as described (Material and Methods, Fig. 2 and Suppl. Fig. 1). For each FRET pair, the figure shows: the fluorescence intensity image of the scanned section (in pseudocolour scale), the phasor plot, and the FLIM image correspondent to the cursor selection of phasors (black circle) illustrating the pixel localization of phasor selection. Two selections are shown for each FRET pair corresponding to phasors at low (11-14%) and high (24%) FRET efficiency.

### uPARmEGFP-ICAM-1mRFP (0% average FRET efficiency)

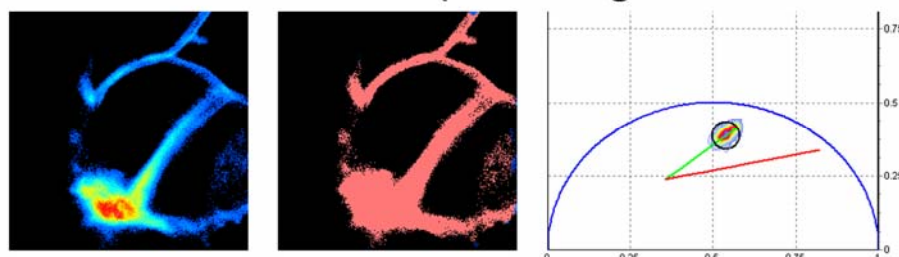


**Figure 28: uPAR/ICAM FRET pair confirming the non interaction of a lipid raft-related protein and an EAP constituent.** FLIM-FRET analysis of uPARmEGFP and ICAM-1-mRFP1 in HEK 293 cells. The intensity image (in pseudocolour scale), the phasor plot and the FLIM image correspondent to the cursor selection (black circle) are shown. This result indicates that FRET does not occur between the two proteins, as the phasor distribution of uPAR-green is identical to that of single transfected cells (data not shown, Caiolfa et al., 2007). It also shows that the localization and distribution of the phasors of mEGFP-constructs is not affected by the kind of protein linked to the fluorophore and by the cells in which they are expressed; while the contribution of other species such as fibronectin (not present in HEK293 samples) and cell autofluorescence varies depending on the cell culture conditions and expression levels of the tagged-proteins.

### Modulation of nanoclustering and diffusion within the endothelial adhesive platforms by tetraspanin blocking peptides

The spatial organization of VCAM-1 and ICAM-1 receptors at the plasma membrane of endothelial cells was studied by immunogold labeling combined with scanning electron microscopy (SEM) (Fig. 29A i). Both ICAM-1 and VCAM-1 form heteroclusters at the plasma membrane (Fig. 29A ii), and localized higher-density clustering was found at the microvilli of docking structures around adherent leukocytes, as shown for ICAM-1 (Fig. 29A iii).

To shed light on the mechanism that controls the tetraspanin-mediated co-clustering of adhesion receptors at the apical plasma membrane of endothelial cells, we used a tetraspanin-derived blocking peptide (CD9-LEL-GST). This soluble peptide interferes with the various functions regulated by CD9-containing tetraspanin microdomains, such as egg-sperm fusion or HIV infection (Ho et al., 2006; Zhu et al., 2002), and decreases VCAM-1- and ICAM-1-mediated lymphocyte adhesion strength

and transmigration under flow conditions (Barreiro et al., 2005). Although the functional effect of these peptides has been well documented, there have been no

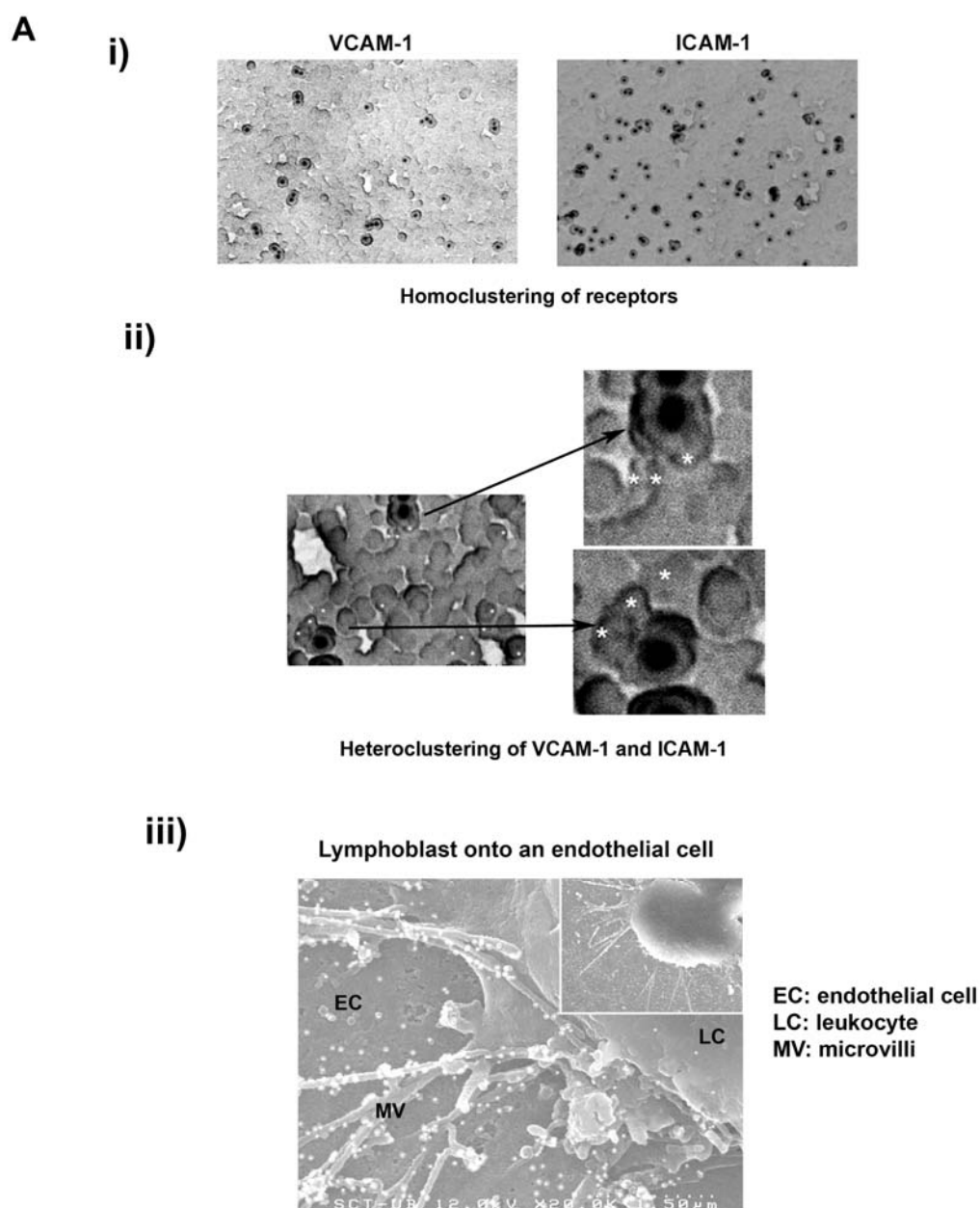


**Figure 29A: Tetraspanin regulates endothelial adhesion receptor nanoclustering.**

**A.** i) TNF- $\alpha$  activated endothelial cells were fixed and stained with anti-VCAM-1 (P8B1) or anti-ICAM-1 (Hu5/3), followed by 40 nm gold-immunolabeling. Then, samples were processed for SEM observation. Representative SEM negative images of  $1.75 \mu\text{m}^2$  areas of the endothelial plasma membrane are shown. ii) TNF- $\alpha$ -activated endothelial cells were fixed and double stained with anti-VCAM-1 (P8B1) and biotinylated anti-ICAM-1 (MEM-111), followed by 40 nm and 15 nm gold-labeling, respectively. Then, samples were processed for SEM observation. The left-hand panel shows a representative SEM negative image of  $0.35 \mu\text{m}^2$  area of the endothelial plasma membrane displaying VCAM-1 (40 nm gold particles) and ICAM-1 (15 nm gold particles, white asterisks). High magnification images show detail of VCAM-1 and ICAM-1 heteroclustering. iii) T lymphoblasts were allowed to adhere to an activated endothelial monolayer for 5 min. Cells were then fixed, stained with anti-ICAM-1 (Hu5/3) followed by 40 nm gold-immunolabeling, and subjected to SEM processing. A representative SEM positive image shows the preferential localization of gold particles at the microvilli of the endothelial docking structure formed around a lymphoblast. The inset shows the leukocyte-endothelial contact area at lower magnification. Scale bar =  $1.50 \mu\text{m}$ .

reported insight into the molecular mechanism through which CD9-LEL-GST exerts its inhibitory action. Nearest neighbour analysis of immunogold-labeled adhesion receptors in the presence of CD9-LEL-GST showed that receptor spacing augmented in

## B

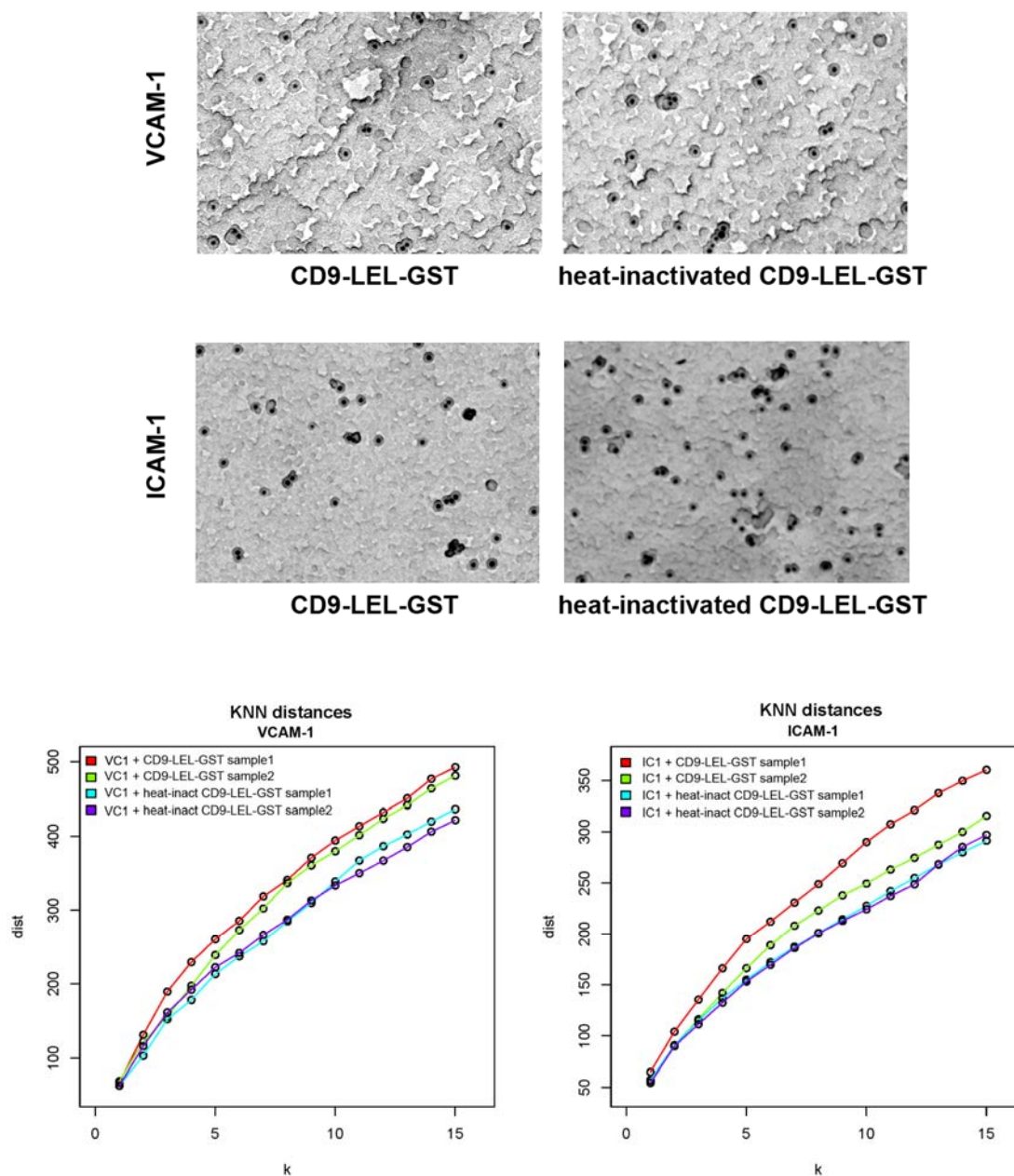


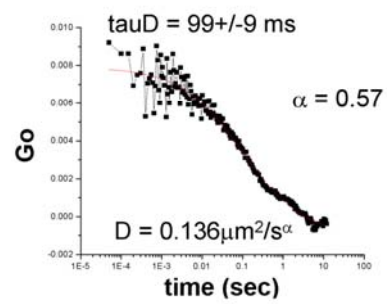
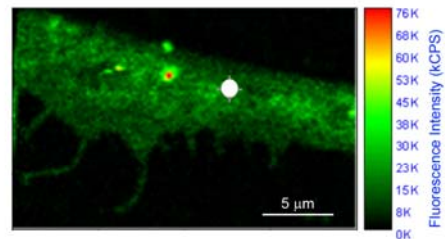
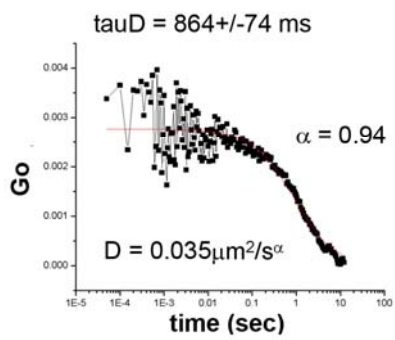
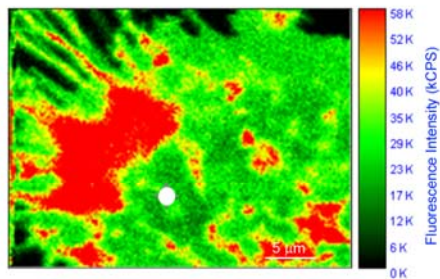
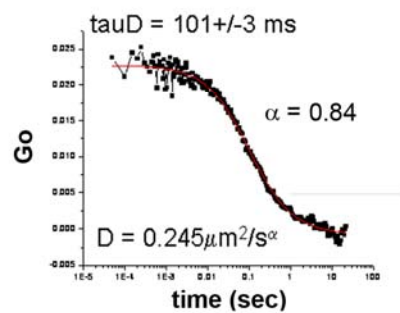
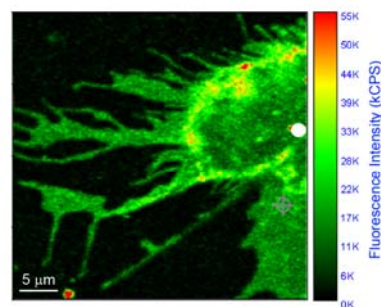
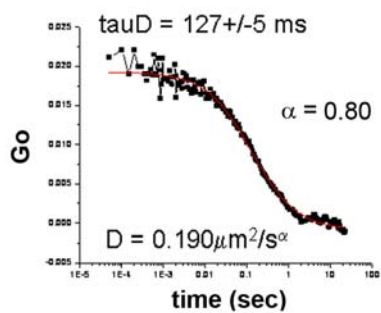
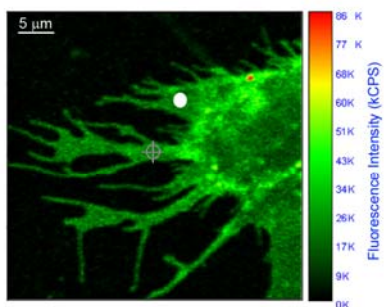
**Figure 29B: Tetraspanin regulates endothelial adhesion receptor nanoclustering.**

**B.** i) Endothelial cells were activated for 20h with TNF- $\alpha$  in the presence of 250  $\mu\text{g}/\text{ml}$  of active or heat-inactivated (5 min 90°C) CD9 blocking peptide (CD9-LEL-GST). Cells were then fixed and stained for VCAM-1 or ICAM-1 as in A i). Representative images of 1.75  $\mu\text{m}^2$  areas of the endothelial plasma membrane are shown. ii) Gold particles in SEM images were counted, and coordinates were assigned to each object using Metamorph software. Inter-particle distances were calculated using a custom-written k-nearest neighbour (knn) distance algorithm based on R software. Graphs show knn distances from 2 representative images of each condition (VCAM-1 or ICAM-1 staining with active or inactive CD9 blocking peptide).

C

i)

## CD9mEGFP + CD9-LEL-GST

CD9mEGFP  
+ heat-inactivated CD9-LEL-GST

ii)

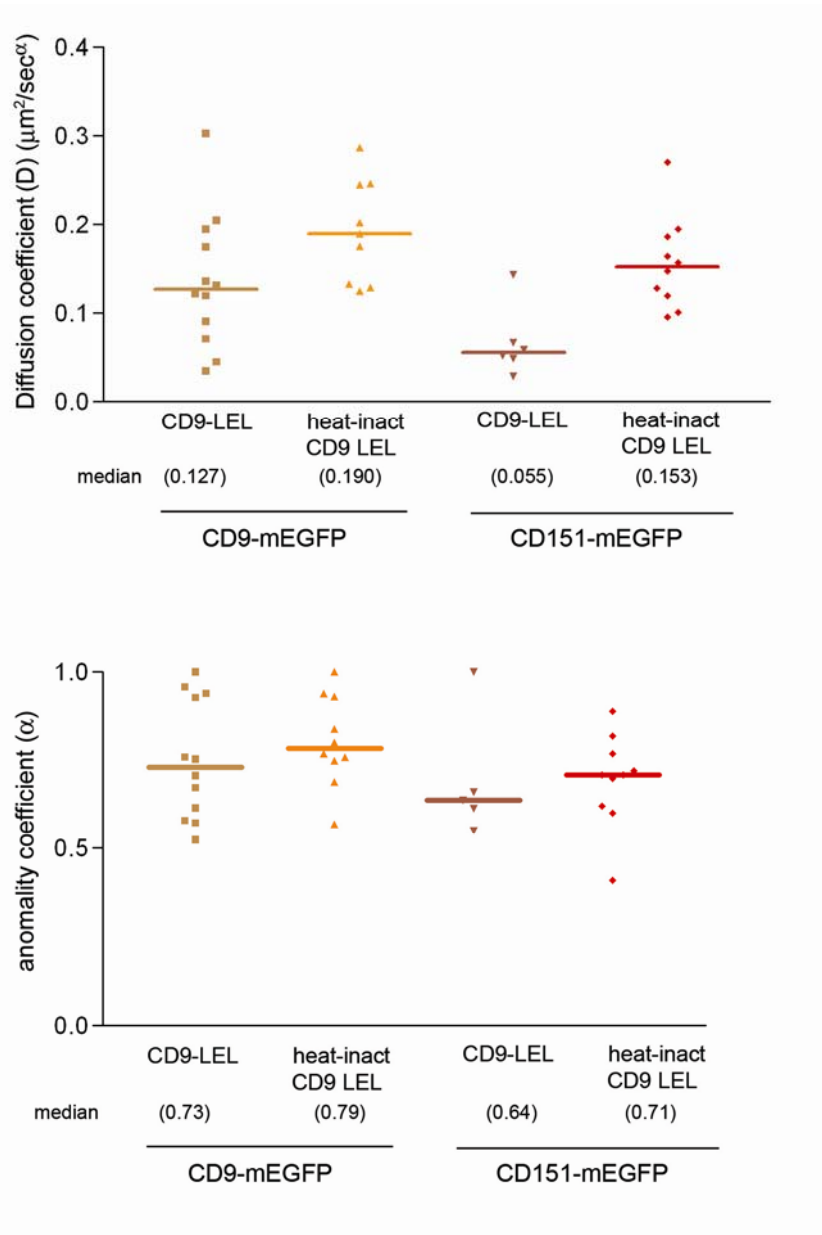


**Figure 29C: Tetraspanin regulates endothelial adhesion receptor nanoclustering.**

C. i) Panels show representative FCS measurements performed at the plasma membrane of endothelial cells transiently-transfected with CD9- or CD151-mEGFP and treated with 250  $\mu\text{g}/\text{ml}$  of active or heat-inactivated CD9-LEL-GST. For each experiment are documented: the fluorescence intensity image, the point in which the laser beam was positioned for the measurement (white circle), the ACF (black line), the best-fitted curve (red line), and the fitted parameters, diffusion time (TauD) and anomaly coefficient ( $\alpha$ ), from which the diffusion coefficient (D) was derived. The corresponding scale bar is shown in each image. kCPS: kilo counts per second. ii) Scatter plots of the diffusion and anomaly coefficients determined by FCS analysis. Each point is an individual measurement. Horizontal lines = medians.

comparison with samples treated with heat-inactivated CD9-LEL-GST. This effect might be due to the insertion of functional blocking peptides within the EAP, competing with endogenous CD9 for association with partners (Fig. 29B). Consistently, FCS analysis revealed that the CD9-LEL peptide, but not heat-inactivated CD9-LEL, decreased the diffusion coefficient of CD9mEGFP molecules. Furthermore, the diffusion coefficient of CD151 was also affected, showing that blocking peptide insertion in EAP modifies the general dynamics within the platforms due to the increasing molecular crowding (Fig. 29C). Together these data suggest that the blocking peptide compete with endogenous CD9 for binding to partners and other tetraspanins. This prevents adequate interactions and imposes steric hindrance, resulting in a net slower diffusion and reduced receptor clustering.

## **DISCUSSION**

### **Identification and characterization of the endothelial docking structure for adherent leukocytes**

VCAM-1 is one of the major endothelial receptors that mediates leukocyte adhesion to the vascular endothelium (Carlos et al., 1990). Recent data obtained with neonatally deficient VCAM-1 mice have strongly suggested that VCAM-1 plays an important role for lymphocyte homing and for T cell-dependent humoral immune responses (Koni et al., 2001; Leuker et al., 2001). In addition, VCAM-1 may play an important role in the pathogenesis of diseases such as atherosclerosis (Cybulsky et al., 2001), rheumatoid arthritis (Carter and Wicks, 2001), and multiple sclerosis (Alon, 2001). Thus, the elucidation of VCAM-1 function in leukocyte adhesion and transmigration is crucial, as this molecule could constitute a molecular target for therapeutic intervention.

The cytoskeletal components involved in the redistribution of VCAM-1 at the leukocyte-endothelial cell contact area have not been studied previously. Among potential candidates, ERM proteins seemed likely to mediate this process as these molecules play an important role in the remodelling of the plasma membrane, as reported for ICAMs (Heiska et al., 1998; Helander et al., 1996; Serrador et al., 1997). We found that endogenous VCAM-1 colocalizes and is physically associated with moesin and ezrin in microspikes and microvilli of the apical surface of cytokine-activated endothelial cells. Furthermore, the cytoplasmic tail of VCAM-1 and the active N-terminal domain of moesin or ezrin are capable to directly bind *in vitro*. These data strongly suggest that ERM proteins are directly involved in the redistribution of VCAM-1. However, it cannot be ruled out completely that adaptor proteins such as EBP50 or E3KARP (Bretscher et al., 2000), also play a role. It has been reported that ERM proteins bind to a positively charged amino acid cluster in the juxta-membrane cytoplasmic domain of CD44, CD43,

and ICAM-2 (Yonemura et al., 1998). In addition, we have found recently that a novel serine-rich motif within the cytoplasmic tail of ICAM-3 is critical for its interaction with ERM proteins (Serrador et al., 2002). The amino acid sequence comparison of VCAM-1 and ICAM-3 cytoplasmic tails suggests that VCAM-1 contains a similar serine-rich motif, likely accounting for ERM association.

To study the VCAM-1/ERM interaction during the extravasation of lymphoblasts, we have made extensive use of a live cell system in combination with time-lapse fluorescence microscopy and GFP fusion proteins. This afforded us with information on dynamic relationships of the two molecules during early adhesion and later stages of TEM. While both, VCAM-1 and moesin, clustered around spreading lymphoblasts on the apical endothelial surface, only moesin remained at lymphoblast-endothelial contacts during the passage of lymphoblasts across the endothelium and their subsequent migration beneath the endothelial monolayer. However, it has been reported that VCAM-1 actively participates in T lymphoblast transmigration across high endothelial venules and monocyte extravasation (Faveeuw et al., 2000; Meerschaert and Furie, 1995). These discrepancies point to a differential role of VCAM-1 that might be both leukocyte and endothelial cell-type specific. Our data on moesin dynamics clearly indicate that another receptor linked to moesin could drive this migration. In this regard, we have found that the dynamic behavior of ICAM-1 is similar to that of moesin during lymphoblast transmigration. The differential dynamic behavior of VCAM-1 and ICAM-1 during lymphoblast adhesion and transmigration on the one hand, and of moesin on the other, could suggest a mechanism by which ERM proteins are able to regulate the distribution of both molecules independently.

As VCAM-1/ERM interaction was mostly restricted to leukocyte tight adhesion and spreading, we took advantage of a cellular model based mainly on VLA-4/VCAM-1. In

this model, leukocytes are restricted to a sustained tight adhesion and are unable to progress to TEM, allowing a detailed study of the endothelial VCAM-1/ERM interaction. In this cell model, VCAM-1 and both, moesin and ezrin, clustered around adherent leukocytes, participating in the formation of an actin-rich docking structure that was attached to and partially engulfed the leukocyte. Similar docking structures were formed around spreading lymphoblasts in static conditions or PBLs adhered to endothelium under flow, in which VCAM-1 and ICAM-1 were concentrated together with ERM proteins. In physiological conditions, these structures rapidly vanished as lymphoblasts or lymphocytes began to migrate through the endothelial monolayer.

Our findings highlight the remarkable active role played by the endothelium during leukocyte adhesion. Thus, the initial VCAM-1 and ICAM-1 engagement trigger their clustering and the subsequent activation and clustering of endothelial moesin and ezrin at the site of cell-cell contact. In turn, phosphorylated active ERM proteins would participate in concert with  $\alpha$ -actinin, an actin-bundling protein, in the rearrangement of the actin cytoskeleton to create the docking structure. Several focal adhesion proteins such as vinculin, talin and paxillin seem to be involved as well. Interestingly, the endothelial docking structure is reminiscent of nascent receptor-mediated phagosomes, in that the subcellular distribution of all these structural proteins is similar in both structures (Allen and Aderem, 1996). In this regard, it has been proposed that focal adhesions and complement receptor-mediated phagosomes could share some conserved mechanisms requiring the same molecules (May and Machesky, 2001). A similar argument could be made to functionally link the former structures and the novel leukocyte-endothelium docking structure described here. On the other hand, VASP is concentrated in the docking structure. This protein is present in actin-based protrusions, where it cooperates with WASp-Arp2/3 complex, as occurs in phagosomes (Castellano et al., 2001). Its

presence at the docking structure could indicate the existence of actin polymerization supporting this endothelial structure, and suggests common mechanisms for *de novo* actin assembly in all these structures. Interestingly, ERM proteins have been also implicated in the *de novo* actin assembly on mature Fc receptor-mediated phagosomes (Defacque et al., 2000).

As ERM activation occurred during the formation of the anchoring structure, we studied the regulatory mechanisms involved. These proteins are regulated by the interplay of PI(4,5)P<sub>2</sub> metabolism and components of the Rho GTPase signaling pathway, thereby linking events occurring at the plasma membrane with cytoskeletal remodelling (Sechi and Wehland, 2000). Interestingly, these regulatory molecules are also important in phagocytosis (Botelho et al., 2000; Chimini and Chavrier, 2000). We found that PI(3,4)P<sub>2</sub>, PI(3,4,5)P<sub>3</sub>, and more abundantly PI(4,5)P<sub>2</sub>, colocalized with VCAM-1 and ERM proteins in the endothelial docking structure. Notably, PI(4,5)P<sub>2</sub> was preferentially concentrated at the microspike tips, whereas the other phosphoinositides exhibited a more diffuse pattern. These observations point to a prominent role of PI(4,5)P<sub>2</sub> in regulating molecular events during endothelial docking of leukocytes. One such event could be the activation of moesin and ezrin through its binding to their N-terminal domain. PI(4,5)P<sub>2</sub> production could be mediated by Rho, since PI4P5K is a down-stream RhoGTPase effector. On the other hand, the presence of PI(3,4)P<sub>2</sub> and PI(3,4,5)P<sub>3</sub> could be related to PI3K activity. Inhibitors of PI3K only mildly affected the generation and maintenance of the docking structure, a finding that is in agreement with its role in phagocytosis, namely to mediate phagosome closure (Cox et al., 1999). In our experimental model, the endothelial anchoring structure does not progress to engulf the leukocyte, and hence, it is less PI3K-dependent. In contrast, the p160 ROCK inhibitor Y27632 inhibited the formation of the anchoring structure and induced its dissolution as well. Abnormal

formation of the endothelial docking structure was also observed under flow conditions after the treatment with Y-27632, which rendered an inhibitory effect in lymphocyte adhesion and transmigration. In addition, the phenomenon of rolling was also decreased. This finding is in agreement with previous reports describing the existence of an E-selectin/actin cytoskeleton adhesion complex induced by leukocyte adhesion (Yoshida et al., 1996; Lorenzon et al., 1998), which it is likely to be also affected by the inhibition of the Rho/p160 ROCK pathway. Our results concur with the previously described regulation of the VCAM-1, ICAM-1, and E-selectin clustering by the GTPase Rho during monocyte adhesion (Wojciak-Stothard et al., 1999). Furthermore, the key role of the Rho/p160 ROCK signaling pathway in the regulation of the adhesion receptor/ERM/actin cytoskeleton interaction and remodelling, which results in the formation of this protrusive structure, is further strengthened by the implication of this pathway in the regulation of CR-mediated phagosomes (Caron and Hall, 1998).

In conclusion, our results provide novel insights into the links between the actin cytoskeleton and adhesion receptors involved in leukocyte adhesion and TEM during inflammation. Further analysis will be focused on molecules involved in the regulation of the endothelial docking structure disruption to allow diapedesis, and the signaling pathways that interconnect both processes.

### **Functional role of the inclusion of endothelial adhesion receptors in tetraspanin-enriched microdomains**

It is well established that tetraspanins interact in multiproteic domains with other transmembrane proteins (Berditchevski, 2001; Boucheix and Rubinstein, 2001; Yanez-Mo et al., 2001; Yauch et al., 1998). Moreover, antibody crosslinking of tetraspanins usually triggers the same cellular responses than antibodies directed to their associated

partners indicating that they conform functional entities (Hemler, 2001; Yauch et al., 1998). Herein, we describe the lateral association of ICAM-1 and VCAM-1 with tetraspanins at the contact area between leukocytes and endothelial cells. Remarkably, the function of these endothelial adhesion molecules can be directly modulated by the tetraspanin-associated moieties.

In contrast to lipid rafts, tetraspanins form a network based on protein-protein interactions, which might be modulated by differential protein expression or post-translational modifications. In addition, tetraspanins are palmitoylated proteins that interact directly with cholesterol (Berditchevski et al., 2002; Charrin et al., 2002; Charrin et al., 2003; Yang et al., 2002) and under certain conditions are also recovered in the light fractions of sucrose gradients (Claas et al., 2001). Thus tetraspanin webs or microdomains could be envisaged as a subtype of lipid rafts. In this regard, it has been suggested that the size of tetraspanin-based microdomains can be as small as lipid rafts (Kropshofer et al., 2002). Moreover, tetraspanin microdomains can be also important for intracellular signalling events, since they are able to associate with PI4-K (Berditchevski et al., 1997) and PKCs (Zhang et al., 2001). Our studies indicate that the composition of endothelial tetraspanin microdomains changes during the transmigration process. Thus, apical domains would be enriched in CD9, whereas in ventral domains CD151 is more highly represented. On the other hand, tetraspanins are also associated with integrin receptors at endothelial intercellular junctions (Chattopadhyay et al., 2003; Yanez-Mo et al., 1998). These data suggest the existence of different tetraspanin microdomains, which might coalesce and diverge during cell activation, adhesion or transmigration. Furthermore, both ICAM-1 and VCAM-1 are anchored to the actin cytoskeleton through the association of ERM proteins to their cytoplasmic tails (Barreiro et al., 2002; Heiska et al., 1998). The linkage of Ig receptors to the cytoskeleton might indicate that tetraspanin

microdomains are not floating freely on the plasma membrane but connected to the cortical actin cytoskeleton.

Tetraspanins have been implicated in several cellular functions, mainly by the use of monoclonal antibodies (Berditchevski, 2001; Boucheix and Rubinstein, 2001; Hemler, 2001; Yanez-Mo et al., 2001). Our results show that soluble CD9-LEL-GST peptides or tetraspanin-specific siRNA inhibit leukocyte transmigration and enhance their detachment by shear stress, supporting the functional role of tetraspanins in transendothelial migration. Similar GST-fusion proteins have been reported to be inhibitory in sperm-egg fusion assays (Higginbottom et al., 2003; Zhu et al., 2002). These LEL-GSTs are a valuable tool, without the effects of detergents or cholesterol depleting agents, which affect the physical properties of the plasma membrane. The tertiary structure of these LEL proteins is very dependent on the proper disulphide bonds formation. Thus, mutation of any of the four Cys in CD9 greatly reduces the recognition in Western blot by an anti-CD9 mAb and completely abolishes functional activity.

Endothelial tetraspanins are highly expressed and show a very slow turnover, so that partial protein knocking down by siRNA is observed only after 3-6 days. Although no complete abrogation of tetraspanin expression is attained, it turned out to be more than sufficient to exert a significant functional effect. Interestingly, a compensatory effect on other tetraspanin expression was observed, suggesting that a tight regulation of the overall tetraspanin load at the plasma membrane exists. Nevertheless, as demonstrated also by the heterologous Colo320 cell system, the repertoire of tetraspanins is also crucial for the proper adhesive function of ICAM-1 and VCAM-1. Tetraspanin siRNA affected ICAM-1 and VCAM-1 expression, which suggest a possible role for tetraspanins in early biosynthetic events. In this regard, it has been previously described that CD9 associates with the  $\beta$ 1 integrin precursor prior to reaching the plasma membrane (Rubinstein et al.,

1997). In a similar way, CD19 expression was selectively reduced in CD81 deficient mice, being the defect located after the endoplasmic reticulum (Shoham et al., 2003). However, tetraspanin interference only affected ICAM-1- and VCAM-1- mediated adhesion when assayed under stringent flow conditions. Moreover, CD9-LEL-GST peptide incubation had no effect on ICAM-1 and VCAM-1 induction but it did also affect their function under shear stress. These data make both experimental approaches complementary and strongly suggest that membrane presentation into the appropriate microdomains of these receptors is functionally relevant for their proper adhesive function. Furthermore, the direct regulation of ICAM-1 and VCAM-1 adhesive function by the proper tetraspanin environment is revealed in the heterologous system of aggregation between Colo320 cells and K562 transfectants. Our data with Colo320 cells also rule out the possible involvement of a putative tetraspanin ligand on leukocytes, since their heterotypic adhesion is completely dependent on ICAM-1 or VCAM-1 expression.

The fact that ICAM-1 and VCAM-1 are included in tetraspanin-based microdomains might favour the efficient transition from the rolling step, in which VCAM-1 is involved (Alon et al., 1995; Berlin et al., 1995), to the firm adhesion of leukocytes via both VCAM-1 and ICAM-1 ligation (Butcher, 1991; Springer, 1994), to finally proceed to diapedesis. The possibility of selectins or other endothelial adhesion molecules being constituents of these endothelial tetraspanin microdomains cannot be ruled out and deserves further analyses. In this scenario, it could be postulated that tetraspanin microdomains would act as specialized platforms that cluster the appropriate adhesion receptors necessary for the rapid kinetics of leukocyte transendothelial migration process.

Inclusion of ICAM-1 and VCAM-1 into tetraspanin domains is necessary for their

proper function under dynamic conditions such as shear stress. This phenomenon could be explained by a possible role of tetraspanins in the preclustering or avidity regulation of endothelial adhesion receptors. Avidity regulation of the mitogenic activity of the membrane-anchored HB-EGF by its association with CD9 has been demonstrated (Higashiyama et al., 1995; Nakamura et al., 2000). Recent observations show that tetraspanin networks are able to cluster class II MHC molecules bearing restricted repertoires of peptides (Kropshofer et al., 2002), thus facilitating antigen peptide presentation. Furthermore, CD81 also regulates VLA-4 and VLA-5-mediated adhesion by enhancing integrin avidity independently of ligand binding (Feigelson et al., 2003). This phenomenon also facilitated leukocyte firm adhesion by strengthening VLA-4/VCAM-1 interaction acting on the leukocyte side.

The inclusion of adhesion receptors into tetraspanin domains could also affect their conformation up-regulating their binding to integrins. In this regard, we have recently described a monoclonal antibody that preferentially recognizes CD9 when associated with  $\alpha 6\beta 1$  integrin (Gutierrez-Lopez et al., 2003). The possibility of reciprocal conformational changes in tetraspanin-associated proteins cannot be excluded. In this regard, CDw78 mAbs recognize HLA-DR only when included into tetraspanin domains (Drbal et al., 1999), although the possibility of a conformational change in HLA-DR due to its interaction with tetraspanins has not been determined. Lately, CD151 knockout mice show a mild deficiency in outside-in activation of  $\alpha IIb\beta III$  integrin in platelets (Lau et al., 2004). Thus, several lines of evidence support a functional role for tetraspanin-based microdomains in different cellular functions. In this report we demonstrate by different complementary experimental approaches, both on primary cells and assessing endogenous proteins, and in an heterologous system, that the adhesive function of ICAM-1 and VCAM-1 is directly modulated by their inclusion in a microdomain containing the

appropriate repertoire of tetraspanins. This effect was shown to be crucial in an important physiological process such as leukocyte extravasation.

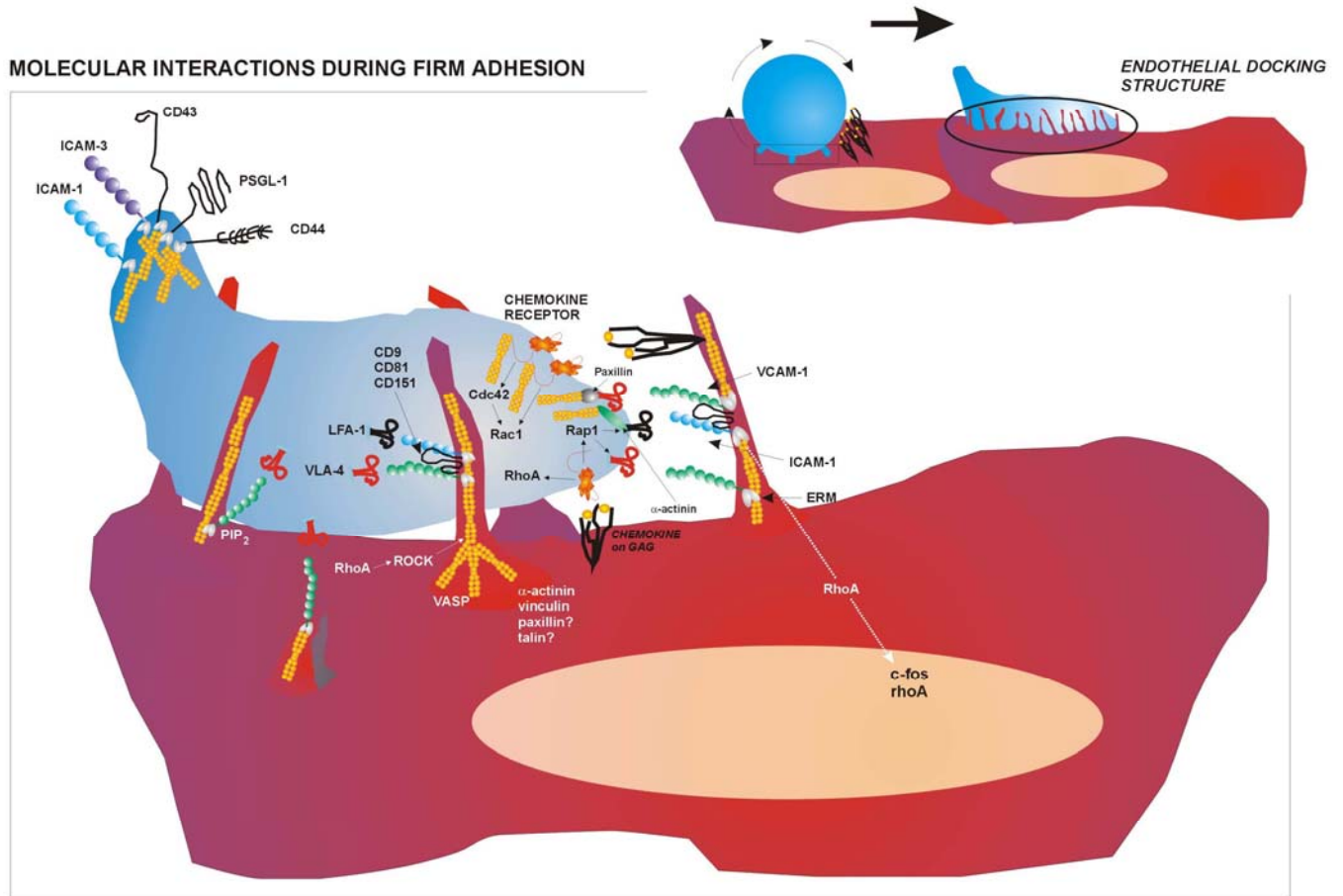


**Figure 30: Model of molecular interactions during firm adhesion.** The slowing-down of leukocytes facilitates their interaction with chemokines exposed on endothelium, triggering the activation of leukocyte integrins by increasing their affinity and avidity to allow the final arrest of adherent leukocytes. This activated state involves a drastic morphological change from the round shape of circulating leukocytes to the polarized shape typical of migrating cells. The acquisition of polarity implies the segregation of adhesion molecules (ICAM-1, ICAM-3, CD43, CD44, PSGL-1, etc) to the rear pole of the cell (uropod), which is lumen-orientated for the recruitment of bystander leukocytes; whereas the integrins localized to the contact area with endothelium to allow the spreading of the cell body onto the vascular wall. On the other hand, the endothelium also plays an active role in firm adhesion by creating docking structures around the attached leukocytes. These endothelial docking structures are formed as a result of VCAM-1 and ICAM-1 engagement by their integrin counterreceptors (VLA-4 and LFA-1, respectively), and are supported by a cortical actin scaffold in which ERM proteins,  $\alpha$ -actinin, vinculin, VASP and other actin-related proteins participate. In addition, members of the tetraspanin family also cooperate with the endothelial adhesion receptors in the docking structure formation. The principal regulatory molecules involved in the formation of the above-mentioned structure and in leukocyte integrin activation are also shown in the inset.

### **Endothelial adhesive platforms as a model for the biophysical study of tetraspanin-enriched microdomains**

The existence of organized membrane domains distinct from those based on lipid-protein interactions (lipid rafts) has not been demonstrated previously in living cells. Biochemical analysis and microscopy studies on fixed samples have indicated that a network of specific protein-protein interactions may occur at cell membranes between tetraspanin members and associated partners (Levy and Shoham, 2005a). In the current study, we have used an array of cutting-edge analytical microscopy and spectroscopy techniques, including single molecular analysis, to characterize in depth the dynamic features and biophysical properties of TEM in living cells. The transiently transfected primary human endothelial cells used in this study are a physiologically relevant cell model that expresses an appropriate repertoire of membrane tetraspanins and adhesion receptors. In addition, the study of four proteins in combination, two tetraspanins and two essential endothelial adhesion receptors, provides a valuable global overview of the behavior of the specialized type of TEM named endothelial adhesive platforms (EAP).

Endogenous expression of CD9 and CD151 tetraspanins and ICAM-1 and VCAM-1 adhesion receptors in endothelial cells reduces the probability of interaction between transiently-transfected tagged proteins in the FLIM-FRET analyses. To minimize this problem, FLIM quantifications were performed in resting HUVEC, in which tetraspanin expression is unaltered, ICAM-1 levels are low and VCAM-1 expression at plasma membrane is negligible. Given that the expression of CD151 and, especially, CD9 is much higher than ICAM-1 in resting cells, it is possible that FRET<sub>eff</sub> values from measurements involving tetraspanin proteins might be underestimated. Furthermore, in the case of CD9, CD151 and ICAM-1, which are able

to homodimerize, the possible association of two green or two red molecular species makes the occurrence of heteroFRET even more improbable. Finally, another potential problem, dimerization of chimeric proteins through their fluorescent tags, was overcome by using monomeric versions of EGFP and mRFP1. Despite the drawbacks of FRET analysis in complex living cell systems, high FRET<sub>eff</sub> was detected for ICAM-1/CD9, VCAM-1/CD151, CD9/CD9, CD9/CD151 and ICAM-1/ICAM-1 pairs and clear-cut differences were detected with respect to non-interacting pairs (VCAM-1/ICAM-1, VCAM-1/VCAM-1). Examination of average FRET<sub>eff</sub> values and the percentage of pixels exhibiting the highest FRET<sub>eff</sub> values for each pair showed that tetraspanin homo- and heterodimers and tetraspanin-partner interactions occur preferentially compared with ICAM-1 dimers, strengthening the concept of EAP as the basic organization of endothelial adhesion receptors on the endothelial apical plasma membrane. In fact, the existence of ICAM-1 dimers had been described before as a small proportion from the whole molecular ICAM-1 population using biochemical approaches (Miller et al., 1995). Besides, BIAcore affinity measurements revealed that a single ICAM-1 monomer, not dimeric ICAM-1, represents the complete, fully competent LFA-1-binding surface (Jun et al., 2001).

The innovative technique used to quantify FRET was completely independent of the concentration of fluorescent species, and is therefore well-suited to analyze and compare data from different transient transfections. Furthermore, the FLIM-FRET approach permitted us to spatially resolve the fretting population within a whole cell, generally yielding a patchwork pattern for the higher FRET<sub>eff</sub> population. To further substantiate the experimental data on the absence of ICAM-1-VCAM-1 heterodimer formation, ICAM-1 or VCAM-1 was indistinctly used as donor in FLIM-FRET experiments. We inverted the labeling fluorophores on the two receptors, showing that

the lack of FRET was not due to artifacts introduced by the fluorescent constructs. Additional control experiments also demonstrated that the protein in the mEGFP constructs affects negligibly the fluorescence lifetime distribution of the fluorophore (i.e., the phasor distribution in phasor-FLIM analysis).

Finally, the observations that the GPI-anchored protein, uPAR, used as a marker of lipid rafts, did not interact with ICAM-1 (used as an EAP marker) in FLIM-FRET experiments, and that the two receptors were sorted to the plasma membrane in different vesicles (data not shown), further sustain the notion that tetraspanins might form discrete and specific microdomains at the cell membrane.

The diffusional behaviour of the EAP components was investigated by combining FRAP and FCS analyses. The possible perturbation of membrane dynamics that might result from exogenous expression of tagged proteins was overcome in FRAP experiments by making a large number of measurements in several batches of transiently-transfected primary cells and making an exhaustive statistical analysis of the data. Photobleaching experiments were all performed under pro-inflammatory conditions (TNF- $\alpha$  treatment) in order to promote proper formation of docking structures around adherent leukocytes mostly through the mediation of endogenous VCAM-1 or ICAM-1. Although the integrin-expressing K562 adhesion model used in our experiments is a simplification of the dynamic physiological firm adhesion process that takes place under hemodynamic flow conditions, this model has allowed us to perform diffusion analyses that would be unfeasible under more physiological but complex conditions.

FRAP analysis examines the diffusion rate of an overall molecular population within a microscopic area. These experiments have provided us with valuable information on the global diffusional behavior of VCAM-1, ICAM-1, CD9, CD151 and

GPI molecular subsets in comparable areas of nude membrane and at sites of leukocyte anchorage. A mixed steady-state molecular population (comprising proteins bound or unbound to cytoskeleton, coupled to partners, in the form of dimers, and so on) is considered for each measurement. From FRAP data collected at nude plasma membrane, we could distinguish differences in the net mobilities of tetraspanins and receptors. Tetraspanins showed the fastest diffusion rate, although this did not differ significantly from the rate for ICAM-1, whereas VCAM-1 population was slower and displayed a higher immobile fraction. The reason for this difference in diffusion behaviour between the two adhesion receptors remains still unsolved. Close interaction between ICAM-1 and CD9 is supported by the experiments with the C-terminally truncated ICAM-1, ICAM-1 $\Delta$ Cyt, which is unable to interact with the actin cytoskeleton via ERM proteins (Barreiro et al., 2002). The lateral mobility of ICAM-1 $\Delta$ Cyt-EGFP was not significantly different from that of CD9, supporting the notion that these molecules can interact in the absence of ICAM-1 cytoplasmic tail. Conversely, GPI-EGFP, a prototypic lipid raft- related molecule widely used in microscopy studies (Kenworthy et al., 2004; Varma and Mayor, 1998), moved much faster and its recovery was complete, with no significant immobile fraction. Moreover, the diffusion properties of CD9, CD151, ICAM-1 and VCAM-1 were altered in the context of docking structures, whereas GPI-EGFP is unaffected by engagement of integrin-bearing leukocytes. These observations strongly argue in favor of these proteins being constituents of physical entities with intrinsic properties and biophysical features distinct from classical lipid rafts.

The delay observed for non-ligand-engaged EAP components at the docking structures could be well due to their transient interaction with ligand-immobilized ICAM-1 or VCAM-1. In this way, these immobile complexes at docking sites could act

as physical constraints on the mobility of the overall molecular populations analyzed, which would produce a net reduction in diffusion rate (Suppl Fig. 3). The fact that VCAM-1 is no more affected than tetraspanins by ligand engagement of ICAM-1 supports a model in which VCAM-1 is co-recruited to ICAM-1/LFA-1-mediated docking structures as a result of both VCAM-1 and ICAM-1 being components of the EAP. The same argument is applicable to the recruitment of ICAM-1 into VCAM-1/VLA-4 induced docking structures.

Remarkably, our data show that CD9 mobility is more strongly affected by the engagement of ICAM-1, while CD151 is more affected by engagement of VCAM-1, confirming the results of previous biochemical analyses, in which ICAM-1 preferentially associated with CD9 and VCAM-1 associated with CD151 (Barreiro et al., 2005). FRET analysis confirmed a degree of specificity inside the preexisting EAP prior to leukocyte binding. The preferential interactions of ICAM-1 with CD9 and VCAM-1 with CD151 are evident in the FRETeff for these pairs, which are close to those of tetraspanin pairs, even though in tetraspanin-partner interactions there are fewer obstacles that can reduce FRETeff.

The diffusional analyses by FCS complemented the FRAP data. Thus, FRAP provided a general view of diffusion within EAP in the presence or absence of adherent leukocytes and in comparison with lipid rafts at a microscopic level, and FCS allowed us to move toward the nanoscopic scale to precisely determine diffusion coefficients of EAP proteins at the single-molecule level. The amounts of exogenously expressed fluorescently-labeled proteins on the surface of cells used for FCS and FCCS analyses was negligible compared with the corresponding endogenous proteins, assuming that there were no alterations in dynamic behaviour due to increased molecular density at the membrane. However, the existence of a mixture of endogenous and exogenous

protein populations precludes determination of the stoichiometry of submicron-size endothelial tetraspanin domains, even though the FCCS studies did provide insights into the lifespan of tetraspanin-partner complexes.

In conclusion, this study performed with this particular type of TEM from the apical membrane of endothelium constitutes the first description of tetraspanin microdomains as physical entities in living cells, with dynamic features that clearly differ from lipid rafts.

### **Regulation of the avidity of endothelial adhesion receptors by their inclusion in tetraspanin-enriched endothelial adhesive platforms**

It is a common error to assume that the demonstration of co-localization of molecules at the microscopic level provides irrefutable evidence of spatial association; the optical resolution limit of classical confocal fluorescence microscopy techniques falls far short that required to identify molecular interactions that take place over a distance of few nanometers. Our data from advanced microscopy techniques demonstrate that the co-localization of two tetraspanins and two receptors at the nude endothelial apical plasma membrane and at specialized adhesive structures does indeed correspond to highly specific and organized interactions among them. Furthermore, this organization confers the appropriate spatial distribution for ICAM-1 and VCAM-1 receptors to exert their efficient adhesion functions.

The regulation of leukocyte integrin activity has been extensively characterized. These proteins can be regulated by conformational changes (affinity) and/or clustering at the plasma membrane (avidity) (Carman and Springer, 2003; Luo et al., 2007). In contrast, no regulatory mechanism, apart from the transcriptional level, has been described previously for the adhesive function of endothelial integrin ligands (Collins

et al., 1995). Our study thus provides novel insights into adhesion receptor regulation, showing how the insertion of two key endothelial receptors, ICAM-1 and VCAM-1, into tetraspanin-enriched microdomains promotes the homo- and hetero-clustering of both molecules at the contact area with the adhered leukocyte, independently of ligand binding and actin cytoskeleton anchorage. The tetraspanin-mediated clustering of endothelial receptors enhances firm adhesion, since disturbance of interactions using tetraspanin blocking peptides or alteration in composition by tetraspanin knock-down decreases the adhesive properties of VCAM-1 and ICAM-1 in transendothelial migration experiments performed under flow conditions and in detachment experiments under increasing shear flows (Barreiro et al., 2005). Whether ICAM-1 or VCAM-1 can undergo any conformational alteration due to their interaction with tetraspanins remains undetermined, in the absence of appropriate reagents to tackle this possibility.

The ability of tetraspanins to mediate the homo- and hetero-clustering of adhesion receptors, which is enhanced by integrin engagement, arises from their ability to laterally associate with each other and with non-tetraspanin partners simultaneously. Therefore, CD9 could promote ICAM-1 homo-avidity by interacting with other CD9 molecules bound to this receptor, whereas CD151 could reproduce the same effect with VCAM-1. Then, the hetero-clustering of ICAM-1 and VCAM-1 could be explained by the interaction of CD9 with CD151. The involvement of other tetraspanins in these organized microdomains cannot be ruled out; indeed, we have observed the inclusion of tetraspanin CD81 at EAP (Barreiro et al., unpublished observations). Conceptually, endothelial receptor homo-avidity would be similar to the avidity phenomenon described for their counter-receptors, the integrins  $\alpha4\beta1$ -VLA-4 (for VCAM-1) and  $\alpha L\beta2$ -LFA-1 (for ICAM-1) integrins. In fact, a role has been reported for CD81 as homeostatic avidity facilitator of multivalent VLA-4 strengthening in the adhesion to

VCAM-1 (Feigelson et al., 2003). Therefore, it is also conceivable that such tetraspanin-mediated co-organization of specific VLA-4 and LFA-1 integrin subsets takes place within leukocyte membranes. Furthermore, the novel concept of hetero-clustering raised here for VCAM-1 and ICAM-1 can be envisaged as a kind of tetraspanin-mediated cross-talk between adhesion receptors; that is, a cellular mechanism to spatio-temporally organize molecules with similar characteristics and functions so as to facilitate their efficient co-ordinated action in critical processes such as extravasation, which occurs over a short time-frame. Moreover, VCAM-1 and ICAM-1 are unlikely to be the only receptors inserted in these tetraspanin microdomains at the apical endothelial plasma membrane; we have also identified other adhesion proteins such as CD44, PECAM-1 and, more importantly, E-selectin in association with EAP (Barreiro et al., unpublished observations). These organized membrane microdomains thus appear to integrate a plethora of adhesion receptors involved in subsequent steps of the extravasation process, and for this reason we have named them endothelial adhesive platforms. These organized platforms are dynamic, since they coalesce or diverge depending on the stimuli received (ligand engagement by tetraspanin partners, and so on).

In sum, our data clearly demonstrate that tetraspanin microdomains account for the specific recruitment of endothelial adhesion receptors to the leukocyte contact area, providing a mechanism to increase avidity at these sites and enhance firm adhesion. This constitutes a novel supramolecular level of regulation in the function of VCAM-1 and ICAM-1 endothelial receptors not envisaged previously for integrin ligands. In the light of these observations, new pharmacological agents that could specifically prevent the interaction of tetraspanin with endothelial adhesion receptors *in vivo* could

constitute novel therapeutical strategies for the treatment of chronic inflammatory and autoimmune diseases.

## **CONCLUSIONS**

- 1.** Endothelial adhesion receptors ICAM-1 and VCAM-1 together with the actin-cytoskeleton and related proteins such as ezrin, moesin,  $\alpha$ -actinin, vinculin and VASP, participate in the formation of a three-dimensional structure that arises from the apical surface of activated endothelial cells to partially embraced and firmly attached adherent lymphocytes, preventing their detachment under physiological hemodynamic conditions. The formation of this cup-like structure is regulated by Rho/ROCK pathway and phosphoinositide PIP<sub>2</sub>.
- 2.** Tetraspanin proteins CD9 and CD151 laterally associate with ICAM-1 and VCAM-1 at the plasma membrane, co-localizing with these adhesion receptors at the endothelial docking structures. The insertion of ICAM-1 and VCAM-1 in tetraspanin microdomains is crucial for the proper adhesive properties of these endothelial receptors.
- 3.** The co-recruitment of ICAM-1 and VCAM-1 adhesion receptors to the docking structures in the absence of ligand engagement, actin anchorage and heterodimer formation, can be explain due to the existence of specific interactions within the tetraspanin microdomains (ICAM-1/CD9, VCAM-1/CD151, CD9/CD151).
- 4.** The biophysical properties of tetraspanin and adhesion receptors demonstrate the existence of these organized microdomains containing CD9, CD151, ICAM-1 and VCAM-1 at the apical plasma membrane of living endothelial cells. This particular kind of microdomains, which presents diffusional properties different from those of lipid rafts, has been termed endothelial adhesive platform.

**5.** Endothelial adhesive platform-induced nanoclustering of VCAM-1 and ICAM-1 represents a novel mechanism of supramolecular organization that regulates the efficient leukocyte integrin-binding capacity of both endothelial receptors.

## **CONCLUSIONES**

- 1.** Los receptores endoteliales de adhesión ICAM-1 y VCAM-1 junto con el citoesqueleto de actina y proteínas relacionadas, tales como ezrina, moesina,  $\alpha$ -actinina, vinculina y VASP, participan en la formación de una estructura tridimensional que emerge de la superficie apical de las células endoteliales activadas para rodear parcialmente y adherir firmemente a los linfocitos, impidiendo su desunión en condiciones hemodinámicas fisiológicas. La formación de esta estructura con forma de copa está regulada por la ruta de señalización Rho/ROCK y el fosfoinosítido PIP<sub>2</sub>.
- 2.** Las tetraspaninas CD9 y CD151 colocalizan con ICAM-1 y VCAM-1 en las estructuras endoteliales de anclaje, asociándose lateralmente a estos receptores en la membrana plasmática. La integración de ICAM-1 y VCAM-1 en microdominios de tetraspaninas es necesaria para el correcto funcionamiento adherente de estos receptores endoteliales.
- 3.** El co-reclutamiento de los receptores de adhesión ICAM-1 y VCAM-1 a las estructuras de anclaje en ausencia de ligando, unión a actina y formación de heterodímeros, puede ser explicado por la existencia de interacciones específicas dentro de los microdominios de tetraspaninas (ICAM-1/CD9, VCAM-1/CD151, CD9/CD151).
- 4.** Las propiedades biofísicas de las tetraspaninas y los receptores de adhesión demuestran la existencia de microdominios organizados en la membrana apical de células endoteliales vivas que contienen CD9, CD151, ICAM-1 y VCAM-1. Este tipo particular

de microdominios presenta propiedades difusivas diferentes a las de las balsas lipídicas, por lo que se les ha denominado “plataformas endoteliales adherentes”.

**5.** La distribución espacial nanométrica de VCAM-1 e ICAM-1 inducida por las plataformas endoteliales adherentes representa un nuevo mecanismo de organización supramolecular que regula la eficiente capacidad de unión a integrinas leucocitarias de ambos receptores endoteliales.

## REFERENCES

- Acevedo, A., M.A. del Pozo, A.G. Arroyo, P. Sanchez-Mateos, R. Gonzalez-Amaro, and F. Sanchez-Madrid. 1993. Distribution of ICAM-3-bearing cells in normal human tissues. Expression of a novel counter-receptor for LFA-1 in epidermal Langerhans cells. *Am J Pathol.* 143:774-83.
- Alon, R., P.D. Kassner, M.W. Carr, E.B. Finger, M.E. Hemler, and T.A. Springer. 1995. The integrin VLA-4 supports tethering and rolling in flow on VCAM-1. *J Cell Biol.* 128:1243-53.
- Alon, R. 2001. Encephalitogenic lymphoblast recruitment to resting CNS microvasculature: a natural immunosurveillance mechanism? *J Clin Invest.* 108:517-9.
- Alon, R., and S. Feigelson. 2002. From rolling to arrest on blood vessels: leukocyte tap dancing on endothelial integrin ligands and chemokines at sub-second contacts. *Sem. Immunol.* 14:93-104.
- Alon, R., V. Grabovsky, and S. Feigelson. 2003. Chemokine induction of integrin adhesiveness on rolling and arrested leukocytes local signaling events or global stepwise activation? *Microcirculation.* 10:297-311.
- Allen, L.A., and A. Aderem. 1996. Molecular definition of distinct cytoskeletal structures involved in complement- and Fc receptor-mediated phagocytosis in macrophages. *J Exp Med.* 184:627-37.
- Amieva, M.R., P. Litman, L. Huang, E. Ichimaru, and H. Furthmayr. 1999. Disruption of dynamic cell surface architecture of NIH3T3 fibroblasts by the N-terminal domains of moesin and ezrin: in vivo imaging with GFP fusion proteins. *J Cell Sci.* 112:111-25.
- Anderson, R.G., and K. Jacobson. 2002. A role for lipid shells in targeting proteins to caveolae, rafts, and other lipid domains. *Science.* 296:1821-5.
- Andre, M., J.P. Le Caer, C. Greco, S. Planchon, W. El Nemer, C. Boucheix, E. Rubinstein, J. Chamot-Rooke, and F. Le Naour. 2006. Proteomic analysis of the tetraspanin web using LC-ESI-MS/MS and MALDI-FTICR-MS. *Proteomics.* 6:1437-49.
- Aplin, A.E., A. Howe, S.K. Alahari, and R.L. Juliano. 1998. Signal transduction and signal modulation by cell adhesion receptors: the role of integrins, cadherins, immunoglobulin-cell adhesion molecules, and selectins. *Pharmacol Rev.* 50:197-263.
- Arpin, M., M. Algrain, and D. Louvard. 1994. Membrane-actin microfilament connections: an increasing diversity of players related to band 4.1. *Curr Opin Cell Biol.* 6:136-41.
- Banks, D.S., and C. Fradin. 2005. Anomalous diffusion of proteins due to molecular crowding. *Biophys J.* 89:2960-71.
- Barreiro, O., M. Yanez-Mo, J.M. Serrador, M.C. Montoya, M. Vicente-Manzanares, R. Tejedor, H. Furthmayr, and F. Sanchez-Madrid. 2002. Dynamic interaction of VCAM-1 and ICAM-1 with moesin and ezrin in a novel endothelial docking structure for adherent leukocytes. *J Cell Biol.* 157:1233-45.
- Barreiro, O., M. Vicente-Manzanares, A. Urzainqui, M. Yanez-Mo, and F. Sanchez-Madrid. 2004. Interactive protrusive structures during leukocyte adhesion and transendothelial migration. *Front Biosci.* 9:1849-63.
- Barreiro, O., M. Yanez-Mo, M. Sala-Valdes, M.D. Gutierrez-Lopez, S. Ovalle, A. Higginbottom, P.N. Monk, C. Cabanas, and F. Sanchez-Madrid. 2005.

- Endothelial tetraspanin microdomains regulate leukocyte firm adhesion during extravasation. *Blood*. 105:2852-61.
- Barret, C., C. Roy, P. Montcourrier, P. Mangeat, and V. Niggli. 2000. Mutagenesis of the phosphatidylinositol 4,5-bisphosphate (PIP(2)) binding site in the NH(2)-terminal domain of ezrin correlates with its altered cellular distribution. *J Cell Biol*. 151:1067-79.
- Beglova, N., S.C. Blacklow, J. Takagi, and T.A. Springer. 2002. Cysteine-rich module structure reveals a fulcrum for integrin rearrangement upon activation. *Nat Struct Biol*. 9:282-7.
- Benjamini, Y., and Y. Hochberg. 1995. Controlling the false discovery rate: a practical and powerful approach to multiple testing. *J. R. Statist. Soc. B.* 57: 289 – 300.
- Berdichevski, F., K.F. Tolias, K. Wong, C.L. Carpenter, and M.E. Hemler. 1997. A novel link between integrins, transmembrane-4 superfamily proteins (CD63 and CD81), and phosphatidylinositol 4-kinase. *J Biol Chem*. 272:2595-8.
- Berdichevski, F. 2001. Complexes of tetraspanins with integrins: more than meets the eye. *J Cell Sci*. 114:4143-51.
- Berdichevski, F., E. Odintsova, S. Sawada, and E. Gilbert. 2002. Expression of the palmitoylation-deficient CD151 weakens the association of alpha 3 beta 1 integrin with the tetraspanin-enriched microdomains and affects integrin-dependent signaling. *J Biol Chem*. 277:36991-7000.
- Berdichevski, F., and E. Odintsova. 2007. Tetraspanins as regulators of protein trafficking. *Traffic*. 8:89-96.
- Berlin, C., E.L. Berg, M.J. Briskin, D.P. Andrew, P.J. Kilshaw, B. Holzmann, I.L. Weissman, A. Hamann, and E.C. Butcher. 1993. Alpha 4 beta 7 integrin mediates lymphocyte binding to the mucosal vascular addressin MAdCAM-1. *Cell*. 74:185-95.
- Berlin, C., R.F. Bargatze, J.J. Campbell, U.H. von Andrian, M.C. Szabo, S.R. Hasslen, R.D. Nelson, E.L. Berg, S.L. Erlandsen, and E.C. Butcher. 1995. alpha 4 integrins mediate lymphocyte attachment and rolling under physiologic flow. *Cell*. 80:413-22.
- Botelho, R.J., M. Teruel, R. Dierckman, R. Anderson, A. Wells, J.D. York, T. Meyer, and S. Grinstein. 2000. Localized biphasic changes in phosphatidylinositol-4,5-bisphosphate at sites of phagocytosis. *J Cell Biol*. 151:1353-1367.
- Boucheix, C., and E. Rubinstein. 2001. Tetraspanins. *Cell Mol Life Sci*. 58:1189-205.
- Bretscher, A., D. Chambers, R. Nguyen, and D. Reczek. 2000. ERM-Merlin and EBP50 protein families in plasma membrane organization and function. *Annu Rev Cell Dev Biol*. 16:113-43.
- Butcher, E.C. 1991. Leukocyte-endothelial cell recognition: three (or more) steps to specificity and diversity. *Cell*. 67:1033-6.
- Butcher, E.C., and L.J. Picker. 1996. Lymphocyte homing and homeostasis. *Science*. 272:60-66.
- Cabanas, C., and N. Hogg. 1993. Ligand intercellular adhesion molecule 1 has a necessary role in activation of integrin lymphocyte function-associated molecule 1. *Proc Natl Acad Sci U S A*. 90:5838-42.
- Caiolfa, V.R., M. Zamai, G. Malengo, A. Andolfo, C.D. Madsen, J. Sutin, M. Digman, E. Gratton, F. Blasi, and N. Sidenius. 2007. Monomer-dimer dynamics and distribution of GPI-anchored uPAR are determined by cell surface protein assemblies. *J Cell Biol*.

- Cairo, C.W., R. Mirchev, and D.E. Golan. 2006. Cytoskeletal regulation couples LFA-1 conformational changes to receptor lateral mobility and clustering. *Immunity*. 25:297-308.
- Cambi, A., B. Joosten, M. Koopman, F. de Lange, I. Beeren, R. Torensma, J.A. Fransen, M. Garcia-Parajo, F.N. van Leeuwen, and C.G. Figdor. 2006. Organization of the integrin LFA-1 in nanoclusters regulates its activity. *Mol Biol Cell*. 17:4270-81.
- Campbell, J.J., J. Hedrick, A. Zlotnik, M.A. Siani, D.A. Thompson, and E.C. Butcher. 1998. Chemokines and the arrest of lymphocytes rolling under flow conditions. *Science*. 279:381-384.
- Campbell, R.E., O. Tour, A.E. Palmer, P.A. Steinbach, G.S. Baird, D.A. Zacharias, and R.Y. Tsien. 2002. A monomeric red fluorescent protein. *Proc Natl Acad Sci U S A*. 99:7877-82.
- Carlos, T.M., A. Dobrina, R. Ross, and J.M. Harlan. 1990. Multiple receptors on human monocytes are involved in adhesion to cultured human endothelial cells. *J Leukoc Biol*. 48:451-6.
- Carlos, T.M., and J.M. Harlan. 1994. Leukocyte-endothelial adhesion molecules. *Blood*. 84:2068-2101.
- Carman, C.V., and T.A. Springer. 2003. Integrin avidity regulation: are changes in affinity and conformation underemphasized? *Curr Opin Cell Biol*. 15:547-56.
- Carman, C.V., and T.A. Springer. 2004. A transmigratory cup in leukocyte diapedesis both through individual vascular endothelial cells and between them. *J Cell Biol*. 167:377-88.
- Carman, C.V., P.T. Sage, T.E. Sciuto, M.A. de la Fuente, R.S. Geha, H.D. Ochs, H.F. Dvorak, A.M. Dvorak, and T.A. Springer. 2007. Transcellular diapedesis is initiated by invasive podosomes. *Immunity*. 26:784-97.
- Caron, E., and A. Hall. 1998. Identification of two distinct mechanisms of phagocytosis controlled by different Rho GTPases. *Science*. 282:1717-1721.
- Carter, R.A., and I.P. Wicks. 2001. Vascular Cell Adhesion Molecule 1 (CD 106). A multifaceted regulator of joint inflammation. *Arthritis Rheum*. 44:985-994.
- Castellano, F., C. Le Clainche, D. Patin, M. Carlier, and P. Chavrier. 2001. A WASp-VASP complex regulates actin polymerization at the plasma membrane. *EMBO J*. 20:5603-14.
- Cinamon, G., V. Shinder, and R. Alon. 2001. Shear forces promote lymphocyte migration across vascular endothelium bearing apical chemokines. *Nat Immunol*. 2:515-522.
- Claas, C., C.S. Stipp, and M.E. Hemler. 2001. Evaluation of prototype transmembrane 4 superfamily protein complexes and their relation to lipid rafts. *J Biol Chem*. 276:7974-84.
- Clayton, A., R.A. Evans, E. Pettit, M. Hallett, J.D. Williams, and R. Steadman. 1998. Cellular activation through the ligation of intercellular adhesion molecule-1. *J Cell Sci*. 111:443-453.
- Clayton, A.H., Q.S. Hanley, and P.J. Verveer. 2004. Graphical representation and multicomponent analysis of single-frequency fluorescence lifetime imaging microscopy data. *J Microsc*. 213:1-5.
- Collins, T., M.A. Read, A.S. Neish, M.Z. Whitley, D. Thanos, and T. Maniatis. 1995. Transcriptional regulation of endothelial cell adhesion molecules: NF-kappa B and cytokine-inducible enhancers. *Faseb J*. 9:899-909.
- Constantin, G., M. Majeed, C. Giagulli, L. Piccio, J.Y. Kim, E.C. Butcher, and C. Laudanna. 2000. Chemokines trigger immediate beta2 integrin affinity and

- mobility changes: differential regulation and roles in lymphocyte arrest under flow. *Immunity*. 13:759-69.
- Cook-Mills, J.M. 2002. VCAM-1 signals during lymphocyte migration: role of reactive oxygen species. *Mol Immunol*. 39:499-508.
- Cox, D., C.C. Tseng, G. Bjekic, and S. Greenberg. 1999. A requirement for phosphatidylinositol 3-kinase in pseudopod extension. *J Biol Chem*. 274:1240-7.
- Cunningham, S.A., J.M. Rodriguez, M.P. Arrate, T.M. Tran, and T.A. Brock. 2002. JAM2 interacts with alpha4beta1. Facilitation by JAM3. *J Biol Chem*. 277:27589-92.
- Cybulsky, M.I., K. Iiyama, H. Li, S. Zhu, M. Chen, M. Iiyama, V. Davis, J.C. Gutierrez-Ramos, P.W. Connelly, and D.S. Milstone. 2001. A major role for VCAM-1, but not ICAM-1, in early atherosclerosis. *J Clin Invest*. 107:1255-1262.
- Charrin, S., S. Manie, M. Oualid, M. Billard, C. Boucheix, and E. Rubinstein. 2002. Differential stability of tetraspanin/tetraspanin interactions: role of palmitoylation. *FEBS Lett*. 516:139-44.
- Charrin, S., S. Manie, C. Thiele, M. Billard, D. Gerlier, C. Boucheix, and E. Rubinstein. 2003. A physical and functional link between cholesterol and tetraspanins. *Eur J Immunol*. 33:2479-89.
- Chattopadhyay, N., Z. Wang, L.K. Ashman, S.M. Brady-Kalnay, and J.A. Kreidberg. 2003. alpha3beta1 integrin-CD151, a component of the cadherin-catenin complex, regulates PTPmu expression and cell-cell adhesion. *J Cell Biol*. 163:1351-62.
- Chavakis, T., A. Bierhaus, N. Al-Fakhri, D. Schneider, S. Witte, T. Linn, M. Nagashima, J. Morser, B. Arnold, K.T. Preissner, and P.P. Nawroth. 2003. The pattern recognition receptor (RAGE) is a counterreceptor for leukocyte integrins: a novel pathway for inflammatory cell recruitment. *J Exp Med*. 198:1507-15.
- Cherukuri, A., T. Shoham, H.W. Sohn, S. Levy, S. Brooks, R. Carter, and S.K. Pierce. 2004. The tetraspanin CD81 is necessary for partitioning of coligated CD19/CD21-B cell antigen receptor complexes into signaling-active lipid rafts. *J Immunol*. 172:370-80.
- Chimini, G., and P. Chavrier. 2000. Function of Rho family proteins in actin dynamics during phagocytosis and engulfment. *Nat Cell Biol*. 2:E191-6.
- Defacque, H., M. Egeberg, A. Habermann, M. Diakonova, C. Roy, P. Mangeat, W. Voelter, G. Marriot, J. Pfannstiel, H. Faulstich, and G. Griffiths. 2000. Involvement of ezrin/moesin in de novo actin assembly on phagosomal membranes. *EMBO J*. 19:199-212.
- del Pozo, M.A., P. Sanchez-Mateos, M. Nieto, and F. Sanchez-Madrid. 1995. Chemokines regulate cellular polarization and adhesion receptor redistribution during lymphocyte interaction with endothelium and extracellular matrix. Involvement of cAMP signaling pathway. *J Cell Biol*. 131:495-508.
- del Pozo, M.A., P. Sanchez-Mateos, and F. Sanchez-Madrid. 1996. Cellular polarization induced by chemokines: a mechanism for leukocyte recruitment? *Immunol Today*. 17:127-31.
- Delaguillaumie, A., J. Harriague, S. Kohanna, G. Bismuth, E. Rubinstein, M. Seigneuret, and H. Conjeaud. 2004. Tetraspanin CD82 controls the association of cholesterol-dependent microdomains with the actin cytoskeleton in T lymphocytes: relevance to co-stimulation. *J Cell Sci*. 117:5269-82.

- Dobereiner, H.G., B.J. Dubin-Thaler, J.M. Hofman, H.S. Xenias, T.N. Sims, G. Giannone, M.L. Dustin, C.H. Wiggins, and M.P. Sheetz. 2006. Lateral membrane waves constitute a universal dynamic pattern of motile cells. *Phys Rev Lett.* 97:038102.
- Doi, Y., M. Itoh, S. Yonemura, S. Ishihara, H. Takano, T. Noda, and S. Tsukita. 1999. Normal development of mice and unimpaired cell adhesion/cell motility/actin-based cytoskeleton without compensatory up-regulation of ezrin or radixin in moesin gene knockout. *J Biol Chem.* 274:2315-21.
- Dominguez-Jimenez, C., M. Yáñez-Mó, A. Carreira, R. Tejedor, R. Gonzalez-Amaro, V. Alvarez, and F. Sánchez-Madrid. 2001. Involvement of  $\alpha 3$  integrin/tetraspanin complexes in the angiogenic response induced by angiotensin II. *FASEB J.* 15.
- Drbal, K., P. Angelisova, A. Rasmussen, I. Hilgert, S. Funderud, and V. Horejsi. 1999. The nature of the subset of MHC class II molecules carrying the CDw78 epitopes. *Int Immunol.* 11:491-498.
- Dustin, M.L., R. Rothlein, A.K. Bhan, C.A. Dinarello, and T.A. Springer. 1986. Induction by IL-1 and interferon-gamma: tissue distribution, biochemistry, and function of a natural adherence molecule (ICAM-1). *J Immunol.* 137:245-54.
- Dwir, O., G.S. Kansas, and R. Alon. 2001. Cytoplasmic anchorage of L-selectin controls leukocyte capture and rolling by increasing the mechanical stability of the selectin tether. *J Cell Biol.* 155:145-56.
- Elices, M.J., L. Osborn, Y. Takada, C. Crouse, S. Luhowskyj, M.E. Hemler, and R.R. Lobb. 1990. VCAM-1 on activated endothelium interacts with the leukocyte integrin VLA-4 at a site distinct from the VLA-4/fibronectin binding site. *Cell.* 60:577-84.
- Engelhardt, B., and H. Wolburg. 2004. Mini-review: Transendothelial migration of leukocytes: through the front door or around the side of the house? *Eur J Immunol.* 34:2955-63.
- Etienne-Manneville, S., J.B. Manneville, P. Adamson, B. Wilbourn, J. Greenwood, and P.O. Couraud. 2000. ICAM-1-coupled cytoskeletal rearrangements and transendothelial lymphocyte migration involve intracellular calcium signaling in brain endothelial cell lines. *J Immunol.* 165:3375-83.
- Evans, E.A., and D.A. Calderwood. 2007. Forces and bond dynamics in cell adhesion. *Science.* 316:1148-53.
- Fagerholm, S.C., T.J. Hilden, S.M. Nurmi, and C.G. Gahmberg. 2005. Specific integrin alpha and beta chain phosphorylations regulate LFA-1 activation through affinity-dependent and -independent mechanisms. *J Cell Biol.* 171:705-15.
- Faveeuw, C., M.E. Di Mauro, A.A. Price, and A. Ager. 2000. Roles of alpha(4) integrins/VCAM-1 and LFA-1/ICAM-1 in the binding and transendothelial migration of T lymphocytes and T lymphoblasts across high endothelial venules. *Int Immunol.* 12:241-51.
- Feigelson, S.W., V. Grabovsky, R. Shamri, S. Levy, and R. Alon. 2003. The CD81 tetraspanin facilitates instantaneous leukocyte VLA-4 adhesion strengthening to vascular cell adhesion molecule 1 (VCAM-1) under shear flow. *J Biol Chem.* 278:51203-12.
- Frenette, P.S., and D.D. Wagner. 1996a. Adhesion molecules--Part I. *N Engl J Med.* 334:1526-9.
- Frenette, P.S., and D.D. Wagner. 1996b. Adhesion molecules---Part II: Blood vessels and blood cells. *N Engl J Med.* 335:43-5.

- Fujita, Y., T. Shiomi, S. Yanagimoto, H. Matsumoto, Y. Toyama, and Y. Okada. 2006. Tetraspanin CD151 is expressed in osteoarthritic cartilage and is involved in pericellular activation of pro-matrix metalloproteinase 7 in osteoarthritic chondrocytes. *Arthritis Rheum.* 54:3233-43.
- Gahmberg, C.G., P. Nortamo, C. Kantor, M. Autero, P. Kotovuori, L. Hemio, R. Salcedo, and M. Patarroyo. 1990. The pivotal role of the Leu-CAM and ICAM molecules in human leukocyte adhesion. *Cell Differ Dev.* 32:239-45.
- Garcia-Lopez, M.A., O. Barreiro, A. Garcia-Diez, F. Sanchez-Madrid, and P.F. Penas. 2005. Role of tetraspanins CD9 and CD151 in primary melanocyte motility. *J Invest Dermatol.* 125:1001-9.
- Geiger, B., and A. Bershadsky. 2002. Exploring the neighborhood: adhesion-coupled cell mechanosensors. *Cell.* 110:139-42.
- Gordon-Alonso, M., M. Yanez-Mo, O. Barreiro, S. Alvarez, M.A. Munoz-Fernandez, A. Valenzuela-Fernandez, and F. Sanchez-Madrid. 2006. Tetraspanins CD9 and CD81 modulate HIV-1-induced membrane fusion. *J Immunol.* 177:5129-37.
- Grabovsky, V., S. Feigelson, C. Chen, D.A. Bleijs, A. Peled, G. Cinamon, F. Baleux, F. Arenzana-Seisdedos, T. Lapidot, Y. van Kooyk, R.R. Lobb, and R. Alon. 2000. Subsecond induction of alpha4 integrin clustering by immobilized chemokines stimulates leukocyte tethering and rolling on endothelial vascular cell adhesion molecule 1 under flow conditions. *J Exp Med.* 192:495-506.
- Gratton, E., D.M. Jameson, and R.D. Hall. 1984. Multifrequency phase and modulation fluorometry. *Annu Rev Biophys Bioeng.* 13:105-24.
- Gray, A., J. van der Kaay, and C.P. Downes. 1999. The pleckstrin homology domains of protein kinase B and GRP1 (general receptor for phosphoinositides-1) are sensitive and selective probes for the cellular detection of phosphatidylinositol 3,4-bisphosphate and/or phosphatidylinositol 3,4,5-triphosphate in vivo. *Biochem J.* 344:929-936.
- Greenwood, J., S. Etienne-Manneville, P. Adamson, and P.O. Couraud. 2002. Lymphocyte migration into the central nervous system: implication of ICAM-1 signalling at the blood-brain barrier. *Vascul Pharmacol.* 38:315-22.
- Gutierrez-Lopez, M.D., S. Ovalle, M. Yáñez-Mó, N. Sánchez-Sánchez, E. Rubinstein, N. Olmo, M.A. Lizarbe, F. Sánchez-Madrid, and C. Cabañas. 2003. A functionally relevant conformational epitope on the CD9 tetraspanin depends on the association with activated beta-1 integrin. *J Biol Chem.* 278:208-218.
- Hakomori, S.I. 2002. Inaugural Article: The glycosynapse. *Proc Natl Acad Sci U S A.* 99:225-32.
- Hayashi, K., S. Yonemura, T. Matsui, and S. Tsukita. 1999. Immunofluorescence detection of ezrin/radixin/moesin (ERM) proteins with their carboxyl-terminal threonine phosphorylated in cultured cells and tissues. *J Cell Sci.* 112:1149-58.
- Heiska, L., K. Alfthan, M. Gronholm, P. Vilja, A. Vaheri, and O. Carpen. 1998. Association of ezrin with intercellular adhesion molecule-1 and -2 (ICAM-1 and ICAM-2). Regulation by phosphatidylinositol 4, 5- bisphosphate. *J Biol Chem.* 273:21893-900.
- Helander, T.S., O. Carpen, O. Turunen, P.E. Kovanen, A. Vaheri, and T. Timonen. 1996. ICAM-2 redistributed by ezrin as a target for killer cells. *Nature.* 382:265-8.
- Hemler, M.E. 2001. Specific tetraspanin functions. *J Cell Biol.* 155:1103-7.
- Hemler, M.E. 2003. Tetraspanin proteins mediate cellular penetration, invasion, and fusion events and define a novel type of membrane microdomain. *Annu Rev Cell Dev Biol.* 19:397-422.

- Hemler, M.E. 2005. Tetraspanin functions and associated microdomains. *Nat Rev Mol Cell Biol.* 6:801-11.
- Henderson, R.B., L.H.K. Lim, P.A. Tessier, F.N.E. Gavins, M. Mathies, M. Perreti, and N. Hogg. 2001. The use of Lymphocyte Function-associated Antigen (LFA-1)-deficient mice to determine the role of LFA-1, Mac-1 and  $\alpha 4$  integrin in the inflammatory response of neutrophils. *J. Exp. Med.* 194:219-226.
- Higashiyama, S., R. Iwamoto, K. Goishi, G. Raab, N. Taniguchi, M. Klagsbrun, and E. Mekada. 1995. The membrane protein CD9/DRAP 27 potentiates the juxtacrine growth factor activity of the membrane-anchored heparin-binding EGF-like growth factor. *J Cell Biol.* 128:929-38.
- Higginbottom, A., Y. Takahashi, L. Bolling, S.A. Coonrod, J.M. White, L.J. Partridge, and P.N. Monk. 2003. Structural requirements for the inhibitory action of the CD9 large extracellular domain in sperm/oocyte binding and fusion. *Biochem Biophys Res Commun.* 311:208-214.
- Hirao, M., N. Sato, T. Kondo, S. Yonemura, M. Monden, T. Sasaki, Y. Takai, and S. Tsukita. 1996. Regulation mechanism of ERM (ezrin/radixin/moesin) protein/plasma membrane association: possible involvement of phosphatidylinositol turnover and Rho-dependent signaling pathway. *J Cell Biol.* 135:37-51.
- Ho, S.H., F. Martin, A. Higginbottom, L.J. Partridge, V. Parthasarathy, G.W. Moseley, P. Lopez, C. Cheng-Mayer, and P.N. Monk. 2006. Recombinant extracellular domains of tetraspanin proteins are potent inhibitors of the infection of macrophages by human immunodeficiency virus type 1. *J Virol.* 80:6487-96.
- Hogg, N., M. Laschinger, K. Giles, and A. McDowall. 2003. T-cell integrins: more than just sticking points. *J Cell Sci.* 116:4695-705.
- Hong, I.K., Y.M. Kim, D.I. Jeoung, K.C. Kim, and H. Lee. 2005. Tetraspanin CD9 induces MMP-2 expression by activating p38 MAPK, JNK and c-Jun pathways in human melanoma cells. *Exp Mol Med.* 37:230-9.
- Hong, I.K., Y.J. Jin, H.J. Byun, D.I. Jeoung, Y.M. Kim, and H. Lee. 2006. Homophilic interactions of Tetraspanin CD151 up-regulate motility and matrix metalloproteinase-9 expression of human melanoma cells through adhesion-dependent c-Jun activation signaling pathways. *J Biol Chem.* 281:24279-92.
- Hordijk, P.L. 2003. Endothelial signaling in leukocyte transmigration. *Cell Biochem Biophys.* 38:305-22.
- Hubbard, A.K., and R. Rothlein. 2000. Intercellular adhesion molecule-1 (ICAM-1) expression and cell signaling cascades. *Free Radic Biol Med.* 28:1379-1386.
- Hynes, R.O. 2002. Integrins: bidirectional, allosteric signaling machines. *Cell.* 110:673-87.
- Ivetic, A., J. Deka, A.J. Ridley, and A. Ager. 2002. The cytoplasmic tail of L-selectin interacts with members of the Ezrin-Radixin-Moesin (ERM) family of proteins: cell activation-dependent binding of Moesin but not Ezrin. *J Biol Chem.* 277:2321-9.
- Jun, C.D., M. Shimaoka, C.V. Carman, J. Takagi, and T.A. Springer. 2001. Dimerization and the effectiveness of ICAM-1 in mediating LFA-1-dependent adhesion. *Proc Natl Acad Sci U S A.* 98:6830-5.
- Kadono, T., G.M. Venturi, D.A. Steeber, and T.F. Tedder. 2002. Leukocyte rolling velocities and migration are optimized by cooperative L-selectin and intercellular adhesion molecule-1 functions. *J Immunol.* 169:4542-50.

- Kenworthy, A.K., B.J. Nichols, C.L. Remmert, G.M. Hendrix, M. Kumar, J. Zimmerberg, and J. Lippincott-Schwartz. 2004. Dynamics of putative raft-associated proteins at the cell surface. *J Cell Biol.* 165:735-46.
- Koni, P.A., S.K. Joshi, U.A. Temann, D. Olson, L. Burkly, and R.A. Flavell. 2001. Conditional vascular cell adhesion molecule 1 deletion in mice: impaired lymphocyte migration to bone marrow. *J Exp Med.* 193:741-753.
- Kovalenko, O.V., D.G. Metcalf, W.F. DeGrado, and M.E. Hemler. 2005. Structural organization and interactions of transmembrane domains in tetraspanin proteins. *BMC Struct Biol.* 5:11.
- Kovalenko, O.V., X.H. Yang, and M.E. Hemler. 2007. A novel cysteine crosslinking method reveals a direct association between claudin-1 and tetraspanin CD9. *Mol Cell Proteomics.*
- Kropshofer, H., S. Spindeldreher, T.A. Rohn, N. Platania, C. Grygar, N. Daniel, A. Wolpl, H. Langen, V. Horejsi, and A.B. Vogt. 2002. Tetraspan microdomains distinct from lipid rafts enrich select peptide- MHC class II complexes. *Nat Immunol.* 3:61-8.
- Lamagna, C., P. Meda, G. Mandicourt, J. Brown, R.J. Gilbert, E.Y. Jones, F. Kiefer, P. Ruga, B.A. Imhof, and M. Aurrand-Lions. 2005. Dual interaction of JAM-C with JAM-B and alpha(M)beta2 integrin: function in junctional complexes and leukocyte adhesion. *Mol Biol Cell.* 16:4992-5003.
- Lammerding, J., A.R. Kazarov, H. Huang, R.T. Lee, and M.E. Hemler. 2003. Tetraspanin CD151 regulates alpha6beta1 integrin adhesion strengthening. *Proc Natl Acad Sci U S A.* 100:7616-21.
- Larson, D.R., J.A. Gosse, D.A. Holowka, B.A. Baird, and W.W. Webb. 2005. Temporally resolved interactions between antigen-stimulated IgE receptors and Lyn kinase on living cells. *J Cell Biol.* 171:527-36.
- Lau, L.M., J.L. Wee, M.D. Wright, G.W. Moseley, P.M. Hogarth, L.K. Ashman, and D.E. Jackson. 2004. The tetraspanin superfamily member, CD151 regulates outside-in integrin  $\alpha$ IIb $\beta$ 3 signalling and platelet function. *Blood.* in press.
- Laudanna, C. 2005. Integrin activation under flow: a local affair. *Nat Immunol.* 6:429-30.
- Laudanna, C., and R. Alon. 2006. Right on the spot. Chemokine triggering of integrin-mediated arrest of rolling leukocytes. *Thromb Haemost.* 95:5-11.
- Le Naour, F., M. Andre, C. Boucheix, and E. Rubinstein. 2006. Membrane microdomains and proteomics: lessons from tetraspanin microdomains and comparison with lipid rafts. *Proteomics.* 6:6447-54.
- Le Naour, F., E. Rubinstein, C. Jasmin, M. Prenant, and C. Boucheix. 2000. Severely reduced female fertility in CD9-deficient mice. *Science.* 287:319-21.
- Lenne, P.F., L. Wawrezynieck, F. Conchonaud, O. Wurtz, A. Boned, X.J. Guo, H. Rigneault, H.T. He, and D. Marguet. 2006. Dynamic molecular confinement in the plasma membrane by microdomains and the cytoskeleton meshwork. *Embo J.* 25:3245-56.
- Leuker, C.E., M. Labow, W. Müller, and N. Wagner. 2001. Neonatally induced inactivation of the vascular cell adhesion molecule 1 gene impairs B Cell Localization and T cell-dependent humoral immune response. *J Exp Med.* 193:755-767.
- Levesque, J.P., A.C. Zannettino, M. Pudney, S. Niutta, D.N. Haylock, K.R. Snapp, G.S. Kansas, M.C. Berndt, and P.J. Simmons. 1999. PSGL-1-mediated adhesion of human hematopoietic progenitors to P-selectin results in suppression of hematopoiesis. *Immunity.* 11:369-78.

- Levy, S., S.C. Todd, and H.T. Maecker. 1998. CD81 (TAPA-1): a molecule involved in signal transduction and cell adhesion in the immune system. *Annu Rev Immunol.* 16:89-109.
- Levy, S., and T. Shoham. 2005a. Protein-protein interactions in the tetraspanin web. *Physiology (Bethesda).* 20:218-24.
- Levy, S., and T. Shoham. 2005b. The tetraspanin web modulates immune-signalling complexes. *Nat Rev Immunol.* 5:136-48.
- Little, K.D., M.E. Hemler, and C.S. Stipp. 2004. Dynamic regulation of a GPCR-tetraspanin-G protein complex on intact cells: central role of CD81 in facilitating GPR56-Galpha q/11 association. *Mol Biol Cell.* 15:2375-87.
- Longo, N., M. Yanez-Mo, M. Mittelbrunn, G. de la Rosa, M.L. Munoz, F. Sanchez-Madrid, and P. Sanchez-Mateos. 2001. Regulatory role of tetraspanin CD9 in tumor-endothelial cell interaction during transendothelial invasion of melanoma cells. *Blood.* 98:3717-26.
- Lorenzon, P., E. Vecile, E. Nardon, E. Ferrero, J.M. Harlan, F. Tedesco, and A. Dobrina. 1998. Endothelial cell E- and P-selectin and vascular cell adhesion molecule-1 function as signaling receptors. *J Cell Biol.* 142:1381-91.
- Luo, B.H., C.V. Carman, and T.A. Springer. 2007. Structural basis of integrin regulation and signaling. *Annu Rev Immunol.* 25:619-47.
- Luscinskas, F.W., G.S. Kansas, H. Ding, P. Pizcueta, B.E. Schleiffenbaum, T.F. Tedder, and M.A.J. Gimbrone. 1994. Monocyte rolling, arrest and spreading on IL-4 activated vascular endothelium under flow is mediated via sequential action of L-selectin, beta-1-integrins, and beta-2-integrins. *J Cell Biol.* 125:1417-27.
- Luster, A.D. 1998. Chemokines--chemotactic cytokines that mediate inflammation. *N Engl J Med.* 338:436-45.
- Maecker, H.T., S.C. Todd, and S. Levy. 1997. The tetraspanin superfamily: molecular facilitators. *Faseb J.* 11:428-42.
- Mangeat, P., C. Roy, and M. Martin. 1999. ERM proteins in cell adhesion and membrane dynamics. *Trends Cell Biol.* 9:187-92.
- Mannion, B.A., F. Berditchevski, S.K. Kraeft, L.B. Chen, and M.E. Hemler. 1996. Transmembrane-4 superfamily proteins CD81 (TAPA-1), CD82, CD63, and CD53 specifically associated with integrin alpha 4 beta 1 (CD49d/CD29). *J Immunol.* 157:2039-47.
- Marlin, S.D., and T.A. Springer. 1987. Purified intercellular adhesion molecule-1 (ICAM-1) is a ligand for lymphocyte function-associated antigen 1 (LFA-1). *Cell.* 51:813-9.
- Marschel, P., and G.W. Schmid-Schonbein. 2002. Control of fluid shear response in circulating leukocytes by integrins. *Ann Biomed Eng.* 30:333-43.
- Martin, F., D.M. Roth, D.A. Jans, C.W. Pouton, L.J. Partridge, P.N. Monk, and G.W. Moseley. 2005. Tetraspanins in viral infections: a fundamental role in viral biology? *J Virol.* 79:10839-51.
- Matsui, T., M. Maeda, Y. Doi, S. Yonemura, M. Amano, K. Kaibuchi, and S. Tsukita. 1998. Rho-kinase phosphorylates COOH-terminal threonines of ezrin/radixin/moesin (ERM) proteins and regulates their head-to-tail association. *J Cell Biol.* 140:647-57.
- May, R.C., and L.M. Machesky. 2001. Phagocytosis and the actin cytoskeleton. *J Cell Sci.* 114:1061-1077.
- Meerschaert, J., and M.B. Furie. 1995. The adhesion molecules used by monocytes for migration across endothelium include CD11a/CD18, CD11b/CD18, and VLA-4

- on monocytes and ICAM-1, VCAM-1, and other ligands on endothelium. *J Immunol.* 154:4099-4112.
- Mehta, P., R.D. Cummings, and R.P. McEver. 1998. Affinity and kinetic analysis of P-selectin binding to P-selectin glycoprotein ligand-1. *J Biol Chem.* 273:32506-13.
- Millan, J., L. Hewlett, M. Glyn, D. Toomre, P. Clark, and A.J. Ridley. 2006. Lymphocyte transcellular migration occurs through recruitment of endothelial ICAM-1 to caveola- and F-actin-rich domains. *Nat Cell Biol.* 8:113-23.
- Miller, J., R. Knorr, M. Ferrone, R. Houdei, C.P. Carron, and M.L. Dustin. 1995. Intercellular adhesion molecule-1 dimerization and its consequences for adhesion mediated by lymphocyte function associated-1. *J Exp Med.* 182:1231-41.
- Min, G., H. Wang, T.T. Sun, and X.P. Kong. 2006. Structural basis for tetraspanin functions as revealed by the cryo-EM structure of uroplakin complexes at 6-A resolution. *J Cell Biol.* 173:975-83.
- Mittelbrunn, M., M. Yanez-Mo, D. Sancho, A. Ursa, and F. Sanchez-Madrid. 2002. Cutting edge: dynamic redistribution of tetraspanin CD81 at the central zone of the immune synapse in both T lymphocytes and APC. *J Immunol.* 169:6691-5.
- Mittelbrunn, M., C. Cabanas, and F. Sanchez-Madrid. 2006. Integrin alpha4. *AfCS-Nature Molecule Pages.* 2006. doi: 10.1038/mp.a001203.01.
- Montoya, M.C., K. Holtmann, K.R. Snapp, E. Borges, F. Sanchez-Madrid, F.W. Luscinskas, G. Kansas, D. Vestweber, and M.O. de Landazuri. 1999. Memory B lymphocytes from secondary lymphoid organs interact with E-selectin through a novel glycoprotein ligand. *J Clin Invest.* 103:1317-27.
- Morelli, A.E., A.T. Larregina, W.J. Shufesky, M.L. Sullivan, D.B. Stolz, G.D. Papworth, A.F. Zahorchak, A.J. Logar, Z. Wang, S.C. Watkins, L.D. Falo, Jr., and A.W. Thomson. 2004. Endocytosis, intracellular sorting, and processing of exosomes by dendritic cells. *Blood.* 104:3257-66.
- Moseley, G.W. 2005. Tetraspanin-Fc receptor interactions. *Platelets.* 16:3-12.
- Muller, J.D., Y. Chen, and E. Gratton. 2003. Fluorescence correlation spectroscopy. *Methods Enzymol.* 361:69-92.
- Munoz, M., J. Serrador, F. Sanchez-Madrid, and J. Teixido. 1996. A region of the integrin VLA alpha 4 subunit involved in homotypic cell aggregation and in fibronectin but not vascular cell adhesion molecule-1 binding. *J Biol Chem.* 271:2696-702.
- Nakamura, F., L. Huang, K. Pestonjamas, E.J. Luna, and H. Furthmayr. 1999. Regulation of F-actin binding to platelet moesin in vitro by both phosphorylation of threonine 558 and polyphosphatidylinositides. *Mol Biol Cell.* 10:2669-85.
- Nakamura, K., T. Mitamura, T. Takahashi, T. Kobayashi, and E. Mekada. 2000. Importance of the major extracellular domain of CD9 and the epidermal growth factor (EGF)-like domain of heparin-binding EGF-like growth factor for up-regulation of binding and activity. *J Biol Chem.* 275:18284-90.
- Nicholson, M.W., A.N. Barclay, M.S. Singer, S.D. Rosen, and P.A. van der Merwe. 1998. Affinity and kinetic analysis of L-selectin (CD62L) binding to glycosylation-dependent cell-adhesion molecule-1. *J Biol Chem.* 273:763-70.
- Nieminen, M., T. Henttinen, M. Merinen, F. Marttila-Ichihara, J.E. Eriksson, and S. Jalkanen. 2006. Vimentin function in lymphocyte adhesion and transcellular migration. *Nat Cell Biol.* 8:156-62.
- Nishida, N., C. Xie, M. Shimaoka, Y. Cheng, T. Walz, and T.A. Springer. 2006. Activation of leukocyte beta2 integrins by conversion from bent to extended conformations. *Immunity.* 25:583-94.

- Nueda, A., C. Lopez-Rodriguez, M.A. Rubio, M. Sotillos, A. Postigo, M.A. del Pozo, M.A. Vega, and A.L. Corbi. 1995. Hematopoietic cell-type-dependent regulation of leukocyte integrin functional activity: CD11b and CD11c expression inhibits LFA-1-dependent aggregation of differentiated U937 cells. *Cell Immunol.* 164:163-9.
- Nydegger, S., S. Khurana, D.N. Kremontsov, M. Foti, and M. Thali. 2006. Mapping of tetraspanin-enriched microdomains that can function as gateways for HIV-1. *J Cell Biol.* 173:795-807.
- Ostermann, G., K.S. Weber, A. Zerneck, A. Schroder, and C. Weber. 2002. JAM-1 is a ligand of the beta(2) integrin LFA-1 involved in transendothelial migration of leukocytes. *Nat Immunol.* 3:151-8.
- Pavalko, F.M., and S.M. LaRoche. 1993. Activation of human neutrophils induces an interaction between the integrin beta 2-subunit (CD18) and the actin binding protein alpha-actinin. *J Immunol.* 151:3795-807.
- Pavalko, F.M., D.M. Walker, L. Graham, M. Goheen, C.M. Doerschuk, and G.S. Kansas. 1995. The cytoplasmic domain of L-selectin interacts with cytoskeletal proteins via alpha-actinin: receptor positioning in microvilli does not require interaction with alpha-actinin. *J. Cell Biol.* 129:1155-1164.
- Penas, P.F., A. Garcia-Diez, F. Sanchez-Madrid, and M. Yanez-Mo. 2000. Tetraspanins are localized at motility-related structures and involved in normal human keratinocyte wound healing migration. *J Invest Dermatol.* 114:1126-35.
- Phair, R.D., and T. Misteli. 2001. Kinetic modelling approaches to in vivo imaging. *Nat Rev Mol Cell Biol.* 2:898-907.
- Pileri, P., Y. Uematsu, S. Campagnoli, G. Galli, F. Falugi, R. Petracca, A.J. Weiner, M. Houghton, D. Rosa, G. Grandi, and S. Abrignani. 1998. Binding of hepatitis C virus to CD81. *Science.* 282:938-41.
- Redford, G.I., and R.M. Clegg. 2005. Polar plot representation for frequency-domain analysis of fluorescence lifetimes. *J Fluoresc.* 15:805-15.
- Rot, A., and U.H. von Andrian. 2004. Chemokines in innate and adaptive host defense: basic chemokines grammar for immune cells. *Annu Rev Immunol.* 22:891-928.
- Rubinstein, E., V. Poindessous-Jazat, F. Le Naour, M. Billard, and C. Boucheix. 1997. CD9, but not other tetraspans, associates with the beta1 integrin precursor. *Eur J Immunol.* 27:1919-1927.
- Rubinstein, E., A. Ziyat, M. Prenant, E. Wrobel, J.P. Wolf, S. Levy, F. Le Naour, and C. Boucheix. 2006. Reduced fertility of female mice lacking CD81. *Dev Biol.* 290:351-8.
- Sachs, N., M. Kreft, M.A. van den Bergh Weerman, A.J. Beynon, T.A. Peters, J.J. Weening, and A. Sonnenberg. 2006. Kidney failure in mice lacking the tetraspanin CD151. *J Cell Biol.* 175:33-9.
- Salas, A., M. Shimaoka, A.N. Kogan, C. Harwood, U.H. von Andrian, and T.A. Springer. 2004. Rolling adhesion through an extended conformation of integrin alphaLbeta2 and relation to alpha I and beta I-like domain interaction. *Immunity.* 20:393-406.
- Sanchez-Madrid, F., and M.A. del Pozo. 1999. Leukocyte polarization in cell migration and immune interactions. *EMBO J.* 18:501-11.
- Sandig, M., E. Negrou, and K.A. Rogers. 1997. Changes in the distribution of LFA-1, catenins, and F-actin during transendothelial migration of monocytes in culture. *J Cell Sci.* 110 ( Pt 22):2807-18.

- Sandig, M., M.L. Korvemaker, C.V. Ionescu, E. Negrou, and K.A. Rogers. 1999. Transendothelial migration of monocytes in rat aorta: distribution of F-actin, alpha-catenin, LFA-1, and PECAM-1. *Biotech Histochem.* 74:276-93.
- Schenkel, A.R., Z. Mamdouh, and W.A. Muller. 2004. Locomotion of monocytes on endothelium is a critical step during extravasation. *Nat Immunol.* 5:393-400.
- Schreiber, T., V. Shinder, D. Cain, R. Alon, and R. Sackstein. 2006. Shear flow-dependent integration of apical and subendothelial chemokines in T cell transmigration: implications for locomotion and the "multi-step paradigm". *Blood.*
- Sechi, A.S., and J. Wehland. 2000. The actin cytoskeleton and plasma membrane connection: PtdIns(4,5)P2 influences cytoskeletal protein activity at the plasma membrane. *J Cell Sci.* 113:3685-3695.
- Serrador, J.M., J.L. Alonso-Lebrero, M.A. del Pozo, H. Furthmayr, R. Schwartz-Albiez, J. Calvo, F. Lozano, and F. Sánchez-Madrid. 1997. Moesin interacts with the cytoplasmic region of intercellular adhesion molecule-3 and is redistributed to the uropod of T lymphocytes during cell polarization. *J Cell Biol.* 138:1409-23.
- Serrador, J.M., M. Vicente-Manzanares, J. Calvo, O. Barreiro, M.C. Montoya, R. Schwartz-Albiez, H. Furthmayr, F. Lozano, and F. Sanchez-Madrid. 2002. A novel serine-rich motif in the intercellular adhesion molecule-3 is critical for its ERM-directed subcellular targeting. *J Biol Chem.*
- Serru, V., F. Le Naour, M. Billard, D.O. Azorsa, F. Lanza, C. Boucheix, and E. Rubinstein. 1999. Selective tetraspan-integrin complexes (CD81/alpha4beta1, CD151/alpha3beta1, CD151/alpha6beta1) under conditions disrupting tetraspan interactions. *Biochem J.* 340:103-11.
- Shamri, R., V. Grabovsky, J.M. Gauguier, S. Feigelson, E. Manevich, W. Kolanus, M.K. Robinson, D.E. Staunton, U.H. von Andrian, and R. Alon. 2005. Lymphocyte arrest requires instantaneous induction of an extended LFA-1 conformation mediated by endothelium-bound chemokines. *Nat Immunol.* 6:497-506.
- Sharma, P., R. Varma, R.C. Sarasij, Ira, K. Gousset, G. Krishnamoorthy, M. Rao, and S. Mayor. 2004. Nanoscale organization of multiple GPI-anchored proteins in living cell membranes. *Cell.* 116:577-89.
- Shaw, R.J., M. Henry, F. Solomon, and T. Jacks. 1998. RhoA-dependent phosphorylation and relocalization of ERM proteins into apical membrane/actin protrusions in fibroblasts. *Mol Biol Cell.* 9:403-19.
- Shaw, S.K., S. Ma, M.B. Kim, R.M. Rao, C.U. Hartman, R.M. Froio, L. Yang, T. Jones, Y. Liu, A. Nusrat, C.A. Parkos, and F.W. Luscinskas. 2004. Coordinated redistribution of leukocyte LFA-1 and endothelial cell ICAM-1 accompany neutrophil transmigration. *J Exp Med.* 200:1571-80.
- Shoham, T., R. Rajapaksa, C. Boucheix, E. Rubinstein, J.C. Poe, T.F. Tedder, and S. Levy. 2003. The tetraspanin CD81 regulates the expression of CD19 during B cell development in a postendoplasmic reticulum compartment. *J Immunol.* 171:4062-4072.
- Simons, P.C., S.F. Pietromonaco, D. Reczek, A. Bretscher, and L. Elias. 1998. C-terminal threonine phosphorylation activates ERM proteins to link the cell's cortical lipid bilayer to the cytoskeleton. *Biochem Biophys Res Commun.* 253:561-5.
- Simons, K., and D. Toomre. 2000. Lipid rafts and signal transduction. *Nat Rev Mol Cell Biol.* 1:31-9.
- Sincock, P.M., S. Fitter, R.G. Parton, M.C. Berndt, J.R. Gamble, and L.K. Ashman. 1999. PETA-3/CD151, a member of the transmembrane 4 superfamily, is

- localised to the plasma membrane and endocytic system of endothelial cells, associates with multiple integrins and modulates cell function. *J Cell Sci.* 112 ( Pt 6):833-44.
- Smith, A., M. Bracke, B. Leitinger, J.C. Porter, and N. Hogg. 2003. LFA-1-induced T cell migration on ICAM-1 involves regulation of MLCK-mediated attachment and ROCK-dependent detachment. *J Cell Sci.* 116:3123-33.
- Springer, T.A. 1994. Traffic signals for lymphocyte recirculation and leukocyte emigration: the multistep paradigm. *Cell.* 76:301-14.
- Sterk, L.M., C.A. Geuijen, L.C. Oomen, J. Calafat, H. Janssen, and A. Sonnenberg. 2000. The tetraspan molecule CD151, a novel constituent of hemidesmosomes, associates with the integrin  $\alpha 6 \beta 4$  and may regulate the spatial organization of hemidesmosomes. *J Cell Biol.* 149:969-82.
- Stewart, M.P., A. McDowall, and N. Hogg. 1998. LFA-1-mediated adhesion is regulated by cytoskeletal restraint and by a  $\text{Ca}^{2+}$ -dependent protease, calpain. *J Cell Biol.* 140:699-707.
- Stipp, C.S., and M.E. Hemler. 2000. Transmembrane-4-superfamily proteins CD151 and CD81 associate with  $\alpha 3 \beta 1$  integrin, and selectively contribute to  $\alpha 3 \beta 1$ -dependent neurite outgrowth. *J Cell Sci.* 113 ( Pt 11):1871-82.
- Stipp, C.S., T.V. Kolesnikova, and M.E. Hemler. 2003. Functional domains in tetraspanin proteins. *Trends Biochem Sci.* 28:106-12.
- Suzuki, K.G., T.K. Fujiwara, M. Edidin, and A. Kusumi. 2007a. Dynamic recruitment of phospholipase C  $\gamma$  at transiently immobilized GPI-anchored receptor clusters induces  $\text{IP}_3$ - $\text{Ca}^{2+}$  signaling: single-molecule tracking study 2. *J Cell Biol.* 177:731-42.
- Suzuki, K.G., T.K. Fujiwara, F. Sanematsu, R. Iino, M. Edidin, and A. Kusumi. 2007b. GPI-anchored receptor clusters transiently recruit Lyn and G  $\alpha$  for temporary cluster immobilization and Lyn activation: single-molecule tracking study 1. *J Cell Biol.* 177:717-30.
- Takahashi, K., T. Sasaki, A. Mammoto, K. Takaishi, T. Kameyama, S. Tsukita, and Y. Takai. 1997. Direct interaction of the Rho GDP dissociation inhibitor with ezrin/radixin/moesin initiates the activation of the Rho small G protein. *J Biol Chem.* 272:23371-5.
- Takeda, Y., A.R. Kazarov, C.E. Butterfield, B.D. Hopkins, L.E. Benjamin, A. Kaipainen, and M.E. Hemler. 2007. Deletion of tetraspanin Cd151 results in decreased pathologic angiogenesis in vivo and in vitro. *Blood.* 109:1524-32.
- Takino, T., H. Miyamori, N. Kawaguchi, T. Uekita, M. Seiki, and H. Sato. 2003. Tetraspanin CD63 promotes targeting and lysosomal proteolysis of membrane-type 1 matrix metalloproteinase. *Biochem Biophys Res Commun.* 304:160-6.
- Thompson, P.W., A.M. Randi, and A.J. Ridley. 2002a. Intercellular adhesion molecule (ICAM)-1, but not ICAM-2, activates RhoA and stimulates c-fos and rhoA transcription in endothelial cells. *J Immunol.* 169:1007-13.
- Thompson, R.E., D.R. Larson, and W.W. Webb. 2002b. Precise nanometer localization analysis for individual fluorescent probes. *Biophys J.* 82:2775-83.
- Tsukita, S., and S. Yonemura. 1997. ERM (ezrin/radixin/moesin) family: from cytoskeleton to signal transduction. *Curr Opin Cell Biol.* 9:70-5.
- Turunen, O., T. Wahlstrom, and A. Vaheri. 1994. Ezrin has a COOH-terminal actin-binding site that is conserved in the ezrin protein family. *J Cell Biol.* 126:1445-53.

- Unternaehrer, J.J., A. Chow, M. Pypaert, K. Inaba, and I. Mellman. 2007. The tetraspanin CD9 mediates lateral association of MHC class II molecules on the dendritic cell surface. *Proc Natl Acad Sci U S A*. 104:234-9.
- Vaheri, A., O. Carpen, L. Heiska, T.S. Helander, J. Jaaskelainen, P. Majander-Nordenswan, M. Sainio, T. Timonen, and O. Turunen. 1997. The ezrin protein family: membrane-cytoskeleton interactions and disease associations. *Curr Opin Cell Biol*. 9:659-66.
- van Wetering, S., J.D. van Buul, S. Quik, F.P. Mul, E.C. Anthony, J.P. ten Klooster, J.G. Collard, and P.L. Hordijk. 2002. Reactive oxygen species mediate Rac-induced loss of cell-cell adhesion in primary human endothelial cells. *J Cell Sci*. 115:1837-46.
- van Wetering, S., N. van Den Berk, J.D. van Buul, F.P. Mul, I. Lommerse, R. Mous, J.P. ten Klooster, J.J. Zwaginga, and P.L. Hordijk. 2003. VCAM-1-mediated Rac signaling controls endothelial cell-cell contacts and leukocyte transmigration. *Am J Physiol Cell Physiol*.
- VanCompernelle, S.E., S. Levy, and S.C. Todd. 2001. Anti-CD81 activates LFA-1 on T cells and promotes T cell-B cell collaboration. *Eur J Immunol*. 31:823-31.
- Varma, R., and S. Mayor. 1998. GPI-anchored proteins are organized in submicron domains at the cell surface. *Nature*. 394:798-801.
- Várnai, P., K.I. Rother, and T. Balla. 1999. Phosphatidylinositol 3-kinase-dependent membrane association of the Bruton's tyrosine kinase pleckstrin homology domain visualized in single living cells. *J Biol Chem*. 274:10983-10989.
- Verfaillie, C.M. 1998. Adhesion receptors as regulators of the hematopoietic process. *Blood*. 92:2609-12.
- Vicente-Manzanares, M., and F. Sanchez-Madrid. 2004. Role of the cytoskeleton during leukocyte responses. *Nat Rev Immunol*. 4:110-22.
- Vogt, A.B., S. Spindeldreher, and H. Kropshofer. 2002. Clustering of MHC-peptide complexes prior to their engagement in the immunological synapse: lipid raft and tetraspan microdomains. *Immunol Rev*. 189:136-51.
- von Andrian, U.H., S.R. Hasslen, R.D. Nelson, S.L. Erlandsen, and E.C. Butcher. 1995. A central role for microvillous receptor presentation in leukocyte adhesion under flow. *Cell*. 82:989-99.
- von Andrian, U.H., and C.R. Mackay. 2000. T-cell function and migration. Two sides of the same coin. *N Engl J Med*. 343:1020-34.
- Wallrabe, H., and A. Periasamy. 2005. Imaging protein molecules using FRET and FLIM microscopy. *Curr Opin Biotechnol*. 16:19-27.
- Wang, Q., and C.M. Doerschuk. 2002. The signaling pathways induced by neutrophil-endothelial cell adhesion. *Antioxid Redox Signal*. 4:39-47.
- Wojciak-Stothard, B., L. Williams, and A.J. Ridley. 1999. Monocyte adhesion and spreading on human endothelial cells is dependent on Rho-regulated receptor clustering. *J Cell Biol*. 145:1293-307.
- Wright, M.D., S.M. Geary, S. Fitter, G.W. Moseley, L.M. Lau, K.C. Sheng, V. Apostolopoulos, E.G. Stanley, D.E. Jackson, and L.K. Ashman. 2004. Characterization of mice lacking the tetraspanin superfamily member CD151. *Mol Cell Biol*. 24:5978-88.
- Yan, Y., K. Shirakabe, and Z. Werb. 2002. The metalloprotease Kuzbanian (ADAM10) mediates the transactivation of EGF receptor by G protein-coupled receptors. *J Cell Biol*. 158:221-6.
- Yanez-Mo, M., A. Alfranca, C. Cabanas, M. Marazuela, R. Tejedor, M.A. Ursa, L.K. Ashman, M.O. de Landazuri, and F. Sanchez-Madrid. 1998. Regulation of

- endothelial cell motility by complexes of tetraspan molecules CD81/TAPA-1 and CD151/PETA-3 with alpha3 beta1 integrin localized at endothelial lateral junctions. *J Cell Biol.* 141:791-804.
- Yanez-Mo, M., R. Tejedor, P. Rousselle, and F. Sanchez -Madrid. 2001. Tetraspanins in intercellular adhesion of polarized epithelial cells: spatial and functional relationship to integrins and cadherins. *J Cell Sci.* 114:577-87.
- Yang, X., Claas C, Kraeft SK, Chen LB, Wang Z, Kreidberg JA, and M. Hemler. 2002. Palmitoylation of tetraspanin proteins: modulation of CD151 lateral interactions, subcellular distribution, and integrin-dependent cell morphology. *Mol Biol Cell.* 13:767-81.
- Yang, X., O.V. Kovalenko, W. Tang, C. Claas, C.S. Stipp, and M.E. Hemler. 2004. Palmitoylation supports assembly and function of integrin-tetraspanin complexes. *J Cell Biol.* 167:1231-40.
- Yang, L., R.M. Froio, T.E. Sciuto, A.M. Dvorak, R. Alon, and F.W. Luscinskas. 2005. ICAM-1 regulates neutrophil adhesion and transcellular migration of TNF-alpha-activated vascular endothelium under flow. *Blood.* 106:584-92.
- Yauch, R.L., F. Berditchevski, M.B. Harler, J. Reichner, and M.E. Hemler. 1998. Highly stoichiometric, stable, and specific association of integrin alpha3beta1 with CD151 provides a major link to phosphatidylinositol 4-kinase, and may regulate cell migration. *Mol Biol Cell.* 9:2751-65.
- Yauch, R.L., and M.E. Hemler. 2000. Specific interactions among transmembrane 4 superfamily (TM4SF) proteins and phosphoinositide 4-kinase. *Biochem J.* 351 Pt 3:629-37.
- Yonemura, S., M. Hirao, Y. Doi, N. Takahashi, T. Kondo, and S. Tsukita. 1998. Ezrin/radixin/moesin (ERM) proteins bind to a positively charged amino acid cluster in the juxta-membrane cytoplasmic domain of CD44, CD43, and ICAM-2. *J Cell Biol.* 140:885-95.
- Yonemura, S., and S. Tsukita. 1999. Direct involvement of ezrin/radixin/moesin (ERM)-binding membrane proteins in the organization of microvilli in collaboration with activated ERM proteins. *J Cell Biol.* 145:1497-509.
- Zacharias, D.A., J.D. Violin, A.C. Newton, and R.Y. Tsien. 2002. Partitioning of lipid-modified monomeric GFPs into membrane microdomains of live cells. *Science.* 296:913-6.
- Zhang, X.A., A.L. Bontrager, and M.E. Hemler. 2001. Transmembrane-4 superfamily proteins associate with activated protein kinase C (PKC) and link PKC to specific beta(1) integrins. *J Biol Chem.* 276:25005-13.
- Zhang, J., R.E. Campbell, A.Y. Ting, and R.Y. Tsien. 2002. Creating new fluorescent probes for cell biology. *Nat Rev Mol Cell Biol.* 3:906-18.
- Zhu, G.Z., B.J. Miller, C. Boucheix, E. Rubinstein, C.C. Liu, R.O. Hynes, D.G. Myles, and P. Primakoff. 2002. Residues SFQ (173-175) in the large extracellular loop of CD9 are required for gamete fusion. *Development.* 129:1995-2002.
- Zwartz, G.J., A. Chigaev, D.C. Dwyer, T.D. Foutz, B.S. Edwards, and L.A. Sklar. 2004. Real-time analysis of very late antigen-4 affinity modulation by shear. *J Biol Chem.* 279:38277-86.

Colyer, R.A., Lee, C.L., and Gratton, E. Time-resolved frequency-domain fluorescence lifetime imaging microscopy in the photon-counting regime (submitted to *Nature Methods*).

Digman, M., V.R. Caiolfa, M. Zamai, and G. Gratton. The Phasor approach to fluorescence lifetime imaging analysis (submitted to *Biophys J*).

R Development Core Team (2006). R: A language and environment for statistical computing. R Foundation for Statistical Computing, Vienna, Austria. ISBN 3-900051-07-0, URL <http://www.R-project.org>.

## **APPENDIX I**

## **SUPPLEMENTAL MATERIAL**

### **Supplemental Figure 1**

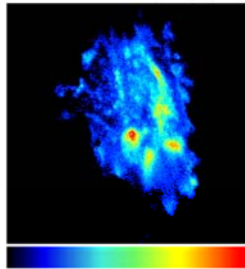
#### **Standards for the phasor-FLIM analysis of FRET.**

Cells expressing only the mEGFP-tagged chimeras of ICAM-1, VCAM-1-or CD9 were used for defining the phasor distributions (i.e., fluorescence lifetime distributions) of each FRET-unquenched donor protein. ICAM-1-mEGFP is the reference for ICAM-1-mEGFP/ICAM-1-mRFP1, ICAM-1mEGFP/VCAM-1mRFP1 and ICAM-1mEGFP/CD9mRFP1 pairs. VCAM-1mEGFP is the reference for VCAM-1mEGFP/VCAM-1mRFP1, VCAM-1mEGFP/ICAMmRFP1 and VCAM-1mEGFP/CD151mRFP1. CD9mEGFP is the reference for CD9mEGFP/CD9mRFP1 and CD9mEGFP/CD151mRFP1.

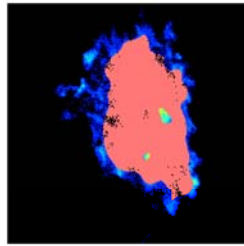
Fluorescence lifetime decays were acquired in the classical TCSPC-FLIM mode and transformed in the phasor representation as described (Digman et al., submitted; Caiolfa et al., 2007). Briefly, by this novel analytical approach, the fluorescence decay in each pixel of the image gives a point in the phasor plot. The phasors ensemble of the image is shown in contour plot. The phasor plot is simply a polar, s.g, coordinate graph, in which only single exponential decays fall on the universal circle (right top panel), and different molecular species occupy distinct positions in the plots (Digman et al., submitted). As in our cells seeded on fibronectin matrices, if the decay at one pixel is a convolution of lifetimes, due to multiple species (i.e., unquenched donor + cell autofluorescence) contributing the fluorescence intensity in that pixel, the phasor falls inside the universal circle, and it is simply the algebraic sum of phasors from each component (Clayton et al., 2004; Gratton et al., 1984; Redford and Clegg, 2005) (right top panel). The phasor distribution in donor-transfected cells indicates the presence of pixels at different contribution of mEGFP and autofluorescence lifetimes. The latter

was evaluated in independent experiments on untransfected cells and the mean of its phasor distribution is reported in the phasor plot (+, right top panel). As it was recently shown (Digman et al., submitted), the phasors corresponding to the fibronectin background and the cellular autofluorescence are spread over a larger area of the phasor plot, due to the low intensity images, the fibronectin background and also the pixel heterogeneity for the cellular autofluorescence are detected. Despite that, the majority (> 95%) of pixels is included in a narrow, distinct area of the plot (black circle in the phasor plot), and are uniformly localized in the image, regardless the variability of the local fluorescence intensity. In these pixels, mEGFP is the predominant species that gives rise to the measured fluorescence lifetime decays. The phasor distribution of the three donor constructs (top, mid and bottom panels) is comparable and depicts the area in the phasor plot in which mEGFP-constructs localize in the presence of fibronectin and cell autofluorescence and in the absence of quenching due to FRET (green line). Once we know the phasors of the unquenched donors and of the fibronectin-cell autofluorescence, we can calculate the FRET trajectory in the phasor plot according to the classical relationship:  $\text{FRET eff} = [1 - (\tau_{\text{donor-acceptor}}/\tau_{\text{donor}})]$ , and define the mean phasors of mEGFP-constructs quenched by 50% FRET and with different contributions of fibronectin-cell autofluorescence (yellow line). In all our experiments, phasors resulting from any combination of unquenched-donors, FRET-quenched-donors and fibronectin-cell autofluorescence have been found within the area delimited by the green and yellow lines in the phasor plot.

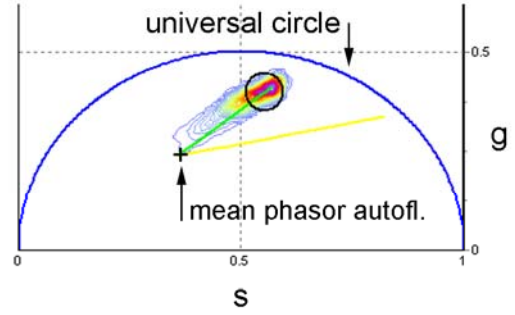
**ICAM-1mEGFP**  
Fl. Intensity (cps)



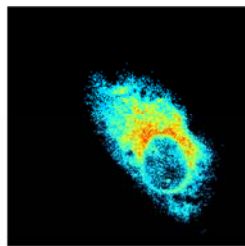
**FLIM**



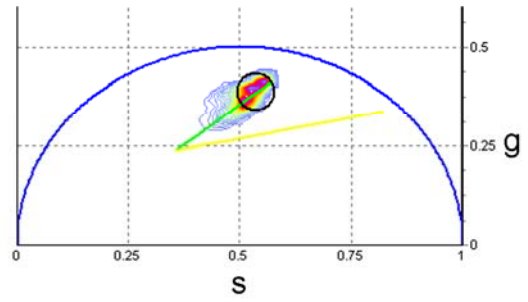
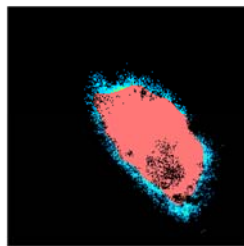
**Phasor Plot**  
universal circle



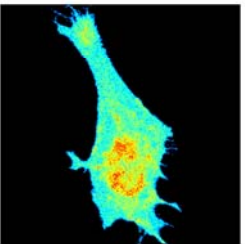
**VCAM-1mEGFP**  
Fl. Intensity (cps)



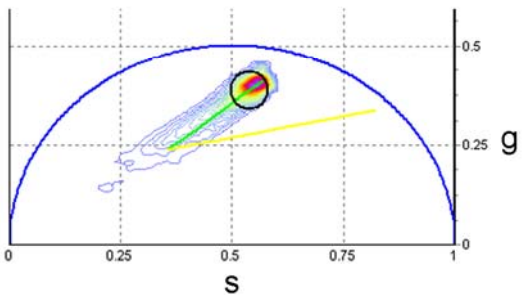
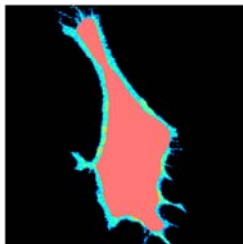
**FLIM**



**CD9mEGFP**  
Fl. Intensity (cps)



**FLIM**



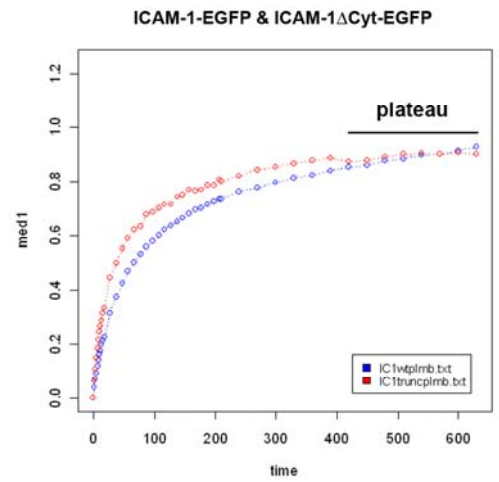
## Supplemental Figure 2

**Example statistical analysis of a FRAP experiments.** For each time point, the table shows mean fluorescence intensities for ICAM-1 and ICAM-1 $\Delta$ Cyt (measured at the plasma membrane) raw p values, and adjusted p values obtained for multiple testing using the Benjamini and Hochberg's (BH) method.

Typically, an acceptance criterion of a single event takes the form of a requirement that the observed data be highly unlikely under a default assumption (null hypothesis). As the number of independent applications of the acceptance criterion begins to outweigh the high unlikelihood associated with each individual test, it becomes increasingly likely that one will observe data that satisfies the acceptance criterion by chance alone (even if the default assumption is true in all cases). These errors are considered false positives because they positively identify a set of observations as satisfying the acceptance criterion while that data in fact represents the null hypothesis. Many mathematical techniques have been developed to counter the false positive error rate associated with making multiple statistical comparisons. To avoid these multiple comparison problems, we used the Benjamini and Hochberg's (BH) method for the statistical analysis of our FRAP experiments.

The accompanying graph shows mean fluorescence recovery curves of ICAM-1 and ICAM-1 $\Delta$ Cyt at the plasma membrane. The adjusted p values shown in the table correspond to the maximum adjusted p value out of the plateau region. The plateau region is marked on the table and the graph and was not considered for the statistical analysis.

time	ICAM-1wt plmb	ICAM-1ΔCyt plmb	raw p value	adj p value
0	0	0	NA	NA
1.672	0.041445203	0.062211154	0.0014295	0.002859
3.36	0.071205925	0.106100321	0.00075684	0.00166505
5.047	0.092905048	0.150995668	5.17E-05	0.00019607
6.735	0.120487324	0.18478153	3.58E-05	0.00018026
8.422	0.143021635	0.217203502	4.10E-05	0.00018026
10.11	0.163590373	0.249126425	3.94E-05	0.00018026
11.797	0.176319104	0.268083712	9.28E-05	0.00030577
13.485	0.199972275	0.289831944	5.35E-05	0.00019607
15.172	0.214441072	0.316964081	2.58E-05	0.00018026
17.094	0.229517518	0.334774979	6.16E-06	9.03E-05
27.078	0.314183443	0.447610567	1.15E-06	5.07E-05
37.078	0.377391664	0.501283786	5.05E-06	9.03E-05
47.078	0.426779613	0.553210547	1.53E-05	0.00016843
57.078	0.469797725	0.589492203	4.00E-05	0.00018026
67.078	0.502283577	0.619902556	2.48E-05	0.00018026
77.078	0.534949608	0.63577203	0.00032832	0.00084976
87.082	0.562564772	0.678234646	9.73E-05	0.00030577
97.082	0.581845775	0.687259253	0.00013012	0.00038169
107.082	0.602027048	0.70335984	0.00031413	0.00084976
117.082	0.621096804	0.714203383	0.00040938	0.00100071
127.082	0.639066925	0.715187329	0.00368559	0.00675692
137.082	0.652297087	0.742437366	0.00100015	0.00209554
147.082	0.664686865	0.748683835	0.00153945	0.00294503
157.082	0.680694429	0.770811837	0.0007483	0.00166505
167.082	0.693920766	0.765796506	0.00732593	0.01289363
177.082	0.702860542	0.769459265	0.01430708	0.02331524
187.082	0.714605595	0.784826263	0.01171529	0.01982588
197.082	0.724695799	0.785534643	0.02043003	0.02899746
207.082	0.734400839	0.807417228	0.01627362	0.02469102
209.082	0.735012048	0.799066984	0.01581788	0.02469102
239.062	0.764013524	0.819702608	0.03431022	0.04574696
269.062	0.776819119	0.843283215	0.01791732	0.02627874
299.062	0.796873596	0.853858873	0.02785973	0.03830713
329.062	0.812796501	0.866630111	0.04062275	0.05257062
359.062	0.824116144	0.875966656	0.06494476	0.08164484
389.062	0.840819443	0.886347376	0.14020416	0.17136064
419.062	0.853145171	0.873160386	0.48201405	0.55812153
449.062	0.860564527	0.877762832	0.57432826	0.64150575
479.082	0.876190491	0.888706725	0.65126562	0.6989192
509.082	0.884239869	0.901876051	0.58318704	0.64150575
539.062	0.895515573	0.902772932	0.82133274	0.85275977
569.062	0.900747269	0.898858818	0.95286216	0.95286216
599.082	0.913658991	0.906393439	0.83337886	0.85275977
629.082	0.926053874	0.900398357	0.44256889	0.52629814



plateau

**Video MOESIN-GFP:** In this video, a lymphoblast that contacts with a moesin-GFP transfected endothelial cell, and immediately transmigrates and moves beneath the endothelium is observed. Moesin is clustered around the lymphoblast along the whole process.

**Video VCAM-1-GFP:** In this video a lymphoblast (upper site) that adheres to, spreads on, and moves towards a lateral junction of the VCAM-1-GFP transfected endothelial cell is observed. Then, it transmigrates and moves beneath the endothelium. Another lymphoblast (lower site) remains spread on the endothelial cell. VCAM-1 is clustered around lymphoblasts adhered to the apical surface of endothelium (arrows), but it is not concentrated around migrating lymphocytes beneath the endothelium (arrowheads).

**Video ICAM-1-GFP:** In this video, a lymphoblast that adheres to, spreads on and moves towards a lateral junction of the ICAM-1-GFP transfected endothelial cell (black arrows) is observed. Then, it transmigrates and moves beneath the endothelium (white arrows). ICAM-1 is clustered around the lymphoblast along the whole process.

In all these three videos, the apical endothelial surface is at a plane remote from the observer.

**Video CD9-GFP:** Dynamics of tetraspanin CD9 during T lymphoblast transendothelial migration. Timelapse video sequence of lymphoblast transmigration through CD9-GFP-transfected TNF- $\alpha$ -activated HUVEC monolayers. The maximal projection of the informative sections from the GFP confocal image stack is merged with DIC image. White arrows mark the position of apically-adhered lymphocytes. Black arrows point to

transmigrated lymphocytes interacting with the ventral surface of endothelium.

**Video CD151-GFP:** Dynamics of tetraspanin CD151 during T lymphoblast transendothelial migration. Time-lapse video sequence of lymphoblast transmigration through CD151-GFP-transfected TNF- $\alpha$ -activated HUVEC monolayers. The maximal projection of the informative sections from the GFP confocal image stack is merged with DIC image. White arrows mark the position of apical adhered lymphocytes. Black arrows point to transmigrated lymphocytes interacting with the ventral surface of endothelium.

**Video CD9 siRNA:** Extravasation under flow with control and CD9 siRNA transfected HUVEC cells. Time-lapse video sequence of an extravasation assay under physiological flow rate conditions of 1.8 dyn/cm<sup>2</sup>. Three different fields, recorded for 30s with a 10x phase contrast objective, starting at min 6:30 of perfusion of PBLs on TNF- $\alpha$ -activated control or CD9 siRNA transfected HUVEC cells are shown.

**Video CD151 siRNA:** Extravasation under flow with control and CD151 siRNA transfected HUVEC cells. Time-lapse video sequence of an extravasation assay under physiological flow rate conditions of 1.8 dyn/cm<sup>2</sup>. Three different fields, recorded for 30s with a 10x phase contrast objective, starting at min 6:30 of perfusion of PBLs on TNF- $\alpha$ -activated control or CD151 siRNA transfected HUVEC cells are shown.

**Video: Dynamics of transendothelial migration under flow conditions:** HUVEC were transiently transfected with ICAM-1-GFP and then mounted on a parallel flow chamber to observe leukocyte-endothelium interactions under physiological flow

conditions. PBLs stained *in vivo* with a neutral monoclonal anti-LFA-1 directly coupled to Alexa 568 (TS2/4) were perfused at  $1.8 \text{ dyn/cm}^2$ . A lymphocyte migrating across an intercellular junction is observed. The ring-like structure of LFA-1 and ICAM-1 in the transmigration passage is shown. As transendothelial migration progresses, the endothelial junction becomes resealed. (This video was performed in collaboration with Ziv Shulman from the laboratory of Dr. Ronen Alon at the Weizmann Institute of Science, Israel).

**Video: Example of extravasation steps under flow conditions.** Freshly isolated PBLs were perfused at physiological rate ( $1.8 \text{ dyn/cm}^2$ ). Rolling, adhered, transmigrating and transmigrated lymphocytes can be observed in the videosequence.

## **APPENDIX II**

## **ABBREVIATIONS:**

ERM: Ezrin, Radixin and Moesin

DIC: Differential Interference Contrast

GFP: Green Fluorescent Protein

GST: Glutathione-S-transferase

HUVEC: Human Umbilical Vein Endothelial Cells

ICAM-1: Intercellular Adhesion Molecule-1

PBL: Peripheral Blood Lymphocyte

PI(4,5)P<sub>2</sub>: Phosphatidylinositol 4,5-bisphosphate

TEM: Transendothelial Migration (according to text)

VCAM-1: Vascular Cell Adhesion Molecule-1

LEL: Large Extracellular Loop

siRNA: Small Interference RNA

LFA-1: Lymphocyte Function-associated Antigen 1

VLA-4: Very Late Antigen-4

FRAP: Fluorescence Recovery After Photobleaching

TCSPC-FLIM-FRET: Time-Correlated Single Photon Counting-Fluorescence Lifetime

Imaging-Fluorescence Resonance Energy Transfer

FCS: Fluorescence Correlation Spectroscopy

FCCS: Fluorescence Cross-correlation Spectroscopy

SEM: Scanning Electron Microscopy

TEM: Tetraspanin-enriched Microdomains (according to text)

EAP: Endothelial Adhesive platforms

## **APPENDIX III**

## LIST OF PUBLICATIONS

1. José L. Alonso-Lebrero, Juan M. Serrador, Carmen Domínguez-Jiménez, **Olga Barreiro**, Alfonso Luque, Miguel A. del Pozo, Karen Snapp, Geoffrey Kansas, Reinhard Schwartz-Albiez, Heinz Furthmayr, Francisco Lozano, and Francisco Sánchez-Madrid: “Polarization and interaction of adhesion molecules P-selectin glycoprotein ligand 1 and intercellular adhesion molecule 3 with moesin and ezrin in myeloid cells” *Blood*. 2000 Apr 1;95(7):2413-9.
2. Juan M. Serrador, Miguel Vicente-Manzanares, Javier Calvo, **Olga Barreiro**, María C. Montoya, Reinhard Schwartz-Albiez, Heinz Furthmayr, Francisco Lozano, and Francisco Sánchez-Madrid: “A novel serine-rich motif in the leukocyte adhesion receptor ICAM-3 is critical for its ERM-directed subcellular targeting” *J Biol Chem*. 2002 Mar 22;277(12):10400-9.
3. Carmen Domínguez-Jiménez, David Sancho, Marta Nieto, María C. Montoya, **Olga Barreiro**, Francisco Sánchez-Madrid, and Roberto González-Amaro: “Effect of Pentoxifylline on Polarization and Migration of Human Leukocytes”. *J Leukoc Biol*. 2002 Apr;71(4):588-96.
4. **Olga Barreiro**, María Yáñez-Mó, Juan M. Serrador, María C. Montoya, Miguel Vicente-Manzanares, Reyes Tejedor, Heinz Furthmayr, and Francisco Sánchez-Madrid: “Dynamic interaction of VCAM-1 and ICAM-1 with moesin and ezrin in a novel endothelial docking structure for adherent leukocytes”. *J Cell Biol*. 2002 Jun 24;157(7):1233-45.
5. Mercedes Rey, Fernando Viedma, Miguel Vicente-Manzanares, María Yáñez-Mó, Ana Urzainqui, **Olga Barreiro**, Jesús Vázquez, and Francisco Sánchez-Madrid: “Association of the Motor Protein Nonmuscle Myosin Heavy Chain-IIA with the C-terminus of the chemokine receptor CXCR4 in T Lymphocytes” *J Immunol*. 2002 Nov 15; 169(10): 5410-4.
6. Miguel Vicente-Manzanares, Mercedes Rey, Manuel Pérez-Martínez, María Yáñez-Mó, David Sancho, José Román Cabrero, **Olga Barreiro**, Toshimasa Ishizaki, Chiharu Higashida, Shuh Narumiya, and Francisco Sánchez-Madrid: “The RhoA effector mDia is induced during T cell activation and regulates actin polymerization and cell migration in T lymphocytes” *J Immunol*. 2003 Jul 15; 171(2): 1023-34.
7. **Olga Barreiro**, Miguel Vicente-Manzanares, Ana C. Urzainqui, María Yáñez-Mó, and Francisco Sánchez-Madrid: “Interactive protrusive structures during leukocyte adhesion and transendothelial migration”. *Front Biosci*. 2004 May 1;9:1849-63.
8. **Olga Barreiro\***, María Yáñez-Mó\*, Mónica Sala-Valdés, María Dolores Gutiérrez-López, Susana Ovalle, Adrian Higginbottom, Peter N. Monk, Carlos Cabañas, and Francisco Sánchez-Madrid: “Endothelial tetraspanin microdomains regulate leukocyte firm adhesion during extravasation”. *Blood*. 2005 Apr 1;105(7):2852-61.

\* Co-authorship.

9. **Olga Barreiro\***, María Ángeles García-López\*, Amaro García-Díez, Francisco Sánchez-Madrid, and Pablo F. Peñas: “Role of tetraspanins CD9, CD81 and CD151 in motility and intercellular contacts of melanocytes”. *J Invest Dermatol.* 2005 Nov;125(5):1001-9. \*Co-authorship.
10. José Román Cabrero, Juan Manuel Serrador, **Olga Barreiro**, María Mittelbrunn, Salvador Naranjo, Miguel Vicente-Manzanares, Ángeles Ursa, Noa Martín-Cófreces, Agustín Valenzuela-Fernández, Jesús Ávila, and Francisco Sánchez-Madrid: “HDAC-6 dependent tubulin acetylation/deacetylation imbalance regulates lymphocyte migration directed by chemokines”. *Mol Biol Cell.* 2006 Aug;17(8):3435-45.
11. Mónica Gordón-Alonso, María Yáñez-Mó, **Olga Barreiro**, Susana Álvarez, M<sup>a</sup> Ángeles Muñoz-Fernández, Agustín Valenzuela-Fernández, and Francisco Sánchez-Madrid: “Tetraspanins CD9 and CD81 modulate HIV-1-induced membrane fusion”. *J Immunol.* 2006 Oct 15;177(8):5129-37.
12. **Olga Barreiro**, Hortensia de la Fuente, María Mittelbrunn, and Francisco Sánchez-Madrid. “Functional insights on the polarized redistribution of leukocyte integrins and their ligands during leukocyte migration and immune interactions”. *Immunol Rev.* 2007 Aug; 218:147-64.
13. Ana Urzainqui, Gloria Martínez del Hoyo, Amalia Lamana, Hortensia de la Fuente, **Olga Barreiro**, Martin K Wild, Dietmar Vestweber, Roberto González Amaro and Francisco Sánchez-Madrid. “PSGL-1/Selectin interaction induces the generation of tolerogenic dendritic cells”. Submitted to *J Immunol.*
14. María Yáñez-Mó, **Olga Barreiro**, Pilar Gonzalo, Alicia Batista, Diego Megías, Laura Genís, Norman Sachs, Mónica Sala-Valdés, Miguel A. Alonso, María C. Montoya, Arnoud Sonnenberg, Alicia G. Arroyo, and Francisco Sánchez-Madrid. “Association of MT1-MMP with tetraspanin CD151 and retention at endothelial junctions: a homeostatic regulatory mechanism of MT1-MMP proteolytic activity”. Submitted to *J Cell Biol.*
15. Petronila Penela, Catalina Ribas, Ivette Aymerich, Niels Eijelkamp, **Olga Barreiro**, Annemieke Kavelaars , Francisco Sánchez-Madrid and Federico Mayor, jr. “G protein-coupled receptor kinase 2 (GRK2) positively regulates epithelial cell migration”. Submitted to *EMBO J.*
16. **Olga Barreiro**, Moreno Zamai, María Yáñez-Mó, Emilio Tejera, Enrico Gratton, Valeria R. Caiolfa, and Francisco Sánchez-Madrid. “Endothelial adhesive platforms: molecular features, dynamics and biophysical properties”. Manuscript in preparation.
17. Sales Ibiza, Andrea Pérez-Rodríguez, Ángel Ortega, Antonio Martínez-Ruiz, **Olga Barreiro**, Carlota A. García-Domínguez, Víctor M. Víctor, Juan V. Espulgues, José M. Rojas, Francisco Sánchez-Madrid, and Juan M. Serrador. “Endothelial nitric oxide synthase regulates N-Ras activation on the Golgi complex of antigen-stimulated T cells”. Manuscript in preparation.

18. **Olga Barreiro**, Río J. Aguilar, Emilio Tejera, Fernando de Torres-Alba, Arturo Evangelista, and Francisco Sánchez-Madrid. “Real Time Imaging of Targeted Microbubbles to Human Endothelium in an ex-vivo model”. Manuscript in preparation.

#### **SCIENTIFIC AWARDS**

- O. Barreiro et al, *J Cell Biol.* 2002 Jun 24;157(7):1233-45. Paper awarded by the Spanish Society of Biochemistry and Molecular Biology as the best publication of a young researcher in 2002.
- P.F. Peñas, M.A. García-López, and O. Barreiro: “Inhibition of motility in melanoma cells using CD9 siRNA”. Study awarded by the Spanish Society of Dermatology in 2004.

# Dynamic interaction of VCAM-1 and ICAM-1 with moesin and ezrin in a novel endothelial docking structure for adherent leukocytes

Olga Barreiro,<sup>1</sup> María Yáñez-Mó,<sup>1</sup> Juan M. Serrador,<sup>1</sup> María C. Montoya,<sup>1</sup> Miguel Vicente-Manzanares,<sup>1</sup> Reyes Tejedor,<sup>1</sup> Heinz Furthmayr,<sup>2</sup> and Francisco Sánchez-Madrid<sup>1</sup>

<sup>1</sup>Servicio de Inmunología, Hospital de la Princesa, Universidad Autónoma de Madrid, 28006 Madrid, Spain

<sup>2</sup>Department of Pathology, Stanford University, Stanford, CA 94305

Ezrin, radixin, and moesin (ERM) regulate cortical morphogenesis and cell adhesion by connecting membrane adhesion receptors to the actin-based cytoskeleton. We have studied the interaction of moesin and ezrin with the vascular cell adhesion molecule (VCAM)-1 during leukocyte adhesion and transendothelial migration (TEM). VCAM-1 interacted directly with moesin and ezrin *in vitro*, and all of these molecules colocalized at the apical surface of endothelium. Dynamic assessment of this interaction in living cells showed that both VCAM-1 and moesin were involved in lymphoblast adhesion and spreading on the endothelium, whereas only moesin participated in TEM, following the same distribution pattern

as ICAM-1. During leukocyte adhesion in static or under flow conditions, VCAM-1, ICAM-1, and activated moesin and ezrin clustered in an endothelial actin-rich docking structure that anchored and partially embraced the leukocyte containing other cytoskeletal components such as  $\alpha$ -actinin, vinculin, and VASP. Phosphoinositides and the Rho/p160 ROCK pathway, which participate in the activation of ERM proteins, were involved in the generation and maintenance of the anchoring structure. These results provide the first characterization of an endothelial docking structure that plays a key role in the firm adhesion of leukocytes to the endothelium during inflammation.

## Introduction

Leukocyte extravasation across the endothelial barrier is a fundamental requirement in a wide variety of physiological and pathological scenarios, including immunity and inflammation. This phenomenon is an active, multistep process that requires drastic morphological changes involving cytoskeletal-directed clustering of adhesion receptors in both leukocytes and endothelial cells (Butcher, 1991). Among adhesion receptors, the integrins  $\alpha 4\beta 1$  (VLA-4) and  $\alpha 1\beta 2$  (LFA-1) play a major role in the tight adhesion of leukocytes to en-

dothelium (González-Amaro and Sánchez-Madrid, 1999). Their main ligands on endothelium are vascular cell adhesion molecule (VCAM)\*-1 and intercellular adhesion molecule (ICAM)-1, respectively (Marlin and Springer, 1987; Elices et al., 1990). ICAM-1 but not VCAM-1 is basally expressed in resting cells, and both molecules are induced upon activation by proinflammatory cytokines such as IL-1 and TNF- $\alpha$  (Carlos and Harlan, 1994). Although it has been described that both VLA-4/VCAM-1 and LFA-1/ICAM-1 interactions mediate the firm adhesion of leukocytes, only the latter molecular pair seems to be required for lymphocyte diapedesis (Oppenheimer-Marks et al., 1991).

The interaction of adhesion molecules with cytoskeletal components is of critical importance for cell-cell and cell-substratum adhesion as well as for receptor internalization. The cortical cytoskeleton regulates the membrane localization of several adhesion receptors, such as ICAMs, CD43, and CD44, through one or more members of the ezrin, radixin, and moesin (ERM) family of proteins (Serrador et al., 1997; Heiska et al., 1998; Yonemura et al., 1998). These molecules function as membrane-actin cytoskeleton linkers regulating cortical morphogenesis and cell adhesion. Accordingly, they

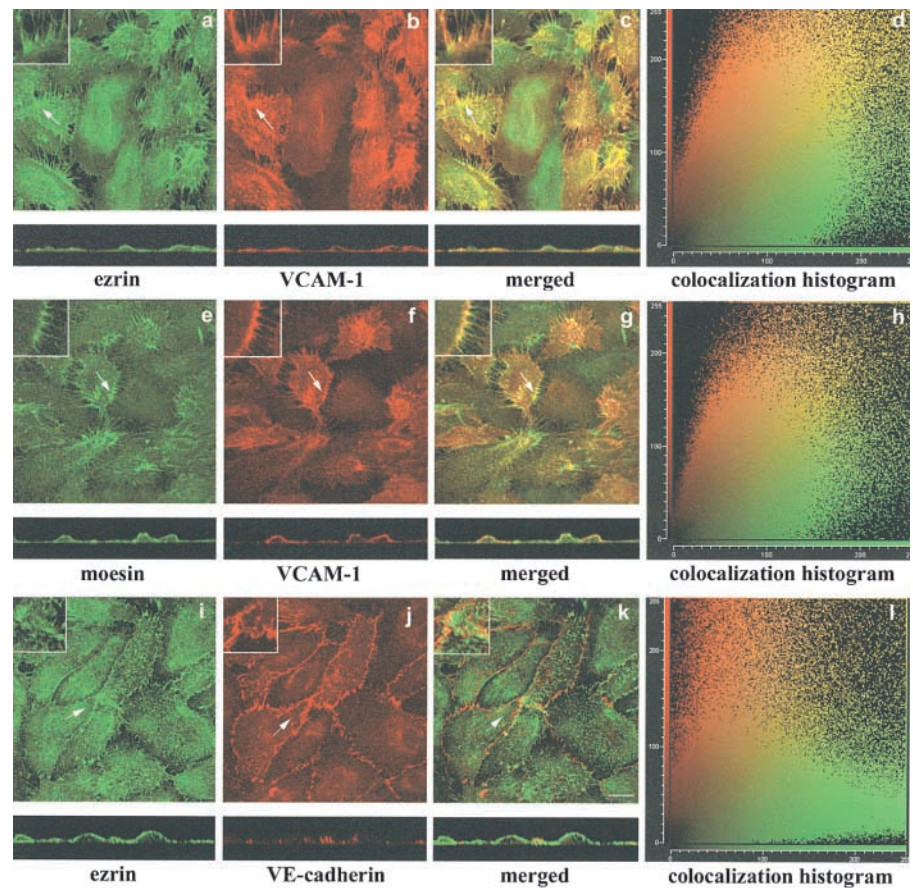
The online version of this article contains supplemental material.

Address correspondence to Servicio de Inmunología, Hospital de la Princesa, Universidad Autónoma de Madrid, C/Diego de León 62, 28006 Madrid, Spain. Tel.: 34-91-309-2115. Fax: 34-91-520-2374. E-mail: fsanchez@hlpr.insalud.es

\*Abbreviations used in this paper: ERM, ezrin, radixin, and moesin; DIC, differential interference contrast; GFP, green fluorescent protein; GST, glutathione-S-transferase; HUVEC, human umbilical vein endothelial cells; ICAM, intercellular adhesion molecule; pAb, polyclonal antibody; PBL, peripheral blood lymphocyte; PI(4,5)P<sub>2</sub>, phosphatidylinositol 4,5-bisphosphate; TEM, transendothelial migration; VCAM, vascular cell adhesion molecule.

Key words: ERM; VCAM-1; ICAM-1; leukocyte adhesion and transendothelial migration; docking structure

**Figure 1. VCAM-1 colocalizes with moesin and ezrin at the apical surface of activated HUVEC.** Confluent HUVEC were activated with 20 ng/ml TNF- $\alpha$  for 20 h. Thereafter, cells were fixed, permeabilized, and stained with the anti-ezrin pAb 90/3 (a and i, green), anti-moesin pAb 95/2 (e, green), anti-VCAM-1 mAb P8B1 (b and f, red), or anti-VE-cadherin mAb Tea1/31 (j, red). Merged images are shown in c, g, and k, where colocalizations are observed (yellow). Images represent confocal laser scanning micrographs showing horizontal projections or the corresponding orthogonal section of the same field. Insets correspond to the amplified image of the zones pointed to by arrows. Colocalization histograms of green and red signals corresponding to these images are shown on the right (d, h, and l). The corresponding colocalization percentages are 65.7% (d), 67.6% (h), and 13.3% (l). Bar, 20  $\mu$ m.



play a key role in the formation of protrusive plasma membrane structures such as filopodia, microspikes, or microvilli (Mangeat et al., 1999; Yonemura and Tsukita, 1999). Structurally, they are closely related to each other and seem to be functionally redundant, as suggested by the apparently normal phenotype of moesin knockout mice (Doi et al., 1999). Their NH<sub>2</sub>-terminal domains interact with integral membrane proteins, whereas their COOH-terminal domains bind F-actin (Turunen et al., 1994). These functions are conformationally regulated by reversible changes from inactive to functionally active forms. Binding of phosphatidylinositol 4,5-bisphosphate (PI[4,5]P<sub>2</sub>) and phosphorylation of a specific COOH-terminal threonine residue unmask the F-actin and membrane binding sites and stabilize the active conformation (Nakamura et al., 1999; Barret et al., 2000). The Rho/p160 ROCK signaling pathway and the phosphatidylinositol turnover are the major regulatory mechanisms for ERM activation, inducing their phosphorylation and translocation into apical membrane/actin protrusions (Hirao et al., 1996; Matsui et al., 1998; Shaw et al., 1998). On the other hand, activated ERM proteins can sequester Rho-GDI to permit Rho activation, providing a positive feedback pathway (Takahashi et al., 1997).

These proteins have been studied in a variety of cellular types, but thus far their functions have not been addressed in endothelial cells. Herein, we describe the direct interaction of VCAM-1 with moesin and ezrin, the two members of the ERM family most highly expressed in endothelium (Menager et al., 1999). We also describe the dynamic distribution of VCAM-1, ICAM-1, and moesin during leukocyte adhesion and lymphoblast transendothelial migration

(TEM), using live time-lapse fluorescence confocal microscopy. Our data indicate that an endothelial docking structure is formed during leukocyte-endothelium interaction in static and under flow conditions. VCAM-1, ICAM-1, and activated ERM proteins participate in this novel anchoring structure together with structural and regulatory molecules typical of nascent phagosomes.

## Results

### VCAM-1 interacts with moesin and ezrin at the apical surface of activated endothelial cells

The subcellular distribution of VCAM-1, ezrin, and moesin, was analyzed by confocal microscopy in TNF- $\alpha$ -activated human umbilical vein endothelial cells (HUVEC). VCAM-1 colocalized with ezrin (Fig. 1, a–c) and moesin (Fig. 1, e–g) in the microspikes and microvilli that protrude from the apical surface of these cells. Colocalization analysis confirmed these observations (Fig. 1, d and h). By contrast, VE-cadherin did not colocalize with ERM proteins (Fig. 1, i–l).

To assess whether this codistribution in activated HUVEC is correlated with the formation of complexes between VCAM-1 molecules and ERM proteins, immunoprecipitation assays were performed. As shown in Fig. 2 A, moesin and ezrin coimmunoprecipitated with VCAM-1. To determine whether these interactions are direct, binding assays were performed using a glutathione-S-transferase (GST) fusion protein containing the cytoplasmic tail of VCAM-1 (GST-VC). The fusion protein containing the cytoplasmic tail of ICAM-3, GST-IC3, which has been demonstrated to bind ERM, as

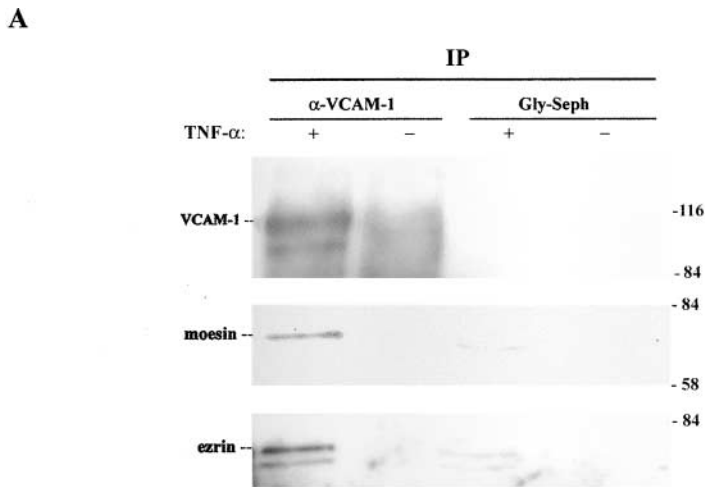
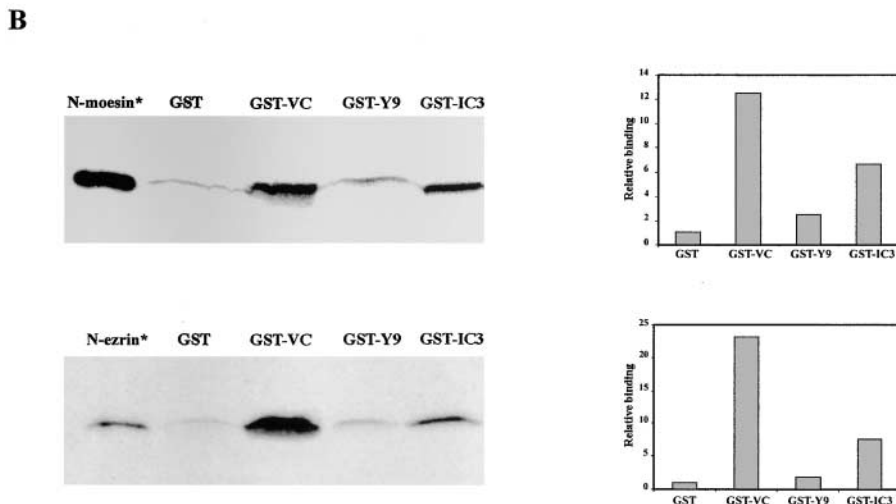


**Figure 2. Association of VCAM-1 with moesin and ezrin.** (A) Cytokine-activated HUVEC were lysed and immunoprecipitated with the anti-VCAM-1 mAb 4B9 or Gly-Sepharose. Immunoprecipitates were then resolved on a 10% SDS-PAGE, and sequentially immunoblotted with the anti-VCAM-1 mAb 4B9, the anti-moesin pAb 95/2, and the anti-ezrin pAb 90/3. Molecular weights (kD) are indicated on the right side. (B) GST or the GST fusion proteins GST-VC, GST-IC3 and GST-Y9 were bound to glutathione-Sepharose beads and incubated with  $^{35}\text{S}$ -Met-N-moesin or  $^{35}\text{S}$ -Met-N-ezrin (top and bottom, respectively). After incubation, beads were boiled in sample buffer and eluted proteins were analyzed by 10% SDS-PAGE, autoradiography, and fluorography. Lanes with isotope-labeled N-moesin and N-ezrin (\*) indicate the molecular mass of these truncated proteins. Densitometric diagrams normalized to the loading controls of GST proteins are shown on the right.



well as the partially truncated form GST-Y9, which shows a considerable reduced binding to moesin and ezrin (Serrador et al., 2002), were used as positive and negative controls, respectively.  $^{35}\text{S}$ -Met-labeled  $\text{NH}_2$ -terminal domain of moesin, N-moesin, and the  $\text{NH}_2$ -terminal domain of ezrin, N-ezrin, were added to Sepharose beads coupled to the GST fusion proteins. Strong binding of VCAM-1 to ezrin and moesin was observed, which was much higher in comparison to ICAM-3 (Fig. 2 B). Altogether, these data demonstrate that VCAM-1 can directly associate with ezrin and moesin *in vitro* and presumably also at the apical membrane sites of endothelial cells.

#### Differential contribution of VCAM-1, ICAM-1, and ERM proteins to the extravasation process

The functional role of the VCAM-1/ERM association in the endothelial cell-lymphocyte interaction was analyzed and compared with another adhesion receptor that also interacts with ERM proteins, namely ICAM-1 (Heiska et al., 1998). For this purpose, we used T lymphoblasts, that express high levels of VLA-4 and LFA-1, ligands of VCAM-1 and ICAM-1, respectively (Fig. 3 A). Both integrins were active since mAb

against them blocked T lymphoblast TEM (Fig. 3 B). These cells were allowed to adhere and migrate across an activated HUVEC monolayer and confocal microscopic analysis of endogenous endothelial VCAM-1 and ICAM-1 distribution was performed. When lymphoblasts were spread on the apical surface of endothelium, VCAM-1 clustered around these cells (Fig. 3 C, a). However, such VCAM-1 clusters were neither observed during the passage of lymphoblasts across the endothelium nor after transmigration (Fig. 3 C, b). The orthogonal section showed two lymphoblasts migrating across adjacent endothelial cells, where clustered VCAM-1 molecules colocalized with endothelial ezrin only at the apical surface of the lymphoblast-endothelial cell contact area (Fig. 3 C, c). On the other hand, ICAM-1 was clustered around lymphoblasts during all the lymphoblast adhesion and transmigration processes (Fig. 3 C, d and e), colocalizing with endothelial ezrin (Fig. 3 C, f).

To dynamically assess the changes in distribution of VCAM-1, ICAM-1, and ERM proteins, HUVEC transiently transfected with VCAM-1-, ICAM-1-, or moesin-green fluorescent protein (GFP) were separately monitored by live

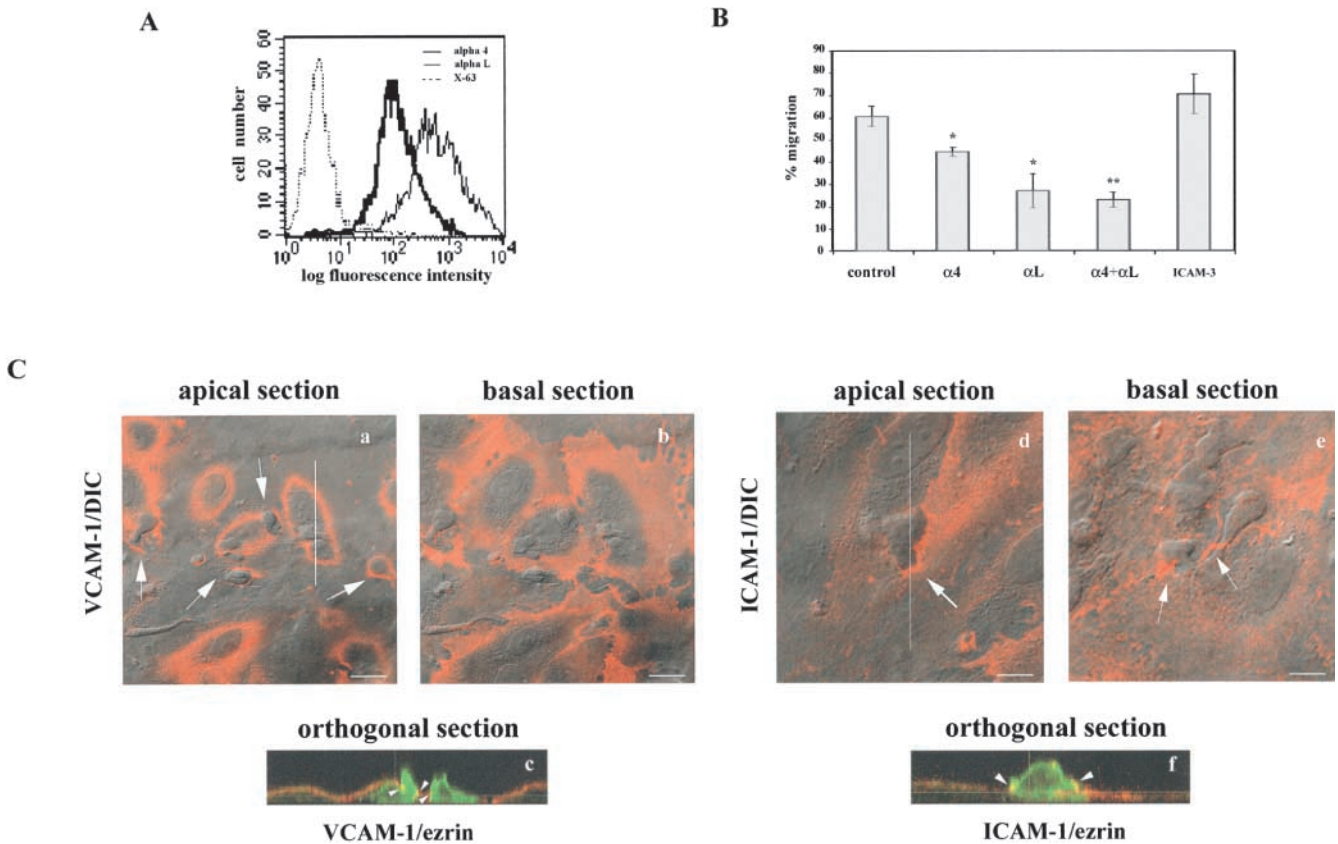


**Figure 3. Distribution of endogenous VCAM-1, ICAM-1, and ezrin during lymphoblast TEM.** (A) Expression of  $\alpha 4$ -integrin (thick line), and  $\alpha L$ -integrin (thin line) on T lymphoblasts as determined by flow cytometry analysis. P3 $\times$ 63 (dotted line) was used as negative control. (B) Transendothelial migration assay of T lymphoblasts pretreated with the blocking anti- $\alpha 4$  mAb HP2/1, the blocking anti- $\alpha L$  mAb TS1/11, the mixture of anti- $\alpha 4$  plus  $\alpha L$  mAb, or the anti-ICAM-3 mAb TP1/24 as negative control. Values correspond to the arithmetic mean  $\pm$  SD of a representative experiment run by duplicate out of three independent ones. Statistically significant values, as defined by unpaired Student's *t* test, are indicated with \* ( $P < 0.05$ ) or \*\* ( $P < 0.015$ ) compared with no mAb treatment. (C) T lymphoblasts were allowed to transmigrate across an activated HUVEC monolayer, and then cells were fixed, permeabilized, and stained with the anti-VCAM-1 mAb P8B1 (a–c, red), the anti-ICAM-1 mAb Hu5/3 (d–f, red), or the anti-ezrin pAb 90/3 (c and f, green). Representative confocal horizontal images showing an apical section of endothelium with adhered lymphoblasts on top (a and d) and a basal section with transmigrated lymphoblasts beneath the endothelium (b and e) are presented. DIC images are shown overlaid with VCAM-1 (a and b) or ICAM-1 staining (d and e). Arrows point to VCAM-1 or ICAM-1 clusters at the contact area. Representative orthogonal sections corresponding to the white line in panel a or panel d are shown in panels c and f, respectively. Green signal corresponds to ezrin staining both in lymphoblasts and endothelium. Arrowheads point to the sites of VCAM-1/ezrin or ICAM-1/ezrin clustering at the apical surface of endothelial cells. Bars: (a and b) 20  $\mu$ m; (d and e) 8  $\mu$ m.

time-lapse confocal microscopy after addition of lymphoblasts. As observed previously for endogenous molecules, VCAM-1- and moesin-GFP fusion proteins redistributed to sites of contact during lymphoblast initial adhesion and spreading. However, only moesin was concentrated in the transmigration cleft and apparently participated in subsequent interactions, when lymphoblasts migrated beneath the activated endothelium (Fig. 4 A). Interestingly, moesin-GFP exhibited a dynamic behavior similar to ICAM-1-GFP (Fig. 4 B), presumably because this adhesion molecule binds to ERM proteins to actively participate in TEM. Digital movies showing more clearly the differential dynamic distribution of these molecules are included as additional material.

#### Redistribution of VCAM-1, ICAM-1, and ERM proteins at a docking structure during endothelium-leukocyte interaction

To focus our study on the role of ERM interaction with endothelial adhesion receptors during the initial adhesion of leuko-

cytes to the endothelium, to which VCAM-1 involvement was mainly restricted, we used K562 cells stably transfected with  $\alpha 4$  integrin (4M7 cells) (Muñoz et al., 1996). These cells expressed high levels of VLA-4, but negligible amounts of LFA-1 (Fig. 5 A). In addition, their adhesion to activated endothelium was dependent on VLA-4, as it was inhibited by the blocking anti- $\alpha 4$  HP2/1 mAb, and induced by the activating anti- $\beta 1$  TS2/16 mAb (Fig. 5 B). 4M7 cells adhered to activated endothelium mainly via VLA-4, but these cells were unable to progress to TEM (unpublished data). When the distribution of endogenous endothelial VCAM-1 was examined during 4M7 cell adhesion, we found that it was strongly concentrated around attached leukocytes (Fig. 5 C, c). Endogenous ezrin colocalized with VCAM-1 at the endothelial-leukocyte contact area (Fig. 5 C, d), and antibodies to ezrin also stained the leukocyte membrane (Fig. 5 C, b). Furthermore, a three-dimensional reconstruction of the site of adhesion showed that VCAM-1 and ezrin were contained in a unique docking structure that was raised above the level of the endo-

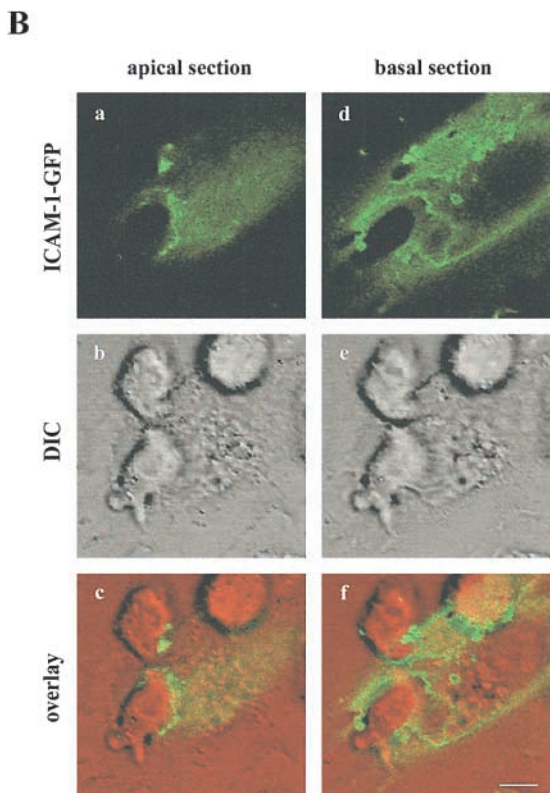
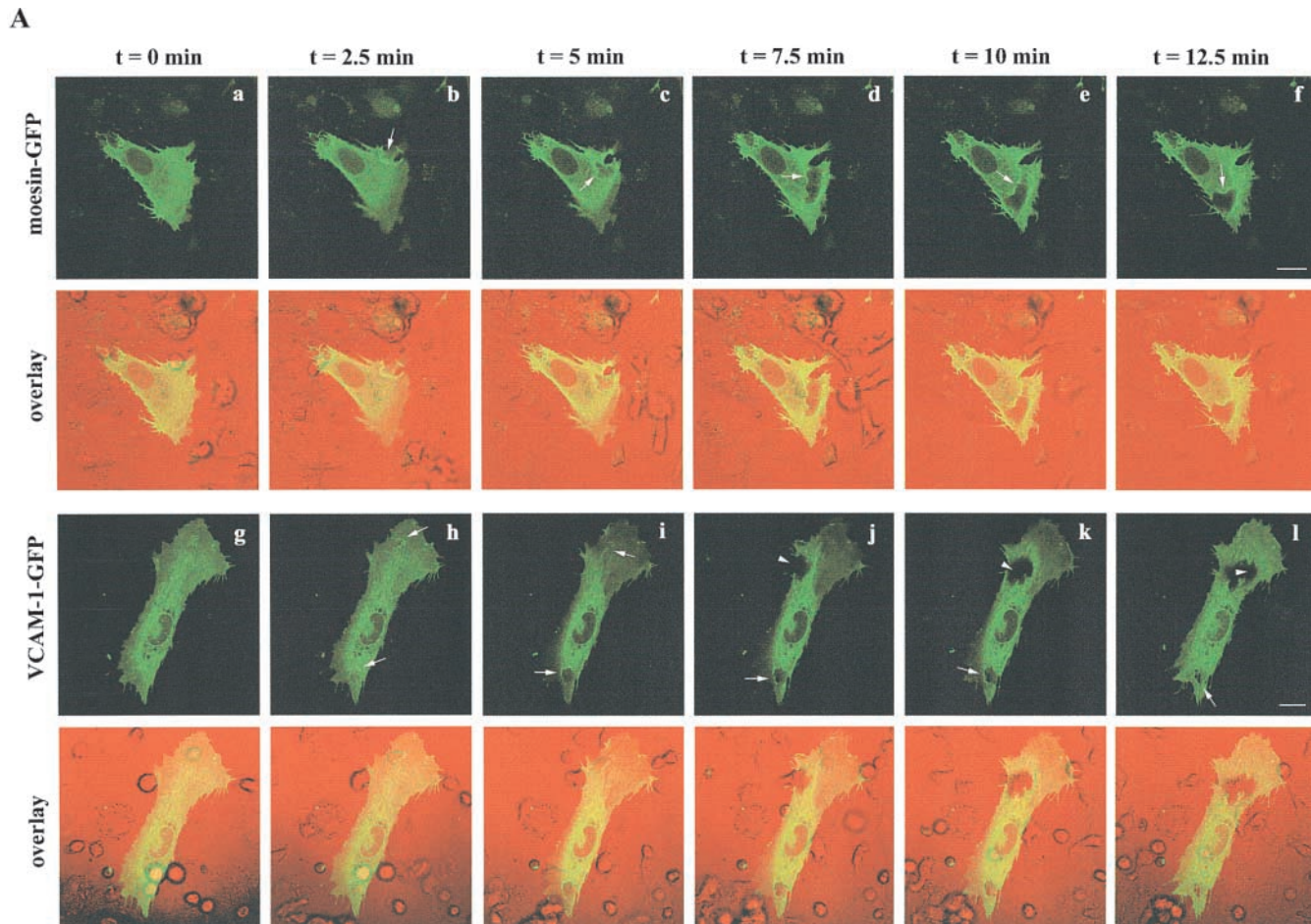


**Figure 4. Dynamic changes in the localization of VCAM-1, ICAM-1, and moesin during lymphoblast TEM.**

(A) Lymphoblasts were allowed to transmigrate across activated HUVEC transfected with moesin- or VCAM-1-GFP. Video sequences tracking the spatial and temporal distribution of moesin (a–f) and VCAM-1 (g–l) were obtained using live time-lapse fluorescence confocal microscopy. Each image represents a projection of several representative horizontal sections of a confocal image stack depicted from the video sequence at the specified times. DIC and fluorescence images are merged and presented at the lower side of each panel. Arrows point to the GFP proteins clustering during the lymphoblast–endothelium interaction. Arrowheads indicate the absence of VCAM-1-GFP from the contact area between the transfected endothelial cell and a migrated lymphoblast placed beneath the endothelial monolayer. Corresponding digital video sequences are available at <http://www.jcb.org/cgi/content/full/jcb.200112126/DC1>. Bars, 20  $\mu$ m.

(B) Lymphoblast transmigration across activated HUVEC transfected with ICAM-1-GFP was analyzed by live time-lapse fluorescence confocal microscopy. Two representative horizontal sections from the apical and the basal side of the endothelial cell belonging to the same confocal stack depicted from the video sequence are presented. ICAM-1-GFP signal is shown in panels a and d. DIC images and the overlaid images are presented in panels b and e, and c and f, respectively. The corresponding video sequence is available at <http://www.jcb.org/cgi/content/full/jcb.200112126/DC1>. Bar, 5  $\mu$ m.

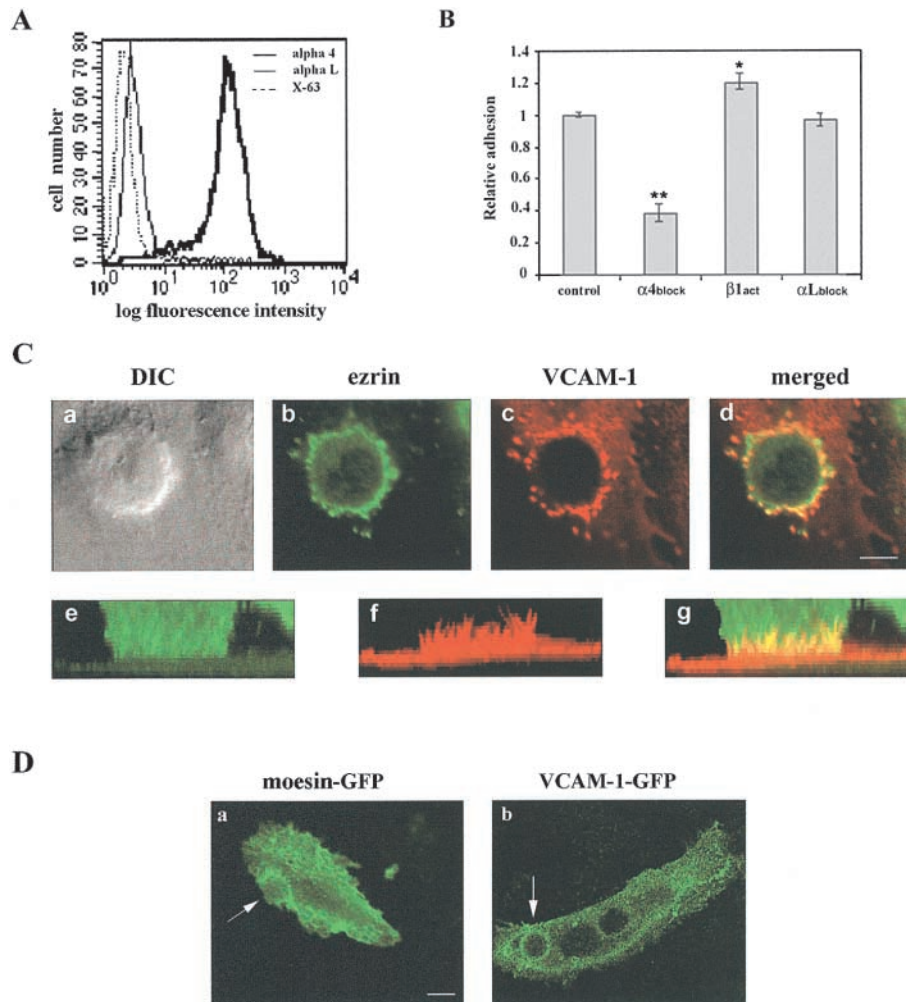
### Figure 5. Localization of VCAM-1 and ezrin at the contact area of activated HUVEC with leukocytes.

(A) Expression of  $\alpha 4$ -integrin (thick line), and  $\alpha L$ -integrin (thin line) on 4M7 cells as determined by flow cytometry analysis. P3 $\times$ 63 (dotted line) was used as negative control.

(B) Adhesion to activated HUVEC of 4M7 cells pretreated with the blocking anti- $\alpha 4$  mAb HP2/1, the activating anti- $\beta 1$  mAb TS2/16, or the blocking anti- $\alpha L$  mAb TS1/11. Values correspond to the arithmetic mean  $\pm$  SD of a representative experiment run by triplicate out of three independent ones. Statistically significant values, as defined by unpaired Student's *t* test, are indicated with \* ( $P < 0.005$ ) or \*\* ( $P < 0.0001$ ), compared with no mAb treatment.

(C) 4M7 cells interacting with activated endothelial cells were fixed, permeabilized, and stained with the anti-ezrin pAb 90/3 (green) and the anti-VCAM-1 mAb P8B1 (red). Representative horizontal sections of confocal laser scanning images (b and c) are merged in d. The corresponding DIC image is shown in a. The corresponding three-dimensional reconstruction is presented in e–g. Bar, 5  $\mu$ m.

(D) 4M7 cells were allowed to adhere to activated HUVEC transfected with moesin- or VCAM-1-GFP. GFP staining was monitored using live time-lapse fluorescence confocal microscopy. Horizontal sections showing the staining of moesin- (a) or VCAM-1-GFP (b) after 60 min of leukocyte–endothelium interaction. Arrows point to the GFP proteins clustered in the anchoring structure. Bar, 20  $\mu$ m.



thelial cell surface and that surrounded the adherent leukocyte in a cup-like fashion. Both proteins were preferentially concentrated in microspikes of this structure that presumably served to anchor the attached leukocyte (Fig. 5 C, e–g). The redistribution of VCAM-1 and moesin to the leukocyte–endothelium contact area was tracked separately by live time-lapse fluorescence confocal microscopy during the interaction of 4M7 cells with VCAM-1- or moesin-GFP transfected HUVEC. The dynamic studies demonstrated that VCAM-1/VLA-4 engagement was associated with the progressive concentration of VCAM-1 and moesin at the specialized anchoring structure formed between the two interacting cells, which was progressively strengthened and sustained with time (Fig. 5 D).

To ascertain the physiological relevance of this docking structure, we analyzed the redistribution of VCAM-1, ICAM-1, and ezrin to the contact area of migrating peripheral blood lymphocytes (PBLs) allowed to adhere under fluid shear conditions, using a physiological wall shear stress (1.8 dyn/cm<sup>2</sup>) for perfusion periods from 30 s to 10 min. We found these endothelial molecules colocalizing in clusters at the docking structures formed around spread PBLs (Fig. 6 A), at early time points during the arrest of lymphocytes. This structure was also observed during the interaction of activated HUVEC with T lymphoblasts in static conditions (Fig. 6 B; unpublished data). Similarities in three-dimensional VCAM-1 distribution around 4M7 cells,

T lymphoblasts or peripheral blood lymphocytes supported the generality of the docking structure (Fig. 6 B).

### Relocation of cytoskeletal components to the endothelial docking structure

The cytoskeletal components involved in the generation of this endothelial structure were analyzed. Samples of 4M7 cells adhered to activated HUVEC and stained for VCAM-1 and F-actin revealed a considerable enrichment of endothelial actin within the docking structure (Fig. 7 A, a–b). Interestingly, this apical actin scaffold appeared not to be connected to basal stress fibers (Fig. 7 A, c–d). On the contrary, tubulin was not present with F-actin at the anchoring structure (Fig. 7 A, e–h). Vinculin and  $\alpha$ -actinin-GFP also redistributed to this structure with a punctuate pattern (Fig. 7 B, c and d, and C, a–c). Likewise, VASP-GFP colocalized with VCAM-1 (Fig. 7 C, f–g), whereas talin and paxillin-GFP were only found colocalizing with VCAM-1 at some adhesion structures (Fig. 7 B, a and b, and C, d and e). These data indicate that the endothelial docking structure was supported by the actin cytoskeleton, actin bundling proteins such as  $\alpha$ -actinin, actin-nucleating proteins such as VASP, and focal adhesion proteins such as vinculin, talin or paxillin. The formation of this structure was associated with a remarkable change in distribution of several of these proteins, in particular vinculin, talin, and paxillin, from their normal

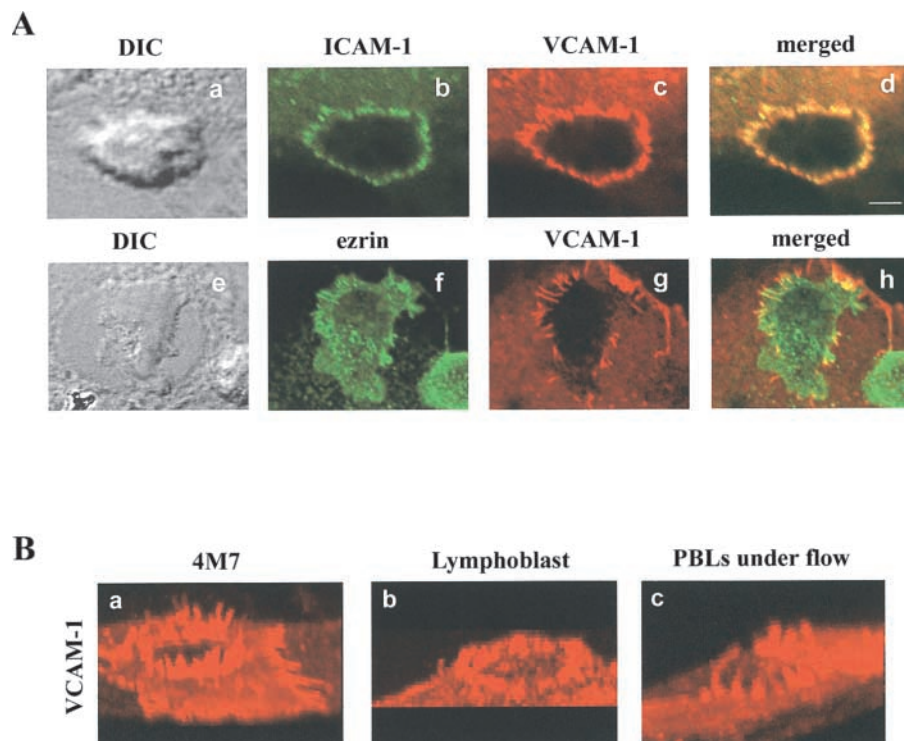


**Figure 6. Formation of the endothelial docking structure for adhered lymphocytes under flow.**

(A) Transendothelial migration assay of peripheral blood lymphocytes under fluid shear conditions. After 10 min of perfusion, cells were fixed and stained for ICAM-1 (b and d, green), VCAM-1 (c, d, g, and h, red), and ezrin (f and h, green). The corresponding DIC images are shown in panels a and e. Merged images are shown in panels d and h. Bar, 3.5  $\mu\text{m}$ . (B) Three-dimensional reconstruction of VCAM-1 staining during 4M7 cell (a), T lymphoblast (b), or PBL under flow (c) adhesion.

subcellular localization at focal adhesions at the basal surface to the docking structure at the apical surface.

### The docking structure is regulated by PI(4,5)P<sub>2</sub> and Rho/p160 ROCK

To assess whether the clustering of ERM proteins at the endothelial-leukocyte contact area is associated with an activated state of these proteins, immunofluorescence studies using the 297S mAb, which recognizes a COOH-terminal threonine phosphorylated in ERM proteins (Matsui et al., 1998), were conducted in the 4M7 cell adhesion model. A high concentration of phosphorylated ERM proteins was evident at the endothelial anchoring structure generated after VCAM-1/VLA-4 interaction (Fig. 8 A). We have also studied two important regulators of ERM activation, namely phosphoinositides and components of the Rho/p160 ROCK pathway. The subcellular localization of different phosphoinositides was determined by using as probes the PH domain of PLC $\delta$ , which binds PI(4,5)P<sub>2</sub>, and that of GRP1, which binds PI(3,4,5)P<sub>3</sub> and PI(3,4)P<sub>2</sub>, fused to GFP (Gray et al., 1999; Várnai et al., 1999). Upon endothelial cell transfection, both probes colocalized with VCAM-1 at the endothelial docking structure (Fig. 8 B, a and b; d and e). PLC $\delta$ -PH-GFP showed a higher concentration at microspike tips (Fig. 8 B, c), whereas GRP1-PH-GFP appeared to be more diffusely distributed and localized throughout the entire structure (Fig. 8 B, f).

Next, blocking studies with chemical inhibitors were performed before and after HUVEC-4M7 cell adhesion. The p160 ROCK inhibitor Y-27632 strongly inhibited the generation and maintenance of the anchoring structure (Fig. 9 A). On the other hand, the PI3K inhibitor Ly 294002 only had a minor effect on the generation of this structure, but moderately inhibited its maintenance (Fig. 9 A). The classical, PKCs

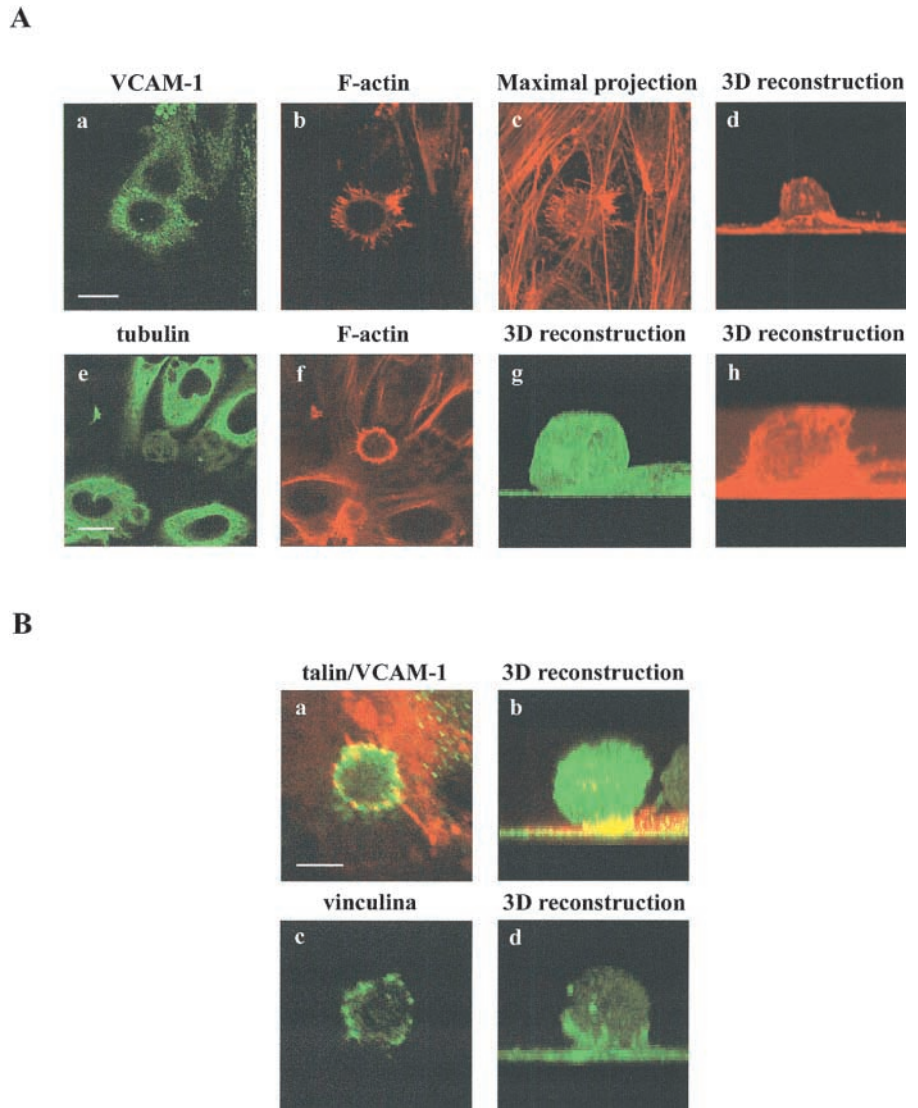
inhibitor Gö6976 did not exert a significant inhibitory effect neither on the generation nor in the maintenance of the anchoring structure (Fig. 9 A). Dynamic studies using VCAM-1-GFP transfected HUVEC showed that the p160 ROCK inhibitor Y-27632 acted by destroying the docking structure formed around 4M7 cells, as observed in Fig. 9 B. Finally, the effect of this inhibitor was assayed on endothelium during peripheral blood lymphocyte adhesion and transmigration under flow conditions. We found a diminished lymphocyte rolling and adhesion after Y-27632 treatment with regard to control conditions. Furthermore, some cells that were initially adhered, began to roll and finally detached from the monolayer, indicating an abnormal adhesion process. Accordingly, all these events led to a significant inhibition of transmigration. The effect of the inhibitor Y-27632 was analyzed at different time periods (3, 6, 8, and 10 min of perfusion), being persistent at any time tested, but only the last time is shown, as representative (Fig. 9 C). Furthermore, immunofluorescence analysis revealed that most of adhered lymphocytes were not tightly anchored by an endothelial docking structure (unpublished data). In conclusion, these findings suggest that both, PI(4,5)P<sub>2</sub> and the Rho/p160 ROCK pathway, are important for the generation as well as for the maintenance of the endothelial docking structure.

## Discussion

VCAM-1 is one of the major endothelial receptors that mediates leukocyte adhesion to the vascular endothelium (Carlos and Harlan, 1994). Recent data obtained with neonatally deficient VCAM-1 mice have strongly suggested that VCAM-1 plays an important role for lymphocyte homing and for T cell-dependent humoral immune responses (Koni et al., 2001; Leuker et al., 2001). In addition, VCAM-1 may play an im-

**Figure 7. Characterization of the endothelial docking structure formed during leukocyte adhesion.**

(A) 4M7 cells were allowed to adhere to activated HUVEC cells, then fixed, permeabilized and stained for VCAM-1 (a, green), F-actin (b–d, f, and h, red), and tubulin (e and g, green). Representative horizontal sections of confocal image-stacks are presented in a and b and e and f. The panel c shows the projection of all the horizontal sections corresponding to the image presented in a and b. Three-dimensional reconstructions of F-actin (d and h) and tubulin (g) stainings are also shown. Bars, 20  $\mu\text{m}$ . (B) 4M7 cells adhered to activated HUVEC were fixed, permeabilized, and stained for talin (a and b, green), VCAM-1 (a and b, red), or vinculin (c and d, green). Representative horizontal sections of confocal images are presented in a and c. Three-dimensional reconstructions are shown in b and d. Bar, 5  $\mu\text{m}$ . (C) 4M7 cells were allowed to adhere to activated HUVEC transfected with  $\alpha$ -actinin, paxillin-, and VASP-GFP. Thereafter, cells were fixed and stained with the anti-VCAM-1 mAb P8B1 (a, d, and f, red). Green signal corresponds to GFP fusion proteins (b, c, e, and g). Representative horizontal sections of confocal image stacks are presented in all panels except for c, which shows the three-dimensional reconstruction of  $\alpha$ -actinin–GFP signal. Bars, 5  $\mu\text{m}$ .



portant role in the pathogenesis of diseases such as atherosclerosis (Cybulsky et al., 2001), rheumatoid arthritis (Carter and Wicks, 2001), and multiple sclerosis (Alon, 2001). Thus, the elucidation of VCAM-1 function in leukocyte adhesion and transmigration is crucial, as this molecule could constitute a molecular target for therapeutic intervention.

The cytoskeletal components involved in the redistribution of VCAM-1 at the leukocyte-endothelial cell contact area have not been studied previously. Among potential candidates, ERM proteins seemed likely to mediate this process as these molecules play an important role in the remodelling of the plasma membrane, as reported for ICAMs (Helander et al., 1996; Serrador et al., 1997; Heiska et al., 1998). We found that endogenous VCAM-1 colocalizes and is physically associated with moesin and ezrin in microspikes and microvilli of the apical surface of cytokine-activated endothelial cells. Furthermore, the cytoplasmic tail of VCAM-1 and the active  $\text{NH}_2$ -terminal domain of moesin or ezrin are capable to directly bind *in vitro*. These data strongly suggest that ERM proteins are directly involved in the redistribution of VCAM-1. However, it cannot be ruled out completely that adaptor proteins such as EBP50 or E3KARP (Bretscher

et al., 2000), also play a role. It has been reported that ERM proteins bind to a positively charged amino acid cluster in the juxta-membrane cytoplasmic domain of CD44, CD43, and ICAM-2 (Yonemura et al., 1998). In addition, we have found recently that a novel serine-rich motif within the cytoplasmic tail of ICAM-3 is critical for its interaction with ERM proteins (Serrador et al., 2002). The amino acid sequence comparison of VCAM-1 and ICAM-3 cytoplasmic tails suggests that VCAM-1 contains a similar serine-rich motif, likely accounting for ERM association.

To study the VCAM-1/ERM interaction during the extravasation of lymphoblasts, we have made extensive use of a live cell system in combination with time-lapse fluorescence microscopy and GFP fusion proteins. This afforded us with information on dynamic relationships of the two molecules during early adhesion and later stages of TEM. Although both VCAM-1 and moesin clustered around spreading lymphoblasts on the apical endothelial surface, only moesin remained at lymphoblast-endothelial contacts during the passage of lymphoblasts across the endothelium and their subsequent migration beneath the endothelial monolayer. However, it has been reported that VCAM-1 actively participates in T lym-

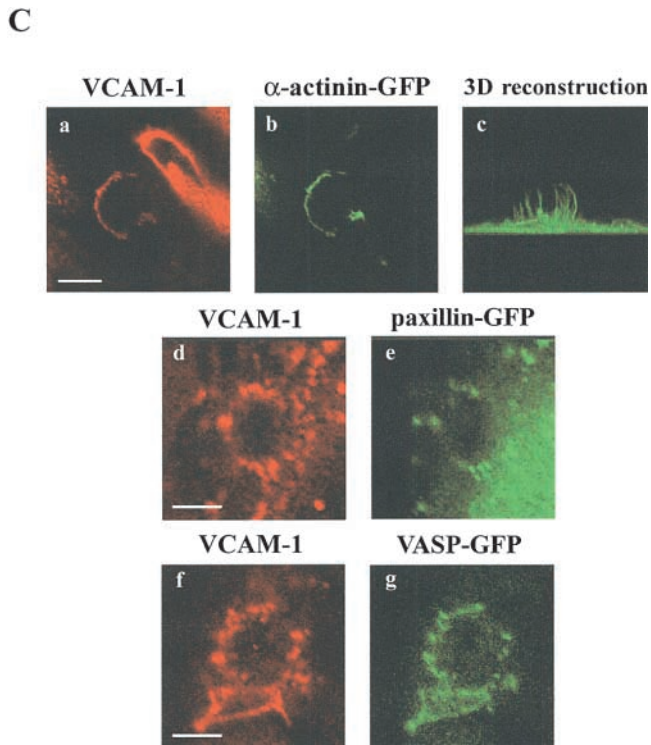
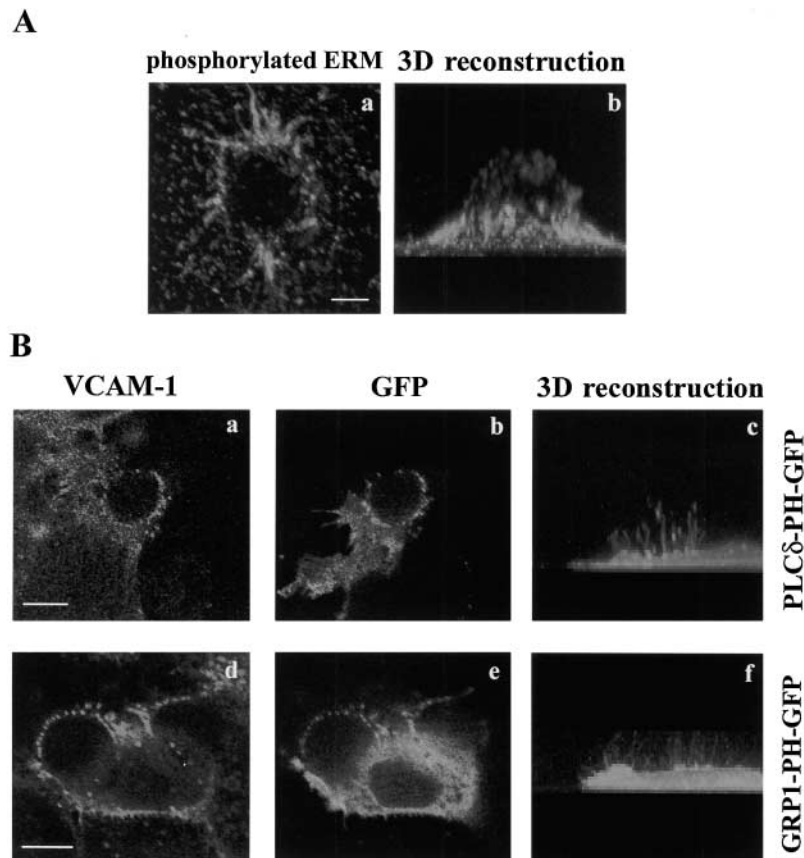


Figure 7 (continued)

phoblast transmigration across high endothelial venules and monocyte extravasation (Meerschaert and Furie, 1995; Fa-veeuw et al., 2000). These discrepancies point to a differential

role of VCAM-1 that might be both leukocyte and endothelial cell-type specific. Our data on moesin dynamics clearly indicate that another receptor linked to moesin could drive this migration. In this regard, we have found that the dynamic behavior of moesin is similar to that of ICAM-1 during lymphoblast transmigration, a finding that is in accordance with previous reports describing the distribution of ICAM-1 on the luminal and basal surfaces of the endothelium and its involvement in TEM (Oppenheimer-Marks et al., 1991; Randolph and Furie, 1996). The differential dynamic behavior of VCAM-1 and ICAM-1 during lymphoblast adhesion and transmigration on the one hand, and of moesin on the other, could suggest a mechanism by which ERM proteins are able to regulate the distribution of both molecules independently.

As VCAM-1/ERM interaction was mostly restricted to leukocyte tight adhesion and spreading, we took advantage of a cellular model based mainly on VLA-4/VCAM-1. In this model, leukocytes are restricted to a sustained tight adhesion and are unable to progress to TEM, allowing a detailed study of the endothelial VCAM-1/ERM interaction. In this cell model, VCAM-1 and both, moesin and ezrin, clustered around adherent leukocytes, participating in the formation of an actin-rich docking structure that was attached to and partially engulfed the leukocyte. Similar docking structures were formed around spreading lymphoblasts in static conditions or PBLs adhered to endothelium under flow, in which VCAM-1 and ICAM-1 were concentrated together with ERM proteins. The fact that both adhesion receptors actively participate in such endothelial structure would reinforce the concept of cross-talk between their ligands VLA-4 and LFA-1



**Figure 8. Localization of phosphorylated ERM proteins and phosphoinositides at the anchoring structure.** (A) 4M7 cells adhered to activated HUVEC were fixed, permeabilized and stained with the mAb 297S. Representative horizontal section of a confocal micrograph (a), and a three-dimensional reconstruction of a series of horizontal sections (b) are shown. Bar, 5  $\mu$ m. (B) HUVEC cells were transfected with PLCs-PH- and GRP1-PH-GFP and then, 4M7 cells were allowed to adhere. Thereafter, cells were fixed, permeabilized and stained with the anti-VCAM-1 mAb P8B1 (a and d). Green signal corresponds to GFP fusion proteins (b and e). Panels c and f show three-dimensional reconstructions of horizontal sections corresponding to the green signal. Bars, 5  $\mu$ m.

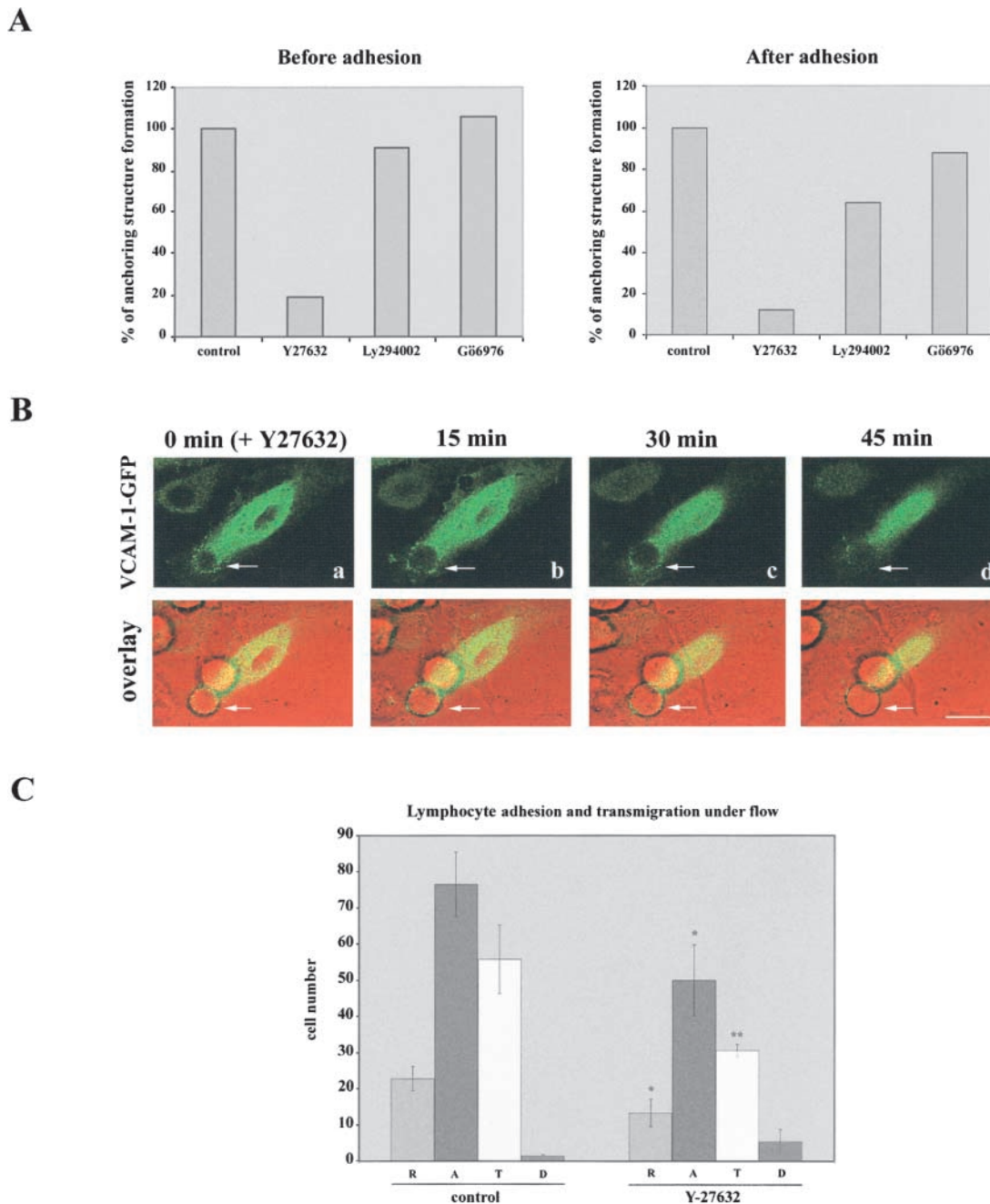


**Figure 9. Rho/p160 ROCK pathway regulates the generation and maintenance of the VCAM-1-mediated docking structure.** (A) Activated HUVEC were pretreated with Y27632 (30  $\mu$ M), Ly294002 (20  $\mu$ M), or Gö6976 (1  $\mu$ M) for 20 min before or 30 min after the addition of 4M7 cells. Total adhesion time was in both cases 60 min. Quantification of leukocyte adhesion and endothelial docking structure formation was carried out by staining with the mAb anti-VCAM-1 P8B1 and counting 300 adhered cells of each treatment. A representative experiment out of four independent ones is presented. (B) Kinetics of the endothelial anchoring structure dissolution after the addition of the p160 ROCK inhibitor Y-27632. The inhibitor Y-27632 (30  $\mu$ M) was added after the formation of the docking structure in a 4M7 adhesion assay performed as above. Representative horizontal sections captured every 15 min are shown in a–d. DIC and fluorescence images are merged and presented in the lower side of each panel. Arrows indicate the clustering of GFP proteins. Bar, 10  $\mu$ m. (C) Effect of Y-27632 on peripheral blood lymphocyte adhesion and TEM under flow conditions. Activated endothelium was pretreated or not with Y-27632 (30  $\mu$ M) for 30 min. Thereafter, PBLs were allowed to adhere and transmigrate under flow conditions for 10 min. Quantification of rolling (R), adhesion (A), transmigration (T), and detachment (D) events during the last minute of perfusion was carried out. Values correspond to the arithmetic mean  $\pm$  SD of four different fields belonging to a representative experiment. Statistically significant values, as defined by unpaired Student's *t* test, are indicated with \* ( $P < 0.01$ ) or \*\* ( $P < 0.002$ ) compared with no inhibitory treatment.

during lymphocyte adhesion (Chan et al., 2000; Rose et al., 2001). Under these physiological conditions, docking structures rapidly vanished as lymphoblasts or lymphocytes began to migrate through the endothelial monolayer.

Our findings highlight the remarkable active role played by the endothelium during leukocyte adhesion. Thus, the initial VCAM-1 and ICAM-1 engagement trigger their clustering and the subsequent activation and clustering of endothelial

moesin and ezrin at the site of cell–cell contact. In turn, phosphorylated active ERM proteins would participate in concert with  $\alpha$ -actinin, an actin-bundling protein, in the rearrangement of the actin cytoskeleton to create the docking structure. Several focal adhesion proteins such as vinculin, talin, and paxillin seem to be involved as well. Interestingly, the endothelial docking structure is reminiscent of nascent receptor-mediated phagosomes, in that the subcellular distribution of all these structural proteins is similar in both structures (Allen and Aderem, 1996). In this regard, it has been proposed that focal adhesions and complement receptor-mediated phagosomes could share some conserved mechanisms requiring the same molecules (May and Machesky, 2001). A similar argument could be made to functionally link the former structures and the novel leukocyte–endothelium docking structure described here. On the other hand, VASP is concentrated in the docking structure. This protein is present in actin-based protrusions, where it cooperates with WASp-Arp2/3 complex, as occurs in phagosomes (Castellano et al., 2001). Its presence at the docking structure could indicate the existence of actin polymerization supporting this endothelial structure, and suggests common mechanisms for *de novo* actin assembly in all these structures. Interestingly, ERM proteins have been also implicated in the *de novo* actin assembly on mature Fc receptor-mediated phagosomes (Defacque et al., 2000).

As ERM activation occurred during the formation of the anchoring structure, we studied the regulatory mechanisms involved. These proteins are regulated by the interplay of PI(4,5)P<sub>2</sub> metabolism and components of the Rho GTPase signaling pathway, thereby linking events occurring at the plasma membrane with cytoskeletal remodelling (Sechi and Wehland, 2000). Interestingly, these regulatory molecules are also important in phagocytosis (Botelho et al., 2000; Chimini and Chavrier, 2000). We found that PI(3,4)P<sub>2</sub>, PI(3,4,5)P<sub>3</sub>, and more abundantly PI(4,5)P<sub>2</sub>, colocalized with VCAM-1 and ERM proteins in the endothelial docking structure. Notably, PI(4,5)P<sub>2</sub> was preferentially concentrated at the microspike tips, whereas the other phosphoinositides exhibited a more diffuse pattern. These observations point to a prominent role of PI(4,5)P<sub>2</sub> in regulating molecular events during endothelial docking of leukocytes. One such event could be the activation of moesin and ezrin through its binding to their NH<sub>2</sub>-terminal domain. PI(4,5)P<sub>2</sub> production could be mediated by Rho, as PI4P5K is a down-stream RhoGTPase effector. On the other hand, the presence of PI(3,4)P<sub>2</sub> and PI(3,4,5)P<sub>3</sub> could be related to PI3K activity. Inhibitors of PI3K only mildly affected the generation and maintenance of the docking structure, a finding that is in agreement with its role in phagocytosis, namely to mediate phagosome closure (Cox et al., 1999). In our experimental model, the endothelial anchoring structure does not progress to engulf the leukocyte; therefore, it is less PI3K dependent. In contrast, the p160 ROCK inhibitor Y27632 inhibited the formation of the anchoring structure and induced its dissolution as well. Abnormal formation of the endothelial docking structure was also observed under flow conditions after the treatment with Y-27632, which rendered an inhibitory effect in lymphocyte adhesion and transmigration. In addition, the phenomenon of rolling was also decreased. This finding is in agreement with previous reports describing the existence of an E-selectin/actin

cytoskeleton adhesion complex induced by leukocyte adhesion (Yoshida et al., 1996; Lorenzon et al., 1998), which it is likely to be also affected by the inhibition of the Rho/p160 ROCK pathway. Our results concur with the previously described regulation of the VCAM-1, ICAM-1, and E-selectin clustering by the GTPase Rho during monocyte adhesion (Wojciak-Stothard et al., 1999). Furthermore, the key role of the Rho/p160 ROCK signaling pathway in the regulation of the adhesion receptor/ERM/actin cytoskeleton interaction and remodelling, which results in the formation of this protrusive structure, is further strengthened by the implication of this pathway in the regulation of complement receptor-mediated phagosomes (Caron and Hall, 1998).

In conclusion, our results provide novel insights into the links between the actin cytoskeleton and adhesion receptors involved in leukocyte adhesion and TEM during inflammation. Further analysis will be focused on molecules involved in the regulation of the endothelial docking structure disruption to allow diapedesis, and the signaling pathways that interconnect both processes.

## Materials and methods

### Cells and cell cultures

HUVEC were obtained and cultured as previously described (Yáñez-Mó et al., 1998). Cells were used up to the third passage in all assays. To activate HUVEC, TNF- $\alpha$  (20 ng/ml; R&D Systems) was added to the culture media 20 h before the assays were performed. Human PBLs and T lymphoblasts were obtained and cultured as described elsewhere (Serrador et al., 1997). K562 cells stably transfected with the  $\alpha 4$  integrin chain gene (4M7 cells) were grown in RPMI 1640 medium (GIBCO BRL) supplemented with 10% FCS, 50 IU/ml penicillin, 50  $\mu$ g/ml streptomycin, and 1 mg/ml of G418 (Calbiochem).

### Antibodies and reagents

The TEA1/31 anti-VE cadherin and TS2/16 anti- $\beta 1$  integrin (Yáñez-Mó et al., 1998), the HP2/1 anti- $\alpha 4$  integrin, TS1/11 anti- $\alpha L$  integrin, and TP1/24 anti-ICAM-3 (Serrador et al., 1997) mAb have been described elsewhere. The 4B9 and P8B1 (anti-VCAM-1), Hu5/3 (anti-ICAM-1), and 297S (antiphosphorylated forms of ERM proteins) mAb were provided by Dr. R.R. Lobb (Biogen Inc.), Dr. E.A. Wayner (Fred Hutchinson Cancer Research Center, Seattle, WA), Dr. F.W. Luscinskas (Brigham and Women's Hospital and Harvard Medical School, Boston, MA), and Dr. S. Sukita (Faculty of Medicine, Kyoto University, Japan), respectively. The moesin-specific polyclonal antiserum 95/2 and the ezrin-polyclonal antiserum 90/3 have been previously described (Serrador et al., 2002). The anti-tubulin and -vinculin mAb were purchased from Sigma-Aldrich. The anti-talin polyclonal antibody (pAb) was a gift of Dr. K. Burrige (University of North Carolina, Chapel Hill, NC). The monoclonal IgG1, $\kappa$  from the P3 $\times$ 63 myeloma cell line was used as negative control. Recombinant human fibronectin was purchased from Sigma-Aldrich. The p160 ROCK inhibitor Y-27632, the PI3K inhibitor Ly 294002, and the classical PKCs inhibitor Gö6976 were purchased from Calbiochem.

### Recombinant DNA constructs and cell transfections

The fusion protein GST-VC, containing the cytoplasmic tail of VCAM-1, was obtained by PCR amplification using as template the human VCAM-1 cDNA, and [TATGGATCCAGAAAAGCCAACATGAAG] and [TGGAAATCATAGATGGGCATTC] as 5' and 3' primers, respectively. The PCR product was cloned as a BamHI/EcoRI fragment into pGEX-4T (Pharmacia LKB Biotechnology). The cytoplasmic tail of ICAM-3 fused to GST (GST-IC3), and a truncated form of it (GST-Y9, Y490stop) have been described elsewhere (Serrador et al., 2002). Expression of GST fusion proteins in BL21 bacteria and purification were performed following the manufacturer's instructions.

VCAM-1-GFP and ICAM-1-GFP were obtained using the corresponding human cDNAs as templates to amplify by PCR the complete encoding region of these molecules without the stop codon. A Xho I site was added to the 5' end and an Xma I site at the 3' end of VCAM-1 cDNA. Likewise, HindIII and BamHI sites were added to the 5' and 3' ends of ICAM-1 cDNA, respectively. The PCR products were then cloned into pEGFP-N1 (CLONTECH Laboratories, Inc.) resulting in an in-frame fusion of enhanced GFP to the COOH terminus of VCAM-1 and ICAM-1. The VCAM-1-

and ICAM-1-GFP proteins behaved similarly to the corresponding endogenous proteins in terms of their binding to ezrin and moesin. The generation of the GFP fusion construct containing the GFP cDNA inserted at the COOH-terminal end of the rat full-length moesin (moesin-GFP, residues 1–577) has been previously described (Amieva et al., 1999).  $\alpha$ -actinin-GFP and paxillin-GFP were gifts of Dr. A.F. Horwitz (University of Virginia, Charlottesville, VA). VASP-GFP, PLC $\beta$ -PH-GFP, and GRP1-PH-GFP, were provided by Dr. J.V. Small (Institute of Molecular Biology, Salzburg, Austria), Dr. T. Balla (National Institutes of Health, Bethesda, MA), and Dr. A. Gray (University of Dundee, Dundee, U.K.), respectively.

Transiently transfected HUVEC were generated by electroporation at 200 V and 975  $\mu$ F using a Gene Pulser (Bio-Rad Laboratories) and adding 20  $\mu$ g of each DNA construct. These cells were used 24–48 h after transfection.

### Flow cytometry analysis, immunofluorescence, and confocal microscopy

For flow cytometry analysis and immunofluorescence experiments, cells were treated as previously described (Yáñez-Mó et al., 1998). Rhodamine Red-X-Affinipure goat anti-mouse IgG (H+L), Alexa Fluor 488 rabbit anti-mouse or goat anti-rabbit IgG (H + L) conjugate highly crossadsorbed, Alexa Fluor 488 streptavidin, and Phalloidin Alexa Fluor 568 were used as fluorescent reagents (Molecular Probes). Staining with the 2975 mAb was performed as previously described (Hayashi et al., 1999). Series of optical sections were obtained with a Leica TCS-SP confocal laser scanning unit equipped with Ar and He/Ne laser beams and attached to a Leica DMIRBE inverted epifluorescence microscope (Leica Microsystems), using a 63 $\times$  oil immersion objective. Colocalization histograms were obtained using the Leica Confocal Software.

### Immunoprecipitation, Western blot, in vitro translation, and protein binding assays

Lysates from activated HUVEC, immunoprecipitation, and Western blot were performed as described (Serrador et al., 2002). The pCR3 plasmids carrying the inserts of untagged moesin and ezrin NH $_2$ -terminal regions (amino acid residues 1–310) were transcribed, translated, and isotope labeled in vitro using a TNT-coupled rabbit reticulocyte lysate system (Promega). Then, binding assays using these isotope-labeled recombinant proteins and the GST fusion proteins (GST-VC, GST-IC3, GST-Y9, and GST alone) were performed as previously described (Serrador et al., 2002).

### Adhesion and transendothelial migration assays

For cellular adhesion assays, HUVEC were grown to confluence in 96-microwell plates (Costar) and activated with TNF- $\alpha$  for 20 h. K562 cells were labeled with 1  $\mu$ M of BCECF-AM for 15 min at 37°C, preincubated with different purified mAb, and allowed to adhere to activated HUVEC for 15 min at 37°C as previously described (Yáñez-Mó et al., 1998). Fluorescence intensity was measured in a microplate reader (Biotek FL500). T lymphoblast migration through a confluent monolayer of activated HUVEC was assayed in 3- $\mu$ m pore Transwell cell culture chambers (Costar). HUVEC were seeded and grown to confluence on these Transwell inserts precoated with 1% gelatin and activated with TNF- $\alpha$  for 20 h. Cultured lymphoblasts ( $2 \times 10^5$  in 100  $\mu$ l of complete 199 medium/well) were incubated with 10  $\mu$ g/ml of different purified mAbs for 20 min at 4°C, and then added to the upper chambers. In the lower well, 600  $\mu$ l of complete 199 medium were poured. Cells were incubated for 90 min at 37°C, and migrated cells were recovered from the lower chamber. The relative number of migrated cells was estimated by flow cytometry.

### Time-lapse fluorescence confocal microscopy

HUVEC transfected with different GFP constructs were grown to confluence on glass-bottom dishes (WillCo Wells) precoated with Fn (20  $\mu$ g/ml). Then, cells were activated with TNF- $\alpha$  for 20 h, and placed on the microscope stage. 4M7 cells or T lymphoblasts resuspended in 500  $\mu$ l of complete 199 medium were added. Plates were maintained at 37°C in a 5% CO $_2$  atmosphere using an incubation system (La-con GBR Pe-con GmbH). Confocal series of fluorescence and differential interference contrast (DIC) images, distanced 0.4  $\mu$ m in the z axis, were simultaneously obtained at 30-s or 1-min intervals, with a 63 $\times$  oil immersion objective. Images were processed and assembled into movies using the Leica Confocal Software.

### Parallel plate flow chamber analysis of endothelial-PMN interactions

The parallel plate flow chamber used for leukocyte adhesion and transmigration under defined laminar flow has been described in detail (Luscinskas et al., 1994). PBLs (10 $^6$ /ml) were drawn across activated confluent monolayers at an estimated wall shear stress of 1.8 dynes/cm $^2$  for perfusion times from 30 s to 10 min. Lymphocyte rolling on the endothelium were easily vi-

sualized as they travelled more slowly than free-flowing cells. Lymphocytes were considered to be adherent after 20 s of stable contact with the monolayer. Transmigrated lymphocytes were determined as being beneath the endothelial monolayer. Lymphocytes were considered to be detached when they returned to free-flowing after having been completely arrested on endothelium. The number of rolling, adhered, transmigrated, and detached cells was quantified by direct visualization of 4 different fields (40 $\times$  phase-contrast objective) at each time point of every independent experiment. Coverslips were fixed immediately in PFA 4% at room temperature for 10 min, washed with HBSS, and stained for VCAM-1, ICAM-1, or ezrin.

### Online supplemental material

All videos are available at <http://www.jcb.org/cgi/content/full/jcb.200112126/DC1>. Video 1 (corresponding to Fig. 4 A, a–f) shows a lymphoblast that contacts with a moesin-GFP-transfected endothelial cell, and immediately transmigrates and moves beneath the endothelium. Moesin is clustered around the lymphoblast along the whole process. Video 2 (corresponding to Fig. 4 A, g–l), shows a lymphoblast (upper site) that adheres to, spreads on, and moves toward a lateral junction of the VCAM-1-GFP-transfected endothelial cell. It then transmigrates and moves beneath the endothelium, whereas another lymphoblast (lower site) remains spread on the endothelial cell. VCAM-1 is clustered around lymphoblasts adhered to the apical surface of endothelium (arrows), but it is not concentrated around migrating lymphocytes beneath the endothelium (arrowheads). Video 3 (corresponding to Fig. 4 B), shows a lymphoblast that adheres to, spreads on, and moves toward a lateral junction of the ICAM-1-GFP-transfected endothelial cell (black arrows). It then transmigrates and moves beneath the endothelium (white arrows). ICAM-1 is clustered around the lymphoblast along the whole process. In all videos, the apical endothelial surface is at a plane remote from the observer.

We thank Drs. R. González-Amaro, D. Sancho, and P. Roda-Navarro for critical reading of the manuscript.

This work was supported by grants SAF99-0034-C01 and FEDER 2FD97-068-C02-02 from the Ministerio de Educación, and grant QLRT-1999-01036 from the European Community to F. Sánchez-Madrid, and a fellowship from the Ministerio de Educación to O. Barreiro.

Submitted: 24 December 2001

Revised: 7 May 2002

Accepted: 7 May 2002

## References

- Allen, L.-A.H., and A. Aderem. 1996. Molecular definition of distinct cytoskeletal structures involved in complement- and Fc receptor-mediated phagocytosis in macrophages. *J. Exp. Med.* 184:627–637.
- Alon, R. 2001. Encephalitogenic lymphoblast recruitment to resting CNS microvasculature: a natural immunosurveillance mechanism? *J. Clin. Invest.* 108:517–519.
- Amieva, M.R., P. Litman, L. Huang, E. Ichimaru, and H. Furthmayr. 1999. Disruption of dynamic cell surface architecture of NIH3T3 fibroblasts by the N-terminal domains of moesin and ezrin: in vivo imaging with GFP fusion proteins. *J. Cell Sci.* 112:111–125.
- Barret, C., C. Roy, P. Montcourrier, P. Mangeat, and V. Niggli. 2000. Mutagenesis of the phosphatidylinositol 4,5-bisphosphate (PIP $_2$ ) binding site in the NH(2)-terminal domain of ezrin correlates with its altered cellular distribution. *J. Cell Biol.* 151:1067–1079.
- Botelho, R.J., M. Teruel, R. Dierckman, R. Anderson, A. Wells, J.D. York, T. Meyer, and S. Grinstein. 2000. Localized biphasic changes in phosphatidylinositol-4,5-bisphosphate at sites of phagocytosis. *J. Cell Biol.* 151:1353–1367.
- Bretscher, A., D. Chambers, R. Nguyen, and D. Reczek. 2000. ERM-Merlin and EBP50 protein families in plasma membrane organization and function. *Annu. Rev. Cell Dev. Biol.* 16:113–143.
- Butcher, E.C. 1991. Leukocyte-endothelial cell recognition: three (or more) steps to specificity and diversity. *Cell.* 67:1033–1036.
- Carlos, T.M., and J.M. Harlan. 1994. Leukocyte-endothelial adhesion molecules. *Blood.* 84:2068–2101.
- Caron, E., and A. Hall. 1998. Identification of two distinct mechanisms of phagocytosis controlled by different Rho GTPases. *Science.* 282:1717–1721.
- Carter, R.A., and I.P. Wicks. 2001. Vascular cell adhesion molecule 1 (CD 106). A multifaceted regulator of joint inflammation. *Arthritis Rheum.* 44:985–994.
- Castellano, F., C. Le Clainche, D. Patin, M.-F. Carlier, and P. Chavrier. 2001. A WASp-VASP complex regulates actin polymerization at the plasma mem-

- brane. *EMBO J.* 20:5603–5614.
- Chan, J.R., S.J. Hyduk, and M.I. Cybulsky. 2000.  $\alpha 4\beta 1$  integrin/VCAM-1 interaction activates  $\alpha L\beta 2$  integrin-mediated adhesion to ICAM-1 in human T cells. *J. Immunol.* 164:746–753.
- Cox, D., C.C. Tseng, G. Bjekic, and S. Greenberg. 1999. A requirement for phosphatidylinositol 3-kinase in pseudopod extension. *J. Biol. Chem.* 274:1240–1247.
- Cybulsky, M.I., K. Iiyama, H. Li, S. Zhu, M. Chen, M. Iiyama, V. Davis, J.C. Gutierrez-Ramos, P.W. Connelly, and D.S. Milstone. 2001. A major role for VCAM-1, but not ICAM-1, in early atherosclerosis. *J. Clin. Invest.* 107:1255–1262.
- Chimini, G., and P. Chavrier. 2000. Function of Rho family proteins in actin dynamics during phagocytosis and engulfment. *Nat. Cell Biol.* 2:E191–E196.
- Defacque, H., M. Egeberg, A. Habermann, M. Diakonova, C. Roy, P. Mangeat, W. Voelter, G. Marriot, J. Pfannstiel, H. Faulstich, and G. Griffiths. 2000. Involvement of ezrin/moesin in de novo actin assembly on phagosomal membranes. *EMBO J.* 19:199–212.
- Doi, Y., M. Itoh, S. Yonemura, S. Ishihara, H. Takano, T. Noda, and S. Tsukita. 1999. Normal development of mice and unimpaired cell adhesion/cell motility/actin-based cytoskeleton without compensatory up-regulation of ezrin or radixin in moesin gene knockout. *J. Biol. Chem.* 274:2315–2321.
- Elices, M.J., L. Osborn, Y. Takada, C. Crouse, S. Luhsowsky, M.E. Hemler, and R.R. Lobb. 1990. VCAM-1 on activated endothelium interacts with the leukocyte integrin VLA-4 at a site distinct from the VLA-4/fibronectin binding site. *Cell.* 60:577–584.
- Faveeuw, C., M.E. Di Mauro, A.A. Price, and A. Ager. 2000. Roles of alpha(4) integrins/VCAM-1 and LFA-1/ICAM-1 in the binding and transendothelial migration of T lymphocytes and T lymphoblasts across high endothelial venules. *Int. Immunol.* 12:241–251.
- González-Amaro, R., and F. Sánchez-Madrid. 1999. Cell adhesion molecules: selectins and integrins. *Crit. Rev. Immunol.* 19:389–429.
- Gray, A., J. van der Kaay, and C.P. Downes. 1999. The pleckstrin homology domains of protein kinase B and GRP1 (general receptor for phosphoinositides-1) are sensitive and selective probes for the cellular detection of phosphatidylinositol 3,4-bisphosphate and/or phosphatidylinositol 3,4,5-triphosphate in vivo. *Biochem. J.* 344:929–936.
- Hayashi, K., S. Yonemura, T. Matsui, and S. Tsukita. 1999. Immunofluorescence detection of ezrin/radixin/moesin (ERM) proteins with their carboxyl-terminal threonine phosphorylated in cultured cells and tissues. *J. Cell Sci.* 112:1149–1158.
- Heiska, L., K. Alfthan, M. Gronholm, P. Vilja, A. Vaheri, and O. Carpen. 1998. Association of ezrin with intercellular adhesion molecule-1 and -2 (ICAM-1 and ICAM-2). Regulation by phosphatidylinositol 4, 5-bisphosphate. *J. Biol. Chem.* 273:21893–21900.
- Helander, T.S., O. Carpen, O. Turunen, P.E. Kovanen, A. Vaheri, and T. Timonen. 1996. ICAM-2 redistributed by ezrin as a target for killer cells. *Nature.* 382:265–268.
- Hirao, M., N. Sato, T. Kondo, S. Yonemura, M. Monden, T. Sasaki, Y. Takai, and S. Tsukita. 1996. Regulation mechanism of ERM (ezrin/radixin/moesin) protein/plasma membrane association: possible involvement of phosphatidylinositol turnover and Rho-dependent signaling pathway. *J. Cell Biol.* 135:37–51.
- Koni, P.A., S.K. Joshi, U.A. Temann, D. Olson, L. Burkly, and R.A. Flavell. 2001. Conditional vascular cell adhesion molecule 1 deletion in mice: impaired lymphocyte migration to bone marrow. *J. Exp. Med.* 193:741–753.
- Leuker, C.E., M. Labow, W. Müller, and N. Wagner. 2001. Neonatally induced inactivation of the vascular cell adhesion molecule 1 gene impairs B cell localization and T cell-dependent humoral immune response. *J. Exp. Med.* 193:755–767.
- Lorenzon, P., E. Vecile, E. Nardon, E. Ferrero, J.M. Harlan, F. Tedesco, and A. Dobrina. 1998. Endothelial cell E- and P-selectin and vascular cell adhesion molecule-1 function as signaling receptors. *J. Cell Biol.* 142:1381–1391.
- Luscinskas, F.W., G.S. Kansas, H. Ding, P. Pizcueta, B.E. Schleiffenbaum, T.F. Tedder, and M.A. Gimbrone Jr. 1994. Monocyte rolling, arrest and spreading on IL-4 activated vascular endothelium under flow is mediated via sequential action of L-selectin, beta-1-integrins, and beta-2-integrins. *J. Cell Biol.* 125:1417–1427.
- Mangeat, P., C. Roy, and M. Martin. 1999. ERM proteins in cell adhesion and membrane dynamics. *Trends Cell Biol.* 9:187–192.
- Marlin, S.D., and T.A. Springer. 1987. Purified inter-cellular adhesion molecule (ICAM-1) is a ligand for lymphocyte-associated antigen 1 (LFA1). *Cell.* 51:813–819.
- Matsui, T., M. Maeda, Y. Doi, S. Yonemura, M. Amano, K. Kaibuchi, and S. Tsukita. 1998. Rho-kinase phosphorylates COOH-terminal threonines of ezrin/radixin/moesin (ERM) proteins and regulates their head-to-tail association. *J. Cell Biol.* 140:647–657.
- May, R.C., and L.M. Machesky. 2001. Phagocytosis and the actin cytoskeleton. *J. Cell Sci.* 114:1061–1077.
- Meerschaert, J., and M.B. Furie. 1995. The adhesion molecules used by monocytes for migration across endothelium include CD11a/CD18, CD11b/CD18, and VLA-4 on monocytes and ICAM-1, VCAM-1, and other ligands on endothelium. *J. Immunol.* 154:4099–4112.
- Menager, C., J. Vassy, C. Doliger, Y. Legrand, and A. Karniguian. 1999. Subcellular localization of RhoA and ezrin at membrane ruffles of human endothelial cells: differential role of collagen and fibronectin. *Exp. Cell Res.* 249:221–230.
- Muñoz, M., J. Serrador, F. Sanchez-Madrid, and J. Teixido. 1996. A region of the integrin VLA alpha 4 subunit involved in homotypic cell aggregation and in fibronectin but not vascular cell adhesion molecule-1 binding. *J. Biol. Chem.* 271:2696–2702.
- Nakamura, F., L. Huang, K. Pestonjampas, E.J. Luna, and H. Furthmayr. 1999. Regulation of F-actin binding to platelet moesin in vitro by both phosphorylation of threonine 558 and polyphosphatidylinositides. *Mol. Biol. Cell.* 10:2669–2685.
- Oppenheimer-Marks, N., L.S. Davis, D.T. Bogue, J. Ramberg, and P.E. Lipsky. 1991. Differential utilization of ICAM-1 and VCAM-1 during the adhesion and transendothelial migration of human T lymphocytes. *J. Immunol.* 147:2913–2921.
- Randolph, G.J., and M.B. Furie. 1996. Mononuclear phagocytes egress from an in vitro model of the vascular wall by migrating across endothelium in the basal to apical direction: role of intercellular adhesion molecule 1 and the CD11/CD18 integrins. *J. Exp. Med.* 183:451–462.
- Rose, D.M., V. Grabovsky, R. Alon, and M.H. Ginsberg. 2001. The affinity of integrin  $\alpha 4\beta 1$  governs lymphocyte migration. *J. Immunol.* 167:2824–2830.
- Sechi, A.S., and J. Wehland. 2000. The actin cytoskeleton and plasma membrane connection: PtdIns(4,5)P2 influences cytoskeletal protein activity at the plasma membrane. *J. Cell Sci.* 113:3685–3695.
- Serrador, J.M., J.L. Alonso-Lebrero, M.A. del Pozo, H. Furthmayr, R. Schwartz-Albiez, J. Calvo, F. Lozano, and F. Sánchez-Madrid. 1997. Moesin interacts with the cytoplasmic region of intercellular adhesion molecule-3 and is redistributed to the uropod of T lymphocytes during cell polarization. *J. Cell Biol.* 138:1409–1423.
- Serrador, J.M., M. Vicente-Manzanares, J. Calvo, O. Barreiro, M.C. Montoya, R. Schwartz-Albiez, H. Furthmayr, F. Lozano, and F. Sanchez-Madrid. 2002. A novel serine-rich motif in the intercellular adhesion molecule-3 is critical for its ERM-directed subcellular targeting. *J. Biol. Chem.* 277:10400–10409.
- Shaw, R.J., M. Henry, F. Solomon, and T. Jacks. 1998. RhoA-dependent phosphorylation and relocalization of ERM proteins into apical membrane/actin protrusions in fibroblasts. *Mol. Biol. Cell.* 9:403–419.
- Takahashi, K., T. Sasaki, A. Mammoto, K. Takaishi, T. Kameyama, S. Tsukita, and Y. Takai. 1997. Direct interaction of the Rho GDP dissociation inhibitor with ezrin/radixin/moesin initiates the activation of the Rho small G protein. *J. Biol. Chem.* 272:23371–23375.
- Turunen, O., T. Wahlstrom, and A. Vaheri. 1994. Ezrin has a COOH-terminal actin-binding site that is conserved in the ezrin protein family. *J. Cell Biol.* 126:1445–1453.
- Várnai, P., K.I. Rother, and T. Balla. 1999. Phosphatidylinositol 3-kinase-dependent membrane association of the Bruton's tyrosine kinase pleckstrin homology domain visualized in single living cells. *J. Biol. Chem.* 274:10983–10989.
- Wojciak-Stothard, B., L. Williams, and A.J. Ridley. 1999. Monocyte adhesion and spreading on human endothelial cells is dependent on Rho-regulated receptor clustering. *J. Cell Biol.* 145:1293–1307.
- Yáñez-Mó, M., A. Alfranca, C. Cabañas, M. Marazuela, R. Tejedor, M.A. Ursa, L.K. Ashman, M.O. de Landázuri, and F. Sánchez-Madrid. 1998. Regulation of endothelial cell motility by complexes of tetraspan molecules CD81/TAPA-1 and CD151/PETA-3 with alpha3beta1 integrin localized at endothelial lateral junctions. *J. Cell Biol.* 141:791–804.
- Yonemura, S., M. Hirao, Y. Doi, N. Takahashi, T. Kondo, and S. Tsukita. 1998. Ezrin/radixin/moesin (ERM) proteins bind to a positively charged amino acid cluster in the juxta-membrane cytoplasmic domain of CD44, CD43, and ICAM-2. *J. Cell Biol.* 140:885–895.
- Yonemura, S., and S. Tsukita. 1999. Direct involvement of ezrin/radixin/moesin (ERM)-binding membrane proteins in the organization of microvilli in collaboration with activated ERM proteins. *J. Cell Biol.* 145:1497–1509.
- Yoshida, M., W.F. Westlin, N. Wang, D.E. Ingber, A. Rosenzweig, N. Resnick, and M.A.J. Gimbrone. 1996. Leukocyte adhesion to vascular endothelium induces E-selectin linkage to the actin cytoskeleton. *J. Cell Biol.* 133:445–455.

## INTERACTIVE PROTRUSIVE STRUCTURES DURING LEUKOCYTE ADHESION AND TRANSENDOTHELIAL MIGRATION

Olga Barreiro, Miguel Vicente-Manzanares, Ana Urzainqui, María Yáñez-Mó, and Francisco Sánchez-Madrid

*Servicio de Inmunología, Hospital de la Princesa, Universidad Autónoma de Madrid, 28006 Madrid, Spain*

### TABLE OF CONTENTS

1. Abstract
2. Introduction
3. Initial interactions between circulating leukocytes and the endothelium: tethering and rolling
  - 3.1. Selectins and their ligands as critical mediators of tethering and rolling
  - 3.2. Membrane topography of adhesion molecules involved in rolling
  - 3.3. Selectins and PSGL-1 as signaling receptors
4. Activation, arrest and firm adhesion of leukocytes
  - 4.1. Chemokines trigger the arrest of leukocytes on endothelium
  - 4.2. Integrin affinity and avidity changes as leukocyte strategies to achieve firm attachment and spreading
  - 4.3. The docking structure: the endothelial contribution to the leukocyte firm adhesion process
    - 4.3.1. VCAM-1 and ICAM-1 play an essential role in leukocyte capture
    - 4.3.2. Structural components and signaling pathways involved in the generation and maintenance of the docking structure
    - 4.3.3. VCAM-1 and ICAM-1 outside-in signaling
5. Transendothelial migration
  - 5.1. Leukocytes undergo drastic cytoskeletal rearrangements to extravasate across the endothelial barrier
  - 5.2. Endothelial cell lateral junctions regulation
    - 5.2.1. Tight junction proteins: role of JAM family in transendothelial migration
    - 5.2.2. Adherens junction disappearance at leukocyte contacts: proteolysis or displacement?
    - 5.2.3. Other molecules with a major role in the passage of leukocytes across endothelium
6. Concluding remarks and perspectives
7. Acknowledgements
8. References

### 1. ABSTRACT

Leukocyte transendothelial migration during homing and inflammation requires drastic cell morphological changes, involving cytoskeletal-directed clustering of adhesion receptors in specialized protrusive membrane structures in leukocytes and endothelial cells. Extravasation is an active process not only for leukocytes but also for endothelial cells, which promote the rapid and efficient entry of leukocytes to the target tissues, without disturbing the integrity of the endothelial barrier. Herein, we have revised the specialized protrusive structures (microvilli, endothelial docking structures, leukocyte lamellipodia and uropod) involved in the different stages of leukocyte extravasation. The adhesion receptor redistribution, cytoskeletal remodelling and intracellular signaling events that participate in this phenomenon are also discussed.

### 2. INTRODUCTION

Cell adhesion receptors regulate many cellular processes such as activation, migration, growth, differentiation and death (1, 2), by both signal transduction and the modulation of intracellular signaling cascades triggered by different growth factors (3). Cellular

interactions are critical for regulation of hematopoiesis (4, 5) and inflammatory responses (6, 7). The coordinate function of adhesion receptors, cytoskeleton and signaling molecules is crucial for leukocyte extravasation, a central process in immunity. Hence, the correct integration of “outside-in” and “inside-out” signals in leukocytes and endothelium during each stage of extravasation is critical to allow the completion of this phenomenon, the so-called “multi-step paradigm” (6, 8). The present review focuses on the molecular mechanisms and the specialized protrusive structures that govern this dynamic process in both leukocytes and endothelial cells.

### 3. INITIAL INTERACTIONS BETWEEN CIRCULATING LEUKOCYTES AND THE ENDOTHELIUM: TETHERING AND ROLLING

Free-flowing leukocytes contact with and adhere to the vascular wall under shear forces to initiate an inflammatory response or to migrate into a secondary lymphoid organ (homing). Leukocyte tethering and rolling on activated endothelial cells are the first steps of the sequential process of extravasation, followed by the firm adhesion and transendothelial migration of leukocytes (9).

## Protrusive structures in leukocyte extravasation

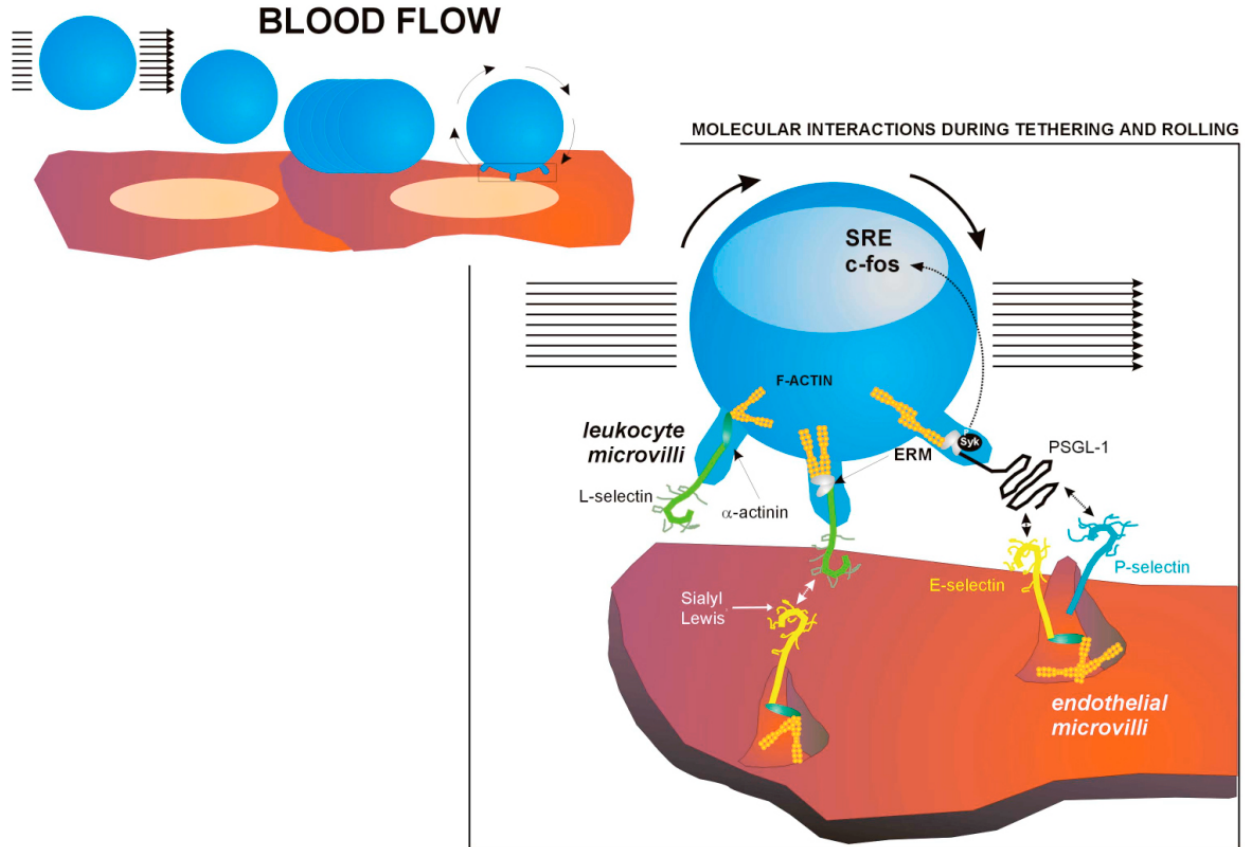


**Figure 1.** The first step of the extravasation process. As shown in the diagram, free-flowing leukocytes establish transient contacts with activated endothelial cells (tethering), being slowed down. These initial contacts allow leukocytes to roll on the endothelial wall to become activated and finally arrest. The main molecules that participate during this process are presented in detail in the inset: E- and P-selectin in endothelium as well as L-selectin and PSGL-1 in leukocytes are localized at specialized protrusions (microvilli) supported by the actin cytoskeleton, which is linked to the adhesion receptors via ERM proteins, alpha-actinin and other cytoskeletal components. All these molecules interact with their corresponding receptors through carbohydrate residues such as Sialyl Lewis<sup>x</sup>. Thus, L-selectin binds to several endothelial counterreceptors (E-selectin among them) and leukocyte PSGL-1 interacts with endothelial E- and P-selectin. In addition, the binding of PSGL-1 with its ligands allows the recruitment of the tyrosine kinase Syk via ERM proteins, which triggers signaling cascades that culminate in the activation of expression of several genes (e.g., SRE and c-fos) in leukocytes.

These initial contacts are largely mediated by selectins and their ligands. All the issues addressed in this chapter are schematically depicted in Figure 1.

### 3.1. Selectins and their ligands as critical mediators of tethering and rolling

Selectins (P-, E- and L-selectin) are cell adhesion molecules that predominantly mediate the initial interactions of leukocytes with endothelium. They are type I transmembrane glycoproteins that bind to sialylated carbohydrate moieties present on ligand molecules in a calcium-dependent manner. Selectins and their ligands interact with variable affinity, and due to their rapid association and dissociation rates mediate transient contacts between leukocytes and endothelium (“tethering”) (10, 11). Tethering results in the slowing of leukocytes in the bloodstream and their rolling on the surface of endothelium, which favors subsequent interactions with endothelial cells mediated by integrins and their ligands,

increasing the adhesiveness of leukocytes, that leads to their final arrest on the vessel wall (12).

P-selectin, which is constitutively expressed by platelets and endothelial cells in secretory granules, is translocated to the cell surface within minutes upon cell activation (13). Once expressed on the surface of endothelial cells, P-selectin is rapidly internalized by endocytosis. Therefore, this adhesion receptor has an important role in early leukocyte recruitment during inflammation (14). E-selectin is also expressed by endothelial cells, but it is synthesized de novo upon cell activation (15). After stimulation with IL-1 or TNF-alpha, it is maximally expressed on the membrane at 4h, and then is slowly internalized and degraded (16). L-selectin is constitutively present in most leukocytes, but it is rapidly shed upon cell activation, thus facilitating the progression to adhesion and transendothelial migration (TEM) (17-19). It was first described as a lymphocyte homing receptor, but

## Protrusive structures in leukocyte extravasation

it also participates in leukocyte recruitment at later stages of the inflammatory response (20).

The best characterized selectin ligand is PSGL-1 (P-selectin glycoprotein ligand-1), a homodimeric sialomucin expressed by almost all leukocytes (21) and platelets (22). PSGL-1 is an important functional ligand *in vivo* for all three selectins (23-26). In addition, CD24 and ESL-1 (E-selectin ligand-1) seem to be ligands in myeloid cells for P-selectin and E-selectin, respectively (27-29). Finally, it has been described that E-selectin, GlyCAM-1, MAdCAM-1, CD34 and Sgp200 specifically interact with L-selectin (reviewed in 30).

Although selectins and their ligands are the primary mediators of leukocyte rolling, alternative cell adhesion pathways are involved in this phenomenon. It has been described that alpha4beta1 (VLA-4) and alpha4beta7 integrins can also mediate leukocyte tethering, rolling and arrest through their interaction with VCAM-1 and MAdCAM-1 in the absence of selectins (31). On the other hand, the interaction of LFA-1(alphaLbeta2)/ICAM-1 cooperates with L-selectin in leukocyte rolling by stabilizing the tethering phase and decreasing the rolling velocity (32, 33). In addition, the chemokines CX3CL1 (fractalkine) and CXCL16 also mediate both rolling and firm adhesion by interacting with CX3CR1 and CXCR6, respectively (34-37).

### 3.2. Membrane topography of adhesion molecules involved in rolling

Adhesion receptor distribution on cell membrane has a key role in leukocyte interactions and is an important regulatory mechanism for leukocyte trafficking (38). Selectins are clustered at the tips of microvilli, and this localization is critical for tethering and rolling.

L-selectin is anchored to the actin cytoskeleton through the constitutive association of its cytoplasmic tail to alpha-actinin, and its cell activation-dependent binding to moesin (39, 40). Although the association with alpha-actinin is not essential for its targeting to microvilli (39), its cytoplasmic anchorage to the actin cytoskeleton is necessary to control L-selectin function (41, 42). PSGL-1 is also localized at the tips of microvilli, and this subcellular distribution has been found to be important for the initiation of tethering and rolling of leukocytes (43, 44). Furthermore, the capability of alpha4, but not beta2 integrins, to initiate leukocyte adhesion under flow is also explained by its selective topographic localization at microvilli (30). Finally, less is known about the involvement of cytoskeleton in the efficient presentation in microvilli of E- and P-selectin by endothelial cells. However, it has been described that leukocyte adhesion induces E-selectin linkage to the actin cytoskeleton through alpha-actinin, paxillin, vinculin, and FAK, but not talin (45).

### 3.3. Selectins and PSGL-1 as signaling receptors

It has been demonstrated that L-selectin activates multiple signaling pathways involved in the reorganization of the actin cytoskeleton, such as the MAPK cascade (46),

the tyrosine kinase p56<sup>lck</sup> and Ras (47) or the Rho GTPase Rac2 (48). In this regard, it has been described that neutrophils from Rac2<sup>-/-</sup> mice show deficient actin polymerization and L-selectin-mediated rolling (49). On the other hand, PSGL-1 activates the MAPK pathway (50), and acts as a negative regulator of human hematopoietic progenitor cells (5). In addition, it has been demonstrated that PSGL-1 induces a rapid synthesis of uPAR and different cytokines such as TNF-alpha, IL-8 and MCP-1 in neutrophils, monocytes and T cells (51-54). Moreover, it has been shown that PSGL-1 induces activation of beta-2 integrins and binding to ICAM-1 in neutrophils (55, 56). Our group has also described the interaction of PSGL-1 with ERM proteins, which link membrane molecules with the actin cytoskeleton (57, 58). This interaction is of critical importance for the leukocyte activation that occurs before extravasation, because it allows the recruitment of the tyrosine kinase Syk by association to ERM proteins through their phosphorylated ITAM-like motifs. Therefore, after PSGL-1 ligation to P-selectin or E-selectin, Syk conveys rolling-emanating signals to the activation of gene expression programs (59). This phenomenon suggests that the intracellular signals induced through PSGL-1 have a priming effect on leukocyte activation, up-regulating the expression of different molecules further involved in extravasation and effector functions (60). Since it has been demonstrated that the cytoplasmic tail of L-selectin also interacts with moesin (40), it is very likely that selectins use a similar strategy to trigger intracellular signaling cascades. In this regard, it has been shown that E-selectin is dephosphorylated upon endothelial cell interaction with leukocytes, supporting its role as a signal transduction molecule (61). In addition, P-selectin also functions as a signaling receptor, mediating stimulation through its interaction with ligands expressed by leukocytes (62).

## 4. ACTIVATION, ARREST AND FIRM ADHESION OF LEUKOCYTES

During their rolling, leukocytes are stimulated by chemokines and integrin ligands expressed on the surface of endothelial cells. These outside-in signals induce an important increase in the affinity and/or avidity of leukocyte integrins (inside-out signals) that allows the shear-resistant arrest of these cells and their firm adhesion to activated endothelium. The adhesion mediated by integrins and their ligands, and their subsequent signaling processes involve a profound remodelling of cytoskeleton in both endothelial cells and leukocytes. In Figure 2, the major adhesive, structural and signaling molecules that participate in the leukocyte firm adhesion to endothelium are summarized.

### 4.1. Chemokines trigger the arrest of leukocytes on endothelium

The main *in situ* modulators of integrin function are chemokines. These chemotactic cytokines act through G-protein-coupled receptors (GPCR), and induce an array of activatory signals within fractions of seconds, leading to an enhancement of adhesion and shape changes in leukocytes (63, 64). Since it is unlikely that soluble chemokine gradients present in the blood flow regulate

## Protrusive structures in leukocyte extravasation

### MOLECULAR INTERACTIONS DURING FIRM ADHESION

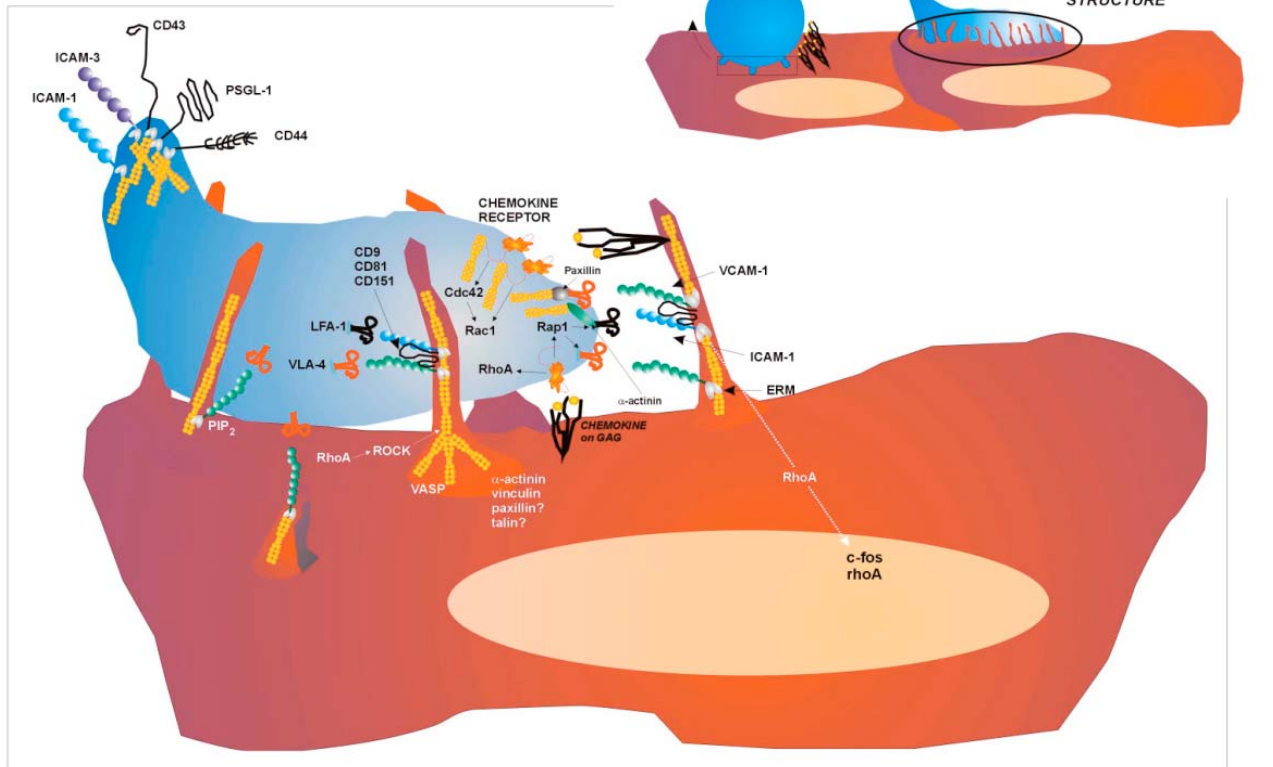


**Figure 2.** Activation, arrest and firm adhesion of leukocytes on endothelium: The slowing-down of leukocytes facilitates their interaction with chemokines exposed on endothelium, triggering the activation of leukocyte integrins by increasing their affinity and avidity to allow the final arrest of adherent leukocytes. This activated state involves a drastic morphological change from the round shape of circulating leukocytes to the polarized shape typical of migrating cells. The acquisition of polarity implies the segregation of adhesion molecules (ICAM-1, ICAM-3, CD43, CD44, PSGL-1, etc) to the rear pole of the cell (uropod), which is lumen-orientated for the recruitment of bystander leukocytes; whereas the integrins localized to the contact area with endothelium to allow the spreading of the cell body onto the vascular wall. On the other hand, the endothelium also plays an active role in firm adhesion by creating docking structures around the attached leukocytes. These endothelial docking structures are formed as a result of VCAM-1 and ICAM-1 engagement by their integrin counterreceptors (VLA-4 and LFA-1, respectively), and are supported by a cortical actin scaffold in which ERM proteins, alpha-actinin, vinculin, VASP and other actin-related proteins participate. In addition, members of the tetraspanin family also cooperate with the endothelial adhesion receptors in the docking structure formation. The principal regulatory molecules involved in the formation of the above-mentioned structure and in leukocyte integrin activation (as discussed in the text) are also shown in the inset.

leukocyte trafficking to specific target tissues, it is thought that chemokines mainly function immobilized at the emigration site (65). At sites of inflammation or in secondary lymphoid tissues, chemokines are present in the subendothelial tissues, as well as in the luminal surface of endothelium. These chemokines are synthesized or transported (transcytosis) by endothelial cells and bound to glycosaminoglycans (GAGs) and, possibly, to the Duffy antigen/receptor for chemokines (DARC) (66). Chemokine-binding sites are concentrated on endothelial microvilli, as occurs with chemokine receptors in leukocytes (67). The presence of particular subsets of chemokines on endothelium contributes to the selective recruitment of leukocytes, a critical phenomenon for the inflammatory response and lymphocyte homing (reviewed in 68). Chemokines may differentially modulate distinct integrins in the same microenvironment, leading to transient or

sustained adhesion of leukocytes (69). Furthermore, CXCL12 (SDF-1alpha), CCL19 (MIP-3beta), CCL21 (SLC) and CCL20 (MIP-3alpha) have all been shown to induce LFA-1-mediated cell arrest in different lymphoid subpopulations (63, 65, 70). In addition, SDF-1alpha up-regulates VLA-4 affinity for VCAM-1, promoting monocyte arrest (71). The mechanism involved in such regulation is not clear, but may involve small Ras GTPases such as Rap1 (72-74), Rho GTPases (75) and other signaling molecules.

#### 4.2. Integrin affinity and avidity changes as leukocyte strategies to achieve firm attachment and spreading

Integrins comprise a family of alpha-beta heterodimeric transmembrane molecules whose activation can be tuned to bind to different Ig-like or extracellular

## Protrusive structures in leukocyte extravasation

matrix ligands. Integrin-mediated cell adhesion is tightly regulated by conformational changes (affinity) and clustering (avidity), being independent of surface expression levels (76). Circulating leukocytes avoid non-specific contacts with vascular walls by maintaining their integrins in non-adhesive states. The *in situ* activation of integrins during leukocyte rolling can be driven by multiple factors. Among affinity regulatory signals, divalent cations such as  $Mn^{2+}$ ,  $Mg^{2+}$  or  $Ca^{2+}$  (77-79) rank as important elements at least *in vitro*. On the other hand, the binding of integrins to endothelial ligands can be enhanced independently of integrin affinity by increasing receptor density (avidity) at the contact area. Integrin avidity can be defined as a rapid interplay between preformed, ligand-induced, and chemokine-triggered avidity states (reviewed in 42). Other potential modulators of VLA-4 and LFA-1 avidity at dynamic contacts, requiring concomitant chemokine triggering, seem to be CD47 and L-selectin (80, 81). There is still another level of regulation known as integrin cross-talk. Thus, the interaction of high affinity VLA-4 with VCAM-1 may trigger LFA-1 clustering, enhancing its avidity to ICAM-1, and promoting leukocyte firm adhesion to endothelium. On the contrary, LFA-1/ICAM-1 engagement decreases the binding of VLA-4 to VCAM-1, allowing leukocyte migration towards the transmigration sites (82, 83).

The clustering of integrins is dependent on their release from the actin cytoskeleton. In this regard, there are relevant differences between VLA-4 and LFA-1. LFA-1 may preform microclusters stabilized by H-ras and cytohesin-1, which are activated via PI3-K or PKC (84-86). However, the macroclustering of LFA-1 prior to ligand engagement is prevented by cytoskeleton anchorage, with the involvement of non-phosphorylated PKC substrates and talin. Consequently, it is necessary the activation of PKC and calpain to release LFA-1 from the actin cytoskeleton (87). Conversely, VLA-4 clustering cannot be induced prior to ligand binding. Furthermore, although PKC signals participate in the release of VLA-4 from cytoskeleton, calpain or PI3-K are not implicated. In addition, it has been described that VLA-4 constitutively interacts with paxillin, while LFA-1 is able to interact with alpha-actinin (reviewed in 42).

Once integrin avidity has been up-regulated and an effective engagement with ligand occurs, the integrin anchorage to actin cytoskeleton is restored and outside-in signaling leads to actin remodelling and cell spreading. Then, leukocytes undergo a profound change in their morphology, acquiring a polarized, motility-related shape (reviewed in 88). This cell shape change favors leukocyte extravasation, and is also involved in the recruitment of bystander leukocytes through the trailing edge (uropod) (89).

### 4.3. The docking structure: the endothelial contribution to the leukocyte firm adhesion process

Endothelium had been considered as a mere physiological barrier, a passive partner for leukocytes during TEM. However, it is now evident that endothelium is a key active element in different physiological processes, including leukocyte extravasation. Our group has

contributed to gain insight into the molecular mechanisms underlying the active role of endothelial cells in the TEM of leukocytes. We have found that activated endothelial cells generate “docking” structures that efficiently attach leukocytes, partially engulfing them. VCAM-1 and ICAM-1, together with cytoskeletal and signaling molecules, are essential constituents of these cup-like structures based on microspikes that emerge from the endothelial apical surface, and which are dynamically involved in capturing leukocytes prior to TEM (90).

#### 4.3.1. VCAM-1 and ICAM-1 play an essential role in leukocyte capture

VCAM-1 and ICAM-1, members of the Ig superfamily, are the two major endothelial adhesion molecules involved in the binding to leukocyte integrins VLA-4 and LFA-1, respectively (91, 92). ICAM-1 but not VCAM-1 is expressed at low levels in resting endothelium, and both molecules are induced upon cell activation by pro-inflammatory cytokines such as IL-1 and TNF- $\alpha$  (93, 94). We have recently found that these integrin ligands are laterally associated with different tetraspanins (CD9, CD81 and CD151), forming protein microdomains in the apical surface of endothelium (Barreiro and Yáñez-Mó, unpublished data). Furthermore, it has been described that VCAM-1 and ICAM-1 are anchored to the actin cytoskeleton through members of the ERM family, mainly ezrin and moesin (90, 95, 96). All these molecules, which are clustered at endothelial microvilli and microspikes, contact and surround the adherent leukocyte, as key elements of the docking structure. The cytoskeletal linkage of VCAM-1 and ICAM-1 is critical for the generation of this structure upon leukocyte adhesion, but it is not necessary for the proper presentation of VCAM-1 and ICAM-1 at the apical surface, since this localization seems to be independent of ligand engagement and actin anchorage (Barreiro and Yáñez-Mó, unpublished data).

Dynamic experiments have demonstrated the involvement of ICAM-1 (through its interaction with LFA-1) not only in the firm adhesion of leukocytes but in their transendothelial migration and subsequent movement underneath the endothelial monolayer. Moesin has a similar behaviour, suggesting that ICAM-1 is anchored to the actin cytoskeleton via ERM proteins during the whole process. On the contrary, VCAM-1 is excluded of the late steps of leukocyte extravasation and only participates in the formation of the endothelial docking structure that firmly attaches the lymphocyte to the endothelium (90).

#### 4.3.2. Structural components and signaling pathways involved in the generation and maintenance of the docking structure

The sequential steps involved in the generation of the endothelial docking structure could be as follows. The initial interaction of VCAM-1 and ICAM-1 with their ligands (VLA-4 and LFA-1 integrins, respectively) triggers their clustering at the leukocyte-endothelium contact area, together with phosphorylated activated ERM proteins. Then, these adaptor proteins in concert with alpha-actinin and vinculin participate in the rearrangement of the actin cytoskeleton to generate the docking structure. The

## Protrusive structures in leukocyte extravasation

participation of other focal adhesion proteins such as talin or paxillin remains to be elucidated. On the other hand, it has been also described that VASP, which cooperates with the WASP-Arp2/3 complex in actin polymerization at nascent protrusions (97), is concentrated at the docking structure (90). These data suggest that this endothelial structure is supported by actin polymerization. However, microtubules do not appear to be involved in this process. Interestingly, the endothelial docking structure seems to be reminiscent of nascent complement receptor-mediated phagosomes, in that the subcellular distribution of all these structural proteins is similar in both structures (98).

Regarding the signaling pathways involved in the generation and maintenance of the docking structure, it has been described the preferential accumulation of PI(4,5)P<sub>2</sub> at the tips of the microspikes of this structure, where could participate in the activation of the ERM proteins. Furthermore, the essential role of the Rho/p160 ROCK signaling pathway in the formation of this protrusive structure, has been also documented (90). These results concur with the regulation of the VCAM-1, ICAM-1, and E-selectin clustering by the GTPase Rho during monocyte adhesion (99). Finally, further analyses are necessary to understand the mechanisms underlying the disruption of the endothelial docking structure to allow leukocyte diapedesis.

### 4.3.3. VCAM-1 and ICAM-1 outside-in signaling

VCAM-1 and ICAM-1 are capable of transducing signals after ligand binding. VCAM-1 is involved in the opening of the “endothelial passage” through which leukocytes can extravasate. In this regard, VCAM-1 ligation induces NADPH oxidase activation and the production of reactive oxygen species (ROS) in a Rac-mediated manner, with subsequent activation of matrix metalloproteinases and loss of VE-cadherin-mediated adhesion. This signaling pathway can be blocked by TGFβ<sub>1</sub> and IFNγ (100-103). On the other hand, cross-linking of both VCAM-1 and ICAM-1 induces a rapid increase in intracellular Ca<sup>2+</sup> concentration (62, 104). ICAM-1-mediated calcium signaling has been mostly studied in brain endothelial cells. In this cellular model, it has been found that ICAM-1-mediated calcium increase triggers activation of Src and subsequent phosphorylation of cortactin (104). ICAM-1 is also able to activate RhoA inducing stress fiber formation (105) and phosphorylation of FAK, paxillin and p130<sup>Cas</sup>, which in turn trigger different signaling pathways involving JNK or p38 (106-108). Moreover, ICAM-1 cross-linking stimulate c-fos and rhoA transcription (105). As reported for PSGL-1 (59), ICAM-1 might enhance c-fos expression through the recruitment of Syk to the ICAM-1/ERM complex, but such possibility deserves further investigation. Finally, the ICAM-1 cross-linking can induce its own expression as well as that of VCAM-1, as a regulatory mechanism to facilitate leukocyte TEM (109).

## 5. TRANSENDOTHELIAL MIGRATION

The signals involved in the firm adhesion of leukocytes to endothelium must be reverted, weakening the original contact sufficiently to allow the migration and

extravasation of leukocytes. During TEM, endothelial junctions must be loosened to a limited extent, thereby avoiding cell monolayer damage or important changes in permeability. Thus, the leukocyte and endothelium membranes are kept in close contact and show prominent associated cytoskeletal structures. Subsequently, the endothelial membranes reseal their connections over the trailing end of the leukocyte.

### 5.1. Leukocytes undergo drastic cytoskeletal rearrangements to extravasate across the endothelial barrier

In leukocytes, integrin-dependent adhesion is required for changes in cytoskeleton plasticity and cell motility (110). In addition, it has been recently described that immobilized chemokines play a pivotal role in this process, since SDF-1α presented on the apical surface of endothelial cells can trigger lymphoid TEM under shear stress conditions in the absence of a chemoattractant gradient across the endothelium, whereas soluble chemotactic gradients do not. This process has been designated as “chemorheotaxis” (111). However, monocytes (112) and neutrophils (113) do not require endothelial apical chemokines to undergo TEM, hence postulating this phenomenon as lymphocyte-specific.

The regulation of the deformation of the leukocyte cytoskeleton during TEM has not been well studied. The possible activation of regulators of the actin cytoskeleton such as small Rho GTPases by integrins or chemokines remains to be elucidated. However, an attractive hypothesis would comprise the activation of Cdc42 by integrins or chemokines, which would cause the extension of a thin exploratory pseudopodium between endothelial cells that, by sequential Rac1 activation, would evolve into a lamella squeezed within an endothelial monolayer gap. This leading lamella and the leukocyte membrane in contact with endothelium are enriched in LFA-1 (114, 115). Finally, the stretching of cell body and tail retraction would result from delayed, tail-oriented RhoA-ROCK activation and actomyosin-based contraction (116).

### 5.2. Endothelial cell lateral junctions regulation

The components of the endothelial lateral junctions can be divided in tight, adherens and gap junctions, each containing distinct molecular constituents, although they do not exhibit a well-organized basolateral organization as in epithelium. These molecular complexes are dynamically organized, associate with the actin cytoskeleton and, except for gap junctions, actively participate in leukocyte TEM. Recent reports strongly suggest that leukocytes and endothelium communicate each other during TEM. The most characterized intracellular signals generated by TEM in endothelium are the mobilization of intracellular Ca<sup>2+</sup> and the reorganization of actin, myosin and associated molecules (117, 118).

Figure 3 establishes a comparison between the interendothelial junctions in the vascular wall and the heterotypic leukocyte-endothelium interactions during transendothelial migration. The morphological changes that leukocytes undergo to pass across the endothelial barrier, as

## Protrusive structures in leukocyte extravasation

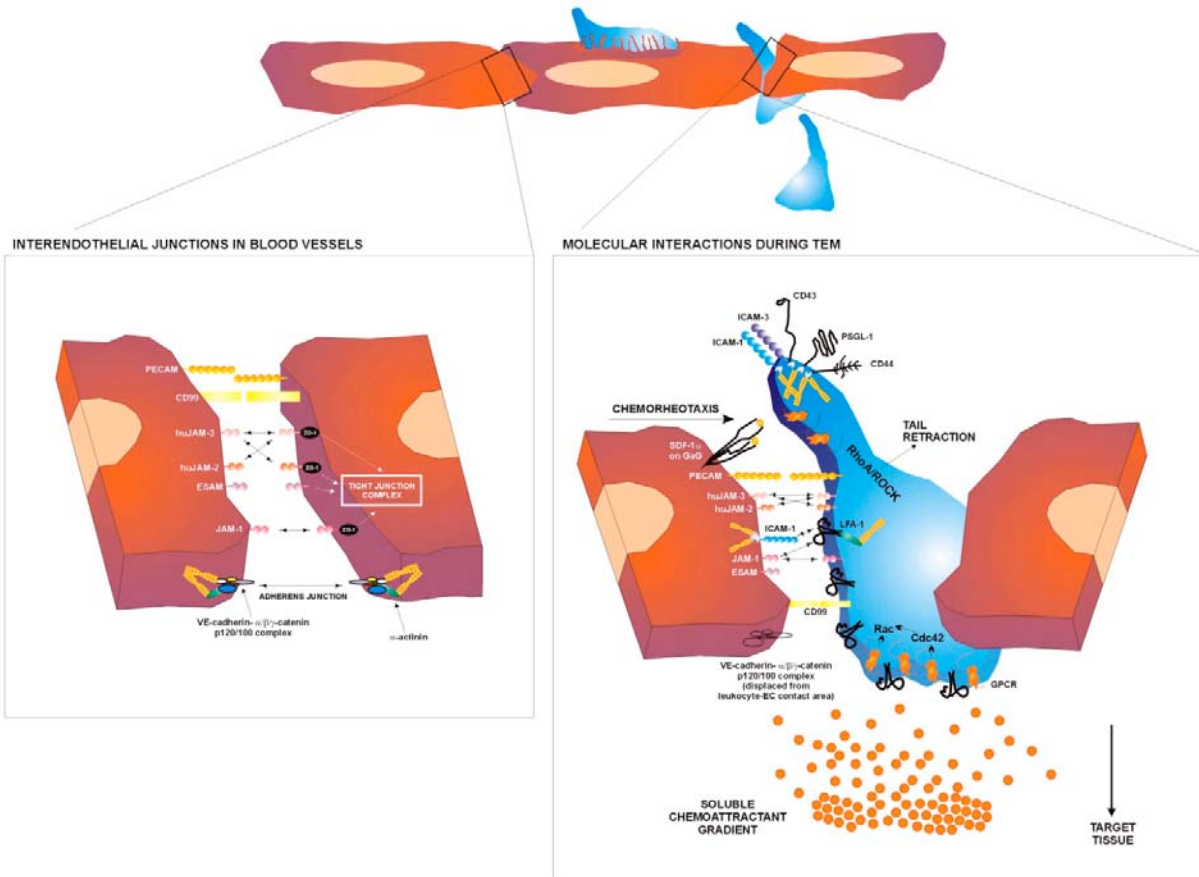


**Figure 3.** Comparison between the interendothelial junctions in the vascular wall and the heterotypic leukocyte-endothelium interactions during transendothelial migration. Only the molecules involved in both processes are shown, including members of the tight junctions (ESAM and the JAM family), the VE-cadherin complex and other molecules such as PECAM-1 and CD99. Most of them interact homophilically, being expressed by the endothelium as well as by leukocytes. On the other hand, the processes of lamellipodia formation at the leukocyte leading edge and tail retraction, the phenomenon of chemorheotaxis and the existence of a subendothelial soluble chemoattractant gradient to guide the extravasated leukocytes to the target tissue are also illustrated.

well as the effect of chemokines and chemoattractant gradients in this process, have been also specified.

### 5.2.1. Tight junction proteins: role of JAM family in transendothelial migration

Among the components of tight junctions (occludin, claudins, ZO-1, -2, -3, etc), two novel groups of adhesion molecules belonging to the Ig superfamily have been recently identified: ESAM (Endothelial cell-Selective Adhesion Molecule) and JAM (Junctional Adhesion Molecule) proteins. In contrast with other members of tight junctions, they play a role in paracellular permeability as well as in lymphocyte homing and TEM. ESAM is involved in the homotypic interaction of endothelial cells, but no heterophilic ligands have been described yet (119, 120). To date, three members of the JAM family have been identified: JAM-1, huJAM-2 (which corresponds to mJAM-3) and huJAM-3 (which corresponds to mJAM-2) (reviewed in 121). JAM-1 is expressed in epithelium, endothelium, erythrocytes, PMNs, monocytes, lymphocytes and platelets; huJAM2 is preferentially expressed in high endothelial venules (HEV); and JAM3 is detected in endothelium and activated T lymphocyte subsets (122-

27). All members of the family contain a PDZ-binding motif in their cytoplasmic tail, which is involved in their association with components of the tight junctions such as ZO-1 and AF-6, suggesting a role for these molecules in recruiting and stabilizing JAMs to site of junction formation (128, 129). The JAM family proteins can interact homophilically at endothelial tight junctions to regulate paracellular permeability or heterophilically with counterreceptors from leukocytes to support TEM. In this regard, it has been described that JAM-1 is capable to interact with itself or with LFA-1 (130). huJAM-2 and huJAM-3 are binding partners, and this interaction could have relevance for lymphocyte homing, due to the restricted expression of huJAM-2 in high endothelial venules (124). Furthermore, huJAM-3 is also capable to interact with itself (131) and with alphaMbeta2 and alphaXbeta2 integrins (132). In turn, huJAM-2 interacts with alpha4beta1 integrin (133). The fact that all the members of the JAM family interact with leukocyte integrins and that are relocated towards the apical surface upon endothelium activation argues for their fundamental role in the regulation of leukocyte adhesion.

### 5.2.2. Adherens junction disappearance at leukocyte contacts: proteolysis or displacement?

Adherens junctions are primarily involved in the regulation of endothelial cell monolayer permeability. The main component of these molecular complexes is VE-cadherin, which mediates  $\text{Ca}^{2+}$ -dependent homophilic adhesion with its extracellular domain and actin cytoskeleton linkage through the interaction of its cytoplasmic tail with alpha-, beta-, gamma-catenin, and p120/100 (134). During leukocyte TEM, VE-cadherin complexes are locally disrupted, generating a localized gap necessary for leukocyte passage, which reseals after TEM. According to these observations, VE-cadherin acts as a "gatekeeper" for leukocyte transmigration. Whether or not this disruption of adherens junctions involves protein degradation has been extensively discussed (135-137). However, the rapid recovery of adherens junctions after the passage of leukocytes seems to point to the existence of a zipper mechanism, which implies the local and transient displacement of molecular complexes from the leukocyte-endothelium area ("trapdoor model") (138, 139). However, the possibility of a certain degree of complex proteolysis cannot be excluded. Moreover, other alternative mechanisms such as transcytosis or preferential passage through tricellular corners, where tight junctions and adherens junctions are less organized, cannot be ruled out (140-142).

### 5.2.3. Other molecules with a major role in the passage of leukocytes across endothelium

Apart from the above-mentioned molecules, there are other endothelial proteins critical for leukocyte TEM that do not belong to tight junctions or adherens junctions complexes. PECAM-1 is another member of the immunoglobulin superfamily that is expressed in endothelium as well as in leukocytes, and that actively participates in TEM (143). It can associate homophilically or with  $\alpha\text{v}\beta_3$  in cis- (144, 145). PECAM-1 transduces negative intracellular signals via the ITIM motif of its cytoplasmic tail (146). In addition, PECAM-1 can regulate adherens junctions by associating to beta-catenin (147). Finally, a recent report describes the existence of a molecular network just below the endothelial plasma membrane that is connected at intervals with the junctional surface. PECAM-1 has been found in this compartment, constitutively recycling along the endothelium borders. During TEM, PECAM-1 recycling molecules are targeted to points of contact with leukocytes. This mechanism could explain how endothelial cells change their borders rapidly and reversely, but remaining tightly apposed to leukocytes to allow their migration (148).

CD99, a highly O-glycosylated type I transmembrane protein, has been found to play a critical role in monocyte TEM, acting at a later stage than PECAM-1 (149). This protein is expressed in leukocytes, where triggers the activation of  $\alpha_4\beta_1$  integrin and regulates the activity of LFA-1, and endothelium, interacting homophilically at interendothelial contacts (reviewed in 145). However, little is known about its precise function on endothelial cells or its involvement in signaling transduction.

## 6. CONCLUDING REMARKS AND PERSPECTIVES

Over the last decade, a huge effort has been made for the study of the basic adhesive mechanisms underlying vascular function. In this regard, the dissection of the phenomena involved in leukocyte extravasation has significantly improved our knowledge of different pathophysiological conditions. The recent description of new molecular complexes and subcellular structures implicated in this process, as well as the characterization of new intracellular signaling pathways or cytoskeletal components, have added more complexity to the extravasation mechanism and opened new insights to future investigations. Furthermore, molecules that are newly being involved in this process could constitute potential molecular targets for therapeutic intervention. Finally, some controversies and obscure points regarding, e.g., differences in the behaviour of monocytes, neutrophils or lymphocytes during TEM or the regulation of interendothelial junctions to allow the passage of leukocytes still remain partially unsolved.

## 7. ACKNOWLEDGEMENTS

We would like to thank Drs. R. González-Amaro, M. Gómez, M. Rey, and D. Sancho for critical reading of the manuscript. The authors' laboratory was supported by grants BMC-2002 00563 from the Ministerio de Ciencia y Tecnología, Ayuda a la Investigación Básica Juan March 2002, FIPSE 36289/02, and FIS CO3/01-Red Cardiovascular to Dr. F. Sánchez-Madrid, and fellowships from Fundación Mapfre Medicina to O. Barreiro, and from Comunidad Autónoma de Madrid to M. Yáñez-Mó.

## 8. REFERENCES

1. Frenette, P. S. & D. D. Wagner: Adhesion molecules--Part I. *N Engl J Med* 334, 1526-9 (1996)
2. Frenette, P. S. & D. D. Wagner: Adhesion molecules---Part II: Blood vessels and blood cells. *N Engl J Med* 335, 43-5 (1996)
3. Aplin, A. E., A. Howe, S. K. Alahari & R. L. Juliano: Signal transduction and signal modulation by cell adhesion receptors: the role of integrins, cadherins, immunoglobulin-cell adhesion molecules, and selectins. *Pharmacol Rev* 50, 197-263 (1998)
4. Verfaillie, C. M.: Adhesion receptors as regulators of the hematopoietic process. *Blood* 92, 2609-12 (1998)
5. Levesque, J. P., A. C. Zannettino, M. Pudney, S. Niutta, D. N. Haylock, K. R. Snapp, G. S. Kansas, M. C. Berndt & P. J. Simmons: PSGL-1-mediated adhesion of human hematopoietic progenitors to P-selectin results in suppression of hematopoiesis. *Immunity* 11, 369-78 (1999)
6. Butcher, E. C.: Leukocyte-endothelial cell recognition: three (or more) steps to specificity and diversity. *Cell* 67, 1033-6 (1991)

## Protrusive structures in leukocyte extravasation

7. Butcher, E. C. & L. J. Picker: Lymphocyte homing and homeostasis. *Science* 272, 60-6 (1996)
8. Springer, T. A.: Traffic signals for lymphocyte recirculation and leukocyte emigration: the multistep paradigm. *Cell* 76, 301-14 (1994)
9. Springer, T. A.: Traffic signals on endothelium for lymphocyte recirculation and leukocyte emigration. *Annu Rev Physiol* 57, 827-72 (1995)
10. Mehta, P., R. D. Cummings & R. P. McEver: Affinity and kinetic analysis of P-selectin binding to P-selectin glycoprotein ligand-1. *J Biol Chem* 273, 32506-13 (1998)
11. Nicholson, M. W., A. N. Barclay, M. S. Singer, S. D. Rosen & P. A. van der Merwe: Affinity and kinetic analysis of L-selectin (CD62L) binding to glycosylation-dependent cell-adhesion molecule-1. *J Biol Chem* 273, 763-70 (1998)
12. Vestweber, D. & J. E. Blanks: Mechanisms that regulate the function of the selectins and their ligands. *Physiol Rev* 79, 181-213 (1999)
13. McEver, R. P., J. H. Beckstead, K. L. Moore, L. Marshall-Carlson & D. F. Bainton: GMP-140, a platelet alpha-granule membrane protein, is also synthesized by vascular endothelial cells and is localized in Weibel-Palade bodies. *J Clin Invest* 84, 92-9 (1989)
14. Mayadas, T. N., R. C. Johnson, H. Rayburn, R. O. Hynes & D. D. Wagner: Leukocyte rolling and extravasation are severely compromised in P selectin-deficient mice. *Cell* 74, 541-54 (1993)
15. Bevilacqua, M. P., J. S. Pober, D. L. Mendrick, R. S. Cotran & M. A. J. Gimbrone: Identification of an inducible endothelial-leukocyte adhesion molecule. *Proc Natl Acad Sci USA* 84, 9238-42 (1987)
16. Subramaniam, M., J. A. Koedam & D. D. Wagner: Divergent fates of P- and E-selectins after their expression on the plasma membrane. *Mol Biol Cell* 4, 791-801 (1993)
17. Kishimoto, T. K., M. A. Jutila, E. L. Berg & E. C. Butcher: Neutrophil Mac-1 and MEL-14 adhesion proteins inversely regulated by chemotactic factors. *Science* 245, 1238-41 (1989)
18. Jung, T. M. & M. O. Dailey: Rapid modulation of homing receptors (gp90MEL-14) induced by activators of protein kinase C. Receptor shedding due to accelerated proteolytic cleavage at the cell surface. *J Immunol* 144, 3130-6 (1990)
19. Walcheck, B., J. Kahn, J. M. Fisher, B. B. Wang, R. S. Fisk, D. G. Payan, C. Feehan, R. Betageri, K. Darlak, A. F. Spatola & T. K. Kishimoto: Neutrophil rolling altered by inhibition of L-selectin shedding *in vitro*. *Nature* 380, 720-3 (1996)
20. Ley, K., D. C. Bullard, M. L. Arbones, R. Bosse, D. Vestweber, T. F. Tedder & A. L. Beaudet: Sequential contribution of L- and P-selectin to leukocyte rolling *in vivo*. *J Exp Med* 181, 669-75 (1995)
21. McEver, R. P. & R. D. Cummings: Role of PSGL-1 binding to selectins in leukocyte recruitment. *J Clin Invest* 100, S97-103 (1997)
22. Frenette, P. S., C. V. Denis, L. Weiss, K. Jurk, S. Subbarao, B. Kehrel, J. H. Hartwig, D. Vestweber & D. D. Wagner: P-selectin glycoprotein ligand 1 (PSGL-1) is expressed on platelets and can mediate platelet-endothelial interactions *in vivo*. *J Exp Med* 191, 1413-22 (2000)
23. Xia, L., M. Sperandio, T. Yago, J. M. McDaniel, R. D. Cummings, S. Pearson-White, K. Ley & R. P. McEver: P-selectin glycoprotein ligand-1-deficient mice have impaired leukocyte tethering to E-selectin under flow. *J Clin Invest* 109, 939-50 (2002)
24. Hirata, T., G. Merrill-Skoloff, M. Aab, J. Yang, B. C. Furie & B. Furie: P-selectin glycoprotein ligand 1 (PSGL-1) is a physiological ligand for E-selectin in mediating T helper 1 lymphocyte migration. *J Exp Med* 192, 1669-76 (2000)
25. Norman, K. E., A. G. Katopodis, G. Thoma, F. Kolbinger, A. E. Hicks, M. J. Cotter, A. G. Pockley & P. G. Hellewell: P-selectin glycoprotein ligand-1 supports rolling on E- and P-selectin *in vivo*. *Blood* 96, 3585-91 (2000)
26. Sperandio, M., M. L. Smith, S. B. Forlow, T. S. Olson, L. Xia, R. P. McEver & K. Ley: P-selectin glycoprotein ligand-1 mediates L-selectin-dependent leukocyte rolling in venules. *J Exp Med* 197, 1355-63 (2003)
27. Levinovitz, A., J. Muhlhoff, S. Isenmann & D. Vestweber: Identification of a glycoprotein ligand for E-selectin on mouse myeloid cells. *J Cell Biol* 121, 449-59 (1993)
28. Steegmaier, M., A. Levinovitz, S. Isenmann, E. Borges, M. Lenter, H. Kocher, B. Kleuser & D. Vestweber: The E-selectin-ligand ESL-1 is a variant of a receptor for fibroblast growth factor. *Nature* 373, 615-20 (1995)
29. Aigner, S., C. L. Ramos, A. Hafezi-Moghadam, M. B. Lawrence, J. Friederichs, P. Altevogt & K. Ley: CD24 mediates rolling of breast carcinoma cells on P-selectin. *FASEB J* 12, 1241-51 (1998)
30. Patel, K. D., S. L. Cuvelier & S. Wiehler: Selectins: critical mediators of leukocyte recruitment. *Semin Immunol* 14, 73-81 (2002)
31. Berlin, C., R. F. Bargatze, J. J. Campbell, U. H. vonAndrian, M. C. Szabo, S. R. Hasslen, R. D. Nelson, E. L. Berg, S. L. Erlandsen & E. C. Butcher: alpha4 integrins mediate lymphocyte attachment and rolling under physiologic flow. *Cell* 80, 413-22 (1995)
32. Henderson, R. B., L. H. K. Lim, P. A. Tessier, F. N. E. Gavins, M. Mathies, M. Perreti & N. Hogg: The use of

## Protrusive structures in leukocyte extravasation

- Lymphocyte Function-associated Antigen (LFA-1)-deficient mice to determine the role of LFA-1, Mac-1 and alpha4 integrin in the inflammatory response of neutrophils. *J Exp Med* 194, 219-26 (2001)
33. Kadono, T., G. M. Venturi, D. A. Steeber & T. F. Tedder: Leukocyte rolling velocities and migration are optimized by cooperative L-selectin and intercellular adhesion molecule-1 functions. *J Immunol* 169, 4542-50 (2002)
34. Bazan, J. F., K. B. Bacon, G. Hardiman, W. Wang, K. Soo, D. Rossi, D. R. Greaves, A. Zlotnik & T. J. Schall: A new class of membrane-bound chemokine with a CX3C motif. *Nature* 385, 640-4 (1997)
35. Matloubian, M., A. David, S. Engel, J. E. Ryan & J. G. Cyster: A transmembrane CXC chemokine is a ligand for HIV-coreceptor Bonzo. *Nat Immunol* 1, 298-304 (2000)
36. Fong, A. M., S. M. Alam, T. Imai, B. Haribabu & D. D. Patel: CX3CR1 tyrosine sulfation enhances fractalkine-induced cell adhesion. *J Biol Chem* 277, 19418-23 (2002)
37. Haskell, C. A., M. D. Cleary & I. F. Charo: Molecular uncoupling of fractalkine-mediated cell adhesion and signal transduction. Rapid flow arrest of CX3CR1-expressing cells is independent of G-protein activation. *J Biol Chem* 274, 10053-8 (1999)
38. von Andrian, U. H., S. R. Hasslen, R. D. Nelson, S. L. Erlandsen & E. C. Butcher: A central role for microvillous receptor presentation in leukocyte adhesion under flow. *Cell* 82, 989-99 (1995)
39. Pavalko, F. M., D. M. Walker, L. Graham, M. Goheen, C. M. Doerschuk & G. S. Kansas: The cytoplasmic domain of L-selectin interacts with cytoskeletal proteins via alpha-actinin: receptor positioning in microvilli does not require interaction with alpha-actinin. *J Cell Biol* 129, 1155-64 (1995)
40. Ivetic, A., J. Deka, A. J. Ridley & A. Ager: The cytoplasmic tail of L-selectin interacts with members of the Ezrin-Radixin-Moesin (ERM) family of proteins: cell activation-dependent binding of Moesin but not Ezrin. *J Biol Chem* 277, 2321-9 (2002)
41. Dwir, O., G. S. Kansas & R. Alon: Cytoplasmic anchorage of L-selectin controls leukocyte capture and rolling by increasing the mechanical stability of the selectin tether. *J Cell Biol* 155, 145-56 (2001)
42. Alon, R. & S. Feigelson: From rolling to arrest on blood vessels: leukocyte tap dancing on endothelial integrin ligands and chemokines at sub-second contacts. *Sem Immunol* 14, 93-104 (2002)
43. Stein, J. V., G. Cheng, B. M. Stockton, B. P. Fors, E. C. Butcher & U. H. von Andrian: L-selectin-mediated leukocyte adhesion *in vivo*: microvillous distribution determines tethering efficiency, but not rolling velocity. *J Exp Med* 189, 37-50 (1999)
44. Shao, J. Y., H. P. Ting-Beall & R. M. Hochmuth: Static and dynamic lengths of neutrophil microvilli. *Proc Natl Acad Sci USA* 95, 6797-802 (1998)
45. Yoshida, M., W. F. Westlin, N. Wang, D. E. Ingber, A. Rosenzweig, N. Resnick & M. A. J. Gimbrone: Leukocyte adhesion to vascular endothelium induces E-selectin linkage to the actin cytoskeleton. *J Cell Biol* 133, 445-55 (1996)
46. Waddell, T. K., L. Fialkow, C. K. Chan, T. K. Kishimoto & G. P. Downey: Signaling functions of L-selectin: enhancement of tyrosine phosphorylation and activation of MAP kinase. *J Biol Chem* 270, 15403-11 (1995)
47. Brenner, B., E. Gulbins, K. Schlottmann, U. Koppenhoefer, G. L. Busch, B. Walzog, M. Steinhausen, K. M. Coggeshall, O. Linderkamp & F. Lang: L-selectin activates the Ras pathway via the tyrosine kinase p56lck. *Proc Natl Acad Sci USA* 93, 15376-81 (1996)
48. Brenner, B., E. Gulbins, G. L. Busch, U. Koppenhoefer, F. Lang & O. Linderkamp: L-selectin regulates actin polymerisation via activation of the small G-protein Rac2. *Biochem Biophys Res Commun* 231, 802-7 (1997)
49. Roberts, A. W., C. Kim, L. Zhen, J. B. Lowe, R. Kapur, B. Petryniak, A. Spaetti, J. D. Pollock, J. B. Borneo, G. B. Bradford, S. J. Atkinson, M. C. Dinauer & D. A. Williams: Deficiency of the hematopoietic cell-specific Rho family GTPase Rac2 is characterized by abnormalities in neutrophil function and host defense. *Immunity* 10, 183-96 (1999)
50. Hidari, K. I., A. S. Weyrich, G. A. Zimmerman & R. P. McEver: Engagement of P-selectin glycoprotein ligand-1 enhances tyrosine phosphorylation and activates mitogen-activated protein kinases in human neutrophils. *J Biol Chem* 272, 28750-6 (1997)
51. Celi, A., G. Pellegrini, R. Lorenzet, A. De Blasi, N. Ready, B. C. Furie & B. Furie: P-selectin induces the expression of tissue factor on monocytes. *Proc Natl Acad Sci USA* 91, 8767-71 (1994)
52. Damle, N. K., K. Klussman, M. T. Dietsch, N. Mohaghehpour & A. Aruffo: GMP-140 (P-selectin/CD62) binds to chronically stimulated but not resting CD4+ T lymphocytes and regulates their production of proinflammatory cytokines. *Eur J Immunol* 22, 1789-93 (1992)
53. Weyrich, A. S., T. M. McIntyre, R. P. McEver, S. M. Prescott & G. A. Zimmerman: Monocyte tethering by P-selectin regulates monocyte chemotactic protein-1 and tumor necrosis factor-alpha secretion. Signal integration and NF-kappa B translocation. *J Clin Invest* 95, 2297-303 (1995)
54. Weyrich, A. S., M. R. Elstad, R. P. McEver, T. M. McIntyre, K. L. Moore, J. H. Morrissey, S. M. Prescott &

## Protrusive structures in leukocyte extravasation

- G. A. Zimmerman: Activated platelets signal chemokine synthesis by human monocytes. *J Clin Invest* 97, 1525-34 (1996)
55. Ruchaud-Sparagano, M. H., T. R. Walker, A. G. Rossi, C. Haslett & I. Dransfield: Soluble E-selectin acts in synergy with platelet-activating factor to activate neutrophil beta 2-integrins. Role of tyrosine kinases and Ca<sup>2+</sup> mobilization. *J Biol Chem* 275, 15758-64 (2000)
56. Simon, S. I., Y. Hu, D. Vestweber & C. W. Smith: Neutrophil tethering on E-selectin activates beta 2 integrin binding to ICAM-1 through a mitogen-activated protein kinase signal transduction pathway. *J Immunol* 164, 4348-58 (2000)
57. Alonso-Lebrero, J. L., J. M. Serrador, C. Dominguez-Jimenez, O. Barreiro, A. Luque, M. A. d. Pozo, K. Snapp, G. Kansas, R. Schwartz-Albiez, H. Furthmayr, F. Lozano & F. Sánchez-Madrid: Polarization and interaction of adhesion molecules P-selectin Glycoprotein Ligand-1 and Intercellular Adhesion Molecule-3 with moesin and ezrin in myeloid cells. *Blood* 95, 2413-9 (2000)
58. Serrador, J. M., A. Urzainqui, J. L. Alonso-Lebrero, J. R. Cabrero, M. C. Montoya, M. Vicente-Manzanares, M. Yañez-Mó & F. Sánchez-Madrid: A juxta-membrane amino acid sequence of P-selectin glycoprotein ligand-1 is involved in moesin binding and ezrin/radixin/moesin-directed targeting at the trailing edge of migrating lymphocytes. *Eur J Immunol* 32, 1560-6 (2002)
59. Urzainqui, A., J. M. Serrador, F. Viedma, M. Yañez-Mó, A. Rodríguez, A. L. Corbí, J. L. Alonso-Lebrero, A. Luque, M. Deckert, J. Vázquez & F. Sánchez-Madrid: ITAM-based interaction of ERM proteins with Syk mediates signaling by the leukocyte adhesion receptor PSGL-1. *Immunity* 17, 401-12 (2002)
60. Gonzalez-Amaro, R. & F. Sanchez-Madrid: Cell adhesion molecules: selectins and integrins. *Crit Rev Immunol* 19, 389-429 (1999)
61. Yoshida, M., B. E. Szente, J. M. Kiely, A. Rosenzweig & M. A. J. Gimbrone: Phosphorylation of the cytoplasmic domain of E-selectin is regulated during leukocyte-endothelial adhesion. *J Immunol* 161, 933-41 (1998)
62. Lorenzon, P., E. Vecile, E. Nardon, E. Ferrero, J. M. Harlan, F. Tedesco & A. Dobrina: Endothelial cell E- and P-selectin and vascular cell adhesion molecule-1 function as signaling receptors. *J Cell Biol* 142, 1381-91 (1998)
63. Campbell, J. J., J. Hedrick, A. Zlotnik, M. A. Siani, D. A. Thompson & E. C. Butcher: Chemokines and the arrest of lymphocytes rolling under flow conditions. *Science* 279, 381-4 (1998)
64. Grabovsky, V., S. Feigelson, C. Chen, D. A. Bleijs, A. Peled, G. Cinamon, F. Baleux, F. Arenzana-Seisdedos, T. Lapidot, Y. van Kooyk, R. R. Lobb & R. Alon: Subsecond induction of alpha4 integrin clustering by immobilized chemokines stimulates leukocyte tethering and rolling on endothelial vascular cell adhesion molecule 1 under flow conditions. *J Exp Med* 192, 495-506 (2000)
65. Stein, J. V., A. Rot, Y. Luo, M. Narasimhaswamy, H. Nakano, M. D. Gunn, A. Matsuzawa, E. J. Quackenbush, M. E. Dorf & U. H. von Andrian: The CC chemokine thymus-derived chemokine agent 4 (TCA-1, secondary lymphoid tissue chemokine, 6Ckine, exodus-2) triggers lymphocyte function-associated antigen 1-mediated arrest of rolling T lymphocytes in peripheral lymph node high endothelial venules. *J Exp Med* 191, 61-76 (2000)
66. Middleton, J., A. M. Patterson, L. Gardner, C. Schmutz & B. A. Ashton: Leukocyte extravasation: chemokine transport and presentation by the endothelium. *Blood* 100, 3853-60 (2002)
67. Singer, I. I., S. Scott, D. W. Kawka, J. Chin, B. L. Daugherty, J. A. DeMartino, J. DiSalvo, S. L. Gould, J. E. Lineberger, L. Malkowitz, M. D. Miller, L. Mitnaul, S. J. Siciliano, M. J. Staruch, H. R. Williams, H. J. Zweerink & M. S. Springer: CCR5, CXCR4, and CD4 are clustered and closely apposed on microvilli of human macrophages and T cells. *J Virol* 75, 3779-90 (2001)
68. Johnston, B. & E. C. Butcher: Chemokines in rapid leukocyte adhesion triggering and migration. *Semin Immunol* 14, 83-92 (2002)
69. Weber, C., J. Kitayama & T. A. Springer: Differential regulation of beta1 and beta2 integrin avidity by chemoattractants in eosinophils. *Proc Natl Acad Sci USA* 93, 10939-44 (1996)
70. Tangemann, K., M. D. Gunn, P. Giblin & S. D. Rosen: A high endothelial cell-derived chemokine induces rapid, efficient and subset-selective arrest of rolling T lymphocytes on a reconstituted endothelial substrate. *J Immunol* 161, 6330-7 (1998)
71. Chan, J. R., S. J. Hyduk & M. I. Cybulsky: Chemoattractants induce a rapid and transient upregulation of monocyte alpha4 integrin affinity for vascular cell adhesion molecule 1 which mediates arrest: an early step in the process of emigration. *J Exp Med* 193, 1149-58 (2001)
72. de Bruyn, K. M. T., S. Rangarajan, K. A. Reequist, C. G. Figdor & J. L. Bos: The small GTPase Rap1 is required for Mn<sup>2+</sup>- and antibody-induced LFA-1- and VLA-4-mediated cell adhesion. *J Biol Chem* 277, 29468-76 (2002)
73. McLeod, S. J., A. H. Y. Li, R. L. Lee, A. E. Burgess & M. R. Gold: The Rap GTPases regulate B cell migration toward the chemokine Stromal Cell-Derived Factor-1 (CXCL12): Potential role for Rap2 in promoting B cell migration. *J Immunol* 169, 1365-71 (2002)
74. Shimonaka, M., K. Katagiri, T. Nakayama, N. Fujita, T. Tsuruo, O. Yoshie & T. Kinashi: Rap1 translates chemokine signals to integrin activation, cell polarization, and motility across vascular endothelium under flow. *J Cell Biol* 161, 417-27 (2003)

## Protrusive structures in leukocyte extravasation

75. Laudanna, C., J. J. Campbell & E. C. Butcher: Role of Rho in chemoattractant-activated leukocyte adhesion through integrins. *Science* 271, 981-3 (1996)
76. Sánchez-Mateos, P., C. Cabañas & F. Sánchez-Madrid: Regulation of integrin function. *Semin Cancer Biol* 7, 99-109 (1996)
77. Day, E. S., L. Osborn & A. Whitty: Effect of divalent cations on the affinity and selectivity of alpha4 integrins towards the integrin ligands vascular cell adhesion molecule-1 and mucosal addressin cell adhesion molecule-1: Ca<sup>2+</sup> activation of integrin alpha4beta1 confers a distinct ligand specificity. *Cell Commun Adhes* 9, 205-19 (2002)
78. Dransfield, I., C. Cabañas, A. Craig & N. Hogg: Divalent cation regulation of the function of the leukocyte integrin LFA-1. *J Cell Biol* 116, 219-26 (1992)
79. van Kooyk, Y., P. Weder, K. Heije & C. G. Figdor: Extracellular Ca<sup>2+</sup> modulates leukocyte function-associated antigen-1 cell surface distribution on T lymphocytes and consequently affects cell adhesion. *J Cell Biol* 124, 1061-70 (1994)
80. Ticchioni, M., V. Raimondi, L. Lamy, J. Wijdenes, F. P. Lindberg, E. J. Brown & A. Bernard: Integrin-associated protein (CD47/IAP) contributes to T cell arrest on inflammatory vascular endothelium under flow. *FASEB J* 15, 341-50 (2001)
81. Hwang, S. T., M. S. Singer, P. A. Giblin, T. A. Yednock, K. B. Bacon, S. I. Simon & S. D. Rosen: GlyCAM-1, a physiologic ligand for L-selectin, activates beta 2 integrins on naive peripheral lymphocytes. *J Exp Med* 184, 1343-8 (1996)
82. Chan, J. R., S. J. Hyduk & M. I. Cybulsky: Alpha 4 beta 1 integrin/VCAM-1 interaction activates alpha L beta 2 integrin-mediated adhesion to ICAM-1 in human T cells. *J Immunol* 164, 746-53 (2000)
83. Porter, J. C. & N. Hogg: Integrin cross talk: activation of lymphocyte function-associated antigen-1 on human T cells alters alpha4beta1- and alpha5beta1-mediated function. *J Cell Biol* 138, 1437-47 (1997)
84. Kolanus, W., W. Nagel, B. Schiller, L. Zeitlmann, S. Godar, H. Stockinger & B. Seed: Alpha L beta 2 integrin/LFA-1 binding to ICAM-1 induced by cytohesin-1, a cytoplasmic regulatory molecule. *Cell* 86, 233-42 (1996)
85. Kolanus, W. & B. Seed: Integrins and inside-out signal transduction: converging signals from PKC and PIP3. *Curr Opin Cell Biol* 9, 725-31 (1997)
86. Tanaka, Y., Y. Minami, S. Mine, H. Hirano, C. D. Hu, H. Fujimoto, K. Fujii, K. Saito, J. Tsukada, Y. van Kooyk, C. G. Figdor, T. Kataoka & S. Eto: H-Ras signals to cytoskeletal machinery in induction of integrin-mediated adhesion of T cells. *J Immunol* 163, 6209-16 (1999)
87. Stewart, M. P., A. McDowall & N. Hogg: LFA-1-mediated adhesion is regulated by cytoskeletal restraint and by a Ca<sup>2+</sup>-dependent protease, calpain. *J Cell Biol* 140, 699-707 (1998)
88. Vicente-Manzanares, M., D. Sancho, M. Yáñez-Mó & F. Sánchez-Madrid: The leukocyte cytoskeleton in cell migration and immune interactions. *Int Rev Cytol* 216, 233-89 (2002)
89. del Pozo, M. A., C. Cabanas, M. C. Montoya, A. Ager, P. Sanchez-Mateos & F. Sanchez-Madrid: ICAMs redistributed by chemokines to cellular uropods as a mechanism for recruitment of T lymphocytes. *J Cell Biol* 137, 493-508 (1997)
90. Barreiro, O., M. Yáñez-Mó, J. M. Serrador, M. C. Montoya, M. Vicente-Manzanares, R. Tejedor, H. Furthmayr & F. Sánchez-Madrid: Dynamic interaction of VCAM-1 and ICAM-1 with moesin and ezrin in a novel endothelial docking structure for adherent leukocytes. *J Cell Biol* 157, 1233-45 (2002)
91. Marlin, S. D. & T. A. Springer: Purified intercellular adhesion molecule-1 (ICAM-1) is a ligand for lymphocyte function-associated antigen 1 (LFA-1). *Cell* 51, 813-9 (1987)
92. Elices, M. J., L. Osborn, Y. Takada, C. Crouse, S. Luhowskyj, M. E. Hemler & R. R. Lobb: VCAM-1 on activated endothelium interacts with the leukocyte integrin VLA-4 at a site distinct from the VLA-4/fibronectin binding site. *Cell* 60, 577-84 (1990)
93. Dustin, M. L., R. Rothlein, A. K. Bhan, C. A. Dinarello & T. A. Springer: Induction by IL-1 and interferon-gamma: tissue distribution, biochemistry, and function of a natural adherence molecule (ICAM-1). *J Immunol* 137, 245-54 (1986)
94. Carlos, T. M. & J. M. Harlan: Leukocyte-endothelial adhesion molecules. *Blood* 84, 2068-101 (1994)
95. Heiska L., K. Alftan, M. Gronholm, P. Vilja, A. Vaheri & O. Carpen: Association of ezrin with intercellular adhesion molecule-1 and -2 (ICAM-1 and ICAM-2). Regulation by phosphatidylinositol 4, 5-bisphosphate. *J Biol Chem* 273, 21893-900 (1998)
96. Vaheri A., O. Carpen, L. Heiska, T.S. Helander, J. Jaaskelainen, P. Majander-Nordenswan, M. Sainio, T. Timonen & O. Turunen: The ezrin protein family: membrane-cytoskeleton interactions and disease associations. *Curr Opin Cell Biol* 9, 659-66 (1997)
97. Castellano, F., C. Le Clainche, D. Patin, M. Carlier & P. Chavrier: A WASp-VASP complex regulates actin polymerization at the plasma membrane. *EMBO J* 20, 5603-14 (2001)
98. Allen, L. A. & A. Aderem: Molecular definition of distinct cytoskeletal structures involved in complement-

## Protrusive structures in leukocyte extravasation

- and Fc receptor-mediated phagocytosis in macrophages. *J Exp Med* 184, 627-37 (1996)
99. Wojciak-Stothard, B., L. Williams & A. J. Ridley: Monocyte adhesion and spreading on human endothelial cells is dependent on Rho-regulated receptor clustering. *J Cell Biol* 145, 1293-307 (1999)
100. van Wetering, S., J. D. van Buul, S. Quik, F. P. Mul, E. C. Anthony, J. P. ten Klooster, J. G. Collard & P. L. Hordijk: Reactive oxygen species mediate Rac-induced loss of cell-cell adhesion in primary human endothelial cells. *J Cell Sci* 115, 1837-46 (2002)
101. van Wetering, S., N. van Den Berk, J. D. van Buul, F. P. Mul, I. Lommerse, R. Mous, J. P. ten Klooster, J. J. Zwaginga & P. L. Hordijk: VCAM-1-mediated Rac signaling controls endothelial cell-cell contacts and leukocyte transmigration. *Am J Physiol Cell Physiol* 285, C343-52 (2003)
102. Cook-Mills, J. M.: VCAM-1 signals during lymphocyte migration: role of reactive oxygen species. *Mol Immunol* 39, 499-508 (2002)
103. Hordijk, P. L.: Endothelial signaling in leukocyte transmigration. *Cell Biochem Biophys* 38, 305-22 (2003)
104. Etienne-Manneville, S., J. B. Manneville, P. Adamson, B. Wilbourn, J. Greenwood & P. O. Couraud: ICAM-1-coupled cytoskeletal rearrangements and transendothelial lymphocyte migration involve intracellular calcium signaling in brain endothelial cell lines. *J Immunol* 165, 3375-83 (2000)
105. Thompson, P. W., A. M. Randi & A. J. Ridley: Intercellular adhesion molecule (ICAM)-1, but not ICAM-2, activates RhoA and stimulates c-fos and rhoA transcription in endothelial cells. *J Immunol* 169, 1007-13 (2002)
106. Greenwood, J., S. Etienne-Manneville, P. Adamson & P. O. Couraud: Lymphocyte migration into the central nervous system: implication of ICAM-1 signalling at the blood-brain barrier. *Vascul Pharmacol* 38, 315-22 (2002)
107. Hubbard, A. K. & R. Rothlein: Intercellular adhesion molecule-1 (ICAM-1) expression and cell signaling cascades. *Free Radic Biol Med* 28, 1379-86 (2000)
108. Wang, Q. & C. M. Doerschuk: The signaling pathways induced by neutrophil-endothelial cell adhesion. *Antioxid Redox Signal* 4, 39-47 (2002)
109. Clayton, A., R. A. Evans, E. Pettit, M. Hallett, J. D. Williams & R. Steadman: Cellular activation through the ligation of intercellular adhesion molecule-1. *J Cell Sci* 111, 443-53 (1998)
110. Sanchez-Madrid, F. & M. A. del Pozo: Leukocyte polarization in cell migration and immune interactions. *EMBO J* 18, 501-11 (1999)
111. Cinamon, G., V. Shinder & R. Alon: Shear forces promote lymphocyte migration across vascular endothelium bearing apical chemokines. *Nat Immunol* 2, 515-22 (2001)
112. Weber, K. S., P. von Hundelshausen, I. Clark-Lewis, P. C. Weber & C. Weber: Differential immobilization and hierarchical involvement of chemokines in monocyte arrest and transmigration on inflamed endothelium in shear flow. *Eur J Immunol* 29, 700-12 (1999)
113. Wan, M., Y. Wang, Q. Liu, R. Schramm & H. Thorlacius: CC chemokines induce P-selectin-dependent neutrophil rolling and recruitment *in vivo*: intermediary role of mast cells. *Br J Pharmacol* 138, 698-706 (2003)
114. Sandig, M., E. Negrou & K. A. Rogers: Changes in the distribution of LFA-1, catenins, and F-actin during transendothelial migration of monocytes in culture. *J Cell Sci* 110, 2807-18 (1997)
115. Sandig, M., M. L. Korvemaker, C. V. Ionescu, E. Negrou & K. A. Rogers: Transendothelial migration of monocytes in rat aorta: distribution of F-actin, alpha-catenin, LFA-1, and PECAM-1. *Biotech Histochem* 74, 276-93 (1999)
116. Worthylake, R. A., S. Lemoine, J. M. Watson & K. Burridge: RhoA is required for monocyte tail retraction during transendothelial migration. *J Cell Biol* 154, 147-60 (2001)
117. Worthylake, R. A. & K. Burridge: Leukocyte transendothelial migration: orchestrating the underlying molecular machinery. *Curr Opin Cell Biol* 13, 569-77 (2001)
118. Johnson-Leger, C., M. Aurrand-Lions & B. A. Imhof: The parting of the endothelium: miracle, or simply a junctional affair? *J Cell Sci* 113, 921-33 (2000)
119. Hirata, K., T. Ishida, K. Penta, M. Rezaee, E. Yang, J. Wohlgemuth & T. Quertermous: Cloning of an immunoglobulin family adhesion molecule selectively expressed by endothelial cells. *J Biol Chem* 276, 16223-31 (2001)
120. Nasdala, I., K. Wolburg-Buchholz, H. Wolburg, A. Kuhn, K. Ebnet, G. Brachtendorf, U. Samulowitz, B. Kuster, B. Engelhardt, D. Vestweber & S. Butz: A transmembrane tight junction protein selectively expressed on endothelial cells and platelets. *J Biol Chem* 277, 16294-303 (2002)
121. Luscinskas, F. W., S. Ma, A. Nusrat, C. A. Parkos & S. K. Shaw: The role of endothelial cell lateral junctions during leukocyte trafficking. *Immunol Rev* 186, 57-67 (2002)
122. Martin-Padura, I., S. Lostaglio, M. Schneemann, L. Williams, M. Romano, P. Fruscella, C. Panzeri, A. Stoppacciaro, L. Ruco, A. Villa, D. Simmons & E. Dejana:

## Protrusive structures in leukocyte extravasation

Junctional adhesion molecule, a novel member of the immunoglobulin superfamily that distributes at intercellular junctions and modulates monocyte transmigration. *J Cell Biol* 142, 117-27 (1998)

123. Palmeri, D., A. van Zante, C. C. Huang, S. Hemmerich & S. D. Rosen: Vascular endothelial junction-associated molecule, a novel member of the immunoglobulin superfamily, is localized to intercellular boundaries of endothelial cells. *J Biol Chem* 275, 19139-45 (2000)

124. Arrate, M. P., J. M. Rodríguez, T. M. Tran, T. A. Brock & S. A. Cunningham: Cloning of human junctional adhesion molecule 3 (JAM3) and its identification as the JAM2 counter-receptor. *J Biol Chem* 276, 45826-32 (2001)

125. Aurrand-Lions, M. A., L. Duncan, L. Du Pasquier & B. A. Imhof: Cloning of JAM-2 and JAM-3: an emerging junctional adhesion molecular family? *Curr Top Microbiol Immunol* 251, 91-8 (2000)

126. Cunningham, S. A., M. P. Arrate, J. M. Rodríguez, R. J. Bjercke, P. Vanderslice, A. P. Morris & T. A. Brock: A novel protein with homology to the junctional adhesion molecule. Characterization of leukocyte interactions. *J Biol Chem* 275, 34750-6 (2000)

127. Aurrand-Lions, M. A., L. Duncan, C. Ballestrem & B. A. Imhof: JAM-2, a novel immunoglobulin superfamily molecule, expressed by endothelial and lymphatic cells. *J Biol Chem* 276, 2733-41 (2001)

128. Bazzoni, G., O. M. Martínez-Estrada, F. Orsenigo, M. Cordenonsi, S. Citi & E. Dejana: Interaction of junctional adhesion molecule with the tight junction components ZO-1, cingulin, and occludin. *J Biol Chem* 275, 20520-6 (2000)

129. Ebnet, K., C. U. Schulz, M. K. Meyer Zu Brickwedde, G. G. Pendl & D. Vestweber: Junctional adhesion molecule interacts with the PDZ domain-containing proteins AF-6 and ZO-1. *J Biol Chem* 275, 27979-88 (2000)

130. Ostermann, G., K. S. Weber, A. Zerneck, A. Schroder & C. Weber: JAM-1 is a ligand of the beta(2) integrin LFA-1 involved in transendothelial migration of leukocytes. *Nat Immunol* 3, 151-8 (2002)

131. Aurrand-Lions, M., C. Johnson-Leger, C. Wong, L. Du Pasquier & B. A. Imhof: Heterogeneity of endothelial junctions is reflected by differential expression and specific subcellular localization of the three JAM family members. *Blood* 98, 3699-707 (2001)

132. Santoso, S., U. J. Sachs, H. Kroll, M. Linder, A. Ruf, K. T. Preissner & T. Chavakis: The junctional adhesion molecule 3 (JAM-3) on human platelets is a counterreceptor for the leukocyte integrin Mac-1. *J Exp Med* 196, 679-91 (2002)

133. Cunningham, S. A., J. M. Rodríguez, M. P. Arrate, T. M. Tran & T. A. Brock: JAM2 interacts with alpha4beta1. Facilitation by JAM3. *J Biol Chem* 277, 27589-92 (2002)

134. Lampugnani, M. G., M. Corada, L. Caveda, F. Breviario, O. Ayalon, B. Geiger & E. Dejana: The molecular organization of endothelial cell to cell junctions: differential association of plakoglobin, beta-catenin, and alpha-catenin with vascular endothelial cadherin (VE-cadherin). *J Cell Biol* 129, 203-17 (1995)

135. Del Maschio, A., A. Zanetti, M. Corada, Y. Rival, L. Ruco, M. G. Lampugnani & E. Dejana: Polymorphonuclear leukocyte adhesion triggers the disorganization of endothelial cell-to-cell adherens junctions. *J Cell Biol* 135, 497-510 (1996)

136. Allport, J. R., H. Ding, T. Collins, M. E. Gerritsen & F. W. Luscinskas: Endothelial-dependent mechanisms regulate leukocyte transmigration: a process involving the proteasome and disruption of the vascular endothelial-cadherin complex at endothelial cell-to-cell junctions. *J Exp Med* 186, 517-27 (1997)

137. Moll, T., E. Dejana & D. Vestweber: *In vitro* degradation of endothelial catenins by a neutrophil protease. *J Cell Biol* 140, 403-7 (1998)

138. Allport, J. R., W. A. Muller & F. W. Luscinskas: Monocytes induce reversible focal changes in vascular endothelial cadherin complex during transendothelial migration under flow. *J Cell Biol* 148, 203-16 (2000)

139. Shaw, S. K., P. S. Bamba, B. N. Perkins & F. W. Luscinskas: Real-time imaging of vascular endothelial-cadherin during leukocyte transmigration across endothelium. *J Immunol* 167, 2323-30 (2001)

140. Feng, D., J. A. Nagy, K. Pyne, H. F. Dvorak & A. M. Dvorak: Neutrophils emigrate from venules by a transendothelial cell pathway in response to FMLP. *J Exp Med* 187, 903-15 (1998)

141. Burns, A. R., D. C. Walker, E. S. Brown, L. T. Thurmon, R. A. Bowden, C. R. Keese, S. I. Simon, M. L. Entman & C. W. Smith: Neutrophil transendothelial migration is independent of tight junctions and occurs preferentially at tricellular corners. *J Immunol* 159, 2893-903 (1997)

142. Burns, A. R., R. A. Bowden, S. D. MacDonell, D. C. Walker, T. O. Odebunmi, E. M. Donnachie, S. I. Simon, M. L. Entman & C. W. Smith: Analysis of tight junctions during neutrophil transendothelial migration. *J Cell Sci* 113, 45-57 (2000)

143. Muller, W. A., S. A. Weigl, X. Deng & D. M. Phillips: PECAM-1 is required for transendothelial migration of leukocytes. *J Exp Med* 178, 449-60 (1993)

144. Wong, C. W., G. Wiedle, C. Ballestrem, B. Wehrle-Haller, S. Etteldorf, M. Bruckner, B. Engelhardt, R. H. Gisler & B. A. Imhof: PECAM-1/CD31 trans-homophilic binding at the intercellular junctions is independent of its cytoplasmic domain; evidence for heterophilic interaction with integrin alphavbeta3 in *Cis*. *Mol Biol Cell* 11, 3109-21 (2000)

## Protrusive structures in leukocyte extravasation

145. Aurrand-Lions, M. A., C. Johnson-Leger & B. A. Imhof: Role of interendothelial adhesion molecules in the control of vascular functions. *Vascul Pharmacol* 39, 239-46 (2002)

146. Newman, D. K., C. Hamilton & P. J. Newman: Inhibition of antigen-receptor signaling by Platelet Endothelial Cell Adhesion Molecule-1 (CD31) requires functional ITIMs, SHP-2, and p56(lck). *Blood* 97, 2351-7 (2001)

147. Ilan, N., L. Cheung, E. Pinter & J. A. Madri: Platelet-endothelial cell adhesion molecule-1 (CD31), a scaffolding molecule for selected catenin family members whose binding is mediated by different tyrosine and serine/threonine phosphorylation. *J Biol Chem* 275, 21435-43 (2000)

148. Mamdouh, Z., X. Chen, L. M. Pierini, F. R. Maxfield & W. A. Muller: Targeted recycling of PECAM from endothelial surface-connected compartments during diapedesis. *Nature* 421, 748-53 (2003)

149. Schenkel, A. R., Z. Mamdouh, X. Chen, R. M. Liebman & W. A. Muller: CD99 plays a major role in the migration of monocytes through endothelial junctions. *Nat Immunol* 3, 143-50 (2002)

**Abbreviations:** ERM: ezrin-radixin-moesin proteins; ESAM: endothelial cell-selective adhesion molecule; ICAM-1: intercellular adhesion molecule-1; JAM: junctional adhesion molecule; LFA-1: lymphocyte function-associated antigen-1; PECAM-1: platelet endothelial adhesion molecule-1; PSGL-1: P-selectin glycoprotein ligand-1; TEM: transendothelial migration; VCAM-1: vascular cell adhesion molecule-1; VLA-4: very-late antigen-4.

**Key Words:** Adhesion, Cytoskeleton, Docking structure Endothelium, Leukocyte, Rolling, Tethering, Transendothelial migration, Review

**Send correspondence to:** Dr. Francisco Sánchez-Madrid: Servicio de Inmunología, Hospital de la Princesa, Universidad Autónoma de Madrid, C/Diego de León 62, 28006 Madrid, Spain. Tel.: 34-91-3092115. Fax: 34-91-5202374. E-mail: fsanchez.hlpr@salud.madrid.org

# Endothelial tetraspanin microdomains regulate leukocyte firm adhesion during extravasation

Olga Barreiro, María Yáñez-Mó, Mónica Sala-Valdés, María Dolores Gutiérrez-López, Susana Ovalle, Adrian Higginbottom, Peter N. Monk, Carlos Cabañas, and Francisco Sánchez-Madrid

**Tetraspanins associate with several transmembrane proteins forming microdomains involved in intercellular adhesion and migration. Here, we show that endothelial tetraspanins relocate to the contact site with transmigrating leukocytes and associate laterally with both intercellular adhesion molecule-1 (ICAM-1) and vascular cell adhesion molecule-1 (VCAM-1). Alteration of endothelial tetraspanin**

**microdomains by CD9–large extracellular loop (LEL)–glutathione S–transferase (GST) peptides or CD9/CD151 siRNA oligonucleotides interfered with ICAM-1 and VCAM-1 function, preventing lymphocyte transendothelial migration and increasing lymphocyte detachment under shear flow. Heterotypic intercellular adhesion mediated by VCAM-1 or ICAM-1 was augmented when expressed exogenously in**

**the appropriate tetraspanin environment. Therefore, tetraspanin microdomains have a crucial role in the proper adhesive function of ICAM-1 and VCAM-1 during leukocyte adhesion and transendothelial migration. (Blood. 2005;105:2852-2861)**

© 2005 by The American Society of Hematology

## Introduction

Plasma membrane contains small organized microdomains (lipid rafts) in which restricted repertoires of proteins are arranged together.<sup>1,2</sup> In resting cells, lipid rafts are estimated to be around 100 nm in diameter, including a few dozen proteins, and are distributed randomly on the cell surface, covering up to 50% of the plasma membrane. Upon cell activation, raft domains coalesce, recruiting and excluding different receptors, and allowing the proper organization of signaling complexes for efficient signal transduction.<sup>1,2</sup>

Tetraspanins comprise a large number of small palmitoylated polypeptides that span the plasma membrane 4 times,<sup>3-6</sup> and form microdomains that contain a restricted repertoire of proteins. Biochemically, they share some properties with lipid rafts, but tetraspanin microdomains are based on protein-protein interactions.<sup>7-10</sup> Tetraspanins have a highly conserved structure with a short and a large extracellular loop (LEL) where 2 or 3 disulfide bonds can be formed.<sup>11</sup> This large loop interacts noncovalently with other tetraspanins and transmembrane proteins, including integrins and adhesion receptors of the immunoglobulin (Ig) superfamily. Although all mammalian cells express different tetraspanins, genetic approaches have been elusive and their function has not yet been fully elucidated. However, their role in antigen presentation and sperm-egg binding has been recently underscored.<sup>12-20</sup>

The association of certain plasma membrane proteins to the cortical actin cytoskeleton is critical for their proper localization and function. Thus, the concentration of selectins and their ligands

on the tip of microvilli<sup>21,22</sup> both at the leukocyte and the apical surface of endothelial cells favors their interaction during the rolling phase of leukocyte extravasation. Likewise, vascular cell adhesion molecule-1 (VCAM-1) and intercellular adhesion molecule-1 (ICAM-1), which are relevant in the subsequent leukocyte firm adhesion step, are also displayed anchored to actin through ezrin-radixin-moesin proteins (ERMs)<sup>23,24</sup> at the apical surface on endothelial cells. Upon leukocyte firm adhesion, the engagement of VCAM-1 and ICAM-1 triggers the reorganization of the endothelial cortical actin cytoskeleton, building up a 3-dimensional docking structure that prevents the detachment of leukocytes by shear stress.<sup>22,23</sup> Here, we show that ICAM-1 and VCAM-1 are included in tetraspanin microdomains that regulate their membrane expression and the efficient adhesive function necessary for proper leukocyte transendothelial migration under flow conditions.

## Materials and methods

### Cells and cell cultures

Human umbilical vein endothelial cells (HUVECs) were obtained and cultured as previously described.<sup>25</sup> Cells were used up to the third passage in all assays. To activate HUVECs, tumor necrosis factor- $\alpha$  (TNF- $\alpha$ ; 20 ng/mL)(R&D Systems, Minneapolis, MN) was added to the culture media 20 hours before the assays were performed. T lymphoblasts were derived

From the Servicio de Inmunología, Hospital de la Princesa, Universidad Autónoma de Madrid, Spain; Instituto de Farmacología y Toxicología, Consejo Superior de Investigaciones Científicas–Universidad Complutense de Madrid (CSIC-UCM), Facultad de Medicina, Universidad Complutense, Madrid, Spain; and Department of Academic Neurology, The Medical School, University of Sheffield, United Kingdom.

Submitted September 17, 2004; accepted November 26, 2004. Prepublished online as *Blood* First Edition Paper, December 9, 2004; DOI 10.1182/blood-2004-09-3606.

Supported by grants BMC-2002 00563 from the Ministerio de Ciencia y Tecnología, Ayuda a la Investigación Básica Juan March 2002, and FIPSE 36289/02 (F.S.-M.), SAF2001-2807 from the Ministerio de Ciencia y Tecnología (C.C.), British Heart Foundation PG/98163 (P.N.M.), and fellowships from Red

Cardiovascular from FIS and EU grant LSHG-CT-2003-502935 (O.B.) and from FIS (M.Y.-M.).

O.B. and M.Y.-M. contributed equally to this manuscript.

The online version of the article contains a data supplement.

**Reprints:** Francisco Sánchez-Madrid, Servicio de Inmunología, Hospital de la Princesa, Universidad Autónoma de Madrid, C/ Diego de León 62, 28006 Madrid, Spain; e-mail: fsanchez.hlpr@salud.madrid.org.

The publication costs of this article were defrayed in part by page charge payment. Therefore, and solely to indicate this fact, this article is hereby marked "advertisement" in accordance with 18 U.S.C. section 1734.

© 2005 by The American Society of Hematology

from freshly isolated human peripheral blood lymphocytes (PBLs) by activation with phytohemagglutinin-L (PHA-L) (1  $\mu\text{g}/\text{mL}$ ; Sigma, St Louis, MO) for 24 hours followed by culture for 7 to 14 days in the presence of recombinant human (rh) interleukin-2 (IL-2; 50 U/mL) obtained from M. Gately (Hoffmann-LaRoche, Nutley, NJ) was provided by the National Institutes of Health AIDS Research and Reference Reagent program, Division of AIDS. Human PBLs, monocytes, neutrophils, and K562 erythroleukemic cells stably transfected with the  $\alpha 4$  or lymphocyte function-associated antigen-1 (LFA-1) integrins were obtained and cultured as described.<sup>23</sup> Adhesion of K562 LFA-1 transfectants to Colo320 colocal carcinoma cell line was performed in the presence of 1 mM  $\text{Mn}^{2+}$  to induce integrin activation. Colo320-CD9 and chimeric Colo320-CD9  $\times$  82 and Colo320-CD82CCG9 are stably transfected clones derived from those previously described.<sup>26</sup> Approval was obtained from the Hospital Universitario de la Princesa institutional review board for these studies. Informed consent was provided according to the Declaration of Helsinki.

### Antibodies and recombinant DNA constructs and proteins

Monoclonal antibodies (mAbs) anti-CD151 (LIA1/1), anti- $\beta 1$  integrin (TS2/16), anti-vascular endothelial (VE)-cadherin (TEA1/31), anti-E-selectin (TEA2/1), anti-CD44 (HP2/9), anti-CD63 (Tea3/18), and anti-CD9 (VJ1/20) have been previously described.<sup>25,27-29</sup> The 4B9 and P8B1 (anti-VCAM-1), Hu5/3 (anti-ICAM-1), 10B1 (anti-CD9), TS82 (anti-CD82), 8C3 (anti-CD151), and I.33.22 (anti-CD81) mAbs were kindly provided by R. Lobb (Biogen, Cambridge, MA), E. A. Wayner (Fred Hutchinson Cancer Research Center, Seattle, WA), F. W. Lusinkas (Brigham and Women's Hospital and Harvard Medical School, Boston, MA), E. Rubinstein (INSERM U268, Villejuif, France), K. Sekiguchi (Osaka University, Japan), and R. Vilella (Hospital Clinic, Barcelona, Spain), respectively. The IgG1, $\kappa$  mAb from the P3  $\times$  63 myeloma cell line was used as negative control. Anti-GST goat polyclonal Ab was purchased from Amersham Biosciences (Uppsala, Sweden), and anti-vimentin mAb was purchased from Sigma.

ICAM-1, VCAM-1, CD9, and CD151-green fluorescent protein (GFP) tagged proteins have been described.<sup>23,30</sup> The LEL-GST peptides of wild-type human CD9 or the mutated forms in the Cys residues have also been described.<sup>31</sup> The corresponding CD151-LEL-GST peptide presented a low rate of proper folding in solution which precluded its use in functional studies.

### Flow cytometry analysis, immunofluorescence, and confocal microscopy

For flow cytometry analysis and immunofluorescence experiments, cells were treated as previously described.<sup>25</sup> Paraformaldehyde solution (4%) was used as a fixative in all samples. Alexa Fluor 488 goat anti-mouse IgG conjugate and rhodamine red-X-Affinipure streptavidin were used as fluorescent reagents (Molecular Probes, Eugene, OR). A series of optical sections were obtained with a Leica TCS-SP confocal laser scanning unit equipped with Ar and He/Ne laser beams and attached to a Leica DMIRBE inverted epifluorescence microscope (Leica Microsystems, Heidelberg, Germany), using a PL APO 63  $\times$  1.32-0.6 oil immersion objective.

### Time-lapse fluorescence confocal microscopy

Transiently transfected HUVECs were generated by electroporation at 200 V and 975  $\mu\text{F}$  using a Gene Pulser (Bio-Rad Labs, Hercules, CA), and adding 20  $\mu\text{g}$  of each DNA construct. These cells were grown to confluence for 24 to 48 hours on glass-bottom dishes (WillCo Wells, Amsterdam, the Netherlands) precoated with fibronectin (20  $\mu\text{g}/\text{mL}$ ; Sigma). Cells were activated with TNF- $\alpha$  for 20 hours; then, T lymphoblasts resuspended in 500  $\mu\text{L}$  of complete 199 medium (BioWhittaker, Verviers, Belgium) were added. During the observation time, plates were maintained at 37°C in a 5%  $\text{CO}_2$  atmosphere using an incubation system (La-con GB Pe-con GmbH, Erbach, Germany). Confocal series of fluorescence and differential interference contrast (DIC) images, distanced 0.4  $\mu\text{m}$  in the z-axis, were simultaneously obtained at 30-second or 1 minute intervals with a  $\times$  63 oil immersion objective. Images were processed and assembled into movies using Leica Confocal software.

### Coimmunoprecipitation assays

Coimmunoprecipitation experiments were performed as previously described<sup>25</sup> with TNF- $\alpha$ -activated HUVEC lysates obtained in 1% Brij96 (Sigma) in 1 mM  $\text{Ca}^{2+}$  and 1 mM  $\text{Mg}^{2+}$  Tris-buffered saline (TBS) with protease inhibitors.

### Small interference RNA assay

To selectively knock down the expression of endothelial tetraspanins CD9 and CD151, a screening of different target sequences for each protein was performed using siRNA expression cassettes (Ambion, Austin, TX). We found the silencing sequences GAGCATCTTCGAGCAAGAA and CATGTGGCACCGTTTGCCCT for CD9 and CD151, respectively. RNA duplexes corresponding to these target sequences, as well as a negative oligonucleotide that does not pair with any human mRNA, designed by Eurogentec (Seraing, Belgium), were used. Oligos were transfected in HUVECs with oligofectamine (Invitrogen, Carlsbad, CA) following manufacturer's instructions. For CD9 interference, cells were transfected on day 0, further split on day 2, and retransfected on day 3. In parallel, on day 3, cells were transfected only once for CD151 knocking down. Then, cells were trypsinized on day 6 and negatively selected with anti-CD9 or anti-CD151 magnetic coated beads (Dynabeads M450 Goat anti-Mouse IgG; DYNAL Biotech ASA, Oslo, Norway) for 3 to 5 minutes at 4°C under rotation to enrich the tetraspanin low-expressing population. Cells thus selected were counted and seeded onto fibronectin to confluence for the different experiments, since its receptor  $\alpha 5\beta 1$  expression was not altered by tetraspanin knocking down (not shown).

### Paracellular monolayer permeability measurements

HUVEC monolayer paracellular permeability measurements were performed in 0.4- $\mu\text{m}$  pore diameter Transwells (Costar, Corning, NY) with 77 kDa fluorescein isothiocyanate (FITC)-labeled dextran (Sigma) as described.<sup>32</sup>

### Adhesion and transendothelial migration assays

Adhesion of human PBLs to HUVEC monolayers was performed in static conditions for 15 minutes at 37°C and measured as described.<sup>23</sup>

PBL migration through a confluent monolayer of activated HUVECs was assayed in 3- $\mu\text{m}$  pore Transwell cell culture chambers (Costar). HUVECs were grown to confluence on Transwell inserts precoated with 1% fixed gelatin or 20  $\mu\text{g}/\text{mL}$  of fibronectin and activated with TNF- $\alpha$  for 20 hours in the presence or not of 150  $\mu\text{g}/\text{mL}$  of the LEL-GST fusion proteins or after knocking down tetraspanin proteins. Monolayers were washed and freshly isolated PBLs ( $2 \times 10^5$  in 100  $\mu\text{L}/\text{well}$ ) were added to the upper chambers. In the lower well, 600  $\mu\text{L}$  of complete 199 medium, with or without 100 ng/mL of human recombinant stromal cell-derived factor-1 $\alpha$  (SDF-1 $\alpha$ ; R&D Systems, Minneapolis, MN) were poured. Chambers were incubated for 2 to 7 hours at 37°C. Migrated lymphocytes, ranging from 5% to 20%, were recovered from the lower chamber and estimated by flow cytometry.

### Parallel plate flow chamber analysis of endothelial-PBL interactions and detachment experiments

The parallel plate flow chamber used for leukocyte adhesion and detachment under defined laminar flow has been described in detail.<sup>33</sup> PBLs ( $1 \times 10^6/\text{mL}$ ) were drawn across activated confluent monolayers at an estimated wall shear stress of 1.8  $\text{dyn}/\text{cm}^2$  for 10 minutes. Lymphocyte rolling on the endothelium was easily visualized since they traveled more slowly than free-flowing cells. Lymphocytes were considered to be adherent after 20 seconds of stable contact with the monolayer. Transmigrated lymphocytes were determined as those being beneath the endothelial monolayer. Lymphocytes were considered to be detached when they returned to a free-flowing state after having established a transient contact with the endothelium. The number of rolling, adhered, transmigrated, and detached cells was quantified by direct visualization of 6 different fields ( $\times$  20 phase-contrast objective) for 30 seconds starting at 3.5 minutes and

ending at 6.5 minutes. Digitalization was performed with Optimas software (Bioscan).

For detachment experiments, peripheral blood lymphocytes were allowed to adhere for 15 minutes at 37°C to activated HUVEC monolayers, either incubated with LEL-GSTs for 20 hours, or transfected with siRNA oligos. Then, shear stress was applied by pulling assay buffer (Hanks balanced salt solution [HBSS] buffer with 2% fetal calf serum [FCS]) through the flow chamber with a programmable syringe pump, starting at 2 dyn/cm<sup>2</sup> and increasing up to 30 dyn/cm<sup>2</sup> at 1-minute intervals. The number of cells attached after each shear stress interval was quantified in 4 to 8 fields ( $\times 20$  phase-contrast objective). Cell detachment was obtained from the difference in adhered cells after subtracting the percentage of cells that had transmigrated during the assay.

### Heterotypic intercellular binding assays

Colo320 colocal carcinoma cells or different stable transfectants derived from this cell line were transiently transfected with ICAM-1-GFP or VCAM-1-GFP by electroporation in an ElectroSquarePorator ECM 830 (BTX, VWR, San Diego, CA). A total of  $5 \times 10^5$  cells of each condition were mixed with  $2 \times 10^5$  of K562 cells, either untransfected or stably transfected with  $\alpha 4$  or LFA-1 integrins, which had been previously loaded with the CM-TMR (5-(and-6)-(((4-chloromethyl)benzoyl)amino)tetramethylrhodamine) red fluorescent dye (Molecular Probes). Then, cells were allowed to adhere at room temperature under rotatory conditions for 90 minutes in RPMI medium without supplements. The relative number of heterotypic intercellular binding was estimated by flow cytometry.

## Results

### Tetraspanins are components of the endothelial docking structure for adherent leukocytes by their association with ICAM-1 and VCAM-1

Tetraspanin proteins are low-molecular-weight polypeptides that are able to associate with a variety of transmembrane proteins via their extracellular domain, forming multiproteic domains in the plasma membrane. They have been involved in several cellular functions including intercellular homotypic and heterotypic adhesion;<sup>6</sup> however, genetic approaches directed to tetraspanins did not render clear-cut information on their individual functional roles. HUVECs express several of these proteins (CD9, CD81, CD151, CD63), both at intercellular contacts and intracellular vesicles.<sup>25,34</sup> On the other hand, T lymphoblasts express CD81 and low levels of CD151, whereas the expression of CD9 is heterogeneous, ranging from completely negative to high expressing cells, and the relative amount of each population varies in different human donors. Upon T lymphoblast adhesion onto activated HUVEC monolayers, endothelial tetraspanins redistributed, together with ICAM-1 and VCAM-1, to the docking structure that emerges from the apical surface to firmly attach the transmigrating cell<sup>22,23</sup> (Figure 1A-B, and data not shown). Tetraspanin redistribution was also observed under flow conditions around adherent peripheral blood lymphocytes, neutrophils, or monocytes (Figure 1C for CD9, and data not shown).

To determine the subcellular localization of endothelial tetraspanins during the whole transendothelial migration process, T lymphoblasts were allowed to transmigrate across TNF- $\alpha$ -activated HUVEC monolayers. CD9 clustering was evident in those lymphocyte-endothelial interactions occurring at the apical surface of the monolayer (Figure 1D, white arrows). In contrast, almost no redistribution of CD9 could be observed at the ventral surface of endothelial cells in contact with transmigrated lymphoblasts (Figure 1D, gray arrows). On the other hand, CD151 relocalization around lymphoblasts was

clearly detected at both the apical and basal surface of the endothelial cell (Figure 1D; white and gray arrows, respectively), paralleling the behavior of ICAM-1. Similarly to that observed with the endogenous protein stainings, CD9-GFP was more clearly relocalized to the contact site with T lymphoblasts at the endothelial apical surface, although some clustering occurred around transmigrated lymphoblasts locomoting underneath the endothelium (Supplemental Video S1; see the Supplemental Video link at the top of the online article on the *Blood* website). On the other hand, CD151-GFP was strongly concentrated at the contact with lymphoblasts throughout all the transmigration process (Video S2). These data point to the existence of different tetraspanin microdomains at the apical and ventral endothelial surfaces and suggest a complex dynamic regulation of these membrane domains.

Tetraspanin interactions are biochemically detected by extraction with Brij 96/97 detergents. Although HUVEC tetraspanins were mostly associated with EWI-F and  $\beta 1$  integrins (Yáñez-Mó et al<sup>25</sup> and data not shown), CD9 and CD151 were also able to pull down ICAM-1 and VCAM-1 (Figure 1E). Conversely, ICAM-1 mAbs were also able to coprecipitate CD9, whereas VCAM-1 mainly coprecipitated CD151. No detectable signal for ICAM-1 was observed in  $\beta 1$  immunoprecipitates (not shown), suggesting that tetraspanin-integrin complexes are different to tetraspanin/ICAM-1/VCAM-1 complexes. Coprecipitation of CD9 and CD151 with ICAM-1 and VCAM-1 could also be faintly detected upon extraction with 1% digitonin (not shown), conditions in which most interactions among tetraspanins are lost and direct tetraspanin-partner associations are observed.<sup>35</sup> These results indicate that ICAM-1 and VCAM-1 are included into tetraspanin microdomains.

### Tetraspanin microdomains are critical for a proper expression and function of ICAM-1 and VCAM-1

In order to gain insights into the relevance of the inclusion of ICAM-1 and VCAM-1 into tetraspanin microdomains at endothelial cells, we used an siRNA approach against tetraspanins CD9 and CD151 in primary human endothelial cells. Endothelial tetraspanin CD9 and CD151 expression was considerably knocked down with specific siRNA oligos. In no case was the expression completely abolished, but a significant reduction (40%-70%) was attained (Figure 2A and B; flow cytometry analysis depicted in logarithmic scale and mean fluorescence quantified in Figure 2C). In immunofluorescence analyses a clear reduction of tetraspanin staining could be observed, with some cells showing expression levels even below the detection threshold (Figure 2D). A compensation effect on the expression of other tetraspanins was observed (Figure 2B-D).

HUVECs thus treated were viable and clearly responded to TNF- $\alpha$ , increasing ICAM-1, VCAM-1, and E-selectin expression over resting levels (ICAM-1 expression increased 10- to 30-fold upon TNF- $\alpha$  treatment, whereas VCAM-1 and E-selectin were undetectable in resting cells; Figure 3A, dotted line). The siRNA transfection procedure slightly affected the inducible expression of these adhesion receptors when compared with untransfected cells, as determined with a negative oligonucleotide control that does not pair with any human mRNA (not shown). In CD9 or CD151 tetraspanin-interfered cells, a selective reduction in the expression of ICAM-1 and VCAM-1, but not that of E-selectin or CD44 was observed (Figure 3A, thick versus thin line). This reduction was of 60%

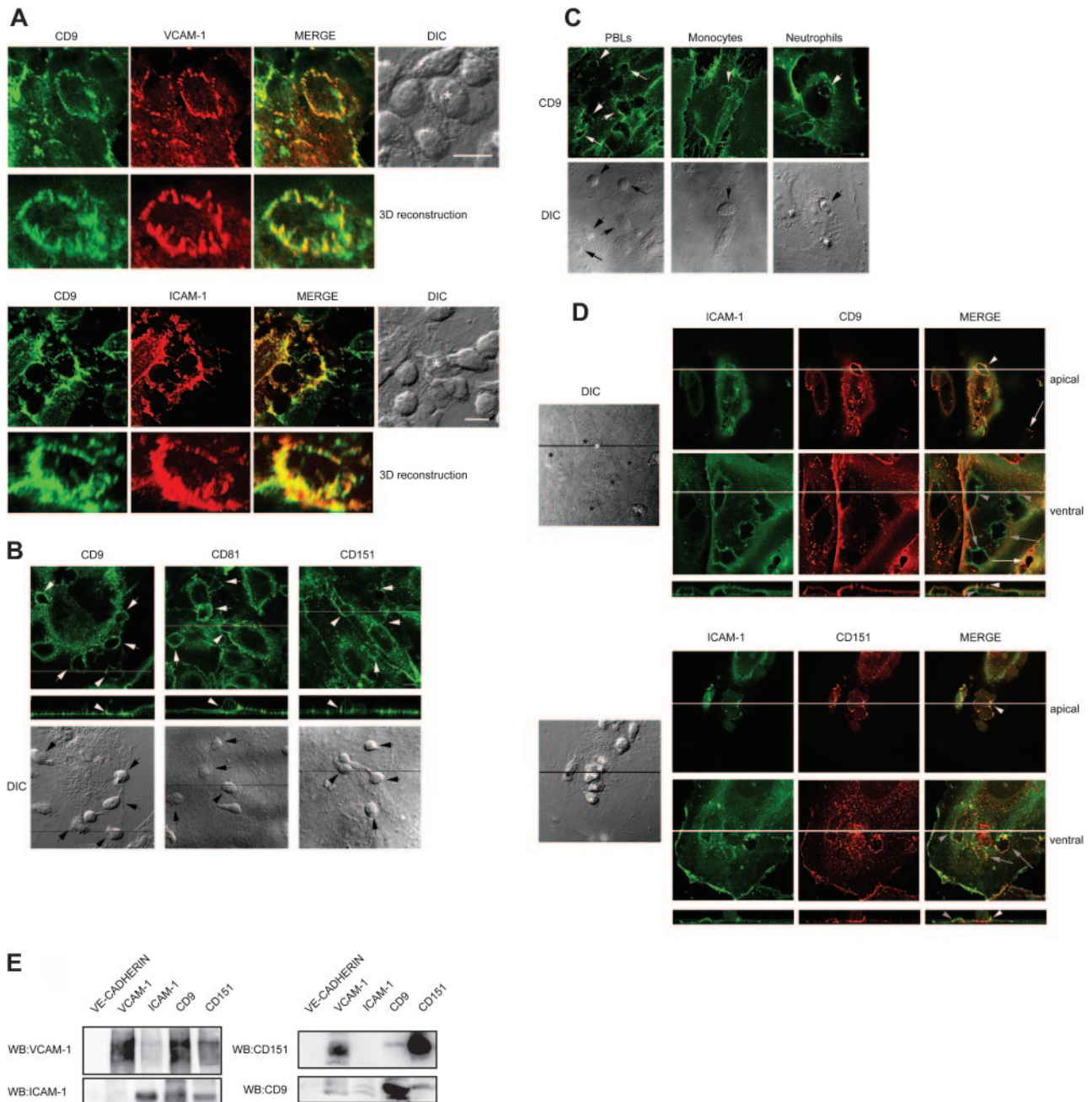


**Figure 1. Endothelial tetraspanin proteins relocalize to the contact site with adherent leukocytes and associate with ICAM-1 and VCAM-1.** (A) T lymphoblasts were adhered to TNF- $\alpha$ -activated HUVEC monolayers, fixed, and double-stained for CD9 and VCAM-1 or ICAM-1. Maximum projections of the relevant sections from the confocal stacks and the merge of both channels are shown. Asterisks in differential interference contrast (DIC) images highlight the T lymphoblasts around which the docking structures shown in the 3-dimensional (3D) reconstructions are formed. Scale bars equal 10  $\mu$ m. (B) T lymphoblasts were adhered to TNF- $\alpha$ -activated HUVEC monolayers, fixed, and stained with antitetraspanin mAbs VJ1/20 (anti-CD9), I.33.2.2 (anti-CD81), and LIA1/1 (anti-CD151). Confocal stacks were obtained and representative apical horizontal and vertical sections together with the corresponding DIC images are shown. Arrows point to the positions of the adhered lymphoblasts. Asterisks in the vertical sections of the adhered lymphoblasts shown in the vertical sections. Scale bar equals 10  $\mu$ m. (C) Human PBLs, neutrophils, or monocytes were perfused at physiologic flow rate (1.8 dyn/cm<sup>2</sup>), fixed, and stained with anti-CD9 VJ1/20 mAb. Confocal stacks were obtained and maximum projections of the whole series or a representative section together with the corresponding DIC images are shown. Arrows point to the position of the adhered leukocytes. Scale bar equals 20  $\mu$ m. (D) Analysis of the localization of endogenous endothelial CD9 or CD151, compared with ICAM-1, at apical and ventral contact sites with transmigrating lymphocytes. Human T lymphoblasts were allowed to transmigrate through TNF- $\alpha$ -activated HUVECs, fixed, and double-stained with antitetraspanin mAbs and biotin-conjugated anti-ICAM-1. Confocal stacks were obtained and representative sections at apical or ventral positions of the same field together with the corresponding DIC image are displayed. White arrows and asterisks mark apically adhered lymphocytes, and gray arrows and black asterisks mark those lymphocytes that have transmigrated. Arrowheads and lines point to the position of the adhered or transmigrated lymphoblast shown in the vertical sections. Scale bar equals 10  $\mu$ m. (E) ICAM-1 and VCAM-1 are associated with tetraspanins in TNF- $\alpha$ -activated HUVECs. Cell lysates were obtained in 1% Brij96 and immunoprecipitated with the different mAbs specific for endothelial adhesion molecules or tetraspanins. After washing, immunoprecipitates were resolved in sodium dodecyl sulfate–polyacrylamide gel electrophoresis (SDS-PAGE) gels and revealed by Western blot for VCAM-1 (P8B1), ICAM-1 (HU5/3), CD151 (8C3) or CD9 (VJ1/20).

for ICAM-1 and 80% for VCAM-1 when compared with their expression in negative oligonucleotide-transfected cells to exclude any off-target effect caused by siRNA transfection (Figure 3B). These data further emphasize the importance of tetraspanin

microdomains in ICAM-1 and VCAM-1 expression and suggest that their association with tetraspanins occurs early in the biosynthetic processing of these Ig adhesion molecules, or that it is necessary for their proper membrane insertion or retention.

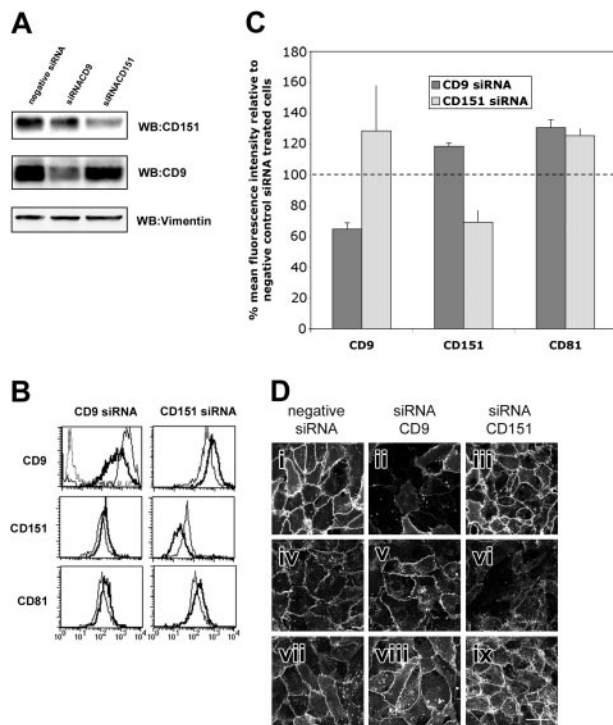


**Figure 2.** siRNA knocking down of tetraspanins CD9 and CD151 in HUVECs. (A) Analysis by Western blot of the expression of tetraspanins CD9 and CD151 in total-cell lysates of siRNA-transfected cells. Loading control for vimentin is also shown. Densitometric analysis of the experiment shown gave a reduction in the total protein amount of 70% for CD151 and 40% for CD9 expression. (B) Flow cytometry analysis of the expression of tetraspanins (anti-CD9 VJ1/20, anti-CD151 LIA1/1, anti-CD81 1.33.2.2) in tetraspanin siRNA-treated HUVECs. Negative siRNA-treated cells are shown in thin lines. Thick lines correspond to the expression in tetraspanin siRNA-transfected cells. Negative control PX63 is shown in dotted lines. The histograms are depicted in a logarithmic scale. (C) Quantitative analysis of the mean fluorescence intensity of CD9, CD151, and CD81 in tetraspanin siRNA-transfected cells. Data represent the mean of 2 independent experiments  $\pm$  SD as the percentage of the expression referred to that of negative control siRNA-transfected cells. (D) Immunofluorescence analysis of CD9 (i-iii), CD151 (iv-vi), and CD81 expression (vi-ix) and localization in HUVECs transfected with siRNA specific for endothelial tetraspanins CD9 and CD151 as well as the negative oligonucleotide. Images were acquired by confocal microscopy using the same photomultiplier parameters in control and tetraspanin-interfered cells. Maximum projection of the whole confocal image stack is shown. Scale bar equals 40  $\mu$ m.

Although ICAM-1 and VCAM-1 expression was lower in tetraspanin-interfered HUVECs, no difference was observed in peripheral blood lymphocyte (PBL) adhesion to interfered monolayers when performed under static conditions (Figure 3C). However, when HUVECs treated with siRNA oligos were seeded onto Transwell insets to perform chemotactic transmigration assays with human PBLs, a strong inhibition of lymphocyte transmigration was observed with both CD9 and CD151 siRNA-treated endothelial monolayers as compared with cells transfected with the negative control oligonucleotide (Figure 3D).

Given that ICAM-1 and VCAM-1 are components of a docking structure whose relevance in leukocyte firm adhesion was unveiled under flow conditions,<sup>23</sup> we assessed the role of tetraspanin microdomains on the strength of lymphocyte adhesion to endothelial cells by measuring their resistance to detachment under increasing shear stress. After 15 minutes, PBL adhesion to TNF- $\alpha$ -activated HUVECs was highly resistant to laminar flow, and most cells still remained attached at 10 dyn/cm<sup>2</sup> (5-fold more than physiologic shear stress) in control HUVEC monolayers (Figure 3E). In contrast, a great proportion of the PBLs adhered on tetraspanin-interfered monolayers started to detach even at low flow rates (Figure 3E).

When extravasation assays using tetraspanin-interfered endothelium were performed under physiologic flow conditions, a significant reduction in the number of adherent lymphocytes was also observed (Figure 3F). Furthermore, a tendency to decrease was consistently observed in rolling and transmigration. All these differences might be related to the lower ICAM-1 and VCAM-1 expression levels in tetraspanin-interfered cells or, additionally, the insertion of these molecules into tetraspanin-based microdomains might be critical for their proper function under shear stress conditions.

#### Tetraspanin-soluble peptides interfere with ICAM-1 and VCAM-1 function without affecting their surface expression

Tetraspanin associations with other transmembrane proteins occur through their LELs.<sup>11</sup> We thus generated soluble GST-LEL peptides from human CD9 (Figure 4A) and point mutants to Ala of any of the 4 Cys residues in the LEL of CD9, which show altered disulphide bond formation and tertiary conformation (Figure 4A). Although some degree of degradation of the soluble peptide occurs, a great proportion of the material eluted from the columns was reactive with CD9 mAb in Western blot under nonreducing conditions (Figure 4A). Incubation of HUVECs with GST-LEL peptides affected neither the expression levels of ICAM-1 and VCAM-1 induced by TNF- $\alpha$  (Figure 4B), nor cell viability (Figure 4C) or monolayer permeability (Figure 4D). The soluble peptides were added to the preparations at the time of addition of TNF- $\alpha$  so that they were accessible at the earliest time of inducible expression of both adhesion receptors. Thus, these peptides allowed us to interfere with tetraspanin-based microdomains without altering the expression levels of ICAM-1 or VCAM-1 induced by TNF- $\alpha$ . Incubation of HUVECs with CD9-LEL-GST, but not the mutated forms, significantly inhibited transendothelial migration of lymphocytes (Figure 5A), whereas they did not affect lymphocyte chemotaxis across nude Transwells (data not shown). When adhered PBLs were subjected to increasing shear stress, a higher PBL detachment rate was also observed upon treatment of HUVECs with CD9-LEL-GST (Figure 5B), but not with the point mutants. In these experiments the number of lymphocytes that transmigrated along the assay was also significantly reduced in those preparations treated with CD9-GST (not shown). All these data demonstrate that tetraspanin microdomains are important not only for proper ICAM-1 and VCAM-1 expression on the plasma membrane but also for their efficient adhesive function under flow conditions.

#### Enhanced ICAM-1 and VCAM-1 adhesive function requires an appropriate tetraspanin environment

To address the relevance of the repertoire of tetraspanin microdomains in the presentation of ICAM-1 and VCAM-1 adhesion molecules, we used Colo320 colocal carcinoma cells and a CD9 stable transfectant in this cell line. Colo320 cells express similar levels of CD151, CD81, CD63, and CD82 on the plasma membrane than endothelial cells, without expression of CD9, ICAM-1, or VCAM-1 (Figure 6A). A down-regulation of CD81 and CD63 was also observed upon stable transfection of these cells with CD9 (Figure 6A). Then, Colo320 and Colo320-CD9 were transiently transfected with VCAM-1 or ICAM-1-GFP to allow their heterotypic binding to  $\alpha$ 4- or LFA-1-transfected K562 cells. The levels of ICAM-1 and VCAM-1 expression attained by transient transfection varied among the different cell lines and experiments, but only cells with comparable high expression were analyzed in functional assays.

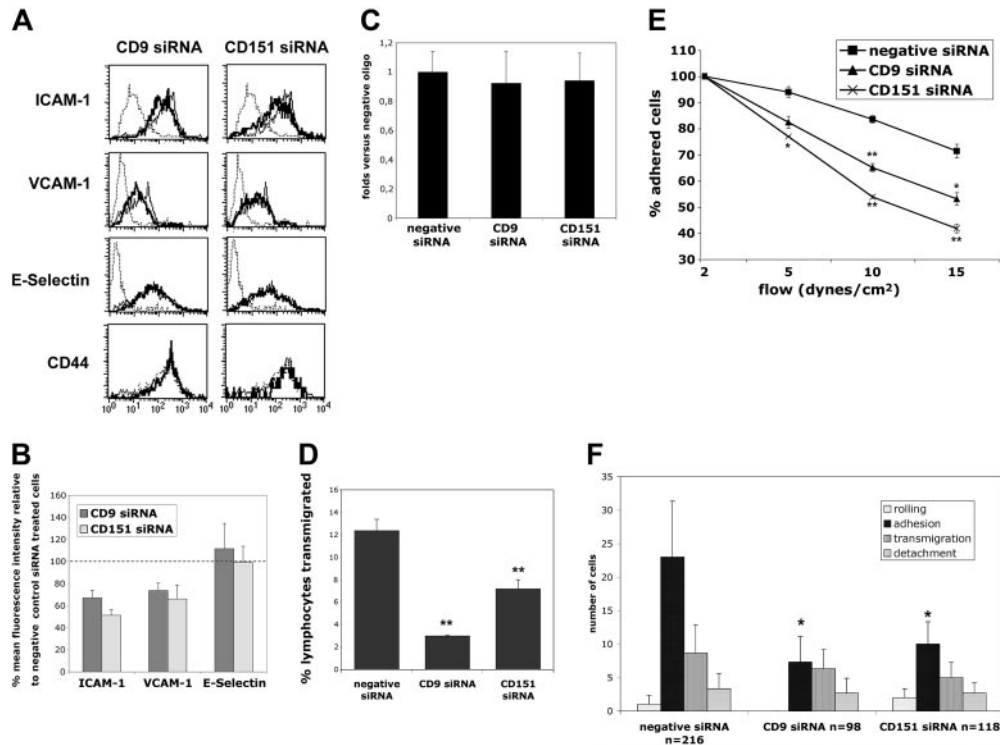


**Figure 3. Tetraspanin interference affects ICAM-1 and VCAM-1 expression and function.** (A) Flow cytometry analysis of the expression of adhesion molecules ICAM-1 (HU5/3), VCAM-1 (P8B1), E-Selectin (TEA2/1), and CD44 (HP2/9) in tetraspanin siRNA-treated HUVECs. TNF- $\alpha$ -activated negative siRNA-treated cells are shown in thin lines. Thick lines correspond to the expression in TNF- $\alpha$ -activated tetraspanin siRNA-transfected cells. Expression of the different adhesion molecules in resting cells is shown in dotted lines. The histograms are depicted in a logarithmic scale. (B) Quantitative analysis of the mean fluorescence intensity of ICAM-1, VCAM-1, and E-selectin in TNF- $\alpha$ -activated tetraspanin siRNA-transfected cells. Data represent the mean of 2 independent experiments  $\pm$ SD as the percentage of the expression referred to that of TNF- $\alpha$ -activated negative control siRNA-transfected cells. (C) Analysis of the adhesion of PBLs to tetraspanin-interfered cells under static conditions. PBLs were loaded with BCECF-AM (2',7'-bis(2-carboxyethyl)-5(6)-carboxyfluorescein acetoxymethyl ester) fluorescent probe and allowed to adhere in serum-free medium on confluent TNF- $\alpha$ -activated HUVEC monolayers for 15 minutes at 37°C. After washing, the percentage of adhesion was quantified in a fluorimeter and depicted as the mean  $\pm$ SD with respect to the adhesion levels of the negative siRNA-transfected cells in 3 different experiments performed in triplicate. (D) siRNA-transfected HUVEC monolayers were seeded onto Transwell insets and activated with 20 ng/mL of TNF- $\alpha$  for 20 hours. Then, human peripheral blood lymphocytes were added to the upper compartment and SDF-1 $\alpha$ -containing medium (100 ng/mL) was added to the lower compartment. Cells were allowed to migrate for 2 hours and analyzed by flow cytometry. Data represent the mean  $\pm$ SD of a representative experiment performed in triplicate. \*\* $P < .005$  in a Student  $t$  test. (E) Tetraspanin interference augments PBL detachment under shear stress. The percentage (mean  $\pm$ SD) of remaining adherent cells is represented for the different flow rates in 4 fields of a representative experiment. ■ indicates negative siRNA; ▲, CD9 siRNA; and ×, CD151 siRNA. \* $P < .02$ ; \*\* $P < .005$  in a Student  $t$  test. (F) Effect of tetraspanin siRNA on lymphocyte adhesion and transmigration under flow conditions. Activated endothelium transfected with specific siRNA oligos for tetraspanins CD9 or CD151 or the negative control oligonucleotide were activated with TNF- $\alpha$ . Thereafter, PBLs were allowed to adhere and transmigrate under physiologic flow conditions (1.8 dyn/cm<sup>2</sup>) for 10 min. Quantification of rolling, adhesion, transmigration, and detachment events was performed from minute 3.5 to minute 6.5 of perfusion. Values correspond to the arithmetic mean  $\pm$ SEM of the total number of PBLs interacting with the endothelial monolayer in the 6 different fields analyzed ( $\times 20$  objective) from a representative experiment. The total number of PBLs ( $n$ ) interacting with the HUVEC monolayer in each condition is depicted in the legend of the x-axis. \* $P < .02$  in a Student  $t$  test.

This cell system allowed us to assess the adhesion mediated independently by ICAM-1 or VCAM-1 in the presence or the absence of CD9. As shown in Figure 6B, binding of K562 transfectants to Colo320 cells was selective and completely dependent on the expression of ICAM-1 or VCAM-1, since no significant binding was observed with untransfected K562 cells or to untransfected Colo320 or Colo320CD9 cells (Figure 6B, and data not shown). Interestingly, VCAM-1- and ICAM-1-mediated binding was augmented by the presence of CD9 on Colo320 cells (Figure 6B). In the case of ICAM-1/LFA-1 binding, the experiments required the addition of Mn<sup>2+</sup> for LFA-1 activation on K562 cells, which resulted in a strong aggregation with Colo320 cells that partially masked the effect of CD9 (Figure 6B).

To further assess the specific contribution of CD9 in the generation of adhesion molecule/tetraspanin microdomains, we assayed the heterotypic binding of K562  $\alpha 4$  transfectants with Colo320 cells that stably express chimeric proteins made up of CD9 and CD82. All chimeric proteins were efficiently expressed at the plasma membrane (Figure 6C, flow cytometry analysis). The first chimera used coded for the N-terminal region of CD9 and the whole LEL and fourth transmembrane region belonged to CD82 (Colo320-CD9  $\times$  82) and behaved as Colo320 wild-type (wt) cells

in regard to VCAM-1-mediated binding (Figure 6C). To map the functionally relevant region of CD9, we used a second chimera with a chimeric LEL comprising the first half of CD82 LEL and the second half of CD9 LEL, where important residues for association with other transmembrane proteins reside (Colo320-CD82CCG9). This chimeric protein was able to enhance VCAM-1-mediated adhesion, even though not to the same extent as wild-type CD9. These data suggest that CD82 is not capable of replacing CD9 in the organization of endothelial-like tetraspanin-based domains in Colo320 cells and confirm that the LEL is an important functional region in CD9. Altogether, these data indicate that proper tetraspanin microdomains are necessary for the adhesive function of VCAM-1 and ICAM-1.

## Discussion

It is well established that tetraspanins interact in multiprotein domains with other transmembrane proteins.<sup>3,4,6,36</sup> Moreover, antibody crosslinking of tetraspanins usually triggers the same cellular responses as antibodies directed to their associated partners, indicating that they conform functional entities.<sup>5,36</sup> Herein, we

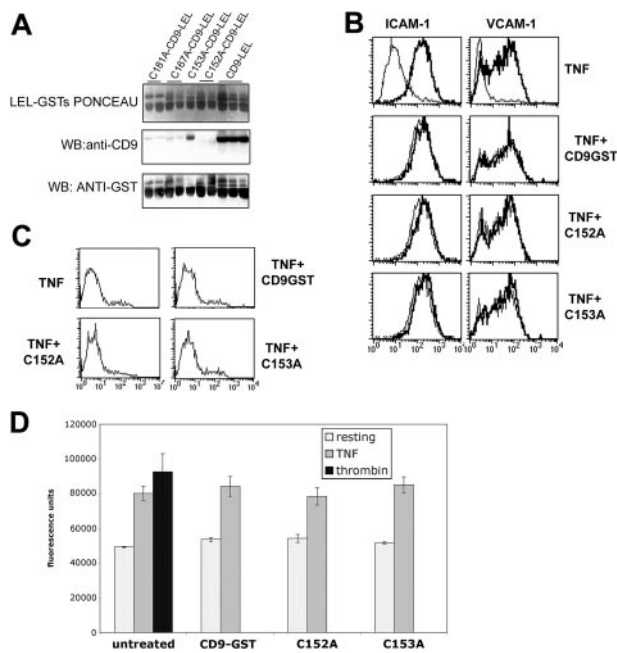


**Figure 4. Characterization of the soluble peptide CD9-LEL-GST and its mutants.** (A) LEL-GST fusion proteins of human CD9, as well as point mutations to Ala of Cys 152, 153, 167, and 181 were generated, produced in bacterial cultures, and isolated by affinity columns of Glutathione-Sepharose. Eluted purified proteins were then analyzed by Ponceau staining and Western blot against CD9 (VJ1/20 mAb) or GST. (B) Flow cytometry analysis of the expression of ICAM-1 and VCAM-1 in HUVECs preincubated with CD9-GST or its point mutants. Thin lines in the upper panels correspond to the expression of resting cells. Thin lines on the following panels correspond to cells treated with TNF- $\alpha$  alone. Thick lines correspond to the expression in cells treated for 20 hours with TNF- $\alpha$  alone (top row) or in combination with the different soluble LEL-GST peptides. (C) Propidium iodide profiles of cells treated for 20 hours with TNF- $\alpha$  alone or in combination with the different soluble LEL-GST peptides. (D) Paracellular permeability analysis of HUVEC monolayers preincubated with the different soluble LEL-GST peptides. Thrombin was added at 0.1 U/mL at the time of addition of the fluorescent dextran. Data represent the mean  $\pm$ SD of a representative experiment performed in duplicate.

describe the lateral association of ICAM-1 and VCAM-1 with tetraspanins at the contact area between leukocytes and endothelial cells. Remarkably, the function of these endothelial adhesion molecules can be directly modulated by the tetraspanin-associated moieties.

In contrast to lipid rafts, tetraspanins form a network based on protein-protein interactions, which might be modulated by differential protein expression or posttranslational modifications. In addition, tetraspanins are palmitoylated proteins that interact directly with cholesterol<sup>8-10,37</sup> and under certain conditions are also recovered in the light fractions of sucrose gradients.<sup>7</sup> Thus, tetraspanin webs or microdomains could be envisioned as a subtype of lipid rafts. In this regard, it has been suggested that the size of tetraspanin-based microdomains can be as small as lipid rafts.<sup>16</sup> Moreover, tetraspanin microdomains can be also important for intracellular signaling events, since they are able to associate with phosphatidylinositol 4-kinase (PI4-K)<sup>38</sup> and protein kinase C (PKC).<sup>39</sup> Our studies indicate that the composition of endothelial tetraspanin microdomains changes during the transmigration process. Thus, apical domains would be enriched in CD9, whereas in ventral domains CD151 is more highly represented. On the other hand, tetraspanins are also associated with integrin receptors at intercellular junctions.<sup>25,40</sup> These data suggest the existence of different tetraspanin microdomains, which might coalesce and diverge during cell activation, adhesion, or transmigration. Furthermore,

both ICAM-1 and VCAM-1 are anchored to the actin cytoskeleton through the association of ERM proteins to their cytoplasmic tails.<sup>23,24</sup> The linkage of Ig receptors to the cytoskeleton might indicate that tetraspanin microdomains are not floating freely on the plasma membrane but are connected to the cortical actin cytoskeleton.

Tetraspanins have been implicated in several cellular functions, mainly by the use of monoclonal antibodies.<sup>3-6</sup> Our results show that soluble CD9-LEL-GST peptides or tetraspanin-specific siRNA inhibit leukocyte transmigration and enhance their detachment by shear stress, supporting the functional role of tetraspanins in transendothelial migration. Similar GST fusion proteins have been reported to be inhibitory in sperm-egg fusion assays.<sup>31,41</sup> These LEL-GSTs are a valuable tool, without the effects of detergents or cholesterol-depleting agents, which affect the physical properties of the plasma membrane. The tertiary structure of these LEL proteins is very dependent on the proper disulphide bond formation. Thus, mutation of any of the 4 Cys in CD9 greatly reduces the recognition in Western blot by an anti-CD9 mAb and completely abolishes functional activity.

Endothelial tetraspanins are highly expressed and show a very slow turnover, so that partial protein knocking down by siRNA is observed only after 3 to 6 days. Although no complete abrogation of tetraspanin expression was attained, it turned out to be more than sufficient to exert a significant functional effect. Interestingly, a compensatory effect on other tetraspanin expression was observed, suggesting that a tight regulation of the overall tetraspanin load at

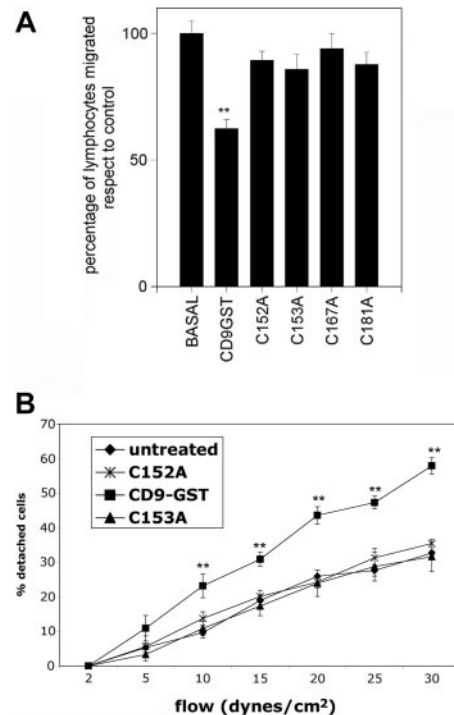


**Figure 5. CD9-LEL-GST inhibits leukocyte transendothelial migration and promotes cell detachment under flow.** (A) CD9-LEL-GST peptide inhibits transendothelial lymphoid migration in Transwells. HUVEC monolayers were activated with TNF- $\alpha$  alone or in combination with the different LEL-GST peptides. Then, human PBLs were added to the upper compartment and allowed to migrate for 5 to 7 hours. Cell migration was analyzed by flow cytometry and represented as the mean  $\pm$ SEM with respect to control untreated monolayers, of 4 independent experiments performed in duplicate. \*\* $P < .005$  in a Student  $t$  test. (B) Preincubation with CD9 LEL-GST fusion protein augments detachment under flow conditions. The percentage of detachment of PBLs was analyzed in 8 to 10 fields under increasing flow rates and represented as the mean  $\pm$ SEM.  $\blacklozenge$  indicates untreated cells;  $\times$ , C152A;  $\blacksquare$ , CD9-GST; and  $\blacktriangle$ , C153A. \*\* $P < .005$  in a Student  $t$  test.

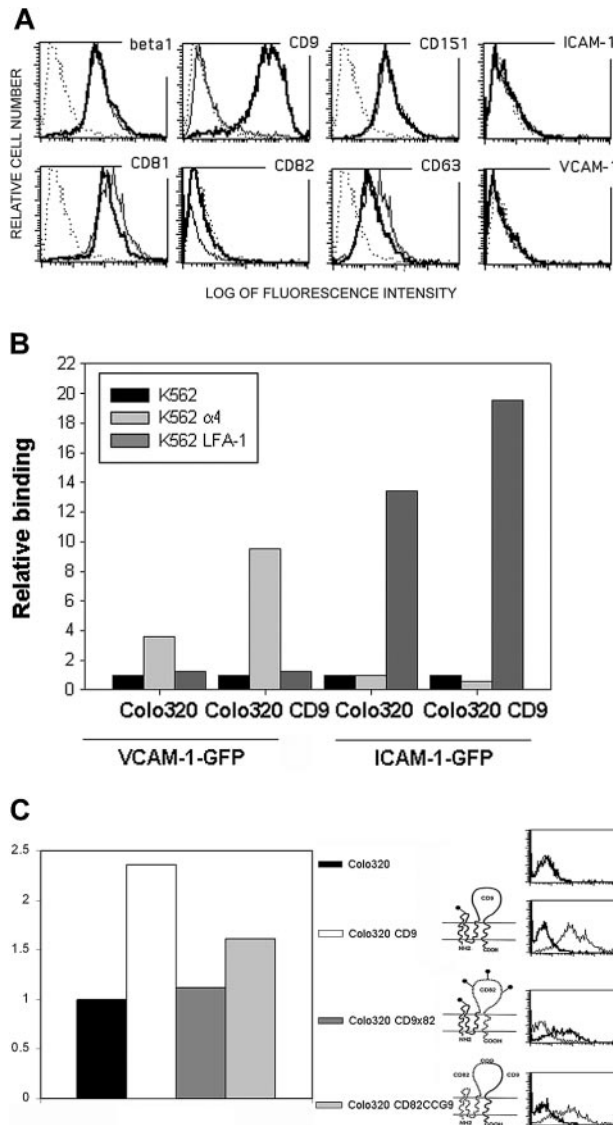


**Figure 6. Enhanced ICAM-1 and VCAM-1 adhesive function requires an appropriate tetraspanin environment.** (A) Flow cytometry analysis of the expression of  $\beta_1$  integrin (TS2/16 mAb), tetraspanins (anti-CD9 VJ1/20, anti-CD151 LIA1/1, anti-CD81 I.33.2.2, anti-CD82 TS82, and anti-CD63 TEA3/18 mAbs), ICAM-1 (HU5/3), and VCAM-1 (P8B1) in Colo320 cells (thin lines) or CD9 stably transfected Colo320 cell line (thick lines). Negative control PX63 is shown in dotted lines. (B) Heterotypic intercellular binding of K562 cell lines (parental and K562  $\alpha 4$  and K562 LFA-1 integrin transfectants) to Colo320 and Colo320CD9 cells transiently transfected with GFP-tagged versions of VCAM-1 and ICAM-1. Data are calculated as the ratio of double-positive aggregates (GFP-Colo320/CM-TMR K562) versus the nonaggregated GFP<sup>+</sup> cells. Graph depicts the relative binding referred to the aggregation obtained with parental K562 cells (that ranged from 10% to 20% of the total GFP<sup>+</sup> cells in the different transient transfections in the experiment shown) in a representative experiment out of 6 performed. (C) Heterotypic intercellular binding of K562 $\alpha 4$  integrin-stable transfectant to VCAM-1-GFP transiently transfected Colo320 cells and the different chimeric clones of CD9/CD82. Data are calculated as the ratio of double-positive aggregates (GFP-Colo320/CM-TMR K562) versus the total number of GFP<sup>+</sup> cells. Graph depicts relative binding referred to the aggregation of Colo320-VCAM-1-GFP cells in a representative experiment out of 3 (11% of the total GFP<sup>+</sup> cells in the experiment depicted). On the right, flow cytometry analysis of the expression with anti-CD9 (10B1, which also recognizes the chimeric CD9/CD82 loop; thin lines) and CD82 (TS82; thick lines) of the different chimeric clones is shown.

the plasma membrane exists. Nevertheless, as demonstrated also by the heterologous Colo320 cell system, the repertoire of tetraspanins is also crucial for the proper adhesive function of ICAM-1 and VCAM-1. Tetraspanin siRNA affected ICAM-1 and VCAM-1 expression, which suggests a possible role for tetraspanins in early

biosynthetic events. In this regard, it has been previously described that CD9 associates with the  $\beta 1$  integrin precursor prior to reaching the plasma membrane.<sup>42</sup> In a similar way, CD19 expression was selectively reduced in CD81-deficient mice, being the defect located after the endoplasmic reticulum.<sup>43</sup> However, tetraspanin interference only affected ICAM-1- and VCAM-1-mediated adhesion when assayed under stringent flow conditions. Moreover, CD9-LEL-GST peptide incubation had no effect on ICAM-1 and VCAM-1 induction but it did affect their function under shear stress. These data make both experimental approaches complementary and strongly suggest that membrane presentation into the appropriate microdomains of these receptors is functionally relevant for their proper adhesive function. Furthermore, the direct regulation of ICAM-1 and VCAM-1 adhesive function by the proper tetraspanin environment is revealed in the heterologous system of aggregation between Colo320 cells and K562 transfectants. Our data with Colo320 cells also rule out the possible involvement of a putative tetraspanin ligand on leukocytes, since their heterotypic adhesion is completely dependent on ICAM-1 or VCAM-1 expression.

The fact that ICAM-1 and VCAM-1 are included in tetraspanin-based microdomains might favor the efficient transition from the rolling step, in which VCAM-1 is involved,<sup>44,45</sup> to the firm adhesion of leukocytes via both VCAM-1 and ICAM-1 ligation,<sup>46,47</sup> to finally proceed to diapedesis. The possibility that selectins or other endothelial adhesion molecules are constituents of these endothelial tetraspanin microdomains cannot be ruled out. Another endothelial Ig adhesion molecule such as PECAM-1, also involved in transmigration,<sup>48</sup> is partially redistributed to the docking structure (not shown). In this regard, the effect of tetraspanin knocking down during the rolling and transmigration steps deserves further analysis using experimental settings specifically designed for the study of these processes. In this scenario, it could be postulated that tetraspanin microdomains would act as specialized platforms that cluster the appropriate adhesion receptors necessary for the rapid kinetics of leukocyte extravasation process.

Inclusion of ICAM-1 and VCAM-1 into tetraspanin domains is necessary for their proper function under dynamic conditions such as shear stress. This phenomenon could be explained by a possible role of tetraspanins in the preclustering or avidity regulation of endothelial adhesion receptors. Avidity regulation of the mitogenic activity of the membrane-anchored heparin-binding epidermal growth factor-like growth factor (HB-EGF) by its association with CD9 has been demonstrated.<sup>49,50</sup> Recent observations show that tetraspanin networks are able to cluster class II major histocompatibility complex (MHC) molecules bearing restricted repertoires of peptides,<sup>16</sup> thus facilitating antigen peptide presentation. Furthermore, CD81 also regulates very late antigen (VLA)-4- and VLA-5-mediated adhesion by enhancing integrin avidity independently of ligand binding.<sup>51</sup> This phenomenon also facilitated leukocyte firm adhesion by strengthening VLA-4-VCAM-1 interaction acting on the leukocyte side.

The inclusion of adhesion receptors into tetraspanin domains could also affect their conformation, up-regulating their binding to integrins. In this regard, we have recently described a monoclonal antibody that preferentially recognizes CD9 when associated with  $\alpha 6\beta 1$  integrin.<sup>26</sup> The possibility of reciprocal conformational changes in tetraspanin-associated proteins cannot be excluded. In this regard, CDw78 mAbs recognize human leukocyte antigen (HLA)-DR only when included into tetraspanin domains,<sup>52</sup> although the possibility of a conformational change in HLA-DR

because of its interaction with tetraspanins has not been determined. Lately, CD151 knock-out mice show a mild deficiency in outside-in activation of  $\alpha_{IIb}\beta_{III}$  integrin in platelets,<sup>53</sup> whereas human CD151 deficiency causes a more aggressive phenotype with renal, skin, hearing, and erythropoiesis defects<sup>54</sup>. Thus, several lines of evidence support a functional role for tetraspanin-based microdomains in different cellular functions. In this report we demonstrate by different complementary experimental approaches, both on primary cells and assessing endogenous proteins, and in an heterologous system, that the adhesive function of ICAM-1 and VCAM-1 is directly modulated by their inclusion in a microdomain containing the appropriate repertoire of tetraspanins. This effect

was shown to be crucial in an important physiologic process such as leukocyte extravasation and may have a great relevance not only in homing and inflammation but also in haematopoietic developmental stages at the bone marrow.<sup>55-57</sup>

## Acknowledgments

We thank E. Rubinstein for the original chimeric constructs of CD9/CD82 and the 10B1 mAb, and R. Gonzalez-Amaro for critical reading of the manuscript.

## References

1. Simons K, Toomre D. Lipid rafts and signal transduction. *Nat Rev Mol Cell Biol*. 2000;1:31-41.
2. Pike LJ. Lipid rafts: bringing order to chaos. *J Lipid Res*. 2003;44:655-667.
3. Berditchevski F. Complexes of tetraspanins with integrins: more than meets the eye. *J Cell Sci*. 2001;114:4143-4151.
4. Boucheix C, Rubinstein E. Tetraspanins. *Cell Mol Life Sci*. 2001;58:1189-1205.
5. Hemler ME. Specific tetraspanin functions. *J Cell Biol*. 2001;276:1103-1107.
6. Yáñez-Mó M, Mittelbrunn M, Sánchez-Madrid F. Tetraspanins and intercellular interactions. *Microcirculation*. 2001;8:153-168.
7. Claas C, Stipp CS, Hemler ME. Evaluation of prototype TM4SF protein complexes and their relation to lipid rafts. *J Biol Chem*. 2001;276:7974-7984.
8. Charrin S, Manie S, Oualid M, Billard M, Boucheix C, Rubinstein E. Differential stability of tetraspanin/tetraspanin interactions: role of palmitoylation. *FEBS Lett*. 2002;516:139-144.
9. Yang X, Claas C, Kraeft SK, et al. Palmitoylation of tetraspanin proteins: modulation of CD151 lateral interactions, subcellular distribution, and integrin-dependent cell morphology. *Mol Biol Cell*. 2002;13:767-781.
10. Berditchevski F, Odintsova E, Sawada S, Gilbert E. Expression of the palmitoylation-deficient CD151 weakens the association of alpha 3 beta 1 integrin with the tetraspanin-enriched microdomains and affects integrin-dependent signaling. *J Biol Chem*. 2002;277:36991-37000.
11. Stipp C, Kolesnikova T, Hemler M. Functional domains in tetraspanin proteins. *Trends Biochem Sci*. 2003;28:106-112.
12. Deng J, Dekruyff RH, Freeman GJ, Umetsu DT, Levy S. Critical role of CD81 in cognate T-B cell interactions leading to Th2 responses. *Int Immunol*. 2002;14:513-523.
13. Chen MS, Tung KS, Coonrod SA, et al. Role of the integrin-associated protein CD9 in binding between sperm ADAM 2 and the egg integrin alpha6beta1: implications for murine fertilization. *Proc Natl Acad Sci U S A*. 1999;96:11830-11835.
14. Mittelbrunn M, Yáñez-Mó M, Sancho D, Urza A, Sánchez-Madrid F. Cutting edge: dynamic redistribution of tetraspanin CD81 at the central zone of the immune synapse in both T lymphocytes and APC. *J Immunol*. 2002;169:6691-6695.
15. Knobloch K, Wright M, Ochslein A, et al. Targeted inactivation of the tetraspanin CD37 impairs T-cell-dependent B-cell response under suboptimal costimulatory conditions. *Mol Cell Biol*. 2000;20:5363-5369.
16. Kropshofer H, Spindeldreher S, Rohn TA, et al. Tetraspan microdomains distinct from lipid rafts enrich select peptide-MHC class II complexes. *Nat Immunol*. 2002;3:61-68.
17. Kaji K, Oda S, Shikano T, et al. The gamete fusion process is defective in eggs of CD9-deficient mice. *Nat Genet*. 2000;24:279-282.
18. Le Naour F, Rubinstein E, Jasmin C, Prenant M, Boucheix C. Severely reduced female fertility in CD9-deficient mice. *Science*. 2000;287:319-321.
19. Miller BJ, Georges-Labouesse E, Primakoff P, Myles DG. Normal fertilization occurs with eggs lacking the integrin alpha6beta1 and is CD9-dependent. *J Cell Biol*. 2000;149:1289-1296.
20. Miyado K, Yamada G, Yamada S, et al. Requirement of CD9 on the egg plasma membrane for fertilization. *Science*. 2000;287:321-324.
21. von Andrian U, Hasslen S, Nelson R, Erlandsen S, Butcher E. A central role for microvillous receptor presentation in leukocyte adhesion under flow. *Cell*. 1995;82:989-999.
22. Barreiro O, Vicente-Manzanares M, Urzainqui A, Yáñez-Mó M, Sánchez-Madrid F. Interactive protrusive structures during leukocyte adhesion and transendothelial migration. *Front Biosci*. 2004;9:1843-1863.
23. Barreiro O, Yáñez-Mó M, Serrador JM, et al. Dynamic interaction of VCAM-1 and ICAM-1 with moesin and ezrin in a novel endothelial docking structure for adherent leukocytes. *J Cell Biol*. 2002;157:1233-1245.
24. Heiska L, Alfthan K, Gronholm M, Vilja P, Vaheri A, Carpen O. Association of ezrin with intercellular adhesion molecule-1 and -2 (ICAM-1 and ICAM-2): regulation by phosphatidylinositol 4, 5-bisphosphate. *J Biol Chem*. 1998;273:21893-21900.
25. Yáñez-Mó M, Alfranca A, Cabañas C, et al. Regulation of endothelial cell motility by complexes of tetraspan molecules CD81/TAPA-1 and CD151/PETA-3 with alpha3beta1 integrin localized at endothelial lateral junctions. *J Cell Biol*. 1998;141:791-804.
26. Gutierrez-Lopez MD, Ovalle S, Yáñez-Mó M, et al. A functionally relevant conformational epitope on the CD9 tetraspanin depends on the association with activated beta-1 integrin. *J Biol Chem*. 2003;278:208-218.
27. Serrador JM, Alonso-Lebrero JL, del Pozo MA, et al. Moesin interacts with the cytoplasmic region of intercellular adhesion molecule-3 and is redistributed to the uropod of T lymphocytes during cell polarization. *J Cell Biol*. 1997;138:1409-1423.
28. Montoya M, Holtmann K, Snapp K, et al. Memory B lymphocytes from secondary lymphoid organs interact with E-selectin through a novel glycoprotein ligand. *J Clin Invest*. 1999;103:1317-1327.
29. Peñas PF, García-Diez A, Sánchez-Madrid F, Yáñez-Mó M. Tetraspanins are localized at motility-related structures and involved in normal human keratinocyte wound healing migration. *J Invest Dermatol*. 2000;114:1126-1135.
30. Longo N, Yáñez-Mó M, Mittelbrunn M, et al. Regulatory role of tetraspanin CD9 in tumor-endothelial cell interaction during transendothelial invasion of melanoma cells. *Blood*. 2001;98:3717-3726.
31. Higginbottom A, Takahashi Y, Bolling L, et al. Structural requirements for the inhibitory action of the CD9 large extracellular domain in sperm/oocyte binding and fusion. *Biochem Biophys Res Commun*. 2003;311:208-214.
32. Dominguez-Jimenez C, Yáñez-Mó M, Carreira A, et al. Involvement of alpha3 integrin/tetraspanin complexes in the angiogenic response induced by angiotensin II. *FASEB J*. 2001;15:1457-1459.
33. Lusinskas FW, Kansas GS, Ding H, et al. Monocyte rolling, arrest and spreading on IL-4 activated vascular endothelium under flow is mediated via sequential action of L-selectin, beta-1-integrins, and beta-2-integrins. *J Cell Biol*. 1994;125:1417-1427.
34. Sincock PM, Fitter S, Parton RG, Berndt MC, Gamble JR, Ashman LK. PETA-3/CD151, a member of the transmembrane 4 superfamily, is localized to the plasma membrane and endocytic system of endothelial cells, associates with multiple integrins and modulates cell function. *J Cell Sci*. 1999;112:833-844.
35. Serru V, Le Naour F, Billard M, et al. Selective tetraspan-integrin complexes (CD81/alpha4beta1, CD151/alpha3beta1, CD151/alpha6beta1) under conditions disrupting tetraspan interactions. *Biochem J*. 1999;340:103-111.
36. Hemler ME. Integrin associated proteins. *Curr Opin Cell Biol*. 1998;10:578-585.
37. Charrin S, Manie S, Thiele C, et al. A physical and functional link between cholesterol and tetraspanins. *Eur J Immunol*. 2003;33:2479-2489.
38. Berditchevski F, Tolias KF, Wong K, Carpenter CL, Hemler ME. A novel link between integrins, transmembrane-4 superfamily proteins (CD63 and CD81), and phosphatidylinositol 4-kinase. *J Biol Chem*. 1997;272:2595-2598.
39. Zhang X, Bontrager A, Hemler M. Transmembrane-4 superfamily proteins associate with activated protein kinase C (PKC) and link PKC to specific beta(1) integrins. *J Biol Chem*. 2001;276:25005-25013.
40. Chattopadhyay N, Wang Z, Ashman LK, Brady-Kalnay SM, Kreidberg J. alpha3beta1 integrin-CD151, a component of the cadherin-catenin complex, regulated PTPase expression and cell-cell adhesion. *J Cell Biol*. 2003;163:1351-1362.
41. Zhu G, Miller B, Boucheix C, et al. Residues SFQ (173-175) in the large extracellular loop of CD9 are required for gamete fusion. *Development*. 2002;129:1995-2002.
42. Rubinstein E, Poindessous-Jazat V, Le Naour F, Billard M, Boucheix C. CD9, but not other tetraspanins, associates with the beta1 integrin precursor. *Eur J Immunol*. 1997;27:1919-1927.
43. Shoham T, Rajapaksa R, Boucheix C, et al. The tetraspanin CD81 regulates the expression of CD19 during B cell development in a postendoplasmic reticulum compartment. *J Immunol*. 2003;171:4062-4072.
44. Berlin C, Bargatzte R, Campbell J, et al. Alpha 4 integrins mediate lymphocyte attachment and

- rolling under physiologic flow. *Cell*. 1995;80:413-422.
45. Alon R, Kassner P, Carr M, Finger E, Hemler M, Springer T. The integrin VLA-4 supports tethering and rolling in flow on VCAM-1. *J Cell Biol*. 1995;128:1243-1253.
  46. Butcher EC. Leukocyte-endothelial cell recognition: three (or more) steps to specificity and diversity. *Cell*. 1991;67:1033-1036.
  47. Springer TA. Traffic signals for lymphocyte recirculation and leukocyte emigration: the multistep paradigm. *Cell*. 1994;76:301-314.
  48. Muller WA, Weigl SA, Deng X, Phillips DM. PECAM-1 is required for transendothelial migration of leukocytes. *J Exp Med*. 1993;178:449-460.
  49. Higashiyama S, Iwamoto R, Goishi K, et al. The membrane protein CD9/DRAP 27 potentiates the juxtacrine growth factor activity of the membrane-anchored heparin-binding EGF-like growth factor. *J Cell Biol*. 1995;128:929-938.
  50. Nakamura K, Mitamura T, Takahashi T, Kobayashi T, Mekada E. Importance of the major extracellular domain of CD9 and the epidermal growth factor (EGF)-like domain of heparin-binding EGF-like growth factor for up-regulation of binding and activity. *J Biol Chem*. 2000;275:18284-18290.
  51. Feigelson S, Grabovsky V, Shamri R, Levy S, Alon R. The CD81 tetraspanin facilitates instantaneous leukocyte adhesion strengthening to vascular cell adhesion molecule 1 (VCAM-1) under shear flow. *J Biol Chem*. 2003;278:51203-51212.
  52. Drbal K, Angelisova P, Rasmussen A, Hilgert I, Funderud S, Horejsi V. The nature of the subset of MHC class II molecules carrying the CDw78 epitopes. *Int Immunol*. 1999;11:491-498.
  53. Lau LM, Wee JL, Wright MD, et al. The tetraspanin superfamily member, CD151 regulates outside-in integrin  $\alpha$ IIb $\beta$ 3 signalling and platelet function. *Blood*. 2004;104:2368-2375.
  54. Karamatic Crew V, Burton N, Kagan A, et al. CD151, the first member of the tetraspanin (TM4) superfamily detected on erythrocytes, is essential for the correct assembly of human basement membranes in kidney and skin. *Blood*. 2004;108:2217-2223.
  55. Leuker CE, Labow M, Müller W, Wagner N. Neonatally induced inactivation of the vascular cell adhesion molecule 1 gene impairs B cell localization and T cell-dependent humoral immune response. *J Exp Med*. 2001;193:755-767.
  56. Koni PA, Joshi SK, Temann UA, Olson D, Burkly L, Flavell RA. Conditional vascular cell adhesion molecule 1 deletion in mice: impaired lymphocyte migration to bone marrow. *J Exp Med*. 2001;193:741-753.
  57. Dittel BN, LeBien TW. Reduced expression of vascular cell adhesion molecule-1 on bone marrow stromal cells isolated from marrow transplant recipients correlates with a reduced capacity to support human B lymphopoiesis in vitro. *Blood*. 1995;86:2833-2841.

# Role of Tetraspanins CD9 and CD151 in Primary Melanocyte Motility

M. Angeles García-López,<sup>\*1</sup> Olga Barreiro,<sup>†1</sup> Amaro García-Díez,<sup>\*</sup> Francisco Sánchez-Madrid<sup>†</sup> and Pablo F Peñas<sup>\*</sup>

Departments of <sup>\*</sup>Dermatology and <sup>†</sup>Immunology, Hospital Universitario de la Princesa, Universidad Autónoma de Madrid, Madrid, Spain

**Tetraspanins CD9 and CD151 have been implicated in cellular motility and intercellular adhesion in several cellular types. Here, we have studied the subcellular localization and the functional role of these molecules in primary melanocytes. We found that endogenous tetraspanins preferentially clustered in areas of melanocyte homotypic intercellular contacts and at the tips of dendrites. These observations were further confirmed using time-lapse fluorescence confocal microscopy of melanocytes transfected with CD9– and CD151–GFP (green fluorescent protein) constructs, suggesting an involvement of these proteins in cellular contacts and migration. Cell adhesion and migration assays performed using blocking monoclonal antibodies against CD9 and CD151 showed no significant effect on cell–extracellular matrix adhesion, whereas the migration of melanocytes was significantly enhanced. The regulation of the migratory capacity of melanocytes by CD9 and CD151 was further confirmed knocking down the endogenous expression of these tetraspanins with small interference RNA oligonucleotides. Therefore, tetraspanin molecules are localized at motile structures in primary human melanocytes regulating the migratory capacity of these cells.**

Key words: CD151/CD9/cell adhesion/cell migration/intercellular contacts/melanocytes  
J Invest Dermatol 125:1001–1009, 2005

Tetraspanins comprise a numerous group of proteins that contain four putative membrane-spanning domains and, characteristically, the presence of a large divergent extracellular loop between the third and fourth membrane-spanning domains (Wright and Tomlinson, 1994). They have been implicated in the regulation of cell development, proliferation, activation, and motility and have been shown to couple to signal transduction pathways (Berditchevski, 2001; Boucheix and Rubinstein, 2001; Hemler, 2001; Stipp *et al*, 2003). In this regard, it has been suggested that the main role of tetraspanins is to organize other proteins into signal-transducing complexes at the cell surface (Berditchevski, 2001; Yáñez-Mó *et al*, 2001; Tarrant *et al*, 2003). Tetraspanins have been shown to coprecipitate with several transmembrane proteins, and with  $\beta$ 1 integrins in particular (Berditchevski *et al*, 1996; Hemler *et al*, 1996; Rubinstein *et al*, 1996; Maecker *et al*, 1997). In epidermal cell adhesion and migration,  $\beta$ 1 integrins play a critical role (Watt and Hertle, 1994). To participate in those functions, integrins may not only bind to intracellular proteins and extracellular ligands (Clark and Brugge, 1995) but may also laterally associate with other transmembrane proteins such as those from the tetraspanin superfamily (Berditchevski, 2001;

Boucheix and Rubinstein, 2001; Hemler, 2001; Stipp *et al*, 2003).

The migration of melanocytes represents a fundamental requirement in a wide variety of physiological and pathological scenarios. Melanocytes migrate from the neural crest to the skin during the first trimester of the embryogenesis. In physiological conditions, melanocytes migrate to display a homogeneous distribution in the epidermis, which have been designated as an “epidermal melanin unit” (Fitzpatrick and Breathnach, 1963). But insights into the cellular and molecular mechanisms underlying such organization, however, remain unknown (Hoath and Leahy, 2003). In adults, melanocytes also migrate during the process of wound healing and to cover the white areas of patients with vitiligo. Although integrins (Morelli *et al*, 1993) and cadherins (Hsu *et al*, 2000) are both implicated in adhesion and movement of melanocytes, little is known about other factors that regulate both functions. Tetraspanins have been found on normal epidermis (Okochi *et al*, 1997; Sincock *et al*, 1997), expressed by keratinocytes (Jones *et al*, 1996; Okochi *et al*, 1997; Peñas *et al*, 2000). We have previously demonstrated that tetraspanin molecules have an important role in keratinocyte motility (Peñas *et al*, 2000). On the other hand, CD9 has been functionally associated with tumor cell motility (Ikeyama *et al*, 1993) and melanoma invasion (Longo *et al*, 2001). Nevertheless, no formal study of tetraspanins has been performed in human primary melanocytes. In this study, we describe the subcellular localization of CD9 and CD151 tetraspanin molecules and their functional role in melanocyte motility.

---

Abbreviations: ECM, extracellular matrix; GFP, green fluorescent protein; mAb, monoclonal antibody; siRNA, small interference RNA  
<sup>1</sup>These authors equally contributed to this work.

## Results

**Melanocytes express CD9 and CD151 tetraspanin proteins at intercellular contacts and tips of dendrites** We analyzed the expression of tetraspanins CD9, CD63, CD81, and CD151, and integrins  $\alpha\beta3$ ,  $\beta1$ ,  $\alpha2$ , and  $\alpha3$  by flow cytometry in normal human melanocytes. These primary cells express high levels of  $\beta1$  integrin and CD9, and lower levels of  $\alpha2$  and  $\alpha3$  chains of integrins and tetraspanins CD81, CD151, and CD63 (Fig 1).

Immunofluorescence studies showed that CD9 and CD151 are distributed throughout the cell body and the dendrites of the melanocyte, their clustering at points of intercellular contact and at the tips of dendrites being remarkable, where they preferentially colocalized with  $\beta1$  integrins (Fig 2a and b). The colocalization percentage obtained considering the overall surface of the melanocytes, however, is rather average (ranging from 14% to 28%), and not all contacts and tips contained accumulation of both molecular types (data not shown). CD81 exhibits a staining pattern similar to that of CD9 and CD151, but no clear CD63 membrane expression was found, although it was highly represented in intracellular vesicles as it has been found in other cell types such as endothelial cells and keratinocytes (data not shown) (Yáñez-Mó *et al*, 1998; Peñas *et al*, 2000).

We found footprints in the immunofluorescence studies with CD9 but almost no staining with CD151 (data not shown). These footprints are made of rests of plasma membrane containing receptors for extracellular matrix proteins that remain attached to the ligands as the cell moves. We and other authors have described this phenomenon, also termed ripping, in keratinocytes (Peñas *et al*, 2000) and other cell types (Palecek *et al*, 1996).

As these findings suggested an implication of tetraspanins in adhesion to the extracellular matrix, we performed adhesion experiments on collagen. We used TS2/16 (an anti-CD29 that activates integrins  $\beta1$ ) and VJ1/14 (an anti-CD29 that inhibits integrins  $\beta1$ ) monoclonal antibodies (mAb) as positive and negative controls of adhesion, respectively. Differences between both TS2/16 (enhancing adhesion) and VJ1/14 (inhibiting adhesion) were significant ( $p < 0.005$ ) but moderate ( $\pm 15\%$  from the control). When melanocytes were incubated with anti-tetraspanin mAb, we also found a reproducible but very mild modification of adhesion ( $\leq 15\%$ ) compared with control cells without antibody treatment, suggesting the lack of implication of CD9 and CD151 in adhesion to collagen (data not shown) as described for other cell types (Yáñez-Mó *et al*, 1998).

**Tetraspanins CD9 and CD151 are involved in melanocyte-melanocyte interactions** To ascertain the kinetics of the localization of tetraspanins in intercellular homotypic contacts of melanocytes, we performed time-lapse fluorescence confocal microscopy with CD9-GFP (green fluorescent protein) and CD151-GFP-tagged proteins. Using CD9-GFP we found that this molecule showed a diffuse pattern of accumulation at transient cell-cell contact sites (Fig 3a, Fig S1). CD151-GFP was rapidly and highly concentrated as soon as dendrites of different melanocytes come into contact (Fig 3b, Fig S2). Both findings

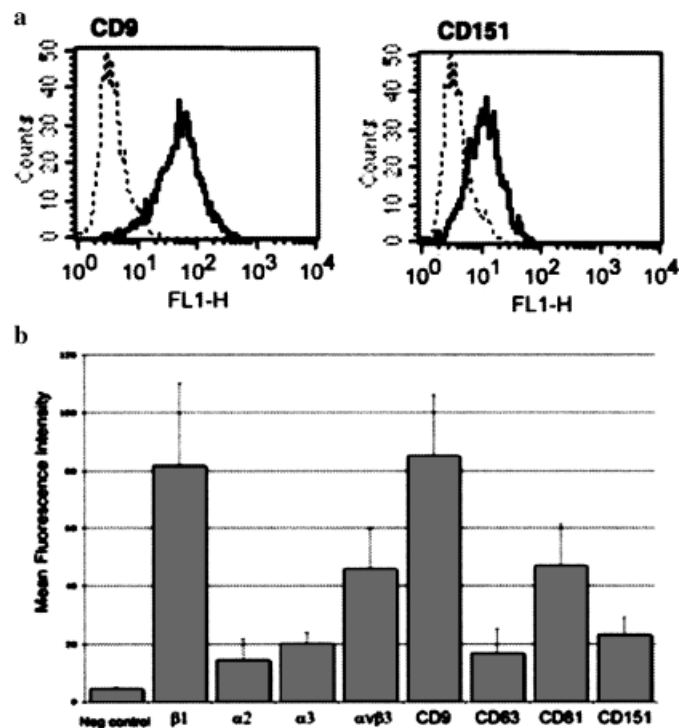


**Figure 1**  
Human primary melanocytes express tetraspanins CD9, CD63, CD81, and CD151. (a) Representative profiles of flow cytometry analysis corresponding to CD9 and CD151 tetraspanins in melanocytes. (b) A quantitative analysis of the membrane expression of  $\beta1$ ,  $\alpha2$ ,  $\alpha3$ , and  $\alpha\beta3$  integrins and CD9, CD63, CD81, and CD151 tetraspanin proteins expressed as mean fluorescence intensity measured by flow cytometry (mean  $\pm$  SEM of six to nine experiments). X-63 was used as negative control.

suggest that CD9 and CD151 transiently cluster at the homotypic intercellular contacts during the scanning of the melanocyte cell surface.

**Tetraspanins are implicated in melanocyte motility** On the other hand, another specific area of accumulation was the tips of the dendrites, which are enriched in ruffles. We found enhanced expression of CD9-GFP (Fig 4a, Figure S3) and CD151-GFP (Fig 4b, Fig S4) at the tip of dendrites when melanocytes explore the surrounding milieu. This localization was dynamic and was displayed by all dendrites; those that directed the movement of the melanocyte and those that were retracting.

As these results suggested that CD9 and CD151 may be involved in the movement of melanocytes, they prompted us to formally explore the functional involvement of tetraspanins in melanocyte motility using Transwell chambers with fibronectin in the lower chamber as a stimulus for melanocyte motility. Blocking monoclonal antibodies against CD9 and CD151, as determined in other cellular types (Yáñez-Mó *et al*, 1998; Peñas *et al*, 2000), enhanced melanocyte motility, whereas anti- $\alpha\beta3$  integrin inhibited the migration of melanocytes. The activatory anti- $\beta1$  integrin TS2/16 decreased the migration of melanocytes, whereas the inhibitory anti- $\beta1$  integrin VJ1/14 increased it (Fig 5a). To evaluate the influence of  $\beta1$  integrins in CD9 and CD151-mediated effect on melanocyte migration, we combined the use of TS2/16 and VJ1/14 with anti-CD9 and anti-CD151 (Fig 5b).

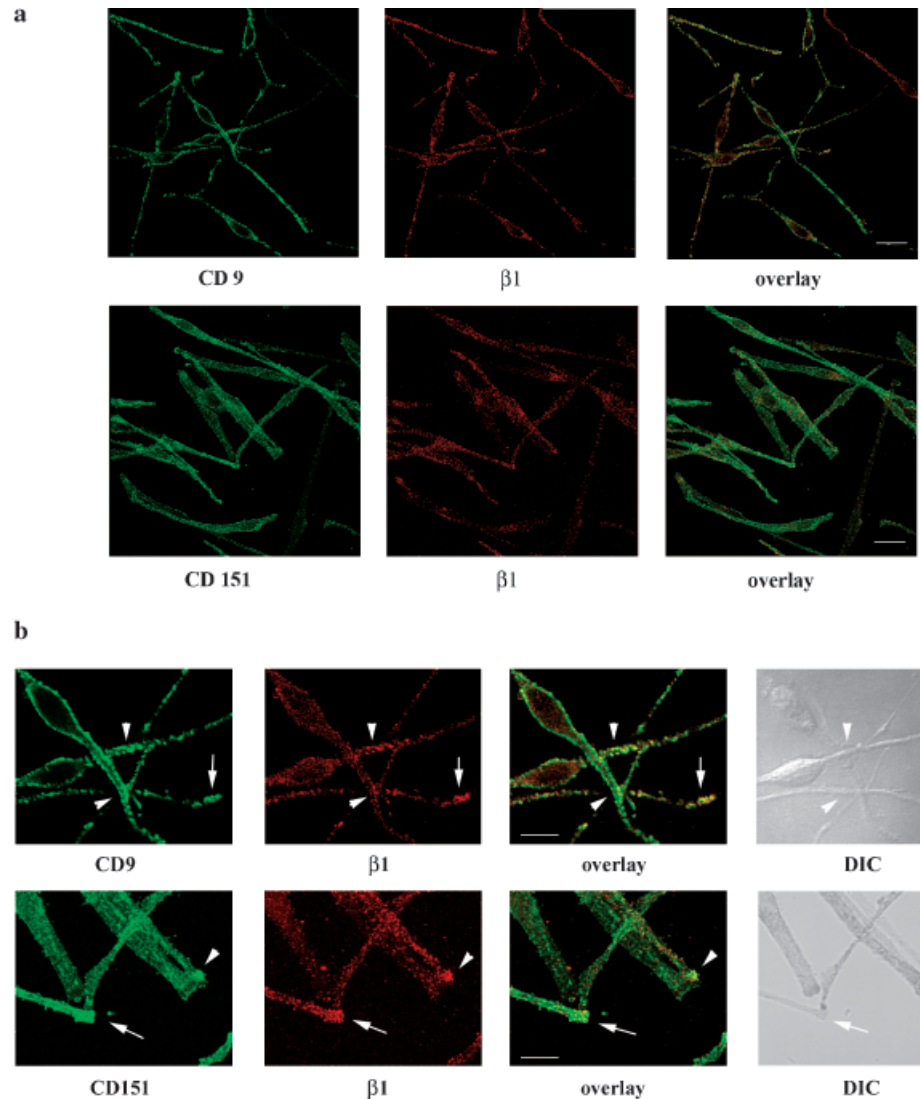


**Figure 2**

**Tetraspanins and  $\beta 1$  integrins colocalize at intercellular contacts of melanocytes and at tips of dendrites.** (a) Representative horizontal confocal sections showing the subcellular distribution of CD9 or CD151 (green fluorescence) compared with  $\beta 1$  integrin (red fluorescence), together with the overlay images are depicted. Scale bar = 20  $\mu\text{m}$ . (b) Zoom images from the representative horizontal confocal sections shown in the previous panel are depicted. Co-clustering of tetraspanin proteins with  $\beta 1$  integrin at intercellular contacts are indicated with white arrowheads and at the tips of the dendrites are indicated with white arrows. Scale bar = 10  $\mu\text{m}$ .

We found that the enhanced effect of CD9 and CD151 on melanocyte migration was more pronounced when combined with VJ1/14, and was partially reversed by TS2/16.

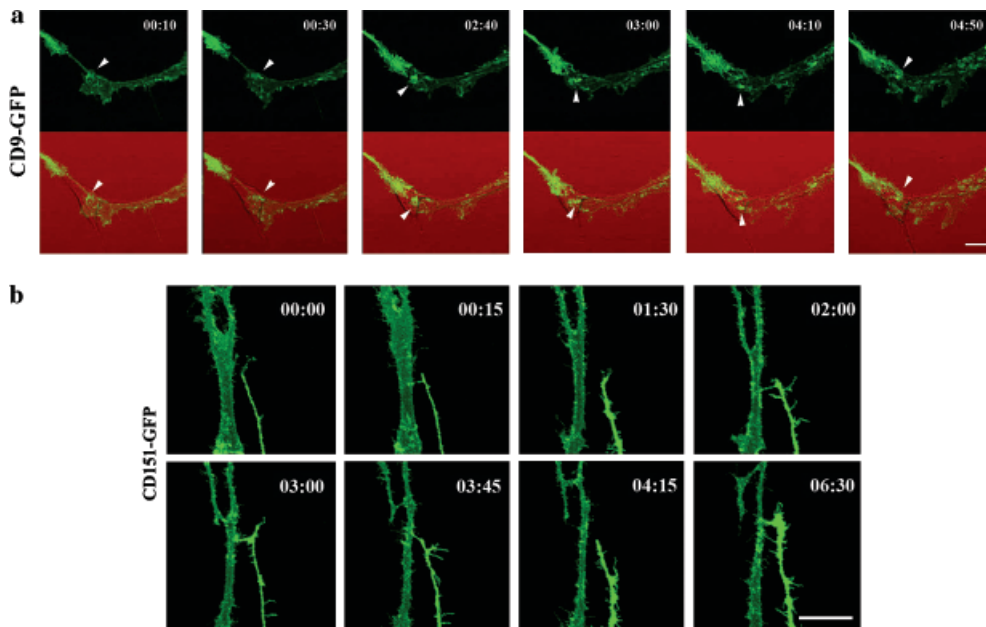
To further assess the functional role of tetraspanins in melanocyte motility, tetraspanin expression was knocked down in melanocytes using small interference RNA (siRNA) against CD9 and CD151. We obtained a significant inhibition in the expression of CD9 and CD151 using specific siRNA (Fig 6a), without affecting the morphological characteristics of siRNA-treated melanocytes (data not shown). We performed similar migration assays using fibronectin as a stimulus of melanocyte motility with these interfered cells and found that siRNA against CD9 and CD151 significantly ( $p < 0.05$ ) stimulates melanocyte migration (Fig 6b). Altogether these data underscore the involvement of tetraspanin in melanocyte migration through regulation of  $\beta 1$  integrin function.

## Discussion

The role of tetraspanins in keratinocytes has been explored previously (Peñas *et al*, 2000). Tetraspanins are implicated in

keratinocyte motility, and a possible implication of these molecules in inter-keratinocyte contacts has been suggested. Although CD9, CD81, and CD151 have been described in melanoma cells (Radford *et al*, 1996; Longo *et al*, 2001), no description of the expression or functional implications of tetraspanins in normal human melanocytes has been reported before.

This work addresses the expression, subcellular distribution, and functional role in cell adhesion and motility of the tetraspanins CD9 and CD151 in primary human melanocytes. The accumulation of both tetraspanins at the tips of the melanocyte dendrites and in the intercellular contacts with other melanocytes was remarkable. Moreover, some ripping was found. These findings suggested the involvement of CD9 and CD151 in melanocyte adhesion to the extracellular matrix, in the exploration of the environment and in homotypic interactions. CD63, a component of melanosomes also known as lysosome-associated membrane protein (LAMP)-3, has been described in melanocytes and melanoma, and implicated in melanoma progression (Ota *et al*, 1998). As expected, CD63 showed low plasma membrane and high intracellular expression in primary melanocytes.

**Figure 3**

**CD9—GFP (green fluorescent protein) and CD151—GFP are dynamically expressed in intercellular contacts.**

Melanocytes transfected with CD9—GFP or CD151—GFP constructs were seeded on coverslips and time-lapse fluorescence confocal microscopy was started after 4 h. Series of optical sections distanced  $0.4 \mu\text{m}$  on the z-axis were acquired every 10 min (CD9) or 15 min (CD151) for a total time of 7 h. a) All the micrographs depicted show the transient accumulation of CD9—GFP at the tip of the dendrite when it contacts with another untransfected melanocyte (white arrowheads). A maximum projection of the relevant sections from the confocal stack of the GFP and the merged image also composed with the corresponding DIC image from each selected time point of the videosequence are shown. Scale bar =  $10 \mu\text{m}$ .

b) The images show the accumulation of CD151—GFP on the membrane of the melanocyte as soon as the cell contacts the dendrite of another highly

transfected melanocyte (T: 00:15, 02:00, 03:00, 03:45, 06:30). When there is no contact, fluorescence intensity returns to basal levels (T: 00:00, 01:30, 04:15). A maximum projection of the relevant sections from the confocal stack of the green signal (GFP) from each corresponding time point of the videosequence is shown. Scale bar =  $20 \mu\text{m}$ .

The role of tetraspanins in adhesion to the ECM varies among different cell types, and it has been suggested that tetraspanins are not involved in cellular adhesion in most cells (Berditchevski, 2001). In this regard, CD9 did not affect MDA-MB 231 (Sugiura and Berditchevski, 1999), human B cells (Shaw *et al*, 1995) or hepatic cells (Mazzocca *et al*, 2002) adhesion. Accordingly, our data show that tetraspanins slightly modulate the adhesion of melanocytes to collagen. But CD151 increased adhesion to collagen and fibronectin of the erytroleukemia cell line HEL (Fitter *et al*, 1999) but did not affect many other cell lines and human primary cells (Yauch *et al*, 1998; Fitter *et al*, 1999; Sugiura and Berditchevski, 1999; Mazzocca *et al*, 2002). It is remarkable that a defective CD151 protein has been implicated as the cause of epidermolysis bullosa in two patients, suggesting that this tetraspanin could play a role in keratinocyte adhesion (Karamatic Crew *et al*, 2004).

Tetraspanins are important in intercellular contacts (Yáñez-Mó *et al*, 2001; Tarrant *et al*, 2003) since they are clearly accumulated in areas of cell–cell contact in most cellular types, both in homo- and heterotypic interactions (Peñas *et al*, 2000; Longo *et al*, 2001). In fact, the CD151- $\alpha 3\beta 1$  integrin complex has been shown to regulate cadherin-mediated adhesion (Chattopadhyay *et al*, 2003). We have found that melanocytes express CD9 and CD151 in melanocyte–melanocyte contacts and in melanocyte–keratinocyte interactions (unpublished results). Immunofluorescence staining of intercellular homotypic interactions was very conspicuous but not constant, suggesting a dynamic and transient clustering of the tetraspanins at these sites. This effect has not been described on keratinocytes or endothelial cells, where the expression was permanent in homotypic interactions and absent in cellular areas with no cell contact. These data, together with the findings of the time-lapse confocal microscopy with CD9—GFP and

CD151—GFP, suggest that tetraspanins are involved in some of the phases of the cell–cell contact, perhaps involved in finding the path of other cells.

Regarding the expression of CD9 and CD151 at the tip of melanocyte dendrites, our findings also suggest a role in the exploration of the external milieu. On cells of neural origin, localized expression of tetraspanins CD9 and CD151 on the tips of the neurites has been implicated in neurite formation (Smith *et al*, 1996; Banerjee *et al*, 1997; Stipp and Hemler, 2000). Our immunofluorescence studies showed that localization of CD9 and CD151 at the tip of melanocyte dendrites was not permanent, and suggested a dynamic clustering of both tetraspanins and  $\beta 1$  integrins. The use of GFP-tagged versions of CD9 and CD151 allowed us to analyze the dynamic clustering of these tetraspanins. Although we cannot exclude that the expression of tetraspanins at the tips of melanocyte dendrites is related to a role in dendrite formation, our data on CD9 and CD151 suggest the involvement of tetraspanins in motility-related structures for the exploration of the environment.

Tetraspanins have been implicated in the motility of many cell types (Berditchevski, 2001), including melanoma cells (Longo *et al*, 2001). The mechanism is still in the process of being elucidated but, as we have previously described in keratinocytes, CD9 and CD151 are present at motility-related structures and not in adhesive contacts to extracellular matrix (Peñas *et al*, 2000). We have found that the anti-CD9 mAb VJ1/10 enhances the motility of melanocytes in migration assays and that it is further enhanced with the anti- $\beta 1$  integrin VJ1/14. Moreover, CD9 siRNA treatment enhances the migration of these cells, supporting our findings that CD9 expression is involved in the negative regulation of melanocyte migration. In human melanoma cells expressing high levels of CD9, anti-CD9 VJ1/10 slightly inhibited cell migration, although anti-CD9 VJ1/10 and VJ1/20

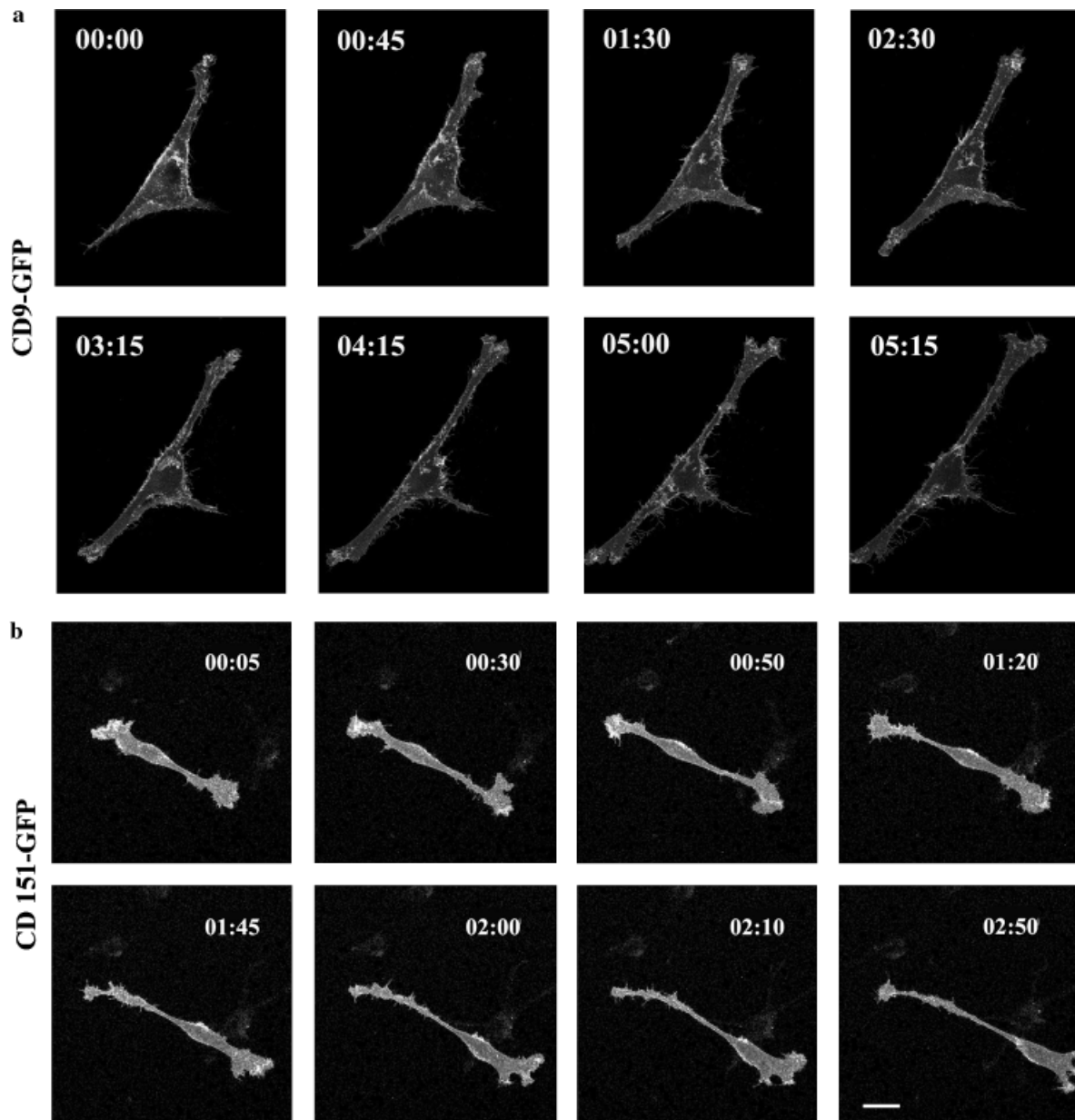


**Figure 4**  
**CD9-GFP (green fluorescent protein) and CD151-GFP are expressed on the tips of dendrites of melanocytes during cell migration.** Melanocytes transfected with CD9-GFP or CD151-GFP constructs were seeded on coverslips and time-lapse fluorescence confocal microscopy was started after 4 h. Series of optical sections distanced  $0.4 \mu\text{m}$  on the z-axis were acquired every 15 min (CD9) or 5 min (CD151) for a total time of 7 h. (a) The micrographs show the dynamic accumulation of CD9-GFP at the tips of the dendrite (T: 00:00, T: 01:30, T: 02:30, T: 04:15) during the exploration of the extracellular environment. A maximum projection of the relevant sections from the confocal stack of the green signal (GFP) from each corresponding time point of the videosequence is shown. Scale bar =  $20 \mu\text{m}$ . (b) The micrographs show the dynamic accumulation of CD151-GFP at the tip of the dendrite as the melanocyte migrates on the coverslip. CD151 clusters can be found both on the front (00:30, 01:20, 1:45, 2:10) and rear (T: 00:05; 00:30, 00:50) dendrites. A maximum projection of the relevant sections from the confocal stack of the green signal (GFP) from each corresponding time point of the videosequence is shown. Scale bar =  $20 \mu\text{m}$ .

presented a strong inhibitory effect of transendothelial migration (Longo *et al*, 2001). Nevertheless, in human and mouse melanoma cells, low CD9 expression has been related to enhanced motility, and transfection of mouse melanoma cells with CD9 lowered their metastatic potential and motility (Ikeyama *et al*, 1993). It is remarkable that mAb anti-CD9 inhibited the migration of human keratinocytes (Peñas *et al*, 2000), endothelial cells (Yáñez-Mó *et al*, 1998), and hepatic stellate cells (Mazzocca *et al*, 2002), whereas it

enhanced the migration of Schwann cells (Anton *et al*, 1995) and melanocytes, both of neuroectodermal origin.

On the other hand, the use of anti-CD151 mAb also enhances the migration of melanocytes. In contrast, anti-CD151 mAb inhibited human keratinocyte (Peñas *et al*, 2000), endothelial (Yáñez-Mó *et al*, 1998), neutrophil (Yauch *et al*, 1998), and hepatic stellate cell (Mazzocca *et al*, 2002) migration. Our finding that CD151 siRNA treatment also increased the migration of melanocytes supports that the role

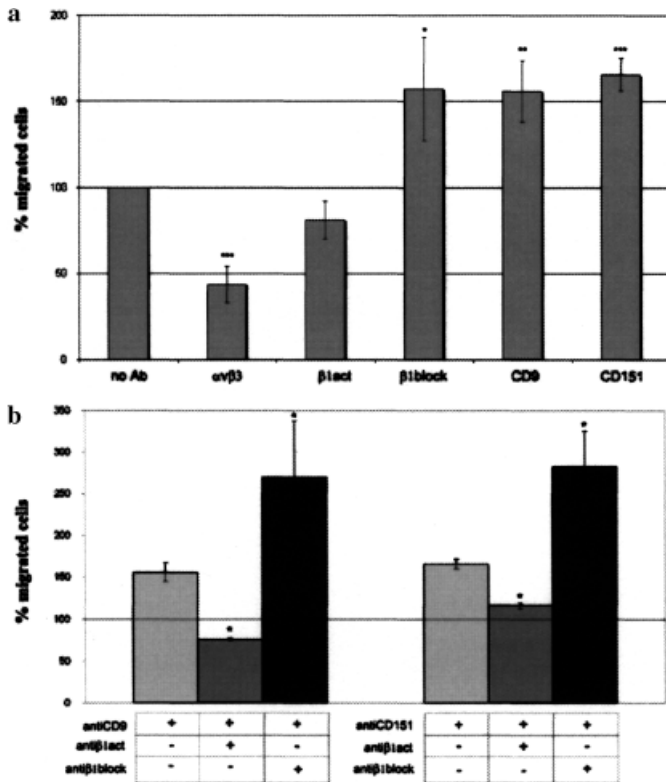


**Figure 5**  
**Anti-CD9 and -CD151 monoclonal antibodies (mAb) influence melanocyte motility.** Melanocyte migration assays were performed in 8- $\mu$ m pore Transwell chambers. Fibronectin was added in the lower chamber as a chemoattractant. The cells that crossed the membrane were counted. (a) Blocking mAb anti-CD9, anti-CD151, and anti- $\beta 1$  stimulated the migration of cells, whereas anti- $\alpha v \beta 3$  and activating anti- $\beta 1$  inhibited the migration. Results were normalized using as control mAb-untreated cells as 100%. Results are depicted as the mean  $\pm$  SEM of seven experiments performed in duplicate. \* $p < 0.05$ , \*\* $p < 0.005$ , and \*\*\* $p > 0.0005$  with respect to no mAb treatment. (b) The same experiment was performed combining the anti-CD9 or anti-CD151 mAb with the activating anti- $\beta 1$  or the blocking anti- $\beta 1$  mAb. Results were normalized using the control with no mAb treatment as 100% (black line). Results are depicted as the mean  $\pm$  SEM of two experiments performed in duplicate. \* $p < 0.05$  with respect to no mAb treatment.

of CD151 in melanocyte motility is different from what has been previously described for other cell types.

We have found that tetraspanins modulate migration of melanocytes. Melanocytes express  $\alpha 2 \beta 1$ ,  $\alpha 3 \beta 1$ ,  $\alpha 5 \beta 1$ , and  $\alpha v \beta 3$  (Zambruno *et al*, 1993; Hara *et al*, 1994). Tetraspanins have been shown to interact with  $\alpha 2 \beta 1$  and  $\alpha 3 \beta 1$  integrins in many cell types, but not with  $\alpha v \beta 3$  (Berditchevski, 2001). The effect of CD9 and CD151 is partially reverted with TS2/16 (activating anti- $\beta 1$  integrin mAb), and it is additive to the effect of VJ1/14 (inhibitory anti- $\beta 1$  integrin mAb).

In conclusion, CD9 and CD151 are dynamically clustered at the tips of dendrites and also in homotypic intercellular contacts of melanocytes. The inhibition of CD9 and CD151 using mAb or siRNA leads to enhanced motility of the cells. Nevertheless, CD9 and CD151 do not seem to be involved in melanocyte adhesion to the extracellular matrix. In keratinocytes, tetraspanins are also involved in motility and are expressed in intercellular contacts (Peñas *et al*, 2000). It is therefore tempting to suggest that the expression of tetra-

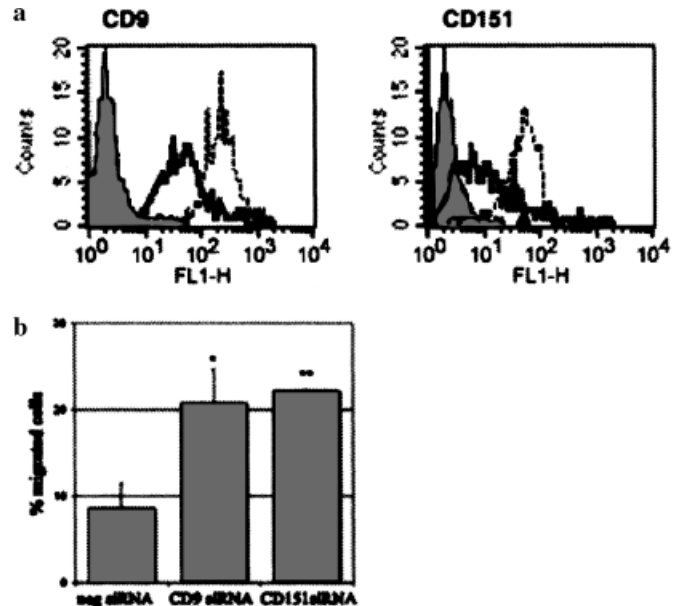


**Figure 6**  
**Knocking down of CD9 and CD151 expression using small interference RNA (siRNA) enhances melanocyte motility.** (a) Melanocytes were transfected with CD9 or CD151 siRNA and negatively selected with anti-CD9 or anti-CD151 magnetic-coated beads, in order to enrich the tetraspanin low-expressing population. We obtained highly interfered melanocyte cells for each tetraspanin. One representative experiment is shown. The mean inhibition was 49% for CD9 and 56% for CD151. Dotted line: negative oligo siRNA-transfected melanocytes, solid line: tetraspanin siRNA-transfected melanocytes, gray area: X-63 used as a negative control of expression. (b) The migratory capacity of these transfected melanocytes was evaluated using 8- $\mu$ m pore Transwell chambers. Fibronectin was added in the lower chamber as a chemoattractant. Negative oligo siRNA-transfected cells were used as control. Results are shown as the mean  $\pm$  SEM of three experiments performed in triplicate. \* $p < 0.05$  and \*\* $p < 0.005$  with respect to negative oligo siRNA treatment.

spanins in cell contacts could be negatively regulating melanocyte migration and, therefore, aiding in the process of homogeneous redistribution of melanocytes in the normal epidermis or in the migration of melanocytes to restore the epidermis damaged during wound healing.

## Materials and Methods

**Cells** Neonatal foreskins obtained within 24 h of elective circumcision were used to culture human melanocytes as described previously (Gilchrist *et al*, 1984; Park *et al*, 1993). In brief, epidermal strips were isolated using dispase 1.2 U per mL (Boehringer Mannheim, Mannheim, Germany) for 12 h at 4°C. After incubation of epidermal strips in 0.05% trypsin/0.02% EDTA (Cambrex, Vervies, Belgium) for 25 min at room temperature, epidermal cells were seeded onto plastic dishes (Corning Incorporated, Corning, New York) at 40,000 cells per  $\text{cm}^2$ . The culture basal medium consisted in 4:1 Dulbecco's modified Eagle's medium (DMEM) with glutamine and pyruvate (Gibco, Paisley, Scotland, UK) and HAM'S F12 (Gibco) complemented with fetal bovine serum 10%, adenine 18 mM (SIGMA, St Louis, Missouri), hydrocortisone 0.5  $\mu$ g per mL (SIGMA), apo-transferrin 5  $\mu$ g per mL (SIGMA, Steinheim, Germany), insulin 5  $\mu$ g per mL (SIGMA), and choleric toxin 10 ng per mL (SIGMA). In the first passage, a selective trypsinization was performed and the melanocytes were cultured in a melanocyte-specific medium: MCDB153 (SIGMA) 5% fetal bovine serum, bovine

pituitary extract (SIGMA) 30  $\mu\text{g}$  per mL,  $\beta$ -fibroblast growth factor (SIGMA) 0.6 ng per mL, insulin 5  $\mu\text{g}$  per mL, hydrocortisone 0.5  $\mu\text{g}$  per mL, and PHA 8 nM (SIGMA). Cultures were used between the second and fourth passages. Approval was obtained from the Hospital Universitario de la Princesa institutional review board for these studies. Informed consent was provided according to the Declaration of Helsinki.

**Antibodies** MAb used in this study have been described previously: the activatory anti- $\beta$ 1 integrin chain TS2/16 (CD29) (Arroyo *et al*, 1992), the inhibitory anti- $\beta$ 1 integrin VJ1/14 (CD29) (Peñas *et al*, 1998), and the anti-CD151 (LIA1/1 and VJ1/16) (Yáñez-Mó *et al*, 1998). Anti-CD63 (TEA3/18), anti-CD9 (VJ1/20 and VJ1/10), anti- $\alpha$ 2 (TEA1/41), and anti- $\alpha$ 3 (VJ1/6) were obtained in our laboratory (Peñas *et al*, 2000). JS-81 (anti-CD81) was purchased from BD Biosciences (San Diego, California). The anti- $\alpha$ v $\beta$ 3 was a kind gift from Dr S. Vilaró (Department of Cell Biology, Universidad de Barcelona, Spain). The monoclonal Ig (IgG1,  $\kappa$ ) from the P3X63 myeloma cell line was used as a negative control, and anti-CD45 antibodies (IgG1, IgG2a, and IgG2b) were used as isotype controls (Pulido *et al*, 1988).

**Flow cytometry** Melanocytes were detached with 0.05% trypsin and 0.02% EDTA, washed, and resuspended in phosphate-buffered saline (PBS). A total of  $5 \times 10^5$  cells were incubated with the corresponding mAb for 30 min at 4°C. After this incubation, cells were washed in PBS and incubated for 20 min at 4°C with the appropriate fluorescein-isothiocyanate (FITC)-conjugated antibody (anti-mouse Ig from DAKOPATTS, Copenhagen, Denmark or anti-rabbit Ig from Pierce Chemical, Rockford, Illinois). Cells were washed and resuspended in PBS with 10  $\mu\text{g}$  per mL propidium iodide and then analyzed in a FACScan flow cytometer (Becton Dickinson Labware, Lincoln Park, New Jersey). Cell analysis was gated both on forward- and size-scatter intensity and propidium iodide fluorescence to discard dead cells.

**Immunofluorescence and laser scanning confocal microscopy** Normal human melanocytes were plated in complete medium on glass coverslips, grown, and fixed in 3.7% paraformaldehyde in PBS. Nonspecific binding sites were blocked by incubation with TNB (0.1 M Tris-HCl, 0.15 M NaCl, 0.5% blocking reagent; Boehringer Mannheim GmbH). Coverslips were incubated with the primary antibody for 1 h at 37°C, washed and incubated with Rhodamine-X goat anti-mouse IgG secondary antibody (Molecular Probes, Leiden, The Netherlands) for 45 min. Coverslips were then blocked with mouse serum, incubated with the corresponding biotinylated antibody for 1 h at 37°C, washed, and incubated with Alexa Fluor488-labelled streptavidin (Molecular Probes, Leiden, The Netherlands) for 45 min. Specimens were examined with a Leica TCS-SP confocal laser scanning unit equipped with Ar and He/Ne laser beams and coupled to a Leica DMIRBE inverted epifluorescence microscope (Leica Microsystems, Heidelberg, Germany), using a  $\times 63/1.4$  NA oil-immersion objective. A series of optical sections distanced 0.4  $\mu\text{m}$  on the z-axis were obtained.

**Migration assay** Melanocyte migration assays were performed in 8- $\mu\text{m}$  pore Transwell chambers (Corning Incorporated, Corning, NY). Fibronectin has been described as a stimulus of melanocyte motility (Zambruno *et al*, 1993); therefore, fibronectin 10  $\mu\text{g}$  per mL was added to the lower chamber and incubated for 1 h at 37°C. Melanocytes, resuspended in serum-free medium MCDB153, were then seeded at 15,000 cells/well on the upper chamber. After 30 min, purified monoclonal antibodies were added to the upper chamber where appropriate. After 18 h, migrated cells onto the lower surface of the filter were stained with toluidine blue and counted. Experiments were carried out in duplicate, and four fields of each transwell were counted with a  $\times 40$  objective in an Eclipse E400 microscope (Nikon, Tokyo, Japan).

Regarding the migration assay using siRNA-transfected cells, cells were recovered from the lower surface of the filter by trypsinization after the incubation period for migration, and the number of migrated cells was estimated by flow cytometry.

**Recombinant DNA constructs, transient transfection, and time-lapse fluorescence confocal microscopy** The CD9-GFP fusion protein construct was obtained by polymerase chain reaction amplification of the CD9 cDNA (a kind gift from Dr E. Rubinstein, INSERM, Villejuif Cedex, France) and cloned in pEGFP-N1 Vector (Clontech Laboratories, Palo Alto, California) in *EcoRI* sites of the cloning site, as described elsewhere (Longo *et al*, 2001). The CD151-GFP fusion protein construct was also obtained by polymerase chain reaction amplification of the CD151 cDNA (a kind gift from Dr S. Fujita, Ehime University, School of Medicine, Shigenobu, Japan) and cloned in pEGFP-N1 Vector (Clontech Laboratories) in *HindIII-KpnI* sites of the cloning site (Barreiro *et al*, 2005).

Primary melanocytes were trypsinized and resuspended in MCDB 153 medium supplemented with 5% FCS, 37.5 mM NaCl, and 20  $\mu\text{g}$  of the vector coding for CD9- or CD151-GFP-tagged proteins. Cells were transfected by electroporation at 975  $\mu\text{F}$  and 200 V in a Gene Pulser II (Bio-Rad, Hercules, California) and were allowed to grow up to 24–48 h after transfection. Then, cells were trypsinized and seeded onto an uncoated 25 mm glass coverslip. Finally, time-lapse videomicroscopy experiments were performed after 4 h of cell adhesion. Samples were maintained at 37°C in a 5% CO<sub>2</sub> atmosphere using an incubation system (La-con GBr Pecon GmbH, Erbach, Germany) coupled to the Leica TCS-SP confocal laser scanning unit. A series of optical sections distanced 0.4  $\mu\text{m}$  on the z-axis were acquired every 5–15 min during a total experimental time of 7 h. Green fluorescence and DIC images were simultaneously obtained using a  $\times 63/1.4$  NA oil-immersion objective. Images were processed and assembled into movies using the Leica Confocal Software.

**siRNA assay** To knock down the expression of CD9 and CD151 selectively, the silencing sequences described previously (Barreiro *et al*, 2005) were used. RNA duplexes corresponding to CD9 and CD151 target sequences, as well as a negative oligonucleotide that does not pair with any human mRNA were produced by Eurogentec (Seraing, Belgium). Oligonucleotides were transfected in primary melanocytes with oligofectamine (Invitrogen, Carlsbad, California) following the manufacturer's instructions. For CD9 interference, melanocytes were transfected on day 0, split on day 2, and retransfected on day 3. For CD151, cells were transfected only once on day 3. Then, cells were trypsinized on day 6 and negatively selected with anti-CD9 or anti-CD151 magnetic-coated beads (DynaBeads M450 Goat anti-Mouse IgG, DYNAL Biotech ASA, Oslo, Norway), in order to enrich the tetraspanin low-expressing population. Cells thus selected were counted and seeded for the different experiments.

**Statistical analysis** Data were compared using the Student's *t* test or one-way analysis of variance.

---

This work was supported by grants from Fondo de Investigación Sanitaria (FIS) 01/1304 and 04/2330 to AGD, a Research Grant from I. F. Cantabria and Centro de Desarrollo Tecnológico e Industrial (CDTI) (01/07047/E) to F. S. M. and A. G. D., Ayuda a la Investigación Básica 2002 from the Juan March Foundation and BMC 2002-00563 to F. S. M., and a fellowship from Red Cardiovascular from FIS and EU grant LSHG-CT-2003-502935 to O. B. We are grateful to María Yáñez-Mó for her critical revision of the manuscript.

### Supplementary Material

The following material is available online for this article.

**Figure S1. Video S1 (from Fig 3a).** Primary human melanocytes transiently transfected with CD9-GFP were seeded on a coverslip for 4 h.

**Figure S2. Video S1 (from Fig 3b).** Primary human melanocytes transiently transfected with CD151-GFP were seeded on a coverslip for 4 h.

**Figure S3. Video S1 (from Fig 4a).** Primary human melanocytes transiently transfected with CD9-GFP were seeded on a coverslip for 4 h.

**Figure S4. Video S1 (from Fig 4b).** Primary human melanocytes transiently transfected with CD151-GFP were seeded on a coverslip for 4 h.

DOI: 10.1111/j.0022-202X.2005.23882.x

Manuscript received January 26, 2005; revised May 30, 2005; accepted for publication June 1, 2005

Address correspondence to: Pablo F. Peñas, Department of Dermatology, Hospital Universitario de la Princesa, Diego de León 62, 28006 Madrid, Spain. Email: pablofp@aedv.es

### References

- Anton ES, Hadjiargyrou M, Patterson PH, Matthew WD: CD9 plays a role in Schwann cell migration *in vitro*. *J Neurosci* 15:584–595, 1995
- Arroyo AG, Sánchez-Mateos P, Campanero MR, Martín-Padura I, Dejana E, Sánchez-Madrid F: Regulation of the VLA integrin-ligand interactions through  $\beta 1$  subunit. *J Cell Biol* 117:659–670, 1992
- Banerjee SA, Hadjiargyrou M, Patterson PH: An antibody to the tetraspanin membrane protein CD9 promotes neurite formation in a partially  $\alpha 3\beta 1$  integrin-dependent manner. *J Neurosci* 17:2756–2765, 1997
- Barreiro O, Yanez-Mo M, Sala-Valdes M, et al: Endothelial tetraspanin microdomains regulate leukocyte firm adhesion during extravasation. *Blood* 105:2852–2861, 2005
- Berditchevski F: Complexes of tetraspanins with integrins: More than meets the eye. *J Cell Sci* 114:4143–4151, 2001
- Berditchevski F, Zutter MM, Hemler ME: Characterization of novel complexes on the cell surface between integrins and proteins with 4 transmembrane domains (TM4 proteins). *Mol Biol Cell* 7:193–207, 1996
- Boucheix C, Rubinstein E: Tetraspanins. *Cell Mol Life Sci* 58:1189–1205, 2001
- Chattopadhyay N, Wang Z, Ashman LK, Brady-Kalnay SM, Kreidberg JA:  $\alpha 3\beta 1$  integrin-CD151, a component of the cadherin-catenin complex, regulates PTPmu expression and cell-cell adhesion. *J Cell Biol* 163:1351–1362, 2003
- Clark EA, Brugge JS: Integrins and signal transduction pathways: The road taken. *Science* 268:233–239, 1995
- Fitter S, Sincoc PM, Jolliffe CN, Ashman LK: Transmembrane 4 superfamily protein CD151 (PETA-3) associates with  $\beta 1$  and  $\alpha 11\beta 3$  integrins in haemopoietic cell lines and modulates cell-cell adhesion. *Biochem J* 338 (Pt 1):61–70, 1999
- Fitzpatrick T, Breathnach A: Das epidermale Melanin-Einheit system. *Dermatol Wochenschr* 147:481–489, 1963
- Gilchrist BA, Vrabel MA, Flynn E, Szabo G: Selective cultivation of human melanocytes from newborn and adult epidermis. *J Invest Dermatol* 83:370–376, 1984
- Hara M, Yaar M, Tang A, Eller MS, Reenstra W, Gilchrist BA: Role of integrins in melanocyte attachment and dendricity. *J Cell Sci* 107:2739–2748, 1994
- Hemler ME: Specific tetraspanin functions. *J Cell Biol* 155:1103–1107, 2001
- Hemler ME, Mannion BA, Berditchevski F: Association of TM4SF proteins with integrins: Relevance to cancer. *Biochim Biophys Acta* 1287:67–71, 1996
- Hoath SB, Leahy DG: The organization of human epidermis: Functional epidermal units and phi proportionality. *J Invest Dermatol* 121:1440–1446, 2003
- Hsu MY, Meier FE, Nesbit M, Hsu JY, Van Belle P, Elder DE, Herlyn M: E-cadherin expression in melanoma cells restores keratinocyte-mediated growth control and down-regulates expression of invasion-related adhesion receptors. *Am J Pathol* 156:1515–1525, 2000
- Ikeyama S, Koyama M, Yamaoko M, Sasada R, Miyake M: Suppression of cell motility and metastasis by transfection with human motility-related protein (MRP-1/CD9) DNA. *J Exp Med* 177:1231–1237, 1993
- Jones PH, Bishop LA, Watt FM: Functional significance of CD9 association with  $\beta 1$  integrins in human epidermal keratinocytes. *Cell Adhes Commun* 4:297–305, 1996
- Karamatic Crew V, Burton N, Kagan A, et al: CD151, the first member of the tetraspanin (TM4) superfamily detected on erythrocytes, is essential for the correct assembly of human basement membranes in kidney and skin. *Blood* 104:2217–2223, 2004
- Longo N, Yanez-Mo M, Mittelbrunn M, de la Rosa G, Munoz ML, Sanchez-Madrid F, Sanchez-Mateos P: Regulatory role of tetraspanin CD9 in tumor-endothelial cell interaction during transendothelial invasion of melanoma cells. *Blood* 98:3717–3726, 2001
- Maecker HT, Todd SC, Levy S: The tetraspanin superfamily: Molecular facilitators. *FASEB J* 11:428–442, 1997
- Mazzocca A, Carloni V, Sciammetta S, et al: Expression of transmembrane 4 superfamily (TM4SF) proteins and their role in hepatic stellate cell motility and wound healing migration. *J Hepatol* 37:322–330, 2002
- Morelli JG, Yohn JJ, Zekman T, Norris DA: Melanocyte movement *in vitro*: Role of matrix proteins and integrin receptors. *J Invest Dermatol* 101:605–608, 1993
- Okochi H, Kato M, Nashiro K, Yoshie O, Miyazono K, Furue M: Expression of tetra-spans transmembrane family (CD9, CD37, CD53, CD63, CD81 and CD82) in normal and neoplastic human keratinocytes: An association of CD9 with  $\alpha 3\beta 1$  integrin. *Br J Dermatol* 137:856–863, 1997
- Ota A, Park JS, Jimbow K: Functional regulation of tyrosinase and LAMP gene family of melanogenesis and cell death in immortal murine melanocytes after repeated exposure to ultraviolet B. *Br J Dermatol* 139:207–215, 1998
- Palecek SP, Schmidt CE, Lauffenburger DA, Horwitz AF: Integrin dynamics on the tail region of migrating fibroblasts. *J Cell Sci* 109:941–952, 1996
- Park HY, Russakovsky V, Ohno S, Gilchrist BA: The  $\beta$  isoform of protein kinase C stimulates human melanogenesis by activating tyrosinase in pigment cells. *J Biol Chem* 268:11742–11749, 1993
- Peñas PF, García-Diez A, Sánchez-Madrid F, Yañez-Mó M: Tetraspanins are localized at motility-related structures and involved in normal human keratinocyte wound healing migration. *J Invest Dermatol* 114:1126–1135, 2000
- Peñas PF, Gomez M, Buezo GF, et al: Differential expression of activation epitopes of  $\beta 1$  integrins in psoriasis and normal skin. *J Invest Dermatol* 111:19–24, 1998
- Pulido R, Cebrián M, Acevedo A, de Landázuri MO, Sánchez-Madrid F: Comparative biochemical and tissue distribution study of four distinct CD45 antigen specificities. *J Immunol* 140:3851–3857, 1988
- Radford KJ, Thorne RF, Hersey P: CD63 associates with transmembrane 4 superfamily members, CD9 and CD81, and with  $\beta 1$  integrins in human melanoma. *Biochem Biophys Res Commun* 222:13–18, 1996
- Rubinstein E, Le Naour F, Lagaudriere-Gesbert C, Billard M, Conjeaud H, Boucheix C: CD9, CD63, CD81, and CD82 are components of a surface tetraspanin network connected to HLA-DR and VLA integrins. *Eur J Immunol* 26:2657–2665, 1996
- Shaw AR, Domanska A, Mak A, et al: Ectopic expression of human and feline CD9 in a human B cell line confers  $\beta 1$  integrin-dependent motility on fibronectin and laminin substrates and enhanced tyrosine phosphorylation. *J Biol Chem* 270:24092–24099, 1995
- Sincoc PM, Mayrhofer G, Ashman LK: Localization of the transmembrane 4 superfamily (TM4SF) member PETA-3 (CD151) in normal human tissues: Comparison with CD9, CD63, and  $\alpha 5\beta 1$  integrin. *J Histochem Cytochem* 45:515–525, 1997
- Smith BE, Bradshaw AD, Choi ES, Rouselle P, Wayner EA, Clegg DO: Human SY5Y neuroblastoma cell interactions with laminin isoforms: Neurite outgrowth on laminin-5 is mediated by integrin  $\alpha 3\beta 1$ . *Cell Adhes Commun* 3:451–462, 1996
- Stipp CS, Hemler ME: Transmembrane-4-superfamily proteins CD151 and CD81 associate with  $\alpha 3\beta 1$  integrin, and selectively contribute to  $\alpha 3\beta 1$ -dependent neurite outgrowth. *J Cell Sci* 113:1871–1882, 2000
- Stipp CS, Kolesnikova TV, Hemler ME: Functional domains in tetraspanin proteins. *Trends Biochem Sci* 28:106–112, 2003
- Sugiura T, Berditchevski F: Function of  $\alpha 3\beta 1$ -tetraspanin protein complexes in tumor cell invasion. Evidence for the role of the complexes in production of matrix metalloproteinase 2 (MMP-2). *J Cell Biol* 146:1375–1389, 1999
- Tarrant JM, Robb L, van Spriel AB, Wright MD: Tetraspanins: Molecular organisers of the leukocyte surface. *Trends Immunol* 24:610–617, 2003

- Watt FM, Hertle MD: Keratinocyte integrins. In: Leight IM, Lane EB, Watt FM (eds). *The Keratinocyte Handbook*. Cambridge: Cambridge University Press, 1994; p 153–164
- Wright MD, Tomlinson MG: The ins and outs of the transmembrane 4 superfamily. *Immunol Today* 15:588–594, 1994
- Yáñez-Mó M, Alfranca A, Cabañas C, *et al*: Regulation of endothelial cell motility by complexes of tetraspan molecules CD81/TAPA-1 and CD151/PETA-3 with alpha3 beta1 integrin localized at endothelial lateral junctions. *J Cell Biol* 141:791–804, 1998
- Yáñez-Mó M, Mittelbrunn M, Sanchez-Madrid F: Tetraspanins and intercellular interactions. *Microcirculation* 8:153–168, 2001
- Yauch RL, Berditchevski F, Harler MB, Reichner J, Hemler ME: Highly stoichiometric, stable, and specific association of integrin alpha3beta1 with CD151 provides a major link to phosphatidylinositol 4- kinase, and may regulate cell migration. *Mol Biol Cell* 9:2751–2765, 1998
- Zambruno G, Marchisio PC, Melchiori A, Bondanza S, Cancedda R, De Luca M: Expression of integrin receptors and their role in adhesion, spreading and migration of normal human melanocytes. *J Cell Sci* 105:179–190, 1993

Olga Barreiro  
Hortensia de la Fuente  
María Mittelbrunn  
Francisco Sánchez-Madrid

# Functional insights on the polarized redistribution of leukocyte integrins and their ligands during leukocyte migration and immune interactions

## Authors' address

Olga Barreiro, Hortensia de la Fuente, María Mittelbrunn,  
Francisco Sánchez-Madrid  
Servicio de Inmunología, Hospital de la Princesa,  
Universidad Autónoma de Madrid, Madrid,  
Spain.  
Departamento de Biología Vasular e Inflamación,  
Centro Nacional de Investigaciones Cardiovasculares,  
Madrid, Spain

## Correspondence to:

Francisco Sánchez-Madrid  
Servicio de Inmunología  
Hospital de la Princesa  
Universidad Autónoma de Madrid  
C/ Diego de León 62  
28006 Madrid, Spain  
Tel.: +34 91 5202370  
Fax: +34 91 5202374  
E-mail: fsanchez.hlpr@salud.madrid.org

## Acknowledgements

We would like to thank Dr R. Gonzalez-Amaro, Dr J. L. Rodriguez-Fernandez, Dr C. Cabanas, Dr M. Vicente-Manzanares and Dr M. Yanez-Mo for critical reading of the manuscript and useful comments. This work has been supported by BFU 2005-08435/BMC, 'Ayuda a la Investigación Básica 2002 de la Fundación Juan March' (to F. S.-M.), Lilly Foundation, and EU grant LSHG-CT-2003-502935 to O. B.

*Immunological Reviews* 2007  
Vol. 218: 147–164  
Printed in Singapore. All rights reserved

© 2007 The Authors  
Journal compilation © 2007 Blackwell Munksgaard  
*Immunological Reviews*  
0105-2896

**Summary:** Cell–cell and cell–matrix interactions are of critical importance in immunobiology. Leukocytes make extensive use of a specialized repertoire of receptors to mediate such processes. Among these receptors, integrins are known to be of crucial importance. This review deals with the central role of integrins and their counterreceptors during the establishment of leukocyte–endothelium contacts, interstitial migration, and final encounter with antigen-presenting cells to develop an appropriate immune response. Particularly, we have addressed the molecular events occurring during these sequential processes, leading to the dynamic subcellular redistribution of adhesion receptors and the reorganization of the actin cytoskeleton, which is reflected in changes in cytoarchitecture, including leukocyte polarization, endothelial docking structure formation, or immune synapse organization. The roles of signaling and structural actin cytoskeleton-associated proteins and organized membrane microdomains in the regulation of receptor adhesiveness are also discussed.

**Keywords:** leukocyte integrins, extravasation, migration, immune synapse, polarization, subcellular localization

## Introduction

Trafficking of leukocytes throughout different tissues and organs and their subsequent interactions with other immune cells are crucial for the development of innate and adaptive immunity (1). Integrins have a central role in cell migration by controlling intercellular and cell–matrix interactions during homing and inflammation. One of the most important features of these receptors relies on the regulation of their adhesion activity independently of their membrane expression. Thus, leukocytes modify their adhesive properties to be properly adapted to every immune scenario (2). Hence, free-flowing leukocytes maintain their integrins in non-adhesive conformation, to avoid unspecific contacts with non-inflamed vascular walls, but upon encountering localized inflammatory foci, a rapid in situ activation of leukocyte integrins by endothelium-displayed activating signals takes place (3). Although integrin-mediated

adhesion contributes to the initial adhesive contacts between a T lymphocyte and an activated antigen-presenting cell (APC), T-cell receptor (TCR) signaling can enhance integrin avidity upon recognition of an agonist peptide–major histocompatibility complex (MHC), which further stabilizes the cell conjugate, allowing the assembly of the immune synapse (IS) (4).

The spatial distribution of integrins and their ligands in specialized membrane structures is also of key importance for the proper accomplishment of their adhesive functions. This topographic organization requires a finely regulated cellular cytoskeleton that also enables the recruitment of signaling intermediates and second messengers that lead to cellular activation (5). This review focuses on the central role of leukocyte integrins and their counterreceptors during inflammation and immunity, paying special attention to the spatiotemporal regulation of their adhesive function.

### Molecular features of leukocyte integrins and their ligands

Integrins constitute a large family of 24 heterodimeric adhesion receptors, each one composed of  $\alpha$  and  $\beta$  subunits. These molecules regulate dynamically their adhesiveness by conformational changes as well as by redistribution on the cell surface (6). Recent data predict the existence of three conformational states for integrins, which differ in their localization on the plasma membrane and in conformation (folded/low affinity, extended with intermediate affinity, and extended with high affinity) (7, 8). The overall strength of adhesiveness (avidity) depends on the affinity of each individual receptor–ligand bond and the number of these interactions. Therefore, the regulation of integrin avidity involves both the modulation of receptor and ligand density and their redistribution on specialized membrane structures (9).

The most relevant integrins for leukocyte adhesion to endothelium are members of the  $\beta 2$  subfamily, particularly leukocyte function-associated antigen-1 (LFA-1) (CD11a/CD18 or  $\alpha L\beta 2$ ) and the myeloid-specific integrin Mac-1 (CD11b/CD18 or  $\alpha M\beta 2$ ), as well as the  $\alpha 4$  integrins very late antigen-4 (VLA-4) ( $\alpha 4\beta 1$ ) and  $\alpha 4\beta 7$ . In addition, LFA-1 plays a central role in the establishment of the IS. Other integrins, such as  $\alpha 5\beta 1$ ,  $\alpha 6\beta 1$ ,  $\alpha 2\beta 1$ , and  $\alpha v\beta 3$ , have a prominent function during interstitial cell migration (10).

Most of the cellular counterreceptors for leukocyte integrins are transmembrane proteins that belong to the immunoglobulin superfamily. LFA-1 binds five distinct intercellular cell adhesion molecules (ICAM-1 to -5), although the most relevant ones seem to be ICAM-1 and ICAM-3 (11). ICAM-1 is found in leukocytes, dendritic cells (DCs), and epithelial cells and is expressed at low levels in resting endothelial cells, becoming

highly upregulated upon inflammatory stimuli (12). ICAM-3 is constitutively expressed by all leukocytes (13), whereas the junctional adhesion molecule-A (JAM-A), an additional ligand for LFA-1, is selectively concentrated at the apical region of intercellular tight junctions in endothelial cells (14). Mac-1 interacts with ICAM-1, JAM-C, and the endothelial receptor RAGE (receptor for advanced glycation end products) (15, 16).

The integrin VLA-4 interacts with vascular cellular adhesion molecule-1 (VCAM-1) (17), which is expressed *de novo* upon endothelial cell activation (18) and also binds JAM-B (19). Alternatively, VLA-4 interacts with ADAM-28 (a disintegrin and metalloproteinase domain-28), fibronectin, osteopontin, thrombospondin, von Willebrand factor, and the bacterial protein invasins (20). Finally, the  $\alpha 4\beta 7$  integrin, apart from its interaction with fibronectin and VCAM-1, specifically recognizes mucosal addressin cell adhesion molecule-1 (MAdCAM-1), a receptor expressed in mucosal lymphoid tissues (21).

### The extravasation process

Leukocyte migration across the vascular barrier into lymphoid or inflamed tissues is a multistep process that requires an orchestrated plethora of adhesion and signaling molecules (22, 23). Blood-borne leukocytes tether and roll over endothelial cells that express different adhesion receptors. During these initial contacts, the slowed-down leukocytes encounter local activation signals for integrins, which trigger their firm adhesion under shear flow, locomotion toward specific transmigration sites, and final diapedesis (24) (Fig. 1).

#### Role of integrins during tethering and rolling

In addition to selectins and their ligands,  $\alpha 4$  integrins, through their interaction with VCAM-1 and MAdCAM-1, support leukocyte tethering, rolling, and arrest (25). Moreover, the interaction of LFA-1–ICAM-1 cooperates with L-selectin in the tethering and rolling steps (26). Other molecules may also participate in the initial steps of extravasation, mainly CD44, which has been recently described as a physiological E-selectin ligand (27). An additional level of molecular complexity during leukocyte migration is introduced by the formation of a cooperative bimolecular complex between CD44 and VLA-4 in activated T cells that reduces CD44-dependent rolling velocity and stabilizes VLA-4-mediated firm adhesion (28).

Adhesion receptor distribution at the plasma membrane has a key role in leukocyte adhesiveness and is another regulatory checkpoint for leukocyte trafficking (29, 30). In leukocytes, selectins, P-selectin glycoprotein ligand-1 (PSGL-1),  $\beta 7$ , and  $\beta 1$  integrins are usually concentrated at surface projections (e.g.

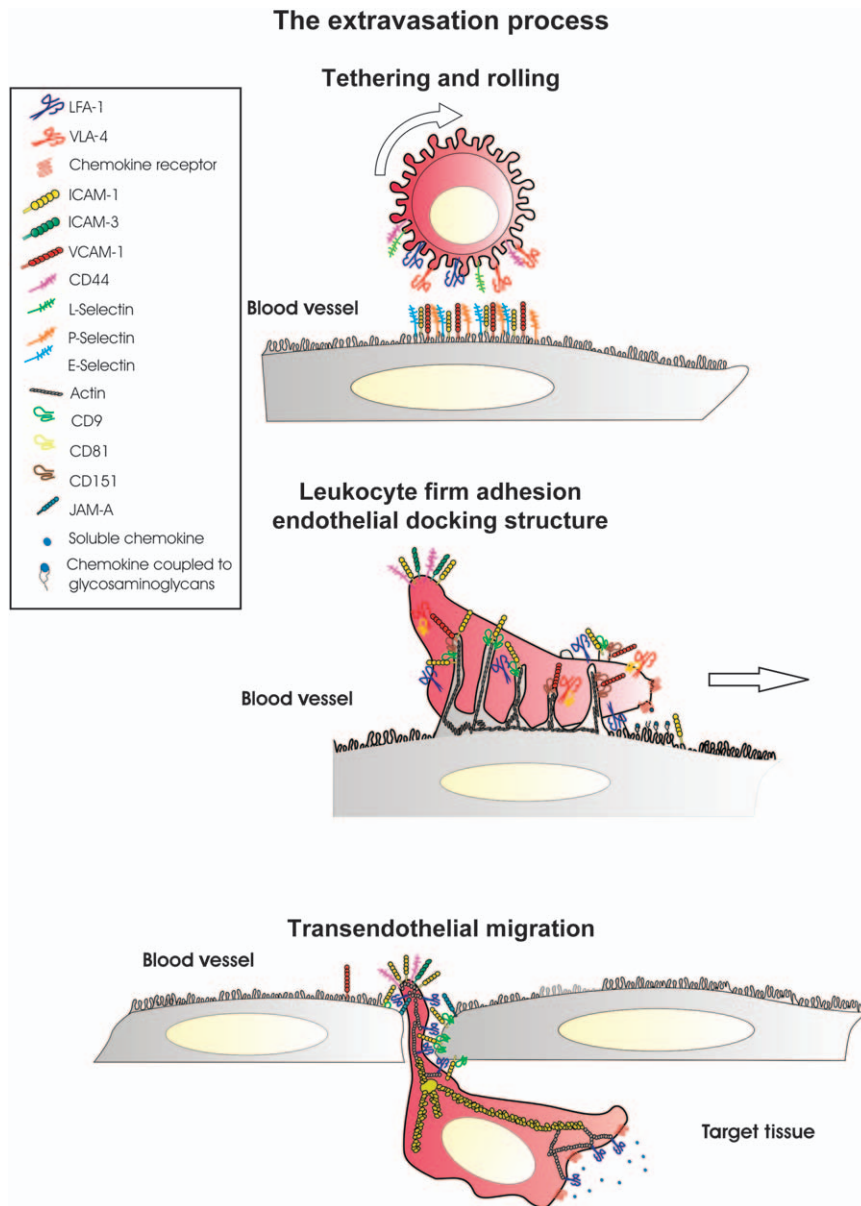


**Fig. 1. Localization of leukocyte integrins and their ligands during the extravasation process.** Upper panel: tethering and rolling of leukocytes onto endothelium. Free-flowing leukocytes establish transient contacts (tethering) with activated endothelial cells and begin to roll on the endothelial wall to become activated and finally arrested. Some of the molecules that participate during this process are displayed: L-selectin, VLA-4, LFA-1, and CD44 in the leukocyte and E-selectin, P-selectin, VCAM-1, and ICAM-1 in the endothelium. All these receptors are localized in specialized protrusions (microvilli), except for LFA-1 and CD44 that are preferentially localized at the leukocyte cell body. Middle panel: leukocyte firm adhesion and endothelial docking structure. The slowing down of leukocytes during the rolling phase facilitates their encountering with chemokines exposed on the apical surface of the endothelium. The inside-out signaling derived from leukocyte chemokine receptors triggers the activation of integrins, which in turn can interact with their endothelial ligands to

mediate leukocyte firm arrest. This step requires drastic morphological changes both in the leukocyte and in the endothelial cell. The round shape of circulating leukocytes changes into a polarized shape typical of migrating cells. The acquisition of polarity implies the segregation of adhesion molecules (ICAM-1, ICAM-3, CD44, etc.) to the rear pole (uropod), whereas the integrins are preferentially localized at the contact area with the endothelium. Additionally, the engagement of endothelial adhesion receptors triggers the formation of docking structures around adherent leukocytes, which also contain tetraspanin proteins and are supported by a cortical actin scaffold. Lower panel: leukocyte transendothelial migration. Upon firm adhesion, leukocytes migrate toward an appropriate site for diapedesis. The classical paracellular route of transmigration is shown in this panel, in which LFA-1 and ICAM-1 actively participate. JAMA, an alternative ligand for LFA-1, is also depicted.

ruffles and microvilli), whereas  $\beta 2$  integrins and CD44 are primarily located on the cell body (31–33) (Fig. 1). Selectin ligand engagements may favor flattening of microvilli, rendering previously inaccessible integrins and G-protein-coupled receptors (GPCRs) on the cell body readily available to their ligands. However, the strict separation of adhesion molecules in microvilli or cell body does not reflect physiology, as the dynamic redistribution of these molecules upon polarization of leukocytes and formation of functional complexes must be taken into account (34).

#### Central involvement of leukocyte integrins in firm adhesion and locomotion to endothelium

During the initial establishment of contacts with the vascular endothelium, leukocytes slow down their rolling velocity and become activated by encountering immobilized chemokines and integrin ligands displayed at the endothelial apical surface. This activation step allows the arrest and firm adhesion of leukocytes to endothelium under shear flow (35). Leukocyte activation involves a marked shape change from the round free-flowing cell to a polarized promigratory morphology with two distinct regions: the leading edge and the uropod (36). Leukocyte polarization enables the cell to turn intracellular forces into net cell locomotion necessary to accomplish the extravasation process (37).

#### Chemokine modulation of integrin activity

During the extravasation process, integrin adhesiveness is modulated by the chemokines coupled to apical endothelial glycosaminoglycans (38). These chemokines act by signaling through GPCRs and induce an array of 'inside-out' signals within fractions of seconds, leading to multiple conformational changes of integrins with important effects on leukocyte adhesion and morphology (34, 39, 40). Both the endothelium-immobilized chemokines and the chemokine receptors expressed on leukocytes are concentrated on microvilli to facilitate their interaction. The presence of specific chemokines on different vascular beds contributes to orchestrate the selective recruitment of leukocyte subsets to inflammation foci or secondary lymphoid organs (41). In addition, chemokines may exert a differential effect on specific integrins within the same microenvironment. Accordingly, it has been described that chemokines can only mediate lymphocyte arrest dependent on VLA-4/VCAM-1 when binding their GPCRs with high affinity and with high relative occupancy, but this signal threshold-dependent effect is not observed with chemokine-stimulated  $\beta 2$  integrins (42).

Small guanosine triphosphatases (GTPases) play a central regulatory role in the integrin activation induced by chemokines, mainly through RhoA activation or/and RhoH inactivation (43–45). It has been also suggested that Rac1 and its guanine nucleotide exchange factors (GEFs) Vav-1 and DOCK2 are involved in the chemokine-mediated activation of integrins in human T and mouse B cells (46–48). However, other authors propose that DOCK2 is mainly involved in microvilli collapse, lamellipodium formation, and lateral mobility induced by chemokines (49). Alternatively, the ras-like small GTPase Rap1 can regulate integrin activation through RapL (regulator of adhesion and cell polarization enriched in lymphoid tissues) that binds to the cytoplasmic tail of the LFA-1  $\alpha$ -chain (50, 51). The important role of Rap1 in integrin activation has been recently underscored by a deficiency in lymphocyte adhesiveness (LAD III), which correlates with a selective impairment in the activation of Rap1 induced by chemokines (52). Furthermore, the activation of phosphatidylinositol 3-OH kinase (PI3K) and protein kinase C  $\zeta$  (PKC- $\zeta$ ) by chemokines is involved in LFA-1 clustering at areas of low ICAM-1 density (39, 43, 53). In addition, the ARF-GEF cytohesin-1 induces LFA-1 activation by direct interaction with its  $\beta 2$  cytoplasmic domain (54, 55). However, there are also negative regulators of integrin activation, such as PKA, H-ras, and integrin-linked kinase (ILK) (56–58). Because of the complexity and time frames of the signaling mechanisms controlling integrin activation, the existence of preformed compartmentalized protein networks ('signalosomes') in leukocytes encountering endothelial chemokines is conceivable (59).

#### Ligand modulation of integrin affinity

Upon the inside-out chemokine-mediated signaling in leukocytes, integrin conformation reversibly and readily switches from the inactive (folded) to the extended conformation with intermediate affinity. This event primes the integrin to bind its endothelial ligand. Integrins containing the 'inserted' I-domain in their  $\alpha$  subunits undergo a further conformational shift from this intermediate affinity extended conformation upon ligand binding, resulting in full integrin activation and leukocyte arrest (60–62). Therefore, high-affinity conformational state for leukocyte immediate arrest requires bidirectional induction from both immobilized chemokines and integrin ligands (40, 63). However,  $\alpha 4$  integrins, which contain an I-like domain in their  $\beta$  subunits, can spontaneously interact with their endothelial ligands without previous chemokine stimulation (64). Therefore, it is possible that these integrins exist in overall extended conformations with high accessibility to their ligands

because of their preferential localization at microvilli. Finally, the 'outside-in' ligand-driven signaling results in further separation of the integrin subunit cytoplasmic tails (unclasp-ing), which favors their association with the cortical actin cytoskeleton (8).

Lateral mobility of integrins at the plasma membrane to promote avidity

Ligand binding enhances the recruitment of additional integrins (microclustering), further increasing the integrin-dependent adhesiveness of leukocytes under shear stress, to support their firm adhesion to endothelium (65). This clustering is dependent on integrin release from the actin cytoskeleton by PKC and calpain to increase their lateral mobility (66). In this regard, it has been suggested that ligand-independent LFA-1 nanoclusters are present at the plasma membrane of leukocytes, which promote the efficient formation of ligand-triggered microclusters (67).

Role of cytoskeleton in regulating integrin adhesiveness

The association of the extended forms of integrins with the cortical cytoskeleton is required to integrate mechanical forces from shear flow and F-actin and to undergo ligand-induced strengthening at endothelial contacts. Accordingly, a recent study has shown that a large proportion of LFA-1 molecules in extended conformation rather than low-affinity folded molecules are anchored to the cytoskeleton prior to ligand binding (68).

However, key differences between  $\alpha 4$  and  $\beta 2$  integrins regarding their increase in avidity mediated by cytoskeleton may occur. The  $\alpha 4$  integrins can bind paxillin upon dephosphorylation of Ser988 in their cytoplasmic domain at the sides and rear pole of the cell, whereas PKA-mediated phosphorylation of these integrins is confined at the leading edge of the cell. Paxillin regulates  $\alpha 4$  integrin function (tethering and firm adhesion) in immune cells (69), enhancing their rate of migration and reducing their spreading. In addition, paxillin- $\alpha 4$  interaction downregulates the formation of focal adhesions, stress fibers, and lamellipodia by triggering the activation of different tyrosine kinases, such as focal adhesion kinase (FAK), Pyk2, Src, and Abl (70). The  $\alpha 4$ -paxillin complex inhibits stable lamellipodia by recruiting an ADP-ribosylation factor (Arf)-GTPase-activating protein that decreases Arf activity, thereby inhibiting Rac, and limiting lamellipodia formation to the cell front (71).

It has been described that LFA-1 and Mac-1 may use the adapter molecules talin,  $\alpha$ -actinin, filamin, and 14-3-3 to properly anchor to the actin cytoskeleton (72, 73). Regarding the subcellular localization, the pattern of LFA-1 varies from low expression in the lamellipodia to high expression in the uropod. However, it has

been reported that high-affinity clustered LFA-1 is restricted to a mid-cell zone, termed the 'focal zone', different from focal adhesions and focal contacts. In addition, talin, properly activated by phosphorylation or phosphatidylinositol-4,5-bisphosphate (PIP2), is essential for the formation and stability of the focal zone and for LFA-1-dependent migration (74).

Effect of mechanical forces on integrin activation

Several studies suggest that integrins are directly regulated by shear stress (75). Shear flow promotes additional stretching of integrin bonds, increasing outside-in signals that coordinate leukocyte and endothelial adhesion machineries to promote productive diapedesis. Recent findings also point to a shear stress-mediated conformational activation of VLA-4, resulting in increased affinity (76). The integration of chemokine- and external force-derived signaling to enhance migration has been defined as the phenomenon of chemorheotaxis (77). In terms of subcellular localization, the integrins displayed on leukocyte microvilli distribute more readily high disruptive forces along the microvillar axis. Remarkably, the importance has been recently addressed of shear forces for the integration of signals from apical and subendothelial chemokines, rendering an increase in chemotaxis toward the subendothelial compartment (78).

Regulation of leukocyte locomotion by integrins

The signals involved in leukocyte firm adhesion to endothelium mediated by integrins are subsequently attenuated to allow leukocyte migration toward an appropriate site of transmigration.  $\beta 2$  Integrins appear to have a critical involvement in this process of locomotion because blockade of these integrins or their correspondent endothelial ligands results in random locomotion, failure in correct positioning at the endothelial junction and defective diapedesis (79).

Integrin-dependent adhesion is required for changes in cytoskeleton plasticity (polarization and spreading) and cell motility (34). Upon interaction with their ligands, integrins activate distinct myosin contractility effectors, actin-remodeling GTPases, and molecules involved in microtubule network regulation at the leading and trailing edges of motile leukocytes (80, 81). During cell polarization, Cdc42, myosin light chain kinase (MLCK), Rac, RapL, Rap1, mDia, myosin-IIA, and chemokine receptors are redistributed to the cellular front, participating in the formation of exploratory filopodia and in the extension of lamellipodia. In contrast, Rho and Rho-associated kinase (ROCK) (both involved in trailing edge retraction), the microtubule-organizing center (MTOC), and the adhesion receptors ICAM-1, ICAM-3, CD44, and CD43 move toward the rear pole (5). The redistribution of integrin

ligands to the uropod seems to be involved in the recruitment of bystander leukocytes through this cellular structure (82). Hence, the integration of signals generated in both cellular poles leads to a coordinated movement of the leukocyte.

#### Integrins during transendothelial migration

Once the leukocyte finds a proper site for transmigration, mostly at intercellular junctions, it extends exploratory pseudopodia in between the two adjacent endothelial cells. Subsequently, pseudopodia evolve into a lamella squeezed into the monolayer gap. During this process, LFA-1 is the integrin with a more prominent role. This molecule is rapidly relocalized, forming a ring-like cluster at the leukocyte–endothelial interface, where it interacts with ICAM-1 and, in some cellular models, with JAM-A (Fig. 1). When the transmigration process is over, LFA-1 is finally concentrated at the uropod (83, 84). The NADase/ADP-ribosyl cyclase CD157 can act in concert with  $\beta 2$  integrins, playing an important role in transendothelial migration (TEM) (85).

#### Endothelial integrin ligands and their contribution to the extravasation process

Endothelium is no longer considered as a passive barrier during TEM. In fact, endothelial cells form 'docking' structures to firmly attach leukocytes upon the binding of VCAM-1 and ICAM-1 to their respective leukocyte ligands, VLA-4 and LFA-1. These cup-like structures are based on microvilli that emerge from the endothelial apical surface, and their essential constituents include endothelial adhesion receptors, together with the actin cytoskeleton, adapter proteins [ezrin–radixin–moesin,  $\alpha$ -actinin, vinculin, vasodilator-stimulated phosphoprotein (VASP)], and signaling molecules (PIP<sub>2</sub>, Rho/ROCK) (86) (Fig. 1). Furthermore, it seems that ICAM-1 and VCAM-1 projections induce linear clusters of integrins along the sides of leukocytes (87). The relevant role of these structures for leukocyte adhesion and transmigration has been unveiled in experiments under flow conditions (86). However, the docking structures should not be envisioned as static structures because experiments using green fluorescent protein-tagged versions of ICAM-1 and VCAM-1 in living cells underscore their dynamic nature (86). These endothelial receptors are clustered around adherent and transmigrating leukocytes. While VCAM-1 remains at the apical endothelial side, ICAM-1 exerts its adhesive function during the whole transmigration process and also relocalizes around the leukocytes moving underneath the endothelium (86). This last observation could point to a role for ICAM-1 and LFA-1 in the egress of monocytes toward the blood flow (88).

Regarding the organization of the apical endothelial plasma membrane, the lateral association of VCAM-1 and

ICAM-1 with different tetraspanin proteins (CD9, CD81, and CD151) as well as the inhibitory effect in leukocyte adhesion and TEM because of the perturbation of the endothelial tetraspanin microdomains have recently been described (89). Tetraspanins form specialized microdomains at the plasma membrane, a kind of multimolecular platform organizing transmembrane receptors in concert with intracellular signaling molecules. The existence is feasible of tetraspanin-enriched adhesive platforms at the apical surface of endothelial cells, containing VCAM-1 and ICAM-1, and a variable proportion of most of the receptors involved in the adhesion and transmigration of leukocytes, including CD44 and platelet-endothelial cell adhesion molecule-1 (PECAM-1), ICAM-2, and JAM molecules (O. Barreiro et al., unpublished data). In addition, tetraspanins can also interact with integrins, regulating their adhesive properties (90).

In the context of leukocyte transmigration, in addition to the classical pathway of diapedesis in which the leukocytes cross through interendothelial junctions without disrupting the integrity of the endothelium (paracellular pathway), there is increasing evidence indicating the existence of an alternative pathway, in which leukocytes could migrate across an individual endothelial cell (transcellular pathway) (91). It has been suggested that endothelial docking structures are involved in the paracellular and transcellular routes of TEM (92). Moreover, new insights into the mechanism of this process have been recently reported, involving the translocation of ICAM-1 to caveolae upon leukocyte adhesion and the subsequent formation of a sort of multivesicular channel, containing ICAM-1 and caveolin-1 around the penetrating leukocyte pseudopod. Both proteins follow the passage of the whole cell, moving toward the basal side of the endothelial membrane (93). In addition, the protein of intermediate filaments, vimentin, also seems to play a role in the transcellular pathway (94). Finally, VCAM-1 and ICAM-1 are also able to transduce signals upon ligand binding, inducing activation of Rac1 or RhoA, respectively, as well as calcium release, and generation of reactive oxygen species and additional signals that cooperate to increase endothelial permeability and facilitate leukocyte transmigration (95).

#### Leukocyte navigation into the tissue

Once leukocytes have passed across the endothelial barrier, they must be able to penetrate the venular wall and migrate into the interstitial extracellular matrix (ECM), following the chemotactic gradient to sites of injury or infection. Although T lymphocytes have been extensively studied regarding their motility and adhesive interactions onto endothelial cells and

ECM components, the mechanisms of T-cell infiltration and its regulation have not been fully characterized. Integrins are the major class of receptors implicated in adhesion to ECM components, mediating a range of different cell functions such as cell attachment and polarity, growth and differentiation, as well as adhesion and migration.

Most ECMs consist of three major classes of macromolecules: collagens, proteoglycans/glycosaminoglycans, and accessory glycoproteins such as fibronectin and laminin. ECM proteins play an important role in the recruitment of inflammatory cells. Monocytes and neutrophils adhere *in vitro* to laminin, thrombospondin, and fibronectin (96), and in *in vivo* animal models of rheumatoid arthritis, the migration of these cells is dependent on the presence of fibronectin (97, 98). The role of ECM in the motility of other leukocyte subsets such as B cells and Langerhans cells (99, 100) as well as the effect on T lymphocyte migration and function have also been described (101–103). In addition, aberrant thymocyte development is observed in the *dy/dy* mutant mouse, which lacks laminin-2, and anti-laminin-5 monoclonal antibodies inhibit mouse thymocyte proliferation as well as their double-negative–double-positive differentiation (104, 105).

#### Mechanisms of leukocyte infiltration through ECM

The perivascular basement membrane is mainly composed of pericytes embedded in a network of ECM proteins, including laminin-8 and -10, type IV collagen, and entactin. This structure constitutes an additional important barrier for migrating leukocytes. Three different mechanisms by which leukocytes may overcome biophysical matrix barriers have been described: cell shape changes, contact-dependent matrix remodeling, and degradation of ECM by proteases. Interestingly, a recent study showed the existence of regions of venule walls where the expression of laminin-10, collagen IV, and nidogen-2 is considerably diminished. Neutrophil transmigration enlarges the size of these regions, and their protein content is further reduced, an effect that appears to involve neutrophil-derived serine proteases (106). Location of proteases at the leukocyte cell surface occurs through two different mechanisms, either by endogenous expression as transmembrane proteins or by binding of extracellular proteases to integral membrane receptors (Fig. 2). Integrins are shown to act as anchoring receptors for several proteases including matrix metalloproteinases (MMPs); such interactions have been detected in caveolae, invadopodia and at the leading edge of migrating cells, where directed proteolytic activity is required (107). In this regard, pro-MMP-2 and pro-MMP-9 are bound to  $\alpha$ L $\beta$ 2 and  $\alpha$ M $\beta$ 2 on the surface of activated leukemic cells, and the inhibition of

these complexes blocks  $\beta$ 2 integrin-dependent leukocyte migration (108). Pro-MMP-9– $\alpha$ M $\beta$ 2 complexes are primarily localized into intracellular granules of resting neutrophils, but after cellular activation, they are relocalized to the cell surface (109). In the case of DC migration, MMP-9 plays a role both *in vivo* and *in vitro* (110–112). In this context, the migration of interferon- $\gamma$ -induced DCs is mediated by MMP-9 and its cell-

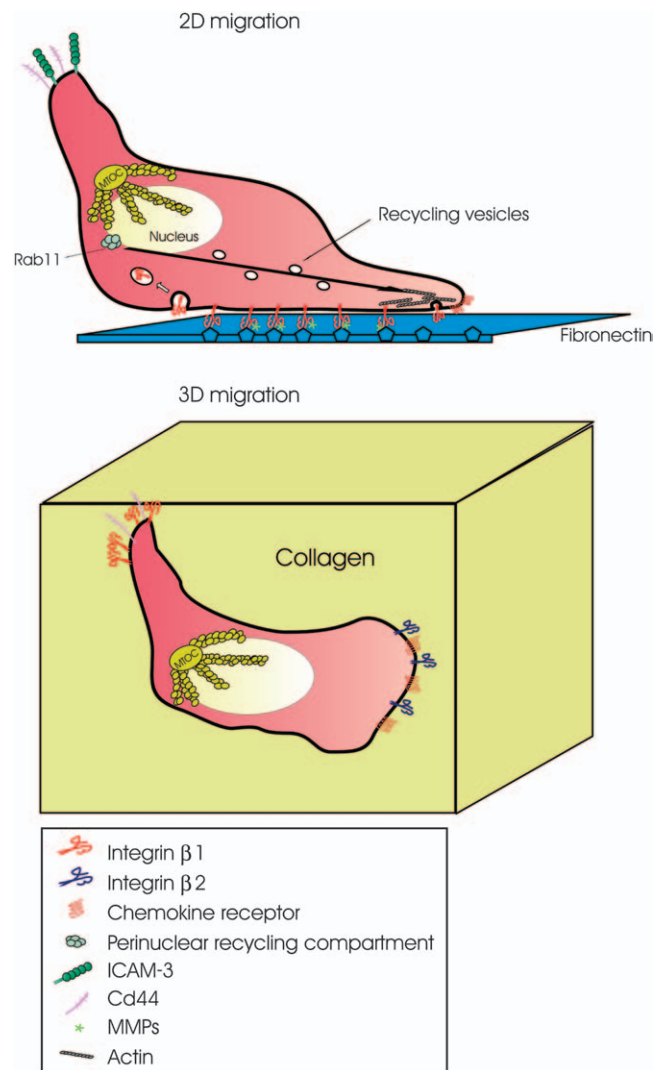


**Fig. 2. Integrin localization on migrating leukocytes on 2D and 3D ECM substrate.** Upper panel: integrin-dependent migration on 2D substrate. Migrating leukocytes on fibronectin show  $\beta$ 1 integrin–ligand interactions and actin cytoskeleton strongly focalized at the basal area and the leading edge. During migration, leukocytes form new attachments at the front and release old ones toward the rear. Released integrins are internalized into endocytic vesicles near the rear and return to the plasma membrane through the traffic from early endosomes to the perinuclear recycling compartment, which can be regulated by Rab11. Lower panel: integrin-independent migration in 3D collagen lattice.  $\beta$ 1 Integrins are redistributed toward the uropod, while  $\beta$ 2 integrins are redistributed to the leading edge. Interactions with collagen occurred independently of coclustering of  $\beta$ 1,  $\beta$ 2, or  $\beta$ 3 integrins with F-actin (118).

surface receptors CD11b and CD44, suggesting a mechanism that involves a synergistic activation of c-Jun N-terminal kinase (JNK) (113). However, it has been described that in three-dimensional (3D) collagen matrices, T-cell and DC migration occur along pre-existing fibrillar strands and that areas of dense network matrix are circummigrated rather than penetrated (114), in a process independent of proteolytic activity (107). Activated T and B lymphocytes, monocytes, and neutrophils synthesize and secrete laminin (115, 116), suggesting that leukocyte-derived matrix proteins might also contribute to the process of transmigration. Of relevance, a defect in neutrophil migration in laminin-8-deficient mice has been reported (116).

#### Role of integrins in leukocyte migration through ECM

Our knowledge about the role of integrins on leukocyte migration through the ECM is scarce and largely controversial, perhaps because of the limitations of the experimental models used to study this phenomenon. In locomotive cells such as leukocytes, properly formed focal adhesions do not exist and are rather replaced by focal contacts, which are frequently of smaller size, incompletely assembled, and less stable, and which may contain molecules not present in focal adhesions, like gelsolin (117). Rapidly migrating leukocytes adopt different morphological shapes during migration, displaying an amoeba-like movement. Interactions of lymphocytes with ECM may be too transient to support the assembly of completely formed focal adhesions (118). Consequently, in T cells, the high migration speed seems to be inversely correlated with focal adhesion formation.

Differences have been described depending not only on the different leukocyte subsets studied but also on the migration model used. The current concept of cell migration and adhesion receptor function is based on the observation of individual fibroblast-like cells migrating on a 2D environment. Because the limited two-dimensional (2D) nature of planar substrates does not reflect the 3D architecture of ECM, the leukocyte–cell matrix interactions have been further investigated in a 3D tissue context. Some models mimicking a 3D tissue environment include collagen lattices, multicomponent matrices that are supplemented with other ECM components, and Matrigel, which mimics the complex basement membrane (119). For direct *in vivo* monitoring of cell behavior in the tissues, intravital microscopy allows the observation of native or fluorescently labeled cells upon TEM or migration in the tissue (120).

It is well known that cross-linking of integrins triggers a motile behavior in T lymphocytes (121). Although leukocyte  $\beta 2$  integrins bind fibrinogen following activation (122), several studies suggest that these integrins are not essential for interactions with other ECM molecules (123, 124). *In vitro*,

activated CD18 null neutrophils adhere to fibronectin and vitronectin through  $\alpha 5\beta 1$  and  $\alpha v\beta 3$  integrins, respectively, while adhesion to endothelial laminin-10 is mediated by  $\alpha 6\beta 1$  (125). Using 3D collagen lattices, it has been found that spontaneously migrating CD4<sup>+</sup> T lymphocytes distribute  $\beta 1$  integrins toward the uropod, while  $\beta 2$  integrins are redistributed toward the leading edge. Simultaneous blockade of  $\beta 1$ ,  $\beta 2$ ,  $\beta 3$ , and  $\alpha v$  integrins did not affect the number or velocity of migrating T lymphocytes in collagen matrices (118). However, the integrin-dependent migration of T cells has also been described on both 2D and 3D collagen substrata (126). In 3D gel reconstituted with major ECM glycoproteins and with gradients formed by RANTES (regulated upon activation, normal T-cell expressed, and presumably secreted) and interleukin-2 (IL-2), directional and random locomotion of T cells requires the activity of  $\alpha 4$ ,  $\alpha 5$ , and to a lesser degree,  $\alpha 2$ , and  $\alpha 6\beta 1$  integrins (127). The critical role of  $\beta 1$  but not  $\beta 2$  integrins in neutrophil locomotion in extravascular tissue has been described *in vivo* by intravital microscopy, in the rat mesentery induced by platelet-activating factor (PAF) (120). In this regard, the integrin  $\alpha 2\beta 1$  has been identified as the main receptor used by neutrophils for migration in extravascular tissue. Furthermore, this integrin is localized at the anterior lamellipodium of neutrophils migrating on collagen in response to N-formyl-methionyl-leucyl-phenylalanine (fMLP) (128). Additional integrins have been studied in the context of polymorphonuclear neutrophil migration, including Mac-1, the effects of which depend on the collagen concentration (129). Moreover, the integrin  $\alpha v\beta 3$  has been described to be concentrated at the leading edge of polymorphonuclear neutrophil migrating on vitronectin (130).

#### Recycling of integrins: role in leukocyte migration

Cell migration involves a dynamic regulation of cell adhesion, in which new adhesions are formed at the cell leading edge, where filipodia and lamellipodia are generated as exploratory projections and, coordinately, adhesions are released from the trailing edge (131). In this context, the supply of adhesion molecules to the site of pseudopodial protrusion must be necessarily replenished in order to enable the cell to move forward.

Recycling assays show that certain integrins are continually internalized from the plasma membrane into the endosomal compartments and that they are then recycled back to the cell surface (132). In addition, there is evidence that the membrane trafficking pathways that recycle adhesion receptors contribute to cell migration (133). In this regard,  $\alpha v\beta 3$  is no longer concentrated at the leading edge of migrating fibroblast but instead in focal adhesions in cells where integrin recycling was disrupted by suppression of PKD1 or Rab4 or by expression of

a mutant  $\beta 3$  integrin that does not bind to PKD1 (134). It has also been described that the inhibition of  $\beta 1$  integrin recycling blocks the migration of epithelial cells on 2D substrates and transmigration chambers (135, 136). Although most of the studies on integrin recycling and the models of polarization in migrating cells use fibroblasts as cell model, there is evidence about the importance of this process in leukocyte migration (130). It has been reported that  $\alpha 5$  integrins are internalized in motile neutrophils; these receptors are colocalized with markers of the endocytic recycling compartment (ERC). Furthermore, as neutrophils migrate, the ERC, which is located at the cell front, reorients to retain its localization behind the leading lamella, indicating that membrane recycling during neutrophil migration has directionality (137) (Fig. 2). In addition, it has been shown recently that LFA-1 is internalized and rapidly recycled in neutrophils upon chemoattractant stimulation by a pathway involving detergent-resistant membrane microdomains (138). A dominant-negative Rab11 mutant induces intracellular accumulation of endocytosed  $\alpha L\beta 2$  and prevents its enrichment in chemoattractant-induced lamellipodia. The importance of the regulation of intracellular trafficking of integrins during leukocyte migration has also been reported in cells from Myo1f-deficient mice, which exhibit a diminished adhesion and reduced motility, as a result of an augmented exocytosis of  $\beta 2$  integrin-containing granules. It is postulated that Myo1f could inhibit granule exocytosis by modulating cortical actin (139).

### Integrins in cognate immune molecular interactions

Establishment of immune contacts between different leukocyte partners, including DC-naive T lymphocyte, follicular dendritic cell (FDC)-B lymphocyte, B lymphocyte-CD4<sup>+</sup> T cells, cytotoxic T lymphocyte (CTL)-target cell, as well as natural killer (NK) lymphocyte-target cell, is required for the development and maintenance of the immune response. All these immune interactions require close and long-lasting, cell-to-cell contact for full activation of the leukocytes. The spatial organization of molecular aggregates of cell-surface receptors and cytoplasmic molecules at the interface between the two interacting cells is referred to as the IS. Integrins, mainly LFA-1, are crucial anchors for maintaining T-APC cell-cell conjugates.

#### Integrins at the Immune Synapse

The IS is characterized by the organization of antigen receptors, costimulatory molecules, and adhesion molecules at the T cell-APC interface. The TCR and peptide-MHC complexes are clustered together with costimulatory molecules (CD4, CD2, and CD28) at the center of the contact zone, the central

supramolecular activating complex (cSMAC) (140). The intracellular signaling molecules PKC- $\theta$ , Ick, Fyn, and  $\zeta$ -associated protein of 70 kDa (Zap70) are also localized at the cSMAC in the inner side of the T-cell membrane. Although signal transduction could occur outside this zone, the organized cSMAC seems to significantly contribute to sustained intracellular signaling and to the internalization of engaged receptors. This cSMAC is surrounded by a ring of LFA-1-ICAM-1 in an area known as the peripheral SMAC (pSMAC) (140). The integrin VLA-4 is also localized at the pSMAC (141), but in contrast to LFA-1, the classical ligands described for VLA-4 are not present at the IS. LFA-1 at the pSMAC is linked to the actin cytoskeletal protein talin (4) and to RapL (142). In addition, other intracellular molecules that regulate integrin function are localized at pSMAC such as Mst1, adhesion and degranulation-promoting adapter protein (ADAP), Src kinase-associated phosphoprotein of 55 kDa (SKAP55), WAVE2, and Tec kinases. In contrast, tetraspanins and integrins are segregated into different regions of the IS; for example, the tetraspanin CD81 is localized at the cSMAC in T and B cells, colocalizing with CD3 and MHC class II molecules, respectively (143).

The concentric cSMAC/pSMAC organization has been described in different ISs, including those formed between T cells and B-cell lines or with lipid bilayers containing ICAM-1 and MHC molecules. Using living T-cell-lipid bilayer models, it has been shown that initially LFA-1-ICAM-1 are concentrated at the center of the IS, surrounded by a ring of TCR-MHC molecules. This organization is rapidly inverted, forming the definitive SMAC, with TCR-MHC at the center and LFA-1-ICAM-1 at the periphery (4). CTLs interacting with target cells show a double cSMAC, where the TCR and secretory apparatus are juxtaposed and surrounded by LFA-1 and talin (144). Localization of LFA-1 at the pSMAC has been corroborated *in vivo* in CTLs during the lysis of virally infected astrocytes (145). In contrast, the cSMAC is not formed by naive CD8<sup>+</sup> T cells during the IS, whereas the formation of the integrin ring has not been addressed in this cellular system (146). The synapses formed between NK lymphocytes and target cells under conditions where killing is prevented by inhibitory receptors adopt several topologies: (i) a concentric structure with a center of adhesion molecules surrounded by a ring of NK receptors, (ii) a multifocal structure, or (iii) a diffuse organization without apparent structure (147). A multifocal IS has been also observed at the cell-to-cell interphase of thymocytes and thymic epithelial cells (148). Similarly, in planar lipid bilayers that contain ICAM-1 and MHC molecules, thymocytes generate multicentric and dynamic MHC clusters that are surrounded by ICAM-1 (149). Although confocal fluorescence studies show that the T cell-DC

IS may form a clear-cut cSMAC/pSMAC segregation (150, 151), it has been reported also that DCs form multifocal ISs (152).

### Integrin functions during the IS

Integrins during the initial scanning of APCs by T cells  
It has been shown that initially, the T cell adheres transiently to the APC, scanning its surface for the presence of specific MHC-peptide complexes (Fig. 3). Several pairs of adhesion molecules are involved in these initial adhesive interactions such as CD2-LFA-3, LFA-1-ICAM-1, LFA-1-ICAM-3, or ICAM-3-DC-SIGN (153). Even when activated, LFA-1 has a relatively low affinity for its ligands, which facilitates a rapid adhesion and cell detachment (154). It has been previously described that ICAM-3 is highly expressed by naive T cells and that, by interacting with its ligand on DCs, LFA-1 provides the weak adhesive contact necessary for the scanning of the APC surface by T cells (155). Interestingly, ICAM-3-LFA-1 interaction on DCs induces the lateral mobility and redistribution of MHC class II molecules to the contact zone. Thus, LFA-1 not only mediates the initial adhesion with DCs but also facilitates the priming of T cells by peptide-MHC class II molecules (151). T-cell scanning of the DC surface *in vitro* occurs rapidly and in a few minutes, and in the presence of cognate antigen, the T cell immediately establishes an IS. However, *in vivo* antigen-specific interactions of T lymphocytes with DCs are unstable the first 8 h, stable between 8 and 24 h, and again transient by 24–36 h (156). The stable interaction observed in the 8- to 24-h period very likely corresponds to the organization and maintenance of the IS, allowing a complete T-cell activation. Whether LFA-1 interactions mediate these initial transitory contacts *in vivo* remain to be determined.

One special feature that distinguishes DCs from other APCs is their ability to trigger antigen-independent responses in T cells. Immature DCs, in the absence of antigen, can induce some responses on T cells, such as increased motility, calcium release, and upregulation of the activation marker CD69. DC-SIGN does not appear to play any role in the induction of these antigen-independent T-cell responses, whereas ICAM-1-LFA-1 interactions and the presence of chemokines CCL17 and CCL22, which are constitutively produced by immature DCs, are required (157). However, LFA-1 does not appear to be necessary *in vivo* for the contact of T lymphocytes and DCs in the absence of antigen (158).

Integrins in conjugate stabilization: on the effector cell side  
Following the initial scanning contacts between the T cell and DC, the signaling through the TCR inhibits T-cell motility (the stop signal) (159), allowing stable cell conjugate, IS formation, and SMAC segregation (Fig. 3). T cells, upon antigen recogni-

tion, rapidly activate the small GTPase Rap1, which binds to RapL forming a multimolecular complex with LFA-1 at the pSMAC, modulating its clustering and adhesion activity (50). Recently, it has been described that the Ser/Thr kinase Mst1 is a downstream effector molecule of RapL and that the silencing of both molecules inhibits conjugate formation (142). Engagement of cytotoxic T-lymphocyte antigen-4 (CTLA-4) (CD154) also induces LFA-1 clustering and adhesion through Rap1 (160), but it also enhances T-cell motility, reducing contact periods between T cells and APCs (161).

Additional signaling molecules that couple TCR occupancy and LFA-1 clustering, promoting T cell-APC conjugation, have been reported, including Vav-1, Src homology 2 leukocyte-specific phosphoprotein of 76 kDa (SLP-76), ADAP, and SKAP55. Upon antigen recognition by the TCR, ADAP is phosphorylated and concentrated at the pSMAC. Overexpression of ADAP and SKAP55 increases T-APC conjugates, whereas knocking-down SKAP55 impairs T cell-APC conjugation. Using a mutant form of ADAP, it has been found that the binding of SLP-76 to ADAP is necessary for pSMAC formation and for IL-2 production (162). Recently, it has been described that the complex ADAP-SKAP55 recruits activated Rap1 to the plasma membrane to mediate integrin activation (163). Moreover, engagement of LFA-1 induces the formation of an F-actin ring-based structure that colocalizes with LFA-1 and tyrosine-phosphorylated proteins. The formation of this structure is dependent on LFA-1 interactions with ADAP (164). Tec kinases (*itk*, *tec*, and *rlk*) also participate in LFA-1 activation upon antigen stimulation. In this regard, *Itk*<sup>-/-</sup> cells show decreased conjugate formation with antigen-loaded APCs and are unable to recruit LFA-1 to the IS (165). An additional role for LFA-1 in the recruitment of Vav-1, PKC- $\theta$ , and Pyk2 to the IS in an *Itk*-dependent manner has been suggested because a defective recruitment of these molecules to the IS is observed in *Itk*<sup>-/-</sup> T cells.

LFA-1 and ICAM-1 also participate in the adhesion of CTLs and target cells and in the formation of the pSMAC. However, cSMAC formation does not seem to be required for cytolytic killing by CD8<sup>+</sup> T cells because killing can be triggered by a single antigenic peptide, far fewer than what is required to form the cSMAC (166). Whereas LFA-1 is in an inactive form in resting CD4<sup>+</sup> T cells, this integrin is constitutively active in CD8<sup>+</sup> CTLs. Binding of LFA-1 on CTLs to target cells initiates the formation of a peripheral ring junction, where LFA-1 and CD3 colocalize. The formation of this ring is antigen independent, but the recognition of antigen by the TCR induces the accumulation of phosphorylated proteins as well as the redistribution of the MTOC toward the contact site (167). In accordance, using planar bilayers containing ICAM-1, it has been described that CTLs form an

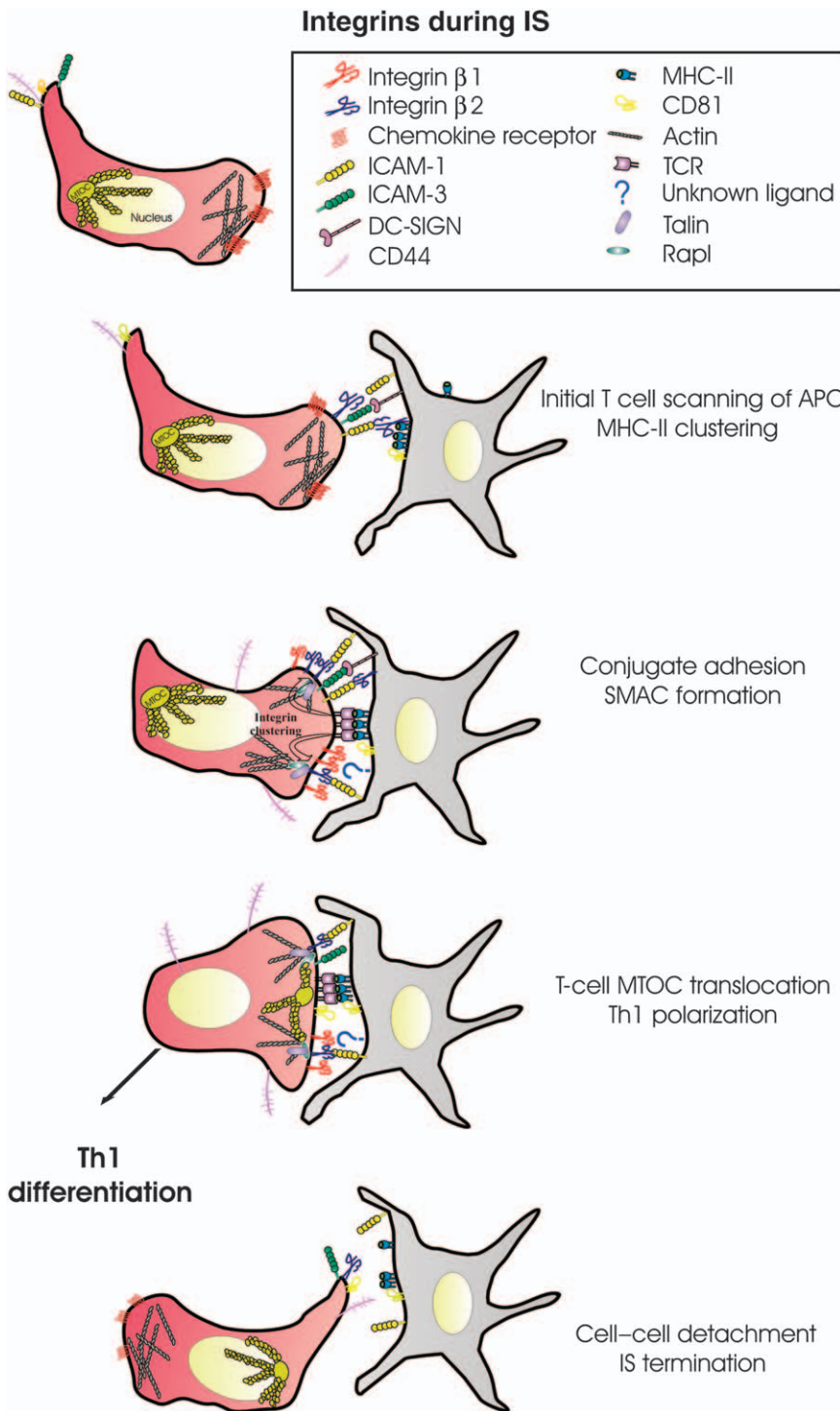


**Fig. 3. Integrin roles during cognate interactions.** Cognate immune interactions require close cell-to-cell contact to permit full activation of the T cell. The interface between the two cells is referred to as the IS. Integrins, mainly LFA-1, are thought to be crucial anchors for maintaining T-APC cell-cell conjugates. Functionally, LFA-1 integrin-mediated adhesion contributes to the initial adhesive contact that the T cell makes when it encounters an activated APC and promotes MHC class II clustering at the DC contact area. Upon recognition of an agonist peptide-MHC complex, TCR signaling can induce integrin clustering, which further stabilizes the conjugate. Once a stable conjugate is formed, the IS assembles and T-cell activation ensues. IS maturation is characterized by the positioning of T-cell MTOC at the vicinity of contact site. Signaling through integrins also promotes costimulatory signals during T-cell activation facilitating Th1 differentiation. Finally, integrin downmodulation could facilitate T-APC detachment and IS termination.

antigen-independent ring junction, where PKC-θ and LFA-1 are colocalized (168). These data suggest that the formation of the antigen-independent ring junction by CTLs constitutes a functional presynapse that favors immune surveillance. When antigen is encountered, CTLs rapidly form an IS, ensuring the release of cytotoxic granules and the lysis of target cells only within an area surrounded by the adhesive gasket.

Integrins in conjugate stabilization: on the target cell side In contrast to T cells, few reports describe the adhesion events that occur in APC during the formation of the IS. *In vitro*, the APC can be mimicked by a lipid bilayer containing peptide-bound MHC class I/II molecules and ICAM-1, and this expression is sufficient for pSMAC and cSMAC segregation (4). However, blockade of ICAM-1-LFA-1 interactions interferes with MHC

class II concentration in synapses. In addition to its role in the accumulation of MHC class II molecules at IS, integrins seem to be necessary for productive contacts of T cells (169–171). Regarding the role of integrins in DCs, it has been described that active  $\beta 2$  integrins are not necessary for the antigen-presenting capacity of DCs (172). However, it has been shown that LFA-1 molecules of DCs are actively concentrated at the IS (151).

The interaction of B cells with FDCs is mediated by VLA-4 and LFA-1 expressed on the B cells and VCAM-1 and ICAM-1 expressed on the FDCs. In addition to establishing physical contact, LFA-1 and VLA-4 of B cells lower the threshold of activation of these cells (173). Although integrins are in a low-avidity state in naive B cells, B-cell receptor (BCR) signaling activates LFA-1 and VLA-4 upon antigen recognition. The inside-out signaling pathway that mediates VLA-4 activation by the BCR involves the consecutive activation and/or generation of lyn, syk, PI3K, Bruton's tyrosine kinase (Btk), phospholipase C $\gamma 2$ , inositol-1,4,5-triphosphate (IP $_3$ ), and PKC (174). In contrast to T lymphocytes, B-cell adhesion is independent of the adapter protein ADAP. Moreover, in the B cell IS, VCAM-1 and ICAM-1 are localized in multiple projections that emerge from the APC (175) resembling the endothelial docking structure (86), while the T cell IS is characterized by a flat interface.

#### Integrins and MTOC translocation

The regulation of MTOC translocation has been previously reviewed (176). It has been reported that engagement of CD3–TCR by antibody-coated beads is sufficient for inducing MTOC translocation on T cells (177). However, different data support a connection between integrins and T cell MTOC translocation during the IS. In T cell–APC conjugates formed by Vav-1-deficient T cells, LFA-1 function is absent, and the MTOC fails to polarize toward the IS (178). In contrast, RapL is able to interact with LFA-1 and microtubules (179), and by regulating these interactions, it could act as a bridge between the pSMAC and the MTOC.

MTOC during IS maturation is polarized to the contact zone, near to the pSMAC ring (180). Dynamic processes of acetylation/deacetylation in microtubules are required for the correct spatial organization of TCR–CD3 and LFA-1 at the IS. Thus, HDAC6 tubulin deacetylase is localized at the pSMAC, and its overexpression in T cells impairs CD3 and LFA-1 localization at the IS, MTOC translocation, and IL-2 production (181). LFA-1 interacts with Mac-MARKS, which binds to microtubules by interacting with dynamin, a subunit of the dynactin complex (182). The scaffolding protein AKAP450, which associates with tubulin and predominately localizes at the MTOC and Golgi complex, is also physically associated with LFA-1 on T cells (183). This association has been described in T cells upon LFA-1

cross-linking, but it could be possible that it also occurs when LFA-1 is concentrated at the pSMAC and thus could be acting as a linker of this integrin and MTOC.

It has been reported recently that the loss of ADAP leads to a severe defect in MTOC translocation and dynein localization at the pSMAC. However, in the same report, it was shown that T cells that lack LFA-1 have no deficiencies in MTOC translocation (184). Moreover, controversial data exist regarding the role of LFA-1 during the polarization of lytic granules in the NK cell IS. The engagement of LFA-1 is sufficient to induce the polarization of lytic granules and perforin release (185). In contrast, it has been reported that CD28 but not LFA-1 signaling is necessary for MTOC and cytolytic granule polarization to the NK cell IS (186). Mac-1 has been reported to be essential for Fc receptor-mediated neutrophil cytotoxicity and conjugate formation between neutrophils and target cells (187).

#### Integrin signals drive T-helper 1 cell differentiation

Several integrins participate in the transduction of costimulatory signals in T cells (188). Engagement of VLA-4 with monoclonal antibody delocalizes this integrin from the pSMAC and delivers costimulatory signals that drive T-helper 1 cell (Th1) polarization (141). Moreover, the administration of an anti- $\alpha 4$  monoclonal antibody *in vivo* dampens Th2-mediated immune diseases (141). LFA-1 signaling also induces a polarization of T cells toward a Th1 phenotype (189), and the blockade of this integrin favors Th2 cytokine production (190) (Fig. 3). LFA-1 promotes Th1 differentiation through two independent signaling pathways involving JAB-1 (Jun activation domain-binding protein 1)–c-Jun and signaling of Erk1/2 (extracellular signal-regulated kinase 1 and 2) through cytohesin-1 (191). DNA accessory molecule 1 (DNAM-1) physically associates with LFA-1 upon CD3 stimulation, and this association is involved in Th1 differentiation (192). Because Fyn is responsible for DNAM-1 phosphorylation induced by LFA-1 signal (193), this kinase may also play an important role in Th1 polarization. In support of this hypothesis, it has been described that Th2 clones in mice express low levels of Fyn (194) and that naive CD4 $^+$  T cells from the Fyn-deficient mice tend to polarize toward the Th2 cells, even in absence of IL-4 and IL-13 (195). Tec kinases could be also involved in Th cell differentiation driven by integrins because in addition to their role in the control of integrin function, these molecules are important in the differentiation of Th cells (196).

With regard to anti-adhesion-based therapies, anti- $\alpha 4$  and anti- $\alpha L$  monoclonal antibodies have been found to be beneficial in several animal models of autoimmune and inflammatory disorders, and humanized antibodies have been

approved for the therapy of multiple sclerosis and psoriasis (197, 198). It has been assumed that their therapeutic effect is a consequence of the inhibition of leukocyte adhesion to endothelium, thus preventing leukocyte extravasation to the inflammatory foci. However, the role of these integrins in mediating leukocyte activation and Th1/Th2 polarization should be also taken into account, mainly because autoimmune and inflammatory diseases are usually associated with Th1/Th2 imbalance (199).

#### Integrins in IS termination

Little information is available on the mechanisms that mediate the detachment of T lymphocytes and APCs and the termination of the IS. One postulated mechanism includes the downmodulation of LFA-1 adhesion. Mature DCs downregulate LFA-1 adhesion by the cytohesin-interacting protein (CYTIP) (200). CYTIP binding to cytohesin-1 results in the relocalization of both from the membrane to the cytosol, which is accompanied by reduced adhesion (201). CYTIP is induced during maturation of DCs, and accumulation of CYTIP at the contact zone of DCs and T cells can be observed with a maximum at 30 min after the onset of cell-to-cell interaction. Accordingly, CYTIP silencing results in stronger adhesion of DCs to T cells. This mechanism seems to be restricted to the DC–T cell interaction because binding of DCs to endothelial cells is not affected by silencing CYTIP (200). However, overexpression of CYTIP in CD4<sup>+</sup> T cells mediates the loss of adhesiveness of LFA-1 to ICAM-1 (201). In contrast, CYTIP-deficient mice have no defects in T-cell and DC activation or differentiation (202).

Signaling through CD4 can downregulate LFA-1 adhesion by dissociation of LFA-1 and cytohesin in a p56lck and PI3K-dependent manner (203, 204). A novel mechanism for LFA-1 downregulation suggests that thromboxane A<sub>2</sub>, produced by

DCs, could negatively regulate DC–T cell interactions and therefore be involved in IS dissolution (205).

The dynamic regulation of integrin adhesiveness is critical for the generation of an immune response. This has been recently shown using a mouse strain with a deletion of the conserved GFFKR sequence in the LFA-1  $\alpha_L$  subunit cytoplasmic domain (*Lfa-1<sup>d/d</sup>* mice). This mutation results in a constitutive activation of LFA-1, associated with a defective disassembly of LFA-1-mediated adhesion. Immune responses, including T-cell proliferation and CTL activation, are impaired by the *Lfa-1<sup>d/d</sup>* mutation (206). Moreover, *Lfa-1<sup>d/d</sup>* mice show a similar phenotype to *Lfa-1<sup>-/-</sup>* mice, with splenomegaly, reduced lymph node sizes, impaired proliferative response of T cells, and reduced NK cell cytotoxicity. These results suggest that the regulation of LFA-1 activation seems to have a key role for the generation of the immune responses. Accordingly, the stabilization of LFA-1 in its active form inhibits the antigen-specific proliferative response of T cells (207). Likewise, the sustained activation of  $\beta_2$  integrins on DCs by divalent cations prolongs contact times of DCs with T cells but inhibits T-cell proliferation (172).

#### Concluding remarks

Over the last 20 years, there has been an intensive effort to understand the complex biology of integrins, including their structure, function, and regulation. The implementation of new biophysical and microscopy techniques will allow investigators to gain further insight in immune adhesion phenomena. Moreover, the development of a new generation of biological agents directed to modulate integrin function will lead to novel therapeutic approaches against inflammatory and autoimmune diseases. Important breakthroughs in this field will come in the near future.

#### References

1. von Andrian UH, Mackay CR. T-cell function and migration. Two sides of the same coin. *N Engl J Med* 2000;**343**:1020–1034.
2. Hynes RO. Integrins: bidirectional, allosteric signaling machines. *Cell* 2002;**110**:673–687.
3. Campbell JJ, Hedrick J, Zlotnik A, Siani MA, Thompson DA, Butcher EC. Chemokines and the arrest of lymphocytes rolling under flow conditions. *Science* 1998;**279**:381–384.
4. Grakoui A, et al. The immunological synapse: a molecular machine controlling T cell activation. *Science* 1999;**285**:221–227.
5. Vicente-Manzanares M, Sanchez-Madrid F. Role of the cytoskeleton during leukocyte responses. *Nat Rev Immunol* 2004;**4**:110–122.
6. Carman CV, Springer TA. Integrin avidity regulation: are changes in affinity and conformation underemphasized? *Curr Opin Cell Biol* 2003;**15**:547–556.
7. Beglova N, Blacklow SC, Takagi J, Springer TA. Cysteine-rich module structure reveals a fulcrum for integrin rearrangement upon activation. *Nat Struct Biol* 2002;**9**:282–287.
8. Nishida N, Xie C, Shimaoka M, Cheng Y, Walz T, Springer TA. Activation of leukocyte beta2 integrins by conversion from bent to extended conformations. *Immunity* 2006;**25**:583–594.
9. Springer TA, Wang JH. The three-dimensional structure of integrins and their ligands, and conformational regulation of cell adhesion. *Adv Protein Chem* 2004;**68**:29–63.
10. Gonzalez-Amaro R, Sanchez-Madrid F. Cell adhesion molecules: selectins and integrins. *Crit Rev Immunol* 1999;**19**:389–429.
11. Gahmberg CG, et al. The pivotal role of the Leu-CAM and ICAM molecules in human leukocyte adhesion. *Cell Differ Dev* 1990;**32**:239–245.
12. Dustin ML, Rothlein R, Bhan AK, Dinarello CA, Springer TA. Induction by IL 1 and interferon-gamma: tissue distribution, biochemistry, and function of a natural adherence molecule (ICAM-1). *J Immunol* 1986;**137**:245–254.

13. Acevedo A, del Pozo MA, Arroyo AG, Sanchez-Mateos P, Gonzalez-Amaro R, Sanchez-Madrid F. Distribution of ICAM-3-bearing cells in normal human tissues. Expression of a novel counter-receptor for LFA-1 in epidermal Langerhans cells. *Am J Pathol* 1993;**143**:774–783.
14. Ostermann G, et al. Involvement of JAM-A in mononuclear cell recruitment on inflamed or atherosclerotic endothelium: inhibition by soluble JAM-A. *Arterioscler Thromb Vasc Biol* 2005;**25**:729–735.
15. Lamagna C, et al. Dual interaction of JAM-C with JAM-B and alpha(M)beta2 integrin: function in junctional complexes and leukocyte adhesion. *Mol Biol Cell* 2005;**16**:4992–5003.
16. Chavakis T, et al. The pattern recognition receptor (RAGE) is a counterreceptor for leukocyte integrins: a novel pathway for inflammatory cell recruitment. *J Exp Med* 2003;**198**:1507–1515.
17. Elices MJ, et al. VCAM-1 on activated endothelium interacts with the leukocyte integrin VLA-4 at a site distinct from the VLA-4/fibronectin binding site. *Cell* 1990;**60**:577–584.
18. Carlos TM, Harlan JM. Leukocyte-endothelial adhesion molecules. *Blood* 1994;**84**:2068–2101.
19. Cunningham SA, Rodriguez JM, Arrate MP, Tran TM, Brock TA. JAM2 interacts with alpha4beta1. Facilitation by JAM3. *J Biol Chem* 2002;**277**:27589–27592.
20. Mittelbrunn M, Cabanas C, Sanchez-Madrid F. Integrin alpha4. *AfCS-Nature Molecule Pages* 2006. doi: 10.1038/mp.a001203.01.
21. Berlin C, et al. Alpha 4 beta 7 integrin mediates lymphocyte binding to the mucosal vascular addressin MAdCAM-1. *Cell* 1993;**74**:185–195.
22. Butcher EC. Leukocyte-endothelial cell recognition: three (or more) steps to specificity and diversity. *Cell* 1991;**67**:1033–1036.
23. Springer TA. Traffic signals for lymphocyte recirculation and leukocyte emigration: the multistep paradigm. *Cell* 1994;**76**:301–314.
24. Barreiro O, Vicente-Manzanares M, Urzainqui A, Yanez-Mo M, Sanchez-Madrid F. Interactive protrusive structures during leukocyte adhesion and transendothelial migration. *Front Biosci* 2004;**9**:1849–1863.
25. Berlin C, et al. Alpha 4 integrins mediate lymphocyte attachment and rolling under physiologic flow. *Cell* 1995;**80**:413–422.
26. Kadono T, Venturi GM, Steeber DA, Tedder TF. Leukocyte rolling velocities and migration are optimized by cooperative L-selectin and intercellular adhesion molecule-1 functions. *J Immunol* 2002;**169**:4542–4550.
27. Katayama Y, Hidalgo A, Chang J, Peired A, Frenette PS. CD44 is a physiological E-selectin ligand on neutrophils. *J Exp Med* 2005;**201**:1183–1189.
28. Nandi A, Estess P, Siegelman M. Bimolecular complex between rolling and firm adhesion receptors required for cell arrest; CD44 association with VLA-4 in T cell extravasation. *Immunity* 2004;**20**:455–465.
29. von Andrian UH, Hasslen SR, Nelson RD, Erlandsen SL, Butcher EC. A central role for microvillous receptor presentation in leukocyte adhesion under flow. *Cell* 1995;**82**:989–999.
30. Finger EB, Bruehl RE, Bainton DF, Springer TA. A differential role for cell shape in neutrophil tethering and rolling on endothelial selectins under flow. *J Immunol* 1996;**157**:5085–5096.
31. Abitorabi MA, Pachynski RK, Ferrando RE, Tidswell M, Erle DJ. Presentation of integrins on leukocyte microvilli: a role for the extracellular domain in determining membrane localization. *J Cell Biol* 1997;**139**:563–571.
32. Erlandsen SL, Hasslen SR, Nelson RD. Detection and spatial distribution of the beta 2 integrin (Mac-1) and L-selectin (LECAM-1) adherence receptors on human neutrophils by high-resolution field emission SEM. *J Histochem Cytochem* 1993;**41**:327–333.
33. Stein JV, Cheng G, Stockton BM, Fors BP, Butcher EC, von Andrian UH. L-selectin-mediated leukocyte adhesion in vivo: microvillous distribution determines tethering efficiency, but not rolling velocity. *J Exp Med* 1999;**189**:37–50.
34. Sanchez-Madrid F, del Pozo MA. Leukocyte polarization in cell migration and immune interactions. *EMBO J* 1999;**18**:501–511.
35. Alon R, Grabovsky V, Feigelson S. Chemokine induction of integrin adhesiveness on rolling and arrested leukocytes. Local signaling events or global stepwise activation? *Microcirculation* 2003;**10**:297–311.
36. del Pozo MA, Sanchez-Mateos P, Nieto M, Sanchez-Madrid F. Chemokines regulate cellular polarization and adhesion receptor redistribution during lymphocyte interaction with endothelium and extracellular matrix. Involvement of cAMP signaling pathway. *J Cell Biol* 1995;**131**:495–508.
37. Geiger B, Bershadsky A. Exploring the neighborhood: adhesion-coupled cell mechanosensors. *Cell* 2002;**110**:139–142.
38. Rot A, von Andrian UH. Chemokines in innate and adaptive host defense: basic chemokines grammar for immune cells. *Annu Rev Immunol* 2004;**22**:891–928.
39. Constantin G, et al. Chemokines trigger immediate beta2 integrin affinity and mobility changes: differential regulation and roles in lymphocyte arrest under flow. *Immunity* 2000;**13**:759–769.
40. Shamri R, et al. Lymphocyte arrest requires instantaneous induction of an extended LFA-1 conformation mediated by endothelium-bound chemokines. *Nat Immunol* 2005;**6**:497–506.
41. Luster AD. Chemokines – chemotactic cytokines that mediate inflammation. *N Engl J Med* 1998;**338**:436–445.
42. Laudanna C. Integrin activation under flow: a local affair. *Nat Immunol* 2005;**6**:429–430.
43. Giagulli C, et al. RhoA and zeta PKC control distinct modalities of LFA-1 activation by chemokines: critical role of LFA-1 affinity triggering in lymphocyte in vivo homing. *Immunity* 2004;**20**:25–35.
44. Cherry LK, Li X, Schwab P, Lim B, Klickstein LB. RhoH is required to maintain the integrin LFA-1 in a nonadhesive state on lymphocytes. *Nat Immunol* 2004;**5**:961–967.
45. Laudanna C, Campbell JJ, Butcher EC. Role of Rho in chemoattractant-activated leukocyte adhesion through integrins. *Science* 1996;**271**:981–983.
46. Garcia-Bernal D, Sotillo-Mallo E, Nombela-Arrieta C, Samaniego R, Fukui Y, Stein JV, Teixido J. DOCK2 is required for chemokine-promoted human T lymphocyte adhesion under shear stress mediated by the integrin alpha4beta1. *J Immunol* 2006;**177**:5215–5225.
47. Garcia-Bernal D, et al. Vav1 and Rac control chemokine-promoted T lymphocyte adhesion mediated by the integrin alpha4beta1. *Mol Biol Cell* 2005;**16**:3223–3235.
48. Nombela-Arrieta C, et al. Differential requirements for DOCK2 and phosphoinositide-3-kinase gamma during T and B lymphocyte homing. *Immunity* 2004;**21**:429–441.
49. Shulman Z, et al. DOCK2 regulates chemokine-triggered lateral lymphocyte motility but not transendothelial migration. *Blood* 2006;**108**:2150–2158.
50. Katagiri K, Maeda A, Shimonaka M, Kinashi T. RAPL, a Rap1-binding molecule that mediates Rap1-induced adhesion through spatial regulation of LFA-1. *Nat Immunol* 2003;**4**:741–748.
51. Katagiri K, et al. Crucial functions of the Rap1 effector molecule RAPL in lymphocyte and dendritic cell trafficking. *Nat Immunol* 2004;**5**:1045–1051.
52. Alon R, Etzioni A. LAD-III, a novel group of leukocyte integrin activation deficiencies. *Trends Immunol* 2003;**24**:561–566.
53. Laudanna C, Mochly-Rosen D, Liron T, Constantin G, Butcher EC. Evidence of zeta protein kinase C involvement in polymorphonuclear neutrophil integrin-dependent adhesion and chemotaxis. *J Biol Chem* 1998;**273**:30306–30315.

54. Kolanus W, et al. Alpha L beta 2 integrin/LFA-1 binding to ICAM-1 induced by cytohesin-1, a cytoplasmic regulatory molecule. *Cell* 1996;**86**:233–242.
55. Weber KS, Weber C, Ostermann G, Dierks H, Nagel W, Kolanus W. Cytohesin-1 is a dynamic regulator of distinct LFA-1 functions in leukocyte arrest and transmigration triggered by chemokines. *Curr Biol* 2001;**11**:1969–1974.
56. Hughes PE, et al. Suppression of integrin activation: a novel function of a Ras/Raf-initiated MAP kinase pathway. *Cell* 1997;**88**:521–530.
57. Friedrich EB, et al. Role of integrin-linked kinase in leukocyte recruitment. *J Biol Chem* 2002;**277**:16371–16375.
58. Laudanna C, Campbell JJ, Butcher EC. Elevation of intracellular cAMP inhibits RhoA activation and integrin-dependent leukocyte adhesion induced by chemoattractants. *J Biol Chem* 1997;**272**:24141–24144.
59. Laudanna C, Alon R. Right on the spot. Chemokine triggering of integrin-mediated arrest of rolling leukocytes. *Thromb Haemost* 2006;**95**:5–11.
60. Cabanas C, Hogg N. Ligand intercellular adhesion molecule 1 has a necessary role in activation of integrin lymphocyte function-associated molecule 1. *Proc Natl Acad Sci USA* 1993;**90**:5838–5842.
61. Salas A, Shimaoka M, Kogan AN, Harwood C, von Andrian UH, Springer TA. Rolling adhesion through an extended conformation of integrin alpha<sub>4</sub>beta<sub>2</sub> and relation to alpha I and beta I-like domain interaction. *Immunity* 2004;**20**:393–406.
62. Shimaoka M, et al. Structures of the alpha I domain and its complex with ICAM-1 reveal a shape-shifting pathway for integrin regulation. *Cell* 2003;**112**:99–111.
63. Grabovsky V, et al. Subsecond induction of alpha<sub>4</sub> integrin clustering by immobilized chemokines stimulates leukocyte tethering and rolling on endothelial vascular cell adhesion molecule 1 under flow conditions. *J Exp Med* 2000;**192**:495–506.
64. Alon R, Kassner PD, Carr MW, Finger EB, Hemler ME, Springer TA. The integrin VLA-4 supports tethering and rolling in flow on VCAM-1. *J Cell Biol* 1995;**128**:1243–1253.
65. Dobereiner HG, et al. Lateral membrane waves constitute a universal dynamic pattern of motile cells. *Phys Rev Lett* 2006;**97**:038102.
66. Stewart MP, McDowall A, Hogg N. LFA-1-mediated adhesion is regulated by cytoskeletal restraint and by a Ca<sup>2+</sup>-dependent protease, calpain. *J Cell Biol* 1998;**140**:699–707.
67. Cambi A, et al. Organization of the integrin LFA-1 in nanoclusters regulates its activity. *Mol Biol Cell* 2006;**17**:4270–4281.
68. Cairo CW, Mirchev R, Golan DE. Cytoskeletal regulation couples LFA-1 conformational changes to receptor lateral mobility and clustering. *Immunity* 2006;**25**:297–308.
69. Alon R, et al. Alpha<sub>4</sub>beta<sub>1</sub>-dependent adhesion strengthening under mechanical strain is regulated by paxillin association with the alpha<sub>4</sub>-cytoplasmic domain. *J Cell Biol* 2005;**171**:1073–1084.
70. Rose DM, Liu S, Woodside DG, Han J, Schlaepfer DD, Ginsberg MH. Paxillin binding to the alpha 4 integrin subunit stimulates LFA-1 (integrin alpha L beta 2)-dependent T cell migration by augmenting the activation of focal adhesion kinase/proline-rich tyrosine kinase-2. *J Immunol* 2003;**170**:5912–5918.
71. Nishiya N, Kiouss WB, Han J, Ginsberg MH. An alpha<sub>4</sub> integrin-paxillin-Arf-GAP complex restricts Rac activation to the leading edge of migrating cells. *Nat Cell Biol* 2005;**7**:343–352.
72. Fagerholm SC, Hilden TJ, Nurmi SM, Gahmberg CG. Specific integrin alpha and beta chain phosphorylations regulate LFA-1 activation through affinity-dependent and -independent mechanisms. *J Cell Biol* 2005;**171**:705–715.
73. Pavalko FM, LaRoche SM. Activation of human neutrophils induces an interaction between the integrin beta 2-subunit (CD18) and the actin binding protein alpha-actinin. *J Immunol* 1993;**151**:3795–3807.
74. Smith A, Carrasco YR, Stanley P, Kieffer N, Batista FD, Hogg N. A talin-dependent LFA-1 focal zone is formed by rapidly migrating T lymphocytes. *J Cell Biol* 2005;**170**:141–151.
75. Marschel P, Schmid-Schonbein GW. Control of fluid shear response in circulating leukocytes by integrins. *Ann Biomed Eng* 2002;**30**:333–343.
76. Zwartz GJ, Chigaev A, Dwyer DC, Foutz TD, Edwards BS, Sklar LA. Real-time analysis of very late antigen-4 affinity modulation by shear. *J Biol Chem* 2004;**279**:38277–38286.
77. Cinamon G, Shinder V, Alon R. Shear forces promote lymphocyte migration across vascular endothelium bearing apical chemokines. *Nat Immunol* 2001;**2**:515–522.
78. Schreiber T, Shinder V, Cain D, Alon R, Sackstein R. Shear flow-dependent integration of apical and subendothelial chemokines in T cell transmigration: implications for locomotion and the “multi-step paradigm.” *Blood* 2007;**109**:1381–1386.
79. Schenkel AR, Mamdouh Z, Muller WA. Locomotion of monocytes on endothelium is a critical step during extravasation. *Nat Immunol* 2004;**5**:393–400.
80. Smith A, Bracke M, Leitinger B, Porter JC, Hogg N. LFA-1-induced T cell migration on ICAM-1 involves regulation of MLCK-mediated attachment and ROCK-dependent detachment. *J Cell Sci* 2003;**116**:3123–3133.
81. Hogg N, Laschinger M, Giles K, McDowall A. T-cell integrins: more than just sticking points. *J Cell Sci* 2003;**116**:4695–4705.
82. del Pozo MA, Cabanas C, Montoya MC, Ager A, Sanchez-Mateos P, Sanchez-Madrid F. ICAMs redistributed by chemokines to cellular uropods as a mechanism for recruitment of T lymphocytes. *J Cell Biol* 1997;**137**:493–508.
83. Sandig M, Negrou E, Rogers KA. Changes in the distribution of LFA-1, catenins, and F-actin during transendothelial migration of monocytes in culture. *J Cell Sci* 1997;**110**:2807–2818.
84. Shaw SK, et al. Coordinated redistribution of leukocyte LFA-1 and endothelial cell ICAM-1 accompany neutrophil transmigration. *J Exp Med* 2004;**200**:1571–1580.
85. Ortolan E, et al. CD157 plays a pivotal role in neutrophil transendothelial migration. *Blood* 2006;**108**:4214–4222.
86. Barreiro O, et al. Dynamic interaction of VCAM-1 and ICAM-1 with moesin and ezrin in a novel endothelial docking structure for adherent leukocytes. *J Cell Biol* 2002;**157**:1233–1245.
87. Carman CV, Jun CD, Salas A, Springer TA. Endothelial cells proactively form microvilli-like membrane projections upon intercellular adhesion molecule 1 engagement of leukocyte LFA-1. *J Immunol* 2003;**171**:6135–6144.
88. Randolph GJ, Furie MB. Mononuclear phagocytes egress from an in vitro model of the vascular wall by migrating across endothelium in the basal to apical direction: role of intercellular adhesion molecule 1 and the CD11/CD18 integrins. *J Exp Med* 1996;**183**:451–462.
89. Barreiro O, et al. Endothelial tetraspanin microdomains regulate leukocyte firm adhesion during extravasation. *Blood* 2005;**105**:2852–2861.
90. Feigelson SW, Grabovsky V, Shamri R, Levy S, Alon R. The CD81 tetraspanin facilitates instantaneous leukocyte VLA-4 adhesion strengthening to vascular cell adhesion molecule 1 (VCAM-1) under shear flow. *J Biol Chem* 2003;**278**:51203–51212.
91. Engelhardt B, Wollburg H. Mini-review: transendothelial migration of leukocytes: through the front door or around the side of the house? *Eur J Immunol* 2004;**34**:2955–2963.
92. Carman CV, Springer TA. A transmigratory cup in leukocyte diapedesis both through individual vascular endothelial cells and between them. *J Cell Biol* 2004;**167**:377–388.

93. Millan J, Hewlett L, Glyn M, Toomre D, Clark P, Ridley AJ. Lymphocyte transcellular migration occurs through recruitment of endothelial ICAM-1 to caveola- and F-actin-rich domains. *Nat Cell Biol* 2006;**8**: 113–123.
94. Nieminen M, Henttinen T, Merinen M, Marttila-Ichihara F, Eriksson JE, Jalkanen S. Vimentin function in lymphocyte adhesion and transcellular migration. *Nat Cell Biol* 2006;**8**:156–162.
95. Hordijk PL. Endothelial signalling events during leukocyte transmigration. *FEBS J* 2006;**273**:4408–4415.
96. Bohnsack JF, Akiyama SK, Damsky CH, Knappe WA, Zimmerman GA. Human neutrophil adherence to laminin in vitro. Evidence for a distinct neutrophil integrin receptor for laminin. *J Exp Med* 1990;**171**:1221–1237.
97. Wahl SM, et al. Synthetic fibronectin peptides suppress arthritis in rats by interrupting leukocyte adhesion and recruitment. *J Clin Invest* 1994;**94**:655–662.
98. Imagawa T, Watanabe S, Katakura S, Boivin GP, Hirsch R. Gene transfer of a fibronectin peptide inhibits leukocyte recruitment and suppresses inflammation in mouse collagen-induced arthritis. *Arthritis Rheum* 2002;**46**:1102–1108.
99. Elenstrom-Magnusson C, Chen W, Clinchy B, Obrink B, Severinson E. IL-4-induced B cell migration involves transient interactions between beta 1 integrins and extracellular matrix components. *Int Immunol* 1995;**7**:567–573.
100. Staquet MJ, Kobayashi Y, Dezutter-Dambuyant C, Schmitt D. Role of specific successive contacts between extracellular matrix proteins and epidermal Langerhans cells in the control of their directed migration. *Eur J Cell Biol* 1995;**66**:342–348.
101. Halvorson MJ, Coligan JE, Sturmhofel K. The vitronectin receptor (alpha V beta 3) as an example for the role of integrins in T lymphocyte stimulation. *Immunol Res* 1996;**15**:16–29.
102. Davis JM, St John J, Cheung HT. Haptotactic activity of fibronectin on lymphocyte migration in vitro. *Cell Immunol* 1990;**129**:67–79.
103. Krivacic KA, Levine AD. Extracellular matrix conditions T cells for adhesion to tissue interstitium. *J Immunol* 2003;**170**:5034–5044.
104. Magner WJ, Chang AC, Owens J, Hong MJ, Brooks A, Coligan JE. Aberrant development of thymocytes in mice lacking laminin-2. *Dev Immunol* 2000;**7**:179–193.
105. Kim MG, et al. Epithelial cell-specific laminin 5 is required for survival of early thymocytes. *J Immunol* 2000;**165**: 192–201.
106. Wang S, et al. Venular basement membranes contain specific matrix protein low expression regions that act as exit points for emigrating neutrophils. *J Exp Med* 2006;**203**:1519–1532.
107. Wolf K, et al. Compensation mechanism in tumor cell migration: mesenchymal-amoeboid transition after blocking of pericellular proteolysis. *J Cell Biol* 2003; **160**:267–277.
108. Stefanidakis M, Bjorklund M, Ihanus E, Gahmberg CG, Koivunen E. Identification of a negatively charged peptide motif within the catalytic domain of progelatinases that mediates binding to leukocyte beta 2 integrins. *J Biol Chem* 2003;**278**: 34674–34684.
109. Stefanidakis M, Ruohtula T, Borregaard N, Gahmberg CG, Koivunen E. Intracellular and cell surface localization of a complex between alphaMbeta2 integrin and promatrix metalloproteinase-9 progelatinase in neutrophils. *J Immunol* 2004;**172**: 7060–7068.
110. Kobayashi Y, Matsumoto M, Kotani M, Makino T. Possible involvement of matrix metalloproteinase-9 in Langerhans cell migration and maturation. *J Immunol* 1999;**163**:5989–5993.
111. Ratzinger G, et al. Matrix metalloproteinases 9 and 2 are necessary for the migration of Langerhans cells and dermal dendritic cells from human and murine skin. *J Immunol* 2002;**168**:4361–4371.
112. Ichiyasu H, McCormack JM, McCarthy KM, Dombkowski D, Preffer FI, Schneeberger EE. Matrix metalloproteinase-9-deficient dendritic cells have impaired migration through tracheal epithelial tight junctions. *Am J Respir Cell Mol Biol* 2004;**30**:761–770.
113. Hu Y, Ivashkiv LB. Costimulation of chemokine receptor signaling by matrix metalloproteinase-9 mediates enhanced migration of IFN-alpha dendritic cells. *J Immunol* 2006;**176**:6022–6033.
114. Gunzer M, Kampgen E, Brocker EB, Zanker KS, Friedl P. Migration of dendritic cells in 3D-collagen lattices. Visualisation of dynamic interactions with the substratum and the distribution of surface structures via a novel confocal reflection imaging technique. *Adv Exp Med Biol* 1997; **417**:97–103.
115. Geberhiwot T, et al. Laminin-8 (alpha4beta1gamma1) is synthesized by lymphoid cells, promotes lymphocyte migration and costimulates T cell proliferation. *J Cell Sci* 2001;**114**: 423–433.
116. Wondimu Z, et al. An endothelial laminin isoform, laminin 8 (alpha4beta1gamma1), is secreted by blood neutrophils, promotes neutrophil migration and extravasation, and protects neutrophils from apoptosis. *Blood* 2004;**104**:1859–1866.
117. Jockusch BM, et al. The molecular architecture of focal adhesions. *Annu Rev Cell Dev Biol* 1995;**11**:379–416.
118. Friedl P, Entschladen F, Conrad C, Niggemann B, Zanker KS. CD4+ T lymphocytes migrating in three-dimensional collagen lattices lack focal adhesions and utilize beta1 integrin-independent strategies for polarization, interaction with collagen fibers and locomotion. *Eur J Immunol* 1998;**28**: 2331–2343.
119. Hendrix MJ, Sefter EA, Sefter RE, Fidler IJ. A simple quantitative assay for studying the invasive potential of high and low human metastatic variants. *Cancer Lett* 1987;**38**:137–147.
120. Werr J, Xie X, Hedqvist P, Ruoslahti E, Lindbom L. Beta 1 integrins are critically involved in neutrophil locomotion in extravascular tissue in vivo. *J Exp Med* 1998;**187**:2091–2096.
121. Hauzenberger D, Klominek J, Holgersson J, Bergstrom SE, Sundqvist KG. Triggering of motile behavior in T lymphocytes via cross-linking of alpha 4 beta 1 and alpha I beta 2. *J Immunol* 1997;**158**: 76–84.
122. Loike JD, et al. CD11c/CD18 on neutrophils recognizes a domain at the N terminus of the A alpha chain of fibrinogen. *Proc Natl Acad Sci USA* 1991;**88**: 1044–1048.
123. Mizgerd JP, et al. Neutrophil emigration in the skin, lungs, and peritoneum: different requirements for CD11/CD18 revealed by CD18-deficient mice. *J Exp Med* 1997;**186**:1357–1364.
124. Henderson RB, et al. The use of lymphocyte function-associated antigen (LFA)-1-deficient mice to determine the role of LFA-1, Mac-1, and alpha4 integrin in the inflammatory response of neutrophils. *J Exp Med* 2001;**194**:219–226.
125. Sixt M, Engelhardt B, Pausch F, Hallmann R, Wendler O, Sorokin LM. Endothelial cell laminin isoforms, laminins 8 and 10, play decisive roles in T cell recruitment across the blood-brain barrier in experimental autoimmune encephalomyelitis. *J Cell Biol* 2001;**153**:933–946.
126. Sundqvist KG, Hauzenberger D, Hultenby K, Bergstrom SE. T lymphocyte infiltration of two- and three-dimensional collagen substrata by an adhesive mechanism. *Exp Cell Res* 1993;**206**:100–110.

127. Franitz S, Alon R, Lider O. Real-time analysis of integrin-mediated chemotactic migration of T lymphocytes within 3-D extracellular matrix-like gels. *J Immunol Methods* 1999;**225**:9–25.
128. Werr J, Johansson J, Eriksson EE, Hedqvist P, Ruoslahti E, Lindbom L. Integrin alpha(2) beta(1) (VLA-2) is a principal receptor used by neutrophils for locomotion in extravascular tissue. *Blood* 2000;**95**:1804–1809.
129. Saltzman WM, Livingston TL, Parkhurst MR. Antibodies to CD18 influence neutrophil migration through extracellular matrix. *J Leukoc Biol* 1999;**65**:356–363.
130. Lawson MA, Maxfield FR. Ca(2+)- and calcineurin-dependent recycling of an integrin to the front of migrating neutrophils. *Nature* 1995;**377**:75–79.
131. Ridley AJ, et al. Cell migration: integrating signals from front to back. *Science* 2003;**302**:1704–1709.
132. Bretscher M. Circulating integrins: alpha 5 beta 1, alpha 6 beta 4 and Mac-1, but not alpha 3 beta 1, alpha 4 beta 1 or LFA-1. *EMBO J* 1992;**11**:405–410.
133. Jones M, Caswell P, Norman J. Endocytic recycling pathways: emerging regulators of cell migration. *Curr Opin Cell Biol* 2006;**18**:549–557.
134. Woods AJ, White DP, Caswell PT, Norman JC. PKD1/PKCmu promotes alphavbeta3 integrin recycling and delivery to nascent focal adhesions. *EMBO J* 2004;**23**:2531–2543.
135. Proux-Gillardeaux V, Gavard J, Irinopoulou T, Mege RM, Galli T. Tetanus neurotoxin-mediated cleavage of cellubrevin impairs epithelial cell migration and integrin-dependent cell adhesion. *Proc Natl Acad Sci USA* 2005;**102**:6362–6367.
136. Tayeb MA, Skalski M, Cha MC, Kean MJ, Scaife M, Coppolino MG. Inhibition of SNARE-mediated membrane traffic impairs cell migration. *Exp Cell Res* 2005;**305**:63–73.
137. Pierini LM, Lawson MA, Eddy RJ, Hendey B, Maxfield FR. Oriented endocytic recycling of alpha5beta1 in motile neutrophils. *Blood* 2000;**95**:2471–2480.
138. Fabbri M, et al. Dynamic partitioning into lipid rafts controls the endo-exocytic cycle of the alphaL/beta2 integrin, LFA-1, during leukocyte chemotaxis. *Mol Biol Cell* 2005;**16**:5793–5803.
139. Kim SV, et al. Modulation of cell adhesion and motility in the immune system by Myo1f. *Science* 2006;**314**:136–139.
140. Monks CRF, Freiberg BA, Kupfer H, Sclaky N, Kupfer A. Three-dimensional segregation of supramolecular activation clusters in T cells. *Nature* 1998;**395**:82–86.
141. Mittelbrunn M, et al. VLA-4 integrin concentrates at the peripheral supramolecular activation complex of the immune synapse and drives T helper 1 responses. *Proc Natl Acad Sci USA* 2004;**101**:11058–11063.
142. Katagiri K, Imamura M, Kinashi T. Spatiotemporal regulation of the kinase Mst1 by binding protein RAP1 is critical for lymphocyte polarity and adhesion. *Nat Immunol* 2006;**7**:919–928.
143. Mittelbrunn M, Yanez-Mo M, Sancho D, Ursa A, Sanchez-Madrid F. Cutting edge: dynamic redistribution of tetraspanin CD81 at the central zone of the immune synapse in both T lymphocytes and APC. *J Immunol* 2002;**169**:6691–6695.
144. Stinchcombe JC, Bossi G, Booth S, Griffiths GM. The immunological synapse of CTL contains a secretory domain and membrane bridges. *Immunity* 2001;**15**:751–761.
145. Barcia C, et al. In vivo mature immunological synapses forming SMACs mediate clearance of virally infected astrocytes from the brain. *J Exp Med* 2006;**203**:2095–2107.
146. O'Keefe JP, Blaine K, Alegre ML, Gajewski TF. Formation of a central supramolecular activation cluster is not required for activation of naive CD8+ T cells. *Proc Natl Acad Sci USA* 2004;**101**:9351–9356.
147. Carlin LM, Eleme K, McCann FE, Davis DM. Inter-cellular transfer and supramolecular organization of human leukocyte antigen C at inhibitory natural killer cell immune synapses. *J Exp Med* 2001;**194**:1507–1517.
148. Richie LI, Ebert PJ, Wu LC, Krummel MF, Owen JJ, Davis MM. Imaging synapse formation during thymocyte selection: inability of CD3zeta to form a stable central accumulation during negative selection. *Immunity* 2002;**16**:595–606.
149. Hailman E, Burack WR, Shaw AS, Dustin ML, Allen PM. Immature CD4(+)CD8(+) thymocytes form a multifocal immunological synapse with sustained tyrosine phosphorylation. *Immunity* 2002;**16**:839–848.
150. Benvenuti F, et al. Dendritic cell maturation controls adhesion, synapse formation, and the duration of the interactions with naive T lymphocytes. *J Immunol* 2004;**172**:292–301.
151. de la Fuente H, et al. Synaptic clusters of MHC class II molecules induced on DCs by adhesion molecule-mediated initial T-cell scanning. *Mol Biol Cell* 2005;**16**:3314–3322.
152. Brossard C, et al. Multifocal structure of the T cell–dendritic cell synapse. *Eur J Immunol* 2005;**35**:1741–1753.
153. Montoya M, Sancho D, Vicente-Manzanares M, Sanchez-Madrid F. Cell adhesion and polarity during immune interactions. *Immunol Rev* 2002;**186**:68–82.
154. Woska JR Jr, Morelock MM, Jeanfavre DD, Bormann BJ. Characterization of molecular interactions between intercellular adhesion molecule-1 and leukocyte function-associated antigen-1. *J Immunol* 1996;**156**:4680–4685.
155. Montoya MC, et al. Role of ICAM-3 in the initial interaction of T lymphocytes and APCs. *Nat Immunol* 2002;**3**:159–168.
156. Mempel TR, Henrickson SE, Von Andrian UH. T-cell priming by dendritic cells in lymph nodes occurs in three distinct phases. *Nature* 2004;**427**:154–159.
157. Real E, et al. Immature dendritic cells (DCs) use chemokines and intercellular adhesion molecule (ICAM)-1, but not DC-specific ICAM-3-grabbing nonintegrin, to stimulate CD4+ T cells in the absence of exogenous antigen. *J Immunol* 2004;**173**:50–60.
158. Westermann J, et al. Naive, effector, and memory T lymphocytes efficiently scan dendritic cells in vivo: contact frequency in T cell zones of secondary lymphoid organs does not depend on LFA-1 expression and facilitates survival of effector T cells. *J Immunol* 2005;**174**:2517–2524.
159. Dustin ML, Bromley SK, Kan Z, Peterson DA, Unanue ER. Antigen receptor engagement delivers a stop signal to migrating T lymphocytes. *Proc Natl Acad Sci USA* 1997;**94**:3909–3913.
160. Schneider H, Valk E, da Rocha Dias S, Wei B, Rudd CE. CTLA-4 up-regulation of lymphocyte function-associated antigen 1 adhesion and clustering as an alternate basis for coreceptor function. *Proc Natl Acad Sci USA* 2005;**102**:12861–12866.
161. Schneider H, et al. Reversal of the TCR stop signal by CTLA-4. *Science* 2006;**313**:1972–1975.
162. Wang H, et al. ADAP-SLP-76 binding differentially regulates supramolecular activation cluster (SMAC) formation relative to T cell-APC conjugation. *J Exp Med* 2004;**200**:1063–1074.
163. Kliche S, et al. The ADAP/SKAP5 signaling module regulates T-cell receptor-mediated integrin activation through plasma membrane targeting of Rap1. *Mol Cell Biol* 2006;**26**:7130–7144.
164. Suzuki JI, Yamasaki S, Wu J, Koretzky GA, Saito T. Actin cloud induced by LFA-1-mediated outside-in signals lowers the threshold for T cell activation. *Blood* 2007;**109**:168–175.
165. Finkelstein LD, Shimizu Y, Schwartzberg PL. Tec kinases regulate TCR-mediated recruitment of signaling molecules and integrin-dependent cell adhesion. *J Immunol* 2005;**175**:5923–5930.

166. Purbhoo MA, Irvine DJ, Huppa JB, Davis MM. T cell killing does not require the formation of a stable mature immunological synapse. *Nat Immunol* 2004;**5**:524–530.
167. Marwali MR, MacLeod MA, Muzia DN, Takei F. Lipid rafts mediate association of LFA-1 and CD3 and formation of the immunological synapse of CTL. *J Immunol* 2004;**173**:2960–2967.
168. Somersalo K, et al. Cytotoxic T lymphocytes form an antigen-independent ring junction. *J Clin Invest* 2004;**113**:49–57.
169. Moy VT, Brian AA. Signaling by lymphocyte function-associated antigen 1 (LFA-1) in B cells: enhanced antigen presentation after stimulation through LFA-1. *J Exp Med* 1992;**175**:1–7.
170. Owens T. A role for adhesion molecules in contact-dependent T help for B cells. *Eur J Immunol* 1991;**21**:979–983.
171. Mentzer SJ, Gromkowski SH, Krensky AM, Burakoff SJ, Martz E. LFA-1 membrane molecule in the regulation of homotypic adhesions of human B lymphocytes. *J Immunol* 1985;**135**:9–11.
172. Varga G, et al. Active MAC-1 (CD11b/CD18) on DC is inhibitory for full T cell activation. *Blood* 2007;**109**:661–669.
173. Carrasco YR, Fleire SJ, Cameron T, Dustin ML, Batista FD. LFA-1/ICAM-1 interaction lowers the threshold of B cell activation by facilitating B cell adhesion and synapse formation. *Immunity* 2004;**20**:589–599.
174. Spaargaren M, et al. The B cell antigen receptor controls integrin activity through Btk and PLCgamma2. *J Exp Med* 2003;**198**:1539–1550.
175. Batista FD, Iber D, Neuberger MS. B cells acquire antigen from target cells after synapse formation. *Nature* 2001;**411**:489–494.
176. Sancho D, et al. Regulation of microtubule-organizing center orientation and actomyosin cytoskeleton rearrangement during immune interactions. *Immunol Rev* 2002;**189**:84–97.
177. Lowin-Kropf B, Shapiro VS, Weiss A. Cytoskeletal polarization of T cells is regulated by an immunoreceptor tyrosine-based activation motif-dependent mechanism. *J Cell Biol* 1998;**140**:861–871.
178. Ardouin L, et al. Vav1 transduces TCR signals required for LFA-1 function and cell polarization at the immunological synapse. *Eur J Immunol* 2003;**33**:790–797.
179. Fujita H, et al. Local activation of Rap1 contributes to directional vascular endothelial cell migration accompanied by extension of microtubules on which RAP1, a Rap1-associated molecule, localizes. *J Biol Chem* 2005;**280**:5022–5031.
180. Kuhn JR, Poenie M. Dynamic polarization of the microtubule cytoskeleton during CTL-mediated killing. *Immunity* 2002;**16**:111–121.
181. Serrador JM, Cabrero JR, Sancho D, Mittelbrunn M, Urzainqui A, Sanchez-Madrid F. HDAC6 deacetylase activity links the tubulin cytoskeleton with immune synapse organization. *Immunity* 2004;**20**:417–428.
182. Zhou X, Li J. Macrophage-enriched myristoylated-alanine-rich C-kinase substrate and its phosphorylation is required for the phorbol ester-stimulated diffusion of beta2 integrin molecules. *J Biol Chem* 2000;**275**:20217–20222.
183. El Din El Homasany BS, et al. The scaffolding protein CG-NAP/AKAP450 is a critical integrating component of the LFA-1-induced signaling complex in migratory T cells. *J Immunol* 2005;**175**:7811–7818.
184. Combs J, et al. Recruitment of dynein to the Jurkat immunological synapse. *Proc Natl Acad Sci USA* 2006;**103**:14883–14888.
185. Perez OD, Mitchell D, Jager GC, Nolan GP. LFA-1 signaling through p44/42 is coupled to perforin degranulation in CD56+CD8+ natural killer cells. *Blood* 2004;**104**:1083–1093.
186. Chen X, Allan DS, Krzewski K, Ge B, Kopcow H, Strominger JL. CD28-stimulated ERK2 phosphorylation is required for polarization of the microtubule organizing center and granules in YTS NK cells. *Proc Natl Acad Sci USA* 2006;**103**:10346–10351.
187. van Spriel AB, et al. Mac-1 (CD11b/CD18) is essential for Fc receptor-mediated neutrophil cytotoxicity and immunologic synapse formation. *Blood* 2001;**97**:2478–2486.
188. Clark EA, Brugge JS. Integrins and signal transduction pathways: the road taken. *Science* 1995;**268**:233–239.
189. Smits HH, et al. Intercellular adhesion molecule-1/LFA-1 ligation favors human Th1 development. *J Immunol* 2002;**168**:1710–1716.
190. Salomon B, Bluestone JA. LFA-1 interaction with ICAM-1 and ICAM-2 regulates Th2 cytokine production. *J Immunol* 1998;**161**:5138–5142.
191. Perez OD, et al. Leukocyte functional antigen 1 lowers T cell activation thresholds and signaling through cytohesin-1 and Jun-activating binding protein 1. *Nat Immunol* 2003;**4**:1083–1092.
192. Shibuya K, et al. CD226 (DNAM-1) is involved in lymphocyte function-associated antigen 1 costimulatory signal for naive T cell differentiation and proliferation. *J Exp Med* 2003;**198**:1829–1839.
193. Shibuya K, et al. Physical and functional association of LFA-1 with DNAM-1 adhesion molecule. *Immunity* 1999;**11**:615–623.
194. Tamura T, et al. Early activation signal transduction pathways of Th1 and Th2 cell clones stimulated with anti-CD3. Roles of protein tyrosine kinases in the signal for IL-2 and IL-4 production. *J Immunol* 1995;**155**:4692–4701.
195. Tamura T, et al. Molecular mechanism of the impairment in activation signal transduction in CD4(+) T cells from old mice. *Int Immunol* 2000;**12**:1205–1215.
196. Dombroski D, et al. Kinase-independent functions for Itk in TCR-induced regulation of Vav and the actin cytoskeleton. *J Immunol* 2005;**174**:1385–1392.
197. Lebwohl M, et al. A novel targeted T-cell modulator, efalizumab, for plaque psoriasis. *N Engl J Med* 2003;**349**:2004–2013.
198. Chaudhuri A, Behan PO. Natalizumab for relapsing multiple sclerosis. *N Engl J Med* 2003;**348**:1598–1599.
199. Gonzalez-Amaro R, Mittelbrunn M, Sanchez-Madrid F. Therapeutic anti-integrin (alpha4 and alphaL) monoclonal antibodies: two-edged swords? *Immunology* 2005;**116**:289–296.
200. Hofer S, et al. Dendritic cells regulate T-cell deattachment through the integrin-interacting protein CYTIP. *Blood* 2006;**107**:1003–1009.
201. Boehm T, et al. Attenuation of cell adhesion in lymphocytes is regulated by CYTIP, a protein which mediates signal complex sequestration. *EMBO J* 2003;**22**:1014–1024.
202. Watford WT, et al. Cytohesin binder and regulator (cybr) is not essential for T- and dendritic-cell activation and differentiation. *Mol Cell Biol* 2006;**26**:6623–6632.
203. Mazerolles F, Barbat C, Hivroz C, Fischer A. Phosphatidylinositol 3-kinase participates in p56(lck)/CD4-dependent down-regulation of LFA-1-mediated T cell adhesion. *J Immunol* 1996;**157**:4844–4854.
204. Trucy M, Barbat C, Sorice M, Fischer A, Mazerolles F. CD4-induced down-regulation of T cell adhesion to B cells is associated with localization of phosphatidylinositol 3-kinase and LFA-1 in distinct membrane domains. *Eur J Immunol* 2004;**34**:2168–2178.
205. Kabashima K, et al. Thromboxane A2 modulates interaction of dendritic cells and T cells and regulates acquired immunity. *Nat Immunol* 2003;**4**:694–701.
206. Semmrich M, et al. Importance of integrin LFA-1 deactivation for the generation of immune responses. *J Exp Med* 2005;**201**:1987–1998.
207. Dransfield I, Cabanas C, Barrett J, Hogg N. Interaction of leukocyte integrins with ligand is necessary but not sufficient for function. *J Cell Biol* 1992;**116**:1527–1535.

**Nanoscale molecular interactions and dynamics of endothelial adhesive platforms  
in primary living cells**

Authors: Olga Barreiro<sup>1,2</sup>, Moreno Zamai<sup>3,4</sup>, María Yáñez-Mó<sup>1,2</sup>, Emilio Tejera<sup>1,2</sup>, Pedro López-Romero<sup>5</sup>, Peter N. Monk<sup>6</sup>, Enrico Gratton<sup>7</sup>, Valeria Caiolfa<sup>3,4</sup> and Francisco Sánchez-Madrid<sup>1,2</sup>.

<sup>1</sup>Servicio de Inmunología, Hospital de la Princesa, Universidad Autónoma de Madrid. Madrid, Spain.

<sup>2</sup>Departamento de Biología Vascular e Inflamación. Centro Nacional de Investigaciones Cardiovasculares. Madrid, Spain.

<sup>3</sup>Department of Molecular Biology and Functional Genomics, San Raffaele Scientific Institute, Milano, Italy.

<sup>4</sup>IIT Network Research, Unit of Molecular Neuroscience, San Raffaele Scientific Institute, Milano, Italy.

<sup>5</sup>Unidad de Genómica. Centro Nacional de Investigaciones Cardiovasculares. Madrid, Spain.

<sup>6</sup>Academic Neurology Unit, School of Medicine and Biomedical Science, University of Sheffield, Sheffield, UK

<sup>7</sup>Laboratory for Fluorescence Dynamics, Biomedical Engineering Department, University of California Irvine, Irvine, CA.

\*Correspondence should be addressed to F. S-M.: Servicio de Inmunología, Hospital de la Princesa, Universidad Autónoma de Madrid, C/ Diego de León 62, 28006. Madrid, Spain.

E-mail: [fsanchez.hlpr@salud.madrid.org](mailto:fsanchez.hlpr@salud.madrid.org) Phone: 34-91-3092115. Fax: 34-91-5202374.

**Running title:** Dynamics of adhesive platforms in endothelium.

**Abbreviations:** ICAM-1: Intercellular Adhesion Molecule-1; VCAM-1: Vascular Cell Adhesion Molecule-1; HUVEC: Human Umbilical Vein Endothelial Cells; LFA-1: Lymphocyte Function-associated Antigen-1; FRAP: Fluorescence Recovery After Photobleaching; TCSPC-FLIM-FRET: Time-Correlated Single Photon Counting-Fluorescence Lifetime Imaging-Fluorescence Resonance Energy Transfer; FCS: Fluorescence Correlation Spectroscopy; FCCS: Fluorescence Cross-correlation Spectroscopy; SEM: Scanning Electron Microscopy; TEM: Tetraspanin-enriched Microdomains; EAP: Endothelial Adhesive Platforms.

**Keywords:** Tetraspanin microdomain, VCAM-1, ICAM-1, adhesion receptor clustering, endothelial adhesive platform.

## **ABSTRACT**

Endothelial VCAM-1 and ICAM-1 are fundamental receptors involved in leukocyte firm adhesion and transendothelial migration during inflammation. These adhesion molecules are recruited toward the leukocyte-endothelium contact site at the apical membrane of activated endothelial cells. Here we show that this recruitment is independent of ligand engagement, actin cytoskeleton anchorage and heterodimer formation, and is instead due to the inclusion of VCAM-1 and ICAM-1 within tetraspanin-enriched microdomains, which act as specialized endothelial adhesive platforms (EAP). Using complementary analytical microscopy techniques (fluorescence recovery after photobleaching, fluorescence correlation and cross-correlation spectroscopy, and fluorescence lifetime imaging-fluorescence resonance energy transfer), we have characterized the diffusional properties, nanoscale organization and specific intra-domain molecular interactions of EAP in primary endothelial living cells. This analysis provides compelling evidence for the existence of EAP as physical entities at the plasma membrane distinct from classical biochemically-defined lipid rafts. Scanning electron microscopy combined with the use of a specific tetraspanin blocking peptide identified EAP-induced nanoclustering of VCAM-1 and ICAM-1 as a novel mechanism of supramolecular organization that regulates the efficient leukocyte integrin binding capacity of both endothelial receptors.

## INTRODUCTION

How cells physically organize and compartmentalize receptors and signaling molecules into specialized, efficient, regulated networks is of critical importance to our understanding of the complexity and dynamics of biological processes. In this regard, cholesterol and sphingolipid-enriched rafts have been proposed as platforms for the sorting of specific membrane components such as glycosylphosphatidylinositol (GPI)-anchored proteins and to provide sites for the assembly of cytoplasmic signaling complexes (Anderson and Jacobson, 2002; Simons and Toomre, 2000). Recent biochemical, proteomics and structural studies bolstered the idea that tetraspanin-enriched microdomains (TEM) at the plasma membrane play a key role in organizing molecular complexes with protein compositions different from those of typical lipid rafts (Hemler, 2005; Le Naour et al., 2006; Min et al., 2006; Nydegger et al., 2006). The existence and physical properties of lipid rafts have been extensively studied using innovative analytical methods (Kenworthy et al., 2004; Larson et al., 2005; Sharma et al., 2004; Suzuki et al., 2007a; Suzuki et al., 2007b). However, there have so far been no documented studies demonstrating the existence of tetraspanin-enriched microdomains on the plasma membrane of living cells and characterizing their dynamic features at molecular level.

Tetraspanins are ubiquitous low molecular weight proteins that span the plasma membrane four times and are able to organize themselves by homo- and hetero-oligomerization (Kovalenko et al., 2005; Stipp et al., 2003). These molecules can also associate laterally at the plasma membrane with a plethora of integral membrane receptors, modulating their functions. These partners include leukocyte and endothelial adhesion molecules (Barreiro et al., 2005; Feigelson et al., 2003; Levy et al., 1998; Mannion et al., 1996; VanCompernelle et al., 2001), intercellular junction- and

extracellular matrix-related integrins (Berditchevski, 2001; Lammerding et al., 2003; Yanez-Mo et al., 1998), CD19/CD21-B cell antigen receptor complex (Cherukuri et al., 2004), MHC-peptide complex (Kropshofer et al., 2002; Vogt et al., 2002), Fc receptors (Moseley, 2005), G-protein-coupled receptors (Little et al., 2004), and metalloproteinases (Andre et al., 2006; Takino et al., 2003; Yan et al., 2002). Tetraspanins also associate intracellularly with a number of cytoplasmic signaling mediators such as type II PI4K or different PKC isoforms (Yauch and Hemler, 2000; Zhang et al., 2001). Thus, the proposed existence of TEM is based on the ability of tetraspanins to simultaneously interact among themselves and with a wide range of molecules, organizing discrete dynamic plasma membrane compartments. Apart from acting as adapters for membrane organization, tetraspanins also regulate trafficking and the biosynthetic processing of associated receptors (reviewed in (Berditchevski and Odintsova, 2007). Although TEM seem to be different from lipid rafts, they are not devoid of lipid interactions, since tetraspanins are highly palmitoylated proteins that bind cholesterol and gangliosides (Charrin et al., 2003; Hakomori, 2002; Yang et al., 2004). The composition of tetraspanins and associated partners, as well as other specific TEM characteristics, may vary with cell type. Gene deletion, knock-down, over-expression, and mutation experiments have revealed key functional roles for tetraspanins in many fundamental physiological processes, among which are egg-sperm fusion (Le Naour et al., 2000; Rubinstein et al., 2006), antigen presentation (Delaguillaumie et al., 2004; Levy and Shoham, 2005b; Mittelbrunn et al., 2002; Unternaehrer et al., 2007), viral cell entry and budding as well as virus-promoted syncytia formation (Gordon-Alonso et al., 2006; Martin et al., 2005; Pileri et al., 1998), metalloproteinase activity (Fujita et al., 2006; Hong et al., 2006; Hong et al., 2005; Takino et al., 2003), angiogenesis (Takeda et al., 2007; Wright et al., 2004), renal

function (Sachs et al., 2006), neurite outgrowth (Stipp and Hemler, 2000), hemidesmosome organization (Sterk et al., 2000), exosome targeting to dendritic cells (Morelli et al., 2004), and cell adhesion, migration and invasion (Barreiro et al., 2005; Chattopadhyay et al., 2003; Garcia-Lopez et al., 2005; Hemler, 2003; Kovalenko et al., 2007; Longo et al., 2001; Yanez-Mo et al., 1998; Yanez-Mo et al., 2001). The fact that there are few ligands suggests that regulation of tetraspanins is likely to occur indirectly, through binding to their laterally-associated partners (Hemler, 2001). However, the molecular mechanisms underlying the regulatory activity of tetraspanins still remain elusive.

Leukocyte extravasation from the bloodstream to sites of infection and inflammation involves a dynamic interaction with the endothelium which is mediated by an array of leukocyte and endothelial cell surface receptors. This process consists of sequential steps of tethering, rolling, firm adhesion, locomotion and diapedesis, with specialized receptor/ligand pairs involved in each (Butcher, 1991; Springer, 1994). Our earlier studies showed that, to prevent leukocyte detachment under hemodynamic flow, endothelial cells form actin-based structures that cluster VCAM-1 and ICAM-1 adhesion molecules, tetraspanins and actin-binding proteins at the contact area with leukocytes (Barreiro et al., 2005; Barreiro et al., 2002). In the present work, we demonstrate the existence, prior to leukocyte binding, of specialized endothelial microdomains containing tetraspanins together with VCAM-1 and ICAM-1, which we have termed endothelial adhesive platforms (EAP). EAP promote nanoclustering of adhesion receptors to enhance their adhesive properties during leukocyte firm adhesion to endothelium. We have used an array of innovative, complementary analytical microscopy techniques to accurately determine the molecular characteristics, dynamics and biophysical properties of EAP. FRAP (fluorescence recovery after photobleaching),

FCS (fluorescence correlation spectroscopy) and FCCS (fluorescence cross-correlation spectroscopy) were used to determine diffusion coefficients, degree of anomaly in diffusion, and multimer formation among EAP components at both microscopic and nanoscopic scale. Furthermore, TCSPC-FLIM (time-correlated single photon counting-fluorescence lifetime imaging) was used to unequivocally determine FRET events within the EAP, thereby unraveling their specific inter-molecular organization. Finally, using scanning electron microscopy in combination with tetraspanin blocking peptides, we show that tetraspanin microdomains make an essential contribution to the avidity regulation of endothelial adhesion receptors, tuning their adhesive properties.

## **MATERIALS AND METHODS**

### **Cells and cell cultures**

Human umbilical vein endothelial cells (HUVEC) were obtained and cultured as previously described (Yanez-Mo et al., 1998). Cells were used up to the third passage in all assays. To activate HUVEC, TNF- $\alpha$  (20 ng/ml) (R&D Systems, Minneapolis, MN) was added to the culture media 20 h before the assays. K562 erythroleukemic cells, which endogenously express  $\beta$ 1 integrin, were stably transfected with integrins  $\alpha$ 4 or LFA-1 (Lymphocyte Function-associated Antigen-1) (Munoz et al., 1996; Nueda et al., 1995) and grown in RPMI 1640 medium (Gibco BRL, Gaithersburg, MD) supplemented with 10% FCS, 50 IU/ml penicillin, 50  $\mu$ g/ml streptomycin, and 1 mg/ml G418 (Calbiochem, La Jolla, CA). T lymphoblasts were derived from freshly isolated human peripheral blood lymphocytes (PBLs) by activation with phytohemagglutinin-L (PHA-L) (1  $\mu$ g/ml; Sigma-Aldrich, St Louis, MO) for 48 h followed by culture for 5-7 days in the presence of recombinant human interleukin-2 (rhIL-2; 100 U/ml) provided by the National Institutes of Health AIDS Research and Reference Reagent Program (Division of AIDS, National Institute of Allergy and Infectious Diseases). Integrin inhibitors BIO5192 and BIRT377 were kindly provided by Biogen Idec (Cambridge, MA) and Boehringer-Ingelheim Pharmaceuticals (Ridgefield, CT), respectively.

### **Antibodies**

Anti-CD151 (LIA1/1), anti-VE-Cadherin (TEA1/31), and anti-CD9 (VJ1/20) monoclonal antibodies (mAb) have been described previously (Yanez-Mo et al., 1998). P8B1 (anti-VCAM-1), MEM-111 and Hu5/3 (anti-ICAM-1), and 8C3 (anti-CD151) mAbs were kindly provided by Dr. E. A. Wayner (Fred Hutchinson Cancer Research

Center, Seattle, WA), Dr. V. Horejsi (Academy of Sciences of the Czech Republic, Prague, Czech Republic), Dr. F. W. Luscinikas (Brigham and Women's Hospital and Harvard Medical School, Boston, MA), and Dr. K. Sekiguchi (Osaka University, Japan), respectively. Anti-caveolin Ab was purchased from Sigma. The 40 nm gold-coupled anti-mouse antibody and 15 nm gold-coupled streptavidin were purchased from British Biocell. International (Cardiff, UK).

### **Recombinant DNA constructs and proteins and transfections**

ICAM-1-, VCAM-1-, CD9-, and CD151-EGFP tagged proteins have been described (Barreiro et al., 2002; Garcia-Lopez et al., 2005; Longo et al., 2001). The construct encoding VCAM $\Delta$ Cyt, a C-terminally truncated VCAM-1 protein in which the first cytoplasmic charged residue is retained to ensure proper membrane insertion, was generated by PCR using the human VCAM-1 cDNA as template, and [CTCGAGTCTCATCACGACAGCAAC] and [CTATCTTGCAAAGTAAATTATC] as 5' and 3' primers, respectively. The PCR product, containing a stop codon at position 722, was cloned into pcDNA3.1/V5-His-TOPO (Invitrogen, Carlsbad, CA) and correct expression of VCAM $\Delta$ Cyt at the plasma membrane was tested. The equivalent ICAM-1-tailless construct was a kind gift of Dr. W.F. Luscinikas (Yang et al., 2005). For the FCS, FCCS, and FLIM-FRET studies, monomeric green and red variants of ICAM-1, VCAM-1, CD9 and CD151 were generated. Monomeric EGFP (mEGFP) constructs were obtained by A206K point mutation (Zacharias et al., 2002; Zhang et al., 2002) using the Quick Mutagenesis Kit (Stratagene, La Jolla, CA). The mRFP1 variants were generated by subcloning the corresponding EGFP constructs into an mRFP1 vector kindly provided by Dr. Tsien (UCSD, La Jolla CA). The GPI-EGFP construct was a kind gift of Dr. M.A. del Pozo (CNIC, Madrid, Spain).

The large extracellular loop (LEL) of wild-type human CD9 was cloned into the pGX-KG vector and expressed in protease negative BL21 cells. LEL-GST fusion proteins were obtained as previously described (Barreiro et al., 2005).

HUVEC were transiently transfected by electroporation at 200 V and 975  $\mu$ F using a Gene Pulser (Bio-Rad Labs, Hercules, CA) with 20  $\mu$ g of each DNA construct, or using lipofectin (Invitrogen) according to the manufacturer's protocol. Transfected cells were grown to confluence for 24-48 h on glass-bottomed dishes (WillCo Wells, Amsterdam, The Netherlands) pre-coated with fibronectin (FN) (Sigma) (20  $\mu$ g/ml). Cells were activated with TNF- $\alpha$  for 20 h and subsequently used for FRAP, FLIM-FRET or FCS experiments.

### **Cell adhesion assays**

HUVEC were grown to confluence on coverslips pre-coated with FN (20  $\mu$ g/ml) and then activated with TNF- $\alpha$  (20 ng/ml) for 20 h. Medium was removed and K562 stable transfectants or T lymphoblasts, resuspended in 500  $\mu$ l of complete 199 medium, were added. Adhesion of K562 LFA-1 transfectants to activated HUVEC monolayers was assayed in the presence of 1mM  $Mn^{2+}$  to activate integrins. Where indicated, T lymphoblasts were treated with BIO5192 (10  $\mu$ g/ml) or BIRT377 (10  $\mu$ M) for 5 min before adhesion assays. After incubation (5-10 min for lymphoblasts, at least 30 min for K562 cells), samples were washed and fixed with 4% paraformaldehyde and processed for immunofluorescence analysis.

Alternatively, TNF- $\alpha$ -activated HUVEC were incubated for 30 min with dynabeads coated with anti-tetraspanin, anti-VCAM-1 or anti-VE-cadherin mAb (DynaL Biotech ASA, Oslo, Norway), and then fixed and stained with biotinylated anti-ICAM-1 mAb.

### **Sucrose density gradient fractionation**

Confluent TNF- $\alpha$ -activated HUVEC were rinsed with phosphate-buffered saline (PBS) and lysed for 20 min in 250  $\mu$ l of 25 mM Tris-HCl, pH 7.5, 150 mM NaCl, 1 % Brij96 at 4°C. The cell lysate was homogenized by passing the sample through a 22-gauge needle. The extract was brought to 40% sucrose (w/w) in a final volume of 4 ml and placed at the bottom of an 8-ml 5-30% linear sucrose gradient. Gradients were ultracentrifuged to equilibrium for 20 h at 39,000 rpm at 4°C in a Beckman SW41 rotor (Beckman Coulter, Fullerton, CA). Fractions (1ml) were harvested from the bottom of the tube. Aliquots from each fraction were subjected to SDS-PAGE and Western blot with appropriate Abs.

### **Immunofluorescence and confocal microscopy**

Immunofluorescence was carried out as previously described (Yanez-Mo et al., 1998). Rhodamine Red-X-Streptavidin and Alexa Fluor 488 highly cross-adsorbed goat anti-mouse IgG (H+L) were used as fluorescent reagents (Molecular Probes, Eugene, OR). Series of optical sections were obtained with a Leica TCS-SP1, SP2 or SP5 confocal laser scanning unit (Leica Microsystems, Heidelberg, Germany), using a 63x oil or glycerol immersion objective (NA: 1.4 or 1.3, respectively). Image analysis was performed with Leica Confocal Software.

### **Fluorescence Recovery after Photobleaching**

Cells transfected with EGFP-fusion proteins (VCAM-1-, ICAM-1-, CD9-, CD151-, ICAM-1 $\Delta$ Cyt-, GPI-EGFP) were plated on 25mm glass coverslips coated with 20  $\mu$ g/ml of FN. After 24h, cells were stimulated with 20 ng/ml TNF- $\alpha$  in the presence

or absence of CD9-LEL-GST and FRAP experiments were performed before 48h after plating. To analyse FRAP at the endothelial docking structure, an adhesion assay was conducted under static conditions using K562 cells expressing VLA-4 ( $\alpha 4\beta 1$ ) or LFA-1 ( $\alpha L\beta 2$ ) at the plasma membrane. Live-cell microscopy was performed with a Leica SP2 laser scanning confocal microscope using the 488-nm Ar laser line and an X 63 glycerol objective. During the observation period, plates were maintained at 37°C in a 5% CO<sub>2</sub> atmosphere using an incubation system (La-con GBr Pe-con GmbH). Laser power for bleaching was maximal, whereas it was attenuated to 10% of the bleach intensity for imaging. Ten single-section prebleach images were acquired, followed by three iterative bleach pulses of 1.686 sec each. Then, ten single-section images were collected at 1.686 sec intervals, followed by 20 images collected every 10 sec and, finally, 15 images every 30 sec for a total experimental time of 650 sec approx.

Fluorescence recovery in the bleached region was measured as average signal intensity. Although the size of the measured region was dependent on docking structure dimension, it was very homogenous. Signal loss in unbleached regions during the recovery period was less than 5 % of the initial fluorescence signal. All recovery curves were generated from background-subtracted and bleaching-corrected images. Fluorescence signal measured in a region of interest (ROI) was normalized to the prebleach signal in the same ROI.

The mobile fraction (Mf) corresponds to the final value of the recovered fluorescence intensity, and the immobile fraction is obtained as 1-Mf. The half-time of recovery is the time from the bleach to the time point where the fluorescence intensity reaches the half of the final recovered intensity. All these three variables were directly obtained from the normalized mean fluorescence recovery curves. To assess the statistical significance of differences found between two given

families of curves characterized by measurements at identical time-points, a point-to-point comparison based on a Student's t-test was implemented. The Benjamini and Hochberg (BH) method (Benjamini and Hochberg, 1995) was employed to control for the false discovery rate associated with multiple testing. The analysis was accomplished using R (R Development Core Team, 2006). A representative example of statistical analysis is shown in Suppl. Fig. 3.

### **Hetero-fluorescence resonance energy transfer by donor fluorescence lifetime imaging microscopy in intact living cells**

HUVEC were single transfected with different mEGFP standards or co-transfected with combinations of mEGFP-mRFP1 pairs and seeded on FN-coated glass-bottomed Petri-dishes as described above. After 24h, and without TNF- $\alpha$  treatment, culture medium was replaced with phenol red-free medium for optimal image acquisition. FLIM was performed using a laser scanning microscope assembled at the Laboratory for Fluorescence Dynamics, (Irvine, CA, USA) using the photon counting regime of the photomultiplier detector in conjunction with time-resolved frequency-domain data acquisition hardware (Colyer et al., submitted). The data is processed automatically by software which accumulates a phase histogram of photon counts across the cross-correlation period, and then automatically calculates the phase and modulation of the emission. From the phase and modulation, the fluorescence lifetime ensembles in live cells was analyzed using the phasor-FLIM approach recently described (Digman et al., submitted; Caiolfa et al., 2007). The system was based on an Olympus Fluoview 1000 microscope, connected to a modulated ISS 471nm diode laser and equipped with a 470 +/- 5 nm excitation filter and a BA 505-525 nm emission filter

(ISS Inc., Champaign, IL, USA). The laser was guided into the microscope by x-y galvano-scanner mirrors (Model 6350; Cambridge Technology, Watertown, MA), driven in a raster scan movement using the ISS 3-axis card (ISS, Inc. Champaign, IL) and synchronized with data acquisition with a Becker and Hickl SPC830 card. Data were acquired and processed by the SimFCS software developed at the LFD. A photomultiplier tube (R7862, Hamamatsu Photonics, Battlesboro, NJ) was used for the detection in the photon counting mode. The objective was a 40X water immersion (Zeiss, Germany) with 1.2 N.A. The scan area (256x256 pixels) corresponds to 32x32  $\mu\text{m}^2$ . Before measurement, a slide with concentrated fluorescein at pH 9 was measured. The lifetime of fluorescein, 4.04 ns, was determined separately in an ISS Inc fluorometer.

### **Fluorescence Correlation Spectroscopy**

Endothelial cells were transiently single or double transfected as for FLIM analysis. The dual-channel confocal fluorescence correlation spectrometer, ALBA (ISS Inc., Champaign, IL, USA), was equipped with avalanche photodiodes and interfaced to a Nikon TE2000 inverted microscope equipped with a dichroic set C-74610 (z488/594 dbx z488/594rpc) + emission filter z 488/594m (Chroma Technology, USA). The objective used was a 60X Plan Apo (1.2 NA, water immersion). Excitation at 488 nm was provided by a tunable argon ion laser (Melles Griot, USA) and at 594 nm by a HeNe Laser (Melles Griot, USA). The diameter and power of the two beams were controlled by the ISS laser launcher system. The two laser lines were combined by a suitable external dichroic mirror (Chroma Technology, USA). Inside the ALBA box an additional dichroic (Chroma Technology, USA) separated the mRFP1 and mEGFP

emissions in the two channels (set C74612 (570 dclp, 520/30m, 610 lp). Every day, the power of the light passing through the objective in the absence of any immersion liquid was adjusted to 1 microW. An x,y,z computer-controlled piezoelectric actuator with a step resolution of less than 50 nm warranted the nanometric positioning. An ISS acquisition card received the data stream from the detectors. Data were stored for further processing by VISTA (ISS Inc.) and simFCS (LFD). Acquisition was in time-mode, and sampling frequency was 20 kHz. The waist ( $\omega_0$ ) of the excitation beam was calibrated before each day's experiments using Rhodamine 110 at 488 nm and Sulphorhodamine at 594 nm. Typical  $\omega_0$  values were 0.34-0.38  $\mu\text{m}$ .

The autocorrelation functions (ACFs) were best-fitted using the anomalous diffusion model (Banks and Fradin, 2005), according to the equation:

$$G(\tau) = \frac{1}{N} \cdot \frac{1}{1 + \left(\frac{\tau}{\tau_D}\right)^\alpha}$$

where N is the average number of molecules in the excitation volume,  $\tau_D$  is the diffusion time, and  $\alpha$  is the anomaly coefficient.

Accordingly, the diffusion coefficient (D) is derived from the relationship:

$$D = \omega^2 / 4\tau^\alpha$$

### **Scanning electron microscopy**

Endothelial monolayers were activated for 20h with TNF- $\alpha$  20 ng/ml in the absence or presence of 250  $\mu\text{g/ml}$  of active or heat-inactivated (5 min, 90°C) CD9-LEL-GST peptide. Cells were then fixed in 2% paraformaldehyde in PBS and subjected to regular immunolabeling with P8B1 (anti-VCAM-1), Hu5/3 (anti-ICAM-1) or biotinylated MEM-111 (anti-ICAM-1) as primary antibodies and 40 nm gold-coupled

anti-mouse antibody or 15 nm gold-coupled streptavidin (BBIInt.) as detection reagents. After immunolabeling, samples were fixed in 2.5% glutaraldehyde in PBS and then dehydrated by sequential passages through 30, 50, 70, 90%, and absolute ethanol. The ethanol was substituted by liquid CO<sub>2</sub>, and the specimens were critical-point dried using a Polaron E3000 apparatus. Then, samples were transferred onto appropriate microscope slides and covered with a carbon layer up to 5 nm using a high vacuum evaporator (Edwards 12E6/1266). Images were obtained with a Hitachi S-4100 scanning electron microscope at an acceleration voltage of 12kV and a working distance of 4mm. Images were processed with Metamorph software (Universal Imaging Corporation, Molecular Devices Corporation, Downingtown, PA). Receptor clustering was evaluated by nearest neighbour analysis using a custom-written software based on R software. The developed method allowed us to establish similarities and discrepancies between different treatments in terms of aggregation and dispersion of the objects (gold particles) in the images.

### **Statistical Analysis**

All statistical analyses were performed with R software or GraphPad Prism (GraphPad Software Inc., San Diego, CA).

## RESULTS

### **Endothelial ICAM-1 and VCAM-1 cluster at the docking structure independently of counterreceptor engagement and actin anchorage**

At contacts with adherent leukocytes, activated endothelial cells form three-dimensional actin-based docking structures which cluster endothelial VCAM-1 and ICAM-1. To analyze the mechanisms regulating the dynamic recruitment of adhesion molecules to these endothelial docking structures, we induced their formation with K562 leukocytes stably expressing either  $\alpha 4\beta 1$  (K562  $\alpha 4$ ) or  $\alpha L\beta 2$  (K562 LFA-1) integrins, which adhere to activated endothelial cells exclusively via VCAM-1 or ICAM-1, respectively. Remarkably, both ICAM-1 and VCAM-1 clustered at the docking structure formed around both types of K562 transfectant cells, regardless of whether they were directly engaged by their corresponding integrin receptor (Fig. 1A). Furthermore, similar co-recruitment effects were observed in a more physiological setting, in which lymphoblasts, which express significant amounts of LFA-1 and VLA-4, were treated with specific inhibitors of either LFA-1 (BIRT377) or VLA-4 (BIO5192) (Fig. 1B).

To assess the extent to which this ligand-independent adhesion molecule clustering is dependent on the actin cytoskeleton, we transiently transfected resting HUVEC with a cytoplasmic tail-truncated mutant of VCAM-1 (VCAM $\Delta$ Cyt). Under these conditions, HUVEC bear low levels of ICAM-1 and negligible levels of endogenous VCAM-1. Upon engagement of VCAM $\Delta$ Cyt by either K562  $\alpha 4$  cells or anti-VCAM-1 coated beads, discrete clusters containing VCAM $\Delta$ Cyt and ICAM-1 were observed around adhered cells, but in no case was a well developed three-dimensional structure formed (Fig. 1C and data not shown). In contrast, when ICAM-1

was directly engaged by K562  $\alpha$ L $\beta$ 2 transfectants, a proper docking structure was formed, also containing VCAM $\Delta$ Cyt (Fig. 1C). These data indicate that the engagement of one endothelial adhesion receptor (ICAM-1 or VCAM-1) by its corresponding leukocyte integrin is sufficient to induce the co-recruitment of the other endothelial receptor towards the contact area with the leukocyte. This co-clustering must involve the extracellular and/or transmembrane domains of both adhesion molecules, because it occurs with cytoplasmic-truncated forms. However, the subsequent reorganization of the endothelial actin cytoskeleton into the protrusive cup depends on actin anchorage of the cytoplasmic tail of the endothelial adhesion molecule bound to its ligand, as indicated by quantitative analysis of the formation of VCAM-1-mediated docking structures in VCAM-1wt- vs. VCAM-1 $\Delta$ Cyt-transfected resting HUVEC (50.33% vs. 6%, respectively).

### **Analysis of ICAM-1 and VCAM-1 hetero- and homo-dimers in living endothelial cells**

Since cytoskeletal anchorage cannot account for adhesion receptor co-recruitment, we investigated the potential formation of VCAM-1/ICAM-1 heterodimers at the apical membrane of intact, living primary endothelial cells. This analysis was based on hetero-FRET, assessed by the donor fluorescence lifetime quenching in TCSPC-FLIM measurements. We generated functional VCAM-1 and ICAM-1 chimaeras fused to monomeric enhanced green (mEGFP, donor, termed also green) or red (mRFP1, acceptor, termed also red) fluorescent proteins (Campbell et al., 2002; Zacharias et al., 2002). The spontaneous dimerization of EGFP, which could interfere with “bona fide” protein-protein interactions, was avoided by introducing the A206K point mutation in the sequence. The constructs were transiently co-transfected into primary HUVEC

under resting conditions, to prevent up-regulation of endogenous VCAM-1 and ICAM-1 expression and thus minimize possible interference that might decrease the efficiency of dimer formation by exogenous molecules. We analyzed the percentage of FRET efficiency (FRET<sub>eff</sub>) of the following pairs: ICAM-1mEGFP/ICAM-1mRFP1, VCAM-1mEGFP/VCAM-1mRFP1, ICAM-1mEGFP/VCAM-1mRFP1 and VCAM-1mEGFP/ICAM-1mRFP1, comparing the fluorescence lifetime of the donor (mEGFP construct) in each co-transfection with that of ICAM-1mEGFP or VCAM-1mEGFP in single transfections. Representative experiments are shown in Fig. 2 and Supplemental Figure 1 (for donor standards). For each donor/acceptor pair in Figure 2, the fluorescence intensity image (in pseudocolour scale), phasor plots and the corresponding FLIM images (pink mask) are shown. As previously described (Caiolfa et al., 2007) for this representation, the fluorescence decay of the donor molecule in each pixel of the image gives a point in the phasor plot. The ensemble of these donor phasors is represented as contour plot. This plot can be scanned by software (Digman et al., submitted) for localizing in the image pixels at high as well as low FRET<sub>eff</sub>. The black circle in the phasor plot selects a sub-population of pixels in which similar FRET efficiencies were observed, and highlights them in the correspondent image. For the ICAM-1-mEGFP/ICAM-1-mRFP1 pair depicted in Fig. 2, the majority of pixels do not show significant FRET (selection average  $\leq 8\%$  FRET). However, a small 16% of the pixels in the image, do show FRET efficiency in the range of  $24 \pm 8\%$  (fairly above the detection limit of the FRET analysis), which are localized in clusters at the membrane. We analyzed 4 replicate experiments and obtained average FRET efficiencies in the range from 5 to 15.5 in 65% of clustered pixels. In contrast, the other pairs of proteins, VCAM-1-mEGFP/VCAM-1-mRFP1, ICAM-1-mEGFP/VCAM-1-mRFP1 and VCAM-1-mEGFP/ICAM-1-mRFP1, did not show any significant quenching of the donor

fluorescence lifetime (i.e., FRET) (Fig. 2), as compared to the phasor distribution of “pure” donor control cells (Suppl. Fig. 1). This analysis demonstrates that, under these conditions, VCAM-1/VCAM-1 homodimers and VCAM-1/ICAM-1 heterodimers are absent from the plasma membrane.

These data thus suggest a separate organization of VCAM-1 and ICAM-1 at the plasma membrane, excluding the formation of VCAM-1/ICAM-1 heterodimers as a prerequisite for the recruitment of one of these receptors to the docking structure in the absence of integrin engagement and cytoskeleton anchorage.

### **Tetraspanin microdomains mediate the association of endothelial adhesion receptors to form specialized endothelial adhesive platforms**

Since ICAM-1 and VCAM-1 co-clustering at the docking structure is dependent on their extracellular and/or transmembrane domains, but does not result from direct interaction, we examined the possible intermediary involvement of tetraspanin proteins. Several tetraspanins, such as CD9 and CD151, are concentrated at docking structures around primary human leukocytes together with VCAM-1 and ICAM-1, and can co-precipitate with these endothelial adhesion receptors (Barreiro et al., 2005). Tetraspanin proteins were also recruited to docking sites in the K562  $\alpha$ 4 and LFA-1 adhesion models (Supplemental Fig. 2). However, no specific tetraspanin ligand has been described in leukocytes. Furthermore, ICAM-1 and VCAM-1 were both recruited when either CD9 or CD151 was engaged with specific antibodies coupled to magnetic beads. In parallel, anti-VCAM-1- and anti-ICAM-1-coated beads were also able to cluster each other and the tetraspanins, whereas anti-VE-cadherin-coated beads did not induce significant recruitment of ICAM-1, VCAM-1 or tetraspanins above basal levels (Fig. 3A, quantified in Fig. 3B, and data not shown).

To assess the relationship between endothelial adhesion molecules and tetraspanin microdomains in more detail, Brij96 lysates of TNF- $\alpha$ -activated HUVEC were fractionated on a continuous 5-40% sucrose gradient. Most tetraspanins were soluble under these conditions and migrated with the heavy fractions (F1-F7) together with ICAM-1 and VCAM-1, which were not found in fractions containing caveolin (used as a marker of detergent-resistant membrane fractions, containing lipid rafts) (Fig. 3C). These results suggest that endothelial tetraspanin microdomains, containing VCAM-1 and ICAM-1 adhesion receptors, clearly stand apart from classical biochemically-defined lipid rafts and are in fact distinct organized membrane structures, which we term endothelial adhesive platforms (EAP).

### **Diffusional properties of endothelial adhesive platforms at nude membrane and at docking structures**

Experimental evidence for the existence of tetraspanin microdomains is mainly based on biochemical approaches or microscopy techniques that analyze fixed cells (Claas et al., 2001; Min et al., 2006; Nydegger et al., 2006). In an attempt to demonstrate the existence of tetraspanin-based EAP in living cells, as physical entities with specific molecular dynamic features distinct from lipid rafts, we made use of the fluorescence recovery after photobleaching (FRAP) technique. First, we analyzed the dynamic behaviors of EGFP-tagged versions of CD9, CD151, VCAM-1 and ICAM-1 at the apical plasma membrane of primary HUVEC and compared these behaviors with that of GPI-EGFP, used as a lipid raft marker (Kenworthy et al., 2004; Sharma et al., 2004) (Fig. 3D). Quantification of recovery half-time data indicated that tetraspanin CD9 and CD151 diffuse 2-3 times more slowly than GPI-EGFP, and that VCAM-1 and ICAM-1 are even slower (3-4 times longer recovery half-time as compared with GPI-

EGFP) (Fig. 3E). The differences observed between the diffusional behaviors of tetraspanin proteins and endothelial adhesion receptors might be due to differential anchorage to the actin cytoskeleton. To examine this possibility, we analyzed the dynamics of a C-terminally truncated EGFP-tagged ICAM-1 protein, ICAM-1 $\Delta$ Cyt-EGFP, which lacks the cytoplasmic domain and, therefore, lacks actin-cytoskeleton linking activity (Fig. 3F). This truncated ICAM-1, freed of cytoskeletal constraints, diffused more rapidly than the full-length receptor. Furthermore, ICAM-1 $\Delta$ Cyt-EGFP diffused faster than CD9, but in this case the difference was not significant, strengthening the notion of EAP as organized lateral-association domains at the plasma membrane.

To assess the influence of leukocyte adhesion on the dynamic behaviour of each EAP component, FRAP was used to examine endothelial docking structures induced by binding of  $\alpha 4^+$ - or LFA-1 $^+$ -K562 cells (Fig. 4A). The most notable effects were that, when endothelial adhesion receptors were dynamically and specifically bound to their ligands, a greater proportion were included in the immobile fraction and the mobility of the mobile fraction was retarded (Fig. 4B and C, for ICAM-1 and VCAM-1, respectively, as well as Suppl. Fig. 3B). The rest of EAP components analyzed were affected to a lesser extent, exhibiting a variable slow-down in fluorescence recovery compared with the FRAP analyses of the same molecules at other regions of the plasma membrane (Suppl. Fig. 3). Statistical analyses showed that the effect on CD9 mobility was greater upon engagement of ICAM-1, while CD151 was more affected by engagement of VCAM-1 (Numerical data on Fig. 4B and C). These data thus reveal a degree of specificity among tetraspanin-partner interactions within the endothelial tetraspanin microdomains. In contrast, GPI-EGFP diffusion was not altered at docking structures (data not shown).

The tailless ICAM-1 mutant IC1 $\Delta$ Cyt-EGFP showed a faster fluorescence recovery rate than the wild-type molecule at docking sites with LFA-1<sup>+</sup>-K562 cells, which indicates that stabilization of the interaction between ICAM-1 and LFA-1 also occurs on the endothelial side, by the anchorage of ICAM-1 to the F-actin cytoskeleton (Fig. 4D).

### **Diffusional characteristics of individual endothelial adhesive platform constituents determined by FCS and FCCS single-molecule measurements**

Because of technical limitations of FRAP, we could not accurately measure the diffusion coefficients of EAP components, which exhibit an anomalous diffusion because of cytoskeleton and ligand binding constraints. To overcome this limitation, we applied fluorescence correlation spectroscopy (FCS) on fluorescent protein-tagged ICAM-1, VCAM-1, CD9 and CD151 expressed in primary human living endothelial cells (Fig. 5A). The autocorrelation functions were always best-fitted using the anomalous diffusion model (see Materials and Methods section). The range of the diffusion ( $D$ ) and anomaly ( $\alpha$ ) coefficients was similar for all tested proteins (Fig. 5B). Nevertheless, the analysis in Fig. 5B indicates that, the diffusion of VCAM-1 and ICAM-1 is overall slower than that of CD9 and CD151. Hence, the FCS measurements of each individual EAP component was in agreement with previous FRAP analyses, indicating that tetraspanins are characterized by faster lateral mobility than adhesion receptors. Further analyses will be performed to sub-classify the results as corresponding to fast and slow molecular subsets. On the other hand, most of the  $D$  coefficients obtained for all these proteins are much slower than those reported for prototypic lipid raft proteins (Lenne et al., 2006). Finally, evidence of dynamic

membrane complexes containing several EAP constituents was attained by fluorescence cross-correlation spectroscopy, as shown in Suppl. Fig. 4.

### **Complexity of inter-molecular interactions within endothelial adhesive platforms**

The colocalization studies previously performed with a conventional spectral confocal microscope, which has an optical resolution limit of 200-250 nm, cannot allow us to further discriminate between direct and indirect interactions within EAP. To explore the complex inter-relationships which might take place within the endothelial adhesive platforms and could account for the recruitment of adhesion receptors, we extended the FLIM-FRET analysis to determine whether direct associations occur among CD9, CD151, ICAM-1 and VCAM-1 molecules. First, we confirmed the formation of tetraspanin homo- and heterodimers (CD9mEGFP-CD9mRFP1 and CD9mEGFP-CD151mRFP1) (Fig. 6A), which was previously suggested mainly on the basis of biochemical studies (Hemler, 2005). We then assessed the direct association of tetraspanins with their endothelial partners. Again, a certain degree of specificity was found inside the microdomains, indicating that CD9 preferentially interacted with ICAM-1 and CD151 with VCAM-1; moreover, the FRET efficiencies of these associations were close to those of tetraspanin pairs (Fig. 6B). In contrast, VCAM-1/CD9 and ICAM-1/CD151 pairs exhibited low occurrence of high FRET<sub>eff</sub>, and FRET in the remaining pixels of the cell was very close to the detection threshold of the technique (data not shown). Control experiments examining interaction between ICAM-1 and uPAR, a cell-surface receptor related to lipid rafts, showed the absence of interaction between these two molecules from distinct membrane microdomains (Suppl. Fig. 1B). These results confirm the suggested specific intra-domain interactions in EAP observed in FRAP analysis and in the fluorescence cross-correlation measurements.

## **Modulation of nanoclustering and diffusion within the endothelial adhesive platforms by tetraspanin blocking peptides**

The spatial organization of VCAM-1 and ICAM-1 receptors at the plasma membrane of endothelial cells was studied by immunogold labeling combined with scanning electron microscopy (SEM) (Fig. 7A i). Both ICAM-1 and VCAM-1 form heteroclusters at the plasma membrane (Fig. 7A ii), and localized higher-density clustering was found at the microvilli of docking structures around adherent leukocytes, as shown for ICAM-1 (Fig. 7A iii).

To shed light on the mechanism that controls the tetraspanin-mediated co-clustering of adhesion receptors at the apical plasma membrane of endothelial cells, we used a tetraspanin-derived blocking peptide (CD9-LEL-GST). This soluble peptide interferes with the various functions regulated by CD9-containing tetraspanin microdomains, such as egg-sperm fusion or HIV infection (Ho et al., 2006; Zhu et al., 2002), and decreases VCAM-1- and ICAM-1-mediated lymphocyte adhesion strength and transmigration under flow conditions (Barreiro et al., 2005). Although the functional effect of these peptides has been well documented, there have been no reported insight into the molecular mechanism through which CD9-LEL-GST exerts its inhibitory action. Nearest neighbour analysis of immunogold-labeled adhesion receptors in the presence of CD9-LEL-GST showed that receptor spacing augmented in comparison with samples treated with heat-inactivated CD9-LEL-GST. This effect might be due to the insertion of functional blocking peptides within the EAP, competing with endogenous CD9 for association with partners (Fig. 7B). Consistently, FCS analysis revealed that the CD9-LEL peptide, but not heat-inactivated CD9-LEL, decreased the diffusion coefficient of CD9mEGFP molecules. Furthermore, the

diffusion coefficient of CD151 was also affected, showing that blocking peptide insertion in EAP modifies the general dynamics within the platforms due to the increasing molecular crowding (Fig. 7C). Together these data suggest that the blocking peptide compete with endogenous CD9 for binding to partners and other tetraspanins. This prevents adequate interactions and imposes steric hindrance, resulting in a net slower diffusion and reduced receptor clustering.

## **DISCUSSION**

### **Endothelial adhesive platforms as a model for the biophysical study of tetraspanin-enriched microdomains**

The existence of organized membrane domains distinct from those based on lipid-protein interactions (lipid rafts) has not been demonstrated previously in living cells. Biochemical analysis and microscopy studies on fixed samples have indicated that a network of specific protein-protein interactions may occur at cell membranes between tetraspanin members and associated partners (Levy and Shoham, 2005a). In the current study, we have used an array of cutting-edge analytical microscopy and spectroscopy techniques, including single molecular analysis, to characterize in depth the dynamic features and biophysical properties of TEM in living cells. The transiently transfected primary human endothelial cells used in this study are a physiologically relevant cell model that expresses an appropriate repertoire of membrane tetraspanins and adhesion receptors. In addition, the study of four proteins in combination, two tetraspanins and two essential endothelial adhesion receptors, provides a valuable global overview of the behavior of the specialized type of TEM named endothelial adhesive platforms (EAP).

Endogenous expression of CD9 and CD151 tetraspanins and ICAM-1 and VCAM-1 adhesion receptors in endothelial cells reduces the probability of interaction between transiently-transfected tagged proteins in the FLIM-FRET analyses. To minimize this problem, FLIM quantifications were performed in resting HUVEC, in which tetraspanin expression is unaltered, ICAM-1 levels are low and VCAM-1 expression at plasma membrane is negligible. Given that the expression of CD151 and, especially, CD9 is much higher than ICAM-1 in resting cells, it is possible that FRET<sub>eff</sub> values from measurements involving tetraspanin proteins might be underestimated. Furthermore, in the case of CD9, CD151 and ICAM-1, which are able

to homodimerize, the possible association of two green or two red molecular species makes the occurrence of heteroFRET even more improbable. Finally, another potential problem, dimerization of chimeric proteins through their fluorescent tags, was overcome by using monomeric versions of EGFP and mRFP1. Despite the drawbacks of FRET analysis in complex living cell systems, high FRET<sub>eff</sub> was detected for ICAM-1/CD9, VCAM-1/CD151, CD9/CD9, CD9/CD151 and ICAM-1/ICAM-1 pairs and clear-cut differences were detected with respect to non-interacting pairs (VCAM-1/ICAM-1, VCAM-1/VCAM-1). Examination of average FRET<sub>eff</sub> values and the percentage of pixels exhibiting the highest FRET<sub>eff</sub> values for each pair showed that tetraspanin homo- and heterodimers and tetraspanin-partner interactions occur preferentially compared with ICAM-1 dimers, strengthening the concept of EAP as the basic organization of endothelial adhesion receptors on the endothelial apical plasma membrane. In fact, the existence of ICAM-1 dimers had been described before as a small proportion from the whole molecular ICAM-1 population using biochemical approaches (Miller et al., 1995). Besides, BIAcore affinity measurements revealed that a single ICAM-1 monomer, not dimeric ICAM-1, represents the complete, fully competent LFA-1-binding surface (Jun et al., 2001).

The innovative technique used to quantify FRET was completely independent of the concentration of fluorescent species, and is therefore well-suited to analyze and compare data from different transient transfections. Furthermore, the FLIM-FRET approach permitted us to spatially resolve the fretting population within a whole cell, generally yielding a patchwork pattern for the higher FRET<sub>eff</sub> population. To further substantiate the experimental data on the absence of ICAM-1-VCAM-1 heterodimer formation, ICAM-1 or VCAM-1 was indistinctly used as donor in FLIM-FRET experiments. We inverted the labeling fluorophores on the two receptors, showing that

the lack of FRET was not due to artifacts introduced by the fluorescent constructs. Additional control experiments also demonstrated that the protein in the mEGFP constructs affects negligibly the fluorescence lifetime distribution of the fluorophore (i.e., the phasor distribution in phasor-FLIM analysis).

Finally, the observations that the GPI-anchored protein, uPAR, used as a marker of lipid rafts, did not interact with ICAM-1 (used as an EAP marker) in FLIM-FRET experiments, and that the two receptors were sorted to the plasma membrane in different vesicles (data not shown), further sustain the notion that tetraspanins might form discrete and specific microdomains at the cell membrane.

The diffusional behaviour of the EAP components was investigated by combining FRAP and FCS analyses. The possible perturbation of membrane dynamics that might result from exogenous expression of tagged proteins was overcome in FRAP experiments by making a large number of measurements in several batches of transiently-transfected primary cells and making an exhaustive statistical analysis of the data. Photobleaching experiments were all performed under pro-inflammatory conditions (TNF- $\alpha$  treatment) in order to promote proper formation of docking structures around adherent leukocytes mostly through the mediation of endogenous VCAM-1 or ICAM-1. Although the integrin-expressing K562 adhesion model used in our experiments is a simplification of the dynamic physiological firm adhesion process that takes place under hemodynamic flow conditions, this model has allowed us to perform diffusion analyses that would be unfeasible under more physiological but complex conditions.

FRAP analysis examines the diffusion rate of an overall molecular population within a microscopic area. These experiments have provided us with valuable information on the global diffusional behavior of VCAM-1, ICAM-1, CD9, CD151 and

GPI molecular subsets in comparable areas of nude membrane and at sites of leukocyte anchorage. A mixed steady-state molecular population (comprising proteins bound or unbound to cytoskeleton, coupled to partners, in the form of dimers, and so on) is considered for each measurement. From FRAP data collected at nude plasma membrane, we could distinguish differences in the net mobilities of tetraspanins and receptors. Tetraspanins showed the fastest diffusion rate, although this did not differ significantly from the rate for ICAM-1, whereas VCAM-1 population was slower and displayed a higher immobile fraction. The reason for this difference in diffusion behaviour between the two adhesion receptors remains still unsolved. Close interaction between ICAM-1 and CD9 is supported by the experiments with the C-terminally truncated ICAM-1, ICAM-1 $\Delta$ Cyt, which is unable to interact with the actin cytoskeleton via ERM proteins (Barreiro et al., 2002). The lateral mobility of ICAM-1 $\Delta$ Cyt-EGFP was not significantly different from that of CD9, supporting the notion that these molecules can interact in the absence of ICAM-1 cytoplasmic tail. Conversely, GPI-EGFP, a prototypic lipid raft- related molecule widely used in microscopy studies (Kenworthy et al., 2004; Varma and Mayor, 1998), moved much faster and its recovery was complete, with no significant immobile fraction. Moreover, the diffusion properties of CD9, CD151, ICAM-1 and VCAM-1 were altered in the context of docking structures, whereas GPI-EGFP is unaffected by engagement of integrin-bearing leukocytes. These observations strongly argue in favor of these proteins being constituents of physical entities with intrinsic properties and biophysical features distinct from classical lipid rafts.

The delay observed for non-ligand-engaged EAP components at the docking structures could be well due to their transient interaction with ligand-immobilized ICAM-1 or VCAM-1. In this way, these immobile complexes at docking sites could act

as physical constraints on the mobility of the overall molecular populations analyzed, which would produce a net reduction in diffusion rate (Suppl Fig. 3). The fact that VCAM-1 is no more affected than tetraspanins by ligand engagement of ICAM-1 supports a model in which VCAM-1 is co-recruited to ICAM-1/LFA-1-mediated docking structures as a result of both VCAM-1 and ICAM-1 being components of the EAP. The same argument is applicable to the recruitment of ICAM-1 into VCAM-1/VLA-4 induced docking structures.

Remarkably, our data show that CD9 mobility is more strongly affected by the engagement of ICAM-1, while CD151 is more affected by engagement of VCAM-1, confirming the results of previous biochemical analyses, in which ICAM-1 preferentially associated with CD9 and VCAM-1 associated with CD151 (Barreiro et al., 2005). FRET analysis confirmed a degree of specificity inside the preexisting EAP prior to leukocyte binding. The preferential interactions of ICAM-1 with CD9 and VCAM-1 with CD151 are evident in the FRETeff for these pairs, which are close to those of tetraspanin pairs, even though in tetraspanin-partner interactions there are fewer obstacles that can reduce FRETeff.

The diffusional analyses by FCS complemented the FRAP data. Thus, FRAP provided a general view of diffusion within EAP in the presence or absence of adherent leukocytes and in comparison with lipid rafts at a microscopic level, and FCS allowed us to move toward the nanoscopic scale to precisely determine diffusion coefficients of EAP proteins at the single-molecule level. The amounts of exogenously expressed fluorescently-labeled proteins on the surface of cells used for FCS and FCCS analyses was negligible compared with the corresponding endogenous proteins, assuming that there were no alterations in dynamic behaviour due to increased molecular density at the membrane. However, the existence of a mixture of endogenous and exogenous

protein populations precludes determination of the stoichiometry of submicron-size endothelial tetraspanin domains, even though the FCCS studies did provide insights into the lifespan of tetraspanin-partner complexes.

In conclusion, this study performed with this particular type of TEM from the apical membrane of endothelium constitutes the first description of tetraspanin microdomains as physical entities in living cells, with dynamic features that clearly differ from lipid rafts.

### **Regulation of the avidity of endothelial adhesion receptors by their inclusion in tetraspanin-enriched endothelial adhesive platforms**

It is a common error to assume that the demonstration of co-localization of molecules at the microscopic level provides irrefutable evidence of spatial association; the optical resolution limit of classical confocal fluorescence microscopy techniques falls far short that required to identify molecular interactions that take place over a distance of few nanometers. Our data from advanced microscopy techniques demonstrate that the co-localization of two tetraspanins and two receptors at the nude endothelial apical plasma membrane and at specialized adhesive structures does indeed correspond to highly specific and organized interactions among them. Furthermore, this organization confers the appropriate spatial distribution for ICAM-1 and VCAM-1 receptors to exert their efficient adhesion functions.

The regulation of leukocyte integrin activity has been extensively characterized. These proteins can be regulated by conformational changes (affinity) and/or clustering at the plasma membrane (avidity) (Carman and Springer, 2003; Luo et al., 2007). In contrast, no regulatory mechanism, apart from the transcriptional level, has been described previously for the adhesive function of endothelial integrin ligands (Collins

et al., 1995). Our study thus provides novel insights into adhesion receptor regulation, showing how the insertion of two key endothelial receptors, ICAM-1 and VCAM-1, into tetraspanin-enriched microdomains promotes the homo- and hetero-clustering of both molecules at the contact area with the adhered leukocyte, independently of ligand binding and actin cytoskeleton anchorage. The tetraspanin-mediated clustering of endothelial receptors enhances firm adhesion, since disturbance of interactions using tetraspanin blocking peptides or alteration in composition by tetraspanin knock-down decreases the adhesive properties of VCAM-1 and ICAM-1 in transendothelial migration experiments performed under flow conditions and in detachment experiments under increasing shear flows (Barreiro et al., 2005). Whether ICAM-1 or VCAM-1 can undergo any conformational alteration due to their interaction with tetraspanins remains undetermined, in the absence of appropriate reagents to tackle this possibility.

The ability of tetraspanins to mediate the homo- and hetero-clustering of adhesion receptors, which is enhanced by integrin engagement, arises from their ability to laterally associate with each other and with non-tetraspanin partners simultaneously. Therefore, CD9 could promote ICAM-1 homo-avidity by interacting with other CD9 molecules bound to this receptor, whereas CD151 could reproduce the same effect with VCAM-1. Then, the hetero-clustering of ICAM-1 and VCAM-1 could be explained by the interaction of CD9 with CD151. The involvement of other tetraspanins in these organized microdomains cannot be ruled out; indeed, we have observed the inclusion of tetraspanin CD81 at EAP (Barreiro et al., unpublished observations). Conceptually, endothelial receptor homo-avidity would be similar to the avidity phenomenon described for their counter-receptors, the integrins  $\alpha 4\beta 1$ -VLA-4 (for VCAM-1) and  $\alpha L\beta 2$ -LFA-1 (for ICAM-1) integrins. In fact, a role has been reported for CD81 as homeostatic avidity facilitator of multivalent VLA-4 strengthening in the adhesion to

VCAM-1 (Feigelson et al., 2003). Therefore, it is also conceivable that such tetraspanin-mediated co-organization of specific VLA-4 and LFA-1 integrin subsets takes place within leukocyte membranes. Furthermore, the novel concept of hetero-clustering raised here for VCAM-1 and ICAM-1 can be envisaged as a kind of tetraspanin-mediated cross-talk between adhesion receptors; that is, a cellular mechanism to spatio-temporally organize molecules with similar characteristics and functions so as to facilitate their efficient co-ordinated action in critical processes such as extravasation, which occurs over a short time-frame. Moreover, VCAM-1 and ICAM-1 are unlikely to be the only receptors inserted in these tetraspanin microdomains at the apical endothelial plasma membrane; we have also identified other adhesion proteins such as CD44, PECAM-1 and, more importantly, E-selectin in association with EAP (Barreiro et al., unpublished observations). These organized membrane microdomains thus appear to integrate a plethora of adhesion receptors involved in subsequent steps of the extravasation process, and for this reason we have named them endothelial adhesive platforms. These organized platforms are dynamic, since they coalesce or diverge depending on the stimuli received (ligand engagement by tetraspanin partners, and so on).

In sum, our data clearly demonstrate that tetraspanin microdomains account for the specific recruitment of endothelial adhesion receptors to the leukocyte contact area, providing a mechanism to increase avidity at these sites and enhance firm adhesion. This constitutes a novel supramolecular level of regulation in the function of VCAM-1 and ICAM-1 endothelial receptors not envisaged previously for integrin ligands. In the light of these observations, new pharmacological agents that could specifically prevent the interaction of tetraspanin with endothelial adhesion receptors *in vivo* could

constitute novel therapeutical strategies for the treatment of chronic inflammatory and autoimmune diseases.

## REFERENCES

- Anderson, R. G., and Jacobson, K. (2002). A role for lipid shells in targeting proteins to caveolae, rafts, and other lipid domains. *Science* 296, 1821-1825.
- Andre, M., Le Caer, J. P., Greco, C., Planchon, S., El Nemer, W., Boucheix, C., Rubinstein, E., Chamot-Rooke, J., and Le Naour, F. (2006). Proteomic analysis of the tetraspanin web using LC-ESI-MS/MS and MALDI-FTICR-MS. *Proteomics* 6, 1437-1449.
- Banks, D. S., and Fradin, C. (2005). Anomalous diffusion of proteins due to molecular crowding. *Biophys J* 89, 2960-2971.
- Barreiro, O., Yanez-Mo, M., Sala-Valdes, M., Gutierrez-Lopez, M. D., Ovalle, S., Higginbottom, A., Monk, P. N., Cabanas, C., and Sanchez-Madrid, F. (2005). Endothelial tetraspanin microdomains regulate leukocyte firm adhesion during extravasation. *Blood* 105, 2852-2861.
- Barreiro, O., Yanez-Mo, M., Serrador, J. M., Montoya, M. C., Vicente-Manzanares, M., Tejedor, R., Furthmayr, H., and Sanchez-Madrid, F. (2002). Dynamic interaction of VCAM-1 and ICAM-1 with moesin and ezrin in a novel endothelial docking structure for adherent leukocytes. *J Cell Biol* 157, 1233-1245.
- Benjamini, Y., and Hochberg, Y. (1995). Controlling the false discovery rate: a practical and powerful approach to multiple testing. *J R Statist Soc B* 57, 289 – 300.
- Berdichevski, F. (2001). Complexes of tetraspanins with integrins: more than meets the eye. *J Cell Sci* 114, 4143-4151.
- Berdichevski, F., and Odintsova, E. (2007). Tetraspanins as regulators of protein trafficking. *Traffic* 8, 89-96.
- Butcher, E. C. (1991). Leukocyte-endothelial cell recognition: three (or more) steps to specificity and diversity. *Cell* 67, 1033-1036.
- Caiolfa, V. R., Zamai, M., Malengo, G., Andolfo, A., Madsen, C. D., Sutin, J., Digman, M., Gratton, E., Blasi, F., and Sidenius, N. (2007). Monomer-dimer dynamics and distribution of GPI-anchored uPAR are determined by cell surface protein assemblies. *J Cell Biol*.
- Campbell, R. E., Tour, O., Palmer, A. E., Steinbach, P. A., Baird, G. S., Zacharias, D. A., and Tsien, R. Y. (2002). A monomeric red fluorescent protein. *Proc Natl Acad Sci U S A* 99, 7877-7882.
- Carman, C. V., and Springer, T. A. (2003). Integrin avidity regulation: are changes in affinity and conformation underemphasized? *Curr Opin Cell Biol* 15, 547-556.
- Claas, C., Stipp, C. S., and Hemler, M. E. (2001). Evaluation of prototype transmembrane 4 superfamily protein complexes and their relation to lipid rafts. *J Biol Chem* 276, 7974-7984.
- Clayton, A. H., Hanley, Q. S., and Verveer, P. J. (2004). Graphical representation and multicomponent analysis of single-frequency fluorescence lifetime imaging microscopy data. *J Microsc* 213, 1-5.
- Collins, T., Read, M. A., Neish, A. S., Whitley, M. Z., Thanos, D., and Maniatis, T. (1995). Transcriptional regulation of endothelial cell adhesion molecules: NF-kappa B and cytokine-inducible enhancers. *Faseb J* 9, 899-909.
- Charrin, S., Manie, S., Thiele, C., Billard, M., Gerlier, D., Boucheix, C., and Rubinstein, E. (2003). A physical and functional link between cholesterol and tetraspanins. *Eur J Immunol* 33, 2479-2489.

Chattopadhyay, N., Wang, Z., Ashman, L. K., Brady-Kalnay, S. M., and Kreidberg, J. A. (2003).  $\alpha 3\beta 1$  integrin-CD151, a component of the cadherin-catenin complex, regulates PTPmu expression and cell-cell adhesion. *J Cell Biol* *163*, 1351-1362.

Cherukuri, A., Shoham, T., Sohn, H. W., Levy, S., Brooks, S., Carter, R., and Pierce, S. K. (2004). The tetraspanin CD81 is necessary for partitioning of coligated CD19/CD21-B cell antigen receptor complexes into signaling-active lipid rafts. *J Immunol* *172*, 370-380.

Delaguillaumie, A., Harriague, J., Kohanna, S., Bismuth, G., Rubinstein, E., Seigneuret, M., and Conjeaud, H. (2004). Tetraspanin CD82 controls the association of cholesterol-dependent microdomains with the actin cytoskeleton in T lymphocytes: relevance to co-stimulation. *J Cell Sci* *117*, 5269-5282.

Feigelson, S. W., Grabovsky, V., Shamri, R., Levy, S., and Alon, R. (2003). The CD81 tetraspanin facilitates instantaneous leukocyte VLA-4 adhesion strengthening to vascular cell adhesion molecule 1 (VCAM-1) under shear flow. *J Biol Chem* *278*, 51203-51212.

Fujita, Y., Shiomi, T., Yanagimoto, S., Matsumoto, H., Toyama, Y., and Okada, Y. (2006). Tetraspanin CD151 is expressed in osteoarthritic cartilage and is involved in pericellular activation of pro-matrix metalloproteinase 7 in osteoarthritic chondrocytes. *Arthritis Rheum* *54*, 3233-3243.

Garcia-Lopez, M. A., Barreiro, O., Garcia-Diez, A., Sanchez-Madrid, F., and Penas, P. F. (2005). Role of tetraspanins CD9 and CD151 in primary melanocyte motility. *J Invest Dermatol* *125*, 1001-1009.

Gordon-Alonso, M., Yanez-Mo, M., Barreiro, O., Alvarez, S., Munoz-Fernandez, M. A., Valenzuela-Fernandez, A., and Sanchez-Madrid, F. (2006). Tetraspanins CD9 and CD81 modulate HIV-1-induced membrane fusion. *J Immunol* *177*, 5129-5137.

Gratton, E., Jameson, D. M., and Hall, R. D. (1984). Multifrequency phase and modulation fluorometry. *Annu Rev Biophys Bioeng* *13*, 105-124.

Hakomori, S. I. (2002). Inaugural Article: The glycosynapse. *Proc Natl Acad Sci U S A* *99*, 225-232.

Hemler, M. E. (2001). Specific tetraspanin functions. *J Cell Biol* *155*, 1103-1107.

Hemler, M. E. (2003). Tetraspanin proteins mediate cellular penetration, invasion, and fusion events and define a novel type of membrane microdomain. *Annu Rev Cell Dev Biol* *19*, 397-422.

Hemler, M. E. (2005). Tetraspanin functions and associated microdomains. *Nat Rev Mol Cell Biol* *6*, 801-811.

Ho, S. H., Martin, F., Higginbottom, A., Partridge, L. J., Parthasarathy, V., Moseley, G. W., Lopez, P., Cheng-Mayer, C., and Monk, P. N. (2006). Recombinant extracellular domains of tetraspanin proteins are potent inhibitors of the infection of macrophages by human immunodeficiency virus type 1. *J Virol* *80*, 6487-6496.

Hong, I. K., Jin, Y. J., Byun, H. J., Jeoung, D. I., Kim, Y. M., and Lee, H. (2006). Homophilic interactions of Tetraspanin CD151 up-regulate motility and matrix metalloproteinase-9 expression of human melanoma cells through adhesion-dependent c-Jun activation signaling pathways. *J Biol Chem* *281*, 24279-24292.

Hong, I. K., Kim, Y. M., Jeoung, D. I., Kim, K. C., and Lee, H. (2005). Tetraspanin CD9 induces MMP-2 expression by activating p38 MAPK, JNK and c-Jun pathways in human melanoma cells. *Exp Mol Med* *37*, 230-239.

Jun, C. D., Shimaoka, M., Carman, C. V., Takagi, J., and Springer, T. A. (2001). Dimerization and the effectiveness of ICAM-1 in mediating LFA-1-dependent adhesion. *Proc Natl Acad Sci U S A* *98*, 6830-6835.

Kenworthy, A. K., Nichols, B. J., Remmert, C. L., Hendrix, G. M., Kumar, M., Zimmerberg, J., and Lippincott-Schwartz, J. (2004). Dynamics of putative raft-associated proteins at the cell surface. *J Cell Biol* *165*, 735-746.

Kovalenko, O. V., Metcalf, D. G., DeGrado, W. F., and Hemler, M. E. (2005). Structural organization and interactions of transmembrane domains in tetraspanin proteins. *BMC Struct Biol* *5*, 11.

Kovalenko, O. V., Yang, X. H., and Hemler, M. E. (2007). A novel cysteine crosslinking method reveals a direct association between claudin-1 and tetraspanin CD9. *Mol Cell Proteomics*.

Kropshofer, H., Spindeldreher, S., Rohn, T. A., Platania, N., Grygar, C., Daniel, N., Wolpl, A., Langen, H., Horejsi, V., and Vogt, A. B. (2002). Tetraspan microdomains distinct from lipid rafts enrich select peptide-MHC class II complexes. *Nat Immunol* *3*, 61-68.

Lammerding, J., Kazarov, A. R., Huang, H., Lee, R. T., and Hemler, M. E. (2003). Tetraspanin CD151 regulates alpha6beta1 integrin adhesion strengthening. *Proc Natl Acad Sci U S A* *100*, 7616-7621.

Larson, D. R., Gosse, J. A., Holowka, D. A., Baird, B. A., and Webb, W. W. (2005). Temporally resolved interactions between antigen-stimulated IgE receptors and Lyn kinase on living cells. *J Cell Biol* *171*, 527-536.

Le Naour, F., Andre, M., Boucheix, C., and Rubinstein, E. (2006). Membrane microdomains and proteomics: lessons from tetraspanin microdomains and comparison with lipid rafts. *Proteomics* *6*, 6447-6454.

Le Naour, F., Rubinstein, E., Jasmin, C., Prenant, M., and Boucheix, C. (2000). Severely reduced female fertility in CD9-deficient mice. *Science* *287*, 319-321.

Lenne, P. F., Wawrezynieck, L., Conchonaud, F., Wurtz, O., Boned, A., Guo, X. J., Rigneault, H., He, H. T., and Marguet, D. (2006). Dynamic molecular confinement in the plasma membrane by microdomains and the cytoskeleton meshwork. *Embo J* *25*, 3245-3256.

Levy, S., and Shoham, T. (2005a). Protein-protein interactions in the tetraspanin web. *Physiology (Bethesda)* *20*, 218-224.

Levy, S., and Shoham, T. (2005b). The tetraspanin web modulates immune-signalling complexes. *Nat Rev Immunol* *5*, 136-148.

Levy, S., Todd, S. C., and Maecker, H. T. (1998). CD81 (TAPA-1): a molecule involved in signal transduction and cell adhesion in the immune system. *Annu Rev Immunol* *16*, 89-109.

Little, K. D., Hemler, M. E., and Stipp, C. S. (2004). Dynamic regulation of a GPCR-tetraspanin-G protein complex on intact cells: central role of CD81 in facilitating GPR56-Galpha q/11 association. *Mol Biol Cell* *15*, 2375-2387.

Longo, N., Yanez-Mo, M., Mittelbrunn, M., de la Rosa, G., Munoz, M. L., Sanchez-Madrid, F., and Sanchez-Mateos, P. (2001). Regulatory role of tetraspanin CD9 in tumor-endothelial cell interaction during transendothelial invasion of melanoma cells. *Blood* *98*, 3717-3726.

Luo, B. H., Carman, C. V., and Springer, T. A. (2007). Structural basis of integrin regulation and signaling. *Annu Rev Immunol* *25*, 619-647.

Mannion, B. A., Berditchevski, F., Kraeft, S. K., Chen, L. B., and Hemler, M. E. (1996). Transmembrane-4 superfamily proteins CD81 (TAPA-1), CD82, CD63, and CD53 specifically associated with integrin alpha 4 beta 1 (CD49d/CD29). *J Immunol* *157*, 2039-2047.

Martin, F., Roth, D. M., Jans, D. A., Pouton, C. W., Partridge, L. J., Monk, P. N., and Moseley, G. W. (2005). Tetraspanins in viral infections: a fundamental role in viral biology? *J Virol* *79*, 10839-10851.

Miller, J., Knorr, R., Ferrone, M., Houdei, R., Carron, C. P., and Dustin, M. L. (1995). Intercellular adhesion molecule-1 dimerization and its consequences for adhesion mediated by lymphocyte function associated-1. *J Exp Med* *182*, 1231-1241.

Min, G., Wang, H., Sun, T. T., and Kong, X. P. (2006). Structural basis for tetraspanin functions as revealed by the cryo-EM structure of uroplakin complexes at 6-Å resolution. *J Cell Biol* *173*, 975-983.

Mittelbrunn, M., Yanez-Mo, M., Sancho, D., Ursa, A., and Sanchez-Madrid, F. (2002). Cutting edge: dynamic redistribution of tetraspanin CD81 at the central zone of the immune synapse in both T lymphocytes and APC. *J Immunol* *169*, 6691-6695.

Morelli, A. E., Larregina, A. T., Shufesky, W. J., Sullivan, M. L., Stolz, D. B., Papworth, G. D., Zahorchak, A. F., Logar, A. J., Wang, Z., Watkins, S. C., *et al.* (2004). Endocytosis, intracellular sorting, and processing of exosomes by dendritic cells. *Blood* *104*, 3257-3266.

Moseley, G. W. (2005). Tetraspanin-Fc receptor interactions. *Platelets* *16*, 3-12.

Munoz, M., Serrador, J., Sanchez-Madrid, F., and Teixido, J. (1996). A region of the integrin VLA alpha 4 subunit involved in homotypic cell aggregation and in fibronectin but not vascular cell adhesion molecule-1 binding. *J Biol Chem* *271*, 2696-2702.

Nueda, A., Lopez-Rodriguez, C., Rubio, M. A., Sotillos, M., Postigo, A., del Pozo, M. A., Vega, M. A., and Corbi, A. L. (1995). Hematopoietic cell-type-dependent regulation of leukocyte integrin functional activity: CD11b and CD11c expression inhibits LFA-1-dependent aggregation of differentiated U937 cells. *Cell Immunol* *164*, 163-169.

Nydegger, S., Khurana, S., Kremmentsov, D. N., Foti, M., and Thali, M. (2006). Mapping of tetraspanin-enriched microdomains that can function as gateways for HIV-1. *J Cell Biol* *173*, 795-807.

Pileri, P., Uematsu, Y., Campagnoli, S., Galli, G., Falugi, F., Petracca, R., Weiner, A. J., Houghton, M., Rosa, D., Grandi, G., and Abrignani, S. (1998). Binding of hepatitis C virus to CD81. *Science* *282*, 938-941.

Redford, G. I., and Clegg, R. M. (2005). Polar plot representation for frequency-domain analysis of fluorescence lifetimes. *J Fluoresc* *15*, 805-815.

Rubinstein, E., Ziyat, A., Prenant, M., Wrobel, E., Wolf, J. P., Levy, S., Le Naour, F., and Boucheix, C. (2006). Reduced fertility of female mice lacking CD81. *Dev Biol* *290*, 351-358.

Sachs, N., Kreft, M., van den Bergh Weerman, M. A., Beynon, A. J., Peters, T. A., Weening, J. J., and Sonnenberg, A. (2006). Kidney failure in mice lacking the tetraspanin CD151. *J Cell Biol* *175*, 33-39.

Sharma, P., Varma, R., Sarasij, R. C., Ira, Gousset, K., Krishnamoorthy, G., Rao, M., and Mayor, S. (2004). Nanoscale organization of multiple GPI-anchored proteins in living cell membranes. *Cell* *116*, 577-589.

Simons, K., and Toomre, D. (2000). Lipid rafts and signal transduction. *Nat Rev Mol Cell Biol* *1*, 31-39.

Springer, T. A. (1994). Traffic signals for lymphocyte recirculation and leukocyte emigration: the multistep paradigm. *Cell* *76*, 301-314.

Sterk, L. M., Geuijen, C. A., Oomen, L. C., Calafat, J., Janssen, H., and Sonnenberg, A. (2000). The tetraspan molecule CD151, a novel constituent of hemidesmosomes, associates with the integrin alpha6beta4 and may regulate the spatial organization of hemidesmosomes. *J Cell Biol* *149*, 969-982.

Stipp, C. S., and Hemler, M. E. (2000). Transmembrane-4-superfamily proteins CD151 and CD81 associate with alpha 3 beta 1 integrin, and selectively contribute to alpha 3 beta 1-dependent neurite outgrowth. *J Cell Sci* *113* ( Pt 11), 1871-1882.

Stipp, C. S., Kolesnikova, T. V., and Hemler, M. E. (2003). Functional domains in tetraspanin proteins. *Trends Biochem Sci* *28*, 106-112.

Suzuki, K. G., Fujiwara, T. K., Edidin, M., and Kusumi, A. (2007a). Dynamic recruitment of phospholipase C gamma at transiently immobilized GPI-anchored receptor clusters induces IP3-Ca2+ signaling: single-molecule tracking study 2. *J Cell Biol* *177*, 731-742.

Suzuki, K. G., Fujiwara, T. K., Sanematsu, F., Iino, R., Edidin, M., and Kusumi, A. (2007b). GPI-anchored receptor clusters transiently recruit Lyn and G alpha for temporary cluster immobilization and Lyn activation: single-molecule tracking study 1. *J Cell Biol* *177*, 717-730.

Takeda, Y., Kazarov, A. R., Butterfield, C. E., Hopkins, B. D., Benjamin, L. E., Kaipainen, A., and Hemler, M. E. (2007). Deletion of tetraspanin Cd151 results in decreased pathologic angiogenesis in vivo and in vitro. *Blood* *109*, 1524-1532.

Takino, T., Miyamori, H., Kawaguchi, N., Uekita, T., Seiki, M., and Sato, H. (2003). Tetraspanin CD63 promotes targeting and lysosomal proteolysis of membrane-type 1 matrix metalloproteinase. *Biochem Biophys Res Commun* *304*, 160-166.

Unternaehrer, J. J., Chow, A., Pypaert, M., Inaba, K., and Mellman, I. (2007). The tetraspanin CD9 mediates lateral association of MHC class II molecules on the dendritic cell surface. *Proc Natl Acad Sci U S A* *104*, 234-239.

VanCompernelle, S. E., Levy, S., and Todd, S. C. (2001). Anti-CD81 activates LFA-1 on T cells and promotes T cell-B cell collaboration. *Eur J Immunol* *31*, 823-831.

Varma, R., and Mayor, S. (1998). GPI-anchored proteins are organized in submicron domains at the cell surface. *Nature* *394*, 798-801.

Vogt, A. B., Spindeldreher, S., and Kropshofer, H. (2002). Clustering of MHC-peptide complexes prior to their engagement in the immunological synapse: lipid raft and tetraspan microdomains. *Immunol Rev* *189*, 136-151.

Wright, M. D., Geary, S. M., Fitter, S., Moseley, G. W., Lau, L. M., Sheng, K. C., Apostolopoulos, V., Stanley, E. G., Jackson, D. E., and Ashman, L. K. (2004). Characterization of mice lacking the tetraspanin superfamily member CD151. *Mol Cell Biol* *24*, 5978-5988.

Yan, Y., Shirakabe, K., and Werb, Z. (2002). The metalloprotease Kuzbanian (ADAM10) mediates the transactivation of EGF receptor by G protein-coupled receptors. *J Cell Biol* *158*, 221-226.

Yanez-Mo, M., Alfranca, A., Cabanas, C., Marazuela, M., Tejedor, R., Ursa, M. A., Ashman, L. K., de Landazuri, M. O., and Sanchez-Madrid, F. (1998). Regulation of endothelial cell motility by complexes of tetraspan molecules CD81/TAPA-1 and CD151/PETA-3 with alpha3 beta1 integrin localized at endothelial lateral junctions. *J Cell Biol* *141*, 791-804.

Yanez-Mo, M., Tejedor, R., Rousselle, P., and Sanchez -Madrid, F. (2001). Tetraspanins in intercellular adhesion of polarized epithelial cells: spatial and functional relationship to integrins and cadherins. *J Cell Sci* *114*, 577-587.

Yang, L., Froio, R. M., Sciuto, T. E., Dvorak, A. M., Alon, R., and Luscinskas, F. W. (2005). ICAM-1 regulates neutrophil adhesion and transcellular migration of TNF-alpha-activated vascular endothelium under flow. *Blood* *106*, 584-592.

Yang, X., Kovalenko, O. V., Tang, W., Claas, C., Stipp, C. S., and Hemler, M. E. (2004). Palmitoylation supports assembly and function of integrin-tetraspanin complexes. *J Cell Biol* *167*, 1231-1240.

Yauch, R. L., and Hemler, M. E. (2000). Specific interactions among transmembrane 4 superfamily (TM4SF) proteins and phosphoinositide 4-kinase. *Biochem J* 351 Pt 3, 629-637.

Zacharias, D. A., Violin, J. D., Newton, A. C., and Tsien, R. Y. (2002). Partitioning of lipid-modified monomeric GFPs into membrane microdomains of live cells. *Science* 296, 913-916.

Zhang, J., Campbell, R. E., Ting, A. Y., and Tsien, R. Y. (2002). Creating new fluorescent probes for cell biology. *Nat Rev Mol Cell Biol* 3, 906-918.

Zhang, X. A., Bontrager, A. L., and Hemler, M. E. (2001). Transmembrane-4 superfamily proteins associate with activated protein kinase C (PKC) and link PKC to specific beta(1) integrins. *J Biol Chem* 276, 25005-25013.

Zhu, G. Z., Miller, B. J., Boucheix, C., Rubinstein, E., Liu, C. C., Hynes, R. O., Myles, D. G., and Primakoff, P. (2002). Residues SFQ (173-175) in the large extracellular loop of CD9 are required for gamete fusion. *Development* 129, 1995-2002.

Ryan A Colyer, Claudia Y Lee, and Enrico Gratton. Time-resolved frequency-domain fluorescence lifetime imaging microscopy in the photon-counting regime (submitted to *Nature Methods*).

Digman, M., V.R. Caiolfa, M. Zamai, and G. Gratton; The Phasor approach to fluorescence lifetime imaging analysis (submitted to *Biophys J*).

R Development Core Team (2006). R: A language and environment for statistical computing. R Foundation for Statistical Computing, Vienna, Austria. ISBN 3-900051-07-0, URL <http://www.R-project.org>.

## LEGENDS TO FIGURES

**Figure 1: VCAM-1 and ICAM-1 are co-presented at lymphocyte-endothelium contact independently of ligand binding and actin anchorage.** **A.** VCAM-1 and ICAM-1 co-localize at the endothelial docking structure in the absence of integrin engagement. K562 transfected with  $\alpha 4$  or LFA-1 integrin were allowed to adhere to TNF- $\alpha$ -activated HUVEC for 30 min, and cells were fixed and double stained with anti-VCAM-1 (P8B1) and biotin-conjugated anti-ICAM-1 (MEM111). Confocal stacks were obtained and orthogonal maximal projections and vertical 3D reconstructions of the whole series are displayed. Scale bars = 20  $\mu\text{m}$ . **B.** VCAM-1 and ICAM-1 are co-recruited to the endothelial contact area with human T lymphoblasts previously treated to inactivate VLA-4 or LFA-1. Human T lymphoblasts were pre-treated for 5 minutes with the LFA-1 inhibitor BIRT377 (10 $\mu\text{M}$ ) or the VLA-4 inhibitor BIO5192 (10 $\mu\text{g}/\text{ml}$ ) and then added to a TNF- $\alpha$  activated HUVEC monolayer for 5 min. Cells were fixed and double stained for VCAM-1 and ICAM-1 as in 1A. Confocal stacks were obtained and a representative section from each treatment is shown together with its corresponding colocalization histogram and a mask showing the distribution within the cell of double green-red pixels from the region marked on the histogram. Scale bars = 10  $\mu\text{m}$ . **C.** VCAM $\Delta$ Cyt is co-recruited to ICAM-1-mediated docking structures but is unable to trigger the formation of VCAM-1-mediated docking structures. Resting HUVEC were transfected with the VCAM $\Delta$ Cyt construct and incubated either with K562 leukocytes expressing VLA-4 (K562  $\alpha 4$ ) or LFA-1 integrin or with T-lymphoblasts. Cells were then fixed and double stained with anti-VCAM-1 (VCAM $\Delta$ Cyt being the only VCAM-1 molecular species detected) and biotin-conjugated anti-ICAM-1. Confocal stacks were obtained and a representative section or

vertical reconstructions of the whole series are displayed. Arrows point to the position of the adhered leukocytes. Scale bars = 20  $\mu\text{m}$ .

**Figure 2: VCAM-1 and ICAM-1 are not displayed as heterodimers at the plasma membrane.** Endothelial cells were co-transfected with different mEGFP-mRFP1 pairs (ICAM-1/ICAM-1, VCAM-1/VCAM-1, ICAM-1/VCAM-1 and VCAM-1/ICAM-1). FLIM-FRET analysis was performed using the phasor-FLIM analysis as explained in Material and Methods. For each pair of proteins, a representative analysis of a co-transfected cell is shown. The fluorescence intensity images of the scanned sections are in pseudocolour scale (left panels) and correspondent mEGFP lifetime distributions are shown in contour plots after the phasor transformation (phasor plots, right panels). In each phasor plot, the experimentally derived green-line represents the mean phasor distribution for unquenched mEGFP fluorescence lifetimes with different contribution of cell autofluorescence (see Suppl. Fig. 1). The yellow line marks the computed trajectory of mEGFP donors quenched by 50% FRET (Föster distance) and at different contribution of autofluorescence (Caiolfa et al., 2007). In the ICAM-1/ICAM-1 cell, two major phasor distributions are observed and selected in the phasor plot (black circles). The first one includes the majority, more than 80%, of the pixels in the image. In these pixels, which are rather homogeneously distributed at the cell membrane (their localization is shown in the FLIM image, pink mask), FRET is negligible ( $\leq 8\%$ ). The second distribution includes only 16% of pixels in which FRET varies from 16 to 32% (mean 24%), and localize few clusters on the cell membrane. The other protein pairs do not show significant quenching due to FRET, as their phasor distributions are not distinguishable from that of the correspondent pure donor cells (Suppl. Fig. 1). In each

of these examples, more than 95% of pixels are selected (black circles) in the non-FRET area of the phasor plot and are localized in the correspondent FLIM image.

**Figure 3: Dynamic behaviour of EAP components at the “nude” plasma membrane.**

**A.** Anti-tetraspanin-coated beads recruit both VCAM-1 and ICAM-1. TNF- $\alpha$ -activated HUVEC were incubated with magnetic beads coated with anti-CD9, anti-CD151, anti-VCAM-1 or anti-VE-cadherin for 30 min and then, stained with biotinylated anti-ICAM-1 mAb. Representative confocal sections are shown. Arrows point to the position of the attached beads. **B.** Quantification of ICAM-1-, VCAM-1- or CD9-EGFP clustering around beads coated with the indicated antibodies and attached to transfected resting or TNF- $\alpha$ -activated HUVEC. Data are the means  $\pm$  S.D. of two independent experiments. **C.** ICAM-1 and VCAM-1 are recovered together with tetraspanins in the heavy fractions of a continuous sucrose gradient. TNF- $\alpha$ -activated HUVEC were lysed in 1% Brij96 and lysates were loaded onto a continuous 5-40% sucrose gradient. After ultracentrifugation, samples were recovered in 1 ml fractions and analyzed by Western blot for VCAM-1, ICAM-1, CD151, CD9, or caveolin. Fractions were recovered from the bottom of the gradient, so that the soluble non-floating fractions were collected first. **D.** FRAP analysis showing differences in the diffusion of tetraspanins and adhesion receptors compared with the lipid raft marker GPI at the plasma membrane. Endothelial cells were transiently transfected with the indicated EGFP-tagged protein constructs and activated with TNF- $\alpha$  20h before microscopy observation. Mean fluorescence recovery curves for CD9-, CD151-, ICAM-1-, VCAM-1- and GPI-EGFP were calculated (n ranged from 5 to 21 independent experiments for each protein) and are depicted together on the same graphic. Statistical significance was assessed by a point-

to-point comparison based on a Student's t-test. p values were adjusted for multiple testing by using the Benjamini and Hochberg method to control for false discovery rate (fdr). Tests were considered to be significant when adjusted p values from 80% of the points out of the plateau were  $< 0.05$ . This ensures that the expected fdr is  $< 5\%$ . (See Suppl. Fig. 3) **E.** Comparison of mobility parameters among tetraspanins, adhesion receptors and GPI-anchored protein at the endothelial plasma membrane. The average half-time recovery rate was calculated considering the mean mobility fraction for each protein. **F.** The retarded mobility of adhesion receptors compared with tetraspanins can be explained by their differential engagement to the actin cytoskeleton. Mean fluorescence recovery curves of ICAM-1 $\Delta$ Cyt-, ICAM-1- and CD9-EGFP were calculated (n ranged from 12 to 21) and are compared on the same graph. Deletion of the ICAM-1 cytoplasmic tail significantly increased recovery rate compared with wild-type protein. Statistical analysis was performed as in D.

**Figure 4: Dynamic behavior of endothelial adhesive platform components within the endothelial docking structure.** **A.** Representative FRAP analysis of an endothelial docking structure. The prebleaching image shows a TNF- $\alpha$ -activated endothelial cell transiently transfected with ICAM-1-EGFP; docking structures formed around attached K562 LFA-1 cells are visible as circles of concentrated EGFP fluorescence. The docking structure in the boxed area, shown at high magnification in the inset, was selected for photobleaching measurements show the fluorescence recovery at the structure over time. Scale bar = 20  $\mu\text{m}$ . **B.** CD9 mobility is tightly regulated in ICAM-1-mediated docking structures. Mean fluorescence recovery curves are shown for ICAM-1-, VCAM-1-, CD9- and CD151-EGFP at docking structures formed around K562 cells expressing LFA-1 (activated by 1 mM  $\text{Mn}^{2+}$ , which does not affect

endothelial molecule mobility); n ranged from 4 to 16 experiments for each transfected protein. Statistical analysis was based on p value adjusted for multiple testing (see Methods and Fig. 3D for details). **C.** CD151 and VCAM-1 mobilities are correlated at VCAM-1-mediated docking structures. Mean fluorescence recovery curves are shown for ICAM-1, VCAM-1-, CD9- and CD151-EGFP at docking structures formed around K562 cells expressing VLA-4 (K562  $\alpha 4$ ); n ranged from 5 to 16 experiments for each protein. Statistical analysis was performed as in B. **D.** Actin-cytoskeleton anchorage stabilizes the interaction of ICAM-1 with its ligand LFA-1. Mean fluorescence recovery curves are shown for ICAM-1 $\Delta$ Cyt- and ICAM-1-EGFP at ICAM-1-mediated docking structures (n=7 for both proteins). Statistical analysis was performed as in B.

**Figure 5. FCS analysis on the components of endothelial adhesive platforms. A.**

The panels show representative FCS measurements performed at the plasma membrane of transiently-transfected primary endothelial cells expressing very low levels of ICAM-1-, VCAM-1-, CD9-, and CD151-mEGFP. For each experiment are documented: the fluorescence intensity image, the point in which the laser beam was positioned for the measurement (white circle), the ACF (black line), the best-fitted curve (red line), and the fitted parameters, diffusion time (TauD) and anomaly coefficient ( $\alpha$ , ranging from 0 to 1), from which the diffusion coefficient (D) was derived as described (See under Materials and Methods section). The corresponding scale bar is shown in each image. kCPS: kilo counts per second. **B.** Scatter plots of the diffusion and anomaly coefficients determined by FCS analysis on the four proteins of interest. Each point is an individual measurement. Horizontal lines = medians.

**Figure 6. Direct and indirect interactions within endothelial adhesive platforms.**

Endothelial cells were co-transfected with different mEGFP-mRFP1 pair constructs (**A**: CD9/CD9 and CD9/CD151; **B**: ICAM-1/CD9 and VCAM-1/CD151). FLIM-FRET analysis was performed as described (Material and Methods, Fig. 2 and Suppl. Fig. 1). For each FRET pair, the figure shows: the fluorescence intensity image of the scanned section (in pseudocolour scale), the phasor plot, and the FLIM image correspondent to the cursor selection of phasors (black circle) illustrating the pixel localization of phasor selection. Two selections are shown for each FRET pair corresponding to phasors at low (11-14%) and high (24%) FRET efficiency.

**Figure 7. Tetraspanin regulates endothelial adhesion receptor nanoclustering.**

**A.** i) TNF- $\alpha$  activated endothelial cells were fixed and stained with anti-VCAM-1 (P8B1) or anti-ICAM-1 (Hu5/3), followed by 40 nm gold-immunolabeling. Then, samples were processed for SEM observation. Representative SEM negative images of  $1.75 \mu\text{m}^2$  areas of the endothelial plasma membrane are shown. ii) TNF- $\alpha$ -activated endothelial cells were fixed and double stained with anti-VCAM-1 (P8B1) and biotinylated anti-ICAM-1 (MEM-111), followed by 40 nm and 15 nm gold-labeling, respectively. Then, samples were processed for SEM observation. The left-hand panel shows a representative SEM negative image of  $0.35 \mu\text{m}^2$  area of the endothelial plasma membrane displaying VCAM-1 (40 nm gold particles) and ICAM-1 (15 nm gold particles, white asterisks). High magnification images show detail of VCAM-1 and ICAM-1 heteroclustering. iii) T lymphoblasts were allowed to adhere to an activated endothelial monolayer for 5 min. Cells were then fixed, stained with anti-ICAM-1 (Hu5/3) followed by 40 nm gold-immunolabeling, and subjected to SEM processing. A representative SEM positive image shows the preferential localization of gold particles

at the microvilli of the endothelial docking structure formed around a lymphoblast. The inset shows the leukocyte-endothelial contact area at lower magnification. Scale bar = 1.50  $\mu\text{m}$ . **B.** i) Endothelial cells were activated for 20h with TNF- $\alpha$  in the presence of 250  $\mu\text{g}/\text{ml}$  of active or heat-inactivated (5 min 90°C) CD9 blocking peptide (CD9-LEL-GST). Cells were then fixed and stained for VCAM-1 or ICAM-1 as in A i). Representative images of 1.75  $\mu\text{m}^2$  areas of the endothelial plasma membrane are shown. ii) Gold particles in SEM images were counted, and coordinates were assigned to each object using Metamorph software. Inter-particle distances were calculated using a custom-written k-nearest neighbour (knn) distance algorithm based on R software. The differences in receptor nanoclustering among samples subjected to different treatments were assessed in terms of aggregation and separation evaluated by means of a knn (k-nearest neighbour) profile. The knn profile is a k-points curve (for our analysis k=15), where each point in the curve is the mean of the nearest neighbour distances for the whole N points in the data set. Dist (title y-axis) corresponds to euclidean distances (considering each point by their x,y coordinates). Graphs show knn distances from 2 representative images of each condition (VCAM-1 or ICAM-1 staining with active or inactive CD9 blocking peptide). **C.** i) Panels show representative FCS measurements performed at the plasma membrane of endothelial cells transiently-transfected with CD9- or CD151-mEGFP and treated with 250  $\mu\text{g}/\text{ml}$  of active or heat-inactivated CD9-LEL-GST. For each experiment are documented: the fluorescence intensity image, the point in which the laser beam was positioned for the measurement (white circle), the ACF (black line), the best-fitted curve (red line), and the fitted parameters, diffusion time (TauD) and anomaly coefficient ( $\alpha$ ), from which the diffusion coefficient (D) was derived. The corresponding scale bar is shown in each image. kCPS: kilo counts

per second. ii) Scatter plots of the diffusion and anomaly coefficients determined by FCS analysis. Each point is an individual measurement. Horizontal lines = medians.

## **LEGENDS TO SUPPLEMENTAL FIGURES**

### **Supplemental Figure 1**

**A. Standards for the phasor-FLIM analysis of FRET.** Cells expressing only the mEGFP-tagged chimeras of ICAM-1, VCAM-1-or CD9 were used for defining the phasor distributions (i.e., fluorescence lifetime distributions) of each FRET-unquenched donor protein. ICAM-1-mEGFP is the reference for ICAM-1-mEGFP/ICAM-1-mRFP1, ICAM-1mEGFP/VCAM-1mRFP1 and ICAM-1mEGFP/CD9mRFP1 pairs. VCAM-1mEGFP is the reference for VCAM-1mEGFP/VCAM-1mRFP1, VCAM-1mEGFP/ICAMmRFP1 and VCAM-1mEGFP/CD151mRFP1. CD9mEGFP is the reference for CD9mEGFP/CD9mRFP1 and CD9mEGFP/CD151mRFP1.

Fluorescence lifetime decays were acquired in the classical TCSPC-FLIM mode and transformed in the phasor representation as described (Digman et al., submitted; Caiolfa et al., 2007). Briefly, by this novel analytical approach, the fluorescence decay in each pixel of the image gives a point in the phasor plot. The phasors ensemble of the image is shown in contour plot. The phasor plot is simply a polar, s.g. coordinate graph, in which only single exponential decays fall on the universal circle (right top panel), and different molecular species occupy distinct positions in the plots (Digman et al., submitted). As in our cells seeded on fibronectin matrices, if the decay at one pixel is a convolution of lifetimes, due to multiple species (i.e., unquenched donor + cell autofluorescence) contributing the fluorescence intensity in that pixel, the phasor falls inside the universal circle, and it is simply the algebraic sum of phasors from each component (Clayton et al., 2004; Gratton et al., 1984; Redford and Clegg, 2005) (right

top panel). The phasor distribution in donor-transfected cells indicates the presence of pixels at different contribution of mEGFP and autofluorescence lifetimes. The latter was evaluated in independent experiments on untransfected cells and the mean of its phasor distribution is reported in the phasor plot (+, right top panel). As it was recently shown (Digman et al., submitted), the phasors corresponding to the fibronectin background and the cellular autofluorescence are spread over a larger area of the phasor plot, due to the low intensity images, the fibronectin background and also the pixel heterogeneity for the cellular autofluorescence are detected. Despite that, the majority (> 95%) of pixels is included in a narrow, distinct area of the plot (black circle in the phasor plot), and are uniformly localized in the image, regardless the variability of the local fluorescence intensity. In these pixels, mEGFP is the predominant species that gives rise to the measured fluorescence lifetime decays. The phasor distribution of the three donor constructs (top, mid and bottom panels) is comparable and depicts the area in the phasor plot in which mEGFP-constructs localize in the presence of fibronectin and cell autofluorescence and in the absence of quenching due to FRET (green line). Once we know the phasors of the unquenched donors and of the fibronectin-cell autofluorescence, we can calculate the FRET trajectory in the phasor plot according to the classical relationship:  $\text{FRET eff} = [1 - (\tau_{\text{donor-acceptor}}/\tau_{\text{donor}})]$ , and define the mean phasors of mEGFP-constructs quenched by 50% FRET and with different contributions of fibronectin-cell autofluorescence (yellow line). In all our experiments, phasors resulting from any combination of unquenched-donors, FRET-quenched-donors and fibronectin-cell autofluorescence have been found within the area delimited by the green and yellow lines in the phasor plot.

**B. uPAR/ICAM FRET pair confirming the non interaction of a lipid raft-related protein and an EAP constituent.** FLIM-FRET analysis of uPARmEGFP and ICAM-1-

mRFP1 in HEK 293 cells. The intensity image (in pseudocolour scale), the phasor plot and the FLIM image correspondent to the cursor selection (black circle) are shown. This result indicates that FRET does not occur between the two proteins, as the phasor distribution of uPAR-green is identical to that of single transfected cells (data not shown, Caiolfa et al., 2007). It also shows that the localization and distribution of the phasors of mEGFP-constructs is not affected by the kind of protein linked to the fluorophore and by the cells in which they are expressed; while the contribution of other species such as fibronectin (not present in HEK293 samples) and cell autofluorescence varies depending on the cell culture conditions and expression levels of the tagged-proteins.

**Supplemental Figure 2. Tetraspanins are localized at docking structures mediated by the engagement of ICAM-1 or VCAM-1.** LFA-1<sup>+</sup> or  $\alpha$ 4<sup>+</sup> K562 cells were allowed to adhere to a TNF- $\alpha$ -activated endothelial monolayer for 30 min. *Left panels:* Cells were fixed and double stained for VCAM-1 (P8B1, red) and CD9 (biotinylated VJ1/20, green). *Right panels:* Cells were stained for CD9 (VJ1/20, green) and ICAM-1 (biotinylated MEM-111, red). Confocal stacks were obtained and orthogonal maximal projections and vertical 3D reconstructions of the whole series are displayed. White arrows point to endothelium-leukocyte contact areas (docking structures).

**Supplemental Figure 3. A. Example statistical analysis of a FRAP experiments.** For each time point, the table shows mean fluorescence intensities for ICAM-1 and ICAM-1 $\Delta$ Cyt (measured at the plasma membrane) raw p values, and adjusted p values obtained for multiple testing using the Benjamini and Hochberg's (BH) method.

Typically, an acceptance criterion of a single event takes the form of a requirement that the observed data be highly unlikely under a default assumption (null hypothesis). As the number of independent applications of the acceptance criterion begins to outweigh the high unlikelihood associated with each individual test, it becomes increasingly likely that one will observe data that satisfies the acceptance criterion by chance alone (even if the default assumption is true in all cases). These errors are considered false positives because they positively identify a set of observations as satisfying the acceptance criterion while that data in fact represents the null hypothesis. Many mathematical techniques have been developed to counter the false positive error rate associated with making multiple statistical comparisons. To avoid these multiple comparison problems, we used the Benjamini and Hochberg's (BH) method for the statistical analysis of our FRAP experiments.

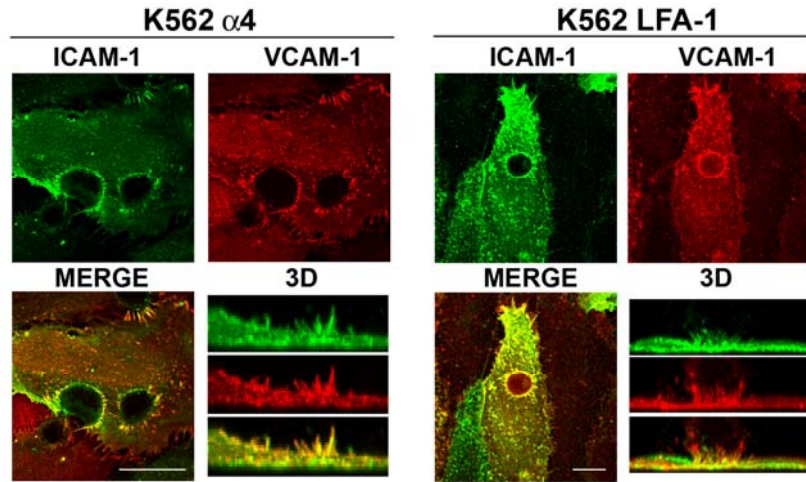
The accompanying graph shows mean fluorescence recovery curves of ICAM-1 and ICAM-1 $\Delta$ Cyt at the plasma membrane. The adjusted p values shown in the table correspond to the maximum adjusted p value out of the plateau region. The plateau region is marked on the table and the graph and was not considered for the statistical analysis.

**B. Comparison of dynamic behaviors of each EAP constituent at nude plasma membrane and at ICAM-1- and VCAM-1-mediated docking structures.** The graphs show the mean fluorescence recovery curves at nude plasma membrane and at ICAM-1 and VCAM-1-mediated docking structures for each EAP component studied: CD9-, CD151-, VCAM-1- or ICAM-1-EGFP. Statistical analysis was performed as indicated in A.

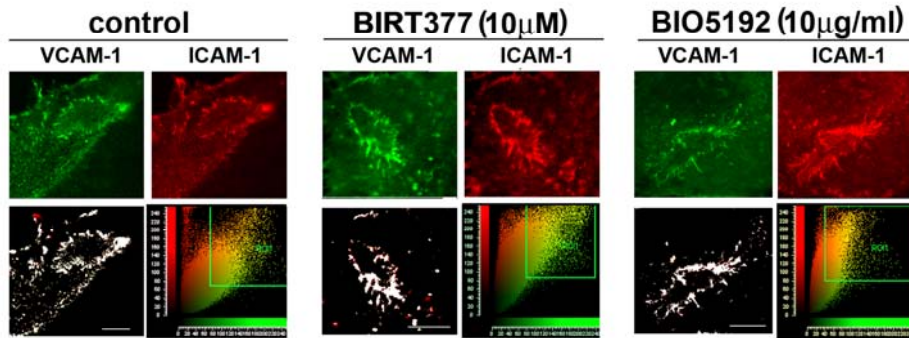
**Supplemental Figure 4. Examples of Fluorescence Cross-correlation Spectroscopy measurements within endothelial adhesive platforms.** The figure shows representative measurements performed at the plasma membrane of HUVEC double transfected with ICAM-1mEGFP/ICAM-mRFP1 (**A**) or CD9mEGFP/CD151mRFP1 (**B**). For each experiment are documented: the fluorescence intensity image from both channels (red and green), the point in which the laser beam was positioned for the measurement (white circle), the ACF (black line), the best-fitted curve (red line), the cross-correlation function for the pair, and the fitted parameters, diffusion time ( $\tau_D$ ) and anomaly coefficient ( $\alpha$ ), from which the diffusion coefficient ( $D$ ) was derived. The corresponding scale bar is shown in the images. kCPS: kilo counts per second.

Figure 1

A



B



C

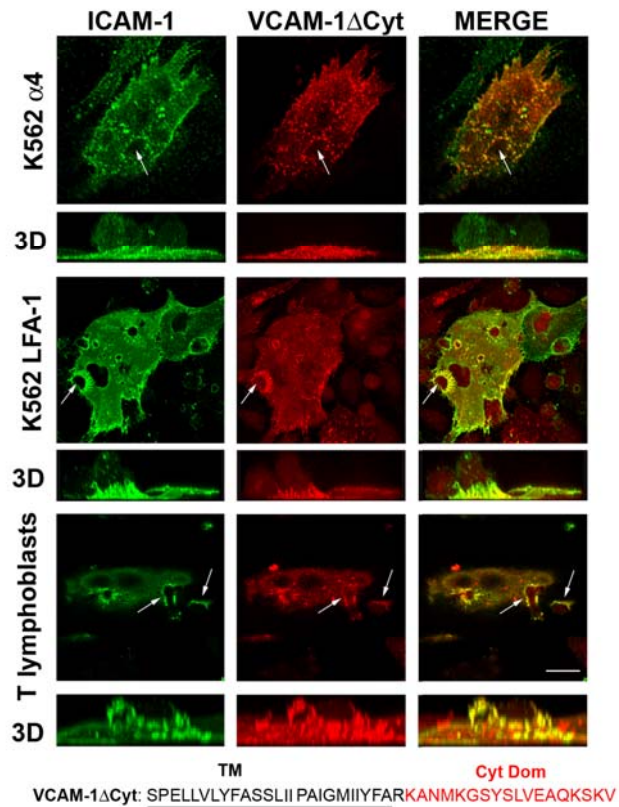


Figure 2

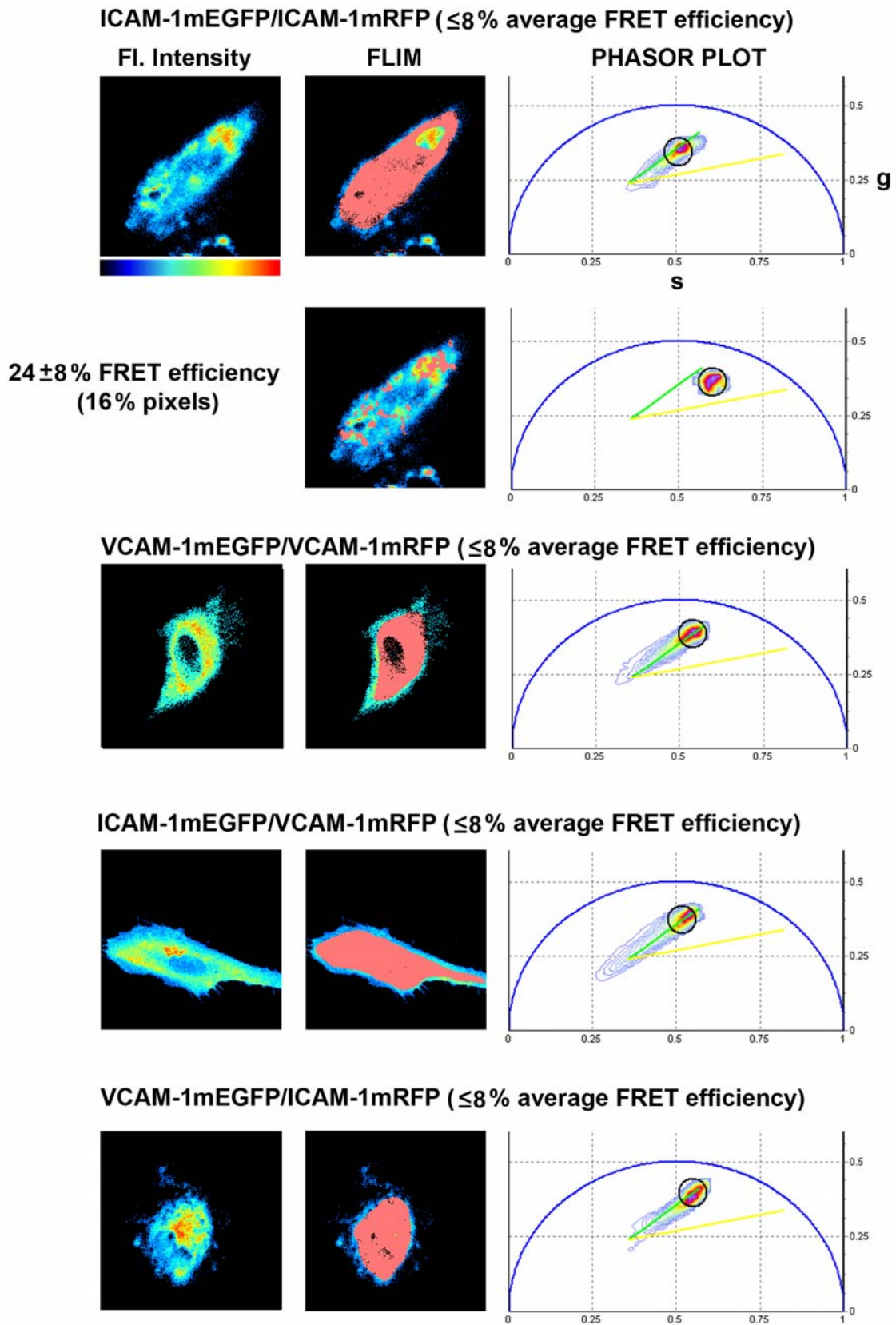
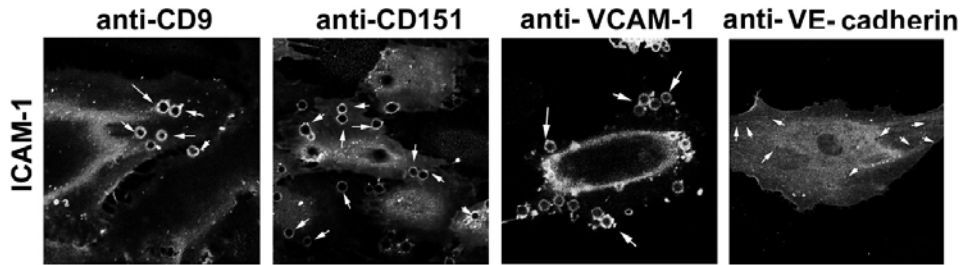
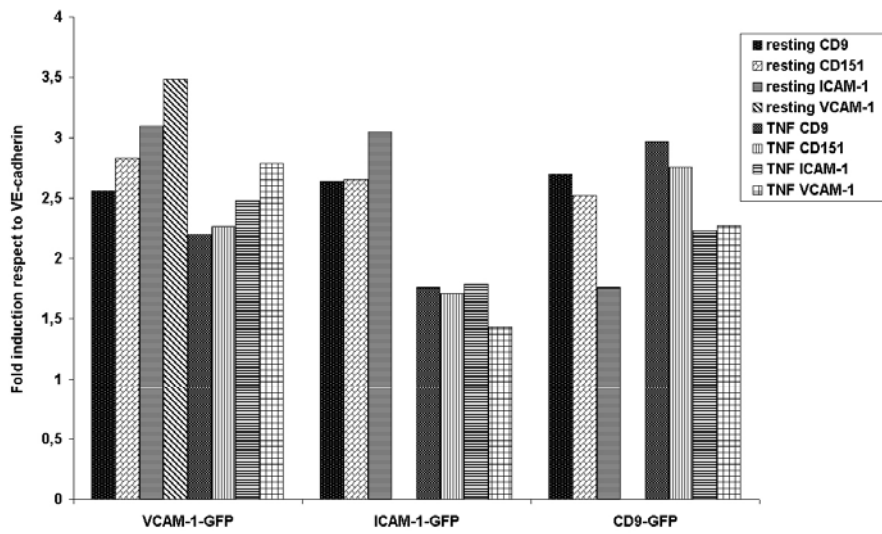


Figure 3

**A**



**B**



**C**

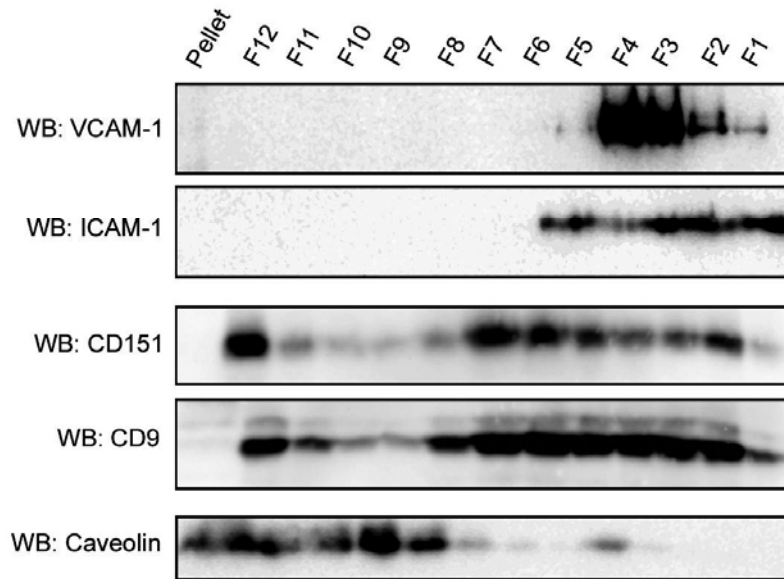
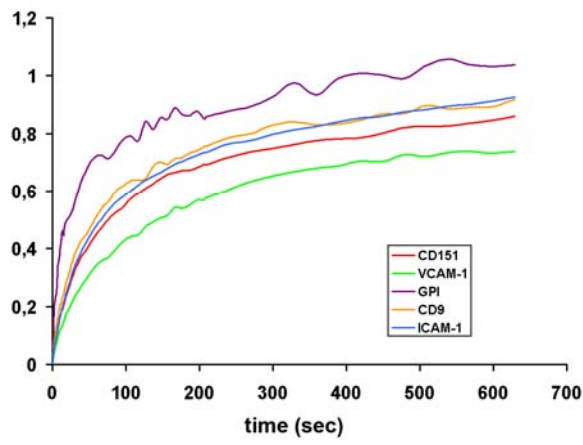


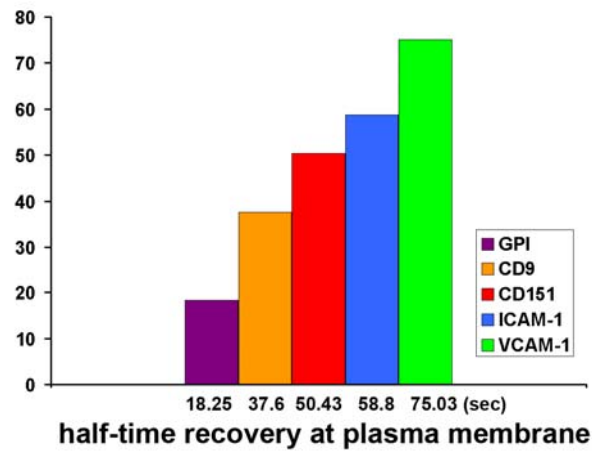
**Figure 3**

**D**

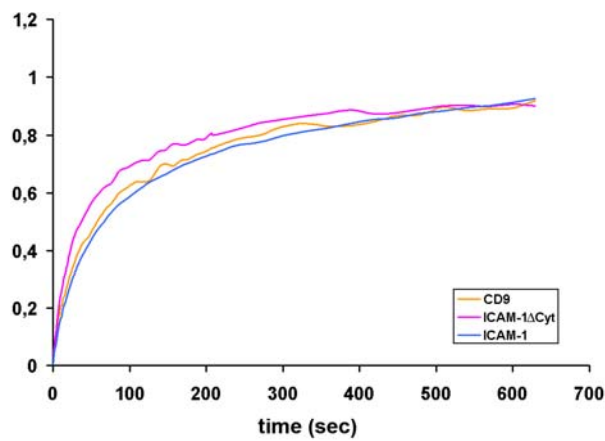


adjusted p-value	GPI
CD9	< 0.05
CD151	<0.005
ICAM-1	< 0.001
VCAM-1	< 0.0005

**E**



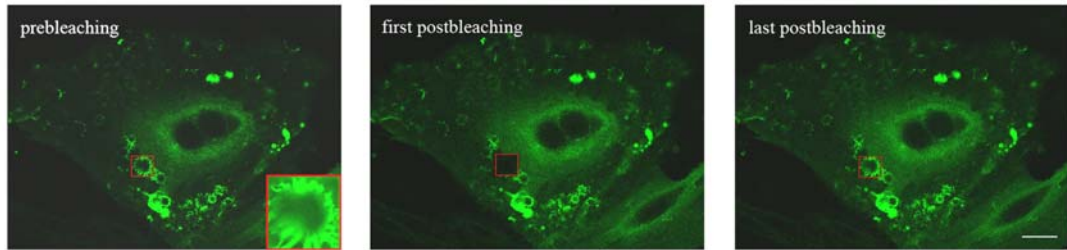
**F**



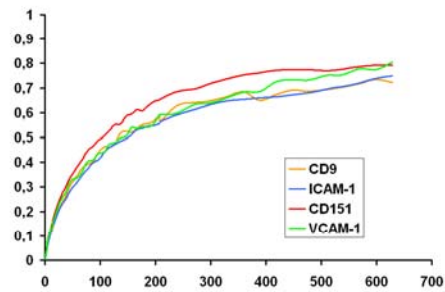
adjusted p-value	ICAM-1 $\Delta$ Cyt
CD9	<0.5
ICAM-1	< 0.0005

Figure 4

A

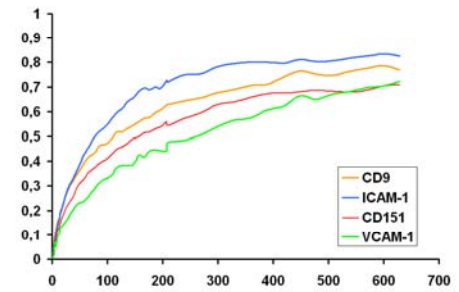


B ICAM-1-mediated docking structures



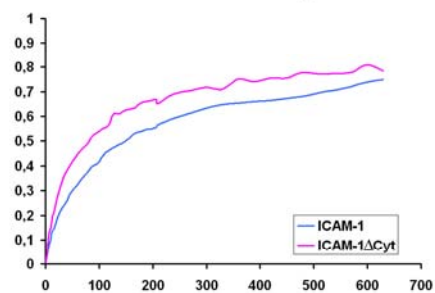
adjusted p-value	ICAM-1
CD9	<0.996
CD151	<0.05
VCAM-1	<0.9

C VCAM-1-mediated docking structures



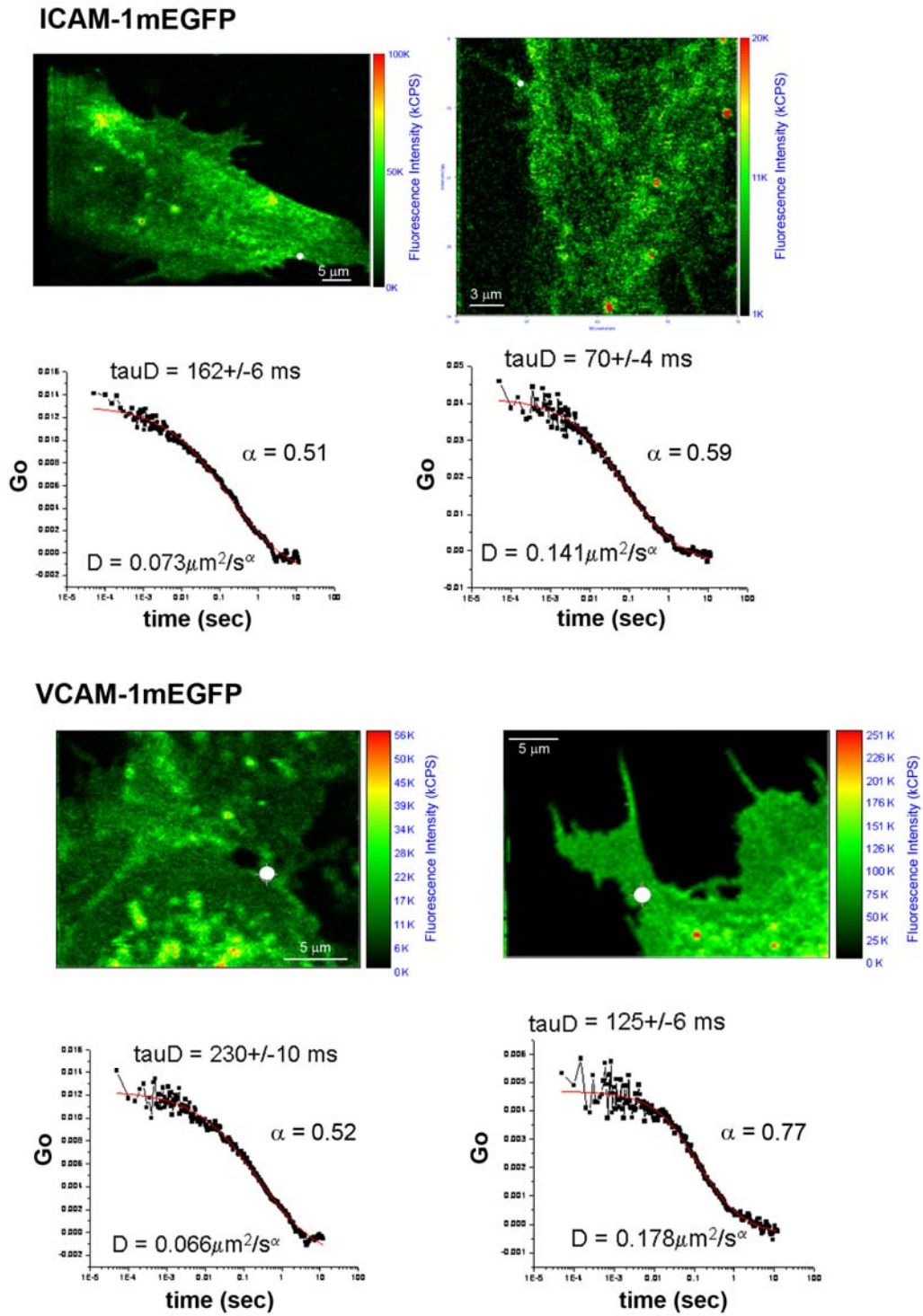
adjusted p-value	VCAM-1
CD9	<0.003
CD151	<0.2
ICAM-1	<0.03

D ICAM-1-mediated docking structures

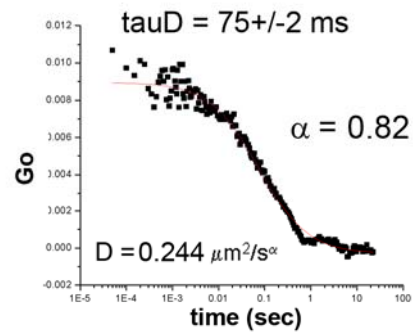
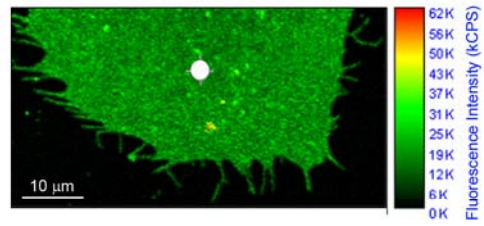
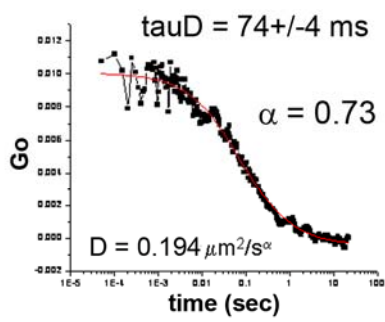
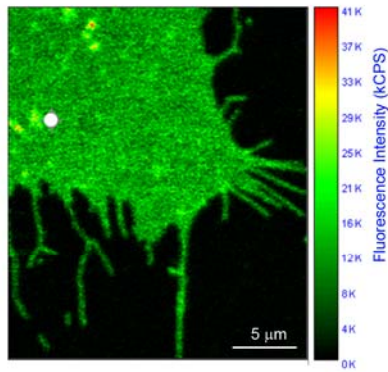


adjusted p-value	ICAM-1ΔCyt
ICAM-1	<0.035

Figure 5A



## CD9 mEGFP



## CD151 mEGFP

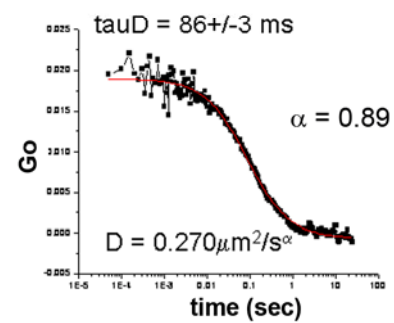
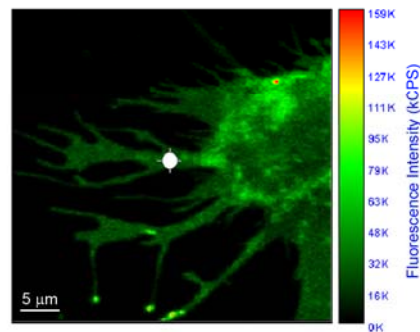
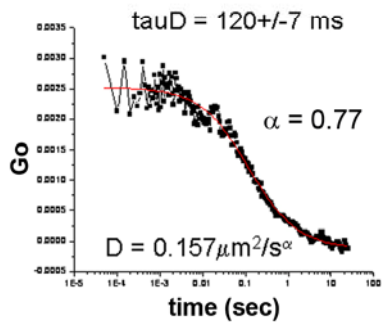
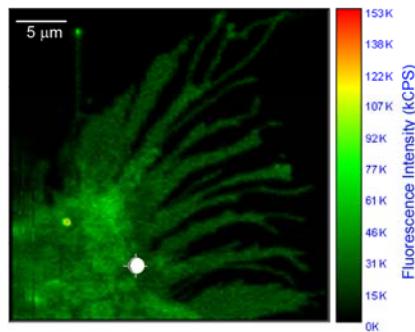


Figure 5B

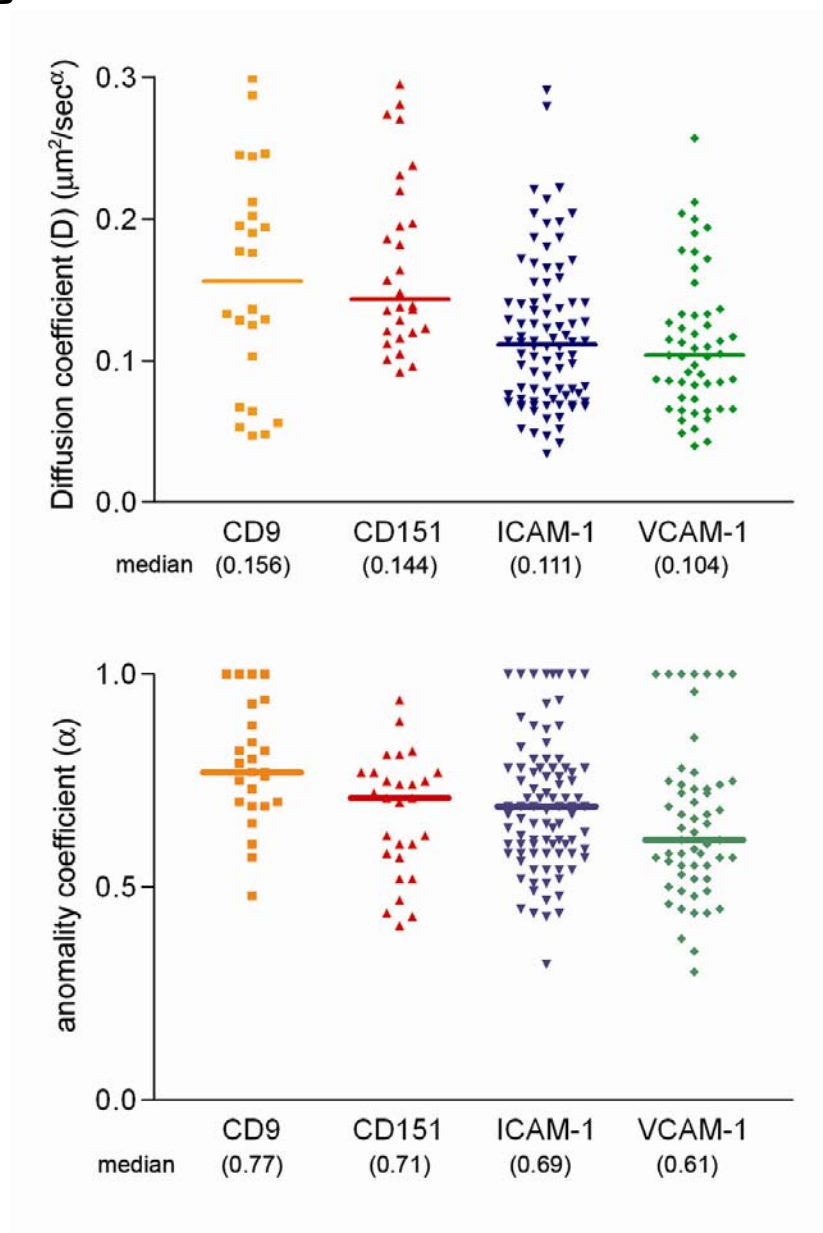


Figure 6A

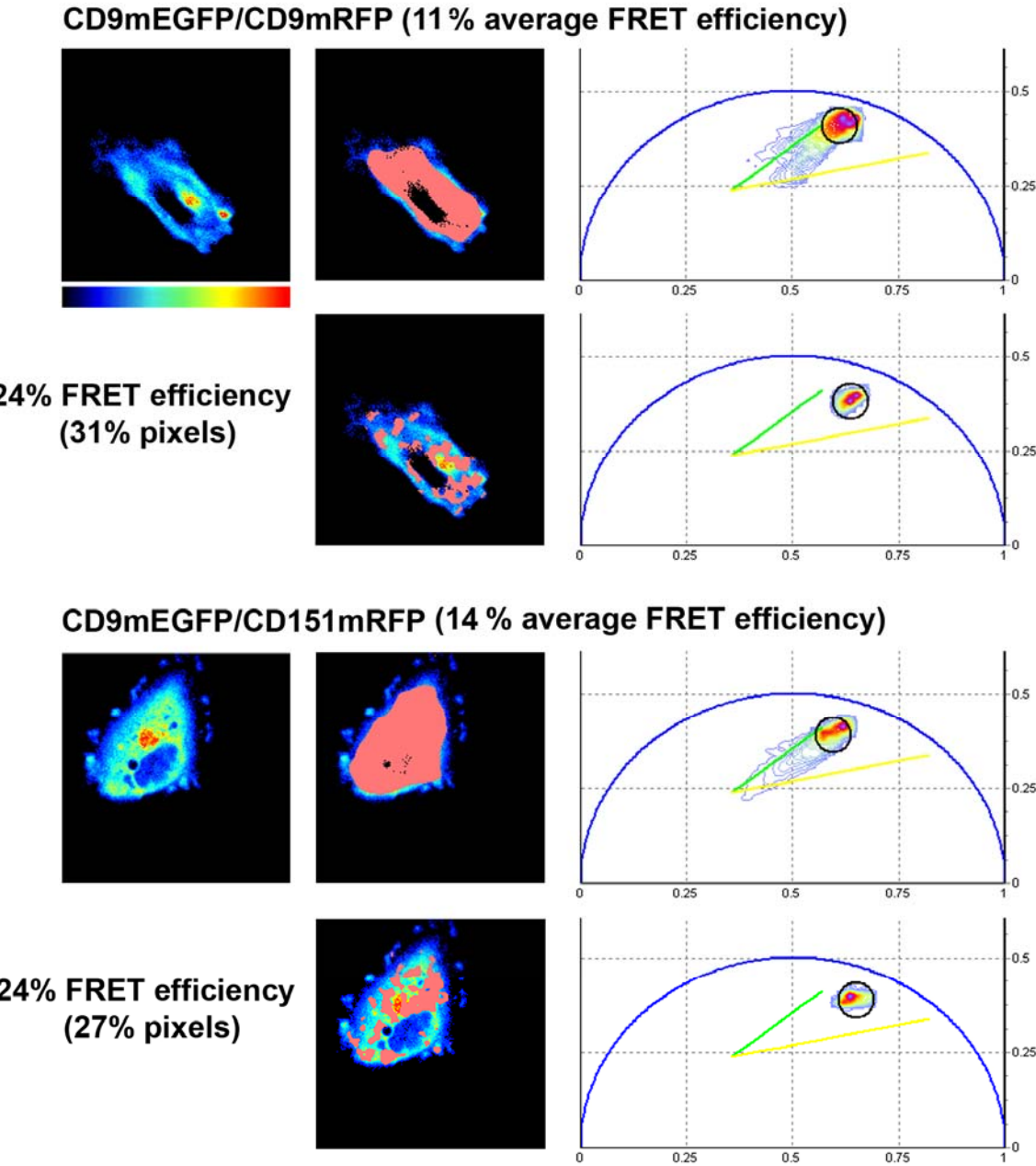
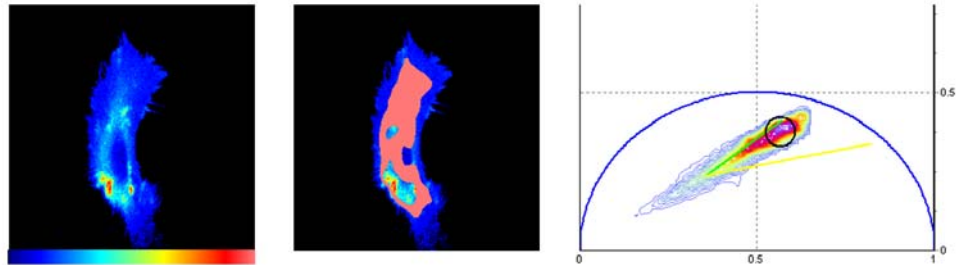
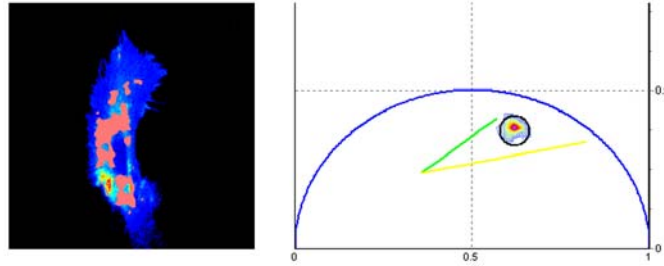


Figure 6B

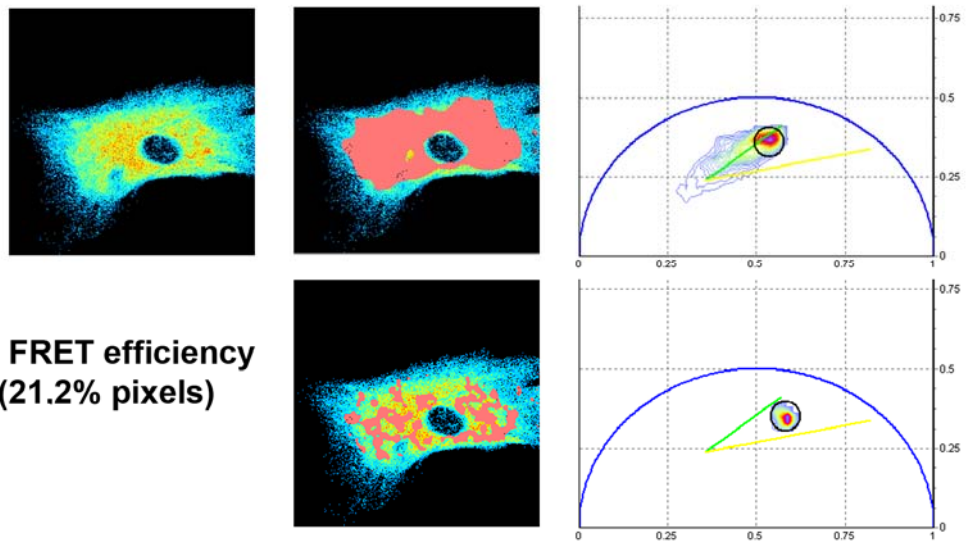
**IC1mEGFP/CD9mRFP (12% average FRET efficiency)**



**24% FRET efficiency  
(12.1% pixels)**



**VCAM-1mEGFP/CD151mRFP (11% average FRET efficiency)**



**24% FRET efficiency  
(21.2% pixels)**

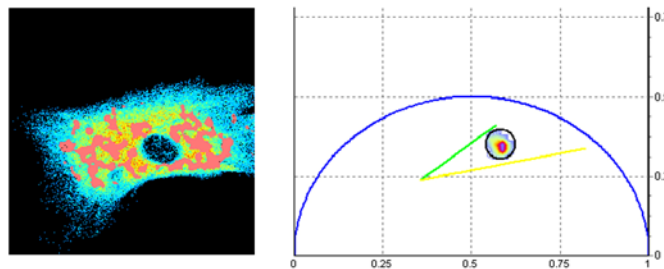
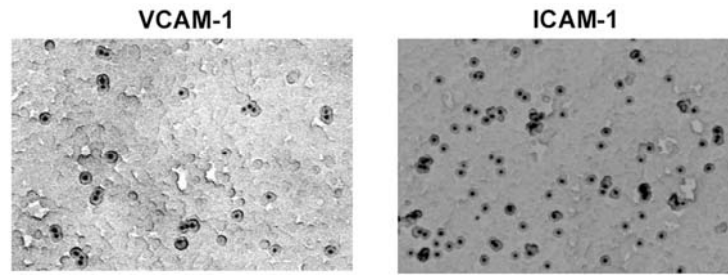


Figure 7

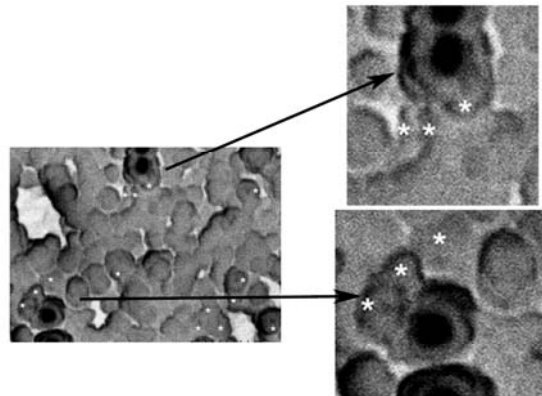
A

i)



Homoclustering of receptors

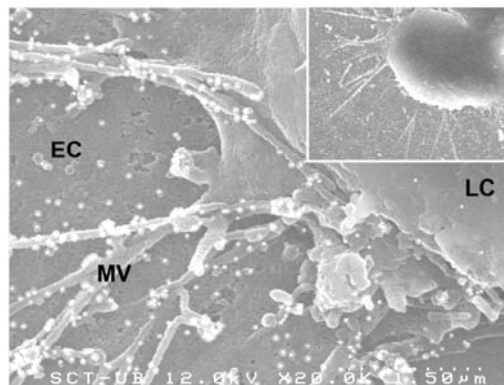
ii)



Heteroclustering of VCAM-1 and ICAM-1

iii)

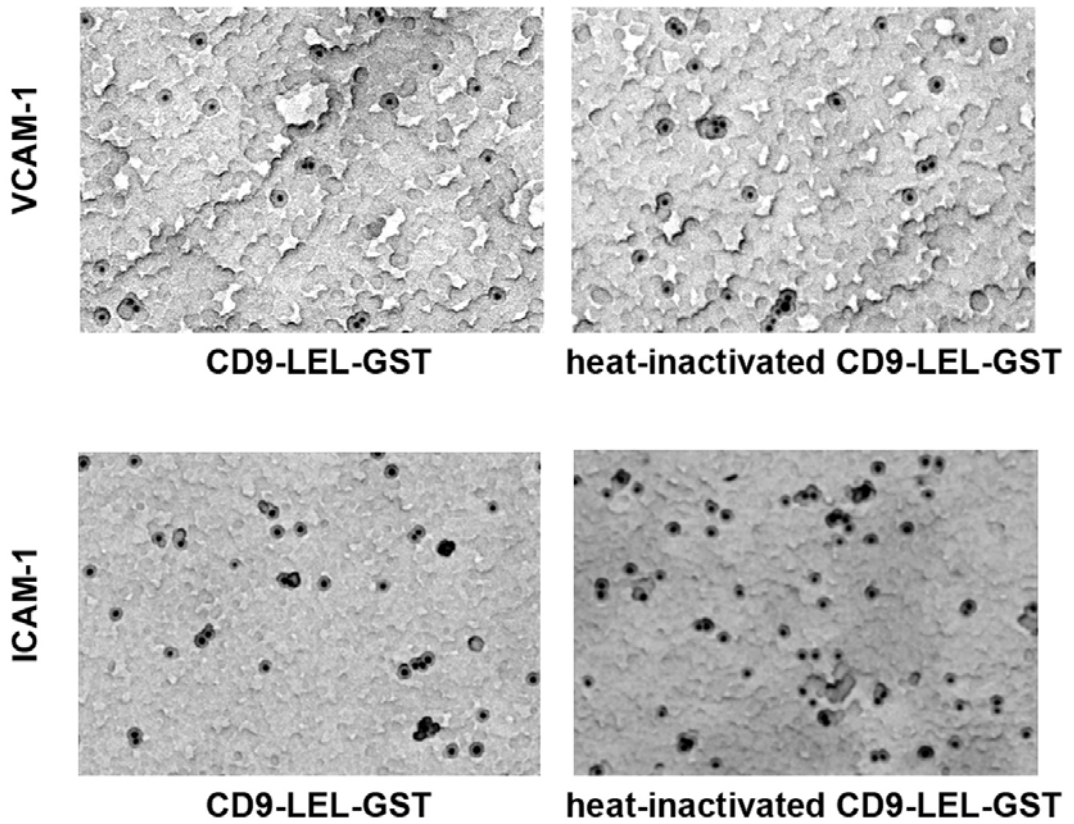
Lymphoblast onto an endothelial cell



EC: endothelial cell  
LC: leukocyte  
MV: microvilli

Figure 7B

i)



ii)

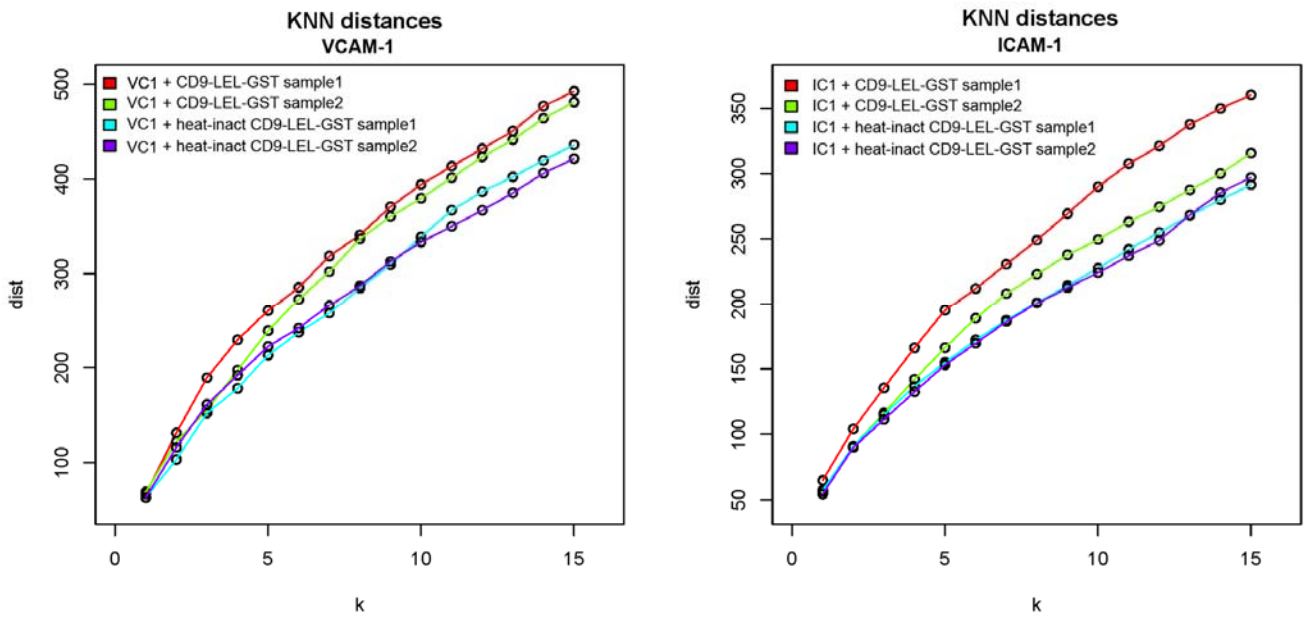
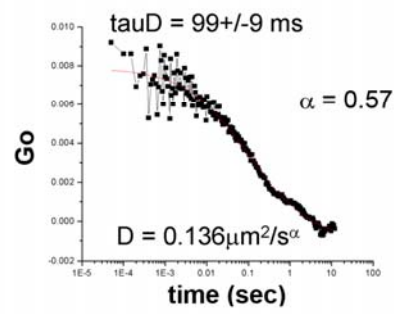
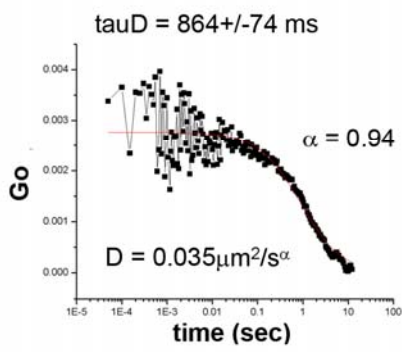
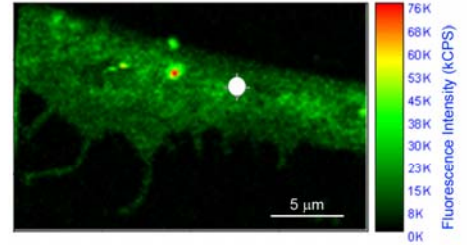
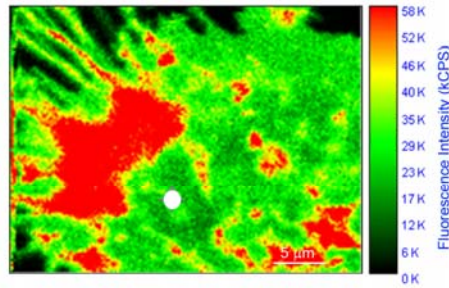
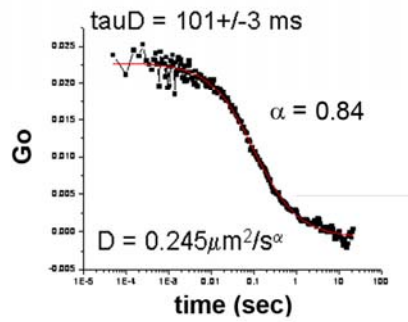
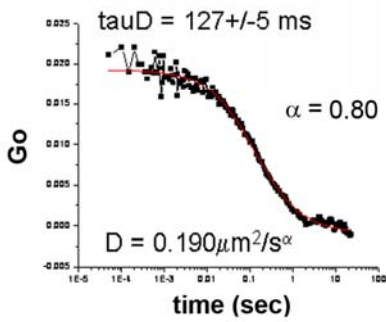
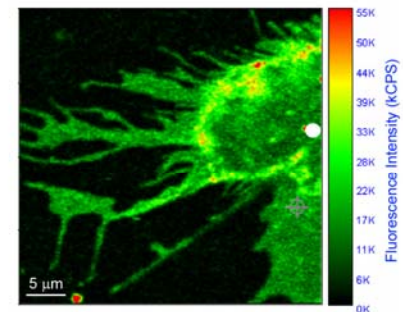
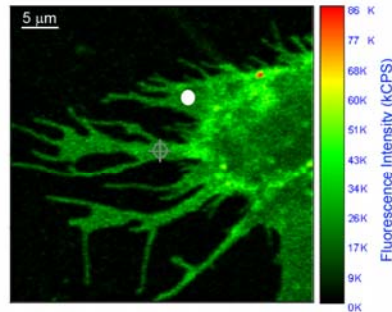


Figure 7C  
i)

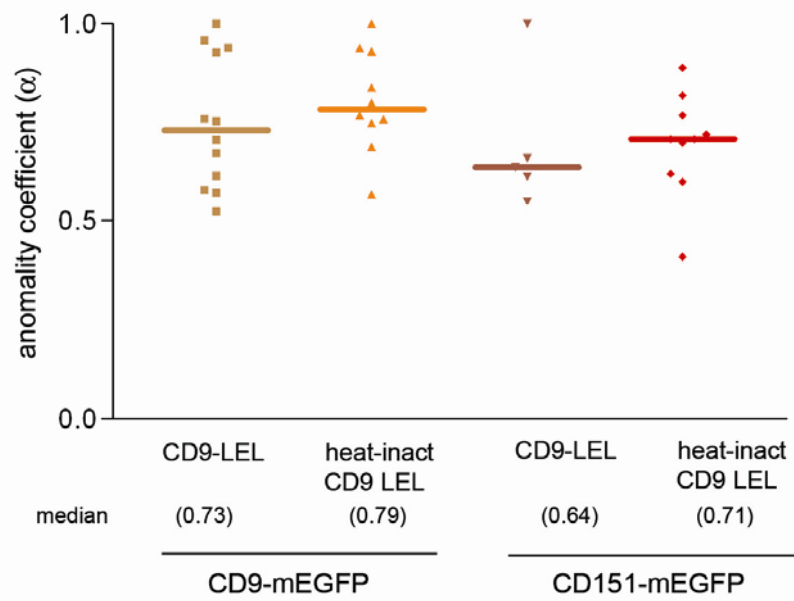
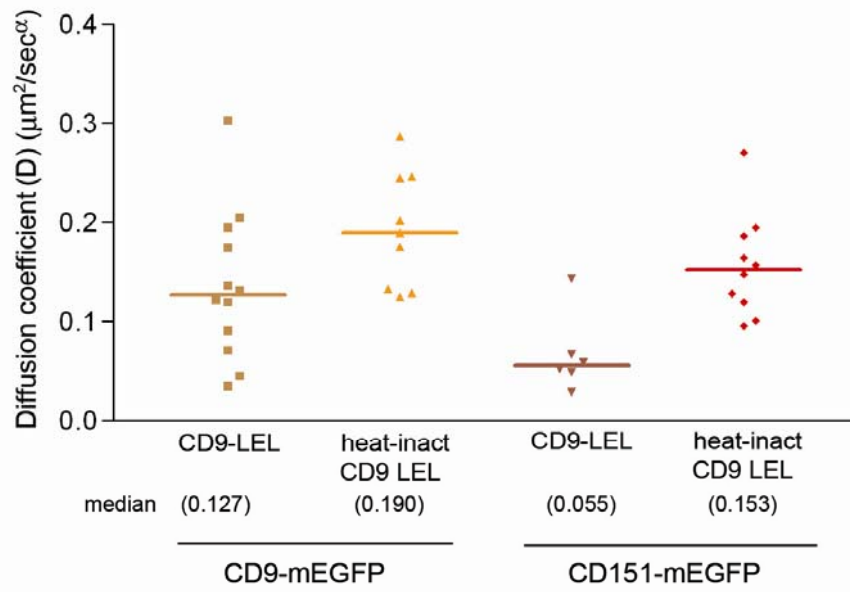
**CD9mEGFP + CD9-LEL-GST**



**CD9mEGFP  
+ heat-inactivated CD9-LEL-GST**

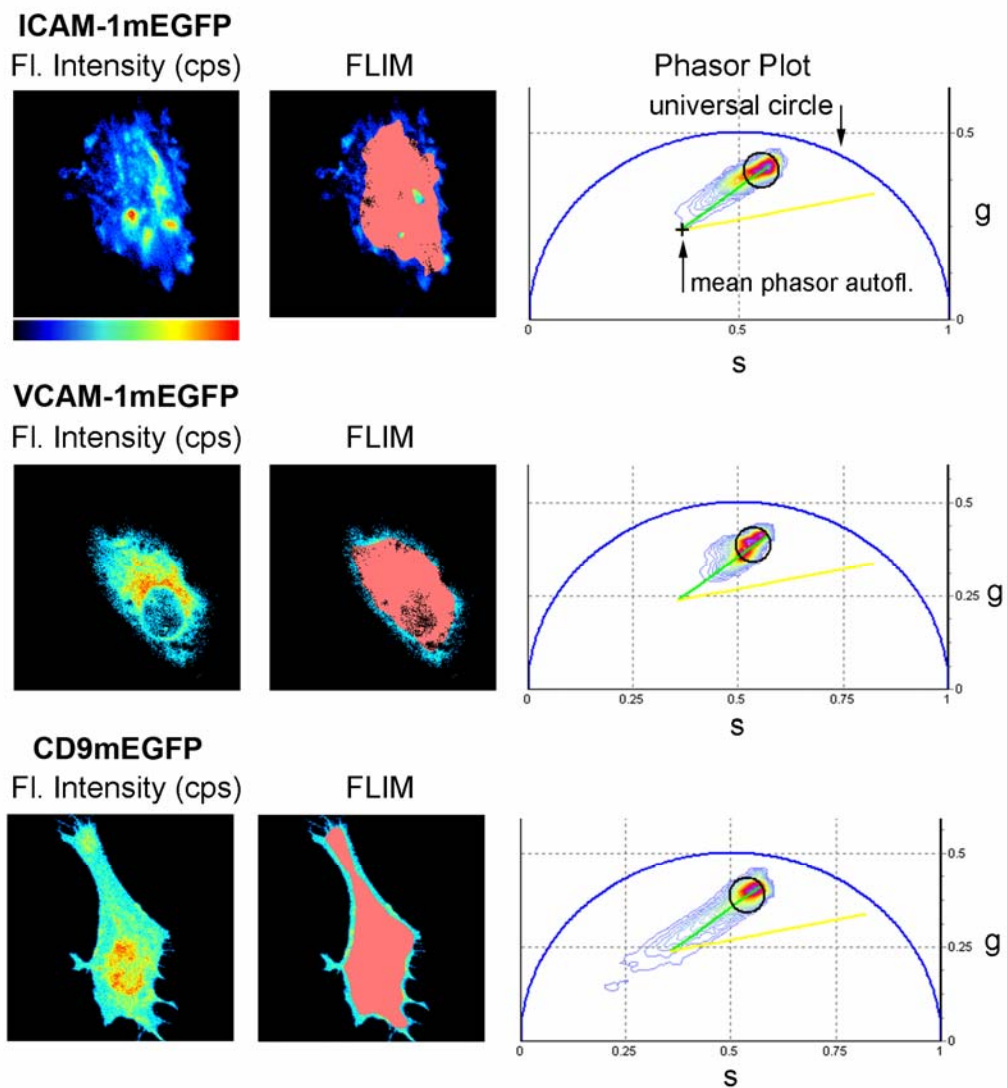


ii)



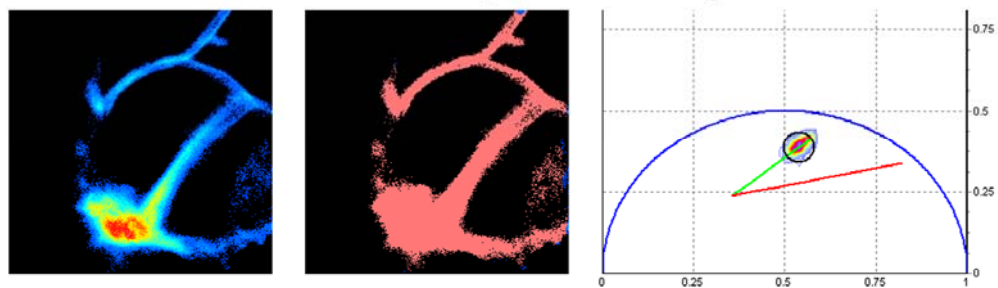
# Supplemental Figure 1

A

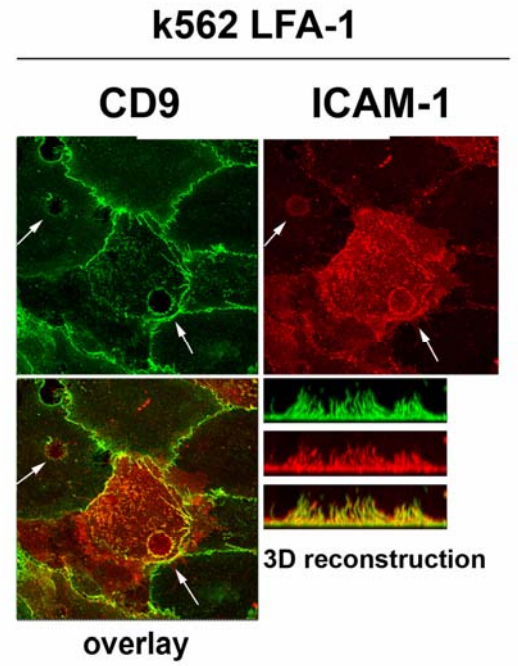
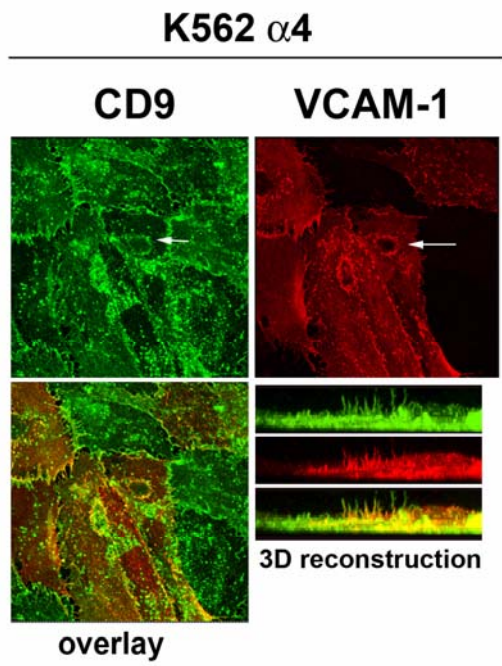


B

uPARmEGFP-ICAM-1mRFP ( $\leq 8\%$  average FRET efficiency)

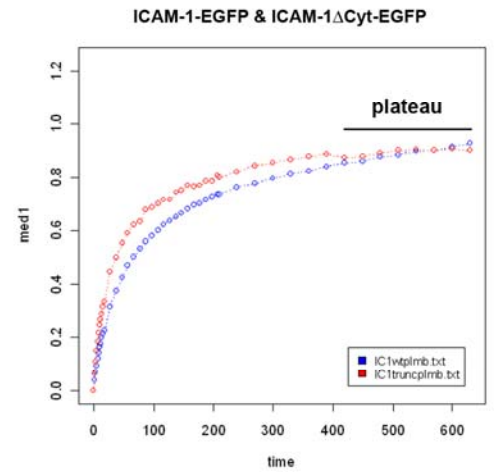


Supplemental Figure 2



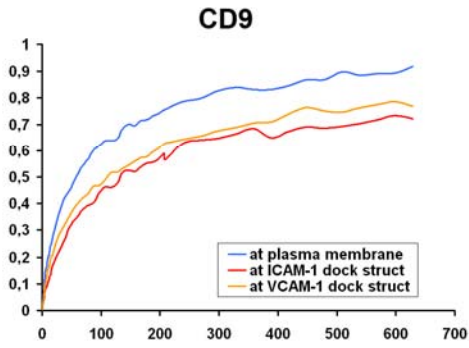
### Supplemental Figure 3A

time	ICAM-1wt plmb	ICAM-1ΔCyt plmb	raw p value	adj p value
0	0	0	NA	NA
1.672	0.041445203	0.062211154	0.0014295	0.002859
3.36	0.071205925	0.106100321	0.00075684	0.00166505
5.047	0.092905048	0.150995668	5.17E-05	0.00019607
6.735	0.120487324	0.18478153	3.58E-05	0.00018026
8.422	0.143021635	0.217203502	4.10E-05	0.00018026
10.11	0.163590373	0.249126425	3.94E-05	0.00018026
11.797	0.176319104	0.268083712	9.28E-05	0.00030577
13.485	0.199972275	0.289831944	5.35E-05	0.00019607
15.172	0.214441072	0.316964081	2.58E-05	0.00018026
17.094	0.229517518	0.334774979	6.16E-06	9.03E-05
27.078	0.314183443	0.447610567	1.15E-06	5.07E-05
37.078	0.377391664	0.501283786	5.05E-06	9.03E-05
47.078	0.426779613	0.553210547	1.53E-05	0.00016843
57.078	0.469797725	0.589492203	4.00E-05	0.00018026
67.078	0.502283577	0.619902556	2.48E-05	0.00018026
77.078	0.534949608	0.63577203	0.00032832	0.00084976
87.082	0.562564772	0.678234646	9.73E-05	0.00030577
97.082	0.581845775	0.687259253	0.00013012	0.00038169
107.082	0.602027048	0.70335984	0.00031413	0.00084976
117.082	0.621096804	0.714203383	0.00040938	0.00100071
127.082	0.639066925	0.715187329	0.00368559	0.00675692
137.082	0.652297087	0.742437366	0.00100015	0.00209554
147.082	0.664686865	0.748683835	0.00153945	0.00294503
157.082	0.680694429	0.770811837	0.0007483	0.00166505
167.082	0.693920766	0.765796506	0.00732593	0.01289363
177.082	0.702860542	0.769459265	0.01430708	0.02331524
187.082	0.714605595	0.784826263	0.01171529	0.01982588
197.082	0.724695799	0.785534643	0.02043003	0.02899746
207.082	0.734400839	0.807417228	0.01627362	0.02469102
209.082	0.735012048	0.799066984	0.01581788	0.02469102
239.062	0.764013524	0.819702608	0.03431022	0.04574696
269.062	0.776819119	0.843283215	0.01791732	0.02627874
299.062	0.796873596	0.853858873	0.02785973	0.03830713
329.062	0.812796501	0.866630111	0.04062275	0.05257062
359.062	0.824116144	0.875966656	0.06494476	0.08164484
389.062	0.840819443	0.886347376	0.14020416	0.17136064
419.062	0.853145171	0.873160386	0.48201405	0.55812153
449.062	0.860564527	0.877762832	0.57432826	0.64150575
479.082	0.876190491	0.888706725	0.65126562	0.6989192
509.082	0.884239869	0.901876051	0.58318704	0.64150575
539.062	0.895515573	0.902772932	0.82133274	0.85275977
569.062	0.900747269	0.898858818	0.95286216	0.95286216
599.082	0.913658991	0.906393439	0.83337886	0.85275977
629.082	0.926053874	0.900398357	0.44256889	0.52629814

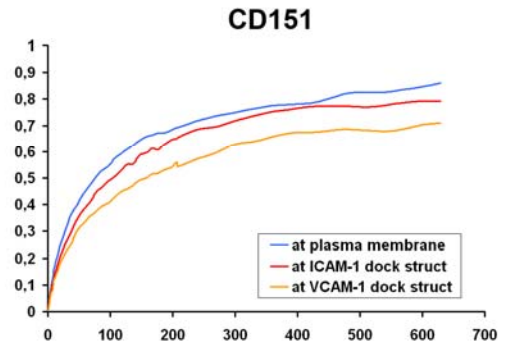


plateau

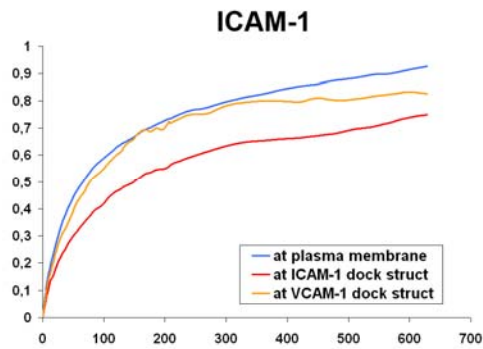
## Supplemental Figure 3B



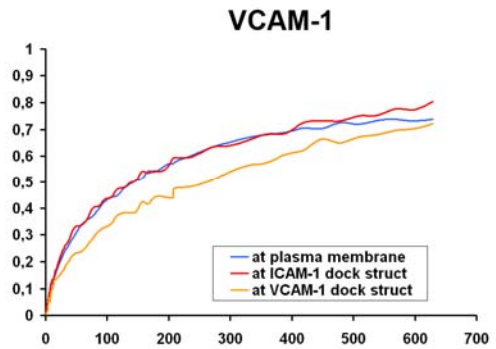
adjusted p-value	CD9 at pl mb
CD9 at ICAM-1 dock str	<0.0045
CD9 at VCAM-1 dock str	<0.03



adjusted p-value	CD151 at pl mb
CD151 at ICAM-1 dock str	<0.35
CD151 at VCAM-1 dock str	<0.025

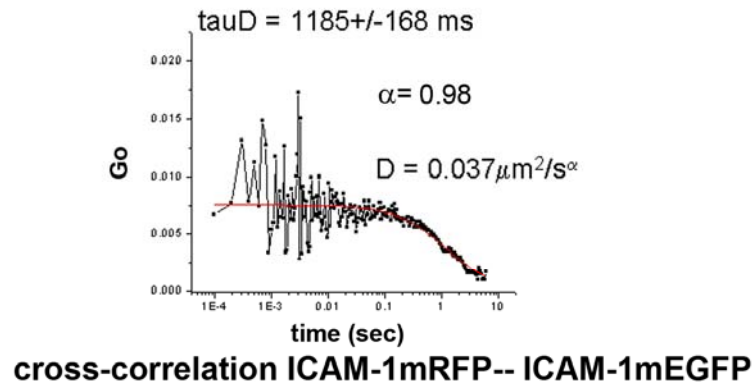
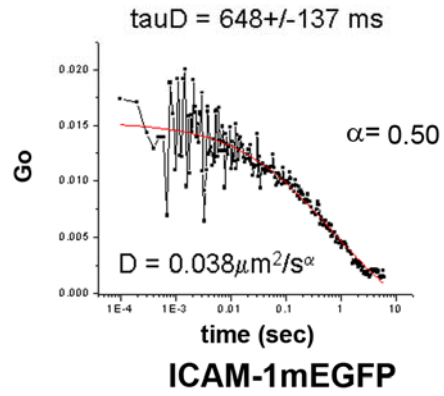
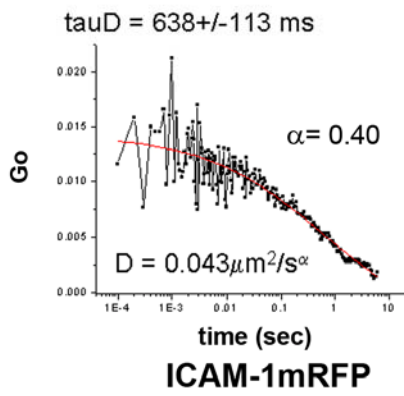
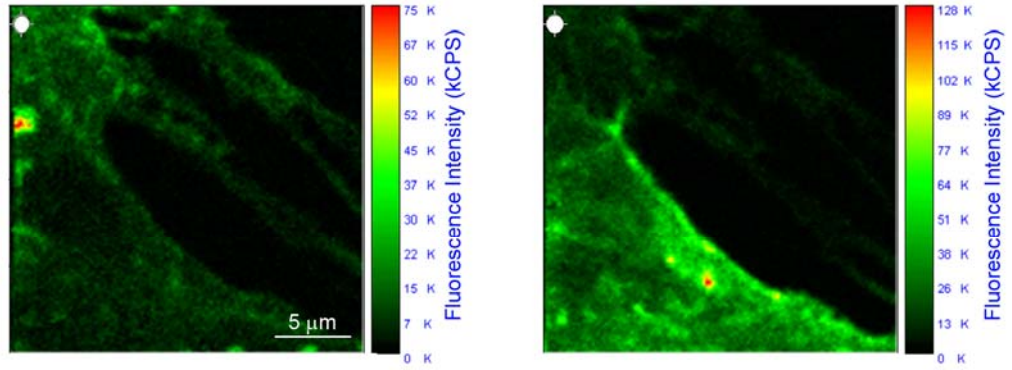


adjusted p-value	ICAM-1 at pl mb
ICAM-1 at ICAM-1 dock str	<0.0001
ICAM-1 at VCAM-1 dock str	<0.6



adjusted p-value	VCAM-1 at pl mb
VCAM-1 at ICAM-1 dock str	<0.996
VCAM-1 at VCAM-1 dock str	<0.025

# Supplemental Figure 4A



Supplemental Figure 4B

